Journal of
...ied Mechanics

...ublication of the A.S.M.E. (Applied Mechanics Division)

...ding 1
...Sokolnikoff, and M. A. Sokolnikoff
...C. F. Kossiakoff 8
...J. S. Rogers 11
...Analysis of Thin Cylindrical Shells, Including Shear and
...E. H. Howe and R. M. Starr 13
...Shell With Small Curvature at the Vertex. . G. D. Gladwell 28
...Axisymmetrically Loaded Anisotropic Elliptical Shells. . . .
...G. Herrey and I. M. Cheng 35
...of Shallow Rectangular Shells . . . . . Eric Reissner 51
...Thin Plastic Plates . . . . . J. P. Sharpe 55
...S. I. Fadle 61
...Cracked Problems Involving Bonded Subject to Dynamic Tension
...M. F. Cheng 68
...G. Herrmann 75
...Compression Molding . . . . . J. R. Stehn 87
...Transverse Vibration of a Tube Containing Flowing Fluid
...R. H. Long, Jr. 95
...Laminated Beams . . . . . B. A. Bolt 99
...Cylindrical Sandwich in the Plastic Range . . . . .
...L. W. Ha and Joseph Kempner 77
...Circular Disks . . . H. Deresiewicz and R. D. Mindlin 86
...Thick Plates . . . . . P. M. Naghdi 89
...Plane Dynamic Problems Involving . . . . . A. P. Boresi 95
...Bending on Compressible Elastic . . . . . Yi-Yuan Yu 103
...Thermal Stresses Symmetric . . . . . T. C. Hsu 107
...Periodic, Elastic Structures . . . . . E. H. Kennard 111
...Shells . . . . . Joseph Kempner 117
...Fins Embedded Within Annular Fins on Round Tubes . . . . .
...H. Zabronsky 119
...Wedges . . . . . I. K. Silverman 123
...Vibrating Beams . . . . . S. Weissenberg-Kaufmann 129
...Flow Around Curved Corners . . . . . H. D. Conway 130
...E. Reissner and S. J. Tsiang . . . . . M. L. Baron and H. H. ...
...Elastic Solids . . . . . F. E. Crandall and C. S. Hsu . . . . . N. J. ...
...Propagation . . . . . and J. G. Kirkwood . . . . . A. H. Shapiro and S. ...
...Compressible Boundary Layer . . . . . and A. M. Wahl, G. O. Sandy, M. J. ...
...Index 151
...Errata 156

MARCH 1953

VOL. 20, NO. 1

...n Society of Mechanical Engineers

Applied Mechanics

Published by the ASME Applied Mechanics Division

E. D. Mountain, Secretary

Applied Mechanics Reviews

The American Society of Mechanical Engineers

Publication Office, Northampton Street, Easton, Pa.
Editorial Department, The American Society of Mechanical Engineers, 29 West Thirty-Ninth Street, New York 18, N. Y.

OFFICERS OF THE SOCIETY
Edward W. E. Meehan, President

C. E. Davies, Secretary

EDITORIAL STAFF

Georges A. Gabriel, Editor
E. W. Comings, Mgr. Editor

By-Laws of the Society ... opinions advanced in papers ... printed in its publications (B13, Par. 4).

Publication office, 20th and Northampton Streets, Easton, Pa. The editorial ... Price ... Subscriptions ... Canada, the United States ... other countries outside the United States, ... on the mailing list. ... published in papers or ... printed in ... Act of August 24, 1912, ... may be made on remittance that will entitle to given

Propagation of Elastic Impact in Beams in Bending[1]

By MARTIN GOLAND,[2] P. D. WICKERSHAM,[3] and M. A. DENGLER,[4] KANSAS CITY, MO.

A theoretical and experimental comparison is made of the strain propagation in steel beams impacted by a sharp, transverse blow. The theoretical analysis is based on an earlier paper by Dengler and Goland, in which a solution based on the Timoshenko bending mechanism is deduced. (An analytical error in this paper is corrected here.) The experimental work was performed on a square beam, impacted by a steel sphere. Measurements are reported both for the strain propagation in the beam and also for the history of forces acting between the ball and beam. The results of the comparison show excellent agreement between the observed and predicted strain propagation, so long as the beam behaves essentially in bending. It is pointed out in the discussion, however, that many impacted beams do not perform essentially in bending, so that the present work does not apply. A small-amplitude high-frequency strain component, not properly predicted by the theory, is also encountered in the experimental data.

Introduction

In a recent paper by Dengler and Goland (1),[5] an analytical solution is derived for the propagation of elastic bending stress in an infinitely long beam subjected to a sharp impact, in the form of a concentrated, lateral load applied to the beam mid-span. The reference (1) result makes use of the Timoshenko bending mechanism, which accounts for the rotatory inertia and shear deformation of cross-sectional beam elements. Unfortunately, an analytical error in this paper has been brought to our attention and suitable corrections are given here. The Dengler and Goland results appear in closed form, but require the evaluation of certain complicated integrals in order to reduce the solution for numerical evaluation.

As a next step in an over-all study of the behavior of beams and plates under sharp impact, the present program was undertaken with the objective of examining the reference (1) results critically by comparing their predictions with experimental observations. In addition to the required experimentation, this necessitated the numerical evaluation of the Dengler and Goland results for the beam configuration under test.

The present report describes the techniques used for the numerical treatment of the Dengler and Goland solution and includes a detailed description of the test program. A critical comparison of the theoretical and experimental results is then undertaken, with a remarkable degree of agreement being shown for beams in bending, even when the impact is of very short duration. The practical significance of this agreement is discussed later.

Some Background on the Investigation

In view of the availability of the reference (1) paper and its associated bibliography, a detailed discussion of the theoretical implications of the Dengler and Goland work is not required here. However, the following remarks may be helpful when considering the ramifications of the present investigation.

The problem of interest is the lateral impact of an infinitely long beam of uniform rectangular cross section by a concentrated force applied to the top surface of the beam. Attention is centered on impacts of short duration, approaching impulsive loading. The mechanism to be studied is that of beam bending, it being assumed that no twisting deformations of the beam cross sections are introduced.

Consider the problem first from the point of view of the theory of elasticity. At the instant the load is applied at a point of the top surface of the beam, stress waves begin to propagate in all directions within the beam. These waves depart from the point of load application and move along the beam length in both directions, the rays reflecting from the top, bottom, and sides of the beam as required. While the load is acting, the stress pattern in the immediate vicinity of the concentrated load is highly three-dimensional in character; away from this localized region, the "beam" action begins to assert itself and the stress distribution becomes approximately two-dimensional, with strong variations of stress occurring only along the beam length and in the direction of the beam height; the stress distribution across the width of the beam is reasonably uniform. Once the load is removed, the beamlike action extends over the loaded region as well.

If the over-all beam behavior is to be studied, a first simplification would appear to be neglect of the three-dimensional character of the stresses immediately near the load. The loss of accuracy implied by this neglect is that the stresses cannot be estimated properly in the immediate vicinity of the applied load, so long as the load is acting. It is to be observed in passing, however, that the situation near the load is of Hertzian character, and it will be shown later that experimental evidence is available to indicate that the classic Hertz impact theory can be used to approximate the stresses acting immediately under the load. Neglect of the three-dimensionality of the stresses in the localized region near the load will not detract appreciably from the accuracy of a study of the over-all beam behavior.

If the stress distribution within the beam is approximated as two-dimensional, then the considerations become those of a problem in plane stress. The normal (vibration) modes for a rectangular bar in plane stress have been established by Lamb (2) and others (see bibliography, reference 1). It is illuminating for the moment to deal with the impact load in terms of its associated

---

[1] The results presented in this paper were obtained in the course of research under the sponsorship of the Office of Naval Research, Contract No. NOnr 704(00).

[2] Director for Engineering Sciences, Midwest Research Institute. Mem. ASME.

[3] Assistant Manager (Instrumentation), Engineering Division, Midwest Research Institute.

[4] Research Mathematician, Midwest Research Institute.

[5] Numbers in parentheses refer to the Bibliography at the end of the paper.

Contributed by the Applied Mechanics Division and presented at the Annual Meeting, New York, N. Y., November 29–December 4, 1953, of The American Society of Mechanical Engineers.

Discussion of this paper should be addressed to the Secretary, ASME, 29 West 39th Street, New York, N. Y., and will be accepted until April 11, 1955, for publication at a later date. Discussion received after the closing date will be returned.

Note: Statements and opinions advanced in papers are to be understood as individual expressions of their authors and not those of the Society. Manuscript received by ASME Applied Mechanics Division, November 13, 1952. Paper No. 53—A-46.

generalized forces which induce appropriate responses in the normal modes of the beam.

Lamb's studies divide the beam normal modes into two sets: Those which have cross-sectional stress distributions which are symmetrical about the beam mid-height plane, and those with antisymmetrical distributions about this plane. Considering the latter, the most fundamental series of modes are those which are related to the elementary beam-bending mechanism in so far as they involve only one "neutral" plane at the mid-height; i.e., the mid-height plane is one of zero stress. For the infinitely long beam, this class of modes displays a continuous natural-frequency variation with change of wave length along the beam. In the low-frequency region, i.e., for long waves, the stress distribution at each beam cross section is closely linear and hence reduces to the modes of the elementary bending theory.

In addition to this fundamental class of modes, an infinite number of higher mode classes also are present. These are characterized by having more than one neutral plane, each class being associated with a certain number of such zero stress planes. The presence of these modes is completely foreign to any elementary bending-type considerations.

In regard to the symmetrical normal modes of the beam, an analogous situation exists. The lowest mode class, which is related to the elementary theory of longitudinal wave transmission, has no neutral plane. The higher mode classes have multiple neutral planes, arranged symmetrically about the beam mid-height.

It has been pointed out by Prof. J. N. Goodier[4] that the application of a downward transverse load of amount P to the top surface of the beam can be thought of as the sum of the following two loadings: (a) downward loads of amount $P/2$ each applied to the top and bottom surfaces of the beam at the loaded cross section, and (b) a downward load of amount $P/2$ applied to the top surface, and an upward load $P/2$ applied to the bottom surface, both at the loaded cross section. The loading (a) is antisymmetrical about the beam mid-plane and hence induces responses only in the antisymmetrical modes. The loading (b), being symmetrical about the beam mid-plane, excites responses only from the symmetrical mode classes.

It thus becomes clear that the transverse impact of a beam by a lateral force applied to the beam top must induce a stress system which has both a symmetrical and an antisymmetrical component about the beam mid-plane. A rather simple physical verification of this fact emerges from the consideration of lateral impact of a very deep beam. The beam being very deep, the problem approaches that of a lateral force application to the straight edge of a semi-infinite solid. Obviously, the action of the force is hardly felt at all at the distant bottom edge of the beam, the entire disturbance being restricted to surface waves propagated along the top (loaded) edge region.

It is not the objective of this study to investigate the lateral impact problem from the comprehensive point of view just outlined. Rather, the scope of the program is restricted to an investigation of beams in "bending;" i.e., to a study of beams which display essentially an antisymmetrical stress distribution at each beam cross section throughout the impact cycle. A corollary to this restriction is that, while a symmetrical stress system must be induced in the beam, it is of negligible importance in comparison with the antisymmetrical counterpart.

As justification for this seemingly arbitrary restriction of scope, it can only be pointed out that such beams in bending can be realized experimentally, as will be shown later. Moreover, these beams have obvious and considerable engineering importance. Unfortunately, definitive rules have not as yet been deduced to discriminate in advance of actual test between beams of bending character, and those where the symmetrical stresses begin to exert an important influence. This should form the objective of continuing study.

Even if it is admitted that only beams in bending are to be dealt with, a thoretical solution to the plane-stress problem from an exact point of view poses great difficulties. Further engineering approximations seem necessary (at least at present) if the impact problem is to be solved in practical fashion. The paper of Dengler and Goland (1) attempts to obtain such a solution by relying on the Timoshenko bending mechanism.

The Timoshenko mechanism differs from the elementary bending theory by introducing approximate corrections for the effects of rotatory inertia and shear deformations of cross-sectional elements of the beam. The fundamental concept of plane cross sections of the beam remaining approximately plane under load is retained. As Cremer (3) and others have shown, the use of the Timoshenko mechanism permits excellent approximation of the transmission characteristics of the fundamental class of beam normal modes and affords a reasonable approximation for the transmission characteristics of the next highest class of modes. Mode classes above these two are ignored entirely. As will be shown later, experimental data appear to confirm the use of the Timoshenko mechanism for the treatment of even the sharpest of beam impacts and hence seem to indicate that the higher mode classes do not contribute significantly to the stresses in beams in bending.

In contrast to the Timoshenko mechanism, the elementary bending theory does not account for the effects of rotatory inertia and shear deformation of the beam cross-sectional elements. This leads to a mathematical theory which restricts its scope to only one mode of transmission; moreover, this mode is a close approximation for the fundamental class of beam normal modes only when the wave length is very long (corresponding to small natural frequencies). It is well known that, because of this characteristic, the elementary bending theory cannot be used for the analysis of sharp beam impacts.

These general remarks are aimed at placing the present program in proper over-all perspective. It is seen that interest is restricted to a particular, though important, phase of the general problem. This discussion also brings out the need for studies directed toward the behavior of beams not exhibiting pure bending characteristics.

Theoretical Calculation of Bending-Stress Propagation in a Uniform Beam Subjected to an Impulsive, Concentrated, Lateral Load

In the theoretical analysis of reference (1), a nondimensional system of co-ordinates is employed, derived as follows: All physical lengths are referred to the height h; all physical masses are referred to ρh^3, where ρ is the density of the beam material; and all physical times are referred to $h(\rho/E)^{1/2}$, where E is the Young's modulus of the beam material. On this basis, all parameters entering the analysis become dimensionless. For example, physical forces are referred to Eh^2, physical moments to Eh^3, physical stresses to E, physical velocities to $(E/\rho)^{1/2}$, and so on.

The reference (1) analysis pertains to the lateral loading of an infinitely long beam of uniform cross section, the loading comprising a concentrated force applied impulsively. The load history thus consists of the product of Dirac functions in time and space.

To arrive at the nature of the bending moment propagation in

[4] Both the theoretical and experimental phases of this program have been discussed with Prof. J. N. Goodier and Dr. E. A. Ripperger, both of Stanford University. The authors wish to acknowledge their most helpful advice.

the beam, reference (1) employs a complicated contour integration entailing consideration of branch points along both the real and imaginary axes. Dr. Julius Miklowitz of the U.S. Naval Ordnance Test Station Inyokern, China Lake, California, has pointed out that the contour analysis of reference (1) is not entirely correct. In particular, referring to the original paper, the cut made along the real axis from $-\infty$ to $+a$ is not sufficient to render the expression λ_3 single-valued. In addition to this cut, a cut along the imaginary axis between $\pm i/k(C)^{1/2}$ is required. This has the effect of making the reference (1) results incorrect for the interval $x < \tau < (C)^{1/2}x$.

The correct results given by Miklowitz, and checked by the present authors, are as follows: For an impulsive loading of unit dimensionless magnitude

(1) For $\tau < x$,

$$m(\tau, x) = 0 \quad [1]$$

(2) For $x < \tau < (C)^{1/2}\, x$,

$$m(\tau, x) = \frac{1}{2\pi}\int_0^b F(\xi, \tau, x)d\xi - \frac{1}{2\pi MN}\int_0^a G(\xi, \tau, x)d\xi \quad [2]$$

(3) For $\tau > (C)^{1/2}\, x$,

$$m(\tau, x) = \frac{1}{2\pi}\int_0^b F(\xi, \tau, x)d\xi \quad [3]$$

where

$$F(\xi, \tau, x) = \left[1 - \frac{\xi}{N(a^2 + \xi^2)^{1/2}}\right]\frac{\cos \xi\tau \cdot \cosh Sx}{S} \quad [4]$$

$$G(\xi, \tau, x) = \frac{1}{\xi(a^2 - \xi^2)^{1/2}}\left\{\zeta \cos (Mx\psi)\cdot\cosh(\xi\tau - Mx\zeta) + \psi \sin (mx\psi)\cdot\sinh(\xi\tau - mx\zeta)\right\} \quad [5]$$

Here $C = E/\lambda G$ where E is Young's modulus and λG is the effective shear modulus of the Timoshenko bending mechanism. Also

$$M = [(C+1)/2]^{1/2};\quad N = (C-1)/(C+1)$$

$$a = 2/k(C-1);\quad b = 1/k(C)^{1/2}$$

$$\zeta = [\xi(R+\xi)/2]^{1/2};\quad \psi = [\xi(R-\xi)/2]^{1/2}$$

$$R = [\xi^2 + N^2(a^2 - \xi^2)]^{1/2}$$

$$S = M\xi^{1/2}[N(a^2 + \xi^2)^{1/2} - \xi]^{1/2}$$

In the numerical evaluation of $m(\tau, x)$ from the above expressions, several difficulties must be overcome. First, it is to be noted that the functions of Equations [4] and [5] must be calculated with great accuracy. A cursory examination shows that the integrands can have magnitudes as large as 10^4, while the magnitude of the bending moment is of the order 10^{-1}.

The integrand of Equation [5] has singularities of order $1/2$ at both ends of the interval of integration. A simple transformation changes the interval from $(0, a)$ to $(0, 1)$. The singularities were removed by substituting $u^2 = \xi$ in the range $0 \leqslant \xi \leqslant 0.64$ and $u^2 = 1 - \xi$ in the range $0.64 \leqslant \xi \leqslant 1$. The integrands were tabulated at close intervals and integration was accomplished using Lagrangian three and five-point quadrature formulas. Spot checks were performed using higher-point integration formulas.

The integrand of Equation [4] is highly oscillatory and in addition has a singularity of order $1/2$ at the origin. Here it was found that the technique of product integration could be used to good advantage. The techniques employed have been previously reported by Luke (8, 9) and need not be detailed here.

For the actual computations, the IBM Card Programmed Computer was used, and better than engineering accuracy was maintained.

The numerical calculations for the present study were undertaken for a beam of square cross section, i.e., $k = 1/2\sqrt{3}$. The value of $C = E/\lambda G$ was fixed in the manner suggested by Mindlin (4) as follows: According to the exact theory, the transmission velocity of very short flexural waves of the fundamental mode variety is the velocity of Rayleigh surface waves. For the Timoshenko bending mechanism, the transmission velocity for this mode class is $(E/\rho C)^{1/2}$ in dimensional form. Accordingly, the value of C is established so as to bring the two velocities into conformance.

For a beam material with Poisson's ratio $1/3$, the resulting value of C is 3.07. Hence the value $C = 3$ was used for the calculations of this paper.

It is interesting to compare this value with the one resulting from elementary bending theory. In view of the parabolic shearing-stress distribution over the cross section of a rectangular beam, the parameter λ equals $2/3$. Hence $C = E/\lambda G = 4$.

The results of bending-moment calculations for the time histories at stations $x = 0$, 4, and 8 are shown in Figs. 1 to 3. For the station $x = 4$, discontinuities of bending moment occur at $\tau = 4$ and $\tau = 4\sqrt{3}$. These correspond to the times of arrival of the two transmission modes of the Timoshenko mechanism at the station in question. A similar performance is observed in the time history for station $x = 8$.

The plots in Figs. 1 to 3 are given in nondimensional terms. It is of interest to note that, for a steel beam, one unit of τ corresponds to a physical time of about $5h$ microsec.

Measurement of Loading Histories and Strain Propagation in Square Beams Subjected to Sharp Lateral Impacts

The second phase of the present study entailed the collection of data regarding the strain propagation in impacted, square-cross-section steel beams. The experimental setup, in general terms, entailed the dropping of a steel ball bearing from a known height onto the top surface of the beam. A force gage (to be described later) measured the force-time history exerted by the ball on the beam, while strain gages at stations $x = 4$ and $x = 8$ (i.e., four and eight beam heights from the impact station) recorded the strain time histories at these locations.

A detailed description of the experiments is now given.

Equipment Setup. The beams used in the tests were of square cross section and were simply supported at their ends in a horizontal plane. The beam dimensions were 1 in. × 1 in. × 8 ft, 6 in. and $2^1/_4$ in. × $2^1/_4$ in. × 11 ft, 7 in. The beams were struck transversely at their mid-spans and their lengths were sufficient to insure that reflections from the beam ends did not return to station $x = 8$ until after the strain recordings of interest were completed.

The steel ball bearings used for the drops were of commercial variety and included sizes between $1/8$ in. and $9/32$ in. diam. A simple release mechanism for the balls consisted of an oversize tube, aligned vertically with its longitudinal axis perpendicular to the longitudinal axis of the beam, and with two small holes drilled in the tube walls along a diameter. A wire inserted in the holes restrained the ball from falling; rapid removal of the wire permitted the ball to drop freely.

Since the theoretical work is based on a knowledge of the forces applied to the beam, a force gage, Fig. 4, was designed to measure this information. The gage consists of a barium-titanate wafer, 0.015 in. thick and 0.250 in. diam. The top and bottom surfaces of the wafer were coated lightly with silver solder. The upper surface of the beam was lapped to provide a smooth flat contact surface for the bottom surface of the wafer. The flat side of a

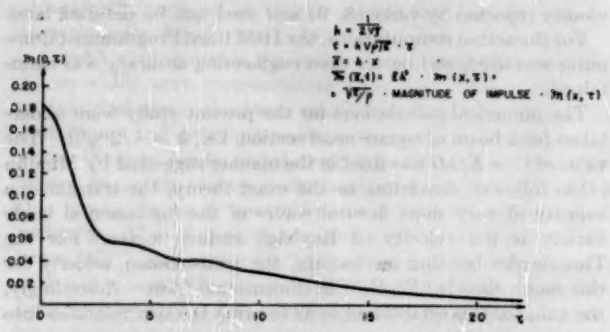

FIG. 1 CALCULATED BENDING MOMENT-TIME HISTORY FOR STATION $x = 0$
(For a concentrated load, impulsively applied to a beam of square cross section with $c = 3$.)

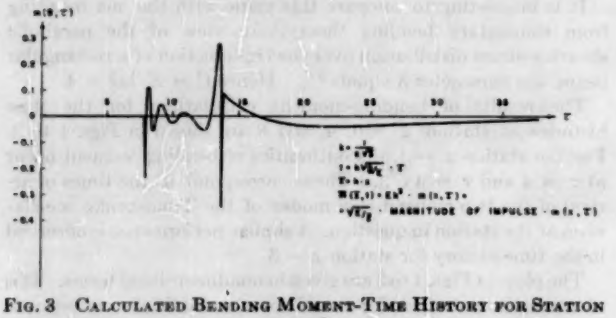

FIG. 3 CALCULATED BENDING MOMENT-TIME HISTORY FOR STATION $x = 8$
(For a concentrated load, impulsively applied to a beam of square cross section with $c = 3$.)

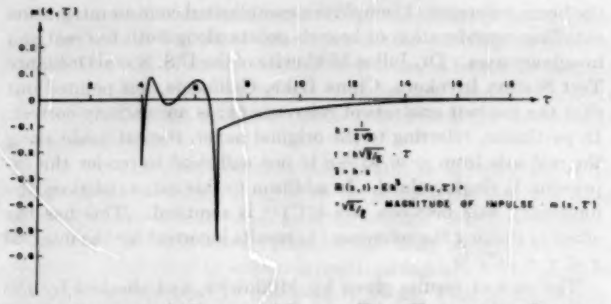

FIG. 2 CALCULATED BENDING MOMENT-TIME HISTORY FOR STATION $x = 4$
(For a concentrated load, impulsively applied to a beam of square cross section with $c = 3$.)

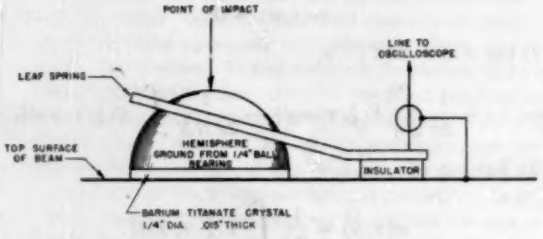

FIG. 4 DIAGRAMMATIC SKETCH OF FORCE GAGE

hemispherical contact button (made from a ball bearing) rests on the top surface of the wafer. A beryllium-copper leaf spring, Fig. 4, affords both positioning and a light preload of the button and wafer on the beam; the spring also serves as the ungrounded electrical contact to the top side of the barium-titanate wafer. The impacting ball strikes the gage at the crown of the contact button.

When the barium-titanate wafer is subjected to compression, it generates a charge between its top and bottom surfaces which is instantaneously proportional to the magnitude of the applied force. Hence the force gage, providing a proper time constant is employed in the circuitry, can be used to generate a voltage versus time curve which is proportional to the impact force-time history.

Calibration of the gage was accomplished by devising a mechanism which suddenly released a known dead load on the gage. The gage constant determined by this method is 0.39 volt per lb applied force. The voltages generated during the test impacts were sufficiently high to be applied without preamplification to the input of a Tektronix type 511 oscilloscope, and then displayed on one trace of a 5SP-11 dual-beam cathode-ray-tube display unit (see later discussion).

To measure the strain time histories at stations $x = 4$ and $x = 8$, four barium-titanate strain gages of $^1/_8$ in. gage length were used; two gages were used at each station, one on the top and one on the bottom surface of the beam. This type gage was employed because of its small size and relatively high signal output (the test impacts induced relatively small strain amplitudes in the beam). The gages consist of barium-titanate bars $^1/_8$ in. $\times$ $^1/_4$ in. $\times$ 0.015 in. thick and have silver-solder coatings on their largest faces to which electrical contacts are made. After cleaning the beam surface with an abrasive and washing it with acetone, the gages were cemented to the beam with nitrocellulose cement in such fashion that a $^1/_8$-in. gage length results for the bending stresses.

It was found that any accumulation of a thin oil-and-dirt film on the gages would cause their gage factors to change appreciably, apparently because of a conducting path being introduced between the gage electrodes. Hence care was exercised to keep the gages clean by frequent acetone washes.

Recording of the strain-gage output was accomplished as follows: The barium-titanate gages generate a charge proportional to the developed strain and the charge then produces a voltage determined by the total of the shunt capacity of the gage itself, the capacity of the signal cable to the preamplifier, the input capacity of the preamplifier, and the capacity which may be placed in shunt across the gage to give any necessary attenuation. The first three of these capacities were measured accurately so that the desired attenuation could be obtained with calibrated capacitors.

The strain-gage signal was first amplified by a Kaylab preamplifier (with a gain of 100) and was then fed into the vertical amplifier of a Tektronix type 512 oscilloscope. This resulted in an over-all frequency band width of 600 kc. A 100-kc square wave was reproduced by this combination with no significant rounding of corners or overshooting. The output from the scope was then applied as one vertical signal to a 5SP-11 dual-beam cathode-ray-tube display unit. (The second vertical signal fed to the display unit was the applied force; hence both force and one strain signal were recorded simultaneously. Unfortunately, equipment to record more than one strain history during a single drop was not available.)

The sweep voltages for the two time bases of the 5SP-11 unit were obtained from two oscilloscopes; a 30-microsec sweep for the force gage was obtained from the Tektronix 511 scope, and a 100-microsec sweep for the strain channel was derived from the Tektronix 512 scope. Photographic recording of the tube traces was accomplished with a Dumont type 296 oscillographic camera. Voltage and time calibrations for the recording system were effected for each drop in routine fashion, the calibration accuracies being within $^1/_2$ per cent. To correlate time on the

TABLE 1 COMPARISON OF OBSERVED AND HERTZIAN CONTACT TIMES AND PEAK FORCES DURING IMPACT OF BALL ON BEAM

Beam size, in.	Ball diam, in.	Drop height, in.	Contact time, microsec		Peak force, lb	
			Observed[a]	Calculated	Observed[a]	Calculated
1	5/32	2	14.0(0.70)	15.2	15.6(0.96)	13.8
1	5/32	4	13.1(0.63)	14.2	25.1(1.25)	21.0
1	5/32	16	11.5(0.24)	12.3	64.3(5.02)	48.0
1	1/4	2	13.2	11.9	8.4	9.3
2 1/4	5/32	0.2	37.0	35.9	9.3	10.7
2 1/4	5/32	0.4	33.5	33.6	16.4	16.1

[a] The data for the 5/32-in. ball are based on eight tests per drop height. The experimental value given is the mean of the eight tests; the number in parentheses, adjacent to the experimental mean, is the standard deviation of the eight test values. The remaining data are for single test points. For the 2 1/4-in-beam tests, the shape of the force versus time curve is non-Hertzian in character, displaying a definite double-peaking.

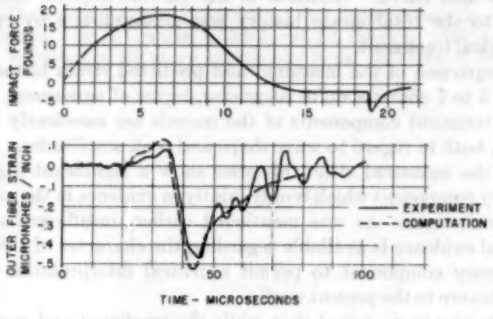

FIG. 5 MEASURED AND CALCULATED HISTORIES OF IMPACT FORCE AND OUTER FIBER STRAIN AT STATION $x = 4$

(For 1-in. beam; 5/32-in. ball; 2-in. drop height. Figs. 5 and 6 represent identical test conditions and show data agreement obtained from various drops.)

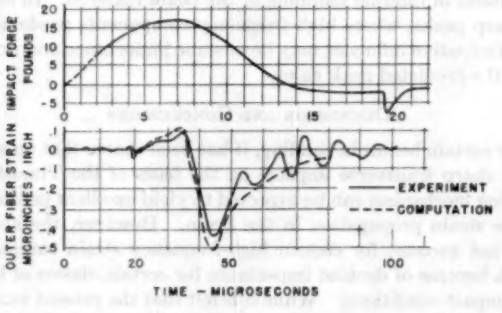

FIG. 6 MEASURED AND CALCULATED HISTORIES OF IMPACT FORCE AND OUTER FIBER STRAIN AT STATION $x = 4$

(For 1-in. beam; 5/32-in. ball; 2-in. drop height. Figs. 5 and 6 represent identical test conditions and show data agreement obtained from various drops.)

two traces, a correlation pip was introduced on both, care being taken to have the pip fall where minimum interference with wave forms results.

The barium-titanate gages were calibrated by comparing their output with those from Baldwin SR-4 type C-7 resistance-wire gages cemented to the beam adjacent to the gages of interest. The beam was excited in sinusoidal bending by means of an electromechanical vibrator and the gage outputs compared. Since the characteristics of the SR-4 gage are known, calibration of the ceramic gages could be accomplished.

An over-all accuracy of ±5 per cent is estimated for the experimental work reported here.

Analysis of the Force Data. Although the basic objective of the present work is to study the bending propagation in beams under known applied loadings, certain interesting information regarding the forces arising from the ball-beam impact was obtained as an experimental dividend. Accordingly, an account of these data is now given.

When designing the force gage, it was realized that the velocity

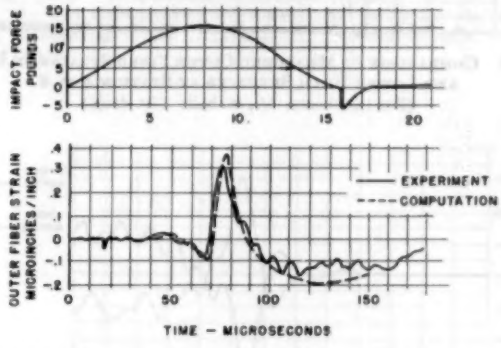

FIG. 7 MEASURED AND CALCULATED HISTORIES OF IMPACT FORCE AND OUTER FIBER STRAIN AT STATION $x = 8$

(For 1-in. beam; 5/32-in. ball; 2-in. drop height.)

of sound in steel is about 0.2 in/microsec. Hence about 10 microsec are required for a stress wave to propagate from the force gage to the bottom surface of the 1-in. beam, and then to be reflected back to the gage. Since the recording times for the force data were considerably in excess of this time interval, it was feared that reflection effects would distort the force measurements. However, no such distortions were immediately evident, save as noted in the next paragraph.

Typical recordings of force-time histories obtained during drops are shown as the solid lines in the upper plots of Figs. 5, 6, and 7. The data show an initial compression history which has the general characteristics to be expected from Hertzian type impact. Following the compression, a small-amplitude tension history is indicated, which obviously cannot arise from the forces between the impacting ball and the beam. Attempts to relate these small-amplitude tensions to either the instrumentation or reflection considerations have thus far been unsuccessful. In the analysis of the data to ascertain the ball-beam forces, the recordings were assumed to be accurate during the compression interval; the indications of tensile forces were ignored.

It having been noted that the force-time histories are Hertzian in character, a comparison was made between the experimental data and Hertz calculations. For the latter, the diameter of the struck body was taken equal to the diameter of the contact button, and the mass of the struck body was taken as infinite. The results of the comparison are shown in Table 1.

It is seen that surprisingly close correlation exists between the calculated and observed values of both contact time and peak force during impact. This seems to imply that the use of the Hertz theory for prediction of the stresses immediately under the concentrated load is a justifiable first approximation, so long as the loading time is relatively short.

It is of interest to note that Christopherson (5) reached similar conclusions based on an approximate analysis. The use of a force gage similar to ours is reported by Crook (6).

Analysis of Strain Data. Strain-time histories measured on

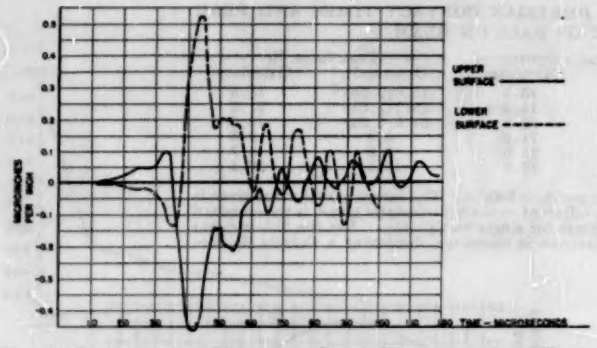

FIG. 8 COMPARISON OF MEASURED OUTER FIBER STRAINS ON UPPER AND LOWER BEAM SURFACES AT STATION $x = 4$
(For 1-in. beam; $^1/_{32}$-in. ball; 2-in. drop.)

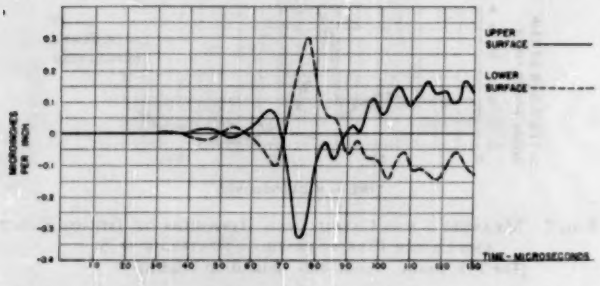

FIG. 9 COMPARISON OF MEASURED OUTER FIBER STRAINS ON UPPER AND LOWER BEAM SURFACES AT STATION $x = 8$
(For 1-in. beam; $^1/_{32}$-in. ball; 2-in. drop.)

beams in the bending class are shown as the solid lines in the lower plots of Figs. 5, 6, and 7. These records are used for comparison with the theory in the manner described in the next section.

In order to insure that the beams used for comparison with the theory were primarily in bending, the records from gages on the top and bottom beam surfaces were compared; for pure bending, they should be mirror images of each other about the time axis. Figs. 8 and 9 show such comparisons at stations $x = 4$ and $x = 8$ for the drop configuration of Figs. 5 to 7.

In general, it is to be noted that the strain histories of Figs. 5 through 9 can be thought of as a basic transient history on which is superimposed certain small-amplitude high-frequency oscillations. It is clear from Figs. 8 and 9 that the basic transients for the Figs. 5 to 7 drop configuration are essentially mirror images of each other; no definite conclusions in this regard can be drawn for the high-frequency oscillation components since the strain records could not be taken simultaneously.

It is of considerable interest to note, however, that the amplitudes of the high-frequency strain components diminish rapidly in going from station $x = 4$ to $x = 8$. This is characteristic of all the data taken, most of which are not reported here.

The degree of reproducibility of records taken during different drops, but for the same drop conditions, is found to be quite excellent. When the force records coincide, the strain records remain identical to within a few per cent, Figs. 5 and 6.

A Comparison of Theoretical and Experimental Results

In order to compare the analytical predictions of Figs. 2 and 3 with the experimental observations, account must be taken of the fact that the former relate to impulsive loading, whereas the test data are for the loading histories shown in Figs. 5 through 7. The most effective way of placing both sets of information on the same footing is to extend the analytical results so that they apply to the experimentally observed load histories. This can be accomplished conveniently by using the Duhamel integral technique (7).

In physical terms, the Duhamel integral approach entails visualization of the load-time history as a series of successive impulses. In view of the linearity of the theory, each impulse contributes to the total strain history as if it acts alone; addition of the effects of the various impulses, due account being taken of the respective impulse amplitudes and time origins, leads to the total strain history for the complete loading.

In the present treatment, the observed loading history was approximated by a series of impulses, the magnitude of each corresponding to the area under a 0.4-microsec interval of the force-versus-time curve. Addition of the various impulse contributions to the total strain history was accomplished by routine numerical treatment.

Comparison of the measured and predicted strain histories in Figs. 5 to 7 shows a quite surprising degree of agreement. The basic transient components of the records are excellently duplicated, both in regard to wave shape and peak amplitudes. However, the measured strain histories show a significant high-frequency component which is only faintly in evidence in the analytical predictions. As was mentioned earlier, insufficient experimental evidence is available regarding the character of the high-frequency component to permit a critical interpretation of its significance to the present work.

It is also to be noted that while the predicted and measured strain amplitudes agree remarkably well, both the histories at $x = 4$ and $x = 8$ show calculated peak values which are slightly higher than the experimental peaks. One possible explanation for this lies in the fact that the present theoretical results neglect the effects of internal damping of the beam material. In regions of sharp peaks, where high frequency components predominate, this dissipative influence may be of some importance and may reduce the predicted peak values.

Discussion and Conclusions

For certain beams in bending, it has been shown that an analysis of sharp transverse impacts on the basis of the Timoshenko bending mechanism can be expected to yield excellent predictions of the strain propagation in the beam. However, the analysis does not account for certain high-frequency strain components which become of decided importance for certain classes of beams and impact conditions. While it is felt that the present work is a contribution to the over-all problem, it suffers from the inability to decide under which circumstances, and in what manner, the high-frequency effects will significantly enter the propagation mechanism.

The present work accounts only approximately for the second class of antisymmetrical transmission modes, omits the contributions from the higher-order antisymmetrical transmission modes, and neglects entirely consideration of the symmetrical transmission modes. It seems desirable, therefore, that further analytical and experimental work be directed toward study of these aspects of the over-all problem. The analytical studies, in so far as possible, should be based on the known results from the theory of elasticity in regard to transmission mode characteristics.

Within the scope of the present work, a practical approach to the analysis of the stresses resulting from sharp impacts is suggested. While the studies reported here pertain to a uniform beam of infinite length, these geometrical restrictions are not inherent in the Timoshenko mechanism. Hence the development of approximate numerical or graphical methods for solution of the Timoshenko beam equation should provide a tool for practical analysis of elastic impact stresses.

Acknowledgment

The authors are indebted to Messrs. Y. L. Luke, E. J. Martin,

Jr., R. H Scheil, and the computations staff, all of Midwest Research Institute, for their aid in carrying out this program.

BIBLIOGRAPHY

1 "Transverse Impact of Long Beams, Including Rotatory Inertia and Shear Effects," by M. A. Dengler and M. Goland, Proceedings of the First National Congress on Applied Mechanics, 1951, published by THE AMERICAN SOCIETY OF MECHANICAL ENGINEERS, New York, N. Y., 1952.

2 "On Waves in an Elastic Plate," by H. Lamb, Proceedings of the Royal Society of London, England, series A, vol. 93, 1916–1917, p. 114.

3 "Bemerkungen zur Ausbreitung von 'Biegewellen' in Stäben und Platten," by L. Cremer, ZAMM, vol. 23, October, 1943. p. 291.

4 "Influence of Rotatory Inertia and Shear on Flexural Motions of Isotropic, Elastic Plates," by R. D. Mindlin, JOURNAL OF APPLIED MECHANICS, Trans. ASME, vol. 73, 1951, pp. 31–38.

5 "Effect of Shear in Transverse Impact on Beams," by D. G. Christopherson, Proceedings of Applied Mechanics, The Institution of Mechanical Engineers, vol. 165, 1951, WEP No. 67.

6 "A Study of Some Impacts Between Metal Bodies by a Piezoelectric Method," by A. W. Crook, Proceedings of the Royal Society of London, England, series A, vol. 212, 1952, pp. 377–390.

7 "Mathematical Methods in Engineering," by T. von Kármán and M. A. Biot, McGraw-Hill Book Company, Inc., New York, N. Y., first edition, 1940, chapter 10.

8 "Mechanical Quadrature Near a Singularity," by Y. L. Luke, Mathematical Tables and Other Aids to Computation, vol. 6, no. 40, October, 1952.

9 "On the Computation of Oscillatory Integrals," by Y. L. Luke, Proceedings of the Cambridge Philosophical Society, vol. 50, Part 2, 1954.

Oil Streamlines in Bearings

By C. F. KETTLEBOROUGH,[1] MELBOURNE, AUSTRALIA

A semigraphical method is given for tracing oil-flow streamlines in bearings. This is illustrated by a typical calculation.

Nomenclature

The following nomenclature is used in the paper:

A = pressure coefficient = $\left(\frac{6\lambda\omega\alpha r_0^2}{h_0^2}\right)$
B = radial width of pad
h = oil-film thickness
h_0 = outlet-film thickness
L = length of rectangular pad in direction of motion
P = oil-film pressure
r = any radius within sector-pad area
r_0 = inner radius of pad
r_1 = nondimensional radius parameter given by $r = r_0 e^{\rho r_1}$
r_m = nondimensional radial position of maximum oil-film pressure
U = velocity of moving member
V_r = radial-velocity component of oil particle
V_t = tangential-velocity component of oil particle
α = angle subtended by sector pad
λ = oil viscosity
θ = angular position of point in oil film
θ_1 = nondimensional angular position given by $\theta = \alpha\theta_1$
ω = angular velocity
$\rho = \log_e\left(\frac{r_0 + B}{r_0}\right)$ from $r = r_0 e^{\rho r_1}$
$F(\theta_1)$ = nondimensional pressure function in circumferential direction
$f(r_1)$ = nondimensional pressure function in radial direction

Development of Graphical Solution

A review of the literature reveals little information on the oil-flow streamlines in a bearing. For a flat slider it is usually illustrated as shown in Fig. 1 (see Norton[2]). However, Gibson's[3] photographs show that the oil flow should be as shown dotted in Fig. 1. In order to elucidate this point a graphical method has been evolved as follows:

The path of a particle of oil situated halfway between the opposite faces of a sector-shaped tilting pad has been traced. It was assumed to remain in this central position. The sector-pad size assumed was 2 1/4 in. ID, 4 1/8 in. OD, and included angle 35°16′.

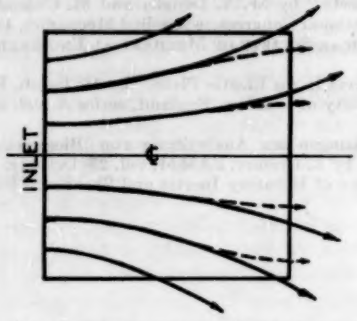

Fig. 1 Oil Streamlines for Rectangular Slider
(Full lines, see Norton;[2] dotted lines, see Gibson.[3])

The radial velocity of such an oil particle is given by

$$\left(-\frac{1}{\lambda}\frac{dP}{dr}\frac{h^2}{8}\right)$$

and the tangential velocity by

$$\left(-\frac{1}{r\lambda}\frac{dP}{d\theta}\frac{h^2}{8} + \frac{\omega r}{2}\right)$$

In order to evaluate these components the slope of the pressure surface and the viscosity must be known. Boswall's[4] approximate method, in which the pressure intensity at any point is given by $P = Ae^{2\rho r}F(\theta_1)f(r_1)$, was used to determine the pressure distribution for a film ratio of 3.4 and a total load of 130 lb, Fig. 2(*a*). Christopherson's[5] relaxation method was then applied to obtain the temperature distribution shown in Fig. 2(*b*). The slopes $dP/d\theta$ and dP/dr are found graphically or by finite-difference formulas from Fig. 2, and the viscosity from Fig. 3, using the viscosity-temperature curve determined by a standard Redwood viscometer. The value of the film thickness at any point is determined from the facts that the film ratio is 3.4 and the computed minimum film thickness is 0.00104 in.

Typical Calculation

Consider the point marked A in Fig. 3.

Radial velocity $V_r = \left(-\frac{1}{\lambda}\frac{dP}{dr}\frac{h^2}{8}\right)$

with $\lambda = 0.77$ poise, $h = 0.00281$ in., $dP/dr = 216$ psi per in., whence $V_r = -19.2$ ips.

Tangential velocity

$$V_t = \left(-\frac{1}{r\lambda}\frac{dP}{d\theta}\frac{h^2}{8} + \frac{\omega r}{2}\right)$$

with

$\lambda = 0.77$ poise, $h = 0.00281$ in., $\omega = -156$ radians/sec (1490

---

[1] Senior Lecturer, University of Melbourne.

[2] "Lubrication," by A. E. Norton, McGraw-Hill Book Company, Inc., New York, N. Y., 1942, fig. 73.

[3] "The Michell Thrust Block," by J. H. Gibson, *Engineering*, vol. 107, June 13, 1919, p. 765.

Contributed by the Applied Mechanics Division and presented at the Annual Meeting, New York, N. Y., November 28–December 3, 1954, of The American Society of Mechanical Engineers.

Discussion of this paper should be addressed to the Secretary, ASME, 29 West 39th Street, New York, N. Y., and will be accepted until April 11, 1955, for publication at a later date. Discussion received after the closing date will be returned.

Note: Statements and opinions advanced in papers are to be understood as individual expressions of their authors and not those of the Society. Manuscript received by ASME Applied Mechanics Division, February 9, 1954. Paper No. 54—A-23.

[4] "The Theory of Film Lubrication," by R. O. Boswall, Longmans, Green and Company, Ltd., London, England, 1928.

[5] "A New Mathematical Method for the Solution of Film Lubrication Problems," by D. G. Christopherson, Proceedings of The Institution of Mechanical Engineers, London, England, vol. 146, 1941, pp. 126–135.

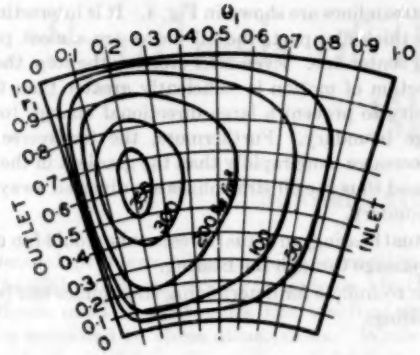

FIG. 2(a) OIL-FILM PRESSURE DISTRIBUTION

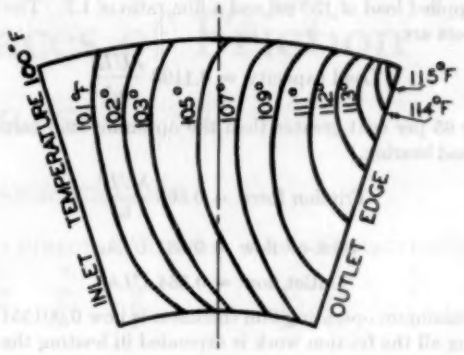

FIG. 2(b) MEAN OIL-FILM TEMPERATURE DISTRIBUTION

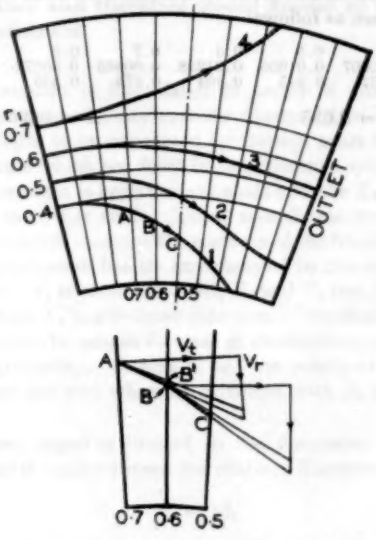

FIG. 3 SHOWING CONSTRUCTION OF AND TYPICAL STREAMLINES FOR SECTOR PAD CONSIDERED

rpm), $r = 1.38$ in., $dP/d\theta = -358$ psi per in., $V_t = 22.9 - 107.8 = -84.9$ ips

With these velocities a velocity triangle is constructed at point A. Assuming the velocity remains constant over the interval $\theta_1 = 0.7$ to $\theta_1 = 0.6$, the particle will move to point B', at which point the velocities are recomputed

$$V_r = -24.5 \text{ ips}$$
$$V_t = -85 \text{ ips}$$

Mean radial velocity over interval $= -21.8$ ips.

Mean tangential velocity over interval $= -85$ ips. With these new velocities a new velocity triangle is constructed at point A and, assuming the oil particle moves with these new velocities over this interval, the particle will move to point B, where the velocities are now $V_r = -26$ ips and $V_t = -85$ ips.

The process could be repeated but it is felt that the second attempt gives sufficient accuracy. A series of such points A, B, C, and so on, are determined and a smooth curve through them gives the approximate streamline.

Four streamlines are shown in Fig. 3 for $r_1 = 0.4$, 0.5, 0.6, 0.7, and clearly show that streamlines 2 and 3 are caused to turn away from the inner radial edge. This is due to two factors:

(*a*) Consider the pressure-induced velocities in the circumferential direction, i.e., in the direction of motion. Between the inlet edge and the point of maximum pressure, the pressure in the oil film reduces the steady velocity component ($\omega r/2$). This pressure-velocity component depends on $dP/d\theta$. Beyond the point of maximum pressure, the pressure-velocity component is very large; i.e., $dP/d\theta$ is large and is in the same direction as the steady component, resulting in a comparatively large increase in the tangential-velocity component.

(*b*) The transverse slope dP/dr decreases more rapidly than the circumferential gradient.

Hence the oil path is deflected away from the inner and outer edges after passing the point of maximum pressure.

Any means which decreases side leakage increases the load capacity. One such bearing is the stepped thrust bearing. Fig. 4 shows the pressure distribution for the step shape as shown and

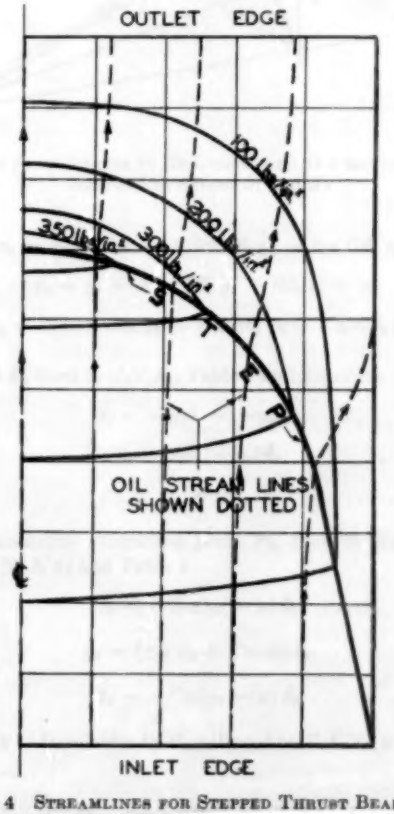

FIG. 4 STREAMLINES FOR STEPPED THRUST BEARING

for an applied load of 130 psi and a film ratio of 1.7. The operating factors are

$$\text{Load capacity} = 0.1193\,\frac{\lambda UL^2}{h_0^2}$$

(This is 65 per cent greater than the optimum load carried by a tilting-pad bearing.)

$$\text{Friction force} = 0.868\,\frac{\lambda UL^2}{h_0}$$

$$\text{Inlet-oil flow} = 0.681\,ULh_0$$

$$\text{Outlet flow} = 0.554\,ULh_0$$

The minimum operating film thickness is now 0.001551 in. and assuming all the friction work is expended in heating the oil, the temperature rise is approximately 13 F. A pad 1 in. square was assumed operating with a moving member having a linear velocity of 250 ips. The viscosity variation through the bearing was assumed to be linear.

The oil streamlines are shown in Fig. 4. It is interesting to note that in the thick-film part, the oil paths are almost parallel to the bearing center line. Even after crossing the step, the velocity in the direction of motion is sufficiently greater than the transverse velocity to prevent a large directional change toward the side-leakage boundary. Furthermore, the transverse pressure gradient decreases more rapidly than the gradient in the direction of motion and thus the oil streamlines are diverted away from the leakage boundary.

In an actual bearing, an actual stream tube would fan out brushlike in its passage through the bearing.

A similar technique for determining streamlines can be used for journal bearings.

Appendix

The essential details given by Boswall's[4] solution for the sector-shaped pad are as follows:

θ_1 or r_1	0	0.1	0.2	0.3	0.4	0.5	0.6	0.7	0.8	0.9	1.0
$-F(\theta_1)$	0	0.02217	0.02594	0.02385	0.02007	0.01606	0.01228	0.00885	0.00572	0.00281	0
$f(r_1)$	0	0.308	0.543	0.716	0.852	0.945	0.994	0.978	0.853	0.562	0

$r_m = 0.635$ $\qquad A = 6690$ psi

Synthesis of the Surfaces of Friction Skew Gears

By JOSEPH STILES BEGGS,[1] LOS ANGELES, CALIF.

The general problem of transmitting motion between two shafts with uniform velocity is discussed in this paper. The methods used to synthesize the teeth of spur gears[2] have been extended to three dimensions. While the present paper is limited to a discussion of friction gears the groundwork is laid for attacking the problem of toothed skew gears. Skew friction gears are shown to slip even under no load and therefore would appear to have a very limited usefulness.

THE problem is formulated in terms of the orthogonal Cartesian co-ordinate systems illustrated in Fig. 1. The two shafts to be connected by friction gears lie along the Z_1 and X_2-axes which are fixed in the reference system $X_0Y_0Z_0$. The $X_1Y_1Z_1$-system is keyed to one shaft and the $X_2Y_2Z_2$-system is fixed on the other shaft. These co-ordinate systems therefore may be used to describe the surfaces of the friction gears.

The $X_3Y_3Z_3$-system has its axes parallel to the corresponding $X_0Y_0Z_0$-axes. Y_4 is coincident with Y_0 and Y_2 but X_4 is rotated an angle α from X_3 in a positive direction. The shafts have been placed in horizontal planes for ease of illustration; this involves no loss of generality. θ_1 and θ_2 are the rotations of the two shafts. They are zero when X_1 coincides with X_0 and Y_2 with Y_4.

The present paper is limited to the discussion of constant angular velocity ratio between the shafts. Therefore

$$\dot{\theta}_1 = k\dot{\theta}_2 \quad \ldots\ldots [1]$$

In order to determine the relative movement at a point of contact of the two gears the motion of any point P_1 fixed in gear 1 is referred to the frame $X_0Y_0Z_0$. The same is done with a momentarily coincident point P_2 fixed in gear 2. To do this the equations of transformation among the sets of co-ordinates involved are derived. These equations may be derived directly from Fig. 1, but they are more readily derived from the direction cosines of the axes involved.

The direction cosines relating the various co-ordinate systems are shown in Tables 1, 2, 3, and 4. Table 4 was obtained by combining Tables 2 and 3. S and C are written for sine and cosine to save space.

The equations of transformation may be written from Fig. 1 and Table 4

TABLE 1 DIRECTION COSINES

	X_0	Y_0	Z_0
X_1	$C\theta_1$	$S\theta_1$	0
Y_1	$-S\theta_1$	$C\theta_1$	0
Z_1	0	0	1

TABLE 2 DIRECTION COSINES

	X_3	Y_3	Z_3
X_4	$C\alpha$	0	$-S\alpha$
Y_4	0	1	0
Z_4	$S\alpha$	0	$C\alpha$

TABLE 3 DIRECTION COSINES

	X_4	Y_4	Z_4
X_2	1	0	0
Y_2	0	$C\theta_2$	$-S\theta_2$
Z_2	0	$S\theta_2$	$C\theta_2$

TABLE 4 DIRECTION COSINES

	X_3	Y_3	Z_3
X_2	$C\alpha$	0	$-S\alpha$
Y_2	$-S\alpha\, S\theta_2$	$C\theta_2$	$-C\alpha\, S\theta_2$
Z_2	$S\alpha\, C\theta_2$	$S\theta_2$	$C\alpha\, C\theta_2$

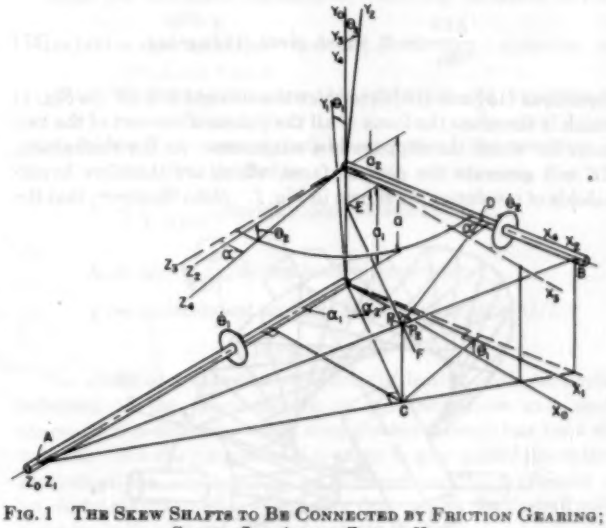

FIG. 1 THE SKEW SHAFTS TO BE CONNECTED BY FRICTION GEARING; SHAFTS LIE ALONG Z_1 AND X_2

$$x_0 = x_3 = C\alpha\, x_2 - S\alpha\, S\theta_2\, y_2 + S\alpha\, C\theta_2\, z_2 \quad \ldots\ldots [2]$$

$$y_0 = y_3 + a = C\theta_2\, y_2 + S\theta_2\, z_2 + a \quad \ldots\ldots [3]$$

$$z_0 = z_3 = -S\alpha\, x_2 - C\alpha\, S\theta_2\, y_2 + C\alpha\, C\theta_2\, z_2 \quad \ldots\ldots [4]$$

For a point P_1 fixed in $X_1Y_1Z_1$, Table 1 and Equation [1]

$$\dot{x}_0 = -y_0\dot{\theta}_1 = -y_0k\dot{\theta}_2 \quad \ldots\ldots [5]$$

$$\dot{y}_0 = x_0\dot{\theta}_1 = x_0k\dot{\theta}_2 \quad \ldots\ldots [6]$$

$$\dot{z}_0 = 0 \quad \ldots\ldots [7]$$

For a momentarily coinciding point P_2, fixed in $X_2Y_2Z_2$, from Equations [2, 3, 4] and Table 4

$$\dot{x}_0 = -S\alpha(y_0 - a)\,\dot{\theta}_2 \quad \ldots\ldots [8]$$

$$\dot{y}_0 = (S\alpha\, x_0 + C\alpha\, z_0)\,\dot{\theta}_2 \quad \ldots\ldots [9]$$

$$\dot{z}_0 = -C\alpha(y_0 - a)\,\dot{\theta}_2 \quad \ldots\ldots [10]$$

The velocity of P_2 relative to P_1, referred to $X_0Y_0Z_0$, when $\dot{\theta}_2 = 1$, is

$$\dot{x}_0 = -S\alpha(y_0 - a) + ky_0 = (k - S\alpha)\, y_0 + aS\alpha \quad \ldots\ldots [11]$$

---

[1] Associate Professor of Engineering, University of California, Los Angeles. Mem. ASME.

[2] "The Synthesis of Gear Tooth Curves," by J. Stiles Beggs, *Physics*, vol. 7, 1936, p. 163.

Contributed by the Applied Mechanics Division and presented at the Annual Meeting, New York, N. Y., November 28–December 3, 1954, of THE AMERICAN SOCIETY OF MECHANICAL ENGINEERS.

Discussion of this paper should be addressed to the Secretary, ASME, 29 West 39th Street, New York, N. Y., and will be accepted until April 11, 1955, for publication at a later date. Discussion received after the closing date will be returned.

NOTE: Statements and opinions advanced in papers are to be understood as individual expressions of their authors and not those of the Society. Manuscript received by ASME Applied Mechanics Division, July 13, 1953. Paper No. 54—A-16.

$$\dot{y}_0 = (S\alpha\, x_0 + C\alpha\, z_0) - kx_0 = -(k - S\alpha)\, x_0 + C\alpha\, z_0 \quad [12]$$

$$\dot{z}_0 = -C\alpha(y_0 - a) = -C\alpha\, y_0 + aC\alpha \quad [13]$$

Calling this relative velocity V, then

$$V^2 = \dot{x}_0^2 + \dot{y}_0^2 + \dot{z}_0^2 \quad [14]$$

If P_1 and P_2 are momentarily typical points of contact of the gear surfaces, their relative velocity represents the slippage of the surfaces at this position. On examining Equations [11], [12], [13], and [14], it is seen that V can be zero only when $\alpha = \pm 90$ deg (spur gears) or $a = 0$ (bevel gears).

If the slippage cannot be zero, the next best solution would be to make it a minimum. For this to be the case

$$\frac{\partial V^2}{\partial x_0} = 0, \text{ which gives } x_0 = \frac{C\alpha}{k - S\alpha}\, z_0 \quad [15]$$

$$\frac{\partial V^2}{\partial y_0} = 0, \text{ which gives } y_0 = \frac{a\,(1 - kS\alpha)}{1 - 2kS\alpha + k^2} \equiv a_1 \quad [16]$$

$$\frac{\partial V^2}{\partial z_0} = 0, \text{ which gives [15] again} \quad [17]$$

Equations [15] and [16] determine the straight line EF (in Fig. 1) which is therefore the locus of all the points of contact of the two gears for which the slippage is a minimum. As the shafts turn, EF will generate the gear surfaces, which are therefore hyperboloids of revolution, as shown in Fig. 2. Note, however, that the

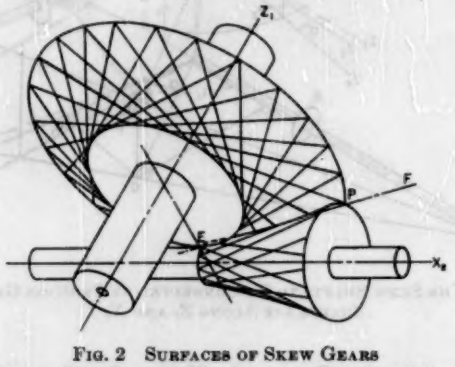

FIG. 2 SURFACES OF SKEW GEARS
(For minimum slippage they are hyperboloids of revolution.)

slip is a minimum for these surfaces only when Equation [1] holds. The question remains will these surfaces produce this velocity ratio between the shafts? In any case if teeth are to be used, and sliding is to be kept to a minimum, the teeth must make contact in the vicinity of these hyperboloids of revolution at their line of contact EF, just as spur-gear teeth make contact in the vicinity of their pitch point where the sliding is zero.

From Fig. 1 and Equation [15]

$$\tan \alpha_1 = \frac{C\alpha}{k - S\alpha} \quad [18]$$

which is recognized as the pitch-cone angle of a bevel gear in terms of the shaft angle (90 deg + α) and the velocity ratio k.

It may be shown that

$$\frac{a_1}{a_2} = \frac{\tan \alpha_1}{\tan \alpha_2} = \frac{(1/k) - S\alpha}{k - S\alpha} \text{ (see Fig. 1)} \quad [19]$$

and

$$k = \frac{S\alpha_2}{S\alpha_1} \quad [20]$$

Substituting Equation [15] in [12]

$$\dot{y}_0 = \frac{-(k - S\alpha)C\alpha}{k - S\alpha}\, z_0 + C\alpha\, z_0 = 0 \quad [21]$$

That is, the component along the common perpendicular to the two shafts, of the relative velocity of the surfaces, is zero at all points of contact. This means that the relative velocity lies in a plane parallel to both shafts. If the value of a_1 from Equation [16] is substituted into the ratio of $\dot{x}_0/\dot{z}_0$ formed from Equations [11] and [13] it is found that this ratio is equal to the expression for tan α_1 given by Equation [18]. The slip of gear 2 on gear 1 is therefore directed along the line of contact from E toward F, and it has the same value all along this line.

If gear 2 is the driver the force it exerts on gear 1 will be in the direction of its slip on gear 1, viz., from E toward F.[3] But this would produce a torque on shaft 1 opposite to the assumed direction of rotation! Apparently the hyperboloids will not transmit the assumed velocity ratio.

Suppose shaft 1 is prevented from rotating. If shaft 2 is rotated in the direction indicated in Fig. 1 the relative velocity at P_1P_2 is in the normal plane to shaft 2 and perpendicular to P_2D. The force on gear 1 will be in this direction and will therefore tend to rotate gear 1 in the direction indicated in Fig. 1. However gear 1, if released, will not reach the speed $k\dot{\theta}_2$ because the torque on it will reverse first. The maximum velocity is reached just as the line containing the relative velocity passes through shaft 1. At this condition the torque is zero because the torque arm is zero. The maximum ratio of $\dot{\theta}_1/\dot{\theta}_2$ may be obtained therefore by setting the torque on gear 1 equal to zero. Since the force of friction acts along the relative velocity this may be done by setting equal to zero the triple scalar product of the following vectors, the position vector from the origin to the point P_1, the relative velocity vector of P_1 and P_2, and the unit vector along the Z_0 axis.

Space does not permit showing this in detail, but suffice it to mention that, as the driving points P_1 and P_2 are taken further from O, the closer will $\dot{\theta}_1/\dot{\theta}_2$ approach k. As the load on the driven gear increases, keeping the normal force between the gear surfaces constant, the driven gear must slow down in order that the relative-velocity vector can move away from the driven shaft and provide sufficient torque arm to drive the load. When the torque arm can increase no further the driven shaft stops. The velocity ratio of these gears therefore depends on the shaft load and the normal force along the line of contact.

CONCLUSION

While the use of spur and bevel friction gearing is growing,[4] due to the use of better steel and better oil,[5] skew friction gearing, because of the inherent limitations mentioned in the paper, seems doomed to limited application.

---

[3] "A Problem in Friction," by F. A. Valentine, *American Mathematical Monthly*, vol. LIII, February, 1946, pp. 83–85.

[4] "Development of the McCulloch Supercharger for Automotive Diesel and Gasoline Engines," by J. W. Oehrli, paper read before the Society of Automotive Engineers, Annual Meeting, January 15, 1954.

[5] "Use of Metallic Traction in Modern Transmissions," by L. A. Graham, paper presented at a meeting of the ASME Machine Design Division, Los Angeles, Calif., Nov. 9, 1953, available from the author, Graham Transmissions, Inc., Menomonee Falls, Wis.

Application of the Electronic Differential Analyzer to the Oscillation of Beams, Including Shear and Rotary Inertia

By C. E. HOWE[1] and R. M. HOWE[2]

The equations for normal modes of lateral vibration of beams are set up on the electronic differential analyzer. Beam deflections due to transverse shear and rotary-inertia forces are included. The differential analyzer is shown to be a fast and accurate method for solving the problem. Analyzer outputs include mode shape, slope, bending moment, and shear force along the beam. Curves showing the normal-mode frequencies for the first three modes of vibration of a uniform free-free beam are presented for a wide range of transverse shear and rotary-inertia parameters. The electronic differential analyzer also is utilized to solve the problem of lateral vibration of nonuniform beams.

Nomenclature

The following nomenclature is used in the paper:

x = horizontal distance from left end of beam
l = length of beam
t = time
ω = frequency of normal-mode oscillation
$y(x, t)$ = transverse deflection of beam at any instant
$y(x)$ = maximum transverse deflection of beam, at x
$\overline{M}(x, t)$ = bending moment at any instant
$M(x)$ = maximum bending moment, at x
$\overline{V}(x, t)$ = transverse shear force at any instant
$V(x)$ = maximum transverse shear force, at x
I = area moment of inertia
E = modulus of elasticity, or Young's modulus
$\overline{EI}(x)$ = fluexural rigidity, at x
EI = constant value of $\overline{EI}(x)$
A = cross-sectional area
G = modulus of shear, or rigidity modulus
k = ratio of average shear stress to stress at neutral axis
$\overline{kAG}\ (x)$ = shear rigidity, at x
kAG = constant value of $\overline{kAG}(x)$
$\overline{\rho}(x)$ = mass per unit length of beam, at x
ρ = constant value of $\overline{\rho}(x)$
$\overline{I}_r(x)$ = mass moment of inertia per unit length of beam, at x
I_r = constant value of $\overline{I}_r(x)$
$\overline{\alpha}(x, t)$ = neutral axis slope due to shear at any instant
$\overline{\alpha}(x)$ = maximum neutral axis slope due to shear, at x
$\overline{\beta}(x, t)$ = neutral axis slope due to bending at any instant
$\overline{\beta}(x)$ = maximum neutral axis slope due to bending, at x
$\left(\overline{\frac{kG}{E}}\right)(x)$ = dimensionless parameter, expressing effect of rotary inertia
$N = \frac{kG}{E}$ = constant value of $\left(\overline{\frac{kG}{E}}\right)(x)$
$\phi_d(x)$ = dimensionless variable, reflecting variation of $\overline{\beta}(x)$ with x
$\phi_r(x)$ = dimensionless variable, reflecting variation of $\overline{I}_r(x)$ with x
$\phi_s(x)$ = dimensionless variable, reflecting the variation of $\overline{kAG}(x)$ with x
$\phi_f(x)$ = dimensionless variable, reflecting the variation of $\overline{EI}(x)$ with x
$S = \frac{EI}{kAGl^2}$, dimensionless parameter
$\lambda = \omega l^2 \sqrt{\frac{\rho}{EI}}$, dimensionless parameter
τ = independent variable for computer, $x = (l/L)\tau$

Introduction

The study of transverse vibrations of beams, with particular reference to the determination of eigenfrequencies and mode shapes, is a problem in which considerable interest has been developed. It is the purpose of this paper to give a brief theoretical analysis of the problem and to demonstrate the usefulness of an electronic differential analyzer in determining the desired solutions for both uniform and nonuniform beams.

The ordinary textbook on vibrations presents a simplified analysis of the vibrating-beam problem. Generally it is assumed that the transverse vibration of the beam takes place in one of the principal planes of flexure of the beam and that the length of the beam is large in comparison with its transverse dimensions. This latter assumption permits the deflection resulting from transverse shear force and from rotary inertia to be neglected without much loss in accuracy. However, if the beam being studied no longer has a length large compared with its cross-sectional dimensions, these simple solutions are not sufficiently accurate.

Lord Rayleigh (1)[3] derived a correction factor to include the effect of rotary inertia. In 1921 Timoshenko (2) set up a group of differential equations which included the effect of transverse shear force as well as that of rotary inertia. From these equations he derived, for the special case of a beam hinged at both ends, a correction factor (2, 3) which could be used to determine an approximately correct frequency. This method of approximation is not readily applicable to beams with other types of end fastenings, as was pointed out by Goens (4). Goens derives exact expressions for the free-free beam with the effects of rotary inertia and transverse shear force included. The roots of these expressions yield the frequencies of vibration if the constants of the beam are known. More recently, Ormondroyd, et al. (5, 6, 7), have pre-

[1] Professor of Physics, Oberlin College, Oberlin, Ohio.
[2] Associate Professor of Aeronautical Engineering, University of Michigan, Ann Arbor, Mich.

Contributed by the Applied Mechanics Division and presented at the Annual Meeting, New York, N. Y., November 28–December 3, 1954, of The American Society of Mechanical Engineers.
Discussion of this paper should be addressed to the Secretary, ASME, 29 West 39th Street, New York, N. Y., and will be accepted until April 11, 1955, for publication at a later date. Discussion received after the closing date will be returned.
Note: Statements and opinions advanced in papers are to be understood as individual expressions of their authors and not those of the Society. Manuscript received by ASME Applied Mechanics Division, September 14, 1953. Paper No. 54—A-18.

[3] Numbers in parentheses refer to the Bibliography at the end of the paper.

sented results of theoretical research on the dynamics of a ship's structure with a view toward the determination of the eigenfrequencies and normal-mode shapes of both uniform and nonuniform beams. In addition, studies were made of forced damped vibrations. In these studies deflection due to transverse shear force is included while the effect of rotary inertia is neglected, and the orthogonality of the modes of vibration is demonstrated. Kruszewski (8) also has analyzed the effects of rotary inertia and transverse shear on the normal-mode frequencies of uniform cantilever and uniform free-free beams.

In all of the foregoing work the solution of the basic equations led to a fourth-order differential equation for the mode shape. This equation was solved, subject to the boundary conditions at the end of the beam, the solutions yielding equations from which the eigenfrequencies were determined. In most cases no attention was given to mode shapes.

Dolph (9) has shown that when the basic equations, including transverse shear and rotary inertia, are solved as simultaneous equations instead of being converted to a single fourth-order equation, the resulting normal-mode solutions for a hinged-hinged beam have two eigenfrequencies associated with a given mode shape. The normal modes are orthogonal in such a way as to allow the most general of initial conditions to be satisfied. It also turns out that when the beam equations are set up on the electronic differential analyzer, it is more convenient to solve the original simultaneous differential equations instead of a single fourth-order equation.

Equations for Transverse Vibration

Basic Equations. By applying the laws of dynamics and elementary strength of materials to a small element of a beam, one obtains the five basic equations

$$\bar{p}(x)\frac{\partial^2 \bar{y}(x,t)}{\partial t^2} + \frac{\partial \bar{V}(x,t)}{\partial x} = 0 \quad [1]$$

$$-\frac{\partial \bar{M}(x,t)}{\partial x} + \bar{I}_r(x)\frac{\partial^2 \bar{\beta}(x,t)}{\partial t^2} + \bar{V}(x,t) = 0 \quad [2]$$

$$\bar{V}(x,t) = -\overline{kAG}(x)\bar{\alpha}(x,t) \quad [3]$$

$$\frac{\partial \bar{\beta}(x,t)}{\partial x} = \frac{\bar{M}(x,t)}{\overline{EI}(x)} \quad [4]$$

$$\frac{\partial \bar{y}(x,t)}{\partial x} = \bar{\alpha}(x,t) + \bar{\beta}(x,t) \quad [5]$$

Equation [1] equates to zero the sum of the transverse forces, while Equation [2] equates to zero the sum of the moments acting on a small element of the beam. Equation [5] states that the neutral axis slope is the sum of $\bar{\beta}$ and $\bar{\alpha}$, where $\bar{\beta}$ is the rotation of a plane normal to the neutral axis, and $\bar{\alpha}$ is the distortion of the angle between this plane and the plane of the neutral axis (6, 7).

If the length l of the beam is very large compared with its transverse dimensions, then the rotary inertia $\bar{I}_r$ and slope $\bar{\alpha}$ due to shear are neglected. Equations [1] to [5] reduce to the simple beam equations

$$\bar{p}(x)\frac{\partial^2 \bar{y}(x,t)}{\partial t^2} + \frac{\partial \bar{V}(x,t)}{\partial x} = 0$$

$$\bar{V}(x,t) = \frac{\partial \bar{M}(x,t)}{\partial x}$$

$$\frac{\partial^2 \bar{y}(x,t)}{\partial x^2} = \frac{\bar{M}(x,t)}{\overline{EI}(x)}$$

Separation of Variables. In Equations [1] to [5] there are two independent variables, distance x along the beam and time t. To separate the two variables x and t, it is assumed that the time variation of all dependent variables is sinusoidal. Thus let

$$\bar{y}(x,t) = y(x)e^{j\omega t}, \quad \bar{M}(x,t) = M(x)e^{j\omega t}, \text{ etc.}$$

Equations [1] to [5] then become a set of simultaneous ordinary differential equations in x, where the normal mode frequency ω appears as an unknown parameter.

Since the equations are to be applied, in general, to the study of a nonuniform beam in which the physical characteristics change along the beam, it will be convenient to define the following relations

$$\bar{p}(x) = \rho\phi_d(x), \quad \bar{I}_r(x) = I_r\phi_r(x),$$
$$\overline{kAG}(x) = kAG\phi_s(x), \quad \overline{EI}(x) = EI\phi_f(x) \quad [6]$$

where ρ, I_r, kAG, and EI are now constants, and the variations of physical properties along the beam are reflected in the ϕ's which are dimensionless. For a uniform beam, $\phi_d = \phi_r = \phi_s = \phi_f = 1$.

It is also convenient to define a frequency parameter λ by

$$\lambda^2 = \frac{\rho\omega^2 l^4}{EI} \quad [7]$$

a shear parameter S by

$$S = \frac{EI}{kAGl^2} \quad [8]$$

and a rotary-inertia parameter N by

$$N = \frac{kAG}{EI}\frac{I_r}{\rho} \quad [9]$$

Since the rotary inertia I_r is given by

$$I_r = \frac{\rho I}{A} \quad [10]$$

an alternate expression for N is

$$N = \frac{kG}{E} \quad [11]$$

In terms of the new parameters defined in Equations [6] to [9] the separated beam equations can be reduced to the following three equations

$$y + \frac{1}{S}\frac{l^2}{\lambda^2}\frac{1}{\phi_d}\frac{d}{dx}(\phi_s\bar{\alpha}) = 0 \quad [12]$$

$$\frac{d}{dx}\left(\phi_f\frac{d\bar{\beta}}{dx}\right) + SN\frac{\lambda^2}{l^2}\phi_r\bar{\beta} + \frac{1}{Sl^2}\phi_s\bar{\alpha} = 0 \quad [13]$$

$$\frac{dy}{dx} = \bar{\alpha} + \bar{\beta} \quad [14]$$

Rewriting Equations for Computer. The electronic differential analyzer integrates with respect to time. Hence it is necessary to change the distance variable x in the beam Equations [12], [13], and [14] to a computer time variable τ. If the range in the distance variable x is $0 \le x \le l$, then the range in the computer time variable τ is $0 \le \tau \le L$, where L is the length of the computer solution in seconds. Thus

$$x = \frac{l}{L}\tau \quad \text{and} \quad \frac{d^n}{dx^n} = \left(\frac{L}{l}\right)^n\frac{d^n}{d\tau^n}$$

Also, let

$$\bar{\alpha}(x) = \frac{L}{l}\alpha(\tau) \quad \text{and} \quad \bar{\beta}(x) = \frac{L}{l}\beta(\tau)$$

Rewriting the beam Equations [12] to [14] in terms of the computer variable τ, we find that

$$y + \frac{1}{S}\frac{L^2}{\lambda^2}\frac{1}{\phi_s}\frac{d}{d\tau}(\phi_s\alpha) = 0 \quad \ldots\ldots [15]$$

$$\frac{d}{d\tau}\left(\phi_f\frac{d\beta}{d\tau}\right) + SN\frac{\lambda^2}{L^2}\phi_s\beta + \frac{1}{SL^2}\phi_s\alpha = 0 \quad \ldots\ldots [16]$$

$$\frac{dy}{d\tau} = \alpha + \beta \quad \ldots\ldots [17]$$

We remember that in the foregoing equations y is the deflection of the beam (volts in the case of the computer) and τ is computer time (corresponding to distance along the beam). S and N are dimensionless parameters which include the effects of transverse shear force and rotary inertia, respectively, and λ is the characteristic root of the equations such that the appropriate boundary conditions are satisfied. Bending moment is proportional to $d\beta/d\tau$ and shear is proportional to α, while the length of the beam is L units of computer time.

The beam equations are subject to boundary conditions, depending on the type of restraint or fastening at each end of the beam. The possible fastenings and the resultant end conditions are summarized in Table 1.

TABLE 1 SUMMARY OF FASTENINGS AND END CONDITIONS

End of beam	Boundary condition for beam	Boundary condition for computer
Free	$M = 0;\ V = 0$	$\phi_f d\beta/d\tau = 0;\ \phi_s\alpha = 0$
Hinged	$y = 0;\ M = 0$	$y = 0;\ \phi_f d\beta/d\tau = 0$
Built-in	$y = 0;\ dy/dz = 0$ or $y = 0;\ \beta = 0$	$y = 0;\ dy/d\tau = 0$ or $y = 0;\ \beta = 0$

In the case of the built-in end, there is some difference of opinion as to whether the slope $dy/d\tau$ of the neutral axis is zero or whether just the fraction β of the slope due to bending moment is zero (2, 3, 7, 8). Equations [15], [16], and [17] form a set of simultaneous linear differential equations which can be solved by the electronic differential analyzer, subject to the appropriate end conditions for a particular type of beam.

Solution of the Vibrating-Beam Problem by the Electronic Differential Analyzer

Theory of Analyzer. Before proceeding with a description of how the vibrating-beam problem can be solved by means of the electronic differential analyzer, it would seem appropriate to review briefly the principles behind the operation of such a computer. For a complete discussion of the theory of electronic differential analyzers, their field of application, and commercially available computers of this type, the reader is directed to references (10, 11).

The basic component of the electronic differential analyzer is the operational amplifier, which is shown schematically in Fig. 1(*a*). It consists of a d-c voltage amplifier of high gain (usually greater than 10,000), an input impedance Z_i, and a feedback impedance Z_f. If we neglect the current into the d-c amplifier itself, i.e., neglect the current to the grid of the input tube, it follows that $i_1 = i_2$. Let us also neglect the voltage input e' to the d-c amplifier in comparison with the output voltage e_2 or the input voltage e_1 to the operational amplifier. We then have

$$i_1 = i_2 \quad \text{or} \quad \frac{e_1}{Z_i} = -\frac{e_2}{Z_f}$$

from which

$$e_2 = -\frac{Z_f}{Z_i}e_1 \quad \ldots\ldots [18]$$

which is the fundamental equation governing the behavior of the operational amplifier. For example, if we wish to multiply a voltage e_1 by a constant k, the feedback and input impedances are made resistors R_f and R_i, respectively, with $R_f/R_i = k$. From Equation [18] the output voltage e_2 of the amplifier will be $-ke_1$ as required, except for a sign reversal.

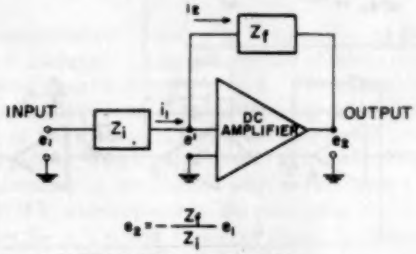

a.) OPERATIONAL AMPLIFIER

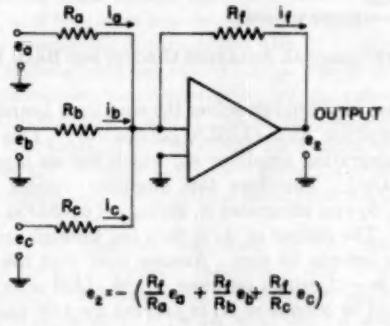

b) OPERATIONAL AMPLIFIER AS A SUMMER

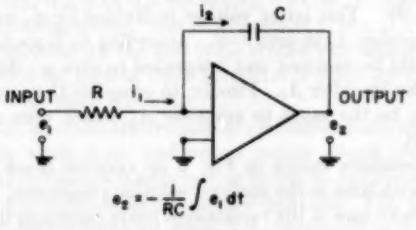

C) OPERATIONAL AMPLIFIER AS AN INTEGRATOR

FIG. 1 ELECTRONIC DIFFERENTIAL ANALYZER

The operational amplifier can be used to sum several voltages, as shown in Fig. 1(*b*). Each voltage to be summed is applied to a separate input resistor. The circuit shown in Fig. 1(*c*) is used for integration. Here the feedback impedance is a capacitor and the input impedance is a resistor; the amplifier output voltage is proportional to the time integral of the input.

Thus it is evident that time represents the independent variable for the electronic differential analyzer, while voltage represents the dependent variables in solving differential equations. In order to demonstrate how operational amplifiers performing the function of multiplication by constant, summation, and integration can be combined to solve ordinary differential equations, we will now set up the amplifier circuits required to solve the beam problem.

Analyzer Circuit for Solving Beam Problem. The equations for lateral vibrations of a beam, including rotary inertia and transverse shear force, were reduced to the three simultaneous ordinary differential Equations [15], [16], and [17]. The computer circuit for solving these three equations is shown in Fig. 2 To under-

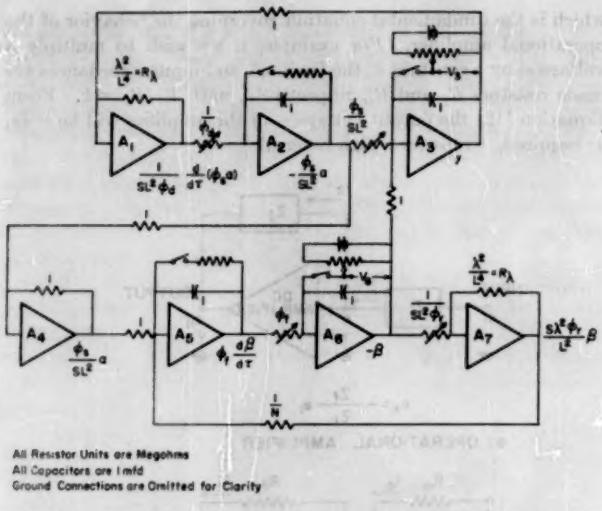

FIG. 2 DIFFERENTIAL ANALYZER CIRCUIT FOR BEAM PROBLEM

stand how the circuit shown solves the equations assume that the output of amplifier A_1 is $(1/SL^2\phi_d)d(\phi_s\alpha)/d\tau$. This voltage is applied to integrating amplifier A_2, which has an input resistor varying as $1/\phi_d$. Therefore this amplifier divides the input voltage by $1/\phi_d$ and integrates it, giving $-(\phi_s/SL^2)\alpha$ as its output voltage. The output of A_2 is then fed through amplifier A_4, which merely inverts its sign. Assume next that the output of amplifier A_6 is $-\beta$, which becomes $(S\lambda^2\phi_r/L^2)\beta$ after being fed through A_7. The output of A_7 is divided by $1/N$ and summed with the output of A_4 to give as the output of A_5 the voltage $-\int[(SN\lambda^2\phi_r/L^2)\beta + (\phi_s/SL^2)\alpha]d\tau$, which from Equation [16] is simply $\phi_f d\beta/d\tau$. This latter voltage is divided by ϕ_f and integrated in amplifier A_6 to give $-\beta$. According to Equation [17] α and β should be summed and integrated to give y; this is the function of the amplifier A_3. Finally, to complete the computing loop we let y be the input to amplifier A_1, which then satisfies Equation [15].

The four resistors shown in Fig. 2 as variable must change their values with time as the analyzer solution progresses. This is necessary to take care of the variation of beam constants with distance along the beam. The way in which this is accomplished is described in the next section. However, in the case of a uniform beam the various ϕ's are equal to unity, and all resistor values are constant.

The initial conditions utilized on the computer depend upon the type of end fastening for the beam in question. For a "free-free" beam the initial conditions (and also the final conditions) are

$$\frac{d\beta}{d\tau} = 0, \quad \alpha = 0 \quad \text{at } \tau = 0 \ldots\ldots\ldots\ldots [19]$$

$$\frac{d\beta}{d\tau} = 0, \quad \alpha = 0 \quad \text{at } \tau = L \ldots\ldots\ldots\ldots [20]$$

The initial conditions given in Equation [19] are imposed by short-circuiting the feedback capacitors of amplifiers A_2 and A_5 in Fig. 2 through initial-condition relays. This is equivalent to making the shear force and bending moment zero at one end of the beam. At the same end the deflection and slope must be finite; these conditions are imposed initially on A_3 and A_6 through voltages V_3 and V_6. The solution of the problem is begun by releasing simultaneously the four initial-condition relays, two of which were holding $d\beta/d\tau = 0$ and $\alpha = 0$, and two of which were holding $y = V_3$ and $-\beta = V_6$.

Trial-and-Error Method for Obtaining Normal-Mode Solutions. Let us consider the case of a uniform, free-free beam. The first trial settings of V_3 and V_6 are arbitrary, and in general a correct solution will not result. For a correct solution $d\beta/d\tau$ must go through zero at precisely the same instant as α goes through zero. The time elapsed between the start of the solution and the instant when $d\beta/d\tau = \alpha = 0$ is then the length L of the computer solution. A typical first trial solution is shown in Fig. 3(a) in which the condition $d\beta/d\tau(L) = \alpha(L) = 0$ obviously is not met. The small pips on the $d\beta/d\tau$-curve indicate when α has passed through zero. By varying V_3 and holding V_6 constant (or vice versa), the ratio V_3/V_6 can be varied until an exact solution is obtained. The trial solutions leading to an exact first-mode solution are shown in Fig. 3. Usually about half a dozen trial solutions are needed until an exact solution is reached. Higher modes are obtained in exactly the same manner. A second-mode solution is shown in Fig. 4.

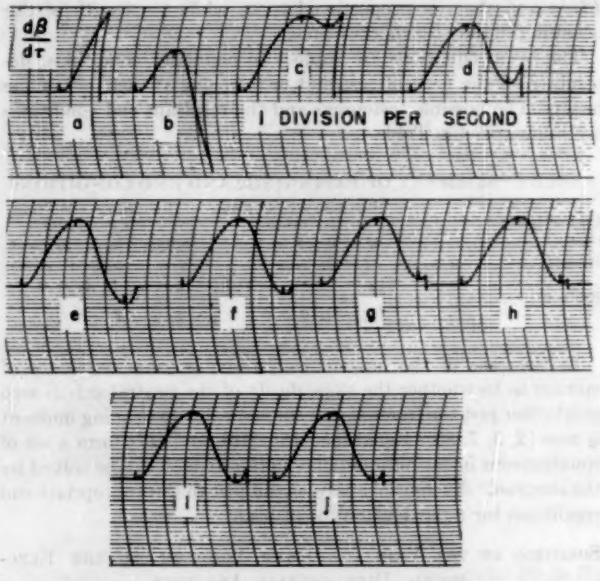

FIG. 3 TRIAL SOLUTIONS FOR FIRST MODES, FREE-FREE BEAM

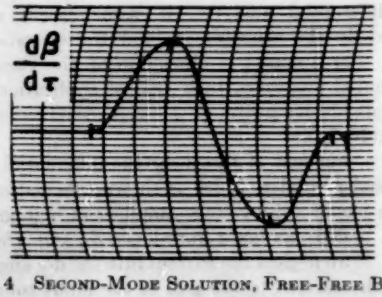

FIG. 4 SECOND-MODE SOLUTION, FREE-FREE BEAM

If we are looking for the solution of a given uniform beam, then we must have chosen originally a suitable computer-solution length L. But the values for the feedback resistor R_λ in A_1 and A_7 (Fig. 2) had to be selected arbitrarily, so that in general the observed computer length L for a correct solution will be different from the L originally chosen. It is then necessary to select a new R_λ and rerun the solution, obtaining a new L. By repeating this process several times and by interpolating, we can arrive at the

value of R_λ which gives a correct solution of the desired length L. The frequency parameter λ is then given by

$$\lambda = L^2 \sqrt{R_\lambda} \quad \ldots\ldots\ldots\ldots\ldots\ldots\ldots\ldots [21]$$

On the other hand, if we are interested in solving the problem for a whole family of uniform beams characterized by different values of the parameter S (i.e., having various thickness-to-length ratios), we may keep R_λ fixed, calculate λ from Equation [21], and S from the formula $1/S = L^2 R_s$. In this procedure every correct solution of length L represents a certain beam, but we cannot choose the exact $1/S$-value for that beam beforehand.

When obtaining solutions of higher modes, one finds that the ratio V_2/V_0 in Fig. 2 becomes extremely critical. A change in these initial voltages of one part in several thousand causes considerable deviation from one solution to the next when a third or fourth mode is being sought. As a result the solutions for higher modes do not repeat from run to run, and it is extremely fortunate ever to get an exact third or fourth-mode solution. However, from several inexact solutions it is fairly easy to interpolate to the length L of an exact solution. Fortunately, when the effects of shear and rotary inertia are included, the initial conditions for obtaining higher modes become much less critical. What actually happens is that for larger and larger values of N and S the mode solutions are characterized more by circular functions than by hyperbolic functions and hence become more stable.

Solutions for a Uniform Free-Free Beam, Neglecting Shear and Rotary Inertia. In order to check the accuracy of the computer, the vibrating-beam problem was first solved for the case in which the length of the beam is very long compared with the thickness. This means that rotary inertia and shear forces are negligible ($N = S = 0$); we might call such a beam "infinitely thin." The frequency parameter λ for the first five modes of an infinitely thin free-free beam are given by Timoshenko (3). To solve this problem on the analyzer the connection between A_2 and A_3 in Fig. 2 was broken, along with the connection between A_7 and A_8. The $1/\phi_d$ and ϕ_f resistors were set equal to unity (1 megohm), as was R_λ, so that $\lambda = L^2$ or $\sqrt{\lambda} = L$. The values for $\sqrt{\lambda}$ are compared with the theoretical values in Table 2.

Evidently the computer solutions are accurate to 0.1 per cent or better. In order to realize this accuracy it is necessary to use very careful calibration techniques (12) in measuring the resistors and capacitors in the computer circuit. The measurement of the length L of the computer solution must also be of considerable accuracy. For a uniform free-free beam the output voltage $d\beta/d\tau$ (proportional to the bending moment) is recorded on one channel of a Brush, Model BL-202, magnetic oscillograph. In order to determine more accurately when the correct end conditions have been realized, the $d\beta/d\tau$ record is "blown up" by a factor of 10

TABLE 2 COMPARISON OF COMPUTER AND THEORETICAL SOLUTIONS FOR A FREE-FREE UNIFORM BEAM, INFINITELY THIN

Mode	$\sqrt{\lambda} = L$ (computer), sec	$\sqrt{\lambda} = L$ (theoretical), sec
1	4.735	4.730
2	7.852	7.853
3	10.997	10.996
4	14.136	14.137

in the region where it is near zero in value, i.e., at the beginning and end of a solution. A correct solution obtained in this manner for a second mode is shown in Fig. 5. The pulses superimposed on the $d\beta/d\tau$-curve occur at the instant α goes through zero. The length L of the solution is just the time elapsed between initial and final pulses. This elapsed time is measured to the order of 1 millisec accuracy by comparison with seconds pulses from Radio Station WWV, which appear on the other recording channel.

Solution for a Uniform Free-Free Beam, Including Shear and Rotary Inertia. The differential Equations [15], [16], and [17] for the vibrating beam include the effects of shear and rotary inertia forces, and hence are representative of a beam whose thickness may be appreciable in comparison with its length. The relative effects of shear force and rotary inertia present in the vibrating beam are represented, respectively, by the values of the dimensionless parameters S and N (see Equations [8] and [11]). For a long, thin beam, S will be small; for a short thick beam, S will be large. On the other hand, for a given shape of beam cross section, N depends only on the ratio of shear modulus G to Young's modulus E.

The differential analyzer was used to find the frequency parameter λ for a considerable range of S and N-values in the case of a uniform free-free beam. The circuit shown in Fig. 2 was used with $\phi_d = \phi_r = \phi_s = \phi_f = 1$; the resistor R_λ was set equal to unity. The value of R_s was chosen arbitrarily, and N was made 0, 0.1, 0.2, and 0.3 by setting $1/N = \infty$, 10, 5, and $3\frac{1}{3}$ megohms, respectively. For each value of $1/N$ and R_s the length L of the solution for the first three modes was determined. The parameter S for each of these solutions is given by $1/S = L^2 R_s$, while $\lambda = L^2$ since $R_\lambda = 1$.

If we let λ_0 equal the frequency parameter for a uniform free-free beam when shear and rotary inertia effects are neglected, then λ/λ_0 represents the correction factor in the frequency when shear and rotary-inertia effects are included. Fig. 6 shows the family of curves obtained when λ/λ_0 is plotted as a function of $1/S$ for the four values of N($N = 0$, 0.1, 0.2, and 0.3). The values chosen for N seemed appropriate for the various types of beams which might be encountered. Variation of λ/λ_0 as a function of N is almost linear, so a much wider range in N can be obtained by interpolation from Fig. 6 without too much loss in accuracy.

The parameter $1/S$ ranges from very high values down to about 14, 35, and 72 in the case of the first, second, and third modes, respectively. These lower limits on $1/S$ correspond to length-thickness ratios of about 2, 3.5, and 5 for a rectangular steel beam; i.e., the length-thickness ratios for the beams represented in Fig. 6 go down to the region where the wave length of vibration is almost the same as the thickness of the beam itself. This is the region where one would expect the assumptions involved in deriving original beam Equations [1] to [5] to break down.

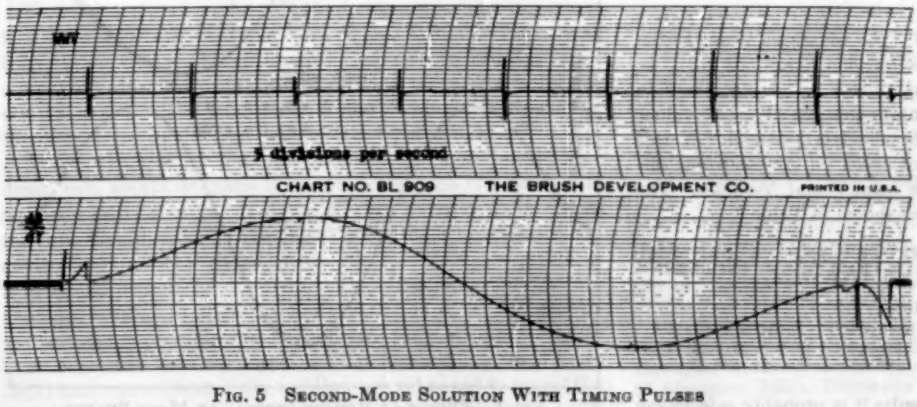

FIG. 5 SECOND-MODE SOLUTION WITH TIMING PULSES

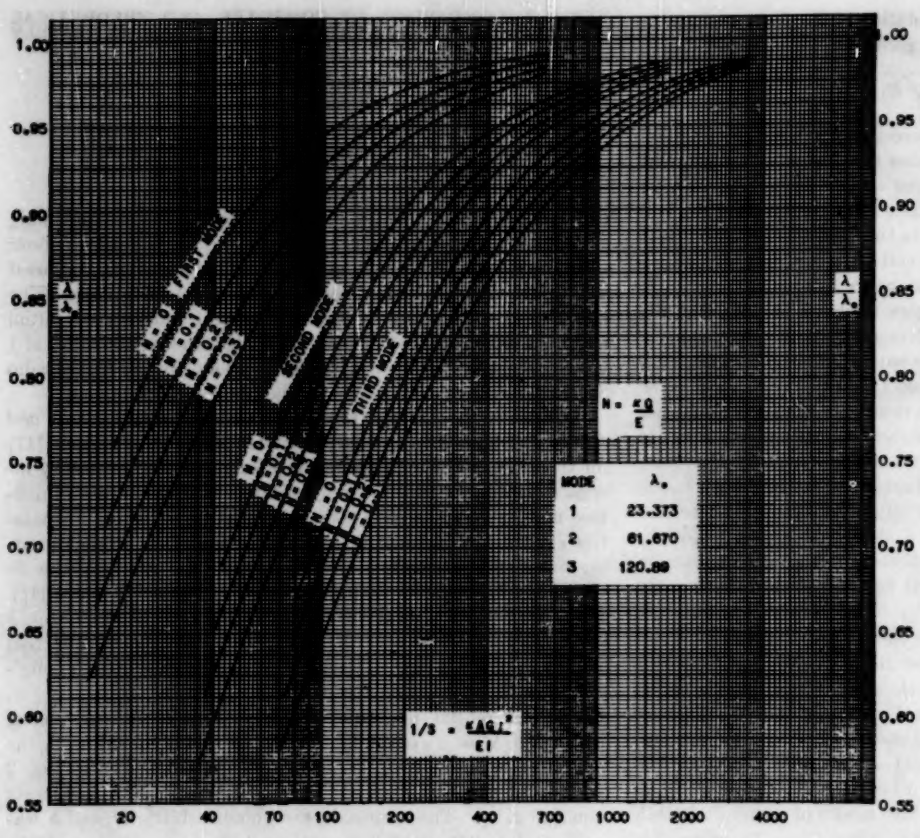

FIG. 6 FREQUENCY PARAMETER FOR FREE-FREE BEAM, INCLUDING EFFECTS OF TRANSVERSE SHEAR AND ROTARY INERTIA

As a matter of general interest, the curves in Fig. 6 were drawn from 11 different values of S for each value of N and each mode. Thus a total of 132 different normal-mode frequency parameters λ were obtained from the electronic differential analyzer. The time required was less than 30 man-hours. When it is remembered that in addition to the frequency parameter λ the deflection, slope, bending moment, and shear force along the beam are obtained from the analyzer, the superiority over hand methods is apparent.

The effect of rotary inertia on the shape of the normal modes is shown in Fig. 7 where the bending moment along the beam is shown for $N = 0$ (no rotary inertia) and $N = 0.3$. When rotary inertia is considered, the shear force is no longer simply the derivative of the bending moment, as can be seen from Equation [2]. This is also evident in Fig. 7 where the shear and bending moment is zero at each end of the beam and yet the slope of the bending-moment curve is not zero at the beam ends when $N = 0.3$.

It is possible to solve analytically the separated beam Equations [15], [16], and [17] for the free-free end conditions (12). In order to compute the frequency parameter λ it is necessary to solve a rather involved transcendental equation. For two values of the shear parameter S and rotary-inertia parameter N this equation was solved for λ as a spot check on the electronic differential analyzer solutions for the same S and N-values. The theoretical and computer results are shown in Table 3.

TABLE 3 COMPARISON OF COMPUTER AND THEORETICAL SOLUTIONS FOR A UNIFORM FREE-FREE BEAM, INCLUDING SHEAR AND ROTARY INERTIA FORCES

		Third Mode	
$1/S$	N	λ(computer)	λ(theoretical)
551	0	111.43	111.32
537	0.2	108.56	108.32

On the basis of the foregoing results it is probably safe to say

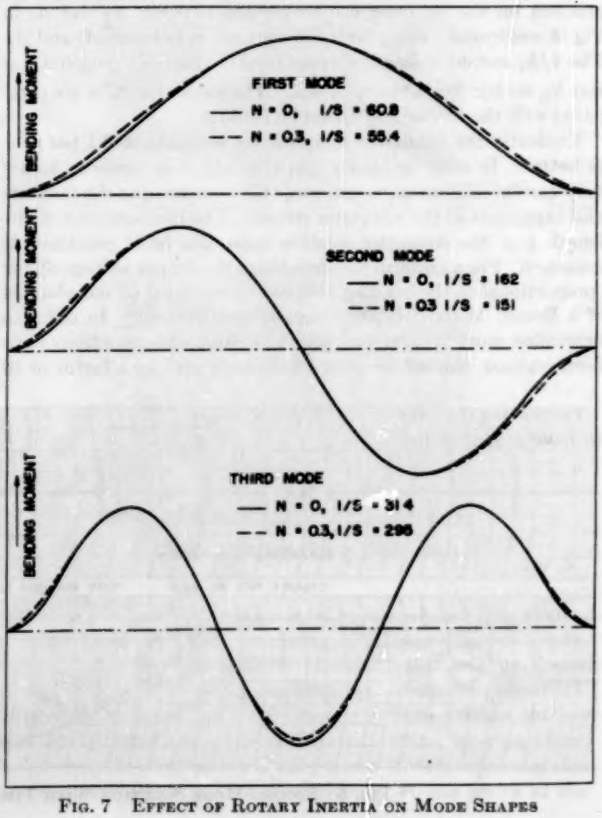

FIG. 7 EFFECT OF ROTARY INERTIA ON MODE SHAPES

that the λ/λ_0-values shown in Fig. 6 are accurate to about 0.2 per cent. It is felt that this accuracy could be improved by a factor of 10 with more careful calibration techniques and by using electronic means instead of hand methods to measure the length of computer solutions. Mode shapes as obtained by the analyzer will be the same order of accuracy as the normal-mode frequencies.

Accuracies of 0.1 per cent or better obviously are of no great engineering significance in this vibrating-beam work. Usually the physical quantities describing the beams themselves are not known to this accuracy, and most engineers would be satisfied with 1 per cent accuracy in normal mode-frequency predictions. The purpose behind these measurements of high accuracy is really twofold; (*a*) to check the accuracies attainable with the electronic differential analyzer, and (*b*) to stimulate further investigation of lateral vibrations of actual beams in the laboratory in order to check the validity of Equations [1] to [5].

Solution of Nonuniform Beams by the Electronic Differential Analyzer. When the electronic differential analyzer is used to find the normal modes of vibration of nonuniform beams, Equations [15], [16], and [17] must again be solved, and the computer circuit shown in Fig. 2 is used. For the nonuniform beam the various ϕ's are functions of computer time τ; i.e., distance along the beam, and four resistors in the computer circuit therefore must vary in a prescribed manner with time. One way of accomplishing this which has been used with considerable success by the authors is to vary each resistor in discrete steps instead of continuously. For example, a linear function of resistance with time can be approximated by the staircase functions shown in Fig. 8. Note that at the end of each step the integral of the step function (the area under the curve) is the same as the integral of the continuous function. When this same integral criteria is used for approximating arbitrary functions by a series of steps, the accuracy of the analyzer solution is surprisingly good (11).

The switching necessary to vary resistors in steps is accomplished by means of 25-position stepping relays (12). This allows one to approximate the variable characteristics along the beam with 25 steps. The techniques for solving the uniform beam are again used to obtain the solution of the nonuniform beam. When a starting button is pressed, the initial condition relays are released and the stepping relays begin changing the appropriate resistors. One of the initial voltages is varied until a solution with the correct end conditions is obtained. In general, this solution will have a length different from the assumed length L for the computer solution. R_λ must then be varied until a correct solution of length L is obtained (or a length close enough to L to allow interpolation of R_λ). The frequency parameter λ is then given by $\lambda = L^2\sqrt{R_\lambda}$, where R_λ is the exact feedback resistance for A_1 and A_7 which gives a correct solution of exact length L.

For solving the nonuniform-beam problem it is quite important to have a good standard-frequency source available for driving the stepping relays. This is necessary not only to insure good accuracy but also to allow solutions to repeat when solving for the critical modes. The time scale of the computer is fixed; so, therefore, must be the time scale of the stepping relays.

As was the case for the uniform-beam computer circuit, here again, care should be taken to maintain the gains of amplifiers in the main loop (A_1-A_2-A_4-A_5-A_6-A_3-A_1) close to unity. This means that one should make an intelligent guess for λ beforehand and choose L so that R_λ is about 1 megohm.

It should perhaps be pointed out that function generators are available which will allow a smooth variation of section properties for nonuniform beams. However, they are considerably more expensive than the stepping-relay method described here; they require more setup time, and they are not as apt to repeat the functions accurately from one run to the next. This latter point is quite important owing to the critical nature of solutions for higher modes.

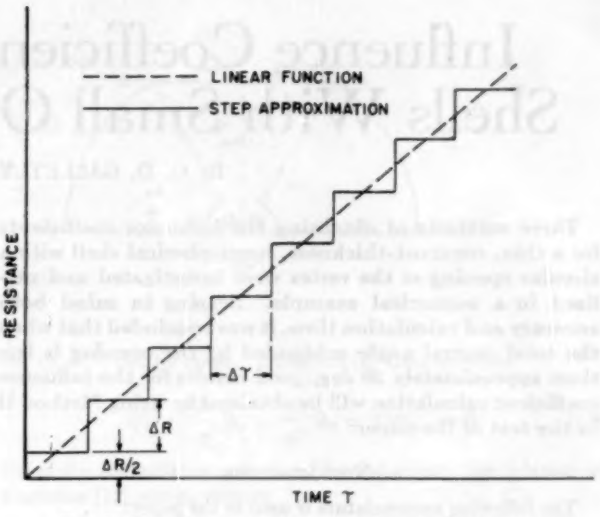

FIG. 8 STEP APPROXIMATION TO A LINEAR FUNCTION

It is in the solution of the nonuniform-beam problem that the electronic differential analyzer should have its greatest utility, for here is a realm in which mathematical solutions that include shear and rotary inertia forces are virtually prohibitive by any hand methods.

BIBLIOGRAPHY

1 "Theory of Sound," by Lord Rayleigh, second edition, The Macmillan Company, London, England, 1894–1896, paragraph 186.

2 "On the Correction for Shear of the Differential Equation for Transverse Vibrations of Prismatic Bars," by S. P. Timoshenko, *London Philosophical Magazine*, series 6, vol. 41, 1921, pp. 744–746.

3 "Vibration Problems in Engineering," by S. P. Timoshenko, second edition, D. Van Nostrand Company, Inc., New York, N. Y., 1937.

4 "Über die Bestimmung der Elastizitätsmodules von Stäben mit Hilfe von Biegungsschwingungen," by E. Goens, *Annalen der Physik*, series 5, vol. 11, 1934, pp. 649–678.

5 "Theoretical Research on the Dynamics of a Ship's Structure," by J. Ormondroyd, R. L. Hess, G. K. Hess, Jr., and J. L. Edman, University of Michigan Engineering Research Institute, Second Progress Report (March 31, 1948), Office of Naval Research Contract N50ri-116 (Univ. of Mich. No. M670-4).

6 "Theoretical Research on the Dynamics of a Ship's Structure," by J. Ormondroyd, R. L. Hess, and G. K. Hess, Jr., University of Michigan Engineering Research Institute, Third Progress Report (March 1, 1949), Office of Naval Research Contract N50ri-116 (Univ. of Mich. No. M670-4).

7 "Theoretical Vibration of Beams," by R. L. Hess, PhD thesis, University of Michigan, 1949.

8 "Effect of Transverse Shear and Rotary Inertia on the Natural Frequency of a Uniform Beam," by E. T. Kruszewski, National Advisory Committee for Aeronautics, TN 1909.

9 "Normal Modes of Oscillation of Beams," by C. L. Dolph, External Memorandum UMM-79 (February 1, 1951), University of Michigan Research Institute.

10 "Electronic Analog Computers," by G. A. Korn and T. M. Korn, McGraw-Hill Book Company, Inc., New York, N. Y., 1952.

11 "Investigation of the Utility of an Electronic Analog Computer in Engineering Problems," by D. W. Hagelbarger, C. E. Howe, and R. M. Howe, External Memorandum UMM-28 (April 1, 1949), University of Michigan Engineering Research Institute, Air Force Contract W33-038-ac-14222 (Project MX-794).

12 "Application of the Electronic Differential Analyzer to the Oscillation of Beams Including Shear and Rotary Inertia," by C. E. Howe, R. M. Howe, and L. L. Rauch, External Memorandum UMM-67 (January, 1951), University of Michigan Engineering Research Institute.

Influence Coefficients for Hemispherical Shells With Small Openings at the Vertex

By G. D. GALLETLY,[1] WASHINGTON, D. C.

Three methods of obtaining the influence coefficients for a thin, constant-thickness, hemispherical shell with a circular opening at the vertex were investigated and utilized in a numerical example. Bearing in mind both accuracy and calculation time, it was concluded that when the total central angle subtended by the opening is less than approximately 30 deg, good results for the influence coefficient calculation will be obtained by using Method II in the text of the paper.

Nomenclature

The following nomenclature is used in the paper:

a = radius of shell
h = thickness of shell
i = $\sqrt{-1}$
n_1, n_2 = complex, nonintegral degrees of associated Legendre functions
u = horizontal deflection of point on shell
A, B, C = constants
D = flexural rigidity of shell = $Eh^3/12(1-\nu^2)$
M_φ = meridional bending moment/unit length
N_θ = stress resultant in θ-direction/unit length
N_φ = stress resultant in φ-direction/unit length
Q_φ = transverse meridional shearing force/unit length
$T_n^1(\ ), q_n^1(\ )$ = associated Legendre functions of 1st and 2nd kinds of order 1 and degree n
V = angle of rotation of tangent to meridian
X_c, X_d, W_c, W_d = functions of φ_0—see Equation [17]
α = $\pi/2 - \varphi_0$
γ, δ = phase angles
λ = $\left[3(1-\nu^2)\dfrac{a^2}{h^2}\right]^{1/4}$
μ = $\cos\varphi$
ν = Poisson's ratio
φ = $\pi/2 - \omega$ (see Fig. 1)
$2\varphi_0$ = total central angle subtended by circular opening
$\psi_1'(\ ), \psi_2'(\ )$, etc. = first derivatives of Schleicher functions $\psi_1(\ ), \psi_2(\ )$, etc.
ρ = $\left[3(1-\nu^2)\dfrac{a^2}{h^2} - \dfrac{\nu^2}{4}\right]^{1/4}$
θ = longitude of point on shell
ω = latitude of point on shell
$\dot{}$ = differentiation with respect to φ
$'$ = differentiation with respect to $\rho\sqrt{2}\varphi$

Introduction

The purpose of this paper is to present briefly a comparison of the results obtained by different methods for the influence coefficients of a thin, constant-thickness, hemispherical shell with a circular opening at the vertex, and loaded with either uniformly distributed moments or forces around the periphery of the opening, Fig. 1. (By influence coefficient is meant the angular rotation or deflection at an edge due to a unit moment or force applied at that edge.)

The methods investigated were those due to Geckeler, Esslinger, and Love, and they were applied to the specific problem of a hemisphere with geometric characteristics as follows: Radius a = 181 in., thickness h = 2 in., total angle subtended by circular opening = 21 deg.

As influence coefficients for cylindrical and conical shells are already available in the literature, it will be seen that their evaluation for hemispheres with circular openings at the vertex will facilitate strength analyses of axisymmetrical cone and cylinder-hemisphere juncture problems.

Differential Equations of Equilibrium

The classical, small-deflection theory of thin shells will be used and also Timoshenko's notation and sign convention. If Q_φ, the transverse shearing force, and V, the rotation of a tangent to a meridian, are selected as dependent variables then the differential equations of equilibrium for the bending of a thin, constant-thickness, hemispherical shell may be written (1)[2]

$$\ddot{Q}_\varphi + \cot_\varphi \dot{Q}_\varphi - (\cot^2\varphi - \nu)Q_\varphi = EhV \quad [1a]$$

$$\ddot{V} + \cot\varphi\ \dot{V} - (\cot^2\varphi + \nu)V = -\frac{a^2 Q_\varphi}{D} \quad [1b]$$

It also can be shown (1) that the differential equation for Q_φ can be put in the following form

$$\ddot{Q}_\varphi + \cot\varphi\ \dot{Q}_\varphi - \cot^2\varphi\ Q_\varphi \pm 2i\rho^2 Q_\varphi = 0 \quad [2]$$

where

$$\rho^4 = 3(1-\nu^2)\frac{a^2}{h^2} - \frac{\nu^2}{4} \quad [3]$$

Method I The Geckeler Approximation

The approximation consists in neglecting the functions Q_φ and V and their first derivatives which are small in comparison with their second derivatives (1). After eliminating V, Equations [1] then reduce to

$$\dddot{Q}_\varphi + 4\lambda^4 Q_\varphi = 0 \quad [4]$$

where

$$\lambda^4 = 3(1-\nu^2)\frac{a^2}{h^2} \quad [5]$$

The general solution of Equation [4] can be written

$$Q_\varphi = Ae^{-\lambda\varphi}\sin(\lambda\varphi + \gamma) + Be^{\lambda\varphi}\sin(\lambda\varphi + \delta) \quad [6]$$

---

[1] Structural Research Engineer, David Taylor Model Basin.

Contributed by the Applied Mechanics Division and presented at the Annual Meeting, New York, N. Y., November 28–December 3, 1954, of The American Society of Mechanical Engineers.

Discussion of this paper should be addressed to the Secretary, ASME, 29 West 39th Street, New York, N. Y., and will be accepted until April 11, 1955, for publication at a later date. Discussion received after the closing date will be returned.

Note: Statements and opinions advanced in papers are to be understood as individual expressions of their authors and not those of the Society. Manuscript received by ASME Applied Mechanics Division, June 11, 1953. Paper No. 54—A-4.

[2] Numbers in parentheses refer to the Bibliography at the end of the paper.

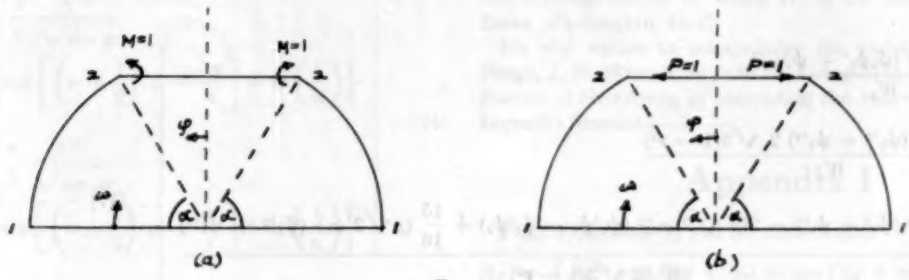

FIG. 1

In this expression φ is measured from the axis of rotation of the shell. For the determination of the constants of integration it is more convenient to introduce a new variable ω, such that

$$\varphi = \pi/2 - \omega \quad \ldots\ldots\ldots\ldots\ldots\ldots [7]$$

Equation [6] then becomes

$$Q_\varphi = A_1 e^{\lambda\omega} \sin(\lambda\omega + \gamma_1) + B_1 e^{-\lambda\omega} \sin(\lambda\omega + \delta_1) \ldots [8]$$

Utilizing the relations

$$\left.\begin{aligned} N_\theta &= -\dot{Q}_\varphi \ldots (a) \\ u &\approx \frac{a \sin\varphi}{Eh} N_\theta \ldots (b) \\ V &\approx \frac{1}{Eh} \ddot{Q}_\varphi \ldots (c) \\ M_\varphi &\approx -\frac{D}{a} \dot{V} \ldots (d) \end{aligned}\right\} \ldots\ldots\ldots [9]$$

and also Equations [7] and [8], it is a simple matter to find the quantities N_θ, u, V, and M_φ. Once these are obtained the problem is to compute the four constants, A_1, B_1, γ_1, and δ_1, for the various cases of edge loading. The cases considered herein are shown in Fig. 1.

The problem is not difficult but involves a fair amount of algebraic manipulation; hence only the final results for the influence coefficients will be given. The final results also will be given in a somewhat simplified form by replacing expressions like $(e^{2\lambda\alpha} + e^{-2\lambda\alpha} - 4\sin^2\lambda\alpha - 2)$ by $e^{2\lambda\alpha}$, which is a reasonable approximation for most shells. Hence there follows:

Owing to uniformly distributed unit horizontal forces at $\omega = \alpha$

$$u = \frac{2\lambda a \cos^2\alpha}{Eh}; \quad V = \frac{2\lambda^2 \cos\alpha}{Eh} \quad \ldots\ldots\ldots [10]$$

Due to uniformly distributed unit moments at $\omega = \alpha$

$$u = \frac{2\lambda^2 \cos\alpha}{Eh}; \quad V = \frac{4\lambda^2}{Eah} \quad \ldots\ldots\ldots [11]$$

The more accurate values for these influence coefficients are given in Appendix 1, where there also is given a brief outline of how they were obtained.

METHOD II THE APPROXIMATION[2] $\cot\varphi = \frac{1}{\varphi}$

For shell sections with small central angles the approximation $\cot\varphi = \frac{1}{\varphi}$ can be made. Equation [2] then becomes

$$\ddot{Q}_\varphi + \frac{1}{\varphi}\dot{Q}_\varphi - \frac{1}{\varphi^2} Q_\varphi \pm 2i\rho^2 Q_\varphi = 0 \quad \ldots\ldots [12]$$

Using the ψ-functions introduced by Schleicher, the solution of Equation [12] can be written

$$\begin{aligned} Q_\varphi = {} & C_1\psi_1'(\rho\sqrt{2}\,\varphi) + C_2\psi_2'(\rho\sqrt{2}\,\varphi) \\ & + C_3\psi_3'(\rho\sqrt{2}\,\varphi) + C_4\psi_4'(\rho\sqrt{2}\,\varphi) \ldots\ldots [13] \end{aligned}$$

where $'$ denotes differentiation with respect to $\rho\sqrt{2}\,\varphi$.

For arguments $\rho\sqrt{2}\,\varphi \leq 6$ the Schleicher functions and their first derivatives have been tabulated (2, 3).

It can be seen from Fig. 169 of reference (1) that ψ_3' and ψ_4' decrease with increasing argument while ψ_1' and ψ_2' increase. Since the stresses resulting from the edge moments and forces decrease with increasing distance from that edge, ψ_1' and ψ_2' are appropriate for edge 1 and ψ_3' and ψ_4' for edge 2, Fig. 1.

Also, as the influence of the perturbational (or edge) loading decreases rapidly, it is convenient for simplification in the calculation of the integration constants to determine the constants for edges 1 and 2 separately. Again, as only a loading around edge 2 is being considered herein, it will suffice to determine the constants C_3 and C_4.

The foregoing method is the approach used by Dr. Maria Esslinger (4) and she determines the constants for the cases shown in Fig. 2.

Utilizing the relations

$$\left.\begin{aligned} N_\varphi &\approx -\frac{1}{\varphi} Q_\varphi \ldots (a) \\ N_\theta &= -\dot{Q}_\varphi \ldots (b) \\ V &\approx \frac{1}{Eh}\left[\ddot{Q}_\varphi + \frac{1}{\varphi}\dot{Q}_\varphi - \frac{1}{\varphi^2} Q_\varphi\right] \ldots (c) \\ M_\varphi &\approx -\frac{D}{a}\left[\dot{V} + \frac{\nu}{\varphi} V\right] \ldots (d) \\ u &= \frac{a\sin\varphi}{Eh}[N_\theta - \nu N_\varphi] \ldots (e) \end{aligned}\right\} \ldots [14]$$

and the relevant boundary conditions, it is possible to determine the influence coefficients. Esslinger gives the following:

Due to uniformly distributed unit horizontal forces at $\varphi = \varphi_0$

$$u = \frac{hW_e}{Eh\varphi_0}; \quad V = \frac{X_e}{Eh\varphi_0} \quad \ldots\ldots\ldots [15]$$

Due to uniformly distributed unit moments at $\varphi = \varphi_0$

$$u = \frac{X_e}{Eh\varphi_0}; \quad V = \frac{X_d}{Eh^2\varphi_0} \quad \ldots\ldots\ldots [16]$$

[2] Since completion of the manuscript it has been drawn to the attention of the author that the use of this approximation in shell theory is also due to Geckeler, vide *Ingenieur-Archiv.*, vol. 1, 1930, p. 260.

where

$$\left.\begin{aligned} X_e &= \frac{(\rho\sqrt{2}\,\varphi_0)^2\,(\psi_3\psi_3' + \psi_4\psi_4')}{W_d} \\ X_d &= \frac{(\rho\sqrt{2}\,\varphi_0)\,(\psi_3'^2 + \psi_4'^2)\,2\sqrt{3(1-\nu^2)}}{W_d} \\ W_e &= \frac{(\rho\sqrt{2}\,\varphi_0)^3\,(\psi_3^2 + \psi_4^2) - 2(\rho\sqrt{2}\,\varphi_0)^2\,(\psi_3'\psi_4 - \psi_4'\psi_3) + \frac{15}{16}\,(\rho\sqrt{2}\,\varphi_0)\,(\psi_3'^2 + \psi_4'^2)}{(W_d)2\sqrt{3(1-\nu^2)}} \\ W_d &= (\psi_3\psi_4' - \psi_4\psi_3') + \frac{0.75}{\rho\sqrt{2}\,\varphi_0}\,(\psi_3'^2 + \psi_4'^2) \end{aligned}\right\} \quad [17]$$

where, in Esslinger's Equation [40], $-N_r$ has been equated to unity as 1 cos $\varphi_0 \approx 1$. It is to be noted that the argument of the foregoing Schleicher functions is $\rho\sqrt{2}\,\varphi_0$. Also X_e, X_d, etc., as defined by Equation [17] are slightly different from Esslinger's definition of these functions.

The functions X_e, X_d, and W_e have been evaluated by Esslinger and incorporated in a chart. However, because of the small scale used, accurate interpolation is rather difficult and evaluation of Equation [17] is necessary.

Method III Love's Method (5)

Setting $U = aQ_\varphi$, introducing two constant multipliers A and B, multiplying Equation [1a] by aA and Equation [1b] by B and adding the resulting equations, one obtains

$$\left(\frac{d^2}{d\varphi^2} + \cot\varphi\,\frac{d}{d\varphi} - \cot^2\varphi\right)(AU + BV) + \nu(AU - BV) + \frac{BUa}{D} - AaEhV = 0 \quad [18]$$

It can be shown (5) that with the substitution

$$\mu = \cos\varphi \quad [19]$$

Equation [18] reduces to

$$\left[(1-\mu^2)\,\frac{d^2}{d\mu^2} - 2\mu\,\frac{d}{d\mu} + n(n+1) - \frac{1}{1-\mu^2}\right][AU + BV] = 0 \quad [20]$$

provided that the relation

$$(n^2 + n - 1)^2 - \nu^2 + 12\,(1-\nu^2)\,\frac{a^2}{h^2} = 0 \quad [21]$$

is satisfied.

Equation [20] is an associated Legendre equation and is satisfied by generalized spherical harmonics of order 1 and degree n (complex and nonintegral for this case).

The solution of Equation [20] is

$$\left.\begin{aligned} U - \frac{Eah}{n_1(n_1+1) + \nu - 1}\,V &= A_1 T_{n1}{}^1(\mu) + B_1 q_{n1}{}^1(\mu) \\ U - \frac{Eah}{n_2(n_2+1) + \nu - 1}\,V &= A_2 T_{n2}{}^1(\mu) + B_2 q_{n2}{}^1(\mu) \end{aligned}\right\} \quad [22]$$

where $T_n{}^1(\mu)$ and $q_n{}^1(\mu)$ are, in Ferrer's notation (6), the associated Legendre functions of the first and second kind.

As the degrees n_1, n_2 of the generalized spherical harmonics are complex the constants A_1 . . . . also will be complex and they can be adjusted so that U and V are real.

The horizontal deflection u and the meridional bending moment M_φ are given by

$$\left.\begin{aligned} u &= -\frac{\sin\varphi}{Eh}\,[\dot{U} - \nu U\cot\varphi] \\ M_\varphi &= -\frac{D}{a}\,[\dot{V} + \nu V\cot\varphi] \end{aligned}\right\} \quad [23]$$

It will be seen that $U(\equiv aQ_\varphi)$, V, u, and M_φ will be functions of four arbitrary constants which can be determined from the boundary conditions.

The main difficulty in this method is the computation of the functions $T_n{}^1(\mu)$, $q_n{}^1(\mu)$, and their first derivatives. To date they have been tabulated only for real degrees n. Love (5) gives series expansions for the functions but, according to Hobson (7), the series are convergent only for $\pi/6 < \varphi < 5\pi/6$. Herein, the functions were calculated by two methods. The first method made use of their asymptotic expansions

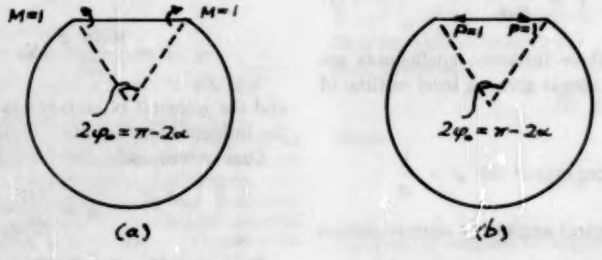

Fig. 2

$$\left.\begin{aligned} T_n^1(\cos\varphi) &\approx \sqrt{\frac{2}{\pi}}\,\frac{n^{1/2}}{\sqrt{\sin\varphi}} \left\{\cos\left[\left(n+\frac{1}{2}\right)\varphi - \frac{3\pi}{4}\right] + 0\left(\frac{1}{n}\right)\right\} \\ Q_n^1(\cos\varphi) &\approx \sqrt{\frac{\pi}{2}}\,\frac{n^{1/2}}{\sqrt{\sin\varphi}} \left\{\sin\left[\left(n+\frac{1}{2}\right)\varphi + \frac{\pi}{4}\right] + 0\left(\frac{1}{n}\right)\right\} \end{aligned}\right\} \quad \ldots [24]$$

The first derivatives were calculated using the recurrence relations between the functions (6, 7).

In the second method, use was made of the relations between the associated Legendre functions and the hypergeometric functions. This method involves gamma and psi functions of complex arguments. The values of the functions were obtained by the Computing Division, National Bureau of Standards, and are given in Appendix 2.

Numerical Example

The geometric characteristics of the hemispherical shell were: Radius $a = 181$ in., thickness $h = 2$ in., total central angle subtended by the circular opening $= 2\varphi_0 = 21$ deg.

The values obtained for the influence coefficients using the different methods are given in Table 1.

TABLE 1 VALUES OF INFLUENCE COEFFICIENTS $Eh\mu$ AND Eh^2V OBTAINED BY DIFFERENT METHODS

	Unit moments at edge, $\varphi = \varphi_0$		Unit horizontal forces at edge, $\varphi = \varphi_0$	
	$Eh\mu$	Eh^2V	$Eh\mu$	Eh^2V
Method I.....	54.50	40.41	147.01	54.50
Method II.....	46.62	35.25	163.45	46.62
Method III(a)...	49.95	37.27	166.16	50.05
Method III(b)...	47.64	36.24	164.66	47.71

Note: Method III(a) used the asymptotic expansions of the associated Legendre functions while Method III(b) utilized the hypergeometric series representation.

The values obtained by the use of Method III(b) are the most accurate and will be taken as the standard for comparison purposes. It can be seen that the values obtained from Method II closely approximate those of Method III(b) while Method I, which is the quickest as far as the time element is concerned, yields a maximum error of approximately +15 per cent. The values obtained from Method III(a) are not as good as those from Method II, although they are better than Method I.

Method III(b), while being the most accurate, is somewhat time-consuming especially if one has to compute the values of the associated Legendre functions. Hence, from the points of view of time-consumption and accuracy, Method II is the one suggested for use.

Conclusions

For cases where the total central angle subtended by the circular opening at the vertex is fairly small, e.g., $<\pi/6$, use of Method II for the calculation of the influence coefficients is recommended. Approximate methods for central angles greater than $\pi/6$ have not been investigated but Love's method [i.e., Method III(b)] will give accurate results for all cases. The calculation for these latter cases, however, is likely to prove laborious until such time as the associated Legendre functions of complex, nonintegral degrees are tabulated.

Acknowledgment

The author wishes to acknowledge the encouragement given to this investigation by E. Wenk, Jr., of the David Taylor Model Basin, Washington, D. C.

He also wishes to acknowledge the assistance of Laura V. Peugh, J. W. Wrench, Jr., and the Computing Division, National Bureau of Standards, in computing the values of the associated Legendre functions.

Appendix 1

From Equations [8] and [9] there results

$$\left.\begin{aligned} N_\theta &= A_1\lambda e^{\lambda\omega}[\sin(\lambda\omega+\gamma_1) + \cos(\lambda\omega+\gamma_1)] \\ &\quad + B_1\lambda e^{-\lambda\omega}[\cos(\lambda\omega+\delta_1) - \sin(\lambda\omega+\delta_1)] \ldots (a) \\ u &= \frac{a\cos\omega}{Eh} N_\theta \ldots (b) \\ V &= \frac{2\lambda^2}{Eh}[A_1 e^{\lambda\omega}\cos(\lambda\omega+\gamma_1) \\ &\quad - B_1 e^{-\lambda\omega}\cos(\lambda\omega+\delta_1)] \ldots (c) \\ M_\varphi &= \frac{a}{2\lambda}[A_1 e^{\lambda\omega}\{\cos(\lambda\omega+\gamma_1) - \sin(\lambda\omega+\gamma_1)\} \\ &\quad + B_1 e^{-\lambda\omega}\{\sin(\lambda\omega+\delta_1) + \cos(\lambda\omega+\delta_1)\}] \ldots (d) \end{aligned}\right\} \quad \ldots [25]$$

For the loading shown in Fig. 1(a), the boundary conditions are

$$(M_\varphi)_{\omega=\alpha} = 1; \quad (Q_\varphi)_{\omega=\alpha} = (Q_\varphi)_{\omega=0} = (M_\varphi)_{\omega=0} = 0 \ldots [26]$$

Substituting these boundary conditions into Equations [8] and [25d] it will be found that the phase angles γ_1 and δ_1 are given by

$$\gamma_1 = \cot^{-1}\left[-\cot\lambda\alpha - \frac{2e^{-2\lambda\alpha}}{1-e^{-2\lambda\alpha}}\right] \equiv \cot^{-1} Y \ldots [27]$$

$$\delta_1 = \cot^{-1}\left[-\cot\lambda\alpha - \frac{2}{1-e^{-2\lambda\alpha}}\right] \equiv \cot^{-1} X \ldots [28]$$

Using the following notation for brevity

$$Z = \left[\frac{e^{2\lambda\alpha} + e^{-2\lambda\alpha} - 4\sin^2\lambda\alpha - 2}{(e^{\lambda\alpha} - e^{-\lambda\alpha})\sin\lambda\alpha}\right] \ldots [29]$$

Then the constants A_1 and B_1 are given by

$$\left.\begin{aligned} A_1 &= -\frac{2\lambda\sqrt{1+Y^2}}{aZ} \\ B_1 &= \frac{2\lambda\sqrt{1+X^2}}{aZ} \end{aligned}\right\} \quad \ldots [30]$$

Substituting Equations [27], [28], [29], and [30] into Equations [25a, b, c], the following expressions for the influence coefficients are obtained

$$u = \frac{2\lambda^2\cos\alpha}{Eh}\left[\frac{e^{2\lambda\alpha} + e^{-2\lambda\alpha} + 4\sin^2\lambda\alpha - 2}{e^{2\lambda\alpha} + e^{-2\lambda\alpha} - 4\sin^2\lambda\alpha - 2}\right] \ldots [31]$$

$$V = \frac{4\lambda^2}{Eah}\left[\frac{e^{2\lambda\alpha} - e^{-2\lambda\alpha} + 2\sin 2\lambda\alpha}{e^{2\lambda\alpha} + e^{-2\lambda\alpha} - 4\sin^2\lambda\alpha - 2}\right] \ldots [32]$$

For the loading shown in Fig. 1 (b), the boundary conditions are

$$(Q_\varphi)_{\omega=\alpha} = \cos\alpha; \quad (Q_\varphi)_{\omega=0} = (M_\varphi)_{\omega=0} = (M_\varphi)_{\omega=\alpha} = 0 \ldots [33]$$

The relations analogous to Equations [27], [28], [29], and [30] are then

$$\gamma_1 = \cot^{-1}\left[1 + \frac{2(1 - e^{-2\lambda\alpha})}{\cot \lambda\alpha(1 - e^{-2\lambda\alpha}) - (1 + e^{-2\lambda\alpha})}\right] \equiv \cot^{-1} y \quad [34]$$

$$\delta_1 = \cot^{-1}\left[-1 + \frac{2(1 - e^{-2\lambda\alpha})}{\cot \lambda\alpha\,(1 - e^{-2\lambda\alpha}) - (1 + e^{-2\lambda\alpha})}\right] \equiv \cot^{-1} x \quad [35]$$

$$Z = -\frac{e^{-\lambda\alpha}}{\sin \lambda\alpha}\left[\frac{e^{2\lambda\alpha} + e^{-2\lambda\alpha} - 4\sin^2 \lambda\alpha - 2}{\cot \lambda\alpha(1 - e^{-2\lambda\alpha}) - (1 + e^{-2\lambda\alpha})}\right] \quad [36]$$

$$A_1 = -\frac{\cos \alpha \sqrt{1 + y^2}}{Z}, \qquad B_1 = \frac{\cos \alpha \sqrt{1 + x^2}}{Z} \quad [37]$$

and for the influence coefficients there results

$$u = \frac{2\lambda a \cos^2 \alpha}{Eh}\left[\frac{e^{2\lambda\alpha} - e^{-2\lambda\alpha} - 2\sin 2\lambda\alpha}{e^{2\lambda\alpha} + e^{-2\lambda\alpha} - 4\sin^2 \lambda\alpha - 2}\right] \quad [38]$$

$$V = \frac{2\lambda^2 \cos \alpha}{Eh}\left[\frac{e^{2\lambda\alpha} + e^{-2\lambda\alpha} + 4\sin^2 \lambda\alpha - 2}{e^{2\lambda\alpha} + e^{-2\lambda\alpha} - 4\sin^2 \lambda\alpha - 2}\right] \quad [39]$$

Appendix 2

Values of the associated Legendre functions for $n = 11.753 + i\,12.204$ (the values of n were obtained by solving Equation [21]).

$$\varphi = \pi/2 \begin{cases} T_n^1 = -2.4670 \times 10^3 + i\,2.4964 \times 10^3 \\ q_n^1 = 3.9214 \times 10^3 + i\,3.8752 \times 10^3 \\ \dot{T}_n^1 = 0.4050 \times 10^3 + i\,60.6960 \times 10^3 \\ \dot{q}_n^1 = 95.3400 \times 10^3 - i\,0.6362 \times 10^3 \end{cases}$$

$$\varphi = 10.5^\circ \begin{cases} T_n^1 = 31.468 + i\,13.238 \\ q_n^1 = 20.312 - i\,48.101 \\ \dot{T}_n^1 = 449.29 - i\,227.25 \\ \dot{q}_n^1 = -365.43 - i\,731.89 \end{cases}$$

The values of the functions and their first derivatives can be checked from the Wronskian, which is

$$T_n^1 \dot{q}_n^1 - q_n^1 \dot{T}_n^1 = \frac{n(n+1)}{\sin \varphi}$$

where the dot, as before, indicates differentiation with respect to φ.

BIBLIOGRAPHY

1 "Theory of Plates and Shells," by S. Timoshenko, McGraw-Hill Book Company, Inc., New York, N. Y., 1940, pp. 454–469.

2 "Beams on Elastic Foundation," by M. Hetenyi, The University of Michigan Press, Ann Arbor, Mich., 1946, pp. 245–255.

3 "Tables of Functions," by E. Jahnke and F. Emde, Dover Publications, Inc., New York, N. Y., fourth edition, 1945, pp. 246–257.

4 "Statische Berechnung von Kesselboden," by Maria Esslinger, Julius Springer, Berlin, Germany, 1952, pp. 1–20.

5 "The Mathematical Theory of Elasticity," by A. E. H. Love, Dover Publications, Inc., New York, N. Y., fourth edition, 1944, pp. 587–589.

6 "Hypergeometric and Legendre Functions With Applications to Integral Equations of Potential Theory," by Chester Snow, AMS 19, National Bureau of Standards, Washington, D. C., 1952, pp. 37 and 42.

7 "Spherical and Ellipsoidal Harmonics," by E. W. Hobson, Cambridge University Press, Cambridge, England, 1931, p. 288.

Membrane and Bending Analysis of Axisymmetrically Loaded Axisymmetrical Shells

By G. HORVAY[1] and I. M. CLAUSEN,[2] SCHENECTADY, N. Y.

Shell formulas are given which are applicable to engineering design.

Nomenclature

The following nomenclature is used in the paper; for notation see Table 1, Fig. 1, and Table 2, Fig. 10.

Forces and Moments:

p_x, p_θ, p_z, or $-p$ = applied loads in x, θ, z-directions, psi
p_H, p_V = applied loads in horizontal and vertical directions, see Equation [1], psi
p = internal pressure, psi
V = vertical force, lb/in.
W = total vertical force, lb
H = horizontal shear force, lb/in.
$Q_x = H \sin \varphi$ = normal shear force, lb/in. (not used)
N_x, N_θ = meridional and hoop tension force, lb/in.
M_x, M_θ = meridional and hoop moment, lb in./in.
$\mathfrak{M}$, $\mathfrak{H}$, $\mathfrak{V}$ = moment lb in./in., horizontal shear force, lb/in., vertical force, lb/in., applied at edge of shell

Co-Ordinates and Geometric Parameters:

x, θ, z = co-ordinates in meridional, azimuthal, and inward normal directions
φ = latitude angle
R_x, R_θ, or R = radii or curvatures of shell middle surface in meridional and azimuthal directions
r = horizontal radius of shell middle surface
h = wall thickness
D = flexural rigidity of shell, see Equation [12]
l = attenuation length, see Equation [11]
l_v = axial component of l
$\mathfrak{L}$ = meridional length of shell between apex (pole) and edge as in Fig. 1
n = distance from edge, in units of l; $n = (\bar{x} - x)/l$
ϵ, f = expansivity and flexibility coefficients, see Equation [13]
Bar over quantity = edge value
Subscripts i, o = inner fiber ($z = +h/2$), outer fiber ($z = -h/2$)

Deformations and Stresses:

u, v, w = displacements in x, θ, z-directions
δ = radial (outward) displacement, positive in same sense as $\mathfrak{H}$
∇ = vertical (upward) displacement
χ = increase in latitude angle (angle of rotation), positive in same sense as $\mathfrak{M}$
κ_x, κ_θ = increase in curvatures, $d\chi/dx$, $\chi \cot\varphi/R$ (not used)
$\epsilon_x, \epsilon_\theta$ = strains in x, θ-directions
σ_x, σ_θ = meridional and hoop stress
F_1, F_2, F_3, F_4 = functions defined in Equation [10d]

The present note serves to supplement the familiar shell formulas of Roark (1).[3] Table 1, item 1, lists general membrane formulas; items 2 to 9 specialize these general formulas to the frequently occurring cases of conical and spherical shells loaded by weight, gas pressure, and liquid pressure.[4]

Table 2, item 10, lists shell-bending formulas in the familiar, Geckeler, approximation. The formulas express the shell displacements δ, χ, ∇, and the shell moments and forces M_x, M_θ, H, N_x, N_θ (per unit length), in terms of the applied edge moment $\mathfrak{M}$ and applied edge shear $\mathfrak{H}$, in the form of decaying sinusoidals $F_1, \ldots, F_4$. The argument n in the formulas denotes distance from the edge in multiples of

$$l = [3(1 - \mu^2)]^{-1/4} (\bar{r}h/\sin \bar{\varphi})^{1/2} \quad [11]$$

Length l thus denotes the distance from the edge in which the exponential factor of F_4 reduces from 1 to $1/e$; l may be called the "attenuation length" of the shell. The functions F_1, F_2, F_3, F_4 are tabulated in reference (2) as functions φ, ζ, ψ, θ, and in reference (3) as functions A, B, C, D.

Shell rotation $\bar{\chi}$ developed at the edge in the absence of force $\mathfrak{H}$, under action of unit applied moment $\mathfrak{M}$, may be called "flexibility," and is assigned the special symbol f. It is related to l, and to the shell stiffness

$$D = Eh^3/12(1 - \mu^2) \quad [12]$$

by the formula[5]

$$f = l/D \quad [13a]$$

Shell displacement $\bar{\delta}$ developed at the edge in the absence of moment $\mathfrak{M}$, under action of unit applied force $\mathfrak{H}$, may be called "expansivity," and is assigned the special symbol ϵ. It is related to f and l_v (the axial component of l) by

$$\epsilon = {}^1/_2 f l_v^2 \quad (l_v = l \sin \bar{\varphi}) \quad [13b]$$

As is well known, the Geckeler approximation replaces the

---

[1] Development Engineer, General Electric Company, Knolls Atomic Power Laboratory. Mem. ASME. The Knolls Atomic Power Laboratory is operated by the General Electric Company for the Atomic Energy Commission. The work reported here was carried out under contract No. W-31-109 Eng-52.

[2] Formerly, Member, Advanced Engineering Program; at present, Technical Engineer, Accessory Turbine Engineering, Aircraft Gas Turbine Division, General Electric Company. Assoc. Mem. ASME

Contributed by the Applied Mechanics Division and presented at the Annual Meeting, New York, N. Y., November 28–December 3, 1954, of The American Society of Mechanical Engineers.

Discussion of this paper should be addressed to the Secretary, ASME, 29 West 39th Street, New York, N. Y., and will be accepted until April 11, 1955, for publication at a later date. Discussion received after the closing date will be returned.

Note: Statements and opinions advanced in papers are to be understood as individual expressions of their authors and not those of the Society. Manuscript received by ASME Applied Mechanics Division, November 17, 1953. Paper No. 54—A-8.

[3] Numbers in parentheses refer to the Bibliography at the end of the paper.

[4] We refer to the equations in items 1 to 10 as Equations [1] to [10]. In the expression of χ, Equation [1c], the closing parenthesis should precede cot φ, thus: R/R_x) cot φ.

[5] Equations [13a, b] are obtained by substituting $n = 0$, $\mathfrak{H} = 0$, $\mathfrak{M} = 1$, and $n = 0$, $\mathfrak{H} = 1$, $\mathfrak{M} = 0$, respectively, into the χ and δ expressions of Equations [10a].

TABLE 1 MEMBRANE ANALYSIS

SHELL DESCRIPTION	TYPE OF LOADING	DESIGN PARAMETERS	DESIGN FORMULAS
General Shell $p_V = p_x \sin\phi + p_z \cos\phi$ $p_H = p_x \cos\phi - p_z \sin\phi$ 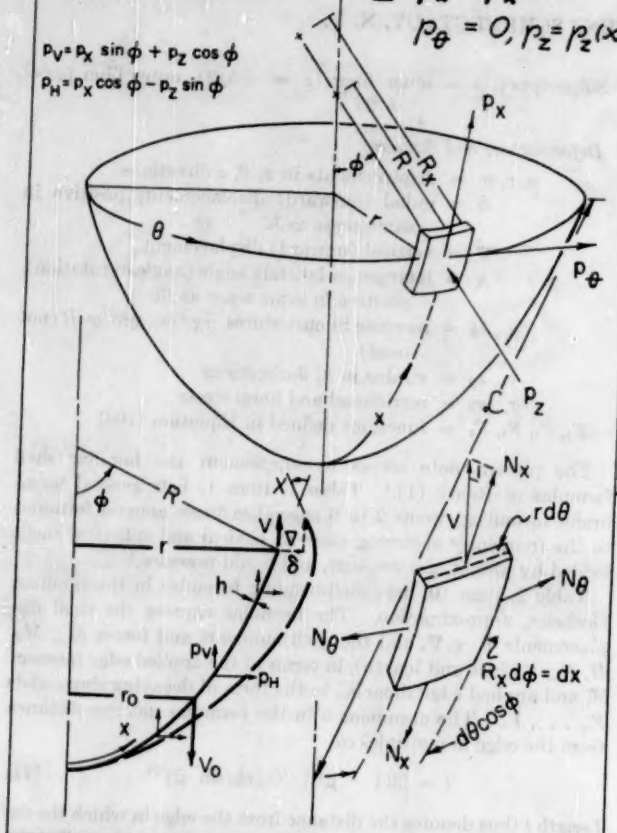	**1.** $p_x = p_x(x)$ $p_\theta = 0,\ p_z = p_z(x)$	(a) forces (lb./in.) $V,\ N_x,\ N_\theta$	$2\pi r V = 2\pi r_0 V_0 - 2\pi \int_{x_0}^{x} r p_x dx$ $N_x = \frac{V}{\sin\varphi},\quad N_x(0) = -\frac{1}{2} R_x(0) p_z(0)$ $N_\theta = -R p_z - \frac{R}{R_x} N_x,\quad N_\theta(0) = -\frac{1}{2} R(0) p_z(0)$
		(b) strains (in./in.) $\varepsilon_x, \varepsilon_\theta$	$\varepsilon_x = \frac{N_x - \mu N_\theta}{E h},\quad \varepsilon_\theta = \frac{N_\theta - \mu N_x}{E h}$
		(c) deformations (in, in/in, in.) δ, χ, ∇	$\delta = r \varepsilon_\theta$ $\chi = (\varepsilon_x - \frac{R}{R_x}\cot\varphi) - \frac{d(R\varepsilon_\theta)}{dx}$ $\nabla\Big|_{x_0}^{x} = \int_{x_0}^{x} (\varepsilon_x \sin\varphi + \chi \cos\varphi)\, dx$ $= -R\cos\varphi \cdot \varepsilon_\theta\Big|_{x_0}^{x} + \int_{x_0}^{x} \frac{\varepsilon_x - R\varepsilon_\theta / R_x}{\sin\varphi} dx$
		(d) stresses (lb./sq.in) σ_x, σ_θ	$\sigma_x = \frac{N_x}{h},\quad \sigma_\theta = \frac{N_\theta}{h}$
Conical Shell 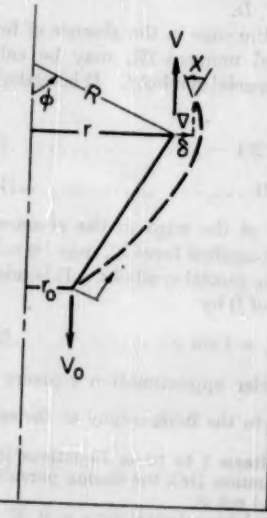	**2.** $p_x = p_x(x)$ $p_\theta = 0$ $p_z = p_z(x)$ $\{ r = R\sin\varphi$ $R_x = \infty$ $dr = dx\cos\varphi$ $r - r_0 = x\cos\varphi \}$	(a) forces	$V = V_0 \frac{r_0}{r} - \frac{1}{r} \int_{r_0}^{r} r(p_x \tan\varphi + p_z) dr$ $\{ = V_0 - \int_0^x p_x dx,\ \text{for } \varphi = \pi/2 \}$ $N_x = \frac{V}{\sin\varphi},\quad N_\theta = -\frac{r p_z}{\sin\varphi}$
		(c) deformations	$\delta = r \varepsilon_\theta$ $\chi = \varepsilon_x \cot\varphi - \frac{d(R\varepsilon_\theta)}{dx} = (\varepsilon_x - \frac{d\delta}{dr})\cot\varphi$ $\nabla = -R\varepsilon_\theta \cos\varphi\Big|_0^x + \frac{1}{\sin\varphi} \int_0^x \varepsilon_x dx$ $= -\delta\cot\varphi\Big|_{r_0}^{r} + \frac{1}{\sin\varphi\cos\varphi} \int_{r_0}^{r} \varepsilon_x dr$

TABLE 1 MEMBRANE ANALYSIS (*Continued*)

SHELL DESCRIPTION	TYPE OF LOADING	DESIGN PARAMETERS	DESIGN FORMULAS
Conical Shell 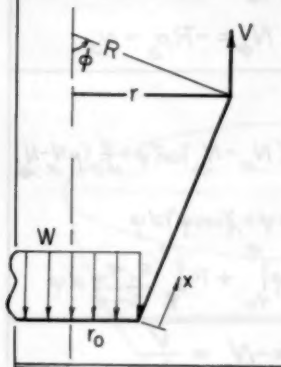	**3. Weight Loading** W (lb.) $p_x = p_\theta = p_z = 0$	(a) forces	$V = \frac{W}{2\pi r}$, $N_x = \frac{V}{\sin\varphi}$, $N_\theta = 0$
		(b) strains	$Eh\varepsilon_x = \frac{V}{\sin\varphi}$, $Eh\varepsilon_\theta = -\mu\frac{V}{\sin\varphi}$
		(c) deformations	$Eh\delta = -\frac{\mu V r}{\sin\varphi}$ $Eh\gamma = \frac{V\cos\varphi}{\sin^2\varphi}$ $Eh\nabla = \frac{W \ln r/r_0}{2\pi \sin^2\varphi\cos\varphi}$ $\{ = \frac{Wx}{2\pi r}$, for $\varphi = \pi/2 \}$
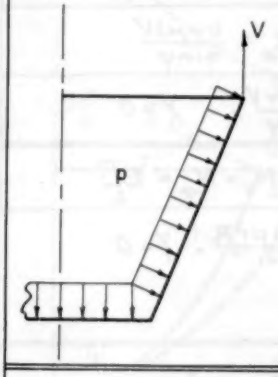	**4. Gas Pressure** p (lb/in²) $p_x = p_\theta = 0$ $p_z = -p$	(a) forces	$V = \frac{pr}{2}$, $N_x = \frac{pr}{2\sin\varphi}$, $N_\theta = \frac{pr}{\sin\varphi}$
		(b) strains	$Eh\varepsilon_x = (\frac{1}{2}-\mu)\frac{pr}{\sin\varphi}$, $Eh\varepsilon_\theta = (1-\frac{\mu}{2})\frac{pr}{\sin\varphi}$
		(c) deformations	$Eh\delta = (1-\mu/2)\,pr^2/\sin\varphi$ $Eh\gamma = -\frac{3}{2}\,pr\cot\varphi/\sin\varphi$ $Eh\nabla = p(r^2-r_0^2)\frac{\cot\varphi}{\sin\varphi}\left[-1+\frac{\mu}{2}+\frac{\frac{1}{2}-\mu/2}{\cos^2\varphi}\right]$ $\{ = (\frac{1}{2}-\mu)prx$, for $\varphi = \pi/2 \}$
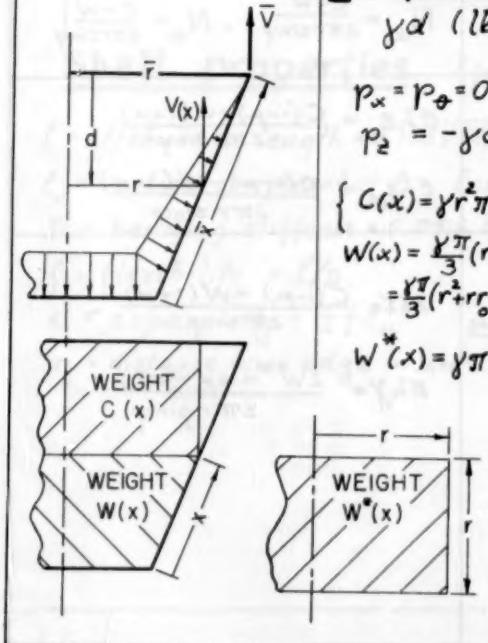	**5. Liquid Pressure** γd (lb/in²) $p_x = p_\theta = 0$ $p_z = -\gamma d$ $\{ C(x) = \gamma r^2 \pi d(x)$, $\bar{C} = 0$ $W(x) = \frac{\gamma\pi}{3}(r^3 - r_0^3)\tan\varphi$ $= \frac{\gamma\pi}{3}(r^2 + r r_0 + r_0^2)x\sin\varphi$ $W^*(x) = \gamma\pi r^3 \}$	(a) forces	$V(x) = \frac{W(x)+C(x)}{2\pi r}$ $N_x = \frac{C+W}{2\pi r\sin\varphi}$, $N_\theta = \frac{2C}{2\pi r\sin\varphi}$
		(b) strains	$Eh\varepsilon_x = \frac{(1-2\mu)C+W}{2\pi r\sin\varphi}$, $Eh\varepsilon_\theta = \frac{(2-\mu)C-\mu W}{2\pi r\sin\varphi}$ { For $\varphi = \pi/2$: $Eh\varepsilon_x = \gamma r(\frac{\bar{x}}{2} - \mu d)$, $Eh\varepsilon_\theta = \gamma r(d - \frac{\mu}{2}\bar{x})$ }
		(c) deformations	$Eh\delta = \frac{(2-\mu)C-\mu W}{2\pi\sin\varphi}$ $Eh\gamma = \frac{2W^* + (W-3C)\cot\varphi}{2\pi r\sin\varphi}$ { For $\varphi = \pi/2$: $Eh\delta = \gamma r^2(d - \frac{\mu}{2}\bar{x})$ $Eh\gamma = \gamma r^2$ $Eh\nabla = \frac{\bar{W}x}{2\pi r}(1 - 2\mu + \mu x/\bar{x})$ }

TABLE 1 MEMBRANE ANALYSIS (*Continued*)

SHELL DESCRIPTION	TYPE OF LOADING	DESIGN PARAMETERS	DESIGN FORMULAS
Spherical Shell	**6.** $p_x = p_x(\varphi)$ $p_\theta = 0$ $p_z = p_z(\varphi)$	(a) forces	$V(\varphi) = V_0 \frac{r_0}{r} - \frac{R}{\sin\varphi}\int_{\varphi_0}^{\varphi}(p_x \sin^2\varphi + p_z \sin\varphi\cos\varphi)d\varphi$ $N_x = \frac{V}{\sin\varphi}$, $N_\theta = -Rp_z - N_x$
		(c) deformations	$Eh\delta = r\varepsilon_\theta$ $Eh\gamma = (1+\mu)\chi N_x - N_\theta)\cot\varphi - \frac{d}{d\varphi}(\mu N_x - N_\theta)$ $\nabla\Big\|_{\varphi_0}^{\varphi} = R\int_{\varphi_0}^{\varphi}(\varepsilon_x \sin\varphi + \chi\cos\varphi)d\varphi$ $= -R\varepsilon_\theta \cos\varphi\Big\|_{\varphi_0}^{\varphi} + R\int_{\varphi_0}^{\varphi}\frac{\varepsilon_x - \varepsilon_\theta}{\sin\varphi}d\varphi$
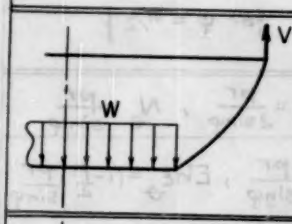	**7. Weight Loading** W (lb.) $p_x = p_\theta = p_z = 0$	(a) forces	$V = \frac{W}{2\pi r}$, $N_x = -N_\theta = \frac{V}{\sin\varphi}$
		(b) strains	$Eh\varepsilon_x = -Eh\varepsilon_\theta = \frac{(1+\mu)V}{\sin\varphi}$
		(c) deformations	$Eh\delta = \frac{-(1+\mu)rV}{\sin\varphi}$, $\gamma = 0$
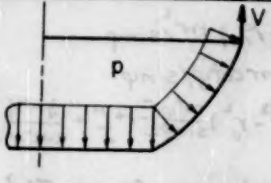	**8. Gas Pressure** p (lb/in²) $p_x = p_\theta = 0$, $p_z = -p$	(a) forces	$V = \frac{pr}{2}$, $N_x = N_\theta = \frac{pR}{2}$
		(c) deformations	$Eh\delta = \frac{(1-\mu)prR}{2}$, $\gamma = 0$
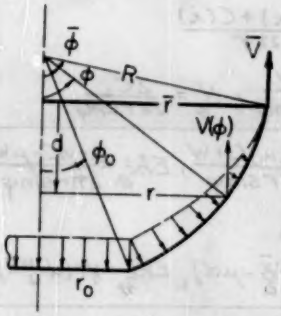 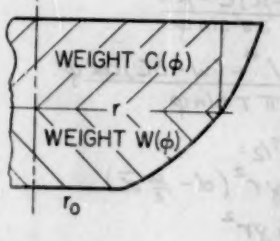 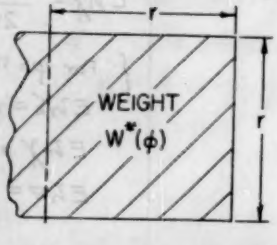	**9. Liquid Pressure** γd (lb/in²) $p_x = p_\theta = 0$ $p_z = -\gamma d = -\gamma r(\cos\varphi - \cos\bar{\varphi})$ $C(\varphi) = \gamma R^3 \pi \sin^2\cdot(\cos\varphi - \cos\bar{\varphi})$ $W(\varphi) = \frac{1}{3}\gamma R^3\pi\left[(1-\cos\varphi)^2\cdot(2+\cos\varphi) - (1-\cos\varphi_0)^2(2+\cos\varphi_0)\right]$ $W^*(\varphi) = \gamma r^3 \pi$	(a) forces	$V = \frac{C+W}{2\pi r}$ $N_x = \frac{C+W}{2\pi r\sin\varphi}$, $N_\theta = \frac{C-W}{2\pi r\sin\varphi}$
		(b) strains	$Eh\varepsilon_x = \frac{C(1-\mu)+W(1+\mu)}{2\pi r\sin\varphi}$ $Eh\varepsilon_\theta = \frac{C(1-\mu)-W(1+\mu)}{2\pi r\sin\varphi}$
		(c) deformations	$Eh\delta = \frac{C(1-\mu)-W(1+\mu)}{2\pi\sin\varphi}$ $Eh\gamma = \frac{2W^* - 4\mu W\cot\varphi}{2\pi r\sin\varphi}$

TABLE 2 EDGE LOAD-ANALYSIS

SHELL DESCRIPTION	TYPE OF LOADING	DESIGN PARAMETERS	DESIGN FORMULAS
General Shell	10. H, M	(a) deformations	$\delta/f\ell_v = -\frac{1}{2}M F_3(n) + \frac{1}{2}H\ell_v F_4(n)$ $\chi/f = M F_4(n) - \frac{1}{2}H\ell_v F_1(n)$ $\nabla = -\delta\cot\varphi$
		(b) moments & forces	$M_x = M F_1(n) - H\ell_v F_2(n)$ $H\ell_v = 2M F_2(n) + H\ell_v F_3(n)$ $M_\theta = \mu M_x$ $N_x = H\cos\varphi$ $N_\theta = Eh\delta/r$ $= \frac{2\sqrt{3(1-\mu^2)}}{h}\left[-M F_3(n) + H\ell_v F_4(n)\right]$ $\left\{2\sqrt{3(1-\mu^2)} = 3.30 \text{ for } \mu = 0.3\right\}$
		(c) stresses	$\sigma_{xo} = \frac{N_x}{h} + \frac{6M_x}{h^2}$, $\sigma_{xi} = \frac{N_x}{h} - \frac{6M_x}{h^2}$ $\sigma_{\theta o} = \frac{N_\theta}{h} + \frac{6M_\theta}{h^2}$, $\sigma_{\theta i} = \frac{N_\theta}{h} - \frac{6M_\theta}{h^2}$

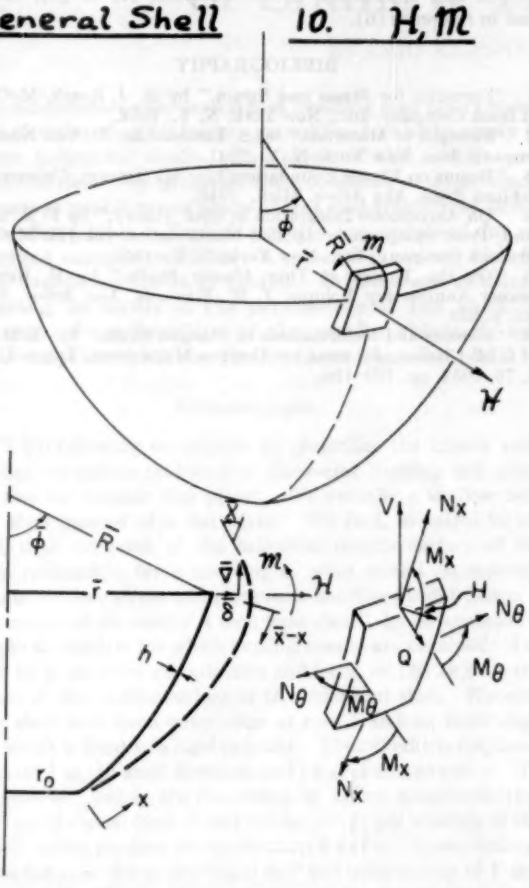

Shell properties (μ=0.3)

ℓ = attenuation length = $0.778\sqrt{\bar{r}\bar{h}/\sin\bar{\varphi}}$

ℓ_v = vertical component of ℓ = $\ell\sin\bar{\varphi}$

D = bending stiffness = $0.0916\,Eh^3$

f = flexibility = ℓ/D

ϵ = expansivity = $\frac{1}{2}f\ell_v^2$

n = distance from edge in units of ℓ = $\frac{\bar{x}-x}{\ell}$

(d) The functions $F_1 = \sqrt{2}\,e^{-n}\cos(n-\frac{\pi}{4})$, $F_2 = e^{-n}\sin n$

$F_3 = -\sqrt{2}\,e^{-n}\sin(n-\frac{\pi}{4})$, $F_4 = e^{-n}\cos n$

n	F_1	F_2	F_3	F_4
0	1	0	1	1
.25	.947	.193	.562	.755
.50	.823	.291	.241	.532
.75	.668	.322	.024	.346
1.0	.508	.310	-.111	.199
1.5	.238	.223	-.207	.016
2.0	.067	.123	-.179	-.056
2.5	-.017	.049	-.115	-.066

arbitrary (axisymmetric) shell by a conical shell tangent at the edge. The shell is then regarded as being made up of "tapered beams on elastic foundation," governed by the equation

$$\frac{r}{\bar{r}}\frac{d^2}{dx^2}\frac{r}{\bar{r}}\frac{d^2\delta}{dx^2} + 4\frac{\delta}{l^4} = 0 \quad \ldots\ldots\ldots\ldots [14]$$

Because our interest is restricted to the edge region, the further approximation is now made that in this equation the variable radius r may be replaced by its edge value $\bar{r}$.

Solution of Equation [14], thus simplified, subject to the boundary conditions

$$\bar{M}_x = \mathfrak{M}, \bar{H} = \mathfrak{C} \quad \ldots\ldots\ldots\ldots\ldots [15]$$

yields the expression of δ listed in Equation [10a]. The expressions of χ, M_x, H then follow from

$$\chi \sin\varphi = -\frac{d\delta}{dx}, \quad M_x = D\frac{d\chi}{dx}, \quad H\sin\varphi = \frac{dM_x}{dx} \quad \ldots [16]$$

A more elaborate derivation of Formulas [10] is given in Hetenyi's book (3). A more accurate treatment of arbitrary axisymmetric shells under edge loads is presented by Hildebrand (4), on the basis of E. Reissner's theory (5). A discussion of the method of determining the edge loads $\mathfrak{M}$ and $\mathfrak{C}$ in a specific shell problem, and application of the Formulas [1] to [10] can be found in reference (6).

BIBLIOGRAPHY

1 "Formulas for Stress and Strain," by R. J. Roark, McGraw-Hill Book Company, Inc., New York, N. Y., 1954.

2 "Strength of Materials," by S. Timoshenko, D. Van Nostrand Company, Inc., New York, N. Y., 1941.

3 "Beams on Elastic Foundation," by M. Hetenyi, University of Michigan Press, Ann Arbor, Mich. 1946.

4 "On Asymptotic Integration in Shell Theory," by F. B. Hildebrand, Proc. Symposia in Applied Mathematics, vol. III, McGraw-Hill Book Company, Inc., New York, N. Y., 1950.

5 "On the Theory of Thin Elastic Shells," by E. Reissner, Reissner Anniversary Volume, J. W. Edwards, Ann Arbor, Mich., 1949, p. 231

6 "Stresses and Deformations of Flanged Shells," by G. Horvay and I. M. Clausen, JOURNAL OF APPLIED MECHANICS, Trans. ASME, vol. 76, 1954, pp. 109–116.

Small Rotationally Symmetric Deformations of Shallow Helicoidal Shells[1]

By ERIC REISSNER,[2] CAMBRIDGE, MASS.

Known solutions for transverse bending and plane stress of flat circular ring plates are generalized so as to apply to shallow helicoidal shells. The pitch of the middle surface of the shell is responsible for a coupling of what would be separate problems of plane stress and transverse bending for flat plates. Explicit results are obtained for an important sample problem. A general property of helicoidal cantilever shells is stated. Criteria are obtained indicating, in terms of the parameters of the shell (*a*) the range of applicability of the results obtained, and (*b*) the range in which the shell behaves like a flat plate.

Introduction

In THE following we propose to generalize the known solutions for certain problems of transverse bending and plane stress for circular ring plates. We consider a shallow helicoidal shell instead of a flat plate. We find, as might be expected, that the pitch of the helicoidal middle surface of the shell is responsible for a coupling of what would be separate problems of plane stress and transverse bending for flat plates.

The nature of the theory is seen most clearly by its application to a sample problem for which explicit results are obtained. Let r and θ be plane polar co-ordinates and let $w_0 = (H/2\pi)\theta$ be the equation of the middle surface of the helicoidal shell. We consider a shell with fixed outer edge at $r = b$ and an inner edge $r = a$ which is fixed to a rigid cylinder. The cylinder is displaced an amount δ in the axial direction and rotated an amount ω. To be determined, within the framework of linear, small-deflection theory, are the axial force P and the torque T, per winding of the ring shell, which produce the movements δ and ω. In the limiting case of a flat plate δ is proportional to P and independent of T and ω is proportional to T and independent of P. For the helicoidal shell we find relations of the form

$$\delta = k_P P + k_{PT} T, \quad \omega = k_T T + k_{TP} P$$

and the coefficients k_P, k_{PT}, k_{TP}, and k_T, contain the influence of the pitch constant H.

As in plate theory, we find here explicit solutions in closed form for the problems of small deformations which are being considered. We know that the same is no longer possible for finite deformations, even for flat plates.[3] This is in contrast to what occurs for the problems of pure bending and twisting of circular ring plates and shallow helicoidal shells which we have considered previously.[4]

The differential equations which form the basis of the present developments are contained in the equations which Marguerre[5] has given for the analysis of finite deflections of shallow shells. We, here, write these equations in polar co-ordinate form and specialized for small deformations. We then obtain appropriate solutions for the problem of the helicoidal shell.

Basic Equations of Small-Deflection Theory, in Polar Co-Ordinates

Let $z = w_0(r, \theta)$ be the equation of the undeflected middle surface of the shell. Let w be the component of displacement in the direction of the axis of the shell measured from the undeflected middle surface. Let u and v be components of displacement in the direction of r and θ, in a plane perpendicular to the axis of the shell. Let ϵ_r, ϵ_θ, and $\gamma_{r\theta}$, be components of strain in the middle surface. Let N_r, N_θ, and $N_{r\theta}$, be stress resultants parallel to the middle surface. Let Q_r and Q_θ, be shear-stress resultants normal to the middle surface. Let M_r, M_θ, and $M_{r\theta}$, be stress couples. Let F be Airy's stress function.

We restrict attention to shells of constant thickness and to cases without body, force components in the r and θ directions. Some of the basic relations of the theory are as in the theory of flat plates, as follows

$$N_r = \frac{1}{r}\frac{\partial F}{\partial r} + \frac{1}{r^2}\frac{\partial^2 F}{\partial \theta^2}, \quad N_\theta = \frac{\partial^2 F}{\partial r^2}, \quad N_{r\theta} = -\frac{\partial}{\partial r}\left(\frac{1}{r}\frac{\partial F}{\partial \theta}\right) \qquad \ldots\ldots [1]$$

$$Q_r = -D\frac{\partial \nabla^2 w}{\partial r}, \quad Q_\theta = -D\frac{1}{r}\frac{\partial \nabla^2 w}{\partial \theta} \qquad \ldots\ldots [2]$$

$$\left.\begin{aligned} M_r &= -D\left(\frac{\partial^2 w}{\partial r^2} + \frac{\nu}{r}\frac{\partial w}{\partial r} + \frac{\nu}{r^2}\frac{\partial^2 w}{\partial \theta^2}\right) \\ M_\theta &= -D\left(\frac{1}{r}\frac{\partial w}{\partial r} + \frac{1}{r^2}\frac{\partial^2 w}{\partial \theta^2} + \nu\frac{\partial^2 w}{\partial r^2}\right) \\ M_{r\theta} &= -(1-\nu)D\frac{\partial}{\partial r}\left(\frac{1}{r}\frac{\partial w}{\partial \theta}\right), \quad D = \frac{Eh^3}{12(1-\nu^2)} \end{aligned}\right\} \ldots [3]$$

The fact that we are dealing with a shell rather than with a plate expresses itself in the form of the differential equations, in the expressions for the axial-stress resultants (as contrasted to those for the transverse-stress resultants Q), and in the expressions for the components of strain in the middle surface.

The differential equations of the theory are

---

[1] The present paper is a report on work done under the sponsorship of the Office of Naval Research under Contract N5-ori-07834 with Massachusetts Institute of Technology.

[2] Professor of Mathematics, Massachusetts Institute of Technology.

[3] "A Problem of Finite Bending of Circular Ring Plates," by E. Reissner, *Quarterly of Applied Mathematics*, vol. 10, 1952, pp. 167–173.

Contributed by the Applied Mechanics Division and presented at the Annual Meeting, New York, N. Y., November 28–December 3, 1954, of The American Society of Mechanical Engineers.

Discussion of this paper should be addressed to the Secretary, ASME, 29 West 39th Street, New York, N. Y., and will be accepted until April 11, 1955, for publication at a later date. Discussion received after the closing date will be returned.

Note: Statements and opinions advanced in papers are to be understood as individual expressions of their authors and not those of the Society. Manuscript received by ASME Applied Mechanics Division, August 24, 1953. Paper No. 54—A-13.

[4] "On Finite Bending and Twisting of Circular Ring Sector Plates and Shallow Helicoidal Shells," by E. Reissner, *Quarterly of Applied Mathematics*, vol. 11, 1953, pp. 473–483.

[5] "Zur Theorie der Gekrümmten Platte Grosser Formänderung," by K. Marguerre, Proceedings of the Fifth International Congress for Applied Mechanics, 1938, pp. 93–101.

$$D\nabla^2\nabla^2 w = p + \frac{1}{r}\frac{\partial}{\partial r}\left[rN_r\frac{\partial w_0}{\partial r}\right] + \frac{1}{r}\frac{\partial}{\partial \theta}\left[N_\theta\frac{1}{r}\frac{\partial w_0}{\partial \theta}\right] + \frac{1}{r}\frac{\partial}{\partial r}\left[N_{r\theta}\frac{\partial w_0}{\partial \theta}\right] + \frac{1}{r}\frac{\partial}{\partial \theta}\left[N_{r\theta}\frac{\partial w_0}{\partial r}\right] \quad [4]$$

$$\nabla^2\nabla^2 F = Eh\left\{2\frac{\partial}{\partial r}\left(\frac{1}{r}\frac{\partial w_0}{\partial \theta}\right)\frac{\partial}{\partial r}\left(\frac{1}{r}\frac{\partial w}{\partial \theta}\right) - \frac{\partial^2 w_0}{\partial r^2}\left(\frac{1}{r^2}\frac{\partial^2 w}{\partial \theta^2} + \frac{1}{r}\frac{\partial w}{\partial r}\right) - \left(\frac{1}{r^2}\frac{\partial^2 w_0}{\partial \theta^2} + \frac{1}{r}\frac{\partial w_0}{\partial r}\right)\frac{\partial^2 w}{\partial r^2}\right\} \quad [5]$$

Axial-stress resultants V_r and V_θ are of the form

$$V_r = Q_r + N_r\frac{\partial w_0}{\partial r} + N_{r\theta}\frac{1}{r}\frac{\partial w_0}{\partial \theta}$$

$$V_\theta = Q_\theta + N_{r\theta}\frac{\partial w_0}{\partial r} + N_\theta\frac{1}{r}\frac{\partial w_0}{\partial \theta} \quad [6]$$

and components of strain in the middle surface are

$$\epsilon_r = \frac{\partial u}{\partial r} + \frac{\partial w_0}{\partial r}\frac{\partial w}{\partial r}, \quad \epsilon_\theta = \frac{u}{r} + \frac{1}{r}\frac{\partial v}{\partial \theta} + \frac{1}{r}\frac{\partial w_0}{\partial \theta}\frac{1}{r}\frac{\partial w}{\partial \theta}$$

$$\gamma_{r\theta} = \frac{1}{r}\frac{\partial u}{\partial \theta} + r\frac{\partial}{\partial r}\left(\frac{v}{r}\right) + \frac{1}{r}\frac{\partial w_0}{\partial \theta}\frac{\partial w}{\partial r} + \frac{\partial w_0}{\partial r}\frac{1}{r}\frac{\partial w}{\partial \theta} \quad [7]$$

In the derivation of the second of the differential equations use has been made of the assumption of an isotropic medium with Hooke's law applicable, that is, of the Relations [3] and of the following relations

$$Eh\epsilon_r = N_r - \nu N_\theta, \quad Eh\epsilon_\theta = N_\theta - \nu N_r, \quad 2(1+\nu)Eh\gamma_{r\theta} = N_{r\theta} \quad [8]$$

Basic Equations for Helicoidal Shells

We take the equation of the middle surface of the helicoidal shell in the form

$$w_0 = \frac{H}{2\pi}\theta \quad [9]$$

The quantity H is the rise per winding of the middle surface of the shell. The differential Equations [4] and [5] may be reduced, after the introduction of w_0 from Equation [9] and N_r, N_θ, and $N_{r\theta}$ from Equation [1] and after some transformations, to the following symmetrical form

$$D\nabla^2\nabla^2 w = p + \frac{H}{\pi}\frac{1}{r^2}\frac{\partial}{\partial r}\left(\frac{1}{r}\frac{\partial F}{\partial \theta}\right) \quad [10]$$

$$\nabla^2\nabla^2 F = -Eh\frac{H}{\pi}\frac{1}{r^2}\frac{\partial}{\partial r}\left(\frac{1}{r}\frac{\partial w}{\partial \theta}\right) \quad [11]$$

Equations [6] for V_r and V_θ reduce to

$$V_r = Q_r + \frac{H}{2\pi}\frac{N_{r\theta}}{r}, \quad V_\theta = Q_\theta + \frac{H}{2\pi}\frac{N_\theta}{r} \quad [12]$$

and Equations [7] for ϵ_r, ϵ_θ, and $\gamma_{r\theta}$ reduce to

$$\left.\begin{aligned}\epsilon_r &= \frac{\partial u}{\partial r}\\ \epsilon_\theta &= \frac{u}{r} + \frac{1}{r}\frac{\partial v}{\partial \theta} + \frac{H}{2\pi}\frac{1}{r^2}\frac{\partial w}{\partial \theta}\\ \gamma_{r\theta} &= \frac{1}{r}\frac{\partial u}{\partial \theta} + r\frac{\partial}{\partial r}\left(\frac{v}{r}\right) + \frac{H}{2\pi}\frac{1}{r}\frac{\partial w}{\partial r}\end{aligned}\right\} \quad [13]$$

Solutions for Rotationally Symmetric Stress Distributions

It is clear that rotationally symmetric stress distributions are obtained if both w and F are assumed to be independent of θ. While solutions of this type are of primary importance for the limiting case of a flat plate, this is found to be no longer so, for the problem of the helicoidal shell. We have previously utilized a special solution of the form[4] $F = F(r)$, $w = k\theta$. We shall see in what follows that a large class of problems can be solved by assuming

$$w = w(r), \quad F = k\theta \quad [14]$$

In a mathematical sense, the solutions of the form, Equations [14], then constitute a specific complement to the solutions discussed in the previous paper.[4] In a physical sense, the Solutions [14] are suggested by the fact that in generalized plane stress the expression $F = k\theta$ is known to apply to the problem of the inner edge of the plate being twisted with respect to the outer edge, and that this specific type of action generally must be considered in rotationally symmetric transverse bending of helicoidal shells.

We note that for $F = k\theta$, we have $N_{r\theta} = k/r^2$ and accordingly the constant k is related to the applied torque T in the form

$$k = T/2\pi \quad [14a]$$

Introduction of Equations [14] into the differential Equations [10] and [11] leaves the following relation to be satisfied

$$D\nabla^2\nabla^2 w(r) = p(r) - \frac{HT}{2\pi^2}\frac{1}{r^4} \quad [15]$$

The solution of Equation [15] may be taken in the form

$$w = \frac{P}{8\pi D}r^2\ln r + \frac{1}{D}[A + Br^2 + C\ln r] - \frac{HT}{2\pi^2}\frac{(\ln r)^2}{8D} + w_p \quad [16]$$

where w_p is a particular solution of $D\nabla^2\nabla^2 w = p$. The first term in Equation [16] will be shown to account for a force P in the axial direction, in the same manner as for a flat plate. The quantities A, B, and C are constants of integration. From Equations [16] and [14] follows for stress resultants and couples

$$N_r = N_\theta = 0, \quad N_{r\theta} = T/2\pi r^2 \quad [17]$$

$$\left.\begin{aligned}Q_r &= -\frac{P}{2\pi r} - \frac{HT}{2\pi^2}\frac{1}{2r^2} + Q_{rp}, \quad Q_\theta = 0\\ V_r &= -\frac{P}{2\pi r} + V_{rp}, \quad V_\theta = 0\end{aligned}\right\} \quad [18]$$

$$M_r = -\frac{P}{8\pi}[(3+\nu) + 2(1+\nu)\ln r] - 2(1+\nu)B + C\frac{(1-\nu)}{r^2} - \frac{HT}{8\pi^2}\left[(1-\nu)\frac{\ln r}{r^2} - \frac{1}{r^2}\right] + M_{rp} \quad [19]$$

$$M_\theta = -\frac{P}{8\pi}[(1+3\nu) + 2(1+\nu)\ln r] - 2(1+\nu)B - C\frac{1-\nu}{r^2} + \frac{HT}{8\pi^2}\left[(1-\nu)\frac{\ln r}{r^2} + \frac{\nu}{r^2}\right] + M_{\theta p} \quad [20]$$

$$M_{r\theta} = 0 \quad [21]$$

In addition to the displacement component w, expressions are needed for the components of displacement u and v. Because of symmetry we have $u = u(r)$ and $v = v(r)$. From $N_r = N_\theta = 0$ follows that $\epsilon_r = \epsilon_\theta = 0$ and therewith, since also $\partial w/\partial\theta = 0$, that

$$u = 0 \quad \text{[22]}$$

From

$$\gamma_{r\theta} = r\frac{d}{dr}\left(\frac{v}{r}\right) + \frac{H}{2\pi}\frac{1}{r}\frac{dw}{dr} = \frac{N_{r\theta}}{Gh} = \frac{T}{2\pi r^2}\frac{1}{Gh}$$

follows as one of the basic relations of this theory

$$\frac{v}{r} = -\frac{T}{4\pi r^2}\frac{1}{Gh} - \frac{H}{2\pi}\int \frac{dw}{dr}\frac{dr}{r^2} \quad \text{[23]}$$

Equations [16] to [23] may be used to solve a variety of specific problems for the shallow helicoidal shell. One general comment suggests itself. As soon as we have for one edge of the ring shell the condition of vanishing $N_{r\theta}$, as, for instance, for cantilever shells, we further have vanishing torque T and therewith disappearance of the pitch constant H in all expressions referring to transverse bending of the ring shell. Accordingly, to the extent that the theory of shallow shells is applicable, we have the result that the helicoidal cantilever shell has the same transverse deflection and the same stress distribution as a flat cantilever plate under the same rotationally symmetric transverse-load condition. The only difference in this case between ring shell and ring plate consists in the fact that, for the ring shell, transverse bending is associated with circumferential displacements v of magnitude

$$v = -(Hr/2\pi)\int (dw/dr)(dr/r^2)$$

Helicoidal Ring Shell With Fixed Outer Edge, Attached Along Its Inner Edge to Movable Rigid Cylinder

Let $r = b$ be the outer edge of the shell and $r = a$ the inner edge. Boundary conditions are

$$\left.\begin{aligned} w(a) &= \delta, & w(b) &= 0 \\ w'(a) &= 0, & w'(b) &= 0 \\ v(a) &= a\omega, & v(b) &= 0 \end{aligned}\right\} \quad \text{[24]}$$

In order to satisfy the six Conditions [24] there are six constants of integration, P, T, A, B, C, and one constant of integration in Equation [23] for v. We have, with $w_p = 0$, upon introducing w from Equation [16] into the first, third, and fourth of Equations [24]

$$\left.\begin{aligned} &\frac{P}{8\pi}(a^2\ln a - b^2\ln b) - B(b^2 - a^2) \\ &- C\ln\frac{b}{a} - \frac{HT}{16\pi^2}[(\ln a)^2 - (\ln b)^2] = D\delta \\ &\frac{P}{8\pi}(2a\ln a + a) + 2Ba + \frac{C}{a} - \frac{HT}{8\pi^2}\frac{\ln a}{a} = 0 \\ &\frac{P}{8\pi}(2b\ln b + b) + 2Bb + \frac{C}{b} - \frac{HT}{8\pi^2}\frac{\ln b}{b} = 0 \end{aligned}\right\} \quad \text{[25]}$$

The fifth and sixth of Equations [24] are combined into one condition by writing, on the basis of Equation [23]

$$\frac{v(b)}{b} - \frac{v(a)}{a} = -\frac{T}{4\pi Gh}\left(\frac{1}{b^2} - \frac{1}{a^2}\right) - \frac{H}{2\pi}\int_a^b \frac{dw}{dr}\frac{dr}{r^2} = -\omega$$

With

$$\int \frac{dw}{dr}\frac{dr}{r^2} = \frac{P}{8\pi D}[(\ln r)^2 + \ln r] + \frac{1}{D}\left[2B\ln r - \frac{C}{2r^2}\right] + \frac{HT}{16\pi^2 D}\left[\frac{\ln r}{r^2} + \frac{1}{2r^2}\right] + \text{const}$$

there follows further

$$\frac{T}{4\pi}\left(\frac{1}{b^2} - \frac{1}{a^2}\right) + \frac{Gh}{D}\frac{H}{2\pi}\left\{\frac{P}{8\pi}\left[(\ln b)^2 - (\ln a)^2 + \ln\frac{b}{a}\right] + 2B\ln\frac{b}{a} - \frac{C}{2}\left(\frac{1}{b^2} - \frac{1}{a^2}\right) + \frac{HT}{16\pi^2}\left[\frac{\ln b}{b^2} - \frac{\ln a}{a^2} + \frac{1}{2}\left(\frac{1}{b^2} - \frac{1}{a^2}\right)\right]\right\} = Gh\omega \quad \text{[26]}$$

It remains to determine the four constants P, T, B, and C from the four Equations [25] and [26]. The last two of Equations [25] are used to express B and C in terms of P and T. The remaining two equations are then, upon elimination of B and C, one of the main results to be obtained, namely, equations expressing force P and torque T in terms of axial and angular displacements δ and ω.

We first obtain for B and C

$$2(b^2 - a^2)B = -\frac{P}{4\pi}\left[b^2\ln b - a^2\ln a + \frac{b^2}{2} - \frac{a^2}{2}\right] + \frac{HT}{8\pi^2}\ln\frac{b}{a}$$

$$\left(\frac{1}{b^2} - \frac{1}{a^2}\right)C = -\frac{P}{4\pi}\ln\frac{b}{a} + \frac{HT}{8\pi^2}\left[\frac{\ln b}{b^2} - \frac{\ln a}{a^2}\right]$$

With this, there are obtained, after some transformations, the following two relations for P, T, δ, and ω

$$\delta = \frac{P}{8\pi D}\left[\frac{b^2 - a^2}{2} - \frac{2a^2b^2}{b^2 - a^2}\left(\ln\frac{b}{a}\right)^2\right] - \frac{HT}{16\pi^2 D}\left[1 - \frac{b^2 + a^2}{b^2 - a^2}\ln\frac{b}{a}\right]\ln\frac{b}{a} \quad \text{[27]}$$

$$\omega = \frac{T}{4\pi}\left[\frac{1}{Gh}\left(\frac{1}{b^2} - \frac{1}{a^2}\right) + \frac{H^2}{4\pi^2 D}\left(\frac{(\ln b/a)^2}{b^2 - a^2} + \frac{1}{4b^2} - \frac{1}{4a^2}\right)\right] + \frac{PH}{16\pi^2 D}\left[1 - \frac{b^2 + a^2}{b^2 - a^2}\ln\frac{b}{a}\right]\ln\frac{b}{a} \quad \text{[28]}$$

For purposes of quantitative discussion it is convenient to write Equations [27] and [28] in the following alternate form

$$\delta = \frac{P(b^2 - a^2)}{16\pi D}f + \frac{TH}{16\pi^2 D}F \quad \text{[27a]}$$

$$\omega = \frac{T(a^2 - b^2)}{4\pi Gha^2b^2}\left[1 + \frac{3(1-\nu)}{8\pi^2}\left(\frac{H}{h}\right)^2 f\right] - \frac{PH}{16\pi^2 D}F \quad \text{[28a]}$$

where

$$\left.\begin{aligned} f &= 1 - \left(\frac{2ab}{b^2 - a^2}\ln\frac{b}{a}\right)^2 \\ F &= \left(\frac{b^2 + a^2}{b^2 - a^2}\ln\frac{b}{a} - 1\right)\ln\frac{b}{a} \end{aligned}\right\} \quad \text{[29]}$$

In order to obtain an idea of the order of magnitude of the influence of pitch of the shell on its stiffness, we consider in particular its axial load-deflection characteristics in the absence of rotation, and its torque-rotation characteristics in the absence of axial deflection. From Equations [27a] and [28a] follow

$$\delta_{\omega=0} = \frac{P(b^2 - a^2)f}{16\pi D}\left[1 - \frac{\lambda g}{1 + \lambda f}\right] \quad \text{[30]}$$

$$\omega_{\delta=0} = \frac{T(a^2 - b^2)}{4\pi Gha^2b^2}\left[1 + \lambda(f - g)\right] \quad \text{[31]}$$

where

$$g = \left(\frac{2ab}{b^2 - a^2}\right)^2 \frac{F^2}{f}, \quad \lambda = \frac{3(1-\nu)}{8\pi^2}\left(\frac{H}{h}\right)^2 \quad \ldots\ldots [32]$$

We shall see that we have for all values of b/a, that $0 < g < f$. Consequently, $\delta_{\omega=0}/P$ is positive and decreases with λ, indicating that the effect of pitch makes the shell stiffer axially than the corresponding flat plate. On the other hand, the effect of pitch makes the shell less stiff circumferentially than the corresponding flat plate. These conclusions are in agreement with what one would expect on the basis of qualitative considerations of the problem.

Further discussion may be carried out with the help of the following parameters

$$R = \frac{1}{2}(b + a), \quad c = \frac{1}{2}(b - a), \quad x = \frac{c}{R} \quad \ldots\ldots [33]$$

As b/a varies from 1 to ∞, the parameter x varies from 0 to 1. We have

$$\left.\begin{aligned}
f &= 1 - \left(\frac{1-x^2}{2x}\ln\frac{1+x}{1-x}\right)^2 \\
&= \frac{4}{3}x^2\left(1 - \frac{2}{15}x^2 + \ldots\right) && f(1) = 1 \\
F &= \left(\frac{1+x^2}{2x}\ln\frac{1+x}{1-x} - 1\right)\ln\frac{1+x}{1-x} \\
&= \frac{8}{3}x^2\left(1 + \frac{11}{15}x^2 + \ldots\right) && F(1) = \infty \\
g &= \left(\frac{1-x^2}{2x}\right)^2\frac{F^2}{f} \\
&= \frac{4}{3}x^2\left(1 - \frac{2}{5}x^2 + \ldots\right) && g(1) = 0 \\
f - g &= \frac{16}{45}x^4 + \ldots && f(1) - g(1) = 1
\end{aligned}\right\} \quad \ldots [34]$$

Numerical values of the functions f, F, g, and $f - g$, may be found in Table 1.[6]

Among qualitative observations, the following are of interest: In the expression for $\delta_{\omega=0}$ the effect of pitch vanishes both for very small values of c/R and for values of c/R near unity, being largest when c/R is about 0.8. For relatively small values of c/R, we have a larger influence of pitch on $\omega_{P=0}$ than on $\omega_{\delta=0}$. For values of c/R very near unity the value of $\omega_{\delta=0}$ approaches $\omega_{P=0}$.

The possible numerical magnitude of these effects, within the range of applicability of the theory of shallow shells, may be seen by considering the largest value of the slope of the shell. We have from $w_0 = (H/2\pi)\theta$ that $(\partial w_0/\tau\partial\theta)_{r=a}$, which will be designated by m, is the largest value of the slope. The expression for m is

$$m = \frac{1}{2\pi}\frac{H}{a} = \frac{1}{2\pi}\frac{H}{R}\frac{1}{1-x} \quad \ldots\ldots [35]$$

It seems reasonable, and is possibly conservative, to restrict m to values of not more than 1/8. We then have

$$\frac{1}{2\pi}\frac{H}{R}\frac{1}{1-x} \le \frac{1}{8}, \quad \frac{H}{R} \le \frac{\pi}{4}(1-x)$$

and

$$\lambda = \frac{3(1-\nu)}{8\pi^2}\left(\frac{H}{h}\right)^2 \le \frac{3(1-\nu)}{128}\left(\frac{R}{h}\right)^2(1-x)^2 \quad \ldots [36]$$

as a limiting relation for the applicability of the theory. As R/h may be quite large compared with unity, it follows that λ may be large enough for the effect of pitch to be quite substantial.

We also have a criterion as to when the effect of pitch is negligible. Sufficient for this to be so is the order-of-magnitude relation

$$\lambda = \frac{3(1-\nu)}{8\pi^2}\left(\frac{H}{h}\right)^2 \ll 1$$

TABLE 1 NUMERICAL VALUES OF FUNCTIONS OCCURRING IN LOAD-DEFLECTION CHARACTERISTICS, EQUATIONS [27a], [28a], [30], AND [31]

x	f	F	g	$f - g$
0	0	0	0	0
0.1	0.013	0.0027	0.013	0.000035
0.2	0.053	0.022	0.052	0.00057
0.3	0.117	0.072	0.115	0.0033
0.4	0.208	0.195	0.198	0.0102
0.5	0.321	0.406	0.295	0.0265
0.6	0.453	0.790	0.393	0.060
0.7	0.601	1.48	0.476	0.124
0.75	0.676	1.99	0.500	0.176
0.8	0.756	2.69	0.507	0.248
0.85	0.831	3.86	0.480	0.351
0.9	0.903	5.70	0.411	0.492
0.95	0.963	9.73	0.274	0.689
1.0	1	∞	0	1

Numerical Example

We choose

$$H/h = 10, \quad b/a = 3, \quad \nu = 1/3$$

and obtain

$$x = 1/2, \quad \lambda = (1/4\pi^2)10^2 = 2.53$$

$$\lambda f = 0.81, \quad \lambda(f - g) = 0.07$$

$$\frac{\lambda g}{1 + \lambda f} = 0.41$$

Accordingly, the effect of pitch modifies the formulas of plate theory by 81 per cent for $\omega_{P=0}$, by 7 per cent for $\omega_{\delta=0}$, and by 41 per cent for $\delta_{\omega=0}$.

[6] It may be noted that f is the function f_3 of reference [4] and $f - g$ is f_1 of reference.[4]

Two-Dimensional Flow About Half Bodies Between Parallel Walls[1]

By JOHN P. BRESLIN,[2] NEW YORK, N. Y.

Two new families of blunt half bodies are derived from the combination of source distributions and a uniform stream. One is obtained from a source lamina placed normal to an infinitely broad free stream, the other family is obtained by using the same source distribution between parallel walls. Formulas for the half-body profiles and the velocity and pressure distributions are given. Results of a calculation for selected values of the parameters are presented in graphical form and applications of the formulas are made to give the pressure distributions on the profile and the walls. The influence of the walls on the pressure distribution and body shape is studied. An approximate relationship (obtained by neglecting the small change in body shape for large wall distances) is derived for the half-body size which may be placed between given walls with a prescribed error in the pressure at one point of the profile. It is concluded that the influence of walls should be considered carefully in the design or use of two-dimensional facilities for study of flows which are of the half-body type.

Introduction

THE literature of hydrodynamics is replete with the derivation and application of the flows of an ideal fluid obtained by various combinations of source and sink distributions along an axis parallel to a uniform flow coming from infinity. Such mathematical flows have been useful in approximating the two-dimensional flow about faired sections and the three-dimensional flow about bodies of revolution. However, these shapes all have fairly sharp forebodies because as noted by Munk (1)[3] it does not seem possible to produce really blunt-nosed bodies by any distribution of sources and sinks on the axis of symmetry. To determine the flow characteristics of blunt-nosed forms, Alexander Weinstein (2) extended the method of sources and sinks by considering distributions of sources on circumferences, rings, and disks arranged in a plane perpendicular to the uniform stream issuing from infinity. Research on the phenomena of cavitation has given impetus to the study of flows about forms of varying fullness of forebody and, consequently, studies have been made of ring and disk distributions by Van Tuyl (3) and Sadowsky and Sternberg (4) which supplement the original work of Weinstein.

All of the afore-mentioned papers treat only the axially symmetric, three-dimensional flows of sources arranged in a plane perpendicular to the main stream. This paper is concerned with the derivation of the two-dimensional counterpart of the disk, that is, the flow about a unit length of an infinite source lamina or sheet taken perpendicular both to the plane of flow and to the direction of the free stream. The flow jointly produced by this source configuration and an infinitely broad free stream will be considered. The flow obtained by the introduction of walls is next derived by the method of images. The effects of channel breadth upon the velocity field and upon some of the dimensions of the blunt half bodies obtained with the orthogonal-line-source distribution are determined.

Flow Produced by a Source Lamina Perpendicular to a Uniform Stream of Infinite Breadth

The complex potential $W(Z)$ of a two-dimensional point source at ($X = 0$, $Y = 0$) in a uniform stream of velocity-U parallel to the X-axis is

$$W = -m \ln Z + UZ \quad \ldots\ldots\ldots\ldots\ldots\ldots [1]$$

where m is the strength of the source and is defined so that the volume rate of flow from the source is $2\pi m$, and ln denotes the natural logarithm.

The complex potential for the infinite source lamina, perpendicular to the XY-plane and the direction of the flow in terms of

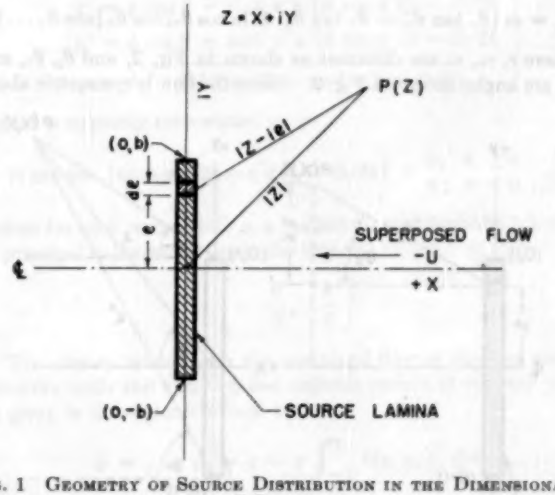

Fig. 1 Geometry of Source Distribution in the Dimensional Z-Plane

the dimensions shown in Fig. 1 is then, by the principle of superposition

$$W_0 = -\int_{-b}^{b} A(e)\ln(Z - ie)de + UZ \quad \ldots\ldots [2]$$

where W_0 is the complex potential, $A(e)$ is the source density, that is, the ratio of strength of an element of the source line to the length of the element, e is the running variable, and $P(Z)$ is any regular point. Switching to dimensionless co-ordinates, the following definitions are adopted: $bx = X$; $by = Y$; $bt = e$;

---

[1] Originally submitted in more detailed form as a thesis for MA in Mathematics, University of Maryland, 1951.

[2] Hydrodynamicist, Gibbs & Cox, Inc.

[3] Numbers in parentheses refer to the Bibliography at the end of the paper.

Contributed by the Applied Mechanics Division and presented at the Annual Meeting, New York, N. Y., November 28–December 3, 1954, of The American Society of Mechanical Engineers.

Discussion of this paper should be addressed to the Secretary, ASME, 29 West 39th Street, New York, N. Y., and will be accepted until April 11, 1955, for publication at a later date. Discussion received after the closing date will be returned.

Note: Statements and opinions advanced in papers are to be understood as individual expressions of their authors and not those of the Society. Manuscript received by ASME Applied Mechanics Division, November 18, 1953. Paper No. 54—A-3.

$bz = Z$; $Ua = A(e)$; and $Ubw_0 = W_0$. Equation [2] may then be written

$$w_0(z) = -\int_{-1}^{1} a(t)\ln(z - it)dt + z \quad [3]$$

This study will now be restricted to the case of constant source strength per unit length so that $a(t) = a = M/bU$ and the total volume rate of flow from the source sheet, $4\pi M$, is for a unit thickness in the direction perpendicular to the XY-plane. The integral of Equation [3] may now be easily obtained. Denoting the complex potential of the source lamina alone by $w_s(z)$ it follows that

$$w_s = \phi_s + i\psi_s = a\{2 - iz\ln[z - i/z + i] - \ln(z^2 + 1)\} \quad [4]$$

The function $w_s(Z)$ is not single valued because of the many-valued character of the argument of the complex logarithm.

The Velocity Potential and Stream Function. The velocity potential and the stream function are obtained by a separation of Equation [4] into real and imaginary parts. Thus the velocity potential is

$$\phi_s = -a\int_{-1}^{1} \ln \rho(x, y, t)dt \quad [5]$$

where

$$\rho = \sqrt{x^2 + (y - t)^2} \quad [6]$$

or

$$\phi_s = a\{r\sin\theta\ln(r_-/r_+) - \ln(r_+)(r_-) + r(\theta_- - \theta_+)\cos\theta\} + 2a \quad [7]$$

and the stream function is

$$\psi_s = -a\int_{-1}^{1} \theta_s(x, y, t)dt \quad [8]$$

or

$$\psi_s = ar\{\theta_-\tan\theta_- - \theta_+\tan\theta_+ + \ln\cos\theta_-/\cos\theta_+\}\cos\theta \quad [9]$$

where r, r_+, r_- are distances as shown in Fig. 2, and θ_s, θ_+, and θ_- are angles shown in Fig. 2. Since the flow is symmetric about

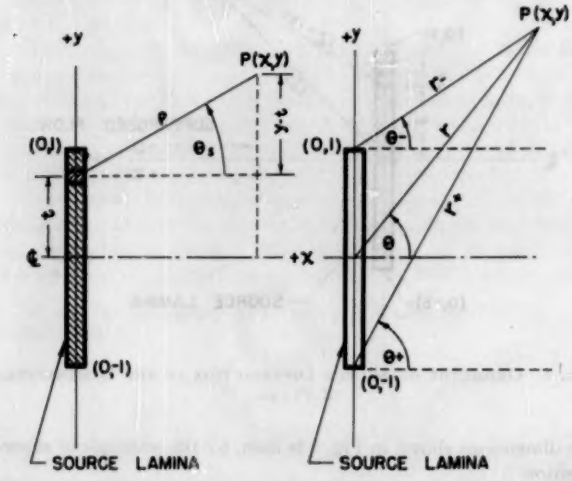

FIG. 2 DEFINITION OF NONDIMENSIONAL POLAR CO-ORDINATES

the x-axis it is sufficient and advantageous to restrict the discussion of the foregoing equations to the upper half plane ($y \geq 0$). The angles, θ, θ_+, and θ_- are made single valued; the angle θ varies between 0 and π; the other angles are contained in the intervals $-\pi/2 \leq \theta_- \leq 3\pi/2$ and $0 \leq \theta_+ \leq \pi$ as the point $P(x, y)$ moves through the upper half plane.

Equation of the Family of Half Bodies. The line $\psi = \psi_s + y = 0$ is the dividing streamline which separates the streaming flow from the source flow. The equation of the half body is derived by using Equation [9] for ψ_s. In terms of rectangular coordinates it is given by

$$y + a\left[x\ln\sqrt{x^2 + (y + 1)^2/x^2 + (y - 1)^2} + (y - 1)\tan^{-1}\left(\frac{y - 1}{x}\right) - (y + 1)\tan^{-1}\frac{y + 1}{x}\right] = 0 \quad [10]$$

The half-breadth of the body y_0 at $x = 0$ is of considerable interest; from Equation [10] it is found to be $y_0 = \pi a$ or in dimensional quantities, $Y_0 = 4\pi M/U$ which is independent of b for a fixed total volume rate of flow $Q = 4\pi M$. This is directly analogous to the result found by Weinstein (2) for the axially symmetric flow due to a source disk in a uniform stream. The asymptotic value of the half-breadth y_∞ approached as $x \to -\infty$ is found from Equation [10] to be $y = 2\pi a = 2y_0$. This same relationship of y_0 and y_∞ is found for two-dimensional half bodies formed from a "point" source in a uniform flow. Consideration of continuity, of course, would give these results directly. Other values of y for $-\infty < x < \xi_0$ (where ξ_0 is the stagnation point or nose position) can be obtained only by numerical methods since Equation [10] involves y implicitly. An approximation for large negative x may be obtained by expanding the functions in Equation [10] and retaining only the first terms. Thus

$$y \approx 2\pi a(1 - 2a/x)^{-1} \quad [11]$$

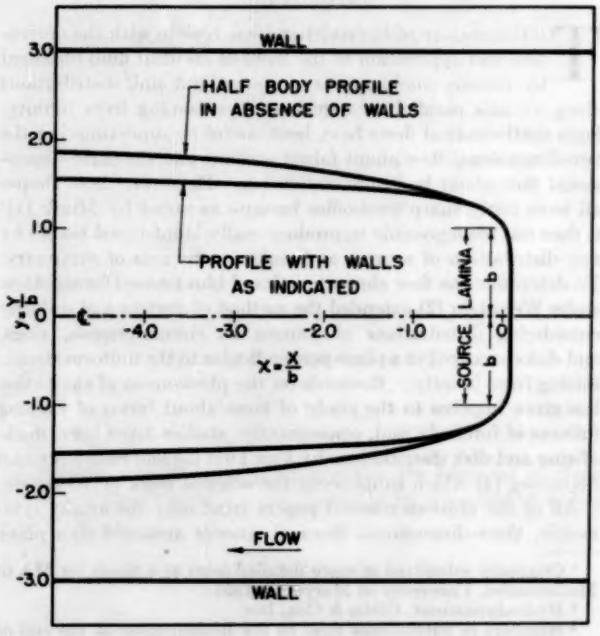

FIG. 3 HALF BODIES GENERATED BY SOURCE LAMINA AND SUPERPOSED FLOW IN INFINITE AND RESTRICTED CHANNELS

Numerical methods were used to produce the half-body shape shown in Fig. 3 for the flow $a = 1/3$, $(3M = bU)$.

Velocity Components and Stagnation Point. The components of velocity parallel to the x and y-axis are given in dimensionless form by

$$u = a(\theta_+ - \theta_-) - 1 \quad [12]$$

$$v = a \ln(r_+/r_-) \quad [13]$$

The stagnation or foremost point on the profile is obtained by setting $u = 0$; v and y being zero from symmetry, there is obtained

$$x = \xi_0 = \cot\left(\frac{1}{2a}\right) \quad [14]$$

The limiting shape having a perfectly flat nose, $\xi_0 = 0$, is obtained for a value of $a = 1/\pi$ or $M = bU$. However, this body is of no practical use since at $x = 0$, $r = 1$, $r_- = 0$, and $v = \infty$. For the flow $a = 1/3$, ξ_0 is found to be 0.0709 which as is seen in Fig. 3 produces a very blunt body. The distance x at which the velocity along $y = 0$ is 99 per cent of the free-stream velocity is $200a$.

Flow Produced by a Linear Array of Discrete Source Lamina Orthogonal to a Uniform Stream

We shall now consider a family of half bodies which are blunter than those derived from the source lamina perpendicular to the flow. This second new family is obtained by placing the same source distribution between walls.

The Complex Potential. The two-dimensional flow about a blunt half body in a stream of finite breadth, i.e., between parallel walls, may be obtained in a direct fashion by the method of images. By distributing source lamina at $Z = \pm i\,2\,nH$ (n integer; $0 \leq n \leq \infty$), as indicated in Fig. 4, one obtains the flow

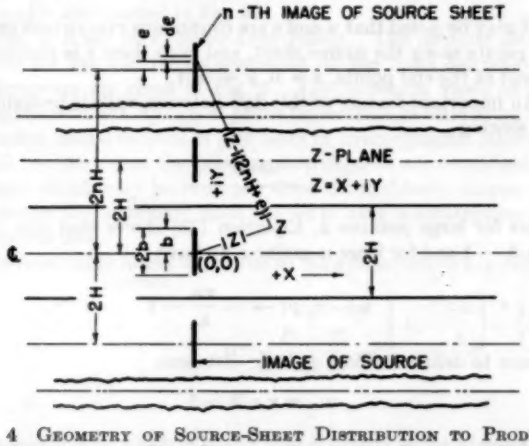

Fig. 4 Geometry of Source-Sheet Distribution to Produce Flow About a Half Body in Channel of Breadth $2H$

about the lamina arranged normal to the stream at $Z = 0$ in a channel of width $2H$. The complex potential for this source flow is found in terms of dimensionless quantities to be

$$w_s = -a \int_{t=-1}^{1} \ln\left\{\sinh\left[\frac{\pi}{2h}(z - it)\right]\right\} dt \quad [15]$$

where H is replaced by bh and all other lengths are defined as before. It can be shown that w_s is analytic and that the conditions of zero normal velocity at the walls is met by Equation [15].

It should be noted at this juncture that the potential function given by Equation [15] is a logical extension of the complex potential function for the two-dimensional point-source flow between parallel walls. This function as given in the standard references (cf. 5) is

$$W' = a' \ln[\sinh(\pi Z/2H)] \quad [16]$$

which is observed to be a special case of the integrated solution for the line source between walls given as Equation [15].

Velocity Potential and Stream Function. The velocity potential and the stream function for the "line" source flows alone are obtained from Equation [15] by separation of real and imaginary parts. The velocity potential is

$$\phi_s = -a \int_{-1}^{1} \ln \rho(x, y, h, t)dt \quad [17]$$

and the stream function is

$$\psi_s = -a \int_{-1}^{1} \theta(x, y, h, t)dt \quad [18]$$

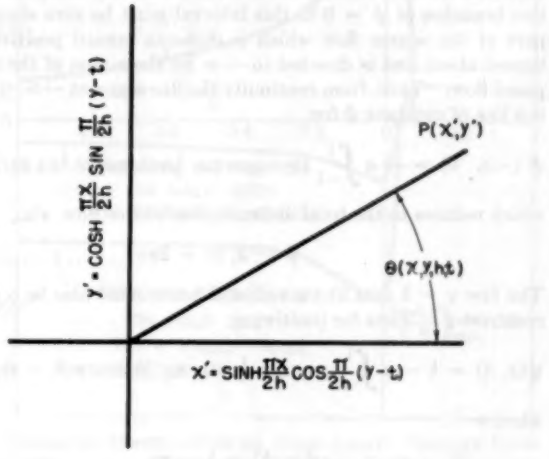

Fig. 5 Angle $\theta(x, y, h, t)$ in $x'y'$-Plane

where ρ and θ are, respectively, the modulus and the argument of the integrand of Equation [15]. In some $x'y'$-plane as shown in Fig. 5, ρ and θ may be represented by

$$\left.\begin{aligned} x' &= \rho\cos\theta = \sinh \pi\, x/2h \cos \pi\,(y - t)/2h \\ y' &= \rho\sin\theta = \cosh \pi\, x/2h \sin \pi\,(y - t)/2h \\ \rho &= \sqrt{\cosh^2 \pi\, x/2h - \cos^2 \pi(y - t)/2h} \end{aligned}\right\} \quad [19]$$

and θ is correctly represented by

$$\theta = \arctan\{\coth \pi x/2h \tan \pi(y - t)/2h\} + \begin{matrix} 0; & x \geq 0 \\ \pi; & x < 0 \end{matrix} \quad [20],\ [20a]$$

where for each regular pair x, y the arc-tangent function takes on a principal value which lies in the interval

$$\left[-\frac{\pi}{2}, \frac{\pi}{2}\right]$$

The stream function for the combined flow of the line source between walls and a superposed uniform stream of velocity $-U$ is given in dimensionless form by

$$\psi = y + \psi_s = y - a \int_{-1}^{1} \theta(x, y, h, t)dt \quad [21]$$

We are interested in some of the lines and curves along which ψ is constant. Thus for the line segment $x > 0$, $y = 0$ there results

$$\psi\,(x, 0) = a \int_{-1}^{1} \arctan\{\coth \pi x/2h \tan \pi t/2h\}\, dt \quad [22]$$

which reduces to

$$\psi\,(x, 0) = 0 \quad [23]$$

since the integrand is an odd function in the interval of integration. The line $x > 0$, $y = 0$ is a streamline which must divide

into two branches at some point, $x = \xi_0$ (to be calculated later). One branch of $\psi = 0$ is the line segment $0 < x \leq \xi_0$, $y = 0$ and the other branch forms a section of the half-body shape. Hence for the interval $0 < x \leq \xi_0$, ψ is zero for $y = 0$ and for such values of y which are solutions of

$$y = a \int_{-1}^{1} \theta\,(x, y, h, t)dt \quad \ldots\ldots [24]$$

That solutions of this integral equation must exist for $0 < x < \xi_0$ follows from the fact that the net flux across any line joining the two branches of $\psi = 0$ in this interval must be zero since that part of the source flow which is directed toward positive x is turned about and is directed to $-\infty$ by the action of the superposed flow. Thus, from continuity the line segment $-\infty \leq x < 0$ is a line of constant ψ for

$$\psi\,(-x,\ 0) = -a \int_{-1}^{1} [\pi + \arctan \{\coth \pi x/2h \tan \pi t/2h\}]dt$$

which reduces to the total dimensionless source flow, viz.,

$$\psi\,(-x, 0) = 2\pi a \quad \ldots\ldots [25]$$

The line $y = h$ acts like a wall and hence must also be a line of constant ψ. Thus for positive x

$$\psi(x, h) = h - a \int_{-1}^{1} \arctan \{\coth \pi x/2h \tan \pi(h - t)/2h\}dt$$

whence

$$\psi(x, h) = h - \pi a \quad \ldots\ldots [26]$$

and for negative x

$$\psi(-x, h) = h - a \int_{-1}^{1} [\pi + \arctan \{\coth(-\pi x/2h) \tan \pi\,(h - t)/2h\}]dt$$

whence

$$\psi(-x, h) = h - \pi a \quad \ldots\ldots [27]$$

The agreement of [26] and [27] checks with the principle of continuity for an incompressible flow since the flux across any line between $\psi(x, y) = 0$ and the wall, $\psi(x, h)$ must be the same for all x.

Equation of the Family of Half Bodies. The equation of a family of half bodies follows from Equation [21] for $\psi(x, y) = 0$ and may be expressed as

$$y = a \int_{-1}^{1} \theta\,(x, y, h, t)dt = a \int_{-1}^{1} \arctan \{\coth \pi\,x/2h \tan \pi(y - t)/2h\}dt \quad \ldots\ldots [28]$$

Since this integral equation has in general no algebraic solution, only a few special values of the half-breadth of the body may be calculated without recourse to numerical methods. Denoting the half-breadth at $x = 0$ by y_0, this value is quickly obtained since $\theta(0, y, h, t) = \pi/2$. Thus

$$y_0 = \pi a \text{ or } Y_0 = \pi\,M/U \quad \ldots\ldots [29]$$

which is exactly the same as for the half body in the absence of walls as shown previously, as it must be by reason of continuity. The asymptotic value y_∞ which is approached as $x \to -\infty$ also is readily derived because for sufficiently large $|x|$, $|\coth \pi x/2h| \to 1.0$ and the integral of Equation [28] is easily obtained. Thus

$$y_\infty = 2\pi a(1 + \pi a/h)^{-1} \quad \ldots\ldots [30]$$

which differs from the result obtained for the flow without walls but is seen to reduce to that value ($y_\infty = 2\pi a$) as $h \to \infty$.

Velocity Components and Stagnation Point. The dimensionless x and y-components of the velocity of the combined source and superposed flow are

$$u = -\frac{\partial \psi}{\partial y} = a \int_{-1}^{1} \frac{\partial \theta}{\partial y}\,(x, y, h, t)dt - 1$$

and

$$v = \frac{\partial \psi}{\partial x} = -\frac{\partial \phi}{\partial y} = a \int_{-1}^{1} \frac{\partial}{\partial y} \ln \rho(x, y, h, t)dt \quad \ldots [31]$$

These expressions may be integrated by inspection (if use is made of the relation of $\partial/\partial y$ and d/dt) to give

$$u = a\,[\theta\,(x, y, h, -1) - \theta\,(x, y, h, 1)] - 1 \quad \ldots\ldots [32]$$

or

$$u = a\,[\arctan \{\coth \pi\,x/2h \tan \pi\,(y + 1)/2h\} - \arctan \{\coth \pi\,x/2h \tan \pi\,(y - 1)/2h\}] - 1 \quad \ldots [33]$$

and

$$v = a \ln \{\rho\,(x, y, h, -1)/\rho\,(x, y, h, 1)\} \quad \ldots\ldots [34]$$

or

$$v = a \ln \sqrt{\left\{\frac{\cosh^2 \pi\,x/2h - \cos^2 \pi\,(y + 1)/2h}{\cosh^2 \pi\,x/2h - \cos^2 \pi\,(y - 1)/2h}\right\}} \quad \ldots [35]$$

It may be noted that u and v are continuous everywhere except for points along the source sheet, and even there v is continuous except at the end points, $x = 0$, $y = \pm 1$.

An important feature of this flow between walls is brought out by seeking

$$\lim_{x \to \infty} u$$

Thus for large positive x, Equation [33] shows that $u(x, y) \to \pi\,a/h - 1$ and for large negative x we have

$$u(-x, y) \to -\frac{\pi a}{h} - 1$$

Hence to define the flow at large distances

$$u_\infty = \pi\,a/h - 1 \quad \ldots\ldots [36]$$

and

$$u_{-\infty} = -\pi\,a/h - 1 \quad \ldots\ldots [37]$$

Contrary to the results of the similar flow without walls, it is seen that the velocity at a great distance is not the superposed velocity. The mathematically imposed "free-stream" velocity is reduced in magnitude at $x = \infty$ by a term $\pi\,a/h$ which may be considered to have been induced by the image flows. At large downstream distances the velocity is greater than the superposed velocity by the same amount. Equation [36] gives a condition on $\pi\,a/h$ in order that the resultant flow may be toward negative x. Thus

$$\pi\,a/h < 1 \quad \ldots\ldots [38]$$

in order that streaming motion from right to left may exist. In dimensional terms, this simply states that the total source flow which is directed toward positive x must be less than the total superposed flow between the walls, or

$$\tfrac{1}{2}Q < 2\,Uh \quad \ldots\ldots [39]$$

This blockage effect would not arise if the body were closed;

i.e., if a sink of strength equal to that of the source were added behind the source sheet.

The stagnation point $x = \xi_0$ may be computed from Equation [32] alone since $v(\xi_0, 0) = 0$. Thus

$$a[\theta(\xi_0, 0, h, -1) - \theta(\xi_0, 0, h, 1)] = 1$$

or

$$2 \text{ arc tan } \{\coth(\pi\xi_0/2h)\tan \pi/2h\} = (a)^{-1}$$

whence

$$\xi_0 = 2h/\pi \coth^{-1} \{(\tan 1/2a)\ (\cot \pi/2h)\} \quad [40]$$

An interesting result of Equation [40] is that the condition for a perfectly flat-nosed profile ($\xi_0 = 0$) is again specified by $a = 1/\pi$ which is entirely independent of the wall-distance parameter h. A limiting position of stagnation is closely approached, viz.

$$\xi_0 = 2h/\pi \quad \text{for } \tan 1/2a \cot \pi/2h \geq 5 \quad [41]$$

Application of Formulas

Form of Half Body. The dividing streamline or half-body shape for the flow between walls specified by $a = 1/3$ and $h = 3$ has been determined by solving Equation [28] by numerical methods. The body shape is given in Fig. 3. For sake of comparison the half body determined by the flow in the absence of walls and specified by $a = 1/3$ has been computed from Equation [10] and is also plotted in Fig. 3.

Effect of Walls on Pressure Distribution. The pressure distributions for the half bodies generated by the flows indicated in the foregoing are given in Fig. 6. The minimum value of the pressure coefficient $\Delta p/q$ is of prime importance in estimating the cavitation characteristics of any body of hydrodynamic interest. It will be noted that the pressure distributions are considerably different which may be expected since the half-body shapes are not similar and moreover since the walls have a constricting effect on the flow.

One reasonably might inquire as to the wall separation required to produce a flow which is nearly that obtained in the absence of walls; i.e., for $h \to \infty$. Inasmuch as the shape of the half body is a function of the wall distance parameter h, the important problem of finding the maximum allowable size of half body for a given two-dimensional parallel-sided channel or tunnel cannot be solved exactly by the formulas derived in the foregoing. However, an approximate answer may be obtained.

A formula for the pressure distribution in the flow about the half body between walls is obtained from Bernoulli's equation in the following form

$$\Delta p/1/2\rho U_\infty^2 = \Delta p/q = 1 - (u^2 + v^2)/(1 - \pi a/h)^2 \quad [42]$$

where u and v are velocity components given by Equations [33], [35], and $\Delta p = p - p_\infty$; p being the pressure at any point x, y; p_∞ the pressure at $x = \infty$ where the velocity is $U_\infty = (\pi a/h - 1)U$; and ρ the mass density of the fluid.

Let the point $x = 0, y_0 = \pi a$ be taken as the control point, then

$$\Delta p/q = C = 1 - (1 - \pi a/h)^{-2} \left\{1 + a^2\left[\ln \frac{\sin \pi(\pi a + 1)/2h}{\sin \pi\ (\pi a - 1)/2h}\right]^2\right\} \quad [43]$$

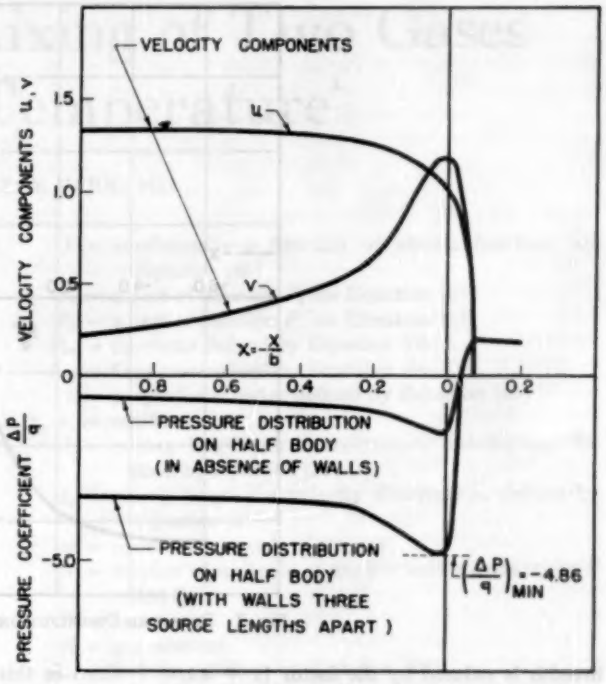

Fig. 6 Pressure Distribution on Half Bodies Derived From Source Lamina and a Superposed Parallel Flow in Presence and Absence of Parallel Walls

The corresponding expression for the pressure-change coefficient C_0 at the same point on the half body without walls ($h = \infty$) is

$$C_0 = -a^2\left[\ln\left(\frac{\pi a + 1}{\pi a - 1}\right)\right]^2 \quad [44]$$

The effect of the walls on the pressure coefficient as a fraction of the pressure coefficient C_0 is given by ΔC; viz.

$$\Delta C = \frac{C - C_0}{C_0} = \frac{\left[1 - \frac{\pi a}{h}\right]^{-2}\left\{1 + a^2\left[\ln \frac{\sin \pi(\pi a + 1)/2h}{\sin \pi(\pi a - 1)/2h}\right]^2\right\} - 1 - a^2\left[\ln\left(\frac{\pi a + 1}{\pi a - 1}\right)\right]^2}{a^2\left[\ln\left(\frac{\pi a + 1}{\pi a - 1}\right)\right]^2} \quad [45]$$

Equation [45] has no exact algebraic solution for the required wall-distance parameter h for a selected error ratio ΔC; however, an approximate formula will suffice since an answer is required for small ΔC. Thus it follows from Equation [45] that for sufficiently large h, the particular value of $h(= h')$ such that the error in pressure coefficient due to walls shall be ΔC is given approximately by

$$h' = (1 - C_0^{-1})\ 2\pi a/\Delta C \quad [46]$$

Conversely, the half-breadth Y_∞ at $X = -\infty$ of that half body which may be symmetrically placed in a two-dimensional channel of half-width h with an allowable error ΔC in C_0 is specified by

$$Y_\infty/h = \Delta C/(1 - C_0^{-1}) \quad [47]$$

It is remarkable that for $\Delta C = 0.02$ and $C_0 = -1.58$, (from Fig. 6) $Y_\infty/h = 0.0122$; for example, a channel of total width $2h = 24$ in. requires that $Y_\infty \leq 0.146$ in. This pronounced effect is primarily due to the "blockage" term $\pi a/h$ which would not arise if the body were closed. It is to be recalled that the body changes shape as the wall separation is changed. The "nose" of the body moves forward slightly and the asymptotic half-

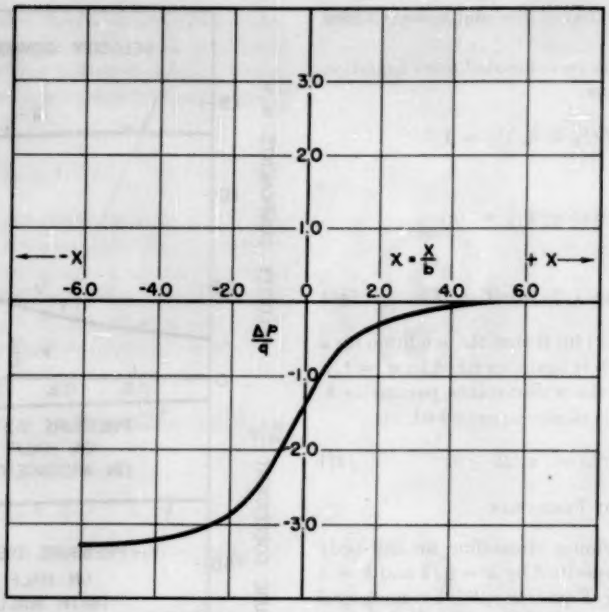

FIG. 7 PRESSURE DISTRIBUTION ON WALL ADJACENT TO HALF BODY

breadth is reduced by the factor $(1 + \pi a/h)^{-1}$ which in this example is only 0.997. This blockage effect is apparently of the same order as that found in a theoretical analysis (6) of plane-cavity flows between walls.

Pressure Distribution on Walls. For some unusual but nonetheless important applications of hydrodynamic flows in restricted channels it is required to estimate a lower bound for the quasi-steady-state pressure distribution along the sea or channel bottom produced by a passing ship. The expression for the pressure coefficient along the walls is

$$(\Delta p/q)_w = 1 - \left\{ \frac{a[\pi - 2\tan^{-1}\{\coth \pi x/2h \cot \pi/2h\}] - 1}{1 - \frac{a\pi}{h}} \right\}^2 \quad \ldots\ldots [48]$$

The distribution along the wall for the flow specified by $a = 1/3$, $h = 3$ is plotted in Fig. 7. It is of interest that the minimum and asymptotic value of $(\Delta p/q)_w = -3.28$ is attained for all practical purposes for $x = -5.0$.

CONCLUSIONS

Two new families of half bodies have been derived from the source lamina of constant-strength distribution placed perpendicular to a uniform stream. One family is obtained for the infinitely broad free stream and the other for the flow between parallel walls. These arrangements of a source sheet and a uniform stream make it possible to obtain very blunt half bodies and the ensuing formulas allow estimates of the velocity and pressure distribution about the forward end of blunt strut shapes.

From the foregoing calculations it is noted that the influence of the walls on the pressure distribution on a half body is very pronounced. This effect should be investigated carefully in the design or use of two-dimensional flow facilities particularly in the case of marine injection-scoop model tests made in closed ducts, where fluid is withdrawn from one duct and introduced into another.

ACKNOWLEDGMENT

The author is indebted to Dr. Alexander Weinstein, Research Professor, Institute for Fluid Dynamics and Applied Mathematics, University of Maryland, for his guidance in this study. Miss Joan Seery is thanked for carefully checking this text.

BIBLIOGRAPHY

1 "Aerodynamic Theory" by M. M. Munk, edited by W. F. Durand, Julius Springer, Berlin, Germany, 1934, vol. 1, p. 266.

2 "On Axially Symmetric Flows," by A. Weinstein, *Quarterly of Applied Mathematics*, vol. 5, 1948, pp. 429–444.

3 "On the Axially Symmetric Flows Around a New Family of Half-Bodies," by A. Van Tuyl, *Quarterly of Applied Mathematics*, vol. 7, 1950, pp. 399–409.

4 "Elliptic Integral Representation of Axially Symmetric Flows," by M. A. Sadowsky and E. Sternberg, *Quarterly of Applied Mathematics*, vol. 8, 1950, pp. 113–126.

5 *Theoretical Hydrodynamics*, by L. M. Milne-Thomson, second edition, The Macmillan Co., New York, N. Y., 1950, p. 259.

6 "Wall Effects in Cavity Flow," by G. Birkhoff, M. Plesset, and N. Simmons, *Quarterly of Applied Mathematics*, vol. 8, 1950, p. 151.

On Turbulent Jet Mixing of Two Gases at Constant Temperature[1]

By S. I. PAI,[2] COLLEGE PARK, MD.

The fundamental equations of both two-dimensional and axially symmetrical turbulent jet mixing of two gases at constant temperature are derived and discussed. A general method of solution of these equations is given. The most important factors in these equations are the turbulent exchange coefficient for velocity distribution and that for density distribution. In general, these coefficients are not equal. If we assume that these coefficients are the same, an analytic solution for the mixing of two uniform streams is found which is an extension of Görtler's solution for the case of homogeneous fluids. The first-order effect of the difference in densities of the two gases in the mixture on the velocity distribution is small. For two-dimensional and axially symmetrical jet from small opening, if the turbulent exchange coefficients are assumed to be the same, the velocity distribution for the case of homogeneous fluid is the first-order approximation of the velocity distribution in the jet of the mixing of two gases and the density distribution is the same as the velocity distribution. Finally, the effect of the difference in the two turbulent exchange coefficients is discussed. It is found that the ratio of turbulent-exchange coefficient for density distribution to that for velocity distribution is larger than 1, and may be as high as 2, and the ratio increases as the difference in density of the two gases increases. The larger this ratio is, the wider the spread of the density distribution than that of velocity distribution will be.

Nomenclature

The following nomenclature is used in the paper:

A = constant of integration, defined by Equation [54]
b = width of mixing region of velocity distribution
b_c = width of mixing region of density distribution
B = constant of integration, defined by Equation [54]
C = concentration of gas 1 in the mixture, defined by Equation [2]
C_m = mass concentration of gas 1 in the mixture, defined by Equation [14]
$d_{0,\nu}$; $d_{1,\nu}$ = constant of integration, see Equations [76] and [85]
E = ratio of turbulent exchange coefficient ϵ_c and ϵ, see Equation [41]
F = nondimensional function of stream function, see Equation [46]
F_0 = a part of function F, see Equation [61]
F_1 = a part of function F, see Equation [61]
$F_{0\nu}$ = functions defined by Equation [65]
$F_{1\nu}$ = functions defined by Equation [66]
h = proportional factor defined by Equation [45]
k_1, k_u, k_c = constants
l_c = mixing length for concentration distribution, defined by Equation [21]
l_u = mixing length for velocity distribution, defined by Equation [31]
m = mass of a molecule of the gas
N = number of molecule of gas per unit volume under P and T
P = pressure
R = gas constant
$R_{0\nu}$ = functions defined by Equation [68]
$\bar{R}_{0\nu}$ = functions defined by Equation [75]
$R_{1\nu}$ = functions defined by Equation [80]
$\bar{R}_{1\nu}$ = functions defined by Equation [84]
t = time
T = temperature
u, v, w = x, y, z- components of velocity
U = mean velocity defined in Equation [46]
u_A = certain constant velocity
x, y, z = Cartesian co-ordinates
y = radial distance in axially symmetrical flow
β = factor defined in Equation [4]
δ = 0 for two-dimensional flow; $\delta = 1$ for axisymmetrical flow
ϵ = turbulent exchange coefficient for velocity distribution
ϵ_c = turbulent exchange coefficient for density distribution
η = y/x
λ = velocity factor defined by Equation [50]
μ = density factor defined by Equation [55]
ξ = $\sigma\eta$
ρ = density
ρ_m = mean density defined by Equation [55]
σ = factor defined by Equation [50]
Φ = error integral defined by Equation [72]
Φ_1 = error function defined by Equation [69]
ψ = stream function defined by Equation [13]

Subscript 1: value for gas 1 except as otherwise specified
Subscript 2: value for gas 2 except as otherwise specified
Bar —: mean value except as otherwise specified
Prime ′: fluctuating value, or differentiation with respect to η in the section Turbulent Mixing of Two Uniform Streams of Different Gases at Constant Temperature.

Introduction

Most of the studies of the problem of jet mixing have been concerned with one fluid; i.e., the fluid in the jet is the same fluid as

[1] This work was carried out under contract AF18(600)86 sponsored by the Air Research and Development Command.

[2] Associate Research Professor, Institute for Fluid Dynamics and Applied Mathematics, University of Maryland.

Contributed by the Applied Mechanics Division and presented at the Annual Meeting, New York, N. Y., Nov. 28–Dec. 3 1954, of The American Society of Mechanical Engineers.

Discussion of this paper should be addressed to the Secretary, ASME, 29 West 39th Street, New York, N. Y., and will be accepted until April 11, 1955, for publication at a later date. Discussion received after the closing date will be returned.

Note: Statements and opinions advanced in papers are to be understood as individual expressions of their authors and not those of the Society. Manuscript received by ASME Applied Mechanics Division, May 11, 1953. Paper No. 54—A-1.

that into which it is injected and with which it mixes. Comparatively little attention appears to have been devoted to problems in which the fluid in the jet is different from that of the surrounding medium. The author has studied the laminar jet mixing of two compressible fluids,[3] in which a new variable, the concentration of one fluid in the other, is introduced; and one more relation, the equation of diffusion, is added in the fundamental equations. In this paper the author extends the theory of laminar jet mixing of two compressible fluids to the case of turbulent flow at isothermal condition.

Hu[4] has extended Tollmien's theory of turbulent jet mixing of incompressible homogeneous fluid to the case in which the mixing fluids are of different densities. Hu confined to the case that the two fluids are immiscible. We shall show later that the assumption of immiscibility is not necessary to derive the fundamental equations of turbulent jet mixing of two fluids of Hu so that the results can be applied to more general cases.

Our basic assumptions are that the mixture may be considered as a continuous medium, that there is no chemical reaction between the fluids, and that the fluids are assumed to be perfect gases so the perfect-gas law holds for each constituent as well as the mixture. Furthermore, the boundary-layer assumptions are assumed to be applicable in the jet-mixing region; i.e., the lateral gradient $\partial/\partial y$ is much larger than the axial gradient $\partial/\partial x$ and the lateral (y-wise) velocity components v are much smaller than the axial (x-wise) velocity component u.

After the derivation of the fundamental equations of turbulent jet mixing of two gases, particularly at isothermal condition, a general discussion of the solution of these equations is given. The most important factors in these equations are the turbulent exchange coefficient for density distribution ϵ_s and that for velocity distribution ϵ. These are not the same, in general. Hypotheses for the expressions of these coefficients in terms of mean velocity are discussed. At first, we find some analytic solutions of these fundamental equations by assuming that these turbulent exchange coefficients are equal. We extend Prandtl-Görtler's theory of the turbulent jet mixing of homogeneous fluid to the present problems. For the mixing of two uniform streams, explicit solutions for the mixing of two gases are obtained. For two-dimensional and axially symmetrical jet from small opening, it has been shown that the velocity distribution of the case of homogeneous fluid is the first-order distribution in this inhomogeneous fluid case and the density distribution is the same as that of velocity. Finally, the effect of the difference in ϵ_s and ϵ is discussed. It is found that the ratio of $E = \epsilon_s/\epsilon$ is always larger than 1 and may be as high as 2. The value of E increases as the difference in density of the two gases in the mixture increases. Further experimental data are necessary to evaluate the value of the ratio E.

Equation of State of Mixture

(*a*) *Temperature T.* The temperature T of the mixture is considered as one of the dependent variables in the present problem. We assume that the temperatures of the two gases at a given point are the same and equal to the temperature of the mixture at that point. It is consistent with our assumption that the mixture may be considered as a continuous medium. In the present analysis we further assume that the temperature T is constant throughout the whole field.

(*b*) *Pressure.* The pressure P of the mixture is considered as another dependent variable in the present problem. Since each constituent of the mixture is considered as a perfect gas, we express here Dalton's law as follows:

"The volume of a mixture of two or more perfect gases is simply the sum of the volume which they would occupy if each is exerted by the same total pressure."

It is well known that in the jet-mixing region, the pressure is approximately constant. In the present analysis, we thus assume that the pressure is constant throughout the whole field.

(*c*) *Density and Concentration.* Let N be the total number of molecules of the mixture of gases 1 and 2 per unit volume under the pressure P and temperature T; N_1 be the corresponding number of molecules of gas 1 per unit volume, and N_2 that of gas 2. We then have

$$N = N_1 + N_2 \quad [1]$$

We define the concentration C of gas 1 in the mixture as

$$C = N_1/N \quad [2]$$

and then the concentration of gas 2 in the mixture is

$$(1 - C) = N_2/N \quad [3]$$

Let m_1 be the mass of a molecule of gas 1 and m_2 that of gas 2. The mass density ρ of the mixture under the pressure P and temperature T is

$$\rho = m_1 N_1 + m_2 N_2 = N m_2 (\beta C + 1) \quad [4]$$

where

$$\beta = \frac{m_1}{m_2} - 1$$

The equation of state of the mixture is then

$$P = NRT \quad [5]$$

where R is Boltzmann's constant.

In the present analysis, both P and T are assumed to be constant throughout the flow field; thus the equation of state, Equation [5], becomes

$$N = \text{const} \quad [6]$$

Equation of Continuity of Mixture

Since the mixture is considered as a definite fluid, the condition of conservation of mass gives the equation of continuity which is

$$\frac{\partial \rho}{\partial t} + \frac{\partial \rho u}{\partial x} + \frac{\partial \rho v}{\partial y} + \frac{\partial \rho w}{\partial z} = 0 \quad [7]$$

where u, v, w are the x-wise, y-wise, and z-wise velocity component of the mixture, respectively.

Substituting Equation [4] into Equation [7] we have

$$\beta \left[\frac{\partial NC}{\partial t} + \frac{\partial NCu}{\partial x} + \frac{\partial NCv}{\partial y} + \frac{\partial NCw}{\partial z} \right] + \left[\frac{\partial N}{\partial t} + \frac{\partial Nu}{\partial x} + \frac{\partial Nv}{\partial y} + \frac{\partial Nw}{\partial z} \right] = 0 \quad [8]$$

The first square bracket is equal to zero because of the equation of diffusion, i.e., Equation [16]. Since N is constant in the present analysis, Equation [8] reduces to

$$\frac{\partial u}{\partial x} + \frac{\partial v}{\partial y} + \frac{\partial w}{\partial z} = 0 \quad [9]$$

The mixture in the present case behaves like an incompressible fluid, even though the density varies in the flow field because the concentration varies.

[3] "The Laminar Jet Mixing of Two Compressible Fluids," by S. I. Pai, Technical Report BT1, Institute for Fluid Dynamics and Applied Mathematics, University of Maryland, February 11, 1952. Also, Proceedings of the Second Midwest Conference on Fluid Mechanics, Ohio State University, 1952, pp. 297–309.

[4] "On Turbulent Mixing of Two Fluids of Different Densities," by N. Hu, Part 2 of PhD thesis, California Institute of Technology, 1944.

If we write

$$u = \bar{u} + u', v = \bar{v} + v', w = \bar{w} + w' \quad [10]$$

where bar represents the mean value and prime, the fluctuating value, Equation [9] may be reduced to

$$\frac{\partial \bar{u}}{\partial x} + \frac{\partial \bar{v}}{\partial y} + \frac{\partial \bar{w}}{\partial z} = 0 \quad [11]$$

In the case of two-dimensional or axisymmetric flow, Equation [11] becomes

$$\frac{\partial \bar{u}}{\partial x} + \frac{\partial \bar{v}}{\partial y} = -\frac{\delta \bar{v}}{y} \quad [12]$$

where y is the radial distance in axisymmetrical case; $\delta = 0$ in two-dimensional case, $\delta = 1$ in axisymmetric case.

From Equation [12] we define stream function ψ such that

$$\frac{\partial \psi}{\partial y} = y^\delta \bar{u}; \quad \frac{\partial \psi}{\partial x} = -y^\delta \bar{v} \quad [13]$$

the equation of continuity, Equation [12], is automatically satisfied. We shall show later that it is convenient to use the stream function ψ as an independent variable instead of y in jet-mixing problems.

Equation of Diffusion of Mixture

Let C_m be the mass concentration of gas 1 in the mixture, i.e.

$$C_m = m_1 N_1 = C N m_1 \quad [14]$$

If the molecular diffusion is neglected, the diffusion of C_m will be mainly due to convection; hence the equation of diffusion is

$$-\frac{\partial C_m}{\partial t} = \frac{\partial u C_m}{\partial x} + \frac{\partial v C_m}{\partial y} + \frac{\partial w C_m}{\partial z} \quad [15]$$

Substituting Equation [14] into Equation [15], we have

$$\frac{\partial CN}{\partial t} + \frac{\partial CNu}{\partial x} + \frac{\partial CNv}{\partial y} + \frac{\partial CNw}{\partial z} = 0 \quad [16]$$

In the case of N = const, we have

$$\frac{\partial C}{\partial t} + \frac{\partial Cu}{\partial x} + \frac{\partial Cv}{\partial y} + \frac{\partial Cw}{\partial z} = 0 \quad [17]$$

Now let us consider the case of two-dimensional or axially symmetrical flow. If we assume that the mean flow is steady and put

$$C = \bar{C} + C' \quad [18]$$

and take the average of various terms in the equation of diffusion, we have

$$\frac{\partial \bar{C}\bar{u}}{\partial x} + \frac{\partial \bar{C}\bar{v}}{\partial y} + \frac{\delta \bar{C}\bar{v}}{y} = -\frac{\partial \overline{C'u'}}{\partial x} - \frac{\partial \overline{C'v'}}{\partial y} - \frac{\delta \overline{C'v'}}{y} \quad [19]$$

According to the boundary-layer assumptions

$$\frac{\partial \overline{C'u'}}{\partial x} << \frac{\partial \overline{C'v'}}{\partial y}$$

Equation [19] becomes

$$\bar{u}\frac{\partial \bar{C}}{\partial x} + \bar{v}\frac{\partial \bar{C}}{\partial y} = -\frac{1}{y^\delta}\frac{\partial y^\delta \overline{C'v'}}{\partial y} \quad [20]$$

By mixing length theory, we may write

$$C' = l_c \frac{\partial \bar{C}}{\partial y} \quad [21]$$

where l_c is the mixing length for concentration distribution. Substituting Equation [21] into Equation [20], we have

$$\bar{u}\frac{\partial \bar{C}}{\partial x} + \bar{v}\frac{\partial \bar{C}}{\partial y} = \frac{1}{y^\delta}\frac{\partial}{\partial y}\left(y^\delta \epsilon_c \frac{\partial \bar{C}}{\partial y}\right) \quad [22]$$

where

$$\epsilon_c = -\overline{l_c v'} \quad [23]$$

ϵ_c is known as the turbulent exchange coefficient for concentration (or density) distribution. Since N is constant, Equation [4] gives

$$\bar{\rho} = N m_2 (\beta \bar{C} + 1) \quad [24]$$

Substituting Equation [24] into Equation [22], we have

$$\bar{u}\frac{\partial \bar{\rho}}{\partial x} + \bar{v}\frac{\partial \bar{\rho}}{\partial y} = \frac{1}{y^\delta}\frac{\partial}{\partial y}\left(y^\delta \epsilon_c \frac{\partial \bar{\rho}}{\partial y}\right) \quad [25]$$

In terms of the variables x and ψ, we obtain

$$\frac{\partial \bar{\rho}}{\partial x} = \frac{\partial}{\partial \psi}\left[y^{2\delta}\epsilon_c \bar{u}\frac{\partial \bar{\rho}}{\partial \psi}\right] \quad [26]$$

Equations of Motion

If the stress tensor due to molecular transfer is neglected, the equations of motion are

$$\frac{\partial \rho u_i}{\partial t} + \frac{\partial \rho u_i u_j}{\partial x_j} = -\frac{\partial P}{\partial x_i} \quad [27]$$

where summation convention is used, with $i = 1, 2,$ or 3; $j = 1, 2,$ or 3, and x_i and x_j are the Cartesian co-ordinates.

For two-dimensional or axisymmetrical flow, Equation [27] is reduced into the following form

$$\frac{\partial \rho u}{\partial t} + \frac{\partial \rho u^2}{\partial x} + \frac{1}{y^\delta}\frac{\partial y^\delta \rho u v}{\partial y} = -\frac{\partial P}{\partial x} \quad [28]$$

$$\frac{\partial \rho v}{\partial t} + \frac{\partial \rho u v}{\partial x} + \frac{1}{y^\delta}\frac{\partial y^\delta \rho v^2}{\partial y} = -\frac{\partial P}{\partial y} \quad [29]$$

Now, we assume that the mean flow is steady, substitute Equations [4], [10], and [18] into Equations [28] and [29], and take average of the resultant equations. Furthermore, we apply the boundary-layer assumptions that

$$\bar{u} >> \bar{v}, \quad \bar{u} \sim \bar{C} \sim 1, \quad \frac{\partial(\ )}{\partial x} << \frac{\partial(\ )}{\partial y}$$

where ( ) may represent any dependent variable,

and assume that

$$\overline{u'^2} << \bar{u}^2, \quad \overline{u'C'} << \bar{u}\,\bar{C}$$

and P is constant in the present problem. Equation [28] then becomes

$$\frac{\partial \bar{\rho}\bar{u}^2}{\partial x} + \frac{1}{y^\delta}\frac{\partial y^\delta \bar{\rho}\bar{u}\bar{v}}{\partial y} = -\frac{1}{y^\delta}\frac{\partial}{\partial y}\left[y^\delta \bar{\rho}\,\overline{l_u v'}\frac{\partial \bar{u}}{\partial y} + y^\delta \bar{u}\,\overline{l_c v'}\frac{\partial \bar{\rho}}{\partial y}\right] \quad [30]$$

where

$$u' = l_u \frac{\partial \bar{u}}{\partial y} \quad [31]$$

with l_u as the mixing length for velocity distribution. If we write

$$\epsilon = -\overline{l_u v'} \quad [32]$$

then ϵ is the turbulent exchange coefficient for velocity distribution. In general, ϵ is different from ϵ_c.

Equation [30] becomes

$$\bar{u}\frac{\partial \bar{\rho}\bar{u}}{\partial x} + \bar{v}\frac{\partial \bar{\rho}\bar{u}}{\partial y} = \frac{1}{y^s}\frac{\partial}{\partial y}\left[y^s \epsilon \bar{\rho}\frac{\partial \bar{u}}{\partial y} + y^s \epsilon_c \bar{u}\frac{\partial \bar{\rho}}{\partial y}\right] \quad [33]$$

Equation [29] is simply reduced to

$$\frac{\partial P}{\partial y} = 0 \quad [34]$$

which is consistent with our assumption that P is constant throughout the flow field.

In terms of x and ψ, we obtain

$$\frac{\partial \bar{\rho}\bar{u}}{\partial x} = \frac{\partial}{\partial \psi}\left[y^{2s}\epsilon\bar{\rho}\bar{u}\frac{\partial \bar{u}}{\partial \psi} + y^{2s}\epsilon_c \bar{u}^2 \frac{\partial \bar{\rho}}{\partial \psi}\right] \quad [35]$$

General Solution of Two-Dimensional or Axially Symmetrical Turbulent Jet Mixing of Two Gases at Constant Temperature

From the foregoing analysis we see that in the present problem there are three unknowns, i.e., density $\bar{\rho}$ (or concentration $\bar{C}$) and velocity components $\bar{u}$ and $\bar{v}$, where P and T (thus N) are assumed to be constant. These unknowns can be obtained by solving the three fundamental Equations [12], [25], [33] with some initial conditions such as follows

$$\left.\begin{array}{l} x = 0 \\ \bar{\rho} = \rho_0(y), \quad \bar{u} = u_0(y), \quad \bar{v} = v_0(y) \end{array}\right\} \quad [36]$$

or

$$\left.\begin{array}{l} [\bar{\rho} = \rho_0(\psi), \quad \bar{u} = u_0(\psi), \quad \bar{v} = v_0(\psi)] \end{array}\right\}$$

If we use ψ as one of the independent variables, Equation [12] is automatically satisfied, and we shall solve only Equations [26] and [35] with the initial conditions in the square bracket of Equations [36].

It is worth while to note that both Equation [26] and [35] are the generalized heat-conduction equations. They can be solved by stepwise numerical procedure, finite-difference method, from the initial conditions [36] without any difficulty, because from the initial conditions it is possible to calculate the rate of change of $\bar{\rho}$ and $\bar{u}$ with respect to x from Equations [26] and [35], respectively. By finite-difference method, the values of $\bar{\rho}$ and $\bar{u}$ at $x = \Delta x$ may be obtained. Hence, by stepwise numerical procedure, the whole flow field can be obtained.

Turbulent Exchange Coefficients

Before we start to solve the fundamental equations such as Equations [26] and [35], we have to make some assumptions on the variations of the turbulent exchange coefficients $\epsilon = -\overline{l_u v'}$ and $\epsilon_c = -\overline{l_c v'}$.

According to Prandtl's momentum transport theory we may assume that

$$v' = -k\, l_u \frac{\partial \bar{u}}{\partial y} \quad [37]$$

where k is a proportional constant. Hence

$$\left.\begin{array}{l} \epsilon = k\, l_u^2 \dfrac{\partial \bar{u}}{\partial y} \\ \epsilon_c = k\, l_u l_c \dfrac{\partial \bar{u}}{\partial y} \end{array}\right\} \quad [38]$$

In general, $l_c \neq l_u$, hence $\epsilon \neq \epsilon_c$. But in Hu's analysis,[4] he assumes that $l_c = l_u$ in order to get some analytic solutions in closed form.

Another hypothesis on turbulent exchange coefficient which also was suggested by Prandtl[5] is that the turbulent exchange coefficient is assumed to be constant over every cross section of the mixing region. Prandtl suggested that

$$\epsilon = k_u\, b\, (\bar{u}_{max} - \bar{u}_{min}) \quad [39]$$

where k_u is a proportional constant, b is the width of the mixing region of velocity distribution, $\bar{u}_{max}$ and $\bar{u}_{min}$ are the maximum and the minimum mean velocities at each cross section.

Similarly, we may write

$$\epsilon_c = k_c\, b_c\, (\bar{u}_{max} - \bar{u}_{min}) \quad [40]$$

where k_c is also a proportional constant; b_c is the width of the mixing region of density distribution. In general, k_c is not equal to k_u and b is not equal to b_c but we may write

$$k_c\, b_c = E k_u b \quad [41]$$

where E is the ratio of ϵ_c to ϵ.

In the following three sections we shall assume that $E = 1$ in order to show some first-order effect of density variation on the turbulent jet mixing problem. We shall discuss the effect of E later.

Turbulent Mixing of Two Uniform Streams of Different Gases at Constant Temperature

Fig. 1 shows the schematic diagram of the problem. If we

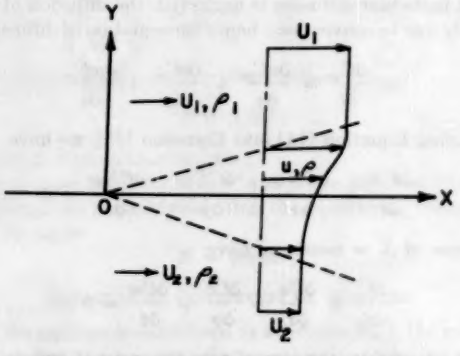

Fig. 1 Mixing of Two Uniform Streams

assume that $E = 1$, the fundamental equations of the present problem are (we drop bar for mean value from here on)

$$\frac{\partial u}{\partial x} + \frac{\partial v}{\partial y} = 0 \quad [42]$$

$$u\frac{\partial \rho}{\partial x} + v\frac{\partial \rho}{\partial y} = \epsilon\frac{\partial^2 \rho}{\partial y^2} \quad [43]$$

$$u\frac{\partial \rho u}{\partial x} + v\frac{\partial \rho u}{\partial y} = \epsilon\frac{\partial^2 \rho u}{\partial y^2} \quad [44]$$

The exchange coefficient ϵ may be written as

$$\epsilon = k_u\, b\, (U_1 - U_2) = k_u\, hx\, (U_1 - U_2);\ [U_1 \geq U_2] \quad [45]$$

because by dimensional analysis we see that in the present problem b must be proportional to x.

For the flow downstream, we may assume that the profiles of both velocity and density are similar; thus we write

[4] "Bemerkungen zur Theorie der freien Turbulenz," by L. Prandtl, ZAMM, vol. 22, October, 1942, pp. 241–243.

$$\psi = xUF(\eta),\ \rho = \rho(\eta) \quad [46]$$

where

$$U = \frac{1}{2}(U_1 + U_2) \quad \text{and} \quad \eta = \frac{y}{x}$$

and then

$$\left.\begin{aligned} \frac{u}{U} &= \frac{\partial \psi}{\partial y} = \frac{dF}{d\eta} = F'(\eta) \\ \frac{v}{U} &= -\frac{\partial \psi}{\partial x} = -F(\eta) + \eta F'(\eta) \end{aligned}\right\} \quad [47]$$

where prime means differentiation with respect to η.

Substituting Equations [45], [46], and [47] into Equations [43] and [44], we have

$$\rho'' = -2\sigma^2 F \rho' \quad [48]$$

$$[\rho F']'' = -2\sigma^2 F [\rho F']' \quad [49]$$

where

$$2\sigma^2 = \frac{1}{2k_m \lambda};\ \lambda = \frac{U_1 - U_2}{U_1 + U_2} \quad [50]$$

Comparing Equations [48] and [49], we have

$$\rho' = A[\rho' F]' \quad [51]$$

where A is a constant. From Equation [51] we find that

$$\rho = \frac{B}{1 - AF'} \quad [52]$$

where B is the constant of integration. Equation [52] was first found by Hu.[4]

The boundary conditions are

$$\left.\begin{aligned} &\rho = \rho_1,\ F' = \frac{U_1}{U} = 1 + \lambda \text{ at } \eta = +\infty \\ &\rho = \rho_2,\ F' = \frac{U_2}{U} = 1 - \lambda \text{ at } \eta = -\infty \end{aligned}\right\} \quad [53]$$

Substituting Equations [53] into [52], we have

$$A = \frac{\mu}{\lambda + \mu};\ B = \frac{\rho_1 \rho_2 \lambda}{\rho_m (\lambda + \mu)} \quad [54]$$

where

$$\mu = \frac{\rho_1 - \rho_2}{\rho_1 + \rho_2};\ \rho_m = \frac{\rho_1 + \rho_2}{2} \quad [55]$$

From Equations [52] and [54] we have

$$\frac{\rho - \rho_2}{\rho_1 - \rho_2} = \frac{\rho_2}{\rho_1} \frac{u - U_2}{U_1 - U_2} \frac{1}{1 - \dfrac{\rho_1 - \rho_2}{\rho_1} \dfrac{u - U_2}{U_1 - U_2}} \quad [56]$$

We see that when $(\rho_1 - \rho_2)$ is small, the density distribution $(\rho - \rho_2)/(\rho_1 - \rho_2)$ is similar to the velocity distribution $(u - U_2)/(U_1 - U_2)$. It is a generalization of Hu's result which is concerned with the special case of $U_2 = 0$, only.

Substituting Equation [52] into [48], we have

$$F''' + 2\sigma^2 FF'' = -\frac{2AF''^2}{1 - AF'} \quad [57]$$

If $\rho_1 = \rho_2 = \text{const}$, $A = 0$, Equation [57] reduces to Görtler's equation[6] for the case of homogeneous fluid, i.e.

$$F''' + 2\sigma^2 FF'' = 0 \quad [58]$$

[6] "Berechung von Aufgaben der freien Turbulenz auf Grund eines neuen Näherungsansatzes," by H. Görtler, ZAMM, vol. 22, October, 1942, pp. 244–254.

We are going to solve Equation [57] by method of small perturbation; i.e., we consider the case of small A, i.e., $\mu << \lambda$.

Equation [57] may be written in the following form

$$F''' + 2\sigma^2 FF'' = -2AF''^2(1 + AF' + A^2 F'^2 + \ldots) \quad [59]$$

If we neglect all the terms of μ^2, we have

$$\lambda F''' + 2\sigma^2 FF''\lambda = -2\mu F''^2 \quad [60]$$

Equation [60] is the fundamental equation of the present problem.

Now we put

$$F = F_0 + \mu F_1 \quad [61]$$

in Equation [60] and neglect the higher-order terms of μ, and we have

$$F_0''' + 2\sigma^2 F_0 F_0'' = 0 \quad [62]$$

$$\lambda F_1''' + 2\sigma^2 \lambda (F_0 F_1'' + F_1 F_0'') = -2F_0''^2 \quad [63]$$

We are going to solve Equations [62] and [63] for F_0 and F_1 with the following boundary conditions

$$\left.\begin{aligned} &F'(\eta) = 1 + \lambda \text{ at } \eta = +\infty \\ &F'(\eta) = 1 - \lambda \text{ at } \eta = -\infty \\ &F'(\eta) = 1 \text{ at } \eta = 0 \end{aligned}\right\} \quad [64]$$

The last condition is obtained by choosing the x-axis, i.e., $y = 0$, passing through the points $u = U$.

We develop both F_0 and F_1 into power series as follows

$$F_0 = \sigma^{-1} \sum_{\nu=0}^{\infty} \lambda^\nu F_{0\nu}(\xi) \quad [65]$$

$$F_1 = \sigma^{-1} \sum_{\nu=0}^{\infty} \lambda^\nu F_{1\nu}(\xi) \quad [66]$$

where $\xi = \sigma\eta$.

Substituting Equations [65] and [66] into Equations [64], we have

$$F_{00}'(\pm\infty) = 1;\ F_{01}'(+\infty) = 1,\ F_{01}'(-\infty) = -1$$

$$\left.\begin{aligned} &F_{0\nu}'(\pm\infty) = 0 \text{ for all } \nu \geq 2 \\ &F_{00}'(0) = 1,\ F_{0\nu}'(0) = 0 \text{ for all } \nu \geq 1 \\ &F_{1\nu}'(\pm\infty) = F_{1\nu}(0) = 0 \text{ for all } \nu \geq 0 \end{aligned}\right\} \quad [67]$$

We see that both the differential Equation [62] and the boundary conditions for F_0 are the same as those of Görtler's case of homogeneous fluids. Hence Görtler's solution may be used for F_0. However, it seems that there are some mistakes in Görtler's original solution, we thus rederive these $F_{0\nu}$ as follows: Substituting Equation [65] into [62] and satisfying the boundary conditions [67], we have

$$\left.\begin{aligned} &F_{00} = \xi \\ &F_{01}''' + 2\xi F_{01}'' = 0 \\ &F_{0\nu}''' + 2\xi F_{0\nu} = \Phi_1(\xi) R_{0\nu}(\xi), \quad \text{for} \quad \nu \geq 2 \end{aligned}\right\} \quad [68]$$

where

$$\Phi_1(\xi) = \frac{2}{\sqrt{\pi}} e^{-\xi^2} \quad [69]$$

and $R_{0\nu}(\xi)$ are known functions of ξ which depend on F_k's where $k \leq \nu - 1$. For instance

$$\Phi_1(\xi) R_{02}(\xi) = -2F_{01}F_{01}'' \quad [70]$$

The solution of F_{01} is

$$F_{01} = \int_0^\xi \Phi(a)\,da + d_{01} \quad [71]$$

where

$$\Phi(a) = \int_0^a \Phi_1(\beta)\, d\beta \quad [72]$$

and d_{01} is an integration constant.

The solution of $F_{0\nu}$ for $\nu \geq 2$ is

$$F_{0\nu} = \int_0^\xi \int_0^\gamma \Phi_1(\beta) \int_0^\beta R_{0\nu}(a)\, da\, d\beta\, d\gamma + C_{0\nu} \int_0^\xi \Phi(a)\, da + D_{0\nu}\xi + d_{0\nu} \quad [73]$$

where $C_{0\nu}$, $D_{0\nu}$, and $d_{0\nu}$ are integration constants.

From the boundary condition $F_{0\nu}'(0) = 0$, $\nu \geq 1$, we have

$$D_{0\nu} = 0;\ \nu \geq 2 \quad [74]$$

and from $F_{0\nu}'(\pm\infty) = 0$ for $\nu \geq 2$, we have

$$C_{0\nu} = 0 \quad [74a]$$

If we write

$$R_{0\nu} = \bar{R}_{0\nu} - 2\, d_{0,\nu-1} \quad [75]$$

then $F_{0\nu}'(\infty) = 0$, for $\nu \geq 2$, gives

$$d_{0,\nu-1} = \frac{\sqrt{\pi}}{2} \int_0^\infty \Phi_1(\beta) \int_0^\beta \bar{R}_{0\nu}(\alpha)\, d\alpha\, d\beta \quad [76]$$

For instance, $d_{01} = -0.16084$ and the rest $d_{0,\nu}$ are even smaller. For practical purpose the velocity distribution of homogeneous fluid may be described simply by the first two terms of Equation [65], i.e.

$$F_0 \cong \frac{1}{\sigma}\left[F_{00} + \lambda F_{01}\right] = \eta + \frac{\lambda}{\sigma}\left[\int_0^\xi \Phi(a)da + d_{01}\right]$$

or the mean velocity distribution u is given by

$$u_0 \cong UF_0' = \frac{U_1 + U_2}{2}\left[1 + \frac{U_1 - U_2}{U_1 + U_2}\int_0^\xi \Phi_1(a)\, da\right] = \frac{U_1 + U_2}{2} + \frac{U_1 - U_2}{2}\frac{2}{\sqrt{\pi}}\int_0^\xi e^{-\xi^2} d\xi \quad [77]$$

The rest terms are minor corrections.

After all $F_{0\nu}$ are known, we substitute Equations [65] and [66] into [63] and collect the terms of same power of λ, and we have

$$F_{10}'''(\xi) + 2\xi F_{10}''(\xi) = 0 \quad [78]$$

Since $F_{10}'(\pm\infty) = 0$

$$F_{10} = d_{10} \quad [79]$$

where d_{10} is a constant.

For $\nu \geq 1$, we have

$$F_{1\nu}''' + 2\xi F_{1\nu}'' = \Phi_1 R_{1\nu}(\xi) \quad [80]$$

where $R_{1\nu}$ are known functions of ξ, which depend on $F_{0\nu}$ and F_{1k} where $k \leq \nu - 1$. For instance

$$\Phi_1 R_{11}(\xi) = -2\left[d_{10} F_{01}'' + F_{01}''^2\right] \quad [81]$$

Similar to the solutions $F_{0\nu}$, we have $\nu \geq 1$

$$F_{1\nu} = \int_0^\xi \int_0^\gamma \Phi_1(\beta) \int_0^\beta R_{1\nu}(\alpha)\, d\alpha\, d\beta\, d\gamma + C_{1\nu} \int_0^\xi \Phi(\xi)\, d\xi + D_{1\nu}\xi + d_{1\nu} \quad [82]$$

By the boundary conditions $F_{1\nu}'(0) = F_{1\nu}'(\pm\infty) = 0$, we have

$$C_{1\nu} = D_{1\nu} = 0 \quad [83]$$

If we write

$$R_{1\nu} = \bar{R}_{1\nu} - 2\, d_{1,\nu-1} \quad [84]$$

then

$$d_{1,\nu-1} = \frac{\sqrt{\pi}}{2} \int_0^\xi \Phi_1(\beta) \int_0^\beta \bar{R}_{1\nu}(\alpha)\, d\alpha\, d\beta \quad [85]$$

By comparison of the solutions of F_1 and F_0, we see that the solution F_1 is of the same order of magnitude as the part of F_0, which has been neglected in Equation [77]. The first-order effect of density variation on the mean velocity distribution of the jet-mixing region is exceedingly small, if we assume that $\epsilon = \epsilon_e$.

Two-Dimensional Jet From a Small Slit

Fig. 2 shows the schematic diagram of the present problem. Since the variation in pressure is small, the momentum across the

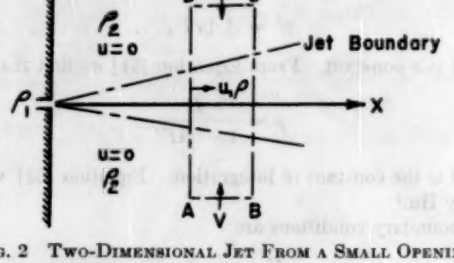

Fig. 2 Two-Dimensional Jet From a Small Opening

different cross sections of the jet (x = const) must be constant, i.e., for every x-station

$$\int_{-\infty}^{\infty} \rho u^2\, dy = \text{const} \quad [86]$$

In general, both ρ and u vary with x. Strictly speaking, it is not possible to obtain similarity in both density and velocity profiles. If we write

$$\rho = \rho_2 + \Delta\rho \quad [87]$$

Equation [86] becomes

$$\rho_2 \int_{-\infty}^{\infty} u^2\, dy + \int_{-\infty}^{\infty} \Delta\rho\, u^2\, dy = \text{const} \quad [88]$$

When $\Delta\rho$ is much smaller than ρ_2, i.e., at far downstream, we have

$$\rho_2 \int_{-\infty}^{\infty} u^2\, dy \cong \text{const} \quad [88a]$$

Then the similarity in profile of velocity may be obtained. By similar procedure to the problem of homogeneous fluid, we have

$$u \sim \frac{1}{\sqrt{x}} \quad [89]$$

and the boundary of the jet is straight line $\eta = y/x$.

From the equation of continuity, if we take a control surface A-B-C-D, Fig. 2, such that C-D and A-B lie in the region of the fluid outside the jet-mixing region, we have, from Equation [7]

$$\int_{AD} \rho u\, dy - \int_{BC} \rho u\, dy = 0 \quad [90]$$

and from Equation [9]

$$\rho_2 \int_{AD} u\,dy - \rho_2 \int_{BC} u\,dy = 0 \quad [91]$$

Subtracting Equation [91] from [90], we have

$$\int_{-\infty}^{\infty} (\rho - \rho_2)\,u\,dy = \text{const} \quad [92]$$

If $\overline{\rho' u'} << \bar{\rho}\bar{u}$, we have by taking average of Equation [92]

$$\int_{-\infty}^{\infty} (\bar{\rho} - \rho_2)\,\bar{u}\,dy = \text{const} \quad [93]$$

Since $\bar{u} \sim 1/\sqrt{x}$, Equation [93] also expresses that $(\bar{\rho} - \rho_2)$ is proportional to $1/\sqrt{x}$. This means that ρ will be very near to ρ_2 when x is very large. This is just what should be expected since at large distance from the slit nearly all the fluid inside the jet is the fluid of density ρ_2 that has been sucked in from both sides of the jet.

Hence if we assume that $E = 1$, and $\bar{\rho} \cong \rho_2$, the equation of motion, Equation [33], becomes

$$\bar{u}\frac{\partial \bar{u}}{\partial x} + \bar{v}\frac{\partial \bar{u}}{\partial y} = \epsilon \frac{\partial^2 \bar{u}}{\partial y^2} \quad [94]$$

It is also the equation of motion for the case of homogeneous fluid. Hence, at large x, the velocity distribution of two-dimensional jet of two gases will be the same as that of homogeneous fluid.

From the equation of diffusion, Equation [25], if we put $E = 1$ nd $\bar{\rho} = \rho_2 + \Delta\bar{\rho}$, we have

$$\bar{u}\frac{\partial \Delta\bar{\rho}}{\partial x} + \bar{v}\frac{\partial \Delta\bar{\rho}}{\partial y} = \epsilon \frac{\partial^2 \Delta\bar{\rho}}{\partial y^2} \quad [95]$$

Comparing Equations [94] and [95], we have

$$\Delta\bar{\rho} = \text{const}\,\bar{u} \quad [96]$$

When $E = 1$, at large distance of x, the distribution of density $\bar{\rho}$ will be the same as the distribution of velocity $\bar{u}$.

Axially Symmetrical Jet From a Small Opening

By the same procedure, it is easy to show that similar results as those of the two-dimensional jet hold for the axially symmetrical case; i. e., strictly speaking, it is not possible to obtain similarity in both density and velocity profiles but at far downstream, and assuming $E = 1$, the velocity distribution of jet mixing of two gases will be the same as that of homogeneous fluid and the density distribution will be the same as that of velocity.

Effect of Factor E

In the preceding three sections we assume that the ratio of the turbulent exchange coefficient for density to that for velocity, i.e., E, is equal to unity. The conclusion drawn is that at far downstream, the distributions for density and velocity are the same. But from experimental evidence,[7] we know that the spread of the concentration distribution is wider than that of velocity. In fact, the factor E is not exactly equal to 1. In order to estimate the value of E approximately, we will consider the two-dimensional case where the x-wise velocity component $\bar{u}$ is nearly constant and we have

$$\bar{u} = u_A + \Delta u,\ \bar{v} = \Delta v \quad [97]$$

where u_A is a constant, $u_A >> \Delta u$ and $\Delta u \sim \Delta v$.

Substituting Equation [97] into Equations [94] and [95], neglecting the higher-order terms, and taking $\Delta u \sim \Delta\rho$ and $E \neq 1$, we have

$$u_A \frac{\partial \Delta u}{\partial x} = \epsilon \frac{\partial^2 \Delta u}{\partial y^2} \quad [98]$$

and

$$u_A \frac{\partial \Delta\rho}{\partial x} = E\epsilon \frac{\partial^2 \Delta\rho}{\partial y^2} \quad [99]$$

Both Equations [98] and [99] are simple linear differential equations of heat conduction. Since these equations are linear, method of superposition is applicable. Of course, since we linearize the original equations, Equations [98] and [99] will yield only approximate results which are only qualitatively correct. Hence it is sufficient to consider a typical solution of these equations.

The elementary solutions of Equations [98] and [99] may be written as follows

$$\Delta u = \frac{u_k}{\sqrt{x}} e^{-\frac{u_A y^2}{4\epsilon x}} \quad [100]$$

and

$$\Delta\bar{\rho} = \frac{\rho_k}{\sqrt{x}} e^{-\frac{u_A y^2}{4\epsilon E x}} \quad [101]$$

where u_k and ρ_k are constants. Keagy[7] has found that at a given x-distance, the experimental distributions of both density and velocity distribution can be approximated by error functions. This qualitatively proves the validity of Equations [100] and [101]. The values of ϵ and E can be determined experimentally. Since the spread of the density distribution is larger than that of velocity, hence E is always larger than 1. The exact value of E depends on the difference of the densities of the two gases in the mixture. Further experimental data are necessary in order to determine the value of E.

From Keagy's and Weller's preliminary data of axially symmetrical jet mixing, we see that E is about 1.2 for nitrogen and air mixture, 1.4 for carbon-dioxide and air mixture, and 2.0 for helium and air mixture. It seems that the larger the difference in density of the two gases in the mixture, the larger the value of E, and the wider the spread of density distribution than that of velocity distribution.

[7] "A Study of Freely Expanding Inhomogeneous Jets," by W. R. Keagy and A. E. Weller, Heat Transfer and Fluid Mechanics Institute, University of California, Berkeley, Calif., June 22–24, 1949, pp. 89–98. Publication of The American Society of Mechanical Engineers, New York, N. Y.

Plastic-Rigid Analysis of a Special Class of Problems Involving Beams Subject to Dynamic Transverse Loading[1]

By MARGARET F. CONROY,[2] LAFAYETTE, IND.

The object of this paper is to show that in certain circumstances the plastic deformation of beams, made of a material with linear strain hardening and subject to dynamic transverse loading, can be determined by the techniques used in solving elastic problems. In particular, the differential equation of motion for such beams is in some instances of the same form as in the corresponding linear elastic case, and so any of the methods employed for solving elastic-beam problems, such as the normal-mode method, Laplace-transform method, or Boussinesq's solutions for infinite beams, can be used. Because of this linear character of the differential equation of motion encountered in the analysis presented here, it also is shown that some initial-motion problems for beams undergoing large plastic deformations due to transverse loading can be solved by superposing solutions. In these problems the disturbance part of the solution is obtained by some elasticity technique and is then superposed on the initial motion of the beam. The method of solution is demonstrated by means of several examples involving finite beams. The first example is an initial-motion problem and illustrates the method of superposition. The second example is an initial-stress problem for a simply supported beam. Again, the method of superposition is used. The last example is a free-boundary problem for a cantilever beam. This problem is solved by an inverse method whereby the form of the solution is assumed and the physical problem associated with this solution is then determined.

Nomenclature

The following nomenclature is used in the paper:

x = distance along beam
y = deflection
K = $\partial^2 y/\partial x^2$, curvature of deflection curve
m = mass per unit length of the beam
M = bending moment
Q = shearing force
t = time
M_0 = limiting value of M for rigid-body motion

Foot-pound-second units are used throughout the paper.

Introduction

The general problem of the determination of the plastic deformation of beams subject to dynamic transverse loading is very difficult to handle. Thus far only one such problem has been solved for a beam made of strain-hardening material. H. F. Bohnenblust (1)[3] has made an elastic-plastic analysis of the problem of an infinite beam subject to a constant-velocity impact. In view, then, of the difficulty encountered in solving problems of this type, the analysis carried out in this paper, while it applies only to a very special class of problems, seems well worth while, since it does add a group of tractable solutions to the literature. It is believed that this analysis represents the first treatment of the plastic deformation of finite beams, made of a strain-hardening material and subject to dynamic transverse loading.

Basic Assumptions

The analysis carried out in this paper is introduced to determine the permanent deformation of beams subjected to transverse loading of such a magnitude that the plastic strains produced are large compared to the elastic strains. It is shown that in some instances a satisfactory approximation to the solution of such problems can be obtained by means of the same techniques used in elastic-beam theory.

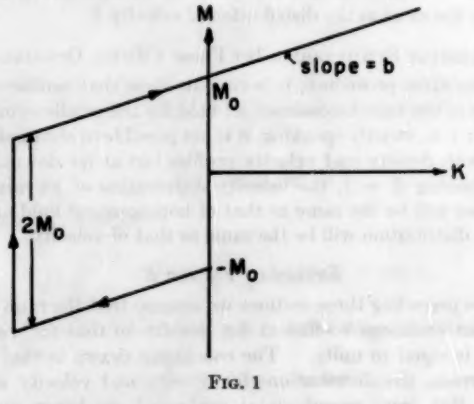

Fig. 1

The analysis is based on the assumption of a linear strain-hardening bending moment-curvature relationship of the type shown in Fig. 1. Thus elastic strains are ignored and the beam is considered to be either rigid or plastic. An approximation for the solution of the actual elastic-plastic problem is then obtained by neglecting the elastic strains and carrying out a plastic-rigid type of analysis. It is expected that this approximation will be satisfactory when the plastic strains are large compared to the elastic strains.

[1] The results presented in this paper were obtained in the course of research sponsored by the Office of Naval Research under Contract N7onr-35801 with Brown University.

[2] Mathematics Instructor, Purdue University.

Contributed by the Applied Mechanics Division and presented at the Annual Meeting, New York, N. Y., November 28–December 3, 1954, of The American Society of Mechanical Engineers.

Discussion of this paper should be addressed to the Secretary, ASME, 29 West 39th Street, New York, N. Y., and will be accepted until April 11, 1955, for publication at a later date. Discussion received after the closing date will be returned.

Note: Statements and opinions advanced in papers are to be understood as individual expressions of their authors and not those of the Society. Manuscript received by ASME Applied Mechanics Division July 1, 1953. Paper No. 54—A-17

[3] Numbers in parentheses refer to the Bibliography at the end of the paper.

The analysis also is based on the assumption that the rate of change of curvature of the beam is everywhere greater than or equal to zero, or everywhere less than or equal to zero, for the range of time considered. This of course places certain restrictions on the initial conditions and boundary conditions for application of this analysis, as described later.

Under these assumptions the bending moment-curvature relationship of the beam for plastic flow is the linear relationship

$$M = \pm M_0 + bK = \pm M_0 + b\frac{\partial^2 y}{\partial x^2} \quad [1]$$

where the sign of M_0 is the same as the sign of the rate of change of curvature of the beam. The differential equation of motion for the beam, which is obtained from the equilibrium conditions

$$Q = \frac{\partial M}{\partial x}, \quad \frac{\partial Q}{\partial x} + m\frac{\partial^2 y}{\partial t^2} = 0$$

becomes

$$\frac{\partial^4 y}{\partial x^4} + \frac{1}{c^2}\frac{\partial^2 y}{\partial t^2} = 0 \quad [2]$$

where

$$\frac{1}{c^2} = \frac{m}{b}$$

This equation of motion is of the same form as in the elastic-beam theory, where the flexural rigidity has been replaced by b. Thus, under the assumptions stated, it is clear that the plastic deformation of a beam can be determined by the same methods used to solve the corresponding elastic problem and, since the equation of motion is linear, superposition of effects is permissible.

The assumptions stated here restrict the application of the analysis to a very special class of problems. However, as mentioned before, the general problem of the plastic deformation of beams subject to dynamic transverse loading has not yielded to theoretical analysis; hence the analysis given here represents definite progress.

The following examples are given to demonstrate the solution.

Initial-Motion Problem

For the application of this method to an initial-motion problem, the initial motion of the beam must be such that the final rate of change of curvature of the beam after loading is everywhere greater than or equal to zero or everywhere less than or equal to zero; that is, the rate of change of curvature of the beam resulting from the initial motion must be such as to eliminate any oscillations in the sign of the rate of change of curvature due to the transverse loading. An example of such an initial motion is afforded by the following problem:

Let a cantilever beam of uniform cross section and length l have one end ($x = 0$) fixed and be subject to an initial motion

$$y = 2.25tx^3 - \frac{x^2}{30} \quad [3]$$

which is maintained for all time by a bending moment, $M_0 + b(4.5t - 1/15)$, applied at the free end of the beam. For $t > 0$ an additional bending moment $9bt$ is applied to the free end ($x = l$) of the beam. The problem is to determine the subsequent motion of the beam.

The initial motion and the applied bending moment given here were chosen rather arbitrarily. Any other choices would serve as well, provided they are such that the rate of change of curvature of the beam after loading is everywhere greater than or equal to zero (or everywhere less than or equal to zero).

Because of the prescribed initial motion, the initial rate of change of curvature of the beam is everywhere greater than zero. Thus the bending moment-curvature relationship is

$$M_I = M_0 + bK_I \quad [4]$$

where K_I and M_I are the bending moment and curvature corresponding to the initial motion. If the final rate of change of curvature of the beam due to the initial motion plus the disturbance remains everywhere positive, the linear bending moment-curvature relationship of Equation [1] remains valid and from Equations [1] and [4] it is clear that

$$M_D = bK_D$$

where K_D and M_D are the additional bending moment and curvature corresponding to the disturbance.

The final deformation of the beam can be obtained by superposing the disturbance deformation onto the initial-motion deformation. The disturbance deformation can be determined by any of the methods used in elastic-beam theory.

The disturbance deformation resulting from the application of the bending moment at $x = l$ can be found readily from Boussinesq's solution for an infinite beam until such time as this solution gives an appreciable disturbance at the fixed end of the beam. While the solution does not satisfy the fixed-end boundary conditions, it yields an approximation to the disturbance deformation until such time as the deflection and slope of the beam at $x = 0$ provided by this solution become significant.

The Boussinesq solution (2) of Equation [2] for a semi-infinite beam, initially ($t = -\infty$) straight and at rest, and subject to the conditions

$$\frac{\partial^2 y}{\partial x^2} = 0, \quad \frac{\partial^2 y}{\partial x^2} = F_1'(ct)$$

at $x = l$, is

$$y = \frac{2}{\sqrt{\pi}}\int_0^\infty F_1\left(ct - \frac{\xi^2}{2\alpha^2}\right)\cos\frac{\alpha^2}{2}\,d\alpha \quad [5]$$

where

$$\xi = l - x$$

and

$$F_1'(ct) = \frac{d}{d(ct)}F_1(ct)$$

hence

$$F_1(ct) = \int_{-\infty}^{ct} F_1'(ct)d(ct)$$

Now, since the bending moment applied at the free end of the cantilever is

$$M_D(t) = \begin{cases} 0 & \text{for } t \le 0 \\ 9bt & \text{for } t \ge 0 \end{cases}$$

and

$$M_D = bK_D$$

it is seen that

$$\frac{\partial^2 y_D}{\partial x^2} \equiv 0, \quad \frac{\partial^2 y_D}{\partial x^2} = F_1'(ct) = \begin{cases} 0 & \text{for } ct \le 0 \\ \dfrac{9}{c}(ct) & \text{for } ct \ge 0 \end{cases}$$

at $x = l$.

It follows from Equation [5] that

$$y_D = \frac{9}{\sqrt{\pi}c}\int_{(l-x)/(2ct)^{1/2}}^{\infty}\left[ct - \frac{(l-x)^2}{2\alpha^2}\right]^2 \cos\frac{\alpha^2}{2}\,d\alpha \quad [6]$$

$$\frac{\partial y_D}{\partial x} = \frac{18}{\sqrt{\pi}c}\int_{(l-x)/(2ct)^{1/2}}^{\infty}\left[ct - \frac{(l-x)^2}{2\alpha^2}\right]\frac{(l-x)}{\alpha^2}\cos\frac{\alpha^2}{2}\,d\alpha$$

and

$$K_D = \frac{\partial^2 y_D}{\partial x^2} = \frac{18}{\sqrt{\pi}c}\int_{(l-x)/(2ct)^{1/2}}^{\infty}\left[ct - \frac{(l-x)^2}{2\alpha^2}\right]^2 \sin\frac{\alpha^2}{2}\,d\alpha \quad [7]$$

From Equations [3] and [7] it is clear that the final rate of change of curvature of the beam resulting from the initial motion plus the disturbance motion is

$$\frac{dK}{dt} = 4.5 + 9\,\{1 - 2S[(l-x)^2/4ct]\}$$

where $S[(l-x)^2/4ct]$ is the Fresnel integral

$$\frac{1}{\sqrt{2\pi}}\int_0^{(l-x)^2/4ct}\frac{\sin\eta}{\sqrt{\eta}}\,d\eta$$

Since $S[(l-x)^2/4ct] < 0.75$ for all values of the argument, it follows that

$$\frac{dK}{dt} > 0$$

everywhere along the beam for all time. Thus Equation [2] is everywhere valid and superposition of effects is allowable. Superposing Equations [3] and [6], we obtain

$$y = 2.25tx^2 - \frac{x^2}{30} + \frac{9}{\sqrt{\pi}c}\int_{(l-x)/(2ct)^{1/2}}^{\infty}\left(ct - \frac{(l-x)^2}{2\alpha^2}\right)^2\cos\frac{\alpha^2}{2}\,d\alpha$$

This Boussinesq solution was calculated (3) at $t = 0.01$ and $t = 0.02$ for the case when $l = 3$ and $c^2 = b/m = 907$. The results are shown in Table 1.

This problem also may be solved by finding y_D by the well-known method of normal modes and then superposing this solution onto the initial motion of the beam.

Simply Supported Beam

Consider a beam of uniform cross section simply supported at the ends $x = 0$ and $x = l$. Initially the beam is at rest and subject to an external bending moment, $M_I \leq -M_0$, at both ends. At time zero an external load distribution

$$q(x, t) = q_0 t \sin\frac{\pi x}{l}$$

is applied to the beam and the resulting deformation is to be determined.

Initially the beam is entirely plastic. If the motion due to the applied load or disturbance is such that the rate of change of curvature of the beam is everywhere negative, for all t, the bending moment-curvature relationship of the beam is

$$M = -M_0 + bK$$

and

$$M_D = bK_D$$

where M_D and K_D are the additional bending moment and curvature resulting from the applied external load. Again, the deformation of the beam can be determined by finding the disturbance deformation by the normal-mode method used in elastic-beam theory and then superposing this onto the initial deformation.

It is assumed in solving this problem that the rate of change of curvature of the beam is everywhere negative, for all t. Once the solution has been obtained, it is readily verified that this assumption is valid.

The initial deformation of the beam is

$$y_I = \frac{M_I + M_0}{2b}(l-x)x$$

and the disturbance deformation of the beam is assumed to be of the form

$$y_D = \sum_{n=1}^{\infty} X_n(x)\varphi_n(t) \quad [8]$$

where the $X_n(x)$ are the normal modes for a beam simply supported at $x = 0$ and $x = l$. These normal modes are readily found to be

$$X_n = (2/ml)^{1/2}\sin\frac{n\pi}{l}x$$

TABLE 1 BOUSSINESQ SOLUTION

	$t = 0.01$			$t = 0.02$		
x	y_I	y_D	y	y_I	y_D	y
0	0	+0.00004	+0.00004	0	+0.00102	+0.00102
0.15	−0.00024	−0.00005	−0.00029	+0.00026	+0.00173	+0.00199
0.30	−0.00098	−0.00015	−0.00113	+0.00105	+0.00223	+0.00328
0.45	−0.00219	−0.00019	−0.00238	+0.00236	+0.00245	+0.00481
0.60	−0.00390	−0.00013	−0.00403	+0.00420	+0.00228	+0.00648
0.75	−0.00609	+0.00005	−0.00604	+0.00656	+0.00146	+0.00802
0.90	−0.00878	+0.00029	−0.00849	+0.00945	+0.00006	+0.00951
1.05	−0.01194	+0.00052	−0.01142	+0.01286	−0.00192	+0.01094
1.20	−0.01560	+0.00062	−0.01498	+0.01680	−0.00438	+0.01242
1.35	−0.01974	+0.00050	−0.01924	+0.02126	−0.00712	+0.01414
1.50	−0.02438	+0.00008	−0.02430	+0.02625	−0.00988	+0.01637
1.65	−0.02949	−0.00064	−0.03013	+0.03176	−0.01230	+0.01946
1.80	−0.03510	−0.00156	−0.03666	+0.03780	−0.01399	+0.02381
1.95	−0.04119	−0.00254	−0.04373	+0.04436	−0.01448	+0.02988
2.10	−0.04778	−0.00332	−0.05110	+0.05145	−0.01330	+0.03815
2.25	−0.05484	−0.00362	−0.05846	+0.05906	−0.00996	+0.04910
2.40	−0.06240	−0.00311	−0.06551	+0.06720	−0.00397	+0.06323
2.55	−0.07044	−0.00142	−0.07186	+0.07586	+0.00509	+0.08095
2.70	−0.07898	+0.00175	−0.07723	+0.08505	+0.01763	+0.10268
2.85	−0.08799	+0.00668	−0.08131	+0.09476	+0.03394	+0.12870
3.00	−0.09750	+0.01355	−0.08395	+0.10500	+0.05421	+0.15921

We have as the equations of motion

$$\ddot{\varphi}_n + p_n^2 \varphi_n = \Phi_n$$

in which Φ_n is the force corresponding to the co-ordinate φ_n and $p_n^2 = c^2\pi^4 n^4/l^4$. If a small increase $\delta\varphi_n$ is given to a co-ordinate φ_n, the work done by the external load will be

$$\Phi_n\,\delta\varphi_n = \int_0^l q_0 t \sin\frac{\pi x}{l}\,(2/ml)^{1/2} \sin\frac{n\pi}{l}\,x\,\delta\varphi_n\,dx$$

and thus

$$\begin{cases} \Phi_n = 0 & \text{for } n \neq 1 \\ \Phi_1 = (2/ml)^{1/2}(l/2)q_0 t \end{cases}$$

Substituting these into the equations of motion and taking into consideration the initial conditions of the problem, we obtain

$$\begin{cases} \varphi_n = 0 & \text{for } n \neq 1 \\ \varphi_1 = (2/ml)^{1/2}(l/2)q_0 \dfrac{1}{p_1^2}\left(t - \dfrac{1}{p_1}\sin p_1 t\right) \end{cases}$$

Finally, substituting X_n and φ_n into Equation [8] and superposing the initial deformation, the following solution for the displacements is obtained

$$y(x,t) = \frac{M_1 + M_0}{2b}(l-x)x + \frac{q_0}{mp_1^2}\sin\frac{\pi x}{l}\left(t - \frac{1}{p_1}\sin p_1 t\right)$$

To insure that this is the solution of the problem, it remains only to verify that $(dK)/(dt) < 0$ for $0 \leq x \leq l$ and all $t > 0$. But, differentiating $y(x, t)$, we find

$$\frac{dK}{dt} = -\frac{q_0}{mp_1^2}\,\frac{\pi^2}{l^2}\sin\frac{\pi x}{l}\,(1 - \cos p_1 t)$$

which is readily seen to be negative for $0 \leq x \leq l$ and all $t > 0$.

Free-Boundary Problem

In the two previous problems the beam was initially entirely plastic and remained entirely plastic for all time. No plastic-rigid boundaries were present. The absence of such boundaries accounts in large measure for the ease with which these problems were solved. However, in the case of a beam which is initially rigid, the application of a load, in general, will produce a moving plastic-rigid boundary. The determination of this free boundary and the solution of such problems does not appear simple. However, by the inverse method to be given, it is possible to find solutions to some free-boundary problems under the assumptions originally given. The method consists essentially of determining what physical problems are associated with simple analytic expressions satisfying Equation [2].

Consider the following solution of Equation [2]

$$y = x^2 t^2 - \frac{x^5}{180c^2} \qquad [9]$$

This expression satisfies the boundary conditions at

$$x = 0 \begin{cases} y = 0 \\ y' = 0 \end{cases} \text{ and at } x = \xi(t) = 12^{1/4}(ct)^{1/2} \begin{cases} K = \dfrac{\partial^2 y}{\partial x^2} = 0 \\ \dfrac{dK}{dt} = 0 \end{cases}$$

That is, the foregoing solution of the differential equation of motion for plastic flow satisfies fixed end conditions at $x = 0$ and free-boundary conditions at $x = \xi(t)$. As t increases from $t = 0$, the position of the free boundary moves from the fixed end ($x = 0$) to larger values of x. Moreover, since $K = 0$ for $x = \xi(t)$, it appears that Equation [9] may be the solution in the plastic region, $0 \leq x \leq \xi(t)$, for a cantilever problem in which the beam is initially straight. For $\xi(t) < x \leq l$ the beam remains rigid; l is the length of the beam. This solution will be valid only until such time as the plastic-rigid boundary reaches the free end of the beam, that is, for $0 \leq t \leq l^2/c(12)^{1/2}$.

The physical problem associated with Equation [9] is now assumed to be that of a cantilever beam, fixed at $x = 0$, initially straight and at rest, and subject at time zero to a force $F(t)$ and a bending moment $M(t)$, both of which are applied at the free end $x = l$.

$F(t)$ and $M(t)$ are determined from the equations of motion for the rigid portion of the beam, i.e.

$$\begin{cases} F(t) + b(y''')_{x=\xi} = \displaystyle\int_\xi^l (R-\xi)\ddot{\theta}\,m\,dR + \int_\xi^l \ddot{y}\,m\,dR \\ M(t) + F(t)\,(l-\xi) = M_0 + \displaystyle\int_\xi^l (R-\xi)\,[(R-\xi)\ddot{\theta}]\,m\,dR + \int_\xi^l (R-\xi)\,\ddot{y}\,m\,dR \end{cases}$$

It follows, then, that

$$F(t) = -b(y''')_{x=\xi} + m(l-\xi)(\ddot{y})_{x=\xi} + m\,\frac{(l-\xi)^2}{2}\,(\ddot{\theta})_{x=\xi}$$

$$M(t) = -F(t)(l-\xi) + M_0 + m\,\frac{(l-\xi)^3}{3}\,(\ddot{\theta})_{x=\xi} + m\,\frac{(l-\xi)^2}{2}\,(\ddot{y})_{x=\xi}$$

where

$$\xi(t) = (12)^{1/4}(ct)^{1/2}$$

$$(\ddot{y})_{x=\xi} = \left[\frac{\partial^2 y}{\partial t^2} + 2\dot{\xi}\,\frac{\partial^2 y}{\partial x \partial t} + (\dot{\xi})^2\,\frac{\partial^2 y}{\partial x^2}\right]_{x=\xi} = 6(12)^{1/2}\,c\dot{t}$$

$$(\ddot{\theta})_{x=\xi} = \left[\frac{\partial^3 y}{\partial t^2 \partial x} + 2\dot{\xi}\,\frac{\partial^3 y}{\partial x^2 \partial t} + (\dot{\xi})^2\,\frac{\partial^3 y}{\partial x^3}\right]_{x=\xi} = 6(12)^{1/4}\,(ct)^{1/2}$$

$$(y''')_{x=\xi} = -\frac{2\xi^2}{3c^2}$$

For any given set of parameters a check must be made to make sure that $M(x) < M_0$ for $\xi < x \leq l$; that is, it must be verified that the yield limit is not exceeded in that portion of the beam which is assumed to be rigid. $M(x)$ is obtained readily from the following equilibrium equation

$$M(x) = M(t) + F(t)(l-x) - \int_x^l (R-x)\,[(R-\xi)\ddot{\theta}]\,m\,dR - \int_x^l m\ddot{y}\,(R-x)\,dR$$

As a specific example, the following practical values of the parameters were chosen: $l = 5$ ft, $M_0 = 17$ ft-lb, $m = 1.2$ lb/ft, $c^2 = 907$ ft^4/sec^2. $M(x)$ was calculated for $\xi \leq x \leq l$ at $t = 0,\ 0.005,\ 0.02,\ 0.05,\ 0.10,\ 0.20$ sec. From the results of these calculations, which are shown in Fig. 2, it appears that for this set of parameters $M(x) < M_0$ for $\xi < x \leq l$. It does not seem feasible to make a rigorous analytic check of this fact.

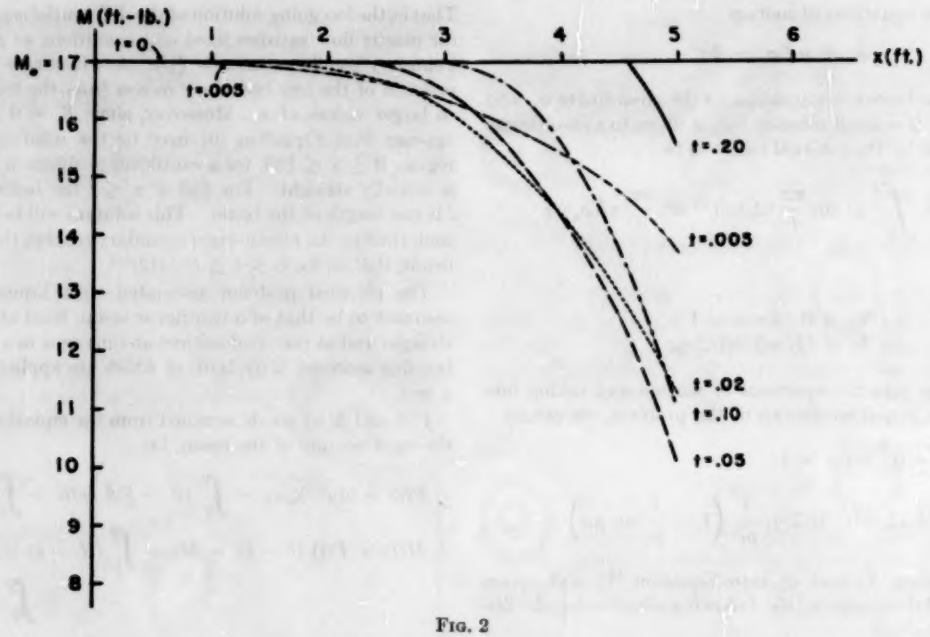

FIG. 2

CONCLUSION

The examples treated in this paper serve to illustrate the fact that, under certain conditions, the plastic deformation of beams subject to dynamic transverse loading can be determined by the same techniques used in solving elastic-beam problems. This is owing to the fact that, under the assumptions given, the equation of motion for a beam undergoing large plastic deformation is of the same linear form as the equation of motion for an elastic beam.

The first two problems were solved readily, largely owing to the fact that in each case the beam was initially entirely plastic and remained entirely plastic for all time. If the beam is initially rigid, an applied load, in general, will produce a moving plastic-rigid boundary. The presence of such free boundaries makes these problems more difficult to handle. The same difficulty arises, of course, in solving problems involving the unloading of external forces, rather than the loading type of problems treated here.

As shown by the third problem, it is possible to find solutions to some free-boundary problems under the original assumptions. The method of solution is essentially an inverse process whereby a simple analytic expression satisfying the differential equation of motion for plastic flow is considered, and the physical problem associated with this solution is then determined. The general problem of a beam subject to prescribed external forces giving rise to free boundaries is not solved so readily.

It was hoped that a numerical technique based on Hartree's method (6) might be devised for locating these free plastic-rigid boundaries at any given time. While there was no free boundary to be determined, Hartree's method was first tried on the first problem of this paper. However, it was found that, owing to the presence of the fourth derivative in the equation of motion of the beam, the results of a finite-difference technique to solve the ordinary differential equation resulting from Hartree's method were poor. In the case of a free-boundary problem, the satisfaction of the boundary conditions, $(dK)/(dt) = 0$, would introduce further high derivatives, and it was virtually impossible to retain sufficient accuracy using finite difference to complete such a problem.

The reader may refer to (7) and (8) for other papers pertaining to the plastic deformation of beams under transverse impact loading.

BIBLIOGRAPHY

1 "The Behavior of Long Beams Under Impact Loading," by P. E. Duwez, D. S. Clark, and H. F. Bohnenblust, JOURNAL OF APPLIED MECHANICS, Trans. ASME, vol. 72, 1950, pp. 27–34.

2 "Application des Potentiels a l'Étude de Équilibre et du Movement des Solides Élastiques," by M. J. Boussinesq, Gauthier-Villars, Paris, France, 1885, p. 444.

3 "Table of Fresnel Integrals," by A. Van Wijngaarden and W. L. Scheen, N. V. Noord-Hollandsche Uitgevers Maatschappij, Amsterdam, Holland, 1949.

4 "Analytical Dynamics," by E. T. Whittaker, Dover Publications, New York, N. Y., 1944, p. 181.

5 "Vibration Problems in Engineering," by S. Timoshenko, D. Van Nostrand Company, Inc., New York, N. Y., 1928, chapter 4.

6 "A Method for the Numerical or Mechanical Solution of Certain Types of Partial Differential Equations," by D. R. Hartree and J. R. Womersley, Proceedings of the Royal Society of London, England, series A, vol. 161, 1937, pp. 353–366.

7 "Large Plastic Deformation of Beams Under Transverse Impact," by E. H. Lee and P. S. Symonds, JOURNAL OF APPLIED MECHANICS, Trans. ASME, vol. 74, 1952, pp. 308–314.

8 "Plastic-Rigid Analysis of Long Beams Under Transverse Impact Loading," by M. F. Conroy, JOURNAL OF APPLIED MECHANICS, Trans. ASME, vol. 74, 1952, pp. 465–470.

Forced Motions of Timoshenko Beams[1]

By G. HERRMANN,[2] NEW YORK, N. Y.

Timoshenko's theory of flexural motions in an elastic beam takes into account both rotatory inertia and transverse-shear deformation and, accordingly, contains two dependent variables instead of the one transverse displacement of classical theory of flexure. For the case of forced motions, the solution involves complications not usually encountered. The difficulties may be surmounted in several ways, one of which is presented in this paper. The method described makes use of the property of orthogonality of the principal modes of free vibration and uses the procedure of R. D. Mindlin and L. E. Goodman in dealing with time-dependent boundary conditions. Thus the most general problem of forced motion is reduced to a free-vibration problem and a quadrature.

Introduction

TIMOSHENKO'S theory of flexural motions of elastic beams, in contrast to the elementary Bernoulli-Euler theory, allows for corrections for shear deformation and rotatory inertia. Though derived more than 30 years ago (1),[3] and attracting the attention of many workers in the field,[4] no complete solution of the most general boundary-value problem of a finite beam with time-dependent boundary conditions of any admissible combination, acted upon by time-dependent normal loads and bending moments with specified arbitrary initial conditions, seems to have been developed to date.

A major difficulty in solving boundary-value problems governed by Timoshenko-type equations (4, 5) consists in finding a proper combination of two (or more) "displacement" components, which would exhibit the property of orthogonality. This property is essential in developing series solutions by the classical (D. Bernoulli) method of separation of variables. In a recent paper (6) it was shown, by means of the example of a Timoshenko-type theory of longitudinal motions of rods, how this difficulty may be overcome by making use of Lagrange's equations of motion.

An additional difficulty, typical of any vibration problem with initial and boundary conditions, arises when one or more boundary conditions are time-dependent. In (6) it was demonstrated, how, in some cases, this complication may be removed by solving certain static problems.

In contrast to the procedure of (6) and as a counterpart of it, we attack here the general forced-vibration problem directly, without recourse to Lagrange's equations. Thereby, the time-dependency of the boundary conditions is dealt with, by making use of the idea of (7).

Thus the most general boundary-value problem of a finite Timoshenko beam will be reduced to the solution of the corresponding free-vibration problem and an integration.

Statement of Problem

Timoshenko's theory of flexural motions of elastic beams is contained[5] in the equations of motion

$$\left.\begin{aligned} k'(y'' - \psi')G/\rho + q/\rho A &= \ddot{y} \\ E\psi''/\rho + k'(y' - \psi)G/\rho r^2 + M_s/\rho A &= \ddot{\psi} \end{aligned}\right\} \quad \ldots\ldots [1]$$

the stress-displacement relations

$$\left.\begin{aligned} M &= -EI\psi' \\ Q &= k'(y' - \psi)AG \end{aligned}\right\} \quad \ldots\ldots\ldots\ldots [2]$$

the boundary conditions

$$\left.\begin{aligned} &1 \quad \text{At each point along length of beam, one member of each of products } \dot{y}q \text{ and } \dot{\psi}M_s \text{ must be specified} \\ &2 \quad \text{At each end of bar, one member of each of products } \dot{y}Q \text{ and } \dot{\psi}M \text{ must be specified} \end{aligned}\right\} \ldots [3]$$

and the initial conditions

Initial displacements and velocities must be specified.... [4]

In [1] to [4] the symbols have the following meanings:

E = Young's modulus
G = shear modulus
k' = shear-deflection coefficient
ρ = mass density
y = transverse displacement of cross section
ψ = angle of rotation of cross section
A = area of cross section
I = area moment of inertia of cross section
r = cross-sectional radius of gyration, $r^2 = I/A$
q = net transverse load, per unit of length
M_s = net (bending) moment, due to applied axial shears
M = bending moment
Q = transverse shear

Primes indicate differentiation with respect to x, the co-ordinate along the centroidal axis of the beam, and dots indicate differentiation with respect to time.

As a convenience in specifying the boundary conditions, the following notation will be employed:

$$\begin{aligned} B_1 &= y \text{ or } Q \quad \text{at } x = 0 \\ B_2 &= \psi \text{ or } M \quad \text{at } x = 0 \\ B_3 &= y \text{ or } Q \quad \text{at } x = l \\ B_4 &= \psi \text{ or } M \quad \text{at } x = l \end{aligned}$$

where l is the length of the beam.

Accordingly, the Boundary Conditions [3] become

---

[1] This investigation was supported by the Office of Naval Research under Contract Nonr-266(09).

[2] Assistant Professor of Civil Engineering, Columbia University. Mem. ASME.

[3] Numbers in parentheses refer to the Bibliography at the end of the paper.

[4] An account of the problem is given in the recent papers (2) and (3) and in the bibliographies to these papers.

Contributed by the Applied Mechanics Division and presented at the Annual Meeting, New York, N. Y., November 28–December 3, 1954, of The American Society of Mechanical Engineers.

Discussion of this paper should be addressed to the Secretary, ASME, 29 West 39th Street, New York, N. Y., and will be accepted until April 11, 1955, for publication at a later date. Discussion received after the closing date will be returned.

Note: Statements and opinions advanced in papers are to be understood as individual expressions of their authors and not those of the Society. Manuscript received by ASME Applied Mechanics Division, June 25, 1953. Paper No. 54—A-6.

[5] For derivation of these equations, consult, for example (8). M_s is the net bending moment, per unit of length, along the beam, due to the application of shear tractions on the cylindrical surface of the beam. This moment usually is omitted and is retained in the present paper for the sake of completeness

$$B_i = f_i(t) \quad i = 1, 2, 3, 4 \ldots\ldots\ldots\ldots [3a]$$

in which the four functions $f_i(t)$ are prescribed.

The Initial Conditions [4] are specified by four arbitrary functions

$$\left.\begin{aligned} y(x, 0) &= y_0(x) \\ \psi(x, 0) &= \psi_0(x) \\ \dot{y}(x, 0) &= \dot{y}_0(x) \\ \dot{\psi}(x, 0) &= \dot{\psi}_0(x) \end{aligned}\right\} \ldots\ldots\ldots\ldots [4a]$$

Free Vibrations

As a preliminary to the study of forced vibrations, we shall be concerned with the problem of free vibration, specified by the homogeneous differential equations of motion

$$\left.\begin{aligned} k'(y'' - \psi')G/\rho &= \ddot{y} \\ E\psi''/\rho + k'(y' - \psi)G/\rho r^2 &= \ddot{\psi} \end{aligned}\right\} \ldots\ldots\ldots [5]$$

and homogeneous boundary conditions

$$B_i = 0, \quad i = 1, 2, 3, 4 \ldots\ldots\ldots\ldots [6]$$

Considering solutions in the form

$$\left.\begin{aligned} y(x, t) &= Y(x) \sin \omega t \\ \psi(x, t) &= \Psi(x) \sin \omega t \end{aligned}\right\} \ldots\ldots\ldots\ldots [7]$$

we may show that the equations of motion, Equations [5], together with the Boundary Conditions [6], are satisfied for an infinite set of discrete frequencies ω_n, each of which corresponds to a mode shape given by functions $Y_n(x)$ and $\Psi_n(x)$. These modes are determined, except for a multiplying factor, common to both functions, from the equations

$$\left.\begin{aligned} Gk'(Y_n'' - \Psi_n') &= -\rho\omega_n^2 Y_n \\ E\Psi_n'' + k'(Y_n' - \Psi_n)G/r^2 &= -\rho\omega_n^2 \Psi_n \end{aligned}\right\} \ldots\ldots\ldots [8]$$

or, because of [2], from the equations

$$\left.\begin{aligned} Q_n' &= -\rho A\omega_n^2 Y_n \\ -M_n' + Q_n &= -\rho I\omega_n^2 \Psi_n \end{aligned}\right\} \ldots\ldots\ldots\ldots [9]$$

We proceed to formulate the property of orthogonality of the principal modes of free vibration, using Rayleigh's method (9).

We multiply the first of Equations [9] by Y_m and the second of Equations [9] by Ψ_m, integrate over the length of the beam and obtain, after integration by parts

$$\left.\begin{aligned} -\rho A\omega_n^2 \int_0^l Y_n Y_m \, dx &= \int_0^l Q_n' Y_m \, dx = Q_n Y_m \Big]_0^l - \int_0^l Q_n Y_m' \, dx \\ -\rho I\omega_n^2 \int_0^l \Psi_n \Psi_m \, dx &= \int_0^l (-M_n' + Q_n)\Psi_m \, dx \\ &= -M_n \Psi_m \Big]_0^l + \int_0^l (M_n \Psi_m + Q_n \Psi_m) \, dx \end{aligned}\right\} \ldots [10]$$

Interchanging the subscripts m and n, a similar set of equations is obtained. Adding the two equations of each set and subtracting the resulting first from the resulting second relationship, we find

$$\left.\begin{aligned} \rho(\omega_n^2 - \omega_m^2) \int_0^l (AY_nY_m + I\Psi_n\Psi_m) \, dx \\ = -Q_nY_m \Big]_0^l + Q_mY_n \Big]_0^l + M_n\Psi_m \Big]_0^l - M_m\Psi_n \Big]_0^l \\ - \int_0^l (M_n\Psi_m' - M_m\Psi_n') \, dx \\ + \int_0^l [Q_n(Y_m' - \Psi_m) - Q_m(Y_n' - \Psi_n)] \, dx \end{aligned}\right\} \ldots [11]$$

The integrated terms in Equation [11] vanish because of Conditions [6] and the two integrands in Equation [11] vanish because of Relations [2]. Thus we obtain the formulation of the property of orthogonality of the principal modes of free vibration

$$\int_0^l (Y_nY_m + r^2\Psi_n\Psi_m) \, dx = 0, \quad \omega_n \neq \omega_m \ldots\ldots [12]$$

Forced Vibrations

The solution of the general forced-vibration problem, specified by Equations [1], [3a], and [4a], will be sought in the form

$$\left.\begin{aligned} y(x, t) &= \sum_{i=1}^{4} g_{iy}(x) f_i(t) + s_y(x, t) \\ \psi(x, t) &= \sum_{i=1}^{4} g_{i\psi}(x) f_i(t) + s_\psi(x, t) \end{aligned}\right\} \ldots\ldots [13]$$

The eight functions g_{iy}, $g_{i\psi}$ correspond to the four functions g_i of (7). They are determined in such a way as to make the boundary conditions on the functions s_y and s_ψ homogeneous. This can be done for all possible combinations of boundary conditions, taking g_{iy} and $g_{i\psi}$ to be polynomials and choosing the coefficients accordingly. It is necessary only to compute those of the g_{iy}, $g_{i\psi}$ for which the corresponding $f_i(t)$ do not vanish.

If, as a first example, the boundary conditions are specified by

$$\begin{aligned} y(0) &= f_1(t) \\ M(0) &= f_2(t) \\ Q(l) &= f_3(t) \\ \psi(l) &= f_4(t) \end{aligned}$$

the functions g_{iy}, $g_{i\psi}$, which make the boundary conditions on s_y, s_ψ homogeneous, are calculated to be

$$\begin{aligned} g_{1y}(x) &= 1 \\ g_{1\psi}(x) &= 0 \\ g_{2y}(x) &= 0 \\ g_{2\psi}(x) &= (l - x)/EI \\ g_{3y}(x) &= x/Ak'G \\ g_{3\psi}(x) &= 0 \\ g_{4y}(x) &= x/l \\ g_{4\psi}(x) &= 1 \end{aligned}$$

If, in the exceptional case, at both ends of the beam time-dependent moments and shears are specified by

$$\begin{aligned} Q(0) &= f_1(t) \\ M(0) &= f_2(t) \\ Q(l) &= f_3(t) \\ M(l) &= f_4(t) \end{aligned} \quad \ldots [10]$$

the functions g_{iy}, $g_{i\psi}$ are found to be

$$\begin{aligned} g_{1y}(x) &= -x^2/2lAk'G \\ g_{1\psi}(x) &= -1/Ak'G \\ g_{2y}(x) &= -x^2/4EI \\ g_{2\psi}(x) &= x^2/2lEI - x/EI \\ g_{3y}(x) &= 0 \\ g_{3\psi}(x) &= 2x^2/Ak'Gl^2 - 3x^2/Ak'Gl^2 \\ g_{4y}(x) &= 0 \\ g_{4\psi}(x) &= -x^2/EIl^2 + x^2/EIl \end{aligned}$$

The remaining problem consists in finding $s_y(x, t)$ and $s_\psi(x, t)$ from the differential equations

$$\left.\begin{aligned}
&\frac{k'G}{\rho}\left(\sum_{i=1}^{4} g_{iy}''f_i - \sum_{i=1}^{4} g_{i\psi}'f_i\right) + \frac{k'G}{\rho}(s_y'' - s_\psi') \\
&\qquad + q/\rho A = \sum_{i=1}^{4} g_{iy}\ddot{f}_i + \ddot{s}_y \\
&\frac{E}{\rho}\sum_{i=1}^{4} g_{i\psi}''f_i + \frac{E}{\rho}s_\psi'' \\
&+ \frac{k'G}{\rho r^2}\left(\sum_{i=1}^{4} g_{iy}'f_i - \sum_{i=1}^{4} g_{i\psi}f_i\right) + \frac{k'G}{\rho r^2}(s_y' - s_\psi) \\
&\qquad + M_a/\rho I = \sum_{i=1}^{4} g_{i\psi}\ddot{f}_i + \ddot{s}_\psi
\end{aligned}\right\} \ldots [14]$$

the boundary conditions

$$B_i = 0, \quad i = 1, 2, 3, 4 \ldots\ldots\ldots\ldots [15]$$

and the initial conditions

$$\left.\begin{aligned}
s_y(x,0) &= y_0(x) - \sum_{i=1}^{4} g_{iy}(x)f_i(0) \\
s_\psi(x,0) &= \psi_0(x) - \sum_{i=1}^{4} g_{i\psi}(x)f_i(0) \\
\dot{s}_y(x,0) &= \dot{y}_0(x) - \sum_{i=1}^{4} g_{iy}(x)\dot{f}_i(0) \\
\dot{s}_\psi(x,0) &= \dot{\psi}_0(x) - \sum_{i=1}^{4} g_{i\psi}(x)\dot{f}_i(0)
\end{aligned}\right\} \ldots\ldots [16]$$

We seek a solution in the form

$$\left.\begin{aligned}
s_y(x,t) &= \sum_{n=1}^{\infty} Y_n(x)\,T_n(t) \\
s_\psi(x,t) &= \sum_{n=1}^{\infty} \Psi_n(x)\,T_n(t)
\end{aligned}\right\} \ldots\ldots [17]$$

assuming[6] that the principal modes form a complete set.

To find $T_n(t)$ we expand first

$$\left.\begin{aligned}
g_{iy} &= \sum_{n=1}^{\infty} G_{in}\,Y_n \\
g_{i\psi} &= \sum_{n=1}^{\infty} G_{in}\,\Psi_n
\end{aligned}\right\} \ldots\ldots [18]$$

Multiplication of the first of Equations [18] by Y_m, of the second of Equations [18] by $r^2\Psi_m$, addition and integration over the length of the beam results, in view of Equation [12], in

$$G_{in} = \frac{\int_0^l (g_{iy}Y_n + r^2 g_{i\psi}\Psi_n)\,dx}{\int_0^l (Y_n^2 + r^2\Psi_n^2)\,dx} \ldots\ldots [19]$$

It may be observed that it is sufficient for the coefficients G_{in}, in the first and second of Equations [18], to be the same.

We expand further

$$\left.\begin{aligned}
\frac{k'G}{\rho}(g_{iy}'' - g_{i\psi}') &= \sum_{n=1}^{\infty} G_{in}^{*}Y_n \\
\frac{E}{\rho}g_{i\psi}'' + \frac{k'G}{\rho r^2}(g_{iy}' - g_{i\psi}) &= \sum_{n=1}^{\infty} G_{in}^{*}\Psi_n
\end{aligned}\right\} \ldots [20]$$

Operations similar to those on Equations [18] and again with the application of Equation [12] yield

$$G_{in}^{*} = \frac{\int_0^l \left\{\frac{k'G}{\rho}(g_{iy}'' - g_{i\psi}')Y_n + \left[\frac{E}{\rho}g_{i\psi}'' + \frac{k'G}{\rho r^2}(g_{iy}' - g_{i\psi})\right] r^2\Psi_n\right\} dx}{\int_0^l (Y_n^2 + r^2\Psi_n^2)\,dx} \ldots [21]$$

Also, we expand the applied time-dependent loads and moments

$$\left.\begin{aligned}
q/\rho A &= \sum_{n=1}^{\infty} Q_n(t)Y_n(x) \\
M_a/\rho I &= \sum_{n=1}^{\infty} Q_n(t)\Psi_n(x)
\end{aligned}\right\} \ldots\ldots [22]$$

In the same manner as in the Expansions [18] and [20] we obtain the (time-dependent) coefficient in Equations [22]

$$Q_n = \frac{\int_0^l \left(\frac{q}{\rho A}Y_n + \frac{M_a r^2}{\rho I}\Psi_n\right) dx}{\int_0^l (Y_n^2 + r^2\Psi_n^2)\,dx} \ldots [23]$$

Thus each term in Equations [14] is an infinite series. Equating the nth terms we obtain

$$\left.\begin{aligned}
&\sum_{i=1}^{4} G_{in}^{*}Y_n f_i - \omega_n^2 Y_n T_n + Q_n Y_n \\
&\qquad = \sum_{i=1}^{4} G_{in}Y_n\ddot{f}_i + \ddot{T}_n Y_n \\
&\sum_{i=1}^{4} G_{in}^{*}\Psi_n f_i - \omega_n^2\Psi_n T_n + Q_n\Psi_n \\
&\qquad = \sum_{i=1}^{4} G_{in}\Psi_n\ddot{f}_i + \ddot{T}_n\Psi_n
\end{aligned}\right\} \ldots [24]$$

where use has been made of Equations [9].

Dividing the first Equation [24] by Y_n and the second by Ψ_n, there result two identical equations on T_n

$$\ddot{T}_n + \omega_n^2 T_n = -\sum_{i=1}^{4} G_{in}\ddot{f}_i + \sum_{i=1}^{4} G_{in}^{*}f_i + Q_n = P_n(t) \ldots [25]$$

the solution being

[6] This assumption could be justified, by generalising the proofs of completeness given by Courant and Hilbert (10) and by Kemble (11) to the case of two dependent variables.

$$T_n = A_n \cos \omega_n t + B_n \sin \omega_n t + \frac{1}{\omega_n} \int_0^t P_n(\tau) \sin \omega_n (t - \tau) d\tau \quad [26]$$

The constants of integration A_n and B_n are determined from the Initial Conditions [16].

Expanding the initial displacements in a series of principal modes

$$\left.\begin{aligned} y_0(x) &= \sum_{n=1}^{\infty} C_n Y_n \\ \psi_0(x) &= \sum_{n=1}^{\infty} C_n \Psi_n \end{aligned}\right\} \quad [27]$$

as well as the initial velocities

$$\left.\begin{aligned} \dot{y}_0(x) &= \sum_{n=1}^{\infty} D_n Y_n \\ \dot{\psi}_0(x) &= \sum_{n=1}^{\infty} D_n \Psi_n \end{aligned}\right\} \quad [28]$$

the expressions for the coefficients C_n and D_n are determined by making use of Equation [12]

$$C_n = \frac{\int_0^l (y_0 Y_n + r^2 \psi_0 \Psi_n)\, dx}{\int_0^l (Y_n^2 + r^2 \Psi_n^2)\, dx} \quad [29]$$

$$D_n = \frac{\int_0^l (\dot{y}_0 Y_n + r^2 \dot{\psi}_0 \Psi_n)\, dx}{\int_0^l (Y_n^2 + r^2 \Psi_n^2)\, dx} \quad [30]$$

Substitution of Equations [27] and [28] in Equations [16] results in

$$\left.\begin{aligned} T_n(0) + \sum_{i=1}^{4} G_{in} f_i(0) &= C_n \\ \dot{T}_n(0) + \sum_{i=1}^{4} G_{in} \dot{f}_i(0) &= D_n \end{aligned}\right\} \quad [31]$$

From Equation [26] we have

$$\left.\begin{aligned} T_n(0) &= A_n \\ \dot{T}_n(0) &= \omega_n B_n \end{aligned}\right\} \quad [32]$$

Thus

$$\left.\begin{aligned} A_n &= C_n - \sum_{i=1}^{4} G_{in} f_i(0) \\ B_n &= \frac{1}{\omega_n} \left[D_n - \sum_{i=1}^{4} G_{in} \dot{f}_i(0) \right] \end{aligned}\right\} \quad [33]$$

This completes the formal solution of the problem.

Acknowledgment

The author wishes to express his gratitude to Prof. R. D. Mindlin of Columbia University for help and advice in the preparation of this paper.

BIBLIOGRAPHY

1 "On the Correction for Shear of the Differential Equation for Transverse Vibrations of Prismatic Bars," by S. Timoshenko, *Philosophical Magazine*, series 6, vol. 41, 1921, pp. 744–746.

2 "Transverse Impact of Long Beams, Including Rotatory Inertia and Shear Effects," by M. A. Dengler and M. Goland, Proceedings of the First U. S. National Congress of Applied Mechanics, 1952, pp. 179–186.

3 "On Traveling Waves in Beams," by R. W. Leonard and B. Budiansky, NACA Technical Note 2874, 1953.

4 "Influence of Rotatory Inertia and Shear on Flexural Motion of Isotropic, Elastic Plates," by R. D. Mindlin, Journal of Applied Mechanics, Trans. ASME, vol. 73, 1951, p. A-31.

5 "A One-Dimensional Theory of Compressional Waves in an Elastic Rod," by R. D. Mindlin and G. Herrmann (Office of Naval Research Project NR-064-388, Contract Nonr-266(09)), Technical Report No. 1, September, 1951. Also published in Proceedings of the First U. S. National Congress of Applied Mechanics, Chicago, Ill., 1951.

6 "Forced Motions of Elastic Rods," by G. Herrmann (Office of Naval Research Project NR-064-388, Contract Nonr-266(09)), Technical Report No. 4, February, 1953. Also published in Journal of Applied Mechanics, Trans. ASME, vol. 76, 1954, pp. 221–224.

7 "Beam Vibrations With Time-Dependent Boundary Conditions," by R. D. Mindlin and L. E. Goodman, Journal of Applied Mechanics, Trans. ASME, vol. 72, 1950, p. 377.

8 "Vibration Problems in Engineering," by S. Timoshenko, D. Van Nostrand Company, Inc., New York, N. Y., second edition, 1937, pp. 337–338.

9 "Theory of Sound," by Lord Rayleigh, Dover Publications, New York, N. Y., second edition, vol. 1, 1945, p. 262.

10 "Methoden der Mathematischen Physik," by R. Courant and D. Hilbert, Julius Springer, Berlin, Germany, vol. 1, 1931, p. 368.

11 "The Fundamental Principles of Quantum Mechanics," by E. Kemble, McGraw-Hill Book Company, Inc., New York, N. Y., 1937, p. 132.

The Stress Problem of Vibrating Compressor Blades

By JAN R. SCHNITTGER,[1] FINSPONG, SWEDEN

In order to demonstrate the general nature of the actual vibrations of compressor and turbine blades, the author undertakes a simplified analysis in which a single stiff blade, with one translational and one pitching mode, is studied. It is shown that all problems of stress in vibrating compressor blades whether they arise from forced or self-sustained vibrations may be related to the magnitude of finite mechanical or aerodynamic disturbances.

Nomenclature

The following nomenclature is used in the paper:

A_x = area of cross section of airfoil
b = semichord of airfoil
$C_L = \dfrac{L}{4bq}$ = lift coefficient
C^*_L = jump in lift coefficient at stall at dynamic conditions
$C_M = \dfrac{M}{4b^2q}$ = moment coefficient
C^*_M = jump in moment coefficient at stall at dynamic conditions
$C_h = m\omega_h^2$ = spring constant of translational motion
$C_\alpha = I_\alpha\omega_\alpha^2$ = spring constant of pitching motion
$c = 2b$ = chord of airfoil
E = modulus of elasticity
F = real part of Theodorsen's function (1)[2]
F_L = aerodynamic reaction in equations of motion due to lift
F_M = aerodynamic reaction in equations of motion due to moment
$F_\sigma = k_h f_\sigma(k_h)$ = stress function due to horizontal velocity disturbance
$F_\beta = k_h f_\beta(k_h)$ = stress function due to angle-of-attack disturbance
$F_p = k_h f_p(k_h)$ = stress function due to mechanical disturbance
$F_{C(L)} = k_h f_{C(L)}(k_h)$ = stress function due to aerodynamic jump at stall
$f_\sigma = (h_0/b)/\sigma\alpha_i$ = amplitude response due to horizontal velocity disturbance $v = v_0(1 + \sigma e^{i\omega t})$
$f_\beta = (h_0/b)/\beta_0$ = amplitude response due to angle-of-attack disturbance $\beta = \beta_0 e^{i[\omega t - k(x-b)]}$
$f_p = (h_0/b)/(p_0/bq)$ = amplitude response due to mechanical disturbance $p = p_0 e^{i\omega t}$
g = acceleration due to gravity
$H = (h_0/b)$ = dimensionless translational deflection
h = translational deflection of center of torsion, positive downward
I_α = moment of inertia of airfoil about center of torsion per unit span
I_x = moment of inertia of cross section of airfoil with respect to neutral axis parallel with chord
$k = (\omega b)/v$ = dimensionless frequency of exciting force
$k_h = (\omega_h b)/v$ = dimensionless natural frequency in translation
$k_\alpha = (\omega_\alpha b)/v$ = dimensionless natural frequency in pitching
L = aerodynamic lift in center of torsion per unit span of airfoil
l = length of airfoil in spanwise direction
M = aerodynamic moment about center of torsion per unit span of airfoil
m = mass of airfoil per unit span
P = force on airfoil at tip
p = mechanical disturbing force per unit span of airfoil
$q = \dfrac{\rho v^2}{2}$ = dynamic pressure
$r_\alpha = \sqrt{\dfrac{I_\alpha}{m}}$ = radius of gyration of airfoil
$r_x = \sqrt{\dfrac{I_x}{A_x}}$ = radius of gyration of cross section of airfoil
s = maximum stress at root section of airfoil
t = time
= maximum thickness of airfoil
v = free-stream velocity
$v_{mtrl} = \sqrt{\dfrac{Eg}{\gamma}}$ = velocity of propagation of waves in solid material of blade
W_{MR} = work per cycle due to moment, positive when going into blade
W_{LR} = work per cycle due to lift, positive when going into blade
x = co-ordinate of dimensionless deflection, that is, $x = \alpha$, respectively, $x = h/b$
= co-ordinate of chordwise distance from leading edge
x_g = chordwise distance from leading edge of center of gravity of airfoil
x_p = chordwise distance from leading edge of center of torsion of airfoil
$x_\alpha = x_g - x_p$
$Z = r_x/t$ = ratio of radius of gyration r_x to maximum thickness t
α = angle of attack, counted from angle of static equilibrium α_i
α_i = initial angle of attack at static equilibrium (flow direction-chord direction)
α_0 = amplitude of angle of attack ($\alpha_i \pm \alpha_0$)
α_1 = angle of attack at which stall occurs when α is increasing

---

[1] Formerly Assistant Professor of Aeronautical Engineering, Massachusetts Institute of Technology, Cambridge, Mass.; presently with the STAL Company.

[2] Numbers in parentheses refer to the Bibliography at the end of the paper.

Contributed by the Applied Mechanics Division and presented at the Annual Meeting, New York, N. Y., November 28–December 3, 1954, of The American Society of Mechanical Engineers.

Discussion of this paper should be addressed to the Secretary, ASME, 29 West 39th Street, New York, N. Y., and will be accepted until April 11, 1955, for publication at a later date. Discussion received after the closing date will be returned.

Note: Statements and opinions advanced in papers are to be understood as individual expressions of their authors and not those of the Society. Manuscript received by ASME Applied Mechanics Division, May 22, 1953. Paper No. 54—A-21.

α_2 = angle of attack at which stall occurs when α is decreasing
β = variation of angle of attack of free stream flow
β_0 = amplitude of variation of angle of attack of free-stream flow
γ = coefficient of aerodynamic damping
δ = dimensionless change of aerodynamic reactions in separated flow at stall proportional to C^*_L, respectively, C^*_M, reference (2)
ϵ = small number $\ll 1$
$\kappa = \rho\frac{\pi b^2}{m}$ = ratio of mass of air contained in a cylinder with the chord as diameter per unit span to mass of airfoil per unit span
Λ = logarithmic damping
$\nu = k/k_h$ = ratio of exciting frequency to natural frequency of airfoil
ρ = density
σ = coefficient of free-stream velocity $v = v_0(1 + \sigma e^{i\omega t})$
ω = frequency radians per sec

Subscripts:

0 = maximum amplitude value
1 = in the part of cycle with increasing positive deflection
2 = in the part of cycle with decreasing positive deflection
g = center of gravity
h = in translational motion
i = initial
L = lift
M = moment
p = center of torsion
= in pitching motion
$(\dot{})$ = first derivative with respect to time
$(\ddot{})$ = second derivative with respect to time
$(')$ = apparent angle of attack
$(*)$ = discontinuity at stall condition

Introduction

The fatigue failures of the blades of advanced axial-flow compressors for aircraft engines are a serious problem. In the past, blade vibrations were attributed to external disturbances acting on the blades (forced vibrations). Recently some failures appeared to be connected with the separation phenomena on the blade surfaces at high aerodynamic loads (stall flutter). These separations can be reproduced for a single blade immersed in a uniform air stream. The arising vibrations are then self-sustained.

The actual cantilever blade of axial-flow compressors possesses an infinite number of degrees of freedom, though only the lowest bending and torsional mode usually cause any trouble. The cascading further increases the complexity. The influence of self-vibrating neighbor blades has been observed as modifications of those vibrations, which are exhibited by a single vibrating blade with two degrees of freedom in an otherwise fixed, two-dimensional cascade. Recent research makes it very likely that the whole phenomenon of stall changes still more, when the arrangement is a complete annular cascade, constituting a part of an axial-flow compressor. In this case, stall propagation along the cascade in the peripheral direction has been observed. Since this latter type of stall may be fairly independent of the motions of the individual blades, it is recognized that the distinction between forced vibrations caused by upstream wakes or flow disturbances, and the so-called stall at high angles of attack, may be unmotivated in the engineering case.

In order to show the general nature of the connected stress problem, the author has undertaken a simplified analysis in which a single, stiff blade with one translational and one pitching mode is studied.

This analysis shows the different nature of the dynamic stability of self-excited compressor blades in comparison with the well-known problem of classical, two-dimensional flutter of airplane wings.

The problem of the self-sustained vibrations has been formulated, however, in a form which coincides with that of the forced vibrations. From the viewpoint of the designer, therefore, the maximum stresses are proportional to the magnitude of certain disturbances and a series of similar stress functions F_σ, F_β, F_{p_i} and $F_{C(L)}$. It is believed that the formulation of the stress problem in this way may prove useful for further research into the actual engineering practice.

Equations of Motion

For the two-dimensional blade system of Fig. 1 the equations of motion may be written

$$\left.\begin{aligned} m\ddot{h} + (x_g - x_p)m\ddot{\alpha} + C_h h &= L \\ (x_g - x_p)m\ddot{h} + I_\alpha\ddot{\alpha} + C_\alpha\alpha &= M \end{aligned}\right\} \quad \ldots\ldots [1]$$

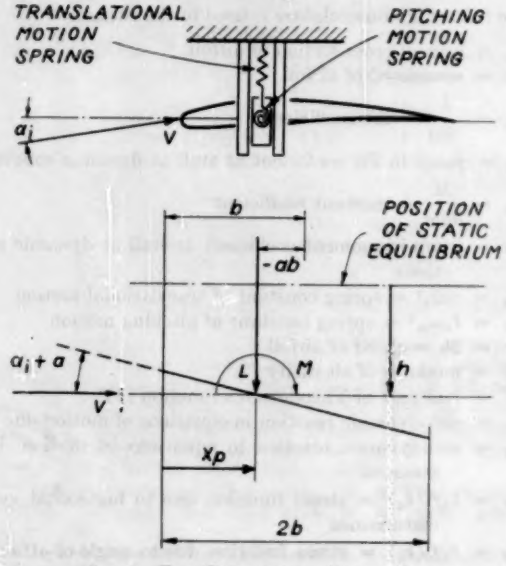

Fig. 1 Two-Dimensional Blade System

The terms on the left-hand side of Equations [1] contain the inertia and elastic forces of the two-dimensional system in translational (h) and pitching (α) motion. L and M are the aerodynamic reactions on the airfoil referred to the center of torsion at x_p. No material damping is considered for the present.

Introducing

$$\left.\begin{aligned} \frac{C_h}{m} &= \omega_h^2 \qquad x_g - x_p = x_\alpha \\ \frac{C_\alpha}{I_\alpha} &= \omega_\alpha^2 \qquad I_\alpha = mr_\alpha^2 \\ \kappa &= \frac{\rho\pi b^2}{m} \quad \text{mass ratio} \\ k &= (\omega b)/v \quad \text{dimensionless frequency} \\ \alpha_i &= \text{initial angle of attack} \end{aligned}\right\} \quad \ldots [2]$$

It is obtained

$$\left.\begin{aligned} \ddot{h} + x_\alpha\ddot{\alpha} + \omega_h^2 h &= \kappa F_L \\ \frac{x_\alpha}{r_\alpha^2}\ddot{h} + \ddot{\alpha} + \omega_\alpha^2\alpha &= \kappa F_M \end{aligned}\right\} \quad \ldots [3]$$

In turbomachinery design the mass ratio

$$\kappa = \frac{\rho \pi b^2}{m}$$

equals about 0.002 (static sea-level condition of axial-flow compressors). The aerodynamic reactions κF_L and κF_M are extremely small in comparison to the inertia and elastic forces of the blade. The typical change of modes into one coupled motion at a common frequency (classical flutter) (1, 3) is unlikely to occur. This is demonstrated by Fig. 2 which is cross-plotted from reference (1), graph I-A. It shows how the reduced velocity $v/\omega b$, at which classical flutter starts, varies with the mass ratio κ. The very

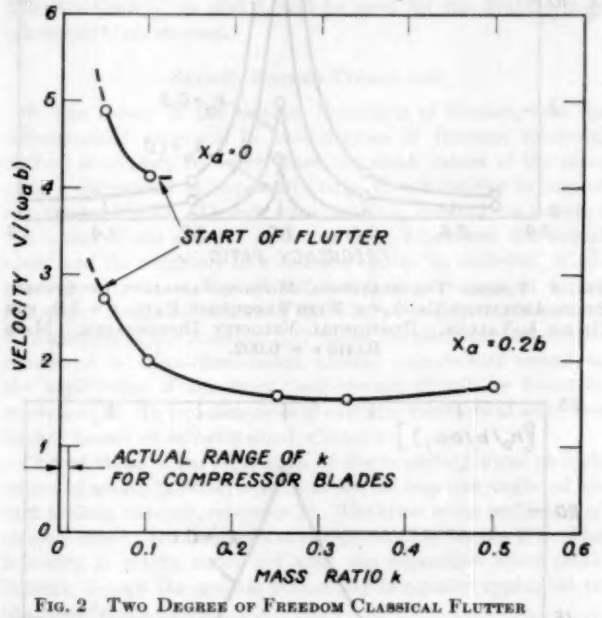

FIG. 2 TWO DEGREE OF FREEDOM CLASSICAL FLUTTER
(Reduced velocity $v/\omega_\alpha b$ is plotted as function of the mass ratio $\kappa = \pi\rho b^2/m$). Fixed variables of diagram are $\omega_\alpha/\omega_h = 5$, center of torsion x_p at 30 per cent chord, radius of gyration $r_\alpha = 0.5$. Two different values of location of center of gravity x_g are shown.)

small κ of current axial-compressor design thus corresponds to exceedingly large reduced velocities $v/\omega b$. The modes of vibration and their frequencies accordingly can be determined with sufficient degree of accuracy by solving the homogeneous part of the System [3].

For the solution it is assumed

$$\left.\begin{aligned} \alpha &= \alpha_0 e^{i\omega t} \\ h &= h_0 e^{i\omega t} \end{aligned}\right\} \quad \ldots\ldots\ldots\ldots\ldots [4]$$

This gives the frequency equation

$$\omega^4 + \frac{\omega_h^2 + \omega_\alpha^2}{1 - \left(\frac{x_\alpha}{r_\alpha}\right)^2}\omega^2 + \frac{\omega_h^2\omega_\alpha^2}{1 - \left(\frac{x_\alpha}{r_\alpha}\right)^2} = 0 \ldots\ldots [5]$$

Equation [5] gives directly two frequency values ω_1 and ω_2 and two amplitude ratios $[(h_0/r_\alpha)/\alpha_0]_1$ and $[(h_0/r_\alpha)/\alpha_0]_2$. Some results are given in Table 1. (Note r_α/b equals about 0.5 for compressor blades.)

The results of Table 1 may be interpreted in the following way:

1 In general, the free modes of the system consist of both translational and angular deflections due to the inertia coupling (which exists when $x_\alpha \neq 0$). A linear transformation defines the

TABLE 1 FREQUENCY AND AMPLITUDE RATIO OF NORMAL MODES OF A TWO-DIMENSIONAL BLADE SYSTEM

Data are given for three ratios of ω_α/ω_h	(ω_α/ω_h) = 4	6	8
ω_1/ω_h for $x_\alpha/r_\alpha = 0.4$	0.995	0.997	1.000
ω_1/ω_h for $x_\alpha/r_\alpha = 0.8$	0.980	0.993	0.993
ω_2/ω_α for $x_\alpha/r_\alpha = 0.4$	1.097	1.094	1.093
ω_2/ω_α for $x_\alpha/r_\alpha = 0.8$	1.70	1.68	1.67
$[(h_0/r_\alpha)/\alpha_0]_1$ for $x_\alpha/r_\alpha = 0.4$	37.6	60.7	746.0
$[(h_0/r_\alpha)/\alpha_0]_1$ for $x_\alpha/r_\alpha = 0.8$	19.2	56.8	56.8
$[(h_0/r_\alpha)/\alpha_0]_2$ for $x_\alpha/r_\alpha = 0.4$	−0.42	−0.41	−0.40
$[(h_0/r_\alpha)/\alpha_0]_2$ for $x_\alpha/r_\alpha = 0.8$	−0.82	−0.81	−0.80

relation between these normal modes and those of the h and α-motion.

2 The degree of inertia coupling is usually small. For NACA 4-digit-series solid blades, the center of torsion appears at x_p equal to 33 to 35 per cent of the chord and the center of gravity x_g at 42 per cent chord. These figures correspond to about 90 per cent of the lower degree of coupling in Table 1 and imply that the free mode of the essentially pitching motion occurs around a point between x_p and x_g. The pure translational motion is very slightly distorted.

Therefore it will be a reasonable step to investigate the case of pure translational motion and a case of pitching motion around a center of torsion in the region of 35 to 45 per cent chord.

The System [3] may thus be written as two independent equations

$$\ddot{h} + \omega_h^2 = \kappa F_L \ldots\ldots\ldots\ldots\ldots [6]$$

$$\ddot{\alpha} + \omega_\alpha^2 = \kappa F_M \ldots\ldots\ldots\ldots\ldots [7]$$

FORCED VIBRATIONS

When a rotating blade row passes through the wakes of upstream objects as blades and struts or through the unsymmetrical flow of divided compressor or turbine intakes, this gives rise to periodic disturbances.

One may possibly express these disturbances as periodic, sinusoidal variations of magnitude v and direction α_i of the free-stream velocity v entering the actual blade row.

For the present the only aerodynamic theory available to treat this case is based on the rather limited premises of classical theory (1, 3), namely, incompressible potential flow around a single airfoil executing a small harmonic motion in the flow leaving behind plane infinitely extended wakes. The problem is divided into two parts. The first consists in finding the aerodynamic reactions to the motion of the airfoil. This is the familiar problem of classical theory (3). The second part deals with the problem of finding the aerodynamic lift and moment acting on a fixed airfoil when the magnitude or direction of the flow velocity varies in front of the airfoil (4, 5).

The most common failure of compressor blades seemingly is due to forced translational motion. Therefore the present investigation concentrated on the pure translational motion.

Consider the two-dimensional blade system at an initial angle of attack α_i and an instantaneous velocity v and restrained so that only pure translational motions are possible, Equation [6]. The reaction F_L then contains both the aerodynamic damping force and the external disturbances (which are of aerodynamic or mechanical nature). These latter will in each case be due to one of the following periodic processes:

Case I. Variation of the magnitude of the free-stream velocity v (horizontal gusts)

$$v = v[1 + \sigma e^{i\omega t}] \ldots\ldots\ldots\ldots\ldots [8]$$

Case II. Variation of the angle of attack of the free-stream velocity v (vertical gusts)

$$\beta = \beta_0 e^{i[\omega t - k(x-b)]} \quad [9]$$

Case III. A mechanical force acting per unit span of the airfoil as a result of unbalances of rotor

$$p = p_0 e^{i\omega t} \quad [10]$$

The solution of the vibration problem by means of Greenberg's expressions is described in the author's paper (2).

The amplitude response may be expressed in the form of the dimensionless amplitude $H_0 = h_0/b$.

The general form of the amplitude response to the foregoing external disturbances is found to be as follows:

Case I

$$H_0/\sigma\alpha_i = f_\sigma(k_h, \kappa, \nu) \quad [11]$$

Case II

$$H_0/\beta_0 = f_\beta(k_h, \kappa, \nu) \quad [12]$$

Case III

$$H_0/(p_0/bq) = f_p(k_h, \kappa, \nu) \quad [13]$$

To the left in Equations [11], [12], and [13] the dimensionless amplitude $H_0 = h_0/b$ is related to the magnitude of the amplitude of actual disturbance, that is, the velocity variation $\pm v_0$ at the angle of attack α_i, the angle of attack variation $\pm\beta_0$, and the mechanical force $\pm p_0$ per unit span per unit "dynamic" pressure force $bq = b(\rho v^2/2)$, respectively. The amplitude responses are functions of the natural dimensionless frequency $k_h = (\omega_h b)/v$, the mass ratio $\kappa = (\rho\pi b^2)/m$, and the ratio $\nu = k/k_h$ of the exciting

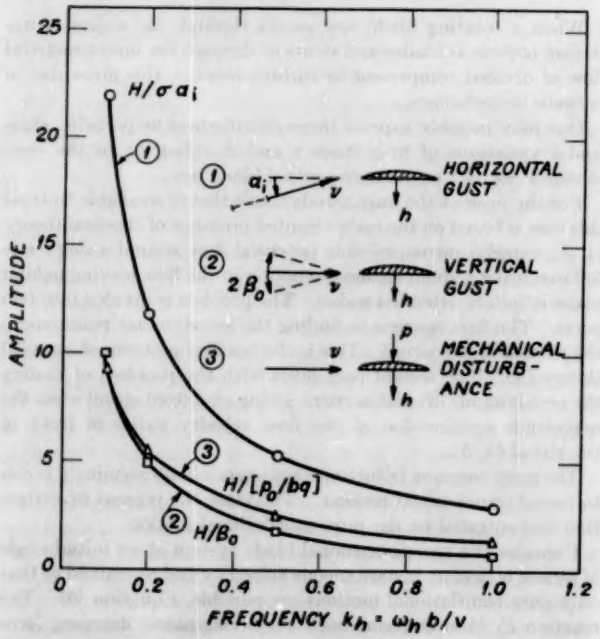

1, Horizontal velocity disturbance
$v = v_0[1 + \sigma e^{i\omega t}]$
2, Vertical velocity disturbance (angle-of-attack variation)
$\beta = \beta_0 e^{i[\omega t - k(x-b)]}$
3, Mechanical disturbance
$p = p_0 e^{i\omega t}$

FIG. 3 FORCED TRANSLATIONAL MOTION—VARIATION OF STEADY-STATE AMPLITUDE $H = h_0/b$ WITH THE FREQUENCY k_h

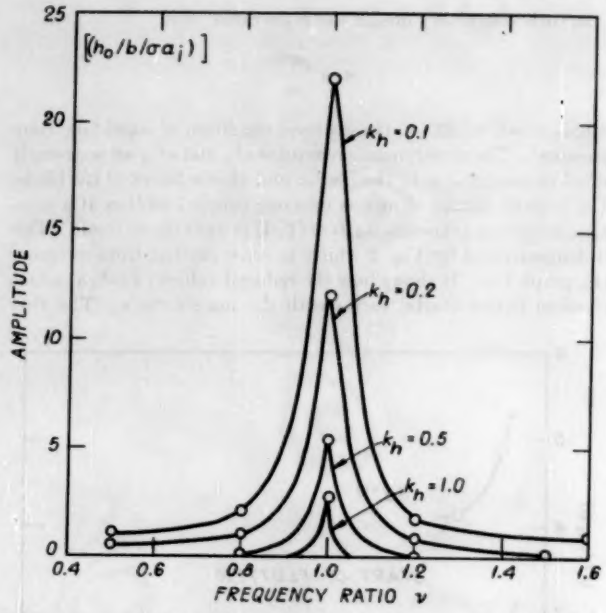

FIG. 4 FORCED TRANSLATIONAL MOTION—VARIATION OF STEADY-STATE AMPLITUDE $(h_0/b)/\sigma\alpha_i$ WITH FREQUENCY RATIO $\nu = k/k_h$ FOR GIVEN k_h-VALUES. HORIZONTAL VELOCITY DISTURBANCE. MASS RATIO $\kappa = 0.002$.

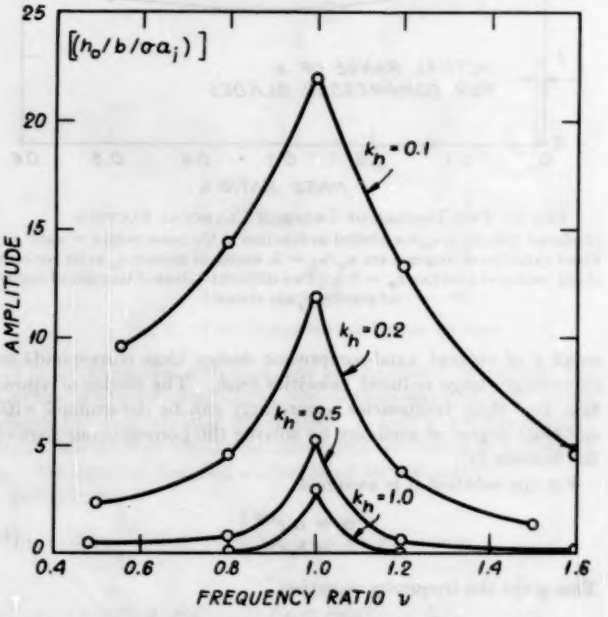

FIG. 5 FORCED TRANSLATIONAL MOTION—VARIATION OF STEADY-STATE AMPLITUDE $(h_0/b)/\sigma\alpha_i$ WITH FREQUENCY RATIO $\nu = k/k_h$ FOR GIVEN k_h-VALUES. HORIZONTAL VELOCITY DISTURBANCE. MASS RATIO $\kappa = 0.02$.

frequency $k = (\omega b)/v$ to the natural frequency $k_h = (\omega_h b)/v$.

The maximum amplitude of any system is obtained when the exciting frequency is tuned to the system, that is, $\nu = 1 + \epsilon$, where ϵ is a small number $\ll 1$.

These cases have been computed and are given in Fig. 3 as functions of k_h, ν being equal to $1 + \epsilon$ and the value of κ varying between 0.002 and 0.02, the exact value having a very small influence at the resonance condition.

It is found that quite generally speaking there is a general increase in the amplitude response with decreasing k_h (that is, for increasing velocity at a given system or decreasing elastic stiffness for a given velocity).

The situation is changed when the frequencies are not tuned. The amplitude response in this case is strongly influenced by the mass ratio, the resonance peak being considerably sharper for the heavier blade (small κ). The resonance curves of case I (Equation [11]) are shown for $\kappa = 0.002$ and 0.02 in Fig. 4 and Fig. 5, respectively. They are quite similar for the other two cases.

The foregoing results constitute the familiar problem of forced vibrations. Resonance occurs whenever any integral multiple of the rotor speed equals the natural frequency of the blade system. The functions f_σ, f_β, and f_p will be used for the evaluation of maximum blade stresses.

Self-Sustained Vibrations

It was shown in the section, Equations of Motion, that the self-sustained vibration in two degrees of freedom (classical flutter) is unlikely to occur, since the small values of the mass ratio κ correspond to impossibly large flow velocities in case of compressor blades. Though some coupling effects both between the modes of one and the same blade, and between the actual blade and its neighbors in a cascade cannot be excluded, it appears possible to explain all self-sustained vibrations in turbomachinery design as motions of essentially one degree of freedom. A discussion of the observed differences between the two-dimensional and the three-dimensional, annular cascade with respect to the implication of the word "self-sustained" will be found in reference (6). In two-dimensional cascades there are at least two known causes of self-sustained vibrations.

One of these is the separation of the boundary layer at high angles of attack (also separation at low or negative angles of attack is likely to occur, reference 2). The other is the oscillation of shock waves at the incidence of compressibility burble (7). The following is chiefly concerned with the separation effect (stall flutter), though the general philosophy is equally applicable to the other (shock flutter).

Recent research (2, 8) has shown that at the separation of the boundary layer there occur changes of the aerodynamic forces so as to feed energy into the blade system. This appears now to be possible both in the translational and the pitching motion.

The simplest way to recognize this is to perform the integrations

$$W_{MR} = \oint M d\alpha \quad [14]$$

$$W_{LR} = \oint L dh \quad [15]$$

It has been found (8) that the aerodynamic reactions retain their usual damping character as they occur in unseparated flow, when the angle of attack is sufficiently remote from the stalling angle, that is, when the angle is either small or very large (sufficiently exceeding the stalling angle). On the other hand, close to the stalling angle the reverse is true: that is, the integrals W_{MR} and W_{LR} form positive values, when the initial angle of attack is close to the stalling angle and the amplitudes are limited (2, 8). Outside a limited region of amplitudes the damping character of the aerodynamic reactions will appear at an increasing amount with increasing amplitudes. Therefore it is conceivable that there exist amplitudes for which

$$W_{MR} = \oint M d\alpha \equiv 0$$

$$W_{LR} = \oint L dh \equiv 0$$

In the translational case the actual angle of attack will be the initial angle of attack α_i plus an apparent angle of attack $\alpha' = h/v$, the amplitude of α' being determined by the translational mode h, if one assumes nearly sinusoidal motion, approximated by $h = h_0 e^{i\omega t}$. The oscillatory motions, for which $W_{MR} \equiv 0$, respectively, $W_{LR} \equiv 0$, are referred to as limit cycles (2, 9). For each completed cycle the aerodynamic reactions in a pitching or a translational motion put a positive amount of work into the blade, when its angle of attack passes forward and back again through the stall region. Since periodic disturbances in the case of forced vibrations also deliver a work corresponding to the energy destroyed in damping, one may conceive that both self-sustained and forced vibrations can be looked upon from the same general aspect. The essential difference between the external disturbances and those connected with the stall is connected with their dependence of the motion of the blade (α, $\dot{\alpha}$, h, $\dot{h}$) and their relation to the aerodynamic conditions, that is, the initial angle of attack α_i, the frequency $k_\alpha = (\omega_\alpha b)/v$, respectively, $k_h = (\omega_h b)/v$, the Mach number, the cascade arrangement, and so on (2).

The author has attempted a rationalization of the behavior of the aerodynamic reactions at stall, Figs. 6 and 7. The following assumptions were made:

(*a*) A certain jump in the aerodynamic lift C^*_L and the aerody-

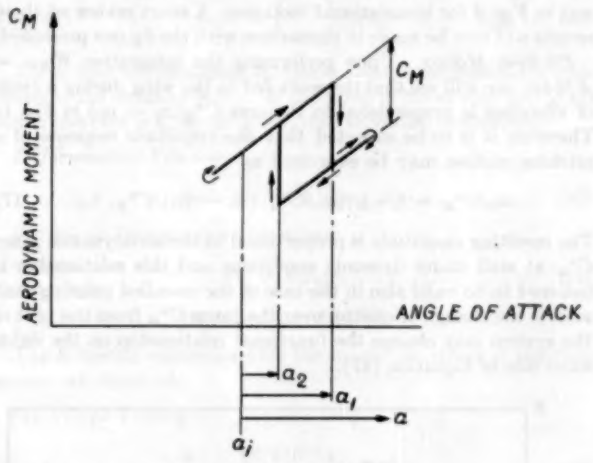

Fig. 6 Pitching Motion

(That part of the aerodynamic moment connected with separation of flow is expressed as an instantaneous change C^*M. This change occurs at different α depending on whether α increases or decreases.)

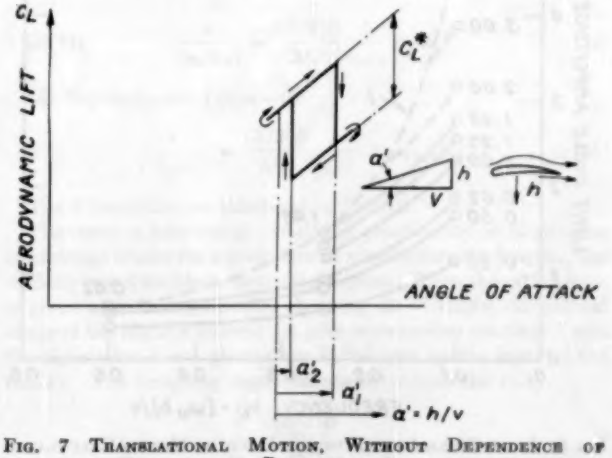

Fig. 7 Translational Motion, Without Dependence of Position

(That part of aerodynamic lift connected with separation of flow is expressed as an instantaneous change C^*_L; this change is dependent on the apparent angle of attack $\alpha' = h/v$ as sketched and occurs at different α' depending on whether α' increases or decreases.)

namic moment C^*_M occurs at an angle of attack equal to α_1 radians above the initial angle of attack α_i, at which latter angle the system is at a state of static equilibrium. Because of hysteresis there will be a delay of the jump C^*_L or C^*_M at decreasing angles of attack (return stroke) so the second jump occurs at an angle $\alpha_2 < \alpha_1$.

(*b*) For the aerodynamic damping forces (which according to the physical situation work mostly in unstalled flow) it is assumed in a first approximation that the classical expressions (3) for the forces in phase with the velocity of the motions still are valid.

The foregoing assumptions lead to the general differential equation in dimensionless quantities

$$\ddot{x} + 2\gamma\dot{x} + x = \begin{cases} 0 \\ \delta \end{cases} \quad \ldots\ldots\ldots\ldots\ldots\ldots [16]$$

Here the coefficient γ corresponds to the aerodynamic damping force and δ is proportional to the jump C^*_M, or C^*_L, depending upon whether pitching or translational motions are studied. The author solved Equation [16] by resorting to the so-called phase plane of nonlinear mechanics (9).

Some practical results are given in Fig. 8 for pitching motions and in Fig. 9 for translational motions. A short review of these results will now be made in connection with the figures presented.

Pitching Motion. Upon performing the integration $W_{MR} = \oint M d\alpha$, one will see that the work fed to the wing during a cycle of vibration is proportional to the area $C^*_M(\alpha_1 - \alpha_2)$ in Fig. 6. Therefore it is to be expected that the amplitude response of a pitching motion may be expressed as

$$\alpha_0/C^*_M = f_{C^*(M)}[\alpha_i/C^*_M, (\alpha_1 - \alpha_2)/C^*_M, k_\alpha] \ldots [17]$$

The resulting amplitude is proportional to the aerodynamic jump C^*_M at stall under dynamic conditions and this relationship is believed to be valid also in the case of the so-called rotating stall even if the change of control over the jump C^*_M from the part of the system may change the functional relationship on the right-hand side of Equation [17].

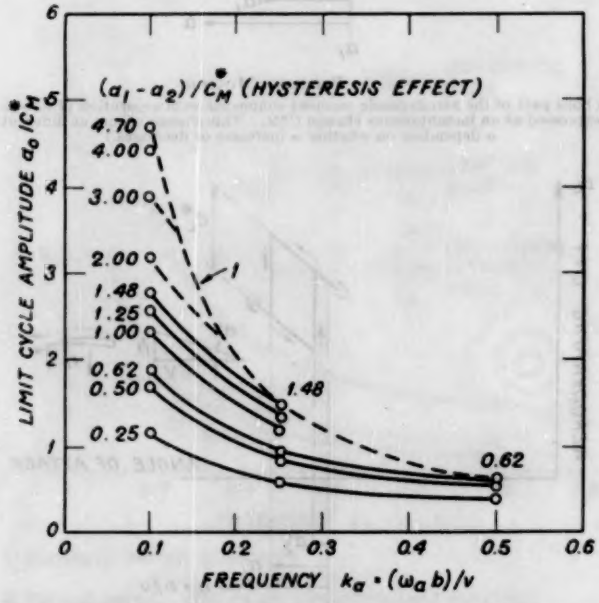

FIG. 8 LIMIT CYCLE AMPLITUDE OF A PITCHING MOTION CALCULATED AS FUNCTION OF FREQUENCY AND HYSTERESIS EFFECT

$\alpha_i = 0$, $\kappa = 0.002$, $r_\alpha/b = 0.5$, $x_p = 35$ per cent chord.

(The important quantity is the assumed jump C^*_M of the aerodynamic moment. Amplitude and hysteresis effect are both expressed in terms of this jump. 1 = locus of maximum possible hysteresis effect.)

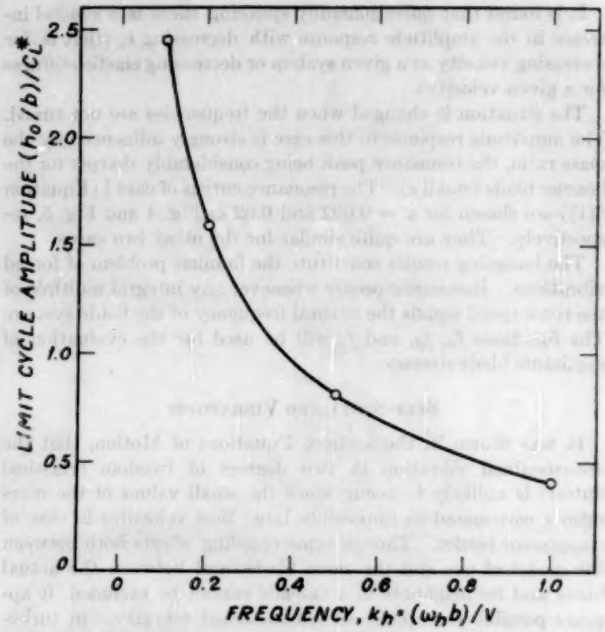

FIG. 9 LIMIT CYCLE AMPLITUDE OF A TRANSLATIONAL MOTION CALCULATED AS A FUNCTION OF FREQUENCY AND WITH $\kappa = 0.002$ AND HYSTERESIS EFFECT EQUAL TO ZERO $\alpha'_1 = \alpha'_2$ AND DISTANCE FROM JUMP EQUAL TO ZERO $\alpha'_1 = 0$

(This latter condition implies a soft, self-excited flutter.)

The jump C^*_M and the hysteresis effect $(\alpha_1 - \alpha_2)/C^*_M$ together describe a rationalized behavior of the aerodynamic reactions in the stall region for all k_α-values. In cases of small natural frequencies $k_\alpha = (\omega_\alpha b)/v$ they constitute a quite realistic concept (2). The variable α_i/C^*_M describes the position of static equilibrium α_i with respect to the actual stalling angle $\alpha_i + \alpha_1$ (see Fig. 6). The dimensionless natural frequency k_α is an important variable. In the relationship of Equation [17] it controls the magnitude of the aerodynamic damping. However, it also can be shown that both C^*_M and $(\alpha_1 - \alpha_2/C^*_M$ are functions of k_α, but it still remains to collect more data on these relations. Equation [17] may then simultaneously be expressed as

$$\alpha_0 = \alpha_0(\alpha_i, k_\alpha) \ldots\ldots\ldots\ldots\ldots\ldots [18]$$

In Fig. 8 it is put $\alpha_i/C_M = 0$; $\kappa = 0.002$, $r_\alpha/b = 0.5$, and $x_p = 35$ per cent chord. It is apparent that the amplitude response α_0/C^*_M of the self-sustained vibration is similar to those forced by the external disturbances.

Translational Motion. It is possible to show that the integral $W_{ML} = \oint L dh$ corresponds to maximum amplitude when there is a zero phase lag in the apparent angle of attack $\alpha' = \dot{h}/v$ and the static equilibrium is close to stall. When this latter is exactly true, that is, when $\alpha_i = 0$ (see Fig. 7) then the system is self-excited in a rather rigorous sense (i.e., oscillations are set up for a very slightly disturbed initial state, soft flutter). This case has been calculated and is reproduced in Fig. 9 which shows the amplitude response $(h_0/b)/C^*_L$ as function of the frequency k_h. In general, however, the response has the form

$$h_0/b = f_{C^*(L)}(\alpha'_1/C^*_L, (\alpha_1' - \alpha_2')/C^*_L, k_h) \ldots [19]$$

The influence of cascading the actual blade may be a dependence of the reactions on the position h, that is, a variable of the form $\int \alpha dt$ enters in Equation [19].

The Stress Problem of Vibrating Compressor Blades

The amplitude response of the elementary blade system being known in terms of the magnitude of the disturbances, it is now possible to make an elementary investigation of the related stress problem of the vibrating cantilever blades in axial turbomachines.

Consider an elastic airfoil of uniform cross section of length l supported as a cantilever beam. Let the cross section have a width c corresponding to the chord and a maximum thickness t. Further, put I_x equal to the moment of inertia of the cross section with respect to the neutral axis parallel with the chord and let A_x be the area of the same cross section and put

$$r_x = \sqrt{\frac{I_x}{A_x}} = Zt$$

The constant Z in the formula $r_x = Zt$ varies with the type of cross section. The rectangular section $c \times t$ has $Z = \sqrt{3}/6 = 0.289$ and the elliptic cross section with the axes c and t has $Z = 1/4 = 0.25$.

As an introduction to the study of the problems of stress of vibrating turbomachine blades, an elementary discussion of pure bending vibrations in the foregoing airfoil will be made. It will be assumed that the cantilever blade is exposed to a uniform flow with the velocity v and an angle of attack α_i with respect to the chord direction. Next, suppose that the blade is subjected to the various disturbances in the previous sections on forced and self-sustained vibrations, and let it be assumed that the aerodynamic conditions at the tip of the blade are completely determining the amplitudes of the tip. It is obvious that this is only approximately true and the integrated reactions may make more correct reference section located somewhere around 75 per cent of the length from the root section. However, it merely means a slight change of a constant numerical value in the discussion which follows.

Assume a force P applied at the tip of the blade. This causes a maximum stress s in the root section

$$s = \frac{Pl/2}{I_x} \quad [20]$$

The deflection at the tip section is

$$h_0 = \frac{Pl^3}{3EI_x} \quad [21]$$

where E = modulus of elasticity.

Elimination of the product Pl gives

$$s = (3/2)E(t/c)\frac{h_0 c}{l^2} \quad [22]$$

The natural frequency may be written

$$\omega_k = \frac{\lambda^2}{l^2}\sqrt{\frac{Eg}{\gamma}}\sqrt{\frac{I_x}{A_x}} = \frac{\lambda^2}{l^2}\sqrt{\frac{Eg}{\gamma}}\, r_x$$

$$\omega_k = \frac{\lambda^2}{l^2}\sqrt{\frac{Eg}{\gamma}}\, Zt \text{ rad/sec} \quad [23]$$

The smallest of the eigenvalues λ equals 1.875 for a straight uniform beam. The factor $\sqrt{Eg/\gamma}$ is a material constant with the dimension of a velocity which can be shown to be the velocity of propagation of waves in the solid material. For convenience we will put

$$\sqrt{\frac{Eg}{\gamma}} = v_{mtrl} \quad [24]$$

It is obtained

$$\omega_k = \lambda^2 Z v_{mtrl}(t/c)\frac{c}{l^2} \quad [25]$$

Elimination of t/l^2 in Equations [22] and [25] gives

$$s = (3/2)E\frac{\omega_k h_0}{\lambda^2 Z v_{mtrl}}$$

and after a slight rearrangement and introduction of $k_k = (\omega_k b)/v$

$$s = \left[\frac{(3/2)E}{\lambda^2 Z}\right]\left(\frac{v}{v_{mtrl}}\right)[k_k(h_0/b)] \quad [26]$$

The functions (h_0/b) of the possible maximum amplitude when the system is in resonance with the various external disturbances are already known from the two preceding sections. Let them be

Forced Vibrations:

Case I $$h_0/b = \sigma\alpha_i f_\sigma(k_k) \quad [27]$$

Case II $$h_0/b = \beta_0 f_\beta(k_k) \quad [28]$$

Case III $$h_0/b = \left(\frac{p_0}{bq}\right) f_p(k_k) \quad [29]$$

For a true self-sustained vibration there is no resonance condition in the ordinary sense. If the jump in lift at stall is $C^*_L(k_k)$ which however is a function of k_k, the following is obtained:

Self-Sustained Vibration:

$$h_0/b = C^*_L(k_k) f_{C^*(L)}(k_k) \quad [30]$$

Put for all four response functions

$$F_m = k_k f_m(k_k) \quad [31]$$

$$m = \sigma,\ \beta,\ p, \text{ and } C^*_L$$

The following expressions for the maximum stress at the root section are obtained:

(*a*) *Forced Vibrations:*

Case I $$\frac{s}{\sigma\alpha_i} = \frac{(3/2)E}{\lambda^2 Z}\frac{v}{v_{mtrl}} F_\sigma(k_k) \quad [32]$$

Case II $$\frac{s}{\beta_0} = \frac{(3/2)E}{\lambda^2 Z}\frac{v}{v_{mtrl}} F_\beta(k_k) \quad [33]$$

Case III $$\frac{s}{(p_0/bq)} = \frac{(3/2)E}{\lambda^2 Z}\frac{v}{v_{mtrl}} F_p(k_k) \quad [34]$$

(*b*) *Self-Sustained Vibrations:*

$$\frac{s}{C^*_L(k_k)} = \frac{(3/2)E}{\lambda^2 Z}\frac{v}{v_{mtrl}} F_{C^*(L)}(k_k) \quad [35]$$

The F-functions are tabulated in Table 2.

The result is interesting. In design practice the problem often is to design blades for a given flow channel where the length l, the velocity v, and the blade material are given. Then the ratio v/v_{mtrl} is given and the modulus of elasticity E. Usually the general shape of the blade is known; i.e., the cross section constant Z and the eigenvalue λ are given (λ is influenced by the taper of the blade). The foregoing requirements determine the ratio

$$\frac{(3/2)E}{\lambda^2 Z}$$

The problem from the point of view of vibratory stresses is then concentrated to the F-functions. This means that one is in-

TABLE 2 STRESS FUNCTIONS $F_\sigma(k_\lambda)$, $F_\beta(k_\lambda)$, $F_p(k_\lambda)$, AND $F_{C^*(L)}(k_\lambda)$

k_λ =	0.1	0.2	0.5	1.0
F_σ =	2.20	2.38	2.65	2.90
F_β =	1.01	1.00	0.88	0.70
F_p =	0.945	1.09	1.30	1.45
$F_{C^*(L)}$ =	0.245	0.318	0.405	0.410

terested in the frequency $k_\lambda = (\omega_\lambda b)/v$. Minimum absolute thickness of blade-tip section and aerodynamical considerations usually predetermine the thickness ratio t/c. Equation [25] then reveals that ω_λ is proportional to the chord $c = 2b$, and that the frequency $k_\lambda = (\omega_\lambda b)/v$ therefore is proportional to the square of the chord, the flow velocity v being a predetermined quantity.

The results of Table 2 now imply that as long as the magnitude of the disturbances, i.e., $\sigma\alpha_i$, β_0, (p_0/bq) and $C^*_L(k_\lambda)$ are unchanged, there are in quite a few situations no objections to the construction of slender blades. In the case of self-sustained vibrations, it must be remembered that the disturbance $C^*_L(k_\lambda)$ is a function of k_λ and Mach number (2, 8), and that $C^*_L(k_\lambda)$ is likely to increase with decreasing k_λ.

It is of great practical interest to compare the order of magnitude of the damping in the blade holder and the internal material damping with the magnitude of the damping of the aerodynamic reactions. Such a comparison already has been made by Shannon (10) who reports some experimental results on the two first kinds of damping.

The damping in the clamping device of the blade depends on the design and pressure of the holder, the internal damping depends on the design (amount of material under high stress), the amplitude or stress, state of condition of material such as temperature (heat-resisting steels increase their damping greatly above a critical temperature), and number of load cycles the actual specimen has passed (the damping usually will be much smaller after a certain time in service).

Obviously, there is no more a simple answer to the question of the magnitude of the root and material damping than there is to that of the aerodynamic damping.

Shannon (10) reports on the internal material logarithmic damping Λ_{mtrl} for two different cases, one with a light alloy for compressor blades and one with a high-temperature alloy.

For both cases, at simulated operating conditions he found $\Lambda_{mtrl} = 0.006$ to 0.007. For the damping in the holder, root damping, he found similarly, $\Lambda_{root} = 0.003$ to 0.01 for the compressor blade and $\Lambda_{root} = 0.03$ for the turbine blade. Taken together, it is obtained for the total structural logarithmic damping, $\Lambda_{strue} = 0.01$ to 0.016 for the compressor blade and $\Lambda_{strue} = 0.036$ for the turbine blade.

Since the root damping at running conditions probably is very small, $\Lambda_{strue} = 0.01$ will be adopted as a figure of comparison for the case of compressor blades.

The comparison of the aerodynamic logarithmic damping Λ_{aero} with the structural damping Λ_{strue} is made for different frequencies k_λ in Table 3 under the assumption that Λ_{strue} stays constant.

Advanced first-stage compressor blades have k_λ of the order of magnitude of 0.1 to 0.2. It is seen that the structural damping for advanced designs appears to be of the order of 10 to 20 per cent of the total damping, thus corresponding to an equal amount of reduction of the stress functions in Table 2 for the actual k_λ-region.

It should be noticed that the internal damping is probably only approximately constant when the absolute frequency ω_λ varies.

It is also probable that a large-size amplitude (the amplitude at the tip of the blade is increasing with decreasing k_λ for the same level of maximum stress) is connected with a nonlinear magnification of the aerodynamic damping. If this is true it corresponds to a tendency to decrease F_σ, F_β, F_p, and $F_{C^*(L)}$ of Table 2 toward decreasing k_λ. This emphasizes even more the interesting possibilities found in connection with these functions.

TABLE 3 RELATIONSHIP BETWEEN STRUCTURAL AND AERODYNAMIC DAMPING AT VARYING NATURAL FREQUENCY

$$\Lambda_{aero} = 2\pi\gamma = 2\pi\kappa\frac{F(k_\lambda)}{k_\lambda}$$

F is here equal to the real part of Theodorsen's function $C(k)$

$\kappa = (\rho\pi b^2)/m = 0.002$

k_λ	0.1	0.5	1.0
Λ_{aero}	0.103	0.015	0.0068
$\Lambda_{strue}/(\Lambda_{strue} + \Lambda_{aero})$, per cent	8.9	40	59.5

The foregoing results were derived from an aerodynamic theory of limited scope under further simplification when applied to the three-dimensional structure. Nevertheless, the results may possibly form the start of a new approach to the stress problem of vibrating compressor blades. More research is necessary, however, both on the aerodynamic and structural side before any more definite advice to the turbomachine designer will be ventured.

Acknowledgments

This paper is an abstract of part of an investigation conducted at the Gas Turbine Laboratory at the Massachusetts Institute of Technology in partial fulfillment of the requirements for the degree of Doctor of Science (1953) in the Mechanical Engineering Department.

The author is greatly indebted to the Department for permission to publish this paper and wishes to express his gratitude to Professors C. R. Soderberg, E. S. Taylor, E. P. Neumann, J. P. Den Hartog, and H. Ashley, and many other members of the Mechanical and Aeronautical Engineering Departments for their help and encouragement.

BIBLIOGRAPHY

1 "Mechanism of Flutter—A Theoretical and Experimental Investigation of the Flutter Problem," by T. Theodorsen and J. E. Garrick, NACA TR 685, 1940.

2 "The Aerodynamic Mechanism of Vibrating Compressor Blades," by J. R. Schnittger, ScD thesis (1953) and Gas Turbine Laboratory Report, Massachusetts Institute of Technology, Cambridge, Mass., 1953.

3 "Introduction to the Study of Aircraft Vibration and Flutter," by R. H. Scanlan and R. Rosenbaum, The MacMillan Company, New York, N. Y., 1951.

4 "Airfoils in Sinusoidal Motion in a Pulsating Airstream," by J. Greenberg, NACA TN 1326, June, 1947.

5 "Some Considerations on an Airfoil in an Oscillating Stream," by J. Greenberg, NACA TN 1372, August, 1947.

6 "Problems of Blade Vibrations in Axial Turbo-Machines," by J. R. Schnittger, in forthcoming vol. XI of "High Speed Aerodynamics and Jet Propulsion," Princeton University Press, Princeton, N. J.

7 "Effect of Compressibility on the Flow Past Thick Airfoil Sections," by B. Daleys and M. Humphreys, NACA TN 1657, July, 1948.

8 "Evaluation of High-Angle-of-Attack Aerodynamic-Derivative Data and Stall Flutter Prediction Techniques," by R. Halfman, H. E. Johnson, and S. M. Haley, NACA TN 2533, November, 1951.

9 "Theory of Oscillations," by A. A. Andronow and E. C. Chaikin, Princeton University Press, Princeton, N. J., 1949.

10 "Vibration Problems in Gas Turbines, Centrifugal and Axial Flow Compressors," by J. F. Shannon, R. and M. No. 2226, British A.R.C., 1946.

Experimental and Theoretical Study of Transverse Vibration of a Tube Containing Flowing Fluid[1]

By R. H. LONG, JR.,[2] COLLEGE PARK, MD.

The free transverse vibrations for the fundamental mode of a single-span tube containing a flowing fluid are investigated analytically and experimentally. An approximate solution of the differential equation of motion is made with an infinite power series. Care must be taken in evaluating the large-order determinant that appears so that erroneous results may be prevented. The solution indicates a slight decrease in frequency and no decaying vibration with an increase in flow rate that can be attributed to the flowing fluid for simply supported, fixed, and fixed-simple ends. For fixed-free ends a decaying vibration due to the flowing fluid is indicated and a slight frequency decrease. The experimental results agree reasonably well with these solutions, although the frequency decrease is within the experimental error. The theory neglects internal damping of the tube and "support" damping. The latter appears significant in magnitude and is evaluated for the constructions used. This paper shows the reason for the incorrect conclusions of previous paper and gives experimental results that tend to verify the analytical results presented here and those in another previous paper by a different procedure.

THE free transverse vibrations for the fundamental mode of a single-span tube containing a flowing fluid are investigated analytically and experimentally for several end conditions.

Analytical Investigation

The differential equation of motion as derived in a previous paper[3] is used.

$$EI\frac{\partial^4 Z}{\partial X^4}+\rho v^2\frac{\partial^2 Z}{\partial X^2}+2\rho v\frac{\partial^2 Z}{\partial T\partial X}+m\frac{\partial^2 Z}{\partial T^2}=0 \quad [1]$$

Here the modulus of elasticity of the tube is E, rectangular moment of inertia I, mass of the fluid per unit length ρ, mass of tube plus fluid per unit length m, and the constant velocity of the fluid relative to the tube is v. The horizontal co-ordinate along the tube is X, the vertical co-ordinate is Z, and time is T.

This equation may be put into nondimensional form by the following substitutions

$$z=Z/L,\ x=X/L,\ t=T\sqrt{EI/mL^4}=Tp$$

Equation [1] becomes

$$\frac{\partial^4 z}{\partial x^4}+w\frac{\partial^2 z}{\partial x^2}+u\frac{\partial^2 z}{\partial t\partial x}+\frac{\partial^2 z}{\partial t^2}=0 \quad [2]$$

where

$$u=\frac{2\rho vL}{\sqrt{mEI}}\quad\text{and}\quad w=\frac{u^2 m}{4\rho}$$

Owing to the great difficulty of obtaining a solution of this equation which will fit the boundary conditions a power-series approximation is used. Assume

$$z=F(x)e^{iDt} \quad [3]$$

with

$$F(x)=\sum_{n=0}^{\infty}a_n x^n \quad [4]$$

Substitution of Equation [3] into Equation [2] gives an ordinary differential equation

$$\frac{d^4F}{dx^4}+w\frac{d^2F}{dx^2}+iuD\frac{dF}{dx}-D^2F=0 \quad [5]$$

Substitution of Equation [4] into [5] gives a set of recurrence equations by placing coefficients of like powers of x equal to zero, as the solution must hold for values of x other than zero.

$$n(n-1)(n-2)(n-3)a_n+(n-2)(n-3)wa_{n-2}+(n-3)iuDa_{n-3}-D^2a_{n-4}=0,\ n=4,5,6\ldots\ldots \quad [6]$$

These equations give four independent solutions for F, in each of which the coefficients may be expressed in terms of a_0, a_1, a_2, a_3, respectively. The boundary conditions determined by the type of support will provide four additional equations for the coefficients a_n.

The significance of D can be seen from Equation [3] or from the equivalent trigonometric form $z=F(x)(\cos Dt+i\sin Dt)$. If D is real then it is related to the circular frequency ω by $\omega=Dp$. When D is complex ($D=R+iS$), Equation [3] becomes $z=F(x)e^{iRt}e^{-St}$ and $\omega=Rp$. S is a measure of the damping that is present. The logarithmic decrement is $\Delta=2\pi S/R$.

The system of equations containing a_n has solutions different from zero if the determinant of the coefficients vanishes. In order to solve this infinite determinant for the exponential factor D the power series is cut off above some finite n. By comparing the known solution for $u=0$ with solutions of the determinant for

---

[1] Portions of this paper were part of a dissertation presented to the faculty of the Yale University School of Engineering in partial fulfillment of the requirements for the degree of Doctor of Engineering, which was awarded in 1952.

[2] Associate Professor, Mechanical Engineering Department, University of Maryland.

[3] "Bending Vibrations of a Pipe Line Containing Flowing Fluid," by G. W. Housner, JOURNAL OF APPLIED MECHANICS, Trans. ASME, vol. 74, 1952, pp. 205–208.

Contributed by the Applied Mechanics Division and presented at the Annual Meeting, New York, N. Y., November 28–December 3, 1954, of THE AMERICAN SOCIETY OF MECHANICAL ENGINEERS.

Discussion of this paper should be addressed to the Secretary, ASME, 29 West 39th Street, New York, N. Y., and will be accepted until April 11, 1955, for publication at a later date. Discussion received after the closing date will be returned.

NOTE: Statements and opinions advanced in papers are to be understood as individual expressions of their authors and not those of the Society. Manuscript received by ASME Applied Mechanics Division, January 22, 1954. Paper No. 54—A-22.

successively greater n it is found that terms up to a certain n must be included for sufficient accuracy. In doing this the convergence of the determinant is demonstrated. With small values of u, convergence is also demonstrated but more terms must be included for sufficient accuracy. With the number of terms used here the solution appears valid at least to $u = 0.3$.

A previous paper[4] used a similar procedure, but the differential equation of motion did not include the term containing w and the dimensionless flow rate was half the u used here. The analysis here deviates from that paper starting with more terms included of the power series. The equation resulting from the determinant is solved for D by a numerical iteration procedure instead of the graphical method mentioned.[4] The erroneous conclusions of that reference were due to cutting off improperly terms of the determinant and not because of the incorrect differential equation used. A proper procedure is discussed in the following.

The determinant is reduced to the second order in successive steps by the method of F. Chio.[5] The resulting equation contains terms in ascending powers of u, w, and D as Equations [7] and [8] in the Appendix indicate. As the order of the determinant is increased some of the terms reach final values and new terms appear with coefficients which are progressively smaller in magnitude. With terms included through u^4D^8 the effect of neglecting the higher-power terms can be shown to be negligible on the value of D with the number of significant figures used.

It also should be noted that care must be taken in cutting off terms of the determinant so that the final value of each term used is included. Otherwise the value of D can be considerably in error, even being negative in some cases. Also, a complex D may be obtained when a real D is actually correct. For simply supported, fixed, and fixed-simple ends D is real. A slight decrease in D (frequency) is indicated with an increase in u. For the extreme

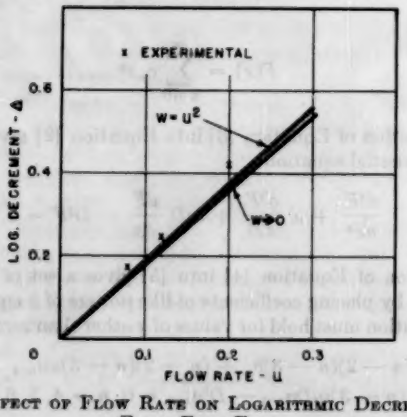

FIG. 1 EFFECT OF FLOW RATE ON LOGARITHMIC DECREMENT FOR FIXED-FREE ENDS

case where $u = 0.840$ and $w = 0.411$ for simply supported ends the decrease in D is only from 9.8696 to 9.6440 (—2.4 per cent). This condition is used as it was the greatest flow rate used in the experimental arrangement and shows the largest decrease percentagewise of the cases investigated.

With fixed-free ends D is complex, indicating a damping effect. The effect of flow rate on the logarithmic decrement is shown by the solid lines in Fig. 1 for two contrasting conditions. They are, first with the term containing w in Equation [5] neglected ($w \to 0$), and then with $w = u^2$ which is for the ratio $m/\rho = 4$. The latter condition is used as the experimental arrangement had a ratio of 3.88. This shows the small contribution to the decaying vibration of the term in Equation [5] containing w over the range of u considered. It may be noted that, for a given value of u, w depends on the m/ρ ratio. As the effect is small with $m/\rho = 4$ the lower limit is for $m/\rho \to 0$ or $w \to 0$. For intermediate values of w the approximate value of the logarithmic decrement may be found by interpolating between the lines. Three points obtained experimentally as described in the following also are shown in the figure.

A slight decrease in frequency is indicated with an increase in u. This effect is shown in Table 1 where the exact condition is the known solution for $u = 0$.

TABLE 1 FREQUENCY DECREASE FOR FIXED-FREE ENDS

		$\omega = Rp$	
u	w	Approx R	Exact R
0	0	3.516	$(1.875)^2 = 3.515625$
0.300	0	3.505	
	u^2	3.485	

It should be noted that the analysis has neglected the internal friction of the pipe material and also the effect of the supports. The order of magnitude of the former as available in the literature is much smaller than that encountered in the experimental arrangements to be described. The damping found for free vibrations with no flow velocity is thus termed support damping. The viscosity of the fluid also has been neglected.

The reason for the decaying vibration for fixed-free ends with the flowing fluid can be seen by considering the origin of the force term containing u. It is the inertia force associated with the Coriolis' acceleration and is due to the fluid moving with a velocity v relative to the tube while the tube has an angular velocity $\partial^2 Z/\partial T \partial X$. The component of this force in the Z-direction is always directed opposite to the velocity as the angular velocity is of the same sense over the entire length of the tube. For the other end conditions considered, the angular velocity of the tube will be of opposite sense over each half span causing the sense of the Z-component inertia force also to be opposite. The net work done per cycle by all these forces is thus zero.

EXPERIMENTAL INVESTIGATION

Tubes with simply supported, fixed, and fixed-free ends were constructed and investigated experimentally.

The simply supported tube was a low-carbon-steel seamless tube with 1 in. OD and a wall thickness of 0.037 in. Two steel support pins were brazed to the tube in the horizontal plane 2 in. from each end. These pins were supported by angles at the upstream end and rollers at the downstream end. Rubber hoses clamped on the ends of the tube permitted water to flow through the tube. Two type A-5, SR4 strain gages were mounted axially on the tube near mid-span, one above and the other below the tube, to pick up the strain in the vibrating tube. A Brush BL-310 strain amplifier and a BL-201 magnetic direct-inking oscillograph were used to record the vibration.

The free vibration was started with no velocity and an initial displacement by hanging a weight at mid-span and cutting the supporting wire. The arrangement used gave good reproducibility.

The effect of the hoses was determined for the empty tube as giving an increase in frequency and decrease in strain of about 2 per cent and thus they do not affect the vibration appreciably.

With the span of the tube of 120.03 in. the natural frequency for the full tube with no flow is 5.70 cycles per sec (cps). The average results of 36 runs for two contrasting conditions are given in Table 2. This shows that there is no effect of a flow rate of $u = 0.84$ on

[4] "Bending Vibrations of a Pipe Line Containing Flowing Fluid," by H. Ashley and G. Haviland, JOURNAL OF APPLIED MECHANICS, Trans. ASME, vol. 72, 1950, pp. 229–232.

[5] "Applied Mathematics for Engineers and Physicists," by L. A. Pipes, McGraw-Hill Book Company, Inc., New York, N. Y., 1946, p. 74.

the frequency and damping within the experimental error. Similar results were found with lower flow rates.

TABLE 2 EXPERIMENTAL RESULTS FOR SIMPLY SUPPORTED ENDS

	Cycles	Log dec.	Cycles	Freq, cps
Full $u = 0$.....	8.9	0.078	8.3	5.64
	18.7	0.075	17.2	5.65
	26.7	0.079	25.5	5.67
	34.8	0.081		
Velocity $u = 0.84$..	8.7	0.081	8.1	5.65
	17.9	0.079	16.6	5.66
	25.7	0.081	25.4	5.67
	33.4	0.085		

NOTE: Values are averages over the number of cycles given.

The results of unpublished, independent experimental work on a simply supported tube, similar to that used here, have been made available by Mr. Erdem Ergin who did the work at the California Institute of Technology. This is presented in Fig. 2 with gratitude for permission to reproduce it. Since the dimensionless flow

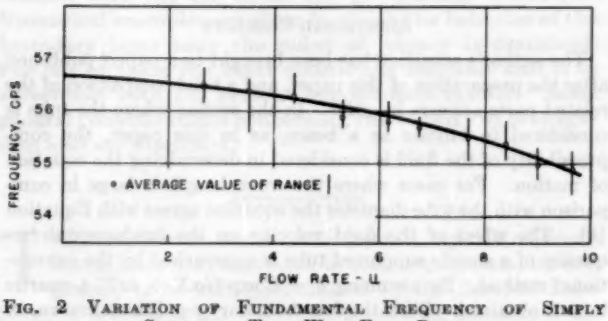

FIG. 2 VARIATION OF FUNDAMENTAL FREQUENCY OF SIMPLY SUPPORTED TUBE WITH FLOW RATE

rate attained is approximately 10 times that used by the author, it shows the effect of the velocity upon the natural frequency of fundamental vibration. Where the range of experiments is the same, it corroborates the author's results. Over the range investigated the frequency decreased about 3.2 per cent. The dural tube used was 0.500 in. OD and 0.453 in. ID with 24 in. between supports. Other values follow:

$\rho = 1.81 \times 10^{4}$ slugs/in.

$m = 2.90 \times 10^{4}$ slugs/in.

$E = 10.5 \times 10^{6}$ psi

$I = 10^{3}$ in.^{4}

The average results for the fixed-ends tube also indicate no effect of the flowing fluid on the frequency and damping as Table 3 shows.

TABLE 3 EXPERIMENTAL RESULTS FOR FIXED ENDS

	Cycles	Log dec.	Cycles	Freq, cps
Full $u = 0$.....	9.4	0.031	43.9	49.43
	22.2	0.031	96.6	49.46
	39.2	0.034		
	52.8	0.034		
	88.7	0.026		
	128.1	0.023		
Velocity $u = 0.36$.....	9.4	0.031	40.0	49.23
	21.8	0.031	91.4	49.02
	38.4	0.036		
	51.0	0.035		
	87.8	0.026		
	120.7	0.024		

NOTE: Values are averages over the number of cycles given.

This was with a 1 in. OD seamless-steel aircraft tubing (SAE 4130) with 0.073 in. wall thickness and 57.95 in. between supports. Steel collars, $2^{7}/_{16}$ in. OD and 12 in. long, were placed on each end of the tube with a slight interference fit. Steel plates ($^{1}/_{2}$ in. × 19 in. × $19^{1}/_{2}$ in.) were welded at the ends of the collars nearest each other. Then supporting pedestals were formed with concrete giving about 12 in. × 24 in. cross section. The vibration was initiated and the strain recorded in the same manner as the foregoing. The theoretical natural frequency for the full tube was 59.8 cps. It may be noted that this tube is farther from being one with fixed ends than the former was from being simply supported.

This tube was converted to fixed-free ends by sawing the tube and removing the downstream pedestal. It was 55.94 in. long and had a natural frequency when filled with water of 10.12 cps. The load used to give the initial deflection was placed 1.94 in. from the free end.

The average results for three different flow rates are given in Table 4.

TABLE 4 EXPERIMENTAL RESULTS FOR FIXED-FREE ENDS

u	Cycles	Log decrement	
0	12.5	0.036	0
0.080	5.0	0.210	0.174
0.118	8.0	0.286	0.250
0.200	11.2	0.457	0.421

NOTE: Values are averages over the number of cycles given.

The first logarithmic-decrement column gives the obtained values, while the second column is the decrement without the support damping of 0.036 included, for plotting in Fig. 1. The average frequency obtained was 10.0 cps for each value of u.

The figure shows reasonable agreement between the analytical and experimental results. The amplitudes on the oscillograph records were difficult to interpret as there was more of a transient effect which persisted longer, believed to be due to the sudden method of starting the vibration, than in the other cases. However, by visual superposition of the records it was found that this transient effect was reproduced on different days. This probably gives part of the experimental error. The effect of fluid viscosity also contributes to this error.

The magnitude of support damping is about 0.08, 0.03, and 0.04 for simply supported, fixed, and fixed-free ends, respectively. This causes the free vibrations to decay in a few seconds with the constructions used.

Appendix

THEORETICAL PROCEDURE

The procedure used will be outlined for simply supported and fixed-free ends. The following equations express the boundary conditions:

Simply supported

$$x = 0 \quad z = \partial^2 z/\partial x^2 = 0$$
$$x = 1 \quad z = \partial^2 z/\partial x^2 = 0$$

Fixed-free

$$x = 0 \quad z = \partial z/\partial x = 0$$
$$x = 1 \quad \partial^2 z/\partial x^2 = \partial^3 z/\partial x^3 = 0$$

When these are substituted into Equation [3] four equations containing the coefficients a_n in addition to Equations [6] are obtained. They are for:

Simply supported

$$a_0 = a_2 = 0$$

$$a_1 + \sum_{n=3}^{\infty} a_n = 0$$

$$\sum_{n=3}^{\infty} n(n-1)a_n = 0$$

Fixed-free $a_0 = a_1 = 0$

$$\sum_{n=2}^{\infty} n(n-1)a_n = 0 \qquad \sum_{n=2}^{\infty} n(n-1)(n-2)\,a_n = 0$$

These equations with Equations [6] give a system of equations containing a_n which has a solution different from zero if the determinant of the coefficients vanishes.

Enough terms are included so that the terms up through u^4D^8 appear in the second-order determinant. This requires starting with the twenty-second-order determinant.

The final equation from evaluating the determinant for simply supported ends is

$$D^2(7{,}567{,}560 + 33{,}783.75u^2 - 540{,}540w + 15{,}015w^2 - 1{,}501.5\,u^2w) = 681{,}080{,}040 - 113{,}513{,}400w + 5{,}675{,}670w^2 + D^4(6006 + 22.75u^2 + u^4/64 - 273w + 5.25w^2 - 54.375u^2w) - D^6(1 + u^2/320 + u^4/391{,}680 - w/30 + w^2/2040 - u^2w/12{,}240) + D^8(1/18{,}360 + u^2/6{,}976{,}800 + u^4/783{,}971{,}436.4 - w/697{,}680 - w^2/817{,}650.7848 - u^2w/389{,}214.3401) \ldots\ldots [7]$$

By starting with the value of D for $u = 0$ an iteration procedure can be used to evaluate D for various values of u and w.

For fixed-free ends the equation has real and imaginary parts so D is complex. The substitution $D = R + iS$ was made for various values of u and w, and R and S were found by an iteration procedure starting with the known value of R at $u = 0$. The following equation resulted from the determinant

$$\ldots D^9(1 + 5u^2/1224 - 4w/153) - iD^7(8u + 28u^3/17 - 2373uw/544) - D^6(10{,}920 + 60u^2 + 5u^4/64 - 360w - 21w^2/4 - 2505u^2w/32) + iD^4(65{,}520u + 210u^3 + 126{,}735uw/4) + D^4(32{,}432{,}400 + 270{,}270u^2 + 1365u^4/4 - 1{,}441{,}440w + 27{,}300w^2 + 589{,}680u^2w) - iD^3(129{,}729{,}600u + 450{,}450u^3 - 107{,}567{,}460uw) - D^2(13{,}621{,}608{,}000 + 227{,}026{,}800u^2 - 908{,}107{,}200w + 24{,}324{,}300w^2 - 348{,}648{,}300u^2w) + iD(27{,}243{,}216{,}000\,u + 10{,}897{,}286{,}400uw) + 163{,}459{,}296{,}000 = 0 \ldots\ldots [8]$$

The reduction of the large order determinant to the second order can be done fairly quickly. The greatest time (several hours) required is in evaluating the second-order determinant for Equation [7] or [8]. The time required to obtain a value of D from Equation [7] by the iteration process depends on the accuracy desired, and by following a systematic procedure, with a little judicious guessing, numerical results may be found in less than an hour usually.

When solving Equation [8] as described, about as much time as required to get Equation [8] from the second-order determinant is needed in making the substitution $D = R + iS$, and this must be done for each combination of values of u and w. The iteration procedure here is about twice as long as for the cases without amplitude decay resulting from fluid flow as there are now two equations to satisfy. Fortunately, the effect of terms containing higher powers of S is negligible compared with the other terms that are present, in the range considered, and such terms can be eliminated during the first iteration simplifying the iteration work following.

Additional Comment

The author's attention has been brought to a paper[4] published after the preparation of this paper, and a brief comparison of the related parts appears in order. In the section where the tube is considered to vibrate as a beam, as in this paper, the compressibility of the fluid is considered in determining the equation of motion. For cases where the wave length is large in comparison with the tube diameter the equation agrees with Equation [1]. The effect of the fluid velocity on the fundamental frequency of a simply supported tube is approached by the conventional method. By assuming $Z = C \exp(i\alpha X + i\omega T)$ a quartic in α is obtained. With the four boundary conditions known, in theory the solution can be found. In order to reduce the complexity some approximations were made and the frequencies for the two limiting conditions of $m/\rho = 0$ and $m/\rho = \infty$ were compared.

This procedure also shows the small effect that fluid flow has in reducing the frequency. The results cover the complete velocity range for a simply supported tube while the author's results have a limit on u as discussed.

---

[4] "Vibrations of a Cylindrical Tube Containing Flowing Fluid," by F. I. N. Niordson, Transactions of the Royal Institute of Technology, Stockholm, Sweden, No. 73, 1953.

An Approximate Theory of Lateral Impact on Beams[1]

By B. A. BOLEY,[2] NEW YORK, N. Y.

The approximate theory derived in this paper describes, by means of a "traveling-wave" approach, the behavior of beams under transverse impact. Lateral impact is considered in detail, namely, one in which a section of the beam undergoes a sudden change in velocity or shear force. The theory considers the effects of shear deformations and of rotatory inertia according to Timoshenko's model, and that of lateral contraction as suggested by Love. The governing equations and the boundary conditions are developed with the aid of an energy-variation technique. Numerical examples are given in which the behavior of the boundary layer near the point of impact is examined. For one of these the exact solution is available and is in agreement with the present approximate results. Some general considerations concerning the velocity of propagation also are discussed.

Introduction

THE behavior of beams under various types of dynamic lateral loads has been found, in some experimental investigations, to be well approximated by the Bernoulli-Euler theory of bending (2, 3, 4, 5).[3] This is not true, however, of the transmission of pulses with very short wave lengths; in such cases it becomes necessary to consider the shearing deformations and the rotatory inertia of the beam. Timoshenko's beam model (6) takes these quantities into account and has been shown by Mindlin (7, 8) to give results which are in good agreement with those obtained either experimentally or from the three-dimensional theory of elasticity (9, 10, 11, 12). A similarly favorable comparison is given by Kolsky (13).

Some exact solutions of the Timoshenko beam equations (which result from the ones used in this paper when lateral contraction terms are neglected) have been obtained for certain special cases (14, 15, 17, 28) but, in general, are quite cumbersome. An attempt is presented here to develop simpler, if approximate, solutions; it employs a traveling-wave approach and is based on Timoshenko's model with an additional correction for lateral contraction analogous to that introduced by Pochhammer (16) in the case of longitudinal impact. The present paper represents a first effort in this direction and consequently is limited in many respects. For example, attention has been concentrated on the behavior of a short portion of the beam close to the point of impact, with generalizations indicated briefly.

Consider a bar, to one end of which is suddenly imparted, for example, a lateral velocity; the ensuing motion of the beam will then certainly contain high-frequency components and therefore will require consideration of the shear and rotatory inertia effects. These effects will be of great importance in the neighborhood of the sudden jump in velocity, but the experimental evidence previously cited [and in particular the work of Vigness (reference 5) who considers the present loading condition] indicates that at some distance from the disturbance front they are not essential for a prediction of the bending stresses.

A consideration of the orders of magnitude of the various terms in the basic equation is carried out in this paper and shows that near the point of impact the shearing deformations and rotatory inertia effect are important, principally in a short "boundary layer" immediately following the disturbance front. The length of this layer is of the order of the cross-sectional dimensions of the bar. Therefore the solution can be set up in two parts; i.e., within the boundary layer the Timoshenko model must be used, but for the remainder of the beam the Bernoulli-Euler theory is adequate.

The behavior of the boundary layer, arising in beams under lateral impact, is described in this paper with an approximate energy theory. Expressions are assumed, in terms of some arbitrary parameters, for the deflection of the beam and for the distance traveled by the disturbance. The parameters are then determined with the aid of the principle of virtual displacements. Four illustrative examples are presented. The exact solution for one of these is known (28) and is in good agreement with the present results.

Basic Assumptions and Relations

Consider a bar, not necessarily uniform in cross section, of length L. Let x measure the distance along the bar, and let y and z be the principal axes of the cross section. Assume that the centroids of all cross sections lie on the x-axis.

The bar is struck at the end where $x = 0$ with a force $P = P(t)$ in the z-direction, the time $t = 0$ being chosen as the beginning of impact. Let the displacements of any point (x, y, z) be u_1, v_1, and w_1, in the x, y, and z-directions, respectively, and denote by $w = w(x, t)$ the displacement, in the z-direction, of points on the x-axis. Assume that displacement w consists of two parts; one, denoted by w_b, taking place with bending, but no shearing, deformations; the other, denoted by w_s, taking place with shearing, but no bending, deformations. Assume further that u_1 and v_1 vanish on the x-axis.

The displacements of points off the x-axis may be related to those of points on this axis, as a first approximation, by means of the formulas for the case of pure bending (18, 19); then

$$\left.\begin{aligned} u_1 &= -w_b' z \\ v_1 &= \nu w_b'' zy \\ w_1 &= w_s + w_b + (\nu/2) w_b'' (z^2 - y^2) \end{aligned}\right\} \quad \ldots\ldots [1]$$

where ν is Poisson's ratio and primes indicate differentiation with respect to x. The strains and stresses at any point in the

---

[1] The work reported here was sponsored by the Office of Naval Research, U. S. Navy, under contract N6-onr-225-29, project NR-064-355 (1).[3]

[2] Associate Professor of Civil Engineering, Columbia University.

[3] Numbers in parentheses refer to the Bibliography at the end of the paper.

Contributed by the Applied Mechanics Division and presented at the Annual Meeting, New York, N. Y., November 28–December 3, 1954, of The American Society of Mechanical Engineers.

Discussion of this paper should be addressed to the Secretary, ASME, 29 West 39th Street, New York, N. Y., and will be accepted until April 11, 1955, for publication at a later date. Discussion received after the closing date will be returned.

Note: Statements and opinions advanced in papers are to be understood as individual expressions of their authors and not those of the Society. Manuscript received by ASME Applied Mechanics Division January 12, 1953. Paper No. 54—A-24.

bar are then, in the usual notation

$$\left.\begin{aligned} \epsilon_x &= -(\epsilon_y/\nu) = -(\epsilon_z/\nu) = (\sigma_x/E) = -w_b''z \\ \gamma_{yz} &= \sigma_y = \sigma_z = \tau_{yz} = 0 \\ \gamma_{xy} &= (\tau_{xy}/G) = w_{bxy}''' \\ \gamma_{xz} &= (\tau_{xz}/G) = w_s' + (\nu/2)\, w_b'''\,(z^2 - y^2) \end{aligned}\right\} \quad . . [2]$$

where E is Young's modulus and $G = E/(2 + 2\nu)$ the shear modulus.

The striking of the bar gives rise to a disturbance which travels along the bar; let the distance traveled in a time t be $L_1 = L_1(t)$; then $L_1(0) = 0$. It follows that

$$w = w_b = w_s = w_b' = 0, \text{ if } x \geq L_1 \ldots\ldots\ldots\ldots [3]$$

is necessary for continuity of the bar, and because sudden changes in slope can only occur with the action of shear. From these equations the kinematical conditions to be satisfied at the head of the disturbance wave (18, art. 205) are easily derived to be

$$w'L_1^{\cdot} + w^{\cdot} = w_b'L_1^{\cdot} + w_b^{\cdot} = w_s'L_1^{\cdot} + w_s^{\cdot} = w_b''L_1^{\cdot} + w_b''^{\cdot} = 0 \ldots\ldots [4]$$

where dots indicate differentiation with respect to time and $L_1^{\cdot}$ represents the velocity of advance of the wave front.

Derivation of Basic Equations

The basic equations of the problem of transverse impact on a bar will now be developed from the principle of virtual displacements, with the aid of D'Alembert's principle. In the present problem

$$\delta(U + V + K_1) = 0 \ldots\ldots\ldots\ldots\ldots [5]$$

where the variation of the strain energy is

$$\delta U = \delta(1/2)\int_0^{L_1}\int\int (\sigma_x\epsilon_x + \sigma_y\epsilon_y + \sigma_z\epsilon_z + \tau_{xy}\gamma_{xy} + \tau_{yz}\gamma_{yz} + \tau_{xz}\gamma_{xz})\, dx\, dy\, dz \ldots\ldots\ldots [6]$$

the variation of the potential of the external forces is

$$\delta V = -P(t)\delta w(0, t) + \int_0^{L_1}\int\int \rho(u_1^{\cdot\cdot}\,\delta\, u_1 + v_1^{\cdot\cdot}\,\delta\, v_1 + w_1^{\cdot\cdot}\,\delta\, w_1)\, dx\, dy\, dz \ldots\ldots [7]$$

the increment in kinetic energy due to the variation of the length L_1 is

$$\delta K_1 = [K_{x\,=\,L_1}]\delta L_1 \ldots\ldots\ldots\ldots\ldots [8]$$

and where the kinetic energy K per unit of length is

$$K = (\rho/2)\int\int [(u_1^{\cdot})^2 + (v_1^{\cdot})^2 + (w_1^{\cdot})^2]\, dy\, dz \ldots\ldots [9]$$

In the foregoing equations $\rho = \rho(x)$ is the mass density of the bar, and the limits of integrations in the y and z-directions must be chosen so as to cover the entire cross section.

The last three terms in Equation [6], which represent the strain energy of shear, cannot be calculated directly from Equations [2] because the shear stress due to w_s is incorrectly given there as constant in any one cross section. A numerical coefficient N is therefore introduced, which differs from the usual one (20, 21) because of the inclusion, in its calculation, of the effect of lateral contraction. The determination of N is carried out in the Appendix for a rectangular section and the results are plotted in Fig. 1. The final form of the strain-energy variation is then

$$\delta U = \delta\int_0^{L_1} (EI_y/2)(w_b'')^2\, dx + \delta\int_0^{L_1} (G/N)(A/2)(w' - w_b')^2\, dx \ldots\ldots [10]$$

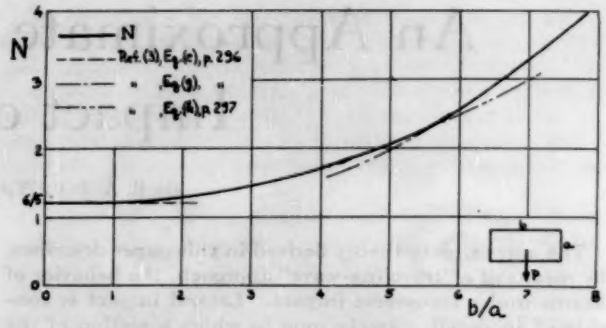

Fig. 1 Values of N for Rectangular Sections

where I_y is the moment of inertia of the cross section about the y-axis.

The various energy quantities can now be evaluated with the aid of Equations [1] and the variations indicated in Equation [5] carried out according to the rules of the calculus of variations. The variation in the length L_1, appearing in the upper limits of the integrals of Equation [10], must be taken into account with the aid of Leibnitz's Formula (22)

$$\delta\int_{f_1}^{f_2} F(x)dx = \int_{f_1}^{f_2} \delta F(x)dx + F(f_2)\,\delta f_2 - F(f_1)\delta f_1 \ldots [11]$$

The final form of Equation [5], correct to terms of the fourth order in the cross-sectional dimensions, is then

$$\left.\begin{aligned} &\int_0^{L_1} \{-(EI_y w_b'')' - (GA/N)(w' - w_b') + \rho I_y w_b''' - (\nu\rho I_y k w^{\cdot\cdot}/2)'\}\, \delta w_b'\, dx \\ &+ \int_0^{L_1} \{-[(GA/N)(w' - w_b')]' + \rho A w^{\cdot\cdot} + (\nu\rho I_y k w_b''^{\cdot\cdot}/2)\}\, \delta w\, dx \\ &+ \{[(EI_y w_b'' + (\nu\rho I_y k w^{\cdot\cdot}/2)]\, \delta w_b' + (GA/N)(w' - w_b')\,\delta w + [(EI_y/2)(w_b'')^2 \\ &+ (G/N)(A/2)(w' - w_b')^2 + (\rho A/2)(w^{\cdot})^2 + (\rho I_y/2)(w_b^{\cdot\cdot})^2 \\ &+ (\nu\rho I_y k w^{\cdot} w_b''^{\cdot}/2)]\,\delta L_1\}_{\text{at } x\,=\,L_1} \\ &- \{[EI_y w_b'' + (\nu\rho I_y k w^{\cdot\cdot}/2)]\, \delta w_b' \\ &+ [(GA/N)(w' - w_b') + P]\,\delta w\}_{\text{at } x\,=\,0} = 0 \end{aligned}\right\} \quad . . [12]$$

where

$$k = 1 - (I_z/I_y) \ldots\ldots\ldots\ldots\ldots [13]$$

and where I_z is the moment of inertia of the cross section about the z-axis. Equation [12] must be satisfied for any arbitrary variation of the displacements; hence the governing equations for the transverse motion of a beam with variable cross section are

$$-(EI_y w_b'')' - (GA/N)(w' - w_b') + \rho I_y w_b''' - (\nu\rho I_y k w^{\cdot\cdot}/2)' = 0$$

$$-[(GA/N)(w' - w_b')]' + \rho A w^{\cdot\cdot} + (\nu\rho I_y k w_b''^{\cdot\cdot}/2) = 0 \ldots [14]$$

In the special case of a uniform bar, w_b and its derivatives may be eliminated; the result is (D indicating a differential operator)

$$Dw = EI_y w^{iv} + \rho A w^{\cdot\cdot} - \rho I_y[1 + (EN/G) - \nu k]w^{\cdot\cdot\cdot\cdot} + (\rho^2 I_y N/G)w^{\cdot\cdot\cdot\cdot} + [(\nu\rho I_y k)^2 N/(4GA)]w^{\cdot\cdot\cdot\cdot} = 0 \ldots [15]$$

It may similarly be shown that this equation takes the form

$$Dw_b' = Dw_s' = 0 \quad \ldots\ldots [16]$$

when written in terms of the bending and shear displacements, respectively. If the terms containing Poisson's ratio are neglected, Equation [15] becomes identical with Timoshenko's equation (6) and very similar to Prescott's (23). If shear deformations are neglected Love's equation (18) results; if both shear and Poisson's ratio terms are neglected the well-known equation for the transverse motion of beams including the effect of rotatory inertia (24) is obtained. The relative importance of the various terms of Equation [15] will be discussed later.

Boundary Conditions

Some of the boundary conditions to be satisfied at the wave front ($x = L_1$) are given by Equations [3]. The remaining conditions there and at $x = 0$ can be obtained from Equation [12]. At $x = 0$ they are either

$$EI_y w_b''' + (\nu\rho I_y k \ddot{w}'/2) = 0 \text{ or } \delta w_b' = 0 \quad \ldots\ldots [17a]$$

and either

$$(GA/N)(w - w_b') + P = 0 \text{ or } \delta w = 0 \quad \ldots\ldots [17b]$$

Thus at the struck end of the bar either the bending moment (modified by a term which vanishes if $I_y = I_z$) or the slope due to bending may be prescribed, and either the shear force or the total displacement.

Consider now the quantities δL_1 and $\delta w_b'$, contained in the boundary conditions at the head of the wave. Since w and $(w + \delta w)$ must vanish at $x = L_1$ and $x = L_1 + \delta L_1$, respectively, it follows that

$$\delta L_1 = -(1/w')\delta w \text{ at } x = L_1 \quad \ldots\ldots [18]$$

and similarly in terms of the bending and shear displacements.

The quantity $\delta w_b'$ stands for the variation of the slope (due to bending) at $x = L_1$, the variation being taken without changing x. It differs from the variation $\delta(w_b')_{\text{total}}$ of the slope at the head of the wave, inasmuch as the latter must be calculated taking into account a change in x equal to δL_1. The relation between the two slope changes is then, with the aid of Equation [18]

$$\delta w_b' = \delta(w_b')_{\text{total}} + (w_b''/w')\delta w \text{ at } x = L_1 \quad \ldots\ldots [19]$$

The bracket of Equation [12] labeled $x = L_1$ indicates that the work done by the shear force and by the moment at $x = L_1$ during the virtual variation of the displacements must balance the total strain plus kinetic energies stored in the portion of the beam defined by $L_1 \leq x \leq (L_1 + \delta L_1)$. It corresponds to the dynamical conditions given by Love (18, art. 206). Use of Equations [18] and [19] gives the boundary conditions as either

$$EI_y w_b''' + (\nu\rho I_y k \ddot{w}'/2) = 0 \text{ or } \delta(w_b')_{\text{total}} = 0 \text{ at } x = L_1 \quad [20]$$

where, because of Equation [3], the latter condition must always be satisfied, and

$$(1 - \alpha^2)(w_b'')^2 - [\alpha^2 - (1/\gamma)](1/r_y)^2(w')^2 + (\nu k/a^2)(\dot{w}'w_b'' - \dot{w}w_b''') = 0 \quad \ldots\ldots [21]$$

at $x = L_1$ with the following notation

$$\alpha = L_1\dot{}/a; \; a = \sqrt{E/\rho}; \; \gamma = EN/G; \; r_y^2 = I_y/A \quad [22]$$

Equations [3], [17a], [17b], and [21] are the boundary conditions of the problem.

Remarks on Role of Shear, Rotatory Inertia, and Lateral Contraction

It is well known (7, 23) that if the effects of shear and rotatory inertia are not considered in the analysis of a beam under lateral impact, the physically impossible result of an infinite velocity of propagation is obtained for very short waves. However, a theory developed by Timoshenko (25) on the basis of the Bernoulli-Euler equation

$$EI_y w^{iv} + \rho A \ddot{w} = 0 \quad \ldots\ldots [23]$$

which results from Equation [15] when all shear, rotatory inertia, and Poisson's ratio effects are neglected, gives stresses and displacements in close agreement with some experiments (2, 3, 4, 5). It therefore appears that shear and rotatory inertia, though essential to a study of the velocity of propagation, play a somewhat limited role. This may be clarified by the following study of the orders of magnitude of the various terms of Equation [15] pertaining to positions of the wave front close to the struck end of the beam.

Consider a portion of the beam, originally at rest, near to and including the end struck laterally. Let order of magnitude of the displacement in this portion of the bar at a time t be denoted by w; in the case of lateral impact w is a finite and nonvanishing quantity. The order of magnitude (denoted by 0) of its time derivative can then be approximated by

$$0(\partial w/\partial t) = w/t \quad \ldots\ldots [24a]$$

The order of magnitude of its x-derivative may be taken as

$$0(\partial w/\partial x) = w/(\lambda L) \quad \ldots\ldots [24b]$$

where the dimensionless coefficient λ appearing in the characteristic length λL will be determined later. The magnitudes of higher derivatives may then be estimated by repeated application of Equations [24]. The orders of magnitude of the various terms in Equation [15] are then (if a common multiplier $[EI_y w/(\lambda L)^4]$ is omitted), respectively

$$\left.\begin{aligned} &0(w^{iv} \text{ — term}) = 1 \\ &0(\ddot{w} \text{ — term}) = \lambda^4 S_y^2 (L/at)^2 \\ &0(w''\ddot{} \text{ — term}) = (1 + \gamma - \nu k)\lambda^2(L/at)^2 \\ &0(\ddot{w}\ddot{} \text{ — term}) = \lambda^4\gamma(L/at)^4 \\ &0(w''\ddot{}\ddot{} \text{ — term}) = (\lambda\nu k/S_y)^2(\gamma/4)(L/at)^4 \end{aligned}\right\} \quad \ldots\ldots [25]$$

In view of the restriction to cases of lateral impact, it is reasonable to suppose that the second of these, which represents the translatory inertia, is important at all times. It is now necessary to determine which of the other terms of Equation [15] are of equal importance.

Assume first, that the w^{iv} — term and the $\ddot{w}$ — term are of the same order of magnitude (as they would have to be if Equation [23] is to hold in good approximation); then

$$0(\lambda^2) = (at/L)(1/S_y) \quad \ldots\ldots [26a]$$

The orders of magnitude of the various terms of Equation [15] are then

$$\left.\begin{aligned} &0(w^{iv} \text{ — term}) = 0(\ddot{w} \text{ — term}) = 1 \\ &0(w''' \text{ — term}) = (1 + \gamma - \nu k)(1/S_y)(L/at) \\ &0(\ddot{w}\ddot{} \text{ — term}) = (\gamma/S_y^2)(L/at)^2 \\ &0(w''\ddot{}\ddot{} \text{ — term}) = (\gamma/4)(\nu^2 k^2/S_y^3)(L/at)^3 \end{aligned}\right\} \quad [26b]$$

The third and fourth terms represent mainly the shear and rotatory inertia effects, and the last term is due principally to lateral contraction. Equations [26b] show that the latter effect is small unless νk is large. The orders of magnitude of these three terms is small compared to 1 unless the time t is very small; specifically, it is more than 1 if, respectively

$$\left.\begin{aligned} &t < [(1 + \gamma - \nu k)/S_y](L/a) \\ &t < [(\gamma)^{1/2}/S_y](L/a) \\ &t < [\gamma\nu^2 k^2/(4S_y^4)]^{1/3}(L/a) \end{aligned}\right\} \quad \ldots\ldots [26c]$$

The largest of the foregoing limiting values is (unless νk is very large) the first; it follows that if t is large compared with the quantity $[(1 + \gamma - \nu k)/S_y](L/a)$, the first two terms of Equation [15] predominate and the others are negligible. If on the other hand, t is small compared with that quantity, it is found from Equations [26b] that the $w^{\prime\prime\prime}$ — term (for instance) is large compared to unity. This is contrary to the hypothesis that the $w^{\prime\prime}$ term always predominates; hence it is necessary to repeat the whole argument on the basis of

$$0(\lambda^2) = (1 + \gamma - \nu k)/S_y^2 \quad [27a]$$

namely, the relation necessary to make the second and third terms of Equations [25] of the same order of magnitude. Equations [26b] are then replaced by

$$\left.\begin{aligned} &0(w^{\prime\prime} - \text{term}) = 1 \\ &0(w^{\prime\prime} - \text{term}) = 0(w^{\prime\prime\prime\prime} - \text{term}) \\ &\qquad = (1 + \gamma - \nu k)^2(1/S_y)^2(L/at)^2 \\ &0(w^{\prime\prime\prime\prime} - \text{term}) = (1 + \gamma - \nu k)^2(1/S_y)^4(L/at)^4 \\ &0(w^{\prime\prime\prime\prime\prime\prime} - \text{term}) = (1 + \gamma - \nu k)(\nu k/S_y^4)(\gamma/4)(L/at)^4 \end{aligned}\right\} . \quad [27b]$$

Here the $w^{\prime\prime\prime}$ term predominates if t is small; similar results may be obtained by equating the order of magnitude of the $w^{\prime\prime\prime\prime}$ term with that of the $w^{\prime\prime}$ term. Considering only the largest of the limiting values of Equations [26c], one may then conclude that if t is very small compared with the quantity $[(1 + \gamma - \nu k)/S_y](L/a)$ the shear and rotatory inertia effects are of paramount importance, and the bending terms secondary. On the other hand, if t is large compared with that quantity, only bending terms need be considered; thus, except for a short interval, Equation [23] will describe with good accuracy the behavior of the bar. If t is of the same order of magnitude as that quantity, all terms should be considered; but because of the large value of a this time is very small. For example, for a 1.7-in-square aluminum or steel bar with $\nu = 0.3$, shear and rotatory inertia may be neglected if $t \gg 10^{-6}$ sec. In the numerical examples which follow, the time t_0 (at which the shear deformations at $x = 0$ become negligible) is 2.1×10^{-5} sec, 6.2×10^{-5} sec, 3.9×10^{-5} sec, in examples I, II(a), and II(b), respectively, for this same bar, and hence in good agreement with that predicted here.

To determine how far the disturbance has traveled in 10^{-5} sec it is necessary to find first the speed of propagation. Immediately after impact the shear (and rotatory inertia) terms predominate, and it is, therefore, reasonable to expect that for a short time the bulk of the disturbance will propagate with the speed

$$L_1^{\cdot} = \sqrt{G/(N\rho)} \quad [28]$$

With this velocity the disturbance will have traveled in the bar approximately 1.1 in. in 10^{-5} sec, that is, less than the cross-sectional dimensions of the bar.

The velocity of propagation given by Equation [28] is identical with one given by the characteristic solution of Equation [15], lateral contraction terms being omitted (15). Such a solution shows that there are two distinct velocities with which a sudden disturbance may be propagated; the slower of these is that given by Equation [28] and corresponds to a sudden change in velocity and in shear force; the other is

$$L_1^{\cdot} = a = \sqrt{E/\rho} \quad [28a]$$

and corresponds to a sudden change in bending moment and in the angular velocity $w_b^{\prime\cdot}$.

The initial shear force at the struck end will now be calculated. The shear force Q is, in general

$$Q = (GA/N)(w^{\prime} - w_b^{\prime}) \quad [29]$$

At $x = L_1$ the quantity $w_b^{\prime}$ is zero; at the beginning of impact $L_1 = 0$ and $w^{\cdot} = v_0$, where v_0 is the velocity with which the beam is struck. The initial force is then (see Equation [4])

$$Q_0 = -GAv_0/(L_1^{\cdot}N) = -Av_0\sqrt{G\rho/N} \quad [30]$$

and the average shear stress

$$\tau_0 = -Gv_0/L_1^{\cdot} \quad [30a]$$

This equation has the same form as that which gives (19) the initial stress in a bar struck axially with a velocity v_0. Equations [30] hold whenever the one point of the beam undergoes a sudden change in velocity of magnitude v_0. The foregoing value for the initial shear force is identical to that given by an exact solution of Equation [15], lateral contraction terms being neglected (28).

The argument has been developed for a region close to the struck end of the bar but could be extended to any position of the wave front at which a sudden change in velocity occurred. Such a wave front travels with a velocity given by Equation [28]; for a wave front traveling with the velocity of Equation [28a] a similar argument could be developed by replacing the displacement w by the rotation $w_b^{\prime}$, and the shear-force discontinuity by one in the bending moment.

Remarks Concerning the Speed of Propagation

Consider first a bar with $I_y = I_z$, for which all terms containing Poisson's ratio vanish. In particular, Condition [21] becomes

$$(1 - \alpha^2)r_y^2(w_b^{\prime\prime})^2 = [\alpha^2 - (1/\gamma)](w^{\prime})^2 \text{ at } x = L_1 \quad [31]$$

Inspection shows that the terms $(1 - \alpha^2)$ and $[\alpha^2 - (1/\gamma)]$ must be of the same sign. Since $\gamma > 1$ they must be positive and must lie in the following region

$$(1/\gamma)^{1/2} \leq \alpha \leq 1 \quad [32]$$

It may be verified that the displacements given by

$$w = c \sin \omega[t - (x/L_1^{\cdot})] \quad [33]$$

satisfy Equation [15] with $k = 0$ if

$$(\omega r_y/a)^2 = \alpha^4/[(1 - \alpha^2)(1 - \alpha^2\gamma)] \quad [33a]$$

Comparison of Equations [32] and [33a] shows that ω must be imaginary. A real value of ω would imply that the condition of continuity of the slope due to bending at $x = L_1$ is violated. Let, in fact, the condition $w_b^{\prime\prime} = 0$ be chosen in Relations [20], rather than $\delta(w_b^{\prime})_{x=L_1} = 0$; then Equation [31] would be replaced by

$$(w_b^{\prime})^2 + (r_y w_b^{\prime\prime}/a)^2 = (1 - \gamma\alpha^2)(w^{\prime})^2 \quad [34]$$

This requires

$$(1/\gamma)^{1/2} \geqslant \alpha \quad [34a]$$

which, when substituted into Equation [33a] gives $\omega^2 > 0$.

The limiting values of α given by Equation [32] are identical with those given by the characteristic solution of the governing equations (see Equations [28]). They correspond to disturbances with very short wave length, i.e. $(1/\omega) = 0$, or, more specifically, to the propagation of discontinuities in bending moment (with $w_b^{\prime} = w^{\prime} = 0$) and in shear force (with $w_b^{\prime\prime} = 0$), respectively, for the upper and lower limit.

To investigate the general case ($k \neq 0$), let the displacement of Equation [33] be again substituted into Equation [15]; then

$$(\omega r_y k\alpha/a)^2(\gamma/2) = b \pm \sqrt{b^2 - \nu^2 k^2 \gamma \alpha^6} \quad [35]$$

where

$$b = (1 - \alpha^2)(1 - \alpha^2\gamma) + \alpha^2\nu k \ldots\ldots\ldots [35a]$$

The quantity $\nu^2k^2\gamma\alpha^6$ is always positive; therefore, ω^2 can be negative (as shall be assumed) only if $b < 0$. However, ω^2 will be real only if $|b| > |\nu k \sqrt{\gamma}\alpha^3|$. These two conditions on b will be satisfied if, and only if

$$(1 - \alpha^2)(1 - \alpha^2\gamma) + \alpha^2\nu k + |\nu k \sqrt{\gamma}\alpha^3| < 0 \ldots [35b]$$

The limiting values of α (namely, those which cause the left-hand side of Relation [35b] to vanish) are plotted in Fig. 2 for rectangular sections of height a and width b, and with $\nu = 0.3$.

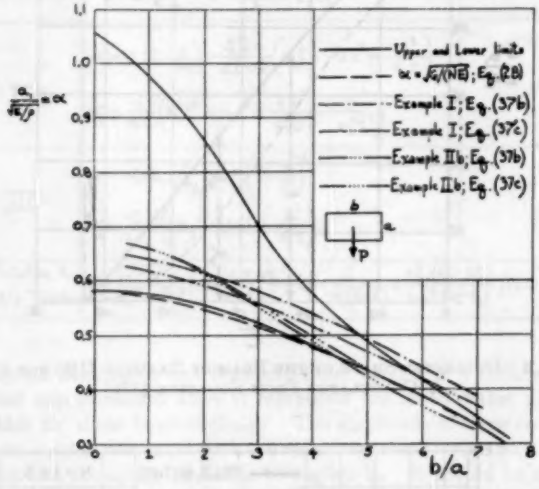

FIG. 2 VARIATION OF VELOCITY OF PROPAGATION WITH SIDE RATIO OF A RECTANGULAR SECTION
(Values for examples I and IIb were calculated for $t = 4$.)

Both the upper and lower limits of α decrease as b/a increases and for large values of b/a they lie so close that they practically establish immediately the value of α. In the numerical examples discussed later the calculated velocity of propagation (whose meaning is discussed later) also decreases with increasing (b/a) and always lies close to the lower limit.

APPROXIMATE METHOD OF SOLUTION

The foregoing theoretical development suggests an approximate method of solution of problems of lateral impact of bars. In this method, expressions are assumed, in terms of some arbitrary parameters, for the deflections of the beam. The parameters are then adjusted so as to approximate a solution of Equation [12]. In general, two wave fronts will arise, each followed by a short region in which shear deformations and rotatory inertia are important. It will then be convenient to assume the displacements in two parts, one vanishing when $x > at$ (see Equation [28a]), the other when $x > at\sqrt{1/\gamma}$ (see Equation [28]). As mentioned in the introduction, however, it is desired to obtain solutions valid for short times only, that is, when the disturbance has affected only a short portion of the beam. During such a period the bulk of the disturbance travels with velocity close to that given by Equation [28]. For such a limited solution it is therefore possible to simplify the problem by assuming that only one wave front exists, traveling with a "mean" velocity L_1 to be calculated from Equation [12]. The details of this method of solution are then as follows:

1 Assume a function $L_1 = L_1(t)$ for the distance traveled by the disturbance at any time t and functions $w = w(x, t)$ and $w_b = w_b(x, t)$ for the displacements of the bar, in terms of n arbitrary parameters. These functions must satisfy the boundary conditions given by Equations [3], [17a], [17b], and [21], and the condition $L_1(0) = 0$.

2 Substitute the assumed functions in Equation [12]. The brackets labeled $x = 0$ and $x = L_1$ will vanish because the boundary conditions already have been satisfied. Note that

$$\delta w = \sum_{i=1}^{n} (\partial w/\partial p_i)\delta p_i \ldots\ldots\ldots\ldots [36]$$

and similarly for w_b', where p_i denotes one of the arbitrary parameters.

3 The result of step 2 is an expression of the form

$$\sum_{i=1}^{n} F_i\,(t, p_1, p_2, \ldots\ldots, p_n)\,\delta p_i = 0 \ldots\ldots [37]$$

Since the δp_i quantities are arbitrary, the exact solution requires that F_i vanish for any i and all t; but in an approximate solution one must be satisfied with adjusting the available parameters to obtain the best possible approximation. The following methods are suggested to obtain an approximate solution in the range $0 < t < T$:

(a) By the method of least squares, that is, by minimizing the sum of the squares of the total errors in each function F_i; then

$$(\partial/\partial p_j)\int_0^T \sum_{i=1}^{n} F_i^2 dt = 0 \quad j = 1, 2, \ldots\ldots, n \ldots\ldots [37a]$$

(b) By setting equal to zero (or minimizing) the average total error in each function F_i; then

$$\int_0^T F_i dt = 0 \quad i = 1, 2, \ldots\ldots, n \ldots\ldots\ldots [37b]$$

(c) By substituting $t = T$ in each function F_i; then

$$F_i(T, p_1, p_2, \ldots\ldots, p_n) = 0 \quad i = 1, 2, 3, \ldots\ldots, n \ldots\ldots [37c]$$

In the numerical examples these three methods were found to yield very similar results. In example I the results of methods (a) and (b) are, for all practical purposes, the same. The results of methods (b) and (c) for the propagation velocity in examples I, II(a), and II(b), respectively, differ by 3.5, 6.8, and 0.0 per cent for a square bar, and by 4.5, 12.0, and 5.3 per cent for a rectangular bar with a width-to-height ratio of 20 to 3. The values given are percentages of the smaller value in each case.

It is probably possible to assume fairly accurate functions for the quantities L_1, w, and w_b, without an excessive number of parameters, if the solution is restricted to the "boundary layer" previously discussed. If, on the other hand, a description of a longer disturbed portion is sought, it may be found that the number of parameters required becomes excessive. In such cases it is suggested that different displacement functions be assumed near the disturbance front and at some distance from it so as to conform with the previous discussion concerning the importance of the shearing deformations and the rotatory inertia effect. This method is illustrated in two of the numerical examples but it should be emphasized that the small number of parameters used still makes the results unreliable outside the boundary layer. The discussion of Fig. 4 indicates, however, that here the Bernoulli-Euler theory provides an adequate approximation.

Expressed in general terms, the choice for the displacement functions is as follows:

Region 1; $(L_1 - L_0) \leq x \leq L_1$

$$\left.\begin{aligned} w &= w_1(x, t) \\ w_b &= w_{b_1}(x, t) \end{aligned}\right\} \quad \ldots\ldots\ldots\ldots\ldots [38a]$$

Region 2; $0 \leq x \leq (L_1 - L_0)$

$$\left.\begin{aligned} w &= w_2(x, t) \\ w_b &= w_2(x, t) - w_1(L_1 - L_0, t) + w_{b_1}(L_1 - L_0, t) \end{aligned}\right\} \quad [38b]$$

These functions must satisfy the conditions of continuity at $x = L_1 - L_0$, namely

$$\left.\begin{aligned} w_1(L_1 - L_0, t) &= w_2(L_1 - L_0, t) \\ w_{b_1}'(L_1 - L_0, t) &= w_2'(L_1 - L_0, t) \end{aligned}\right\} \quad \ldots\ldots\ldots [38c]$$

as well as the following requirements on the shear force and bending moment

$$\left.\begin{aligned} (GA/N)[w_1'(L_1 - L_0, t) - w_{b_1}'(L_1 - L_0, t)] &= 0 \\ EI_y w_{b_1}''(L_1 - L_0, t) &= EI_y w_2''(L_1 - L_0, t) \end{aligned}\right\} \quad [38d]$$

Within the distance $(L_1 - L_0)$, which varies as the disturbance progresses along the bar, the effects of shear, rotatory inertia, and lateral contraction are important. The shear-strain energy vanishes in Region 2. The distance L_0 may be taken as a parameter or may be expressed in terms of other parameters. If the time elapsed after the start of impact is very small ($t \leq t_0$), only Region 1 will be present. The numerical examples show that for large values of time ($L_1 - L_0$) is small compared with L_1, and that in Region 2 the (constant) shearing displacements constitute only a small fraction of the total displacements. In general, the order of magnitude of $(L_1 - L_0)$ is $(1 + \gamma - \nu k)(L_1'/a)(L/S_y)$, where the value for the propagation velocity L_1' may be taken in good approximation from Equation [28].

Numerical Examples

Four numerical examples, described in Table 1, were solved by the foregoing procedure. The details of the solutions, omitted here, have been presented more fully in reference (1). The assumed displacements are given in Table 2, together with the expression for the time $t = t_0$ at which the disturbance has traveled a distance equal to the length of Region 1. Typical results of the calculations are plotted in Figs. 2 to 5.

In each example the velocity of propagation $L_1' = a_1$ was taken as one of the parameters, and therefore, the values obtained represent mean velocities within the range of validity of the solution. In other words, a_1 is a weighted average of the velocities of propagation of all the component wave lengths contained in the disturbance and, as expected, was close to the velocity, given by Equation [28], for the propagation of sudden jumps in velocity and shear force.

TABLE 1 DESCRIPTION OF NUMERICAL EXAMPLES

	Example I	Example II(a)	Example II(b)	Example III
Boundary conditions at $x = 0$	$w = v_0 t$	$w = v_0 t$		$w = v_0 t + v_1 t^2$
	$w_b' = 0$	$w_b' = 0$		$w_b' = 0$
Arbitrary parameters	α	α, c		α
Equations used in solution	[37a], [37b], [37c]	[37b], [37c]		[37b]
Restrictions on calculations	Lateral contraction neglected	Lateral contraction neglected	Lateral contraction considered, $t \leq t_0$	$k = 0$, $t \leq t_0$

Notes: (a) $\alpha = a_1/\sqrt{E/\rho}$, where distance traveled by disturbance is $L_1 = a_1 t$. (b) Quantities v_0 and v_1 are constants: v_1 is given in Equation [40a]. (c) At $t = t_0$ disturbance has traveled a distance equal to length of Region 1 of Equations [38a]

The variation of the shear force at the struck end of the bar of example I is plotted in Fig. 4 together with that obtained from the exact solution, Equation [28]. It may be seen that the two curves are in good agreement within the boundary layer previously discussed. It should be noted that (taking as an example a rectangular section), a wave traveling with the velocity of Equation [28] will have traveled a distance equal to the height of the bar when the abscissa of Fig. 4 equals approximately 6.2.

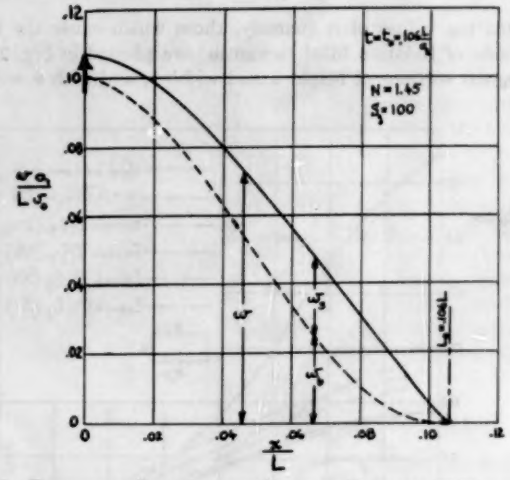

Fig. 3 Deflected Shape of the Beam of Example II(b) for $t = t_0$, Calculated From Equation [37c]

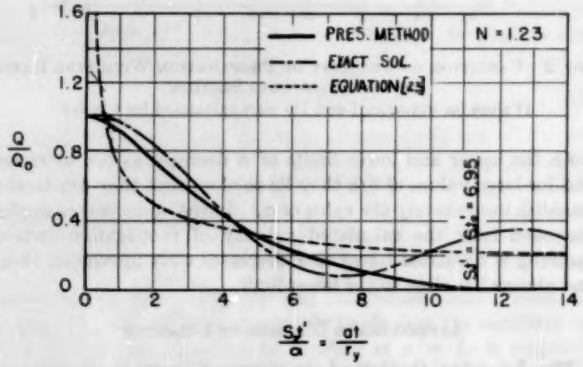

Fig. 4 Variation of Shear Force at Point of Impact for Example I

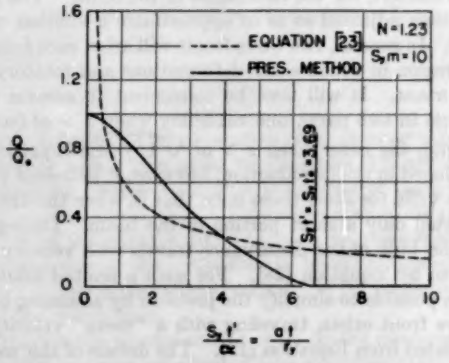

Fig. 5 Variation of Shear Force at Point of Impact for Example III

TABLE 2 EXPRESSIONS FOR ASSUMED DEFLECTIONS AND FOR t_0

Example No.	Displacements of Region 1 ($a_2t - t_0 \leq x \leq a_1 t$)	Displacements of Region 2 ($0 \leq x \leq a_1 t - t_0$)	Expressions for $t_0 = L_0/a_1$ when $t \leq t_0$	Expressions for $t_0 = L_0/a_1$ when $t \geq t_0$
I	$w = v_0\left(t - \frac{x}{a_1}\right)$ $w_b = \frac{v_0 K}{6r_g}\left(2a_1 t^2 - 3xt + \frac{x^3}{a_1^2 t}\right)$	$w = w_2 = v_0\left(t - \frac{x}{a_1}\right) - \frac{v_0 K}{r_g}\left[\frac{x^3 - 3a_1(t-t_0)x^2 + a_1^2(t-t_0)^2 x^3}{2a_1^2 t(t-t_0)^2}\right]$ $w_b = w_2 - v_0 t_0 + \frac{v_0 a_1 t_0^2 K(3t-t_0)}{6r_g t}$	$t_0 = \frac{2r_g}{Ka_1}$	$t_0 = t - \sqrt{t^2 - \frac{2tr_g}{Ka_1}}$
IIa	$w = v_0\left(t - \frac{x}{a_1}\right) + \frac{v_0 c}{aL}\left(a_1 t x - 2x^2 + \frac{x^3}{a_1 t}\right)$ $w_b = \frac{v_0 K}{6r_g}\left(a_1 t - \frac{3x^2}{a_1} + \frac{2x^3}{a_1^2 t}\right)$	$w = w_2 = v_0\left[t + Px^2 + \frac{Nx^3}{a_1(t-t_0)} + \frac{Mx^4}{a_1^2(t-t_0)^2}\right]$ $w_b = w_2 - v_0\left[t_0 + \frac{ca_1 t_0^2(t-t_0)}{aLt} - \frac{Ka_1 t_0^2(3t-2t_0)}{6r_g t}\right]$	$t_0 = \frac{aL}{ca_1^2}$	$t_0 = \frac{1}{2}\left[t - \sqrt{t^2 - \frac{4tr_g}{Ka_1}}\right]$
IIb	$w = v_0\left(t - \frac{x}{a_1}\right) - \frac{v_0 Rc}{aLvk}\left(a_1 t x - 2x^2 + \frac{x^3}{a_1 t}\right)$ $w_b = \frac{v_0 c}{aL}\left(a_1^2 t^2 - 4x^2 + \frac{4x^3}{a_1 t} - \frac{x^4}{a_1^2 t^2}\right)$	—	$t_0 = -\frac{vkaL}{Rca_1^2}$	—
III	$w = v_0\left(t - \frac{x}{a_1}\right) + v_1\left(t - \frac{x}{a_1}\right)^2$ $w_b = \frac{v_0 K}{6r_g}\left(2a_1 t^2 - 3xt + \frac{x^3}{a_1^2 t}\right)$	—	$t_0 = \frac{2v_0 r_g}{v_0 a_1 K - 4r_g v_1}$	—
Notation for this Table	$K = \frac{\sqrt{\alpha\gamma - 1}}{\sqrt{\beta(1-\alpha)}}$; $M = \frac{KS_g}{a_1 Lt}\left(\frac{t}{2} - t_0\right) - \frac{1}{a_1^2(t-t_0)} + \frac{ct_0(3t-3t_0)}{aLt(t-t_0)}$; $N = -\frac{2KS_g}{a_1 Lt}\left(\frac{t}{2} - t_0\right) + \frac{3}{a_1^2(t-t_0)} + \frac{ct_0(-4t+3t_0)}{aLt(t-t_0)}$; $P = \frac{ct_0^2\alpha a_1 - L}{a_1^2 L(t-t_0)} - M - N$; $R = \frac{2(1-\alpha^2)}{\alpha^2} + \frac{S_g^2(1-\alpha\gamma)}{8\alpha^2\beta}$			

Beyond that point the Bernoulli-Euler theory is a sufficiently good approximation since it represents the mean value about which the shear force oscillates. The amplitude of these oscillations is small compared with the maximum shear force and it was therefore thought permissible to neglect it. It should be mentioned, however, that these oscillations arise because of the presence of shear deformations, which therefore in reality affect the entire beam. Only if they are neglected is it possible to carry out the order-of-magnitude considerations as in Equation [24]; consequently, the use of the Bernoulli-Euler theory in this region is consistent with the accuracy employed throughout this development.

Examples II(a) and II(b) represent solutions of the same problem using two different deflected shapes, respectively, neglecting and considering the effect of lateral contraction. For $k = 0$, however, all lateral contraction terms vanish; hence, in this particular case, the discrepancy between the results of those examples is due to the variation in deflected shape alone. The difference between the two velocities of propagation is only 4.7 per cent of the smaller value, indicating that, in this case at least, a change in assumed shape does not influence greatly the results.

For other values of k examples II(a) and II(b) give widely varying results, indicating that the importance of lateral contraction increases with k. Thus, for a rectangular bar with a width-to-height ratio of 20 to 3, the foregoing error increases to 46.4 per cent of the smaller velocity.

In example III the quantity v_0 was determined by assuming that the beam is struck at $x = 0$ by a rigid mass M moving with an initial velocity v_0. The assumption was made that the beam and the mass remain in contact; therefore this solution holds only within the duration of the subimpacts described in references (2, 3, 4). However, the time t_0 is considerably smaller than the measured duration of the subimpacts. It may be remarked, incidentally, that it is difficult to find direct experimental proof for these solutions within the boundary layer because of the extremely short distance covered by it. The only verification possible appears to be that concerning the accuracy of the basic equations at high frequencies (8, 13).

Returning to example III, let the displacements of the struck end of the beam be expressed as

$$w(0, t) = \sum_{i=0}^{\infty} v_i t^{(i+1)} \quad \ldots\ldots\ldots\ldots\ldots [39]$$

where v_0 is the initial velocity, and $2v_1$ the initial acceleration. The equation of motion of the striking mass is

$$(GA/N)(w' - w_b') = M\ddot{w} \quad \text{at } x = 0 \quad \ldots\ldots\ldots [40]$$

When the various displacement functions are substituted in this equation, the quantities v_i can be determined in terms of v_0 by equating coefficients of like powers of t. If only the two lowest powers are kept, the result is

$$v_1/v_0 = -GA/(2NMa_1) \quad \ldots\ldots\ldots\ldots [40a]$$

The results of example III depend on the parameter $(S_g m)$, where S_g is the slenderness ratio of the bar, and m is the ratio of the mass of the striking body to the mass of the bar. If m is very large, or the bar very slender, the end of the bar moves with constant velocity, thus approaching the conditions of example I. The results of the two examples are, in fact, identical if $(1/S_g m)$ vanishes. The variation of the shear force of the struck end of the beam of example III is shown in Fig. 5 for a value $S_g m = 10$. The variation is similar to that of Fig. 4 but the shear force of course decreases more rapidly than in example I. Again, the Bernoulli-Euler theory may be used for regions beyond the boundary layer.

In conclusion, it is felt that the present approach is in certain respects different from the methods usually employed in this type of problem and therefore may be of some interest. Of course the applications presented are limited in scope; it is, nevertheless, hoped that they may prove of value as a basis for further work.

Acknowledgment

The author gratefully acknowledges the contributions to the development described of Robert E. Heninger, Vincent P.

Zimnoch, and Chi-Chang Chao and wishes to thank the Office of Naval Research, U. S. Navy, for its support of the investigation.

BIBLIOGRAPHY

1 "An Energy Theory of Transverse Impact on Beams, Including the Effects of Shear, Rotatory Inertia and Lateral Contraction," by B. A. Boley, R. E. Heninger, and V. P. Zimnoch, Technical Report submitted to the Office of Naval Research, U. S. Navy, under contract N6-onr-225-29, project NR-064-355, January, 1952.

2 "Photoelastic Study of Stresses Due to Impact," by F. Tuzi and M. Nisida, *Philosophical Magazine*, vol. 21, 1936, p. 448.

3 "Impact Stresses in a Freely Supported Beam," by R. N. Arnold, Proceedings of The Institution of Mechanical Engineers, London, England, vol. 137, 1937, pp. 217–281.

4 "Impact on Beams," by H. L. Mason, JOURNAL OF APPLIED MECHANICS, Trans. ASME, vol. 58, 1936, p. A-55.

5 "Transverse Waves in Beams," by I. Vigness, Proceedings of the Society for Experimental Stress Analysis, vol. 8, 1951, pp. 69–82.

6 "On the Correction for Shear of the Differential Equation for Transverse Vibrations of Prismatic Bars," by S. Timoshenko, *Philosophical Magazine*, vol. 41, 1921, pp. 744–746.

7 "Influence of Rotatory Inertia and Shear on Flexural Motions of Isotropic Elastic Plates," by R. D. Mindlin, JOURNAL OF APPLIED MECHANICS, Trans. ASME, vol. 73, 1951, pp. 31–38.

8 "Timoshenko's Shear Coefficient for Flexural Vibrations of Beams," by R. D. Mindlin and H. Deresiewicz, Technical Report No. 10, Office of Naval Research Contract Nonr-266(09), June, 1953.

9 "The Dispersion of Supersonic Waves in Cylindrical Rods of Polycrystalline Silver, Nickel and Magnesium," by S. Shear and A. B. Focke, *Physical Review*, vol. 57, 1940, p. 532.

10 "The Velocity of Longitudinal Waves in Cylindrical Bars," by D. Bancroft, *Physical Review*, vol. 59, 1941, p. 588.

11 "Dispersion of Elastic Waves in Solid Circular Cylinders," by G. E. Hudson, *Physical Review*, vol. 63, 1943, p. 46.

12 "A Critical Study of the Hopkinson Pressure Bar," by R. M. Davies, Philosophical Transactions of the Royal Society of London, England, vol. 240, 1948, p. 375.

13 "Stress Waves in Solids," by H. Kolsky, Clarendon Press, Oxford, England, 1953.

14 "Transverse Impact of Long Beams, Including Rotatory Inertia and Shear Effects," by M. A. Dengler and M. Goland, Proceedings of the First U. S. National Congress of Applied Mechanics, 1952, p. 179.

15 "On Traveling Waves in Beams," by R. W. Leonard and B. Budiansky, NACA TN 2874, January, 1953.

16 "Über Fortpflanzungageschwindigkeiten Kleiner Schwingungen in Einem Unbegrenzten Isotropen Kreiscylinder," by L. Pochhammer, *Crelle Journal für Mathematik*, vol. 81, 1876, pp. 324–336.

17 "Flexural Waves in Beams According to More Exact Theory of Bending," by J. Miklowitz, NAYORD Report 2049, 1953.

18 "The Mathematical Theory of Elasticity," by A. E. H. Love, fourth edition, Dover Publications, New York, N. Y., 1944.

19 "Theory of Elasticity," by S. Timoshenko and J. N. Goodier, second edition, McGraw-Hill Book Company, Inc., New York, N. Y., 1951.

20 "Theory of Elastic Stability," by S. Timoshenko, McGraw-Hill Book Company, Inc., New York, N. Y., 1936.

21 "Numerical Procedures for the Calculation of the Stresses in Monocoques," by N. J. Hoff, B. Klein, and P. A. Libby, NACA TN 999.

22 "Higher Mathematics for Engineers and Physicists," by I. S. Sokolnikoff and E. S. Sokolnikoff, McGraw-Hill Book Company, Inc., New York, N. Y., 1941.

23 "Elastic Waves and Vibrations of Thin Rods," by J. Prescott, *Philosophical Magazine*, vol. 33, seventh series, 1942, pp. 703–754.

24 "Theory of Sound," by J. W. S. Rayleigh, Dover Publications, New York, N. Y., 1945.

25 "Vibration Problems in Engineering," by S. Timoshenko, second edition, D. Van Nostrand Company, Inc., New York, N. Y., 1937.

26 "The Application of Saint-Venant's Principle in Some Problems of Impact," by B. A. Boley, Technical Report No. 2, U. S. Navy Contract Nonr-266(20), Columbia University, 1953. Also, paper to be published in the JOURNAL OF APPLIED MECHANICS.

27 "The Propagation of Elastic Waves in a Rod," by J. L. B. Cooper, *Philosophical Magazine*, vol. 38, seventh series, 1953, p. 147.

28 "Some Solutions of the Timoshenko-Beam Equations," by B. A. Boley and Chi-Chang Chao, Technical Report No. 3, U. S. Navy Contract Nonr-266(20), Columbia University, 1954.

Appendix

DETERMINATION OF N

The quantity N is defined by the equation

$$2GU_s = \int\int (\tau_{xz}^2 + \tau_{yz}^2)\, dy\, dz = (N/A)(\int\int \tau_{zz} dy\, dz)^2$$

for a beam bent by a force in the z-direction. In this equation U_s is the shear-strain energy per unit of length, and the limits of integration must be chosen so as to cover the entire cross section. For a rectangular section, sufficiently accurate values of the shear stresses may be obtained from the approximate formulas given by Timoshenko.[4] The results are plotted in Fig. 1.

These values of N correspond to the stress distribution at some distance from the point of load application, and there is some question as to whether they are applicable in the portion of the beam immediately behind the disturbance front (Region 1 of Equation [38*a*]). For very small values of time, Region 1 is close to the point of impact, and therefore (according to Saint Venant's principle) strongly affected by the details of load application. Whether this is true of Region 1 for other values of time is the subject of an investigation in progress at present (26).

The coefficient N cannot be used to account for normal stress distributions radically different from that of Equations [3], such as arise when skin waves become prominent (19). In such case a more accurate theory, similar to Prescott's (23, 27), would be required, or the present approach might be modified by the introduction of some arbitrary parameters in the stress variation within the cross section of the bar. The coefficient N was calculated in the foregoing from statical considerations; the correction suggested by Mindlin (8, 14) was not included in the calculations.

[4] Reference (19), p. 327 ff.

Anisotropic Loading Functions for Combined Stresses in the Plastic Range

By L. W. HU[1] AND JOSEPH MARIN,[2] STATE COLLEGE, PA.

A loading function is a relation between combined stresses for which the beginning of plastic flow takes place. The loading function for a given material is different depending upon the initial plastic strains produced. That is, the initial stress or strain history influences the subsequent loading function. This paper gives the results of an experimental investigation to determine the validity of certain loading functions proposed for anisotropic materials. The study reported was conducted for an aluminum alloy 24S-T and the state of stress covered was biaxial tension. These stresses were produced in the usual way by subjecting thin-walled tubular specimens to axial tension and internal pressure. The test results showed that none of the existing loading functions is adequate for interpreting the plastic stress-strain relations obtained. Tests also were made to determine the change in the loading function with increase in plastic flow. It was found that the loading function did not remain symmetrical with respect to the original function, nor was the new loading function the same as the original except for a shift of origin. However, the test results support in a qualitative way the concept of the so-called "yield corner."

Introduction

VARIOUS theories of plasticity have been proposed for expressing theoretically the stress-strain relations for metals subjected to combined stresses in the plastic range. To express specifically these plastic stress-strain relations it is necessary to assume a so-called "loading function." This function also may be called a "yielding function" when it is used to define the beginning of plastic deformation (1, 2).[3] A yielding function is a relation between the combined stresses and the simple tension yield strength of the material and defines the beginning of yielding for states of combined stress.

A loading function is a relation between the combined stresses for materials which have been stressed initially beyond yielding; that is, the loading function considers the strain history of the material. For stress states within the limits defined by the loading function, plastic deformation does not occur. (For example, in Fig. 3, the ellipse shown represents a loading function for two-dimensional stresses based upon the distortion-energy criterion.) For a loading function correctly to represent the behavior of the material, stressing of the material along the path represented by the loading function should result in changes in the elastic strains only, with no change in the plastic deformation. For three-dimensional stresses, the loading function may be represented by a surface in space with the co-ordinates representing the three principal stresses. Two different types of these functions or surfaces have been used in conjunction with theories of plasticity. In one type, such as the distortion-energy criterion, the loading surface has a unique normal at all points. In a second type, such as the maximum-shear criterion, there are points on the loading surface where discontinuities occur and where there is no unique normal (2).

In addition to specifying conditions of limiting plastic flow, the concept of the loading function provides a means of distinguishing between certain plasticity theories. For example, a consequence of the slip theory (3) is the existence of a so-called yield corner where a unique normal to the loading surface is not required. On the other hand, the usual formulations of the flow theory (4) require that the loading surface have a unique normal everywhere. Other characteristics of the loading functions are described in references (5) and (6).

Previous Experimental Investigations

Few experimental studies have been made to verify the concept of the loading function. The first extensive study was made by Taylor and Quinney (7) in 1931, and a few experimental results have been reported by other investigators since that time. In 1947, Cunningham, Dorn, and Thomsen (8) reported the variation in the distortion-energy ellipse for different stages of straining. These results indicated that a loading function existed and could be expressed in terms of a number of concentric distortion-energy ellipses for different stages of straining. However, the foregoing test results were restricted to biaxial stresses with constant principal stress ratios during loading.

Shaw and Wycherley (9) conducted a biaxial-stress test with variable principal stress ratios. This test was made by loading a thin-walled tubular steel specimen under axial loading and internal pressure in such a manner that the octahedral shear stress or distortion energy was maintained constant. The results of this test showed that the octahedral shear or distortion-energy loading function was not adequate. Variable biaxial tensile-stress tests for an aluminum alloy 14S-T4 were made by the authors (10) to determine the accuracy of both the distortion-energy and maximum shear-stress criterion. In these tests either the distortion energy or the maximum shear stress was maintained constant. The results showed that appreciable plastic deformation occurred and that neither criterion was adequate as a loading function. Other similar tests, made by the authors on an aluminum alloy 14S-T6 (11) and on a cold-drawn mild steel, also show that the distortion-energy loading function is not adequate.

Purpose of Investigation

The purpose of this investigation was to investigate for an aluminum alloy 24S-T, the validity of various loading functions, such as distortion-energy criterion, the maximum shear-stress criterion, and a criterion suggested by Prager (1). In addition, tests were conducted to study the changes in the loading function

---

[1] Assistant Professor of Engineering Research, Department of Engineering Mechanics, The Pennsylvania State University.

[2] Head, Department of Engineering Mechanics, The Pennsylvania State University. Mem. ASME.

[3] Numbers in parentheses refer to the Bibliography at the end of the paper.

Contributed by the Applied Mechanics Division and presented at the Annual Meeting, New York, N. Y., November 28–December 3, 1954, of The American Society of Mechanical Engineers.

Discussion of this paper should be addressed to the Secretary, ASME, 29 West 39th Street, New York, N. Y., and will be accepted until April 11, 1955, for publication at a later date. Discussion received after the closing date will be returned.

Note: Statements and opinions advanced in papers are to be understood as individual expressions of their authors and not those of the Society. Manuscript received by ASME Applied Mechanics Division, July 11, 1953. Paper No. 54—A-9.

with increase in stress. Three possible types of change were considered and will be designated as (*a*) isotropic expansion, (*b*) shifting of origin, and (*c*) yield corner. One of the purposes of this study was to determine which of these types of loading-function change represents the actual behavior.

The loading functions will be considered and tested for the vicinity of the proportional limit, since for the condition of yield the loading function is not dependent on the strain history (2) and therefore can be applied.

For the material tested in this study initial isotropy of the material was not present and it was necessary to modify the usual form of the loading functions to provide for this anisotropy. For this purpose, an anisotropic loading function suggested by Hill (15) was modified and used for the present investigation.

Anisotropic Loading Functions

Initial anisotropy is said to exist in a material when it has different mechanical properties in different directions. Another type of anisotropy in materials may be produced during the straining of a material in the plastic range. The loading function in the case of initial anisotropy may not be of symmetrical form with the yield stress in simple tension equal to that in compression. Furthermore, if anisotropy also occurs during straining, then the loading function does not remain geometrically similar to the initial yielding function.

Assuming the initial isotropy of materials, Reuss (14) first proposed an anisotropic loading function, in which the anisotropy due to straining was described by containing the plastic-strain components in the formulation of the loading function. In 1948, Hill (15) suggested a loading function to describe the initial anisotropy of materials by introducing six material constants in the formulation of this function. Studying the plastic behavior of metal sheets, Jackson, Smith, and Lankford (16) proposed a loading function having the same form as the one suggested by Hill. Other similar relations also were presented by Fisher (17), and by Hazlett, Robinson, and Dorn (18). In this paper new loading functions for initially anisotropic materials will be suggested based upon the general form of Hill's loading function (15). The relation proposed by Hill is

$$2f = F(\sigma_{22} - \sigma_{33})^2 + G(\sigma_{33} - \sigma_{11})^2 + H(\sigma_{11} - \sigma_{22})^2 + 2(L\sigma_{23}^2 + M\sigma_{31}^2 + N\sigma_{12}^2) = 1 \quad [1]$$

where F, G, H, L, M, and N are experimental constants and the σ-values are stress components.

For isotropic materials, the loading or yielding funtions for strain-independent materials and two-dimensional stresses are

$$\bar{\sigma}^2 = \sigma_1^2 - \sigma_1\sigma_2 + \sigma_2^2 = \sigma_y^2 \quad [2]$$

for the distortion-energy criterion.

$$\left.\begin{array}{l} \text{For } \sigma_1 > \sigma_2 > 0 \text{ or } \sigma_1 < \sigma_2 < 0,\ \sigma_1 = \pm\sigma_y \\ \text{For } \sigma_2 > \sigma_1 > 0 \text{ or } \sigma_2 < \sigma_1 < 0,\ \sigma_2 = \pm\sigma_y \\ \text{For } \sigma_1 > 0 > \sigma_2 \text{ or } \sigma_2 > 0 > \sigma_1,\ \sigma_1 - \sigma_2 = \pm\sigma_y \end{array}\right\} \quad [3]$$

for the maximum-shear criterion, and

$$\frac{3}{2}\left[(\sigma_1^2 - \sigma_2\sigma_1 + \sigma_2^2)^2 - \frac{1}{12}(\sigma_1 + \sigma_2)^2(\sigma_1 - 2\sigma_2)^2(\sigma_2 - 2\sigma_1)^2\right] = \sigma_y^6 \quad [4]$$

for Prager's criterion. In Equations [1] to [4], σ_y is the yield stress in simple tension or compression (assumed equal for all directions) and σ_1 and σ_2 are the principal stresses.

Dividing Equations [2] and [4] by σ_y

$$\left(\frac{\sigma_1}{\sigma_y}\right)^2 - \left(\frac{\sigma_1}{\sigma_y}\right)\left(\frac{\sigma_2}{\sigma_y}\right) + \left(\frac{\sigma_2}{\sigma_y}\right)^2 = 1 \quad [2a]$$

$$\left.\begin{array}{ll} \dfrac{\sigma_1}{\sigma_y} = \pm 1 & \text{for } \sigma_1 > \sigma_2 > 0 \text{ or } \sigma_1 < \sigma_2 < 0 \\ \dfrac{\sigma_2}{\sigma_y} = \pm 1 & \text{for } \sigma_2 > \sigma_1 > 0 \text{ or } \sigma_2 < \sigma_1 < 0 \\ \left(\dfrac{\sigma_1}{\sigma_y}\right) - \left(\dfrac{\sigma_2}{\sigma_y}\right) = \pm 1 & \text{for } \sigma_1 > 0 > \sigma_2 \text{ or } \sigma_1 < 0 < \sigma_2 \end{array}\right\} \quad [3a]$$

$$\frac{3}{2}\left\{\left[\left(\frac{\sigma_1}{\sigma_y}\right)^2 - \left(\frac{\sigma_1}{\sigma_y}\right)\left(\frac{\sigma_2}{\sigma_y}\right) + \left(\frac{\sigma_2}{\sigma_y}\right)^2\right]^3 - \frac{1}{12}\left(\frac{\sigma_1}{\sigma_y} + \frac{\sigma_2}{\sigma_y}\right)^2\left(\frac{\sigma_1}{\sigma_y} - \frac{2\sigma_2}{\sigma_y}\right)^2\left(\frac{\sigma_2}{\sigma_y} - \frac{2\sigma_1}{\sigma_y}\right)^2\right\} = 1 \quad [4a]$$

The dimensionless loading functions given by Equations [2*a*], [3*a*], and [4*a*] can be represented geometrically by using the dimensionless ratios σ_1/σ_y and σ_2/σ_y as co-ordinates. For anisotropic materials, the geometrical symmetry of the loading surface can be retained, if the yield stresses in both directions are considered; that is, the anisotropic loading functions for the different criteria can be obtained from Equations [2*a*], [3*a*], and [4*a*] by rewriting these relations in the form

$$\left(\frac{\sigma_1}{\sigma_{1y}}\right)^2 - \left(\frac{\sigma_1}{\sigma_{1y}}\right)\left(\frac{\sigma_2}{\sigma_{2y}}\right) + \left(\frac{\sigma_2}{\sigma_{2y}}\right)^2 = 1 \quad [5]$$

$$\left.\begin{array}{ll} \dfrac{\sigma_1}{\sigma_{1y}} = \pm 1 & \text{for } \sigma_1 > \sigma_2 > 0 \text{ or } \sigma_1 < \sigma_2 < 0 \\ \dfrac{\sigma_2}{\sigma_{2y}} = \pm 1 & \text{for } \sigma_2 > \sigma_1 > 0 \text{ or } \sigma_2 < \sigma_1 < 0 \\ \dfrac{\sigma_1}{\sigma_{1y}} - \dfrac{\sigma_2}{\sigma_{2y}} = \pm 1 & \text{for } \sigma_1 > 0 > \sigma_2 \text{ or } \sigma_1 < 0 < \sigma_2 \end{array}\right\} \quad [6]$$

$$\frac{3}{2}\left[\left(\frac{\sigma_1}{\sigma_{1y}}\right)^2 - \left(\frac{\sigma_1}{\sigma_{1y}}\right)\left(\frac{\sigma_2}{\sigma_{2y}}\right) + \left(\frac{\sigma_2}{\sigma_{2y}}\right)^2\right]^3 - \frac{1}{8}\left(\frac{\sigma_1}{\sigma_{1y}} + \frac{\sigma_2}{\sigma_{2y}}\right)^2\left(\frac{\sigma_1}{\sigma_{1y}} - \frac{2\sigma_2}{\sigma_{2y}}\right)^2\left(\frac{\sigma_2}{\sigma_{2y}} - \frac{2\sigma_1}{\sigma_{1y}}\right)^2 = 1 \quad [7]$$

where the yield stresses in directions 1 and 2 are represented by σ_{1y} and σ_{2y}, respectively. By the foregoing modification in the loading functions simple tensile strengths in the σ_1 and σ_2 directions can be made to agree with the actual values; that is from Equation [5], [6], or [7], for $\sigma_2 = 0$, $\sigma_1 = \sigma_{1y}$ and for $\sigma_1 = 0$, $\sigma_2 = \sigma_{2y}$.

In the foregoing derivation, the tensile and compressive yield stresses in one direction were assumed equal to each other. For materials such as cast iron, this is not the case. However, the same principles can be applied to the formulation of anisotropic loading functions for such materials, if the following rules are observed:

1 The tensile stress is assumed to be positive, and the compressive stress is assumed to be negative.

2 The yield stress σ_y in the above equations has a positive value equal to the tensile yield stress and has a negative value equal to the compressive yield stress in the same direction.

3 The ratios σ_1/σ_{1y} and σ_2/σ_{2y} are always positive.

In this manner, the geometrical symmetry of loading surface

can be retained, even when the material has different yield stresses in tension and compression for various directions.

The loading functions as expressed by Equations [5], [6], and [7] will now be checked experimentally by using tension-tension tests on an aluminum alloy 24S-T.

Loading-Function Tests on Alcoa 24S-T

The material tested was an aluminum alloy designated as 24S-T. The mechanical properties and plastic stress-strain relations of this material for various tensile biaxial-stress ratios are given in reference (12). The testing machine used to apply combined internal pressure and axial loading to a tubular specimen is described in reference (13) and the dimensions of the specimen used are shown in Fig. 1.

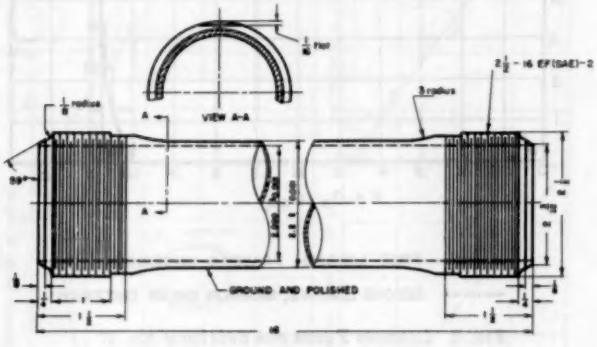

Fig. 1 Biaxial-Stress Specimen

(All dimensions are in inches.)

The specimens were subjected to a specific manner of loading based on predetermined values for each test. The average values of the axial and tangential stresses were used assuming a thin-walled tube. Since the plastic strains were small, the values of the stresses were calculated based upon the initial specimen dimensions; that is, the axial and tangential-stress values were determined by the equations

$$\left.\begin{aligned} \sigma_a &= \frac{P}{\pi(d_i + t)t} \\ \text{and} \qquad \sigma_t &= \frac{pd_i}{2t} \end{aligned}\right\} \qquad \text{[8]}$$

where P = the total axial load, p = the internal pressure, d_i = the initial internal diameter, and t = the initial wall thickness.

The radial stress σ_r is small and was assumed to be zero. Both the tangential and axial strains were measured by using an SR-4 electric resistance-wire strain gage, since the plastic strains were of the order of magnitude of the elastic strains. The elastic values of the radial strains were determined by the use of Hooke's law and the plastic strains were calculated by considering that the volume remains constant as assumed in the theories of plasticity. Nominal stresses and strains were calculated based upon the initial dimensions and the original gage length since the plastic strains produced were relatively small.

Based upon the simple stress-strain relations reported in reference (12), a loading path *O-A-B-C-O*, as shown in Fig. 2, was selected for determining the proportional limits in the axial and tangential directions of the tubular specimens. Since the loading surface must be concave toward the origin, the paths *A-B* and *B-C* must be either on or within the yielding surface. To determine the proportional limits four tests were conducted at different stress levels. In Table 1, the plastic strains produced during the loading path *O-A-B-O* are given. The proportional limits were found to be 34,000 psi in the axial direction, and 30,000 psi in the tangential direction. Using these values of stresses, the loading paths for the following tests were computed.

TABLE 1 PLASTIC STRAINS PRODUCED ALONG LOADING PATH *O-A-B-O* IN FIG. 2

Stress component, psi		Plastic-strain component, 10^{-3} in/in	
Axial, σ_a	Tangential, σ_t	Axial, ϵ_a^p	Tangential, ϵ_t^p
40000	40000	0.18	2.20
39000	35000	0.19	0.32
36000	32000	0	0.12
34000	30000	0	0

To check the validity of the distortion-energy criterion, a test was conducted by subjecting a specimen to biaxial tension along the loading path 0-1-2 . . . . . 19-20-0 as shown in Fig. 3. If the

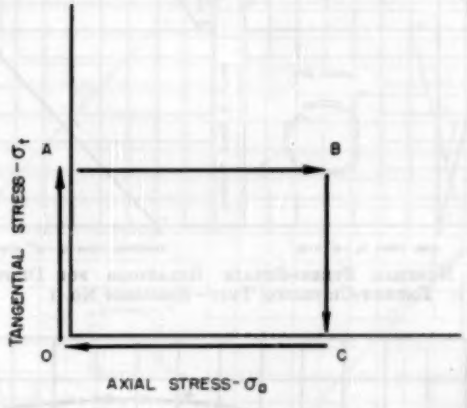

Fig. 2 Loading Path for Determination of Proportion Limit

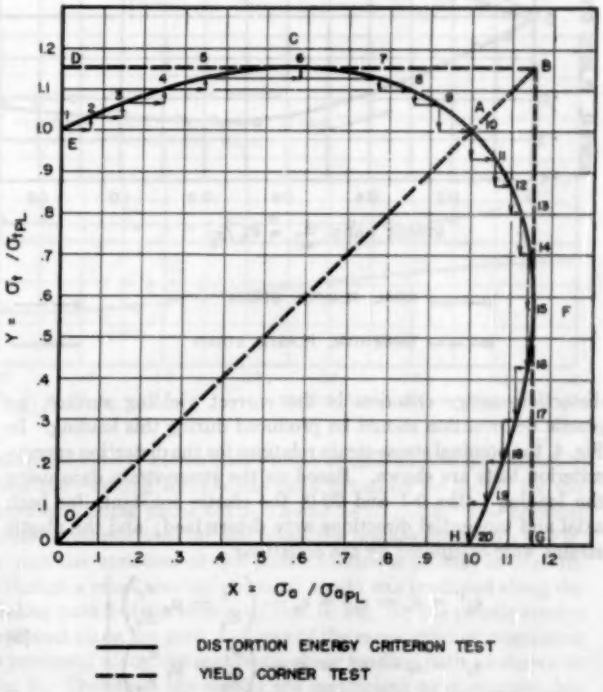

Fig. 3 Loading Path for Distortion Energy-Criterion Test and Yield-Corner Test

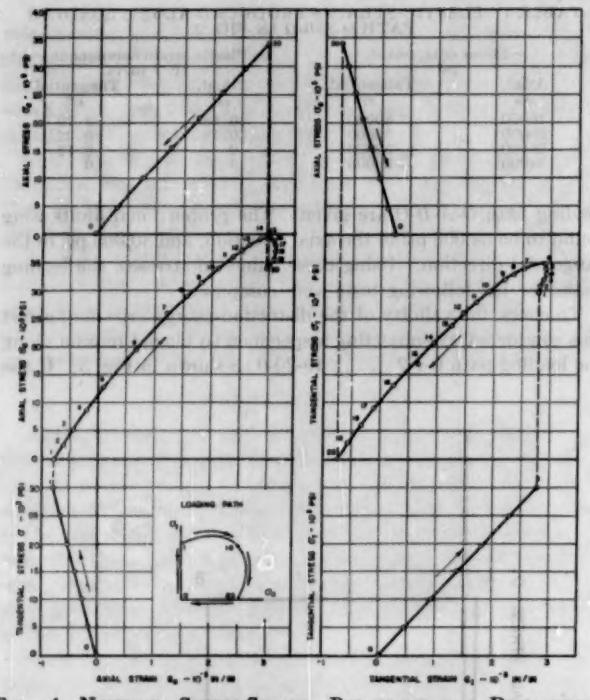

FIG. 4 NOMINAL STRESS-STRAIN RELATIONS FOR DISTORTION ENERGY-CRITERION TEST—SPECIMEN NO. 1

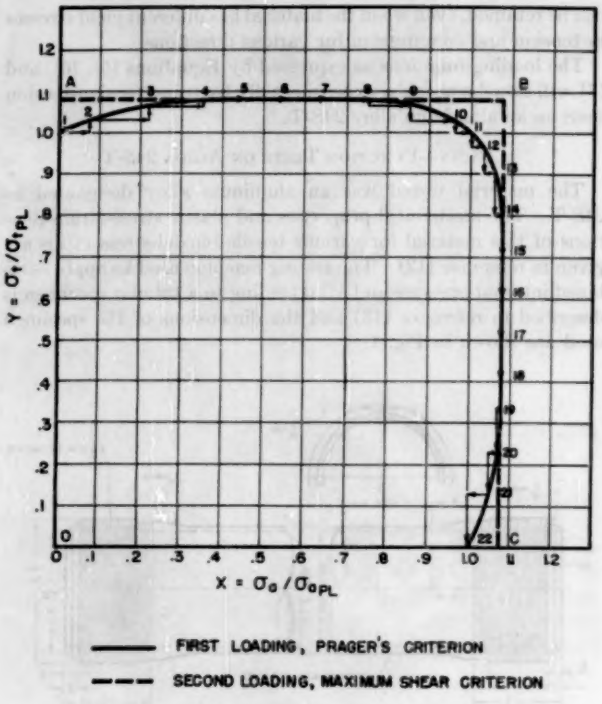

FIG. 6 LOADING PATHS FOR SPECIMEN NO. 27

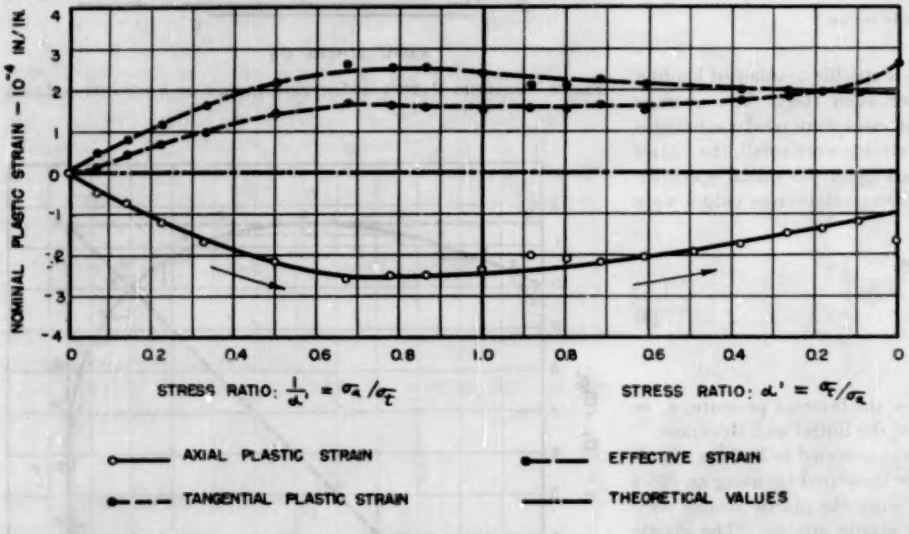

FIG. 5 VARIATION OF PLASTIC-STRAIN COMPONENTS AND EFFECTIVE STRAIN FOR DISTORTION ENERGY-CRITERION TEST—SPECIMEN NO. 1

distortion-energy criterion is the correct yielding surface, no plastic deformation should be produced during this loading. In Fig. 4, the nominal stress-strain relations for the distortion energy-criterion tests are shown. Based on the stress-strain data using the loading paths 0-1 and 20-0, the elastic constants for both axial and tangential directions were determined; and the plastic strains were calculated by the equations

$$\left.\begin{aligned} \epsilon_a'' &= \epsilon_a - \epsilon_a' = \epsilon_a - \left(\frac{\sigma_a}{E_a} - \mu_a \frac{\sigma_t}{E_t}\right) \\ \epsilon_t'' &= \epsilon_t - \epsilon_t' = \epsilon_t - \left(\frac{\sigma_t}{E_t} - \mu_t \frac{\sigma_a}{E_a}\right) \end{aligned}\right\} \quad \ldots\ldots [9]$$

where ϵ is the total strain, ϵ' is the elastic-strain component, and ϵ'' is the plastic-strain component; E is the modulus of elasticity and μ is Poisson's ratio. The subscripts a and t indicate the axial and tangential direction, respectively. The variations of the plastic strains and the effective strain along the loading path 0–1–2 . . . . . 19–20–0 are given in Fig. 5. As reported by previous investigations (8, 11), the test results did not agree with the distortion-energy criterion. In other words, the correct yielding surface must be inside the distortion-energy ellipse.

Using test data on Alcoa 24S-T obtained by Osgood (19), Drucker (20) claimed that the Prager criterion (as given by Equation [4] for biaxial stresses) gives the best agreement with test results. For anisotropic materials, Equation [4] can be reduced to the dimensionless form of Equation [7], and represented graphically by the curve 1–2 . . . . . 21–22 in Fig. 6. Using the

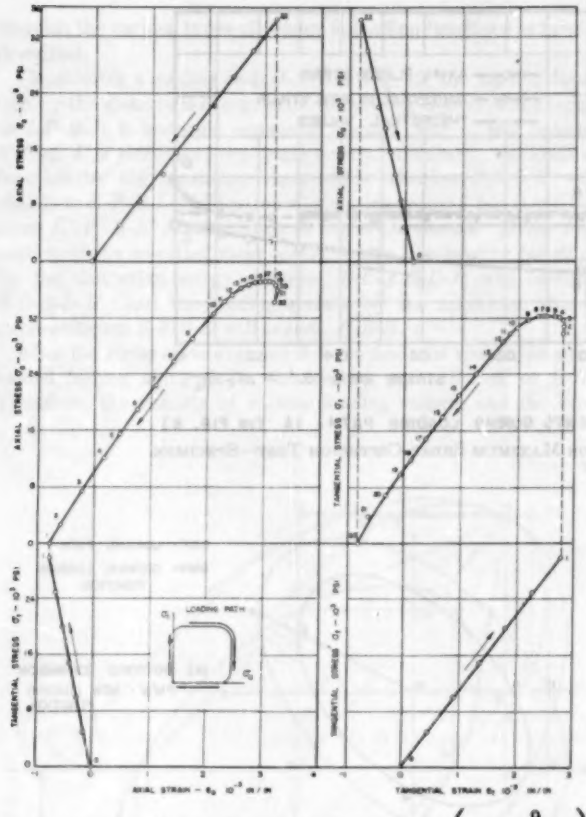

FIG. 7 NOMINAL STRESS-STRAIN RELATIONS FOR $\left(J_2^3 - \frac{9}{4} J_3^2\right)$ CRITERION TEST—SPECIMEN NO. 27

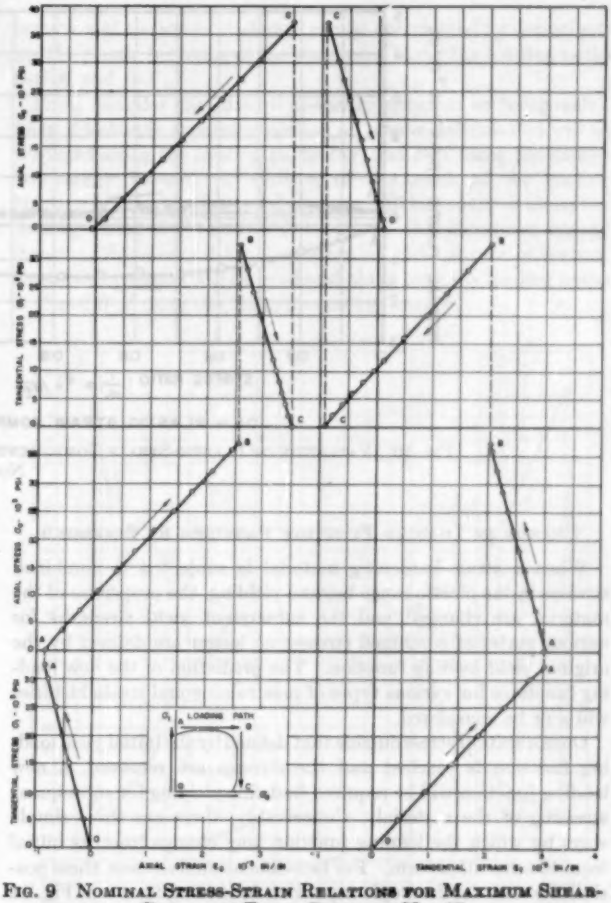

FIG. 9 NOMINAL STRESS-STRAIN RELATIONS FOR MAXIMUM SHEAR-CRITERION TEST—SPECIMEN NO. 27

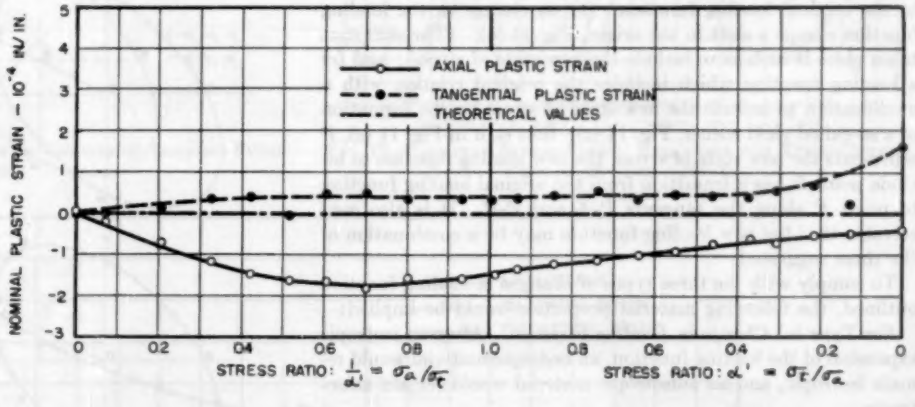
AXIAL PLASTIC STRAIN
TANGENTIAL PLASTIC STRAIN
THEORETICAL VALUES
NOMINAL PLASTIC STRAIN — 10^{-4} IN/ IN.
STRESS RATIO: $\frac{1}{\alpha'} = \sigma_a/\sigma_t$
STRESS RATIO: $\alpha' = \sigma_t/\sigma_a$

FIG. 8 VARIATION OF PLASTIC-STRAIN COMPONENTS FOR $\left(J_2^3 - \frac{9}{4} J_3^2\right)$ CRITERION TEST—SPECIMEN NO. 27

loading path 0–1–2 . . . 21–22–0, a test was conducted in order to verify the validity of the Prager criterion. In Fig. 7, the nominal stress-strain relations for Prager's criterion are shown. The plastic strains were calculated by Equation [9]. The variation in the strains is represented by the plot in Fig. 8.

In order to distinguish between the maximum-shear criterion and the Prager criterion, the same specimen, after stressing along the loading path 0–1 . . . 21–22–0, was reloaded by following a different loading path *O-A-B-C-O*. If the Prager criterion is correct, plastic strains would be produced during the loading path from 1 to *A*, since the path 1-*A* is outside the yielding surface postulated by the Prager criterion. However, if the maximum-shear criterion is correct, no plastic strains should be produced, since the yielding surface has been extended to *A-B-C* by the previous loading paths 4-5 . . . 8 and 14 . . . . 19. The nominal stress-strain relations for this reloading process are shown in Fig. 9; and the variation of the plastic strains is plotted in Fig. 10. Although a small amount of plastic strain was produced along the loading path 1-*A*, as shown by *O-A* in Fig. 10, the plastic strains produced along the path *A-B* was of the same order of magnitude as produced along the maximum-shear loading path as shown in Fig. 8. Therefore, the results are insufficient to distinguish between Prager's criterion and the maximum-shear criterion, since neither can be considered satisfactory.

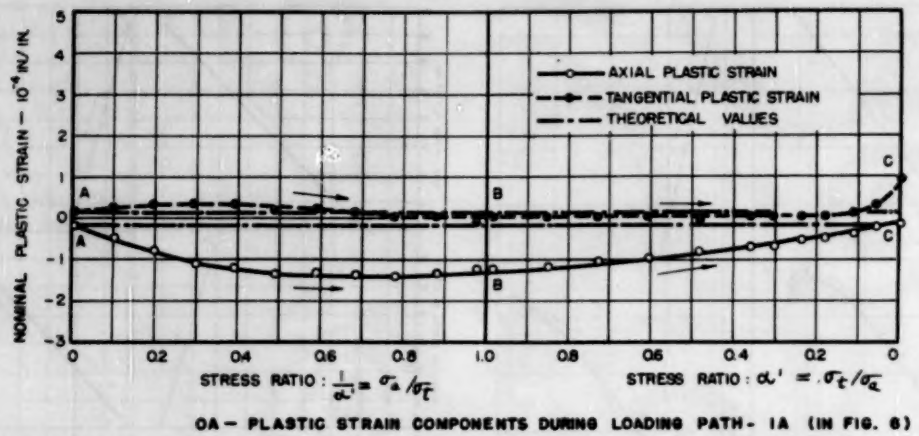
NOMINAL PLASTIC STRAIN — 10^{-6} IN./IN.
AXIAL PLASTIC STRAIN
TANGENTIAL PLASTIC STRAIN
THEORETICAL VALUES
A
B
C
STRESS RATIO : $\frac{1}{\alpha'} = \sigma_a/\sigma_t$
STRESS RATIO : $\alpha' = \sigma_t/\sigma_a$
OA — PLASTIC STRAIN COMPONENTS DURING LOADING PATH - IA (IN FIG. 6)

FIG. 10 VARIATION OF PLASTIC-STRAIN COMPONENTS FOR MAXIMUM SHEAR-CRITERION TEST—SPECIMEN NO. 27

CHANGE IN LOADING FUNCTION PROVIDED BY STRESSING

When a strain-hardening material is subjected to combined stresses in the plastic range beyond yielding, the properties of the material are changed and the subsequent yield strengths for various states of combined stresses no longer are defined by the original yield loading function. The prediction of the new loading functions for various types of prestraining and strain histories will now be considered.

Once a state of stress outside that defined by the initial yield loading function is reached and the stresses are removed, a new loading function will be required to define yielding for subsequent stressing of the material. Conceivably, there are three simple ways by which the loading function may change from its initial form to some other form. For two-dimensional stresses, these possibilities are: (*a*) Isotropic expansion in loading function, Fig. 11 (*a*), in which the loading function remains geometrically similar to the original loading function; (*b*) no change in the loading function except a shift in the origin, Fig. 11 (*b*). (The shift that takes place is such as to include the new state of stress); and (*c*) a loading function which includes the original relation with a modification to include the new state of stress by the formation of a so-called yield corner, Fig. 11 (*c*); that is, if in Fig. 11 (*c*), P represents the new state of stress, the new loading function to include point P has a transition from the original loading function to point P along the tangents P-A and P-B. It is also conceivable that the new loading function may be a combination of the three suggested.

To comply with the three types of changes in loading function outlined, the following material properties would be implied:

For Type (*a*) *Change in Loading Function.* After an isotropic expansion of the loading function, an isotropic material would remain isotropic, and an anisotropic material would remain anisotropic,

For Type (*b*) *Change in Loading Function.* After a shifting of the loading function, an isotropic material would become anisotropic, and an anisotropic material would have a higher degree of anisotropy than before. However, the changes in properties in different directions would bear a definite geometrical relation to the loading path.

For Type (*c*) *Change in Loading Function.* After the formation of a yield corner, an isotropic material would become anisotropic, although the material properties in certain directions may not be affected at all. Furthermore, an anisotropic material would have a higher degree of anisotropy than before, although the mechanical properties of the material in certain directions may retain their initial anisotropy. However, the significant change is that the loading function having unique normals everywhere originally, no longer have unique normals at all points.

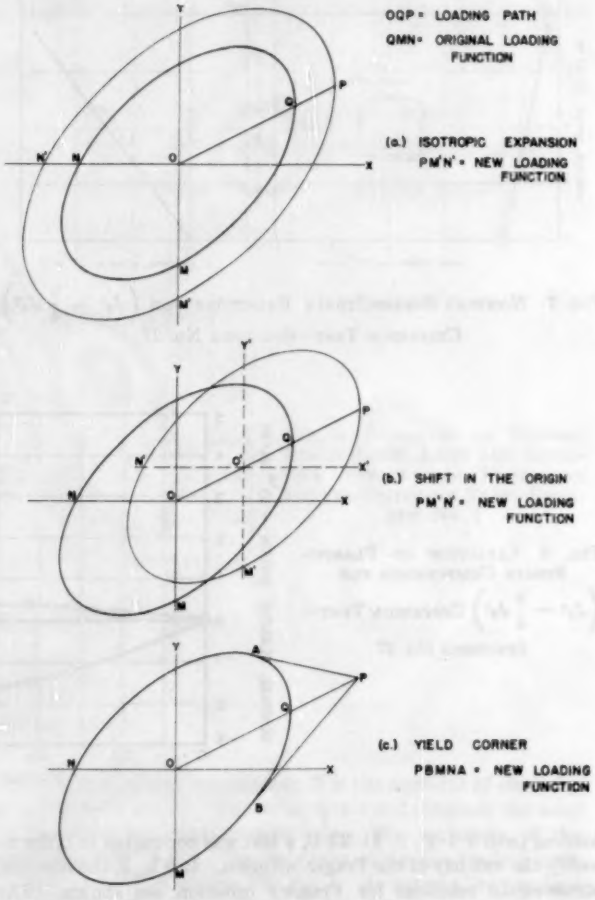
OQP = LOADING PATH
QMN = ORIGINAL LOADING FUNCTION
(a.) ISOTROPIC EXPANSION
PM'N' = NEW LOADING FUNCTION
(b.) SHIFT IN THE ORIGIN
PM'N' = NEW LOADING FUNCTION
(c.) YIELD CORNER
PBMNA = NEW LOADING FUNCTION

FIG. 11 BASIC MODES OF CHANGE OF LOADING FUNCTIONS

In order to understand the process involved in changing of load functions, various experiments should be conducted. In this investigation, only preliminary tests were conducted to dis-

tinguish the various types of change in loading functions as herein described.

Considering a loading path *O-A-B* in Fig. 12, the loading function by the distortion-energy criterion *E-C-A-G-D-H* will change to *I-P-B-J*, if isotropic expansion occurs; but it will become *I'-P'-B-J'* if shifting of the origin occurs. Similarly, the loading function by the maximum shear-stress criterion *E-F-G-H* will change to *K-P-B-L-M* if isotropic expansion occurs; but it will become *K'-P'-B-L'-M'* if shifting of the origin occurs. If the formation of the so-called yield corner occurs, the loading function by the distortion-energy criterion *E-C-A-G-D-H* will become *E-C-B-D-H;* and the loading surface by the maximum shear-stress criterion *E-F-G-H* will become *E-B-H*.

After the stress state at point *B* is reached, the specimens were loaded further along either the loading paths *B-P-K* or *B-N*. Therefore, the validity of various loading criteria and the confirmation of the mode of change can be determined by investigating the plastic behavior of the specimens along the loading paths *B-P-K* and *B-N*.

First, consider the distortion-energy criterion as being valid. Then if isotropic expansion occurs, no plastic deformation will be produced along the loading paths *B-P* and *B-N* using the distortion-energy theory. If shifting of the origin of the loading function occurs, no plastic deformation will be produced along the loading paths *B-P'* and *B-Q* based on the distortion energy theory. Moreover, if the formation of yield corner is correct, plastic deformation will be produced along both the loading paths *B-K* and *B-N* using the distortion-energy theory.

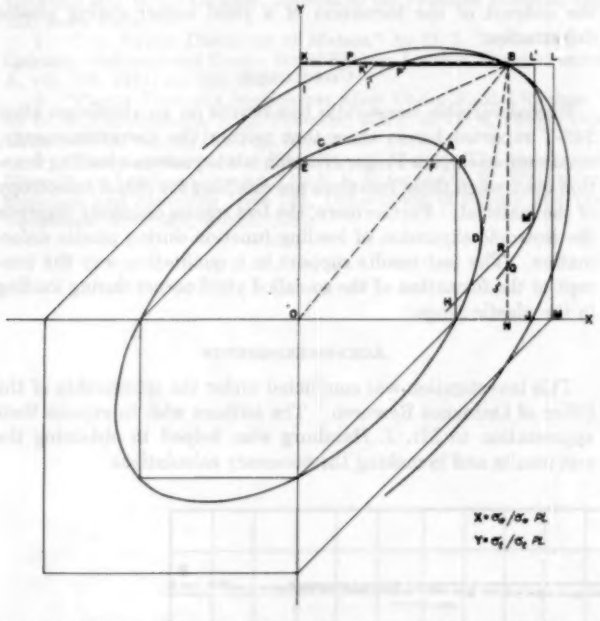

FIG. 12 LOADING PATHS FOR TESTS ON CHANGE OF LOADING FUNCTIONS

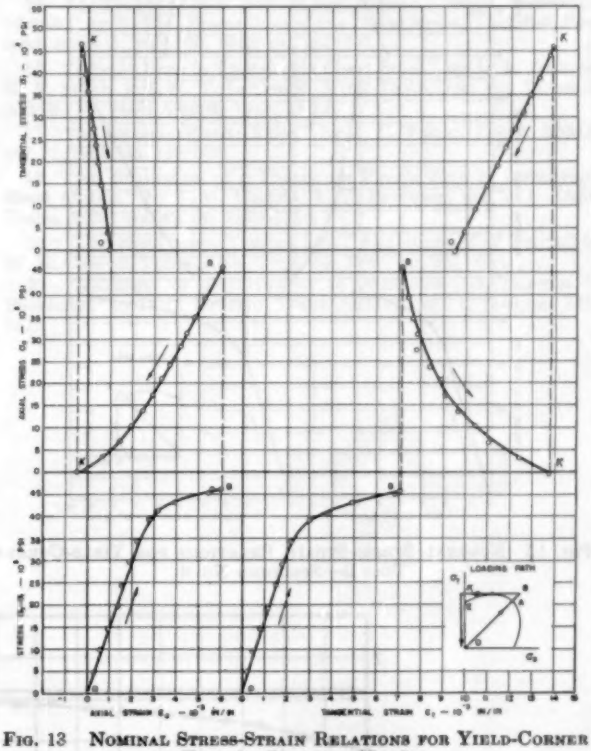

FIG. 13 NOMINAL STRESS-STRAIN RELATIONS FOR YIELD-CORNER TEST A—SPECIMEN NO. 6

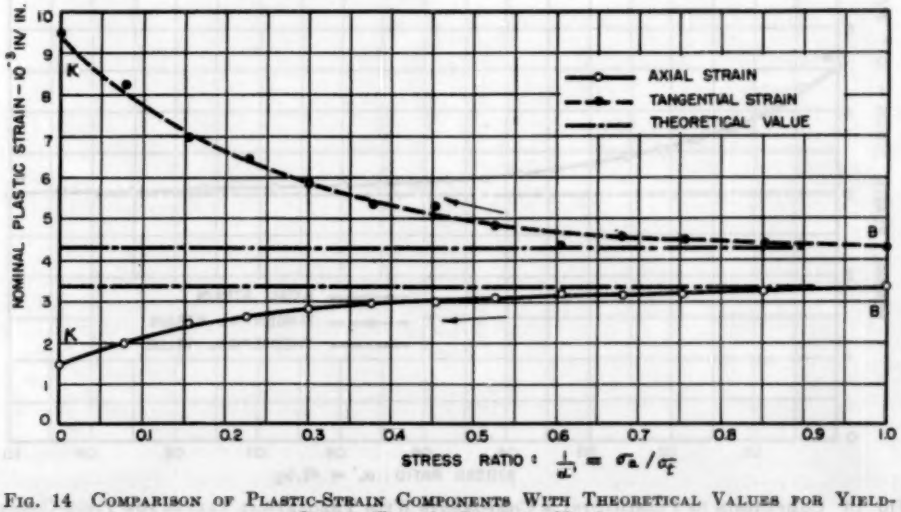

FIG. 14 COMPARISON OF PLASTIC-STRAIN COMPONENTS WITH THEORETICAL VALUES FOR YIELD-CORNER TEST A—SPECIMEN NO. 6

For the isotropic expansion of loading function to be valid, then in Fig. 12, no plastic deformation will be produced along the loading paths *B-K* and *B-N* if the maximum shear-stress criterion is used. Also if the shifting of the origin of the loading function is valid, no plastic strain will be produced along the loading paths *B-K'* and *B-R* by the shear-stress theory. If the formation of the so-called yield corner is correct, plastic deformation will be produced along both the loading paths *B-K* and *B-N* based on the maximum shear-stress criterion.

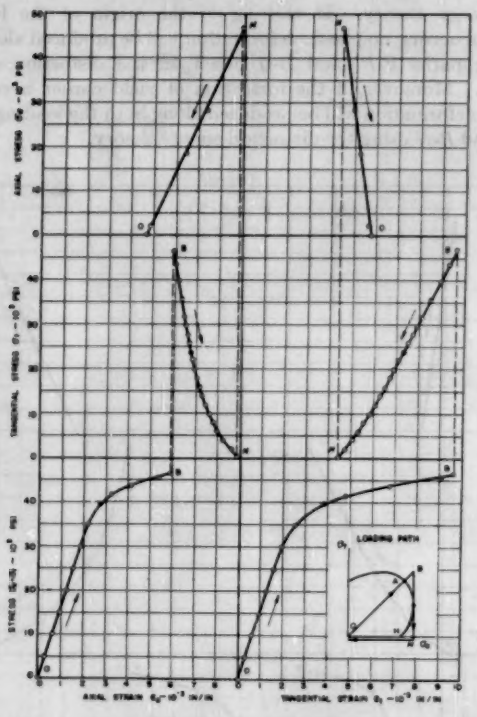

FIG. 15 NOMINAL STRESS-STRAIN RELATIONS FOR YIELD-CORNER TEST B—SPECIMEN NO. 4

To verify the foregoing statements two tests were conducted. In one test the specimen was loaded along the path *O-A-B-P-K-O*, and in the other test the specimen was loaded along the path *O-A-B-N-O* (Fig. 12). The nominal stress-strain relations for these tests are shown in Figs. 13 and 15, and the variations of the plastic deformations along the loading paths *B-P-K* and *B-N* are represented in Figs. 14 and 16. The test results in Figs. 14 and 16, show that plastic deformation definitely developed during both the loading paths *B-P-K* and *B-N*. Therefore, only one conclusion can be reached; namely, the isotropic expansion of the loading function is not likely to occur during stressing in the plastic range. However, the test results also qualitatively support the concept of the formation of a yield corner during plastic deformation.

CONCLUSION

Biaxial variable stress-ratio test results on an aluminum alloy 24S-T reported herein show that neither the distortion-energy, maximum-shear, nor Prager criterion is adequate as a loading function even when these functions are modified for initial anisotropy of the material. Furthermore, the test results definitely disprove the isotropic expansion of loading function during plastic deformation. The test results support in a qualitative way the concept of the formation of the so-called yield corner during loading in the plastic range.

ACKNOWLEDGMENTS

This investigation was conducted under the sponsorship of the Office of Ordnance Research. The authors wish to express their appreciation to Mr. J. Hamburg who helped in obtaining the test results and in making the necessary calculations

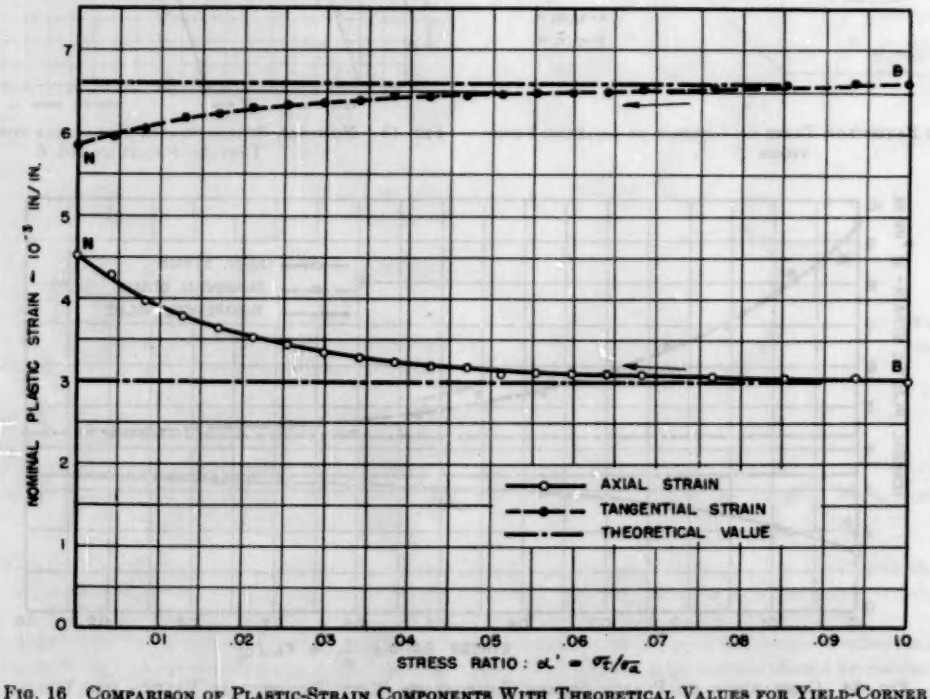

FIG. 16 COMPARISON OF PLASTIC-STRAIN COMPONENTS WITH THEORETICAL VALUES FOR YIELD-CORNER TEST B—SPECIMEN NO. 4

BIBLIOGRAPHY

1 "Strain Hardening Under Combined Stresses," by W. Prager, *Journal of Applied Physics*, vol. 16, 1945, pp. 837–840.

2 "Stress-Strain Relations in the Plastic Range, A Survey of Theory and Experiment," by D. C. Drucker, A-11 S-1, Brown University, Providence, R. I., December, 1950.

3 "A Mathematical Theory of Plasticity Based on the Concept of Slip," by S. B. Batdorf and B. Budiansky, NACA, TN 1871, April, 1949, 33 pp.

4 "Mémoire sur l'établissement des équations differentielles des movements interieurs opérés dans les corps solides ductiles au delà des limites on l'élasticité pourrait les ramener à leur premier état," *Comptes Rendus*, Paris, France, vol. 70, 1870, pp. 473–480.

"On the Use of Singular Yield Conditions and Associated Flow Rules," by William Prager, JOURNAL OF APPLIED MECHANICS, Trans. ASME, vol. 75, 1953, pp. 317–320.

5 "Effective Stress and Effective Strain in Relation to Stress Theories of Plasticity," by G. N White, Jr. and D. C. Drucker, *Journal of Applied Physics*, vol. 21, 1950, pp. 1013–1021.

6 "Some Extensions of Elementary Plasticity Theory," by F. Edelman and D. C. Drucker, *Journal of the Franklin Institute*, vol. 251, June, 1951.

7 "The Plastic Distortion of Metals," by G. I. Taylor and H. Quinney, Philosophical Trans., Royal Society, London, England, series A, vol. 230, 1931, pp. 323–362.

8 "Plastic Flow of a Magnesium Alloy Under Biaxial Stresses," by D. M. Cunningham, E. G. Thomsen, and J. E. Dorn, Proceedings of the ASTM, vol. 47, 1947, pp. 546–553.

9 "Experiments on the Plasticity of Metals, The Octahedral Shear Stress Loading Criterion," by F. S. Shaw and G. W. Wycherley, Structure and Materials Note 181, Department of Supply and Development, Australia, March, 1950.

10 "Plastic Stress-Strain Relations for Biaxial Tension and Variable Stress Ratios," by J. Marin and L. W. Hu, Proceedings of the ASTM, vol. 52, 1952, pp. 1095–1125.

11 "On the Validity of Assumptions Made in Theories of Plastic Flow for Metals," by J. Marin and L. W. Hu, Trans. ASME, vol. 75, 1953, pp. 1181–1190.

12 "Biaxial Plastic Stress-Strain Relations for 24S-T Aluminum Alloy," by J. Marin, F. H. Faupel, V. L. Dutton, and M. W. Brossman, NACA, TN 1536, 1948.

13 "Plastic Stress-Strain Relations for 75S-T6 Aluminum Alloy Subjected to Biaxial Tensile Stresses," by J. Marin, B. H. Ulrich, and W. P. Hughes, NACA, TN 2425, August, 1951.

14 "Recent Developments in the Mathematical Theory of Plasticity," by W. Prager, *Journal of Applied Physics*, vol. 20, no. 3, 1949, pp. 235–241.

15 "A Theory of the Yielding and Plastic Flow of Anisotropic Metals," by R. Hill, Proceedings of the Royal Society, London, England, series A, vol. 193, 1948, pp. 281–297.

16 "Plastic Flow in Anisotropic Sheet Steel," by L. R. Jackson, K. F. Smith, and W. T. Lankford, *Metal Technology*, vol. 15, no. 5, AIME, TP 2440, August, 1948, 15 pp.

17 "Anisotropic Plastic Flow," by J. C. Fisher, Trans. ASME, vol. 71, 1949, pp. 349–356.

18 "An Evaluation of a Theory for Plastic Flow in Anisotropic Sheet Metals," by T. H. Haslett, A. T. Robinson, and J. E. Dorn, Trans. ASM, vol. 42, pp. 1326–1356.

19 "Combined Stress Tests on 24S-T Aluminum Alloy Tubes," by W. R. Osgood, Trans. ASME, vol. 69, 1947, pp. 247–253.

20 "Relations of Experiments to Mathematical Theories of Plasticity," by D. C. Drucker, Trans. ASME, vol. 71, 1949, pp. 349–357.

Axially Symmetric Flexural Vibrations of a Circular Disk[1]

By H. DERESIEWICZ[2] and R. D. MINDLIN,[3] NEW YORK, N. Y.

At high frequencies, the flexural vibrations of a plate are described very poorly by the classical (Lagrange) theory because of neglect of the influence of coupling with thickness-shear vibrations. The latter may be taken into account by inclusion of rotatory inertia and shear-deformation terms in the equations. The resulting frequency spectrum is given, in this paper, for the case of axially symmetric vibrations of a circular disk with free edges and is compared with the spectrum predicted by the classical theory.

Introduction

THE problem of free vibrations of a thin, isotropic, elastic, circular disk, of constant thickness, was first attacked by Poisson (1)[4] over a century ago. Basing his investigation on the classical (Lagrange) theory of plates, he obtained the lower frequencies of the axially symmetric flexural motions of such a disk with a traction-free boundary.

It is well known that the classical theory satisfactorily predicts actual behavior only for the first few flexural modes of motion of a plate whose thickness is small in comparison with its other dimensions. For the higher flexural modes the influence of coupling with the thickness-shear mode of motion becomes increasingly important. Hence, the classical theory, in which this effect is not taken into account, ceases to yield reliable information (2). In particular, at the frequency of pure thickness-shear vibration of an infinite plate (i.e., displacement constant in direction and parallel to the plane of the plate) a drastic change occurs in the frequency spectrum of a finite plate (3, 4).

The influence of coupling between flexure and shear is taken into account by inclusion of rotatory inertia and shear-deformation terms in the equations. The resulting change in the frequency spectrum has been given previously for the case of a free-free beam (3) and a class of antisymmetric modes of motion of a circular disk (4). The present paper contains a discussion of the axially symmetric, flexural vibrations of a free disk, with emphasis on behavior in the neighborhood of the thickness-shear frequency. The spectrum obtained with consideration of the effects of rotatory inertia and shear deformation is compared with that predicted by the classical theory.

Plate Equations

If account is taken of rotatory inertia and shear deformation, the plate stress-displacement relations in polar co-ordinates, for the axially symmetric case,[5] become

$$\left.\begin{aligned} M_r &= D\left(\frac{\partial \psi}{\partial r} + \frac{\nu}{r}\psi\right) \\ M_\theta &= D\left(\nu\frac{\partial \psi}{\partial r} + \frac{\psi}{r}\right) \\ Q_r &= \kappa^2\mu h\left(\psi + \frac{\partial w}{\partial r}\right) \\ M_{r\theta} &= Q_\theta = 0 \end{aligned}\right\} \quad \ldots\ldots\ldots\ldots [1]$$

where $D = Eh^3/12(1-\nu^2)$, E, μ, ν, and h are Young's modulus, the shear modulus, Poisson's ratio, and the thickness, respectively, and $\kappa^2 = \pi^2/12$. The functions ψ and w are related to the radial and axial components of the displacement according to the approximations

$$\left.\begin{aligned} u_r &\approx z\psi(r, t) \\ u_z &\approx w(r, t) \end{aligned}\right\} \quad \ldots\ldots\ldots\ldots\ldots [2]$$

u_θ, the circumferential component of the displacement, is zero.

The plate equations of motion,[6] for the present problem, are

$$\left.\begin{aligned} \frac{\partial M_r}{\partial r} + \frac{M_r - M_\theta}{r} - Q_r &= \frac{\rho h^3}{12}\frac{\partial^2 \psi}{\partial t^2} \\ \frac{\partial Q_r}{\partial r} + \frac{Q_r}{r} &= \rho h\frac{\partial^2 w}{\partial t^2} \end{aligned}\right\} \quad \ldots\ldots\ldots [3]$$

where ρ is the density of the plate.

If we now insert Equations [1] in [3] we obtain the plate displacement equations of motion. Omitting the time factor e^{ipt}, these become

$$\left.\begin{aligned} &\left(\frac{d^2}{dr^2} + \frac{1}{r}\frac{d}{dr} - \frac{1}{r^2} + \frac{\rho p^2 h^2}{12D}\right)\psi \\ &\qquad - \frac{\kappa^2\mu h}{D}\left(\psi + \frac{dw}{dr}\right) = 0 \\ &\left(\frac{d}{dr} + \frac{1}{r}\right)\psi + \left(\frac{d^2}{dr^2} + \frac{1}{r}\frac{d}{dr} + \frac{\rho p^2}{\kappa^2\mu}\right)w = 0 \end{aligned}\right\} \quad \ldots [4]$$

Equations [4] may be uncoupled by differentiating the second equation once and subtracting the result from the first one. This procedure yields an expression for ψ in terms of w, which, when inserted into the second of Equations [4], gives a single equation on w only

$$\left(\frac{d^2}{dr^2} + \frac{1}{r}\frac{d}{dr} + \delta_1^2\right)\left(\frac{d^2}{dr^2} + \frac{1}{r}\frac{d}{dr} + \delta_2^2\right)w = 0 \quad \ldots [5]$$

---

[1] This investigation was supported by the Office of Naval Research under Contract Nonr-266(09).

[2] Assistant Professor of Civil Engineering, Columbia University. Assoc. Mem. ASME.

[3] Professor of Civil Engineering, Columbia University. Mem. ASME.

[4] Numbers in parentheses refer to the Bibliography at the end of the paper.

Contributed by the Applied Mechanics Division and presented at the Annual Meeting, New York, N. Y., November 28–December 3, 1954, of The American Society of Mechanical Engineers.

Discussion of this paper should be addressed to the Secretary, ASME, 29 West 39th Street, New York, N. Y., and will be accepted until April 11, 1955, for publication at a later date. Discussion received after the closing date will be returned.

Note: Statements and opinions advanced in papers are to be understood as individual expressions of their authors and not those of the Society. Manuscript received by ASME Applied Mechanics Division, February 5, 1954. Paper No. 54—A-15.

[5] These are given, in the general case, by equations [3] of reference (4).

[6] For the general case, see equations [2] of reference (4).

where

$$\delta_1^2, \delta_2^2 = \frac{\delta_0^4}{2}\left[R + S \pm \sqrt{(R-S)^2 + 4\delta_0^{-4}}\right]$$

$$S = D/\kappa^2\mu h, \quad \delta_0^4 = \rho p^2 h/D, \quad R = h^2/12$$

The expression for ψ in terms of w is given by

$$\psi = (R\delta_0^4 - S^{-1})^{-1}\frac{d}{dr}\left[\frac{d^2}{dr^2} + \frac{1}{r}\frac{d}{dr} + (S\delta_0^4 + S^{-1})\right]w \quad [6]$$

Solution of Equations of Motion

Equation [5] may be solved for w by noting that

$$w = w_1 + w_2 \quad [7]$$

where w_1 and w_2 satisfy, respectively, the equations

$$\left(\frac{d^2}{dr^2} + \frac{1}{r}\frac{d}{dr} + \delta_i^2\right)w_i = 0, \quad i = 1, 2 \quad [8]$$

Hence, the shear displacement ψ is found to be

$$\psi = (\sigma_1 - 1)\frac{dw_1}{dr} + (\sigma_2 - 1)\frac{dw_2}{dr} \quad [9]$$

where

$$\sigma_1, \sigma_2 = (\delta_2^2, \delta_1^2)(R\,\delta_0^4 - S^{-1})^{-1}$$

Both of Equations [8] are Bessel equations of zero order. In dealing with a solid disk, their appropriate solutions are

$$\left.\begin{aligned} w_1 &= A_1 J_0(\delta_1 r) \\ w_2 &= A_2 J_0(\delta_2 r) \end{aligned}\right\} \quad [10]$$

where A_1, A_2 are arbitrary constants.

For a plate with a traction-free edge, the boundary conditions are

$$M_r = Q_r = 0 \quad \text{at } r = a \quad [11]$$

where a is the radius of the plate.

Inserting Equations [1], [9], and [10] in Equations [11], the boundary conditions become

$$\left.\begin{aligned} &(\sigma_1 - 1)[\delta_1^2 a^2 J_0''(\delta_1 a) + \nu\delta_1 a J_0'(\delta_1 a)]A_1 \\ &\quad + (\sigma_2 - 1)[\delta_2^2 a^2 J_0''(\delta_2 a) + \nu\delta_2 a J_0'(\delta_2 a)]A_2 = 0 \\ &A_1\sigma_1\delta_1 J_0'(\delta_1 a) + A_2\sigma_2\delta_2 J_0'(\delta_2 a) = 0 \end{aligned}\right\} \quad [12]$$

where primes indicate differentiation with respect to the argument.

Frequency Equation

The secular equation, governing the frequency, is obtained by setting the determinant of Equations [12] equal to zero. The resulting equation may be written in the form

$$\frac{g - \beta^2}{1 + g}\gamma\Gamma_1 + \frac{1 - g\beta^2}{1 + g}\beta\gamma\Gamma_2 - (1 - \nu)(1 - \beta^2) = 0 \quad [13a]$$

where

$$\beta = \delta_2/\delta_1, \quad \gamma = \delta_1 a, \quad g = R/S$$

$$\Gamma_1 = J_0(\gamma)/J_1(\gamma), \quad \Gamma_2 = J_0(\beta\gamma)/J_1(\beta\gamma)$$

It may be observed that g is a material constant, depending only on Poisson's ratio, while the remaining functions in Equation [13a] depend on the frequency.

Since δ_1 is real for all positive values of the frequency p, while δ_2 is real or imaginary, depending on whether p is greater or less than $\bar{p} = \pi(\mu/\rho)^{1/2}/h$, β will be real or imaginary according as $p \gtrless \bar{p}$.[7] For the range $p < \bar{p}$, if we let $\beta = i\beta_1$, the frequency equation may be transformed to the more convenient form

$$\frac{g + \beta_1^2}{1 + g}\gamma\Gamma_1 + \frac{1 + g\beta_1^2}{1 + g}\beta_1\gamma G_2 - (1 - \nu)(1 + \beta_1^2) = 0 \quad [13b]$$

where $G_2 = I_0(\beta_1\gamma)/I_1(\beta_1\gamma)$, and $I_0(x)$, $I_1(x)$ are modified Bessel functions of the first kind.

We may find an explicit formula for the frequency by means of the relation $\beta = \delta_2/\delta_1$ and the expressions for δ_1 and δ_2 which immediately follow Equation [5]. Thus

$$\left.\begin{aligned} p/\bar{p} &= [1 - \beta^2(1 + g)^2/g\,(1 + \beta^2)^2]^{-1/2}, \quad p > \bar{p} \\ p/\bar{p} &= [1 + \beta_1^2(1 + g)^2/g(1 - \beta_1^2)^2]^{-1/2}, \quad p < \bar{p} \end{aligned}\right\} \quad [14]$$

In addition, from the relation $\gamma = \delta_1 a$, we find

$$\left.\begin{aligned} d/h &= \gamma(\bar{p}/p)[(1 + \beta^2)/3(1 + g)]^{1/2}, \quad p > \bar{p} \\ d/h &= \gamma(\bar{p}/p)[(1 - \beta_1^2)/3(1 + g)]^{1/2}, \quad p < \bar{p} \end{aligned}\right\} \quad [15]$$

where d is the diameter of the disk.

The complete solution of the problem is contained in Equations [13], [14], and [15]. With the value of ν specified for the material of the plate, a choice of β or β_1 determines $p/\bar{p}$ by Equations [14] and yields an infinite set of roots γ of Equations [13]. For the chosen β or β_1 each of these roots furnishes a ratio d/h through Equations [15], so that there results an infinite set of values of d/h corresponding to each value of $p/\bar{p}$.

Frequency Spectrum

The resonant frequencies of axially symmetric flexural vibrations of a circular plate with free boundaries, as predicted by the present theory, are shown, for the range $0.80 \leq p/\bar{p} \leq 1.12$, in Fig. 1. The computations were made for $g = 0.283$, corresponding to $\nu = 0.312$. These curves are characteristic of a frequency spectrum arising from the coupling of two infinite systems.[8] The first system consists of the flexural modes, whose frequency spectrum may be visualized as an extension, into the region $p > \bar{p}$, of the curves in the region $p < \bar{p}$. The second system is comprised of the fundamental thickness-shear mode and its overtones. Their spectrum may be discerned as formed by the loci of the flat, nearly horizontal portions of the resonance curves in the region above the thickness-shear frequency. They are, clearly, asymptotic to this frequency.

Comparison With Classical Theory

In order to observe the effect, on the resonant frequencies, of the coupling with thickness-shear motion, it is necessary to make a comparison with the corresponding frequency spectrum obtained from the classical theory, in which this effect is absent. Here, the relation between frequency and diameter to thickness ratio is,[9] in the present notation

$$d/h = \gamma(\bar{p}/p)^{1/2}[8/3\pi^2(1 - \nu)]^{1/4} \quad [16]$$

where the values of γ are given by the roots of the secular equation[10]

$$\gamma(\Gamma_1 + G_1) - 2(1 - \nu) = 0 \quad [17]$$

---

[7] $\bar{p}$ is the frequency of the first thickness-shear mode of an infinite plate.

[8] See, for example, Fig. 1 of reference (3).

[9] Reference (5), article 217, equations [1] and [4].

[10] Reference (5), article 219, equation [2].

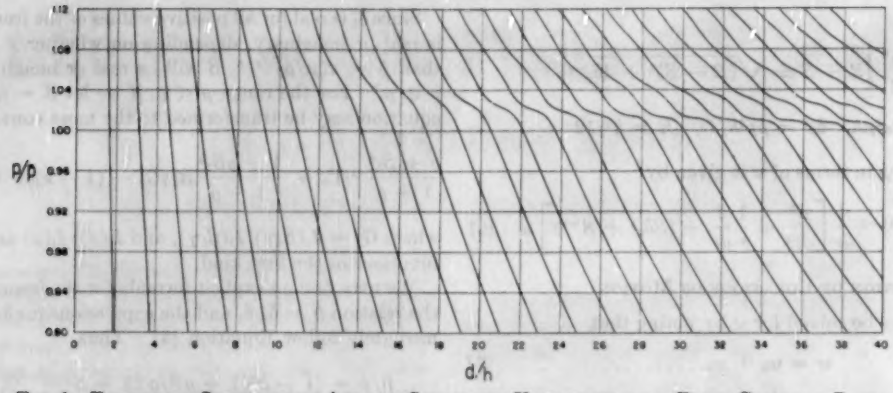

FIG. 1 FREQUENCY SPECTRUM OF AXIALLY SYMMETRIC VIBRATIONS OF A FREE, CIRCULAR DISK, ILLUSTRATING RESULTS OF COUPLING OF FLEXURE AND THICKNESS SHEAR

(d/h = ratio of diameter to thickness; $p/\bar{p}$ = ratio of resonant frequency to frequency of pure thickness-shear vibration of an infinite plate of thickness h; $\nu = 0.312$.)

in which

$$G_1 = I_0(\gamma)/I_1(\gamma)$$

The resulting curves, for $\nu = 0.312$ (corresponding to $g = 0.283$), are shown in Fig. 2.

The presence of the thickness-shear mode is represented, in the present theory, by the rotatory-inertia coefficient R and the shear-deformation coefficient S. (In the sequel, this theory is referred to as RS and the classical theory as C.) It may be verified that the secular equation of RS (Equation [13]) degenerates to that of C (Equation (17]) for the limiting case $R = S = 0$ (so that $\delta_1^2, \delta_2^2 = \pm\delta_0^2$). Hence the curves in Fig. 1, when extended down to $p/p = 0$, approach those of Fig. 2 asymptotically. The suppression of shear deformation in C serves as a constraint which raises the frequencies, in that theory, above those of RS. As a result, for a given plate, RS reveals that there are many more resonances, in a given frequency range, than are predicted by C. For example, for $d/h = 40$, there are 25 resonances in the range $0 < p/p < 1$, whereas C predicts only 16.

Furthermore, in designing a plate to resonate at a certain frequency, in its fundamental mode, one would be led to choose too large a plate on the basis of C. For example, for $p/p = 0.05$, the diameter would be in excess by 2.61 per cent. This discrepancy increases with the ratio of plate thickness to wave length of mode and, hence, with the order of the mode. For example, if the second mode of the plate is to vibrate at $p/p = 0.05$, the error in diameter chosen on the basis of C would be 2.86 per cent. The discrepancies are more pronounced at higher frequencies. Thus, the error in diameter of a plate designed, according to C, to resonate at $p/p = 0.1$, in the first mode, is 5.33 per cent and, in the second mode, 5.79 per cent.

The most striking difference between the two theories occurs at frequencies above that of the fundamental thickness-shear mode, as may be seen from Figs. 1 and 2.

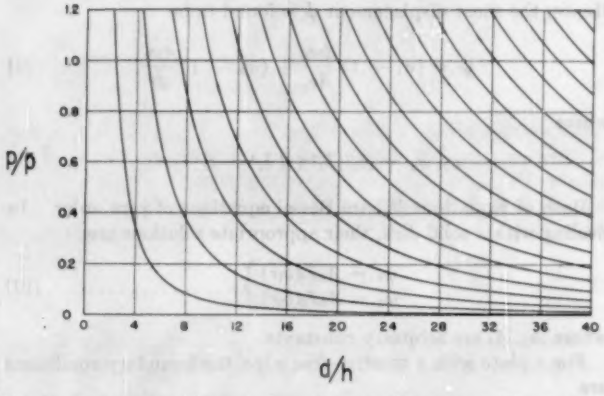

FIG. 2 FREQUENCY SPECTRUM OF AXIALLY SYMMETRIC VIBRATIONS OF A FREE, CIRCULAR DISK ACCORDING TO THE CLASSICAL (LAGRANGE) THEORY OF FLEXURE OF PLATES ($\nu = 0.312$)

BIBLIOGRAPHY

1 "Mémoire sur l'équilibre et le mouvement des corps élastiques," by S. D. Poisson, Paris, Mémoires de l'Académie, vol. 8, 1829; see also "A History of the Theory of Elasticity," by I. Todhunter and K. Pearson, Cambridge University Press, England, 1886, vol. 1, p. 262f.

2 "Influence of Rotatory Inertia and Shear on Flexural Motions of Isotropic, Elastic Plates," by R. D. Mindlin, JOURNAL OF APPLIED MECHANICS, Trans. ASME, vol. 73, 1951, pp. 31–38.

3 "Thickness-Shear and Flexural Vibrations of Crystal Plates," by R. D. Mindlin, *Journal of Applied Physics*, vol. 22, 1951, pp. 316–323.

4 "Thickness-Shear and Flexural Vibrations of a Circular Disk," by R. D. Mindlin and H. Deresiewicz, *Journal of Applied Physics*, vol. 25, 1954, pp. 1329–1332.

5 "Theory of Sound," by Lord Rayleigh, Dover Publications, New York, N. Y., 1944.

The Effect of Elliptic Holes on the Bending of Thick Plates

By P. M. NAGHDI,[1] ANN ARBOR, MICH.

The effects of an elliptic hole on both plain bending and pure twist of an elastic plate are investigated by application of the recent theory for bending of plates due to E. Reissner, where the influence of shear deformation and transverse-normal stress is taken into account. The stress-concentration factors are given for both cases mentioned. The solution, which is approximate in character, involves modified Mathieu functions of the second kind. In limiting cases, the results reduce exactly to the solution of corresponding problems with circular hole, as well as to the predictions of the classical theory of plates.

Introduction

THE recent extension and improvement of the classical (Poisson-Kirchhoff) theory of bending of thin elastic plates by E. Reissner[2] (1, 2, 3) has led to a theory which accounts for the effect of shear deformation and transverse-normal stress; Reissner's theory was obtained by use of the principle of virtual work.[3] This theory subsequently was rederived from the general equations of elasticity by A. E. Green (6) who also indicated a series method for the three-dimensional solution of flexure of plates (7). An analogous theory to that of Reissner also has been developed by Mindlin (8) for flexural motion of elastic plates where the influence of rotary inertia and shear deformation has been taken into account.

In the absence of surface loading according to Reissner (2), the problem of bending of isotropic elastic plates is equivalent to establishing the deflection w of the plate which satisfies

$$D(\nabla^4 w) = \phi \quad \ldots\ldots [1]$$

and an associated stress function χ given by

$$\chi = \psi_1 - \psi \quad \ldots\ldots [2]$$

where ϕ and ψ are conjugate harmonic functions, and ψ_1 is the solution of

$$\nabla^2\psi_1 - \frac{10}{h^2}\psi_1 = 0 \quad \ldots\ldots [3]$$

In Equations [1] and [3], ∇^2 is the two-dimensional Laplacian, h is the thickness of the plate, and D denotes the rigidity of the plate given by

$$\frac{Eh^3}{12(1-\nu^2)}$$

where E and ν are Young's modulus and Poisson's ratio, respectively.

It should be mentioned that, contrary to the classical theory where the existence of only two boundary conditions at each edge is necessary, the present theory requires the satisfaction of three boundary conditions at each edge of the plate.[4]

Using appropriate solutions of Equations [1] and [3], Reissner (2) considered the effect of a circular hole in an infinite plate under the state of both plain bending and pure twist. The stress (stress couple) concentration factors as given by Reissner for the case of plain bending and experimental results (9) were in very good agreement. The corresponding solution for the case of a rigid circular inclusion in an infinite plate subjected to plain bending is given by Hirsch (10). More recently Reissner's theory has been applied to problems of rectangular plates with variable load by Schafer (11) and to axially symmetric plates on elastic foundations by the present author and Rowley (12).

In the present paper, using Reissner's theory, the effect of an elliptic hole in an infinite plate in the state of both plain bending and pure twist is considered. The solution, which is approximate in character, involves modified Mathieu functions of the second kind. Stress-concentration factors are given for both cases mentioned, and the solutions for limiting cases are discussed.

In contrast to the present study, it should be mentioned that the influence of circular and elliptic holes on the bending of thin plates, using the classical theory, was investigated by Goodier (13) and the solutions to corresponding problems of the effect of circular and elliptic inclusions on the bending of plates have been given by Goland (14). It is noteworthy that the experimental results for plates with circular holes have confirmed the predictions of the classical theory for only large values of hole-diameter-plate thickness ratios (15, 16, 17).

The Basic Equations in Orthogonal Curvilinear Co-Ordinates

In order to render manageable the boundary conditions at the hole, it is necessary to introduce elliptic cylindrical co-ordinates. For this purpose, however, it is convenient to transform Reissner's equations to orthogonal curvilinear co-ordinates and then to deduce those for the elliptic co-ordinate system. We recall that a curvilinear co-ordinate system is defined by a transformation[5]

$$x = x(\alpha_1, \alpha_2), \quad y = y(\alpha_1, \alpha_2), \quad z = z \quad \ldots\ldots [4]$$

and the corresponding co-ordinate surfaces $\alpha_1, \alpha_2 = \text{const}$, which are mutually orthogonal provided

---

[1] Professor of Engineering Mechanics, University of Michigan. Assoc. Mem. ASME.

[2] Also see reference (4). Numbers in parentheses refer to the Bibliography at the end of the paper.

[3] See also reference (5) for the derivation of the basic equations of this theory by means of a new variational theorem.

Contributed by the Applied Mechanics Division and presented at the Annual Meeting, New York, N. Y., November 28–December 3, 1954, of The American Society of Mechanical Engineers.

Discussion of this paper should be addressed to the Secretary, ASME, 29 West 39th Street, New York, N. Y., and will be accepted until April 11, 1955, for publication at a later date. Discussion received after the closing date will be returned.

Note: Statements and opinions advanced in papers are to be understood as individual expressions of their authors and not those of the Society. Manuscript received by ASME Applied Mechanics Division, March 4, 1954. Paper No. 54—A-26.

[4] For axisymmetrical problems, there are two boundary conditions at each edge, although they are not the same as those appropriate for the classical theory. In this connection, see reference (12).

[5] For an exposition of curvilinear co-ordinates, see reference (18), articles 19–22C.

$$\frac{\partial x}{\partial \alpha_i}\frac{\partial x}{\partial \alpha_j} + \frac{\partial y}{\partial \alpha_i}\frac{\partial y}{\partial \alpha_j} = 0;\ (i \neq j) \quad [5]$$

The differential arc length is given by

$$(ds)^2 = \frac{1}{h_1^2}\,d\alpha_1^2 + \frac{1}{h_2^2}\,d\alpha_2^2 + dz^2 \quad [6]$$

where

$$\frac{1}{h_i^2} = \left(\frac{\partial x}{\partial \alpha_i}\right) + \left(\frac{\partial y}{\partial \alpha_i}\right)^2;\ (i = 1, 2) \quad [7]$$

Reissner's Equations [I] to [IV], as given in reference (2), upon transformation to curvilinear cylindrical co-ordinates, read as follows[4]

$$h_1 h_2\left[\frac{\partial}{\partial \alpha_1}\left(\frac{V_1}{h_2}\right) + \frac{\partial}{\partial \alpha_2}\left(\frac{V_2}{h_1}\right)\right] = -p \quad [8]$$

$$M_1 - \frac{h^2}{5}\left[h_1\frac{\partial V_1}{\partial \alpha_1} + h_1 h_2 V_2\frac{\partial}{\partial \alpha_2}\left(\frac{1}{h_1}\right)\right] + \frac{\nu h^2}{10(1-\nu)}\,p = -D\left\{\left[h_1^2\frac{\partial^2 w}{\partial \alpha_1^2} + h_1\frac{\partial h_1}{\partial \alpha_1}\frac{\partial w}{\partial \alpha_1} - \frac{h_2^2}{h_1}\frac{\partial h_1}{\partial \alpha_2}\frac{\partial w}{\partial \alpha_2}\right] + \nu\left[h_2^2\frac{\partial^2 w}{\partial \alpha_2^2} + h_2\frac{\partial h_2}{\partial \alpha_2}\frac{\partial w}{\partial \alpha_2} - \frac{h_1^2}{h_2}\frac{\partial h_2}{\partial \alpha_1}\frac{\partial w}{\partial \alpha_1}\right]\right\} \quad [9]$$

$$M_2 - \frac{h^2}{5}\left[h_2\frac{\partial V_2}{\partial \alpha_2} + h_1 h_2 V_1\frac{\partial}{\partial \alpha_1}\left(\frac{1}{h_2}\right)\right] + \frac{\nu h^2}{10(1-\nu)}\,p = -D\left\{\left[h_2^2\frac{\partial^2 w}{\partial \alpha_2^2} + h_2\frac{\partial h_2}{\partial \alpha_2}\frac{\partial w}{\partial \alpha_2} - \frac{h_1^2}{h_2}\frac{\partial h_2}{\partial \alpha_1}\frac{\partial w}{\partial \alpha_1}\right] + \nu\left[h_1^2\frac{\partial^2 w}{\partial \alpha_1^2} + h_1\frac{\partial h_1}{\partial \alpha_1}\frac{\partial w}{\partial \alpha_1} - \frac{h_2^2}{h_1}\frac{\partial h_1}{\partial \alpha_2}\frac{\partial w}{\partial \alpha_2}\right]\right\} \quad [10]$$

$$M_{12} - \frac{h^2}{10}\left[\frac{h_2}{h_1}\frac{\partial}{\partial \alpha_2}(h_1 V_1) + \frac{h_1}{h_2}\frac{\partial}{\partial \alpha_1}(h_2 V_2)\right] = -(1-\nu)D\left(h_1 h_2\frac{\partial^2 w}{\partial \alpha_1 \partial \alpha_2} + h_2\frac{\partial h_1}{\partial \alpha_2}\frac{\partial w}{\partial \alpha_1} + h_1\frac{\partial h_2}{\partial \alpha_1}\frac{\partial w}{\partial \alpha_2}\right) \quad [11]$$

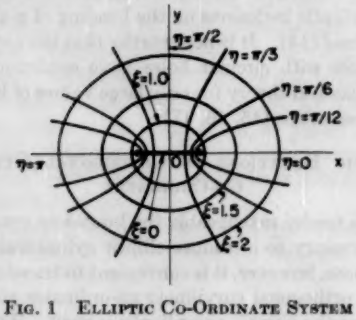

FIG. 1 ELLIPTIC CO-ORDINATE SYSTEM

where M_1, M_2, M_{12} denote the stress couples, V_1 and V_2 are the shear-stress resultants, and p is the surface load at $z = h/2$.

The elliptic co-ordinates shown in Fig. 1 are defined by

$$x + iy = c\cosh\rho;\ \rho = \xi + i\eta \quad (i = \sqrt{-1})$$

Hence

$$x = c\cosh\xi\cos\eta,\ y = c\sinh\xi\sin\eta \quad [12]$$

[4] In Equations [8] to [11] subscripts 1 and 2 refer to directions α_1 and α_2, respectively.

and

$$\frac{1}{h_1^2} = \frac{1}{h_2^2} = J^2 = \frac{1}{2}\,c^2(\cosh 2\xi - \cos 2\eta) \quad [13]$$

In accordance with the Transformations [12] and [13], and in the absence of the surface load p, Equations [8] to [11] in elliptic co-ordinates reduce in order to

$$\frac{\partial}{\partial \xi}(JV_\xi) + \frac{\partial}{\partial \eta}(JV_\eta) = 0 \quad [14]$$

$$J^4 M_\xi - \frac{h^2}{5}J^2\left[J\frac{\partial V_\xi}{\partial \xi} + V_\eta\frac{\partial J}{\partial \eta}\right] = -D\left[J^2\left(\frac{\partial^2 w}{\partial \xi^2} + \nu\frac{\partial^2 w}{\partial \eta^2}\right) - \frac{1-\nu}{2}\frac{\partial J^2}{\partial \xi}\frac{\partial w}{\partial \xi} + \frac{1-\nu}{2}\frac{\partial J^2}{\partial \eta}\frac{\partial w}{\partial \eta}\right] \quad [15]$$

$$J^4 M_\eta - \frac{h^2}{5}J^2\left(J\frac{\partial V_\eta}{\partial \eta} + V_\xi\frac{\partial J}{\partial \xi}\right) = -D\left[J^2\left(\frac{\partial^2 w}{\partial \eta^2} + \nu\frac{\partial^2 w}{\partial \xi^2}\right) - \frac{1-\nu}{2}\frac{\partial J^2}{\partial \eta}\frac{\partial w}{\partial \eta} + \frac{1-\nu}{2}\frac{\partial J^2}{\partial \xi}\frac{\partial w}{\partial \xi}\right] \quad [16]$$

$$J^4 M_{\xi\eta} - \frac{h^2}{10}J\left[J^2\left(\frac{\partial V_\xi}{\partial \eta} + \frac{\partial V_\eta}{\partial \xi}\right) - \frac{1}{2}\left(V_\xi\frac{\partial J^2}{\partial \eta} + V_\eta\frac{\partial J^2}{\partial \xi}\right)\right] = -(1-\nu)D\left(J^2\frac{\partial^2 w}{\partial \xi \partial \eta} - \frac{1}{2}\frac{\partial J^2}{\partial \eta}\frac{\partial w}{\partial \xi} - \frac{1}{2}\frac{\partial J^2}{\partial \xi}\frac{\partial w}{\partial \eta}\right) \quad [17]$$

Following Reissner, introduction of a stress function χ into Equation [14] yields

$$V_\xi = \frac{1}{J}\frac{\partial \chi}{\partial \eta},\quad V_\eta = -\frac{1}{J}\frac{\partial \chi}{\partial \xi} \quad [18]$$

Substituting these results into Equations [15], [16], [17], we obtain

$$J^4 M_\xi = -D\left[J^2\left(\frac{\partial^2 w}{\partial \xi^2} + \nu\frac{\partial^2 w}{\partial \eta^2}\right) - \frac{1-\nu}{2}\frac{\partial J^2}{\partial \xi}\frac{\partial w}{\partial \xi} + \frac{1-\nu}{2}\frac{\partial J^2}{\partial \eta}\frac{\partial w}{\partial \eta}\right] + \frac{h^2}{5}\left(J^2\frac{\partial^2 \chi}{\partial \xi \partial \eta} - \frac{1}{2}\frac{\partial J^2}{\partial \xi}\frac{\partial \chi}{\partial \eta} - J\frac{\partial J}{\partial \eta}\frac{\partial \chi}{\partial \xi}\right) \quad [19]$$

$$J^4 M_\eta = -D\left[J^2\left(\frac{\partial^2 w}{\partial \eta^2} + \nu\frac{\partial^2 w}{\partial \xi^2}\right) - \frac{1-\nu}{2}\frac{\partial J^2}{\partial \eta}\frac{\partial w}{\partial \eta} + \frac{1-\nu}{2}\frac{\partial J^2}{\partial \xi}\frac{\partial w}{\partial \xi}\right] + \frac{h^2}{5}\left(-J^2\frac{\partial^2 \chi}{\partial \xi \partial \eta} + \frac{1}{2}\frac{\partial J^2}{\partial \eta}\frac{\partial \chi}{\partial \xi} + J\frac{\partial J}{\partial \xi}\frac{\partial \chi}{\partial \eta}\right) \quad [20]$$

$$J^4 M_{\xi\eta} = -(1-\nu)D\left(J^2\frac{\partial^2 w}{\partial \xi \partial \eta} - \frac{1}{2}\frac{\partial J^2}{\partial \eta}\frac{\partial w}{\partial \xi} - \frac{1}{2}\frac{\partial J^2}{\partial \xi}\frac{\partial w}{\partial \eta}\right) + \frac{h^2}{10}\left[J^2\left(\frac{\partial^2 \chi}{\partial \eta^2} - \frac{\partial^2 \chi}{\partial \xi^2}\right) - \left(\frac{\partial J^2}{\partial \eta}\frac{\partial \chi}{\partial \eta} - \frac{\partial J^2}{\partial \xi}\frac{\partial \chi}{\partial \xi}\right)\right] \quad [21]$$

General Solution in Elliptic Co-Ordinates

Writing Equation [1] as

$$D(\nabla^2 w) = A_0 + B_0\xi + C_0\eta + \sum_{n=1}^{\infty}\left\{A_n e^{-n\xi} + B_n e^{n\xi}\right\}\begin{matrix}\sin n\eta \\ \cos n\eta\end{matrix} \quad \ldots [22]$$

where the right-hand side is harmonic in elliptic co-ordinates, then its conjugate is

$$\psi = B_0\eta - C_0\xi + \sum_{n=1}^{\infty}\left\{A_n e^{-n\xi} + B_n e^{n\xi}\right\}\begin{matrix}\cos n\eta \\ -\sin n\eta\end{matrix} \quad \ldots [23]$$

Integration of the differential Equation [22], suitable for our present purposes, results in

$$\left.\begin{aligned} Dw = {} & \bar{E}_0 + \bar{F}_0\xi + \bar{A}_0(\cosh 2\xi + \cos 2\eta) \\ & + \sum_{n=1}^{\infty}\left[\bar{E}_n e^{-n\xi} + \bar{F}_n e^{n\xi}\right]\begin{matrix}\sin n\eta \\ \cos n\eta\end{matrix} \\ & + \sum_{n=1}^{\infty}\left[\bar{A}_n e^{-(n+1)\xi} + \bar{B}_n e^{(n+1)\xi}\right]\begin{matrix}\sin(n-1)\eta \\ \cos(n-1)\eta\end{matrix} \\ & + \sum_{n=1}^{\infty}\left[\bar{A}_n e^{-(n-1)\xi} + \bar{B}_n e^{(n-1)\xi}\right]\begin{matrix}\sin(n+1)\eta \\ \cos(n+1)\eta\end{matrix} \end{aligned}\right\} \quad \ldots [24]$$

where the barred constants are related to the unbarred constants as follows

$$\left.\begin{aligned} & \bar{A}_0 = \frac{c^2}{16}A_0,\ \bar{A}_1 = -\frac{c^2}{16}A_2,\ \bar{B}_1 = -\frac{c^2}{16}B_2 \\ & \bar{A}_n = \frac{c^2}{16n}(A_{n-1} - A_{n+1}),\ \bar{B}_n = \frac{c^2}{16n}(B_{n-1} - B_{n+1}); \quad (n \geq 2) \\ & \bar{E}_n = c^2 E_n,\quad \bar{F}_n = c^2 F_n;\ (n \geq 0) \end{aligned}\right\} \quad \ldots [25]$$

Solution of the differential Equation [3] in elliptic co-ordinates may be written as follows[7]

$$\psi_1 = \sum_{n=0}^{\infty} G_n\,\mathrm{Fek}_n(\xi, -q)\mathrm{ce}_n(\eta, -q) + \sum_{n=1}^{\infty} H_n\,\mathrm{Gek}_n(\xi, -q)\mathrm{se}_n(\eta, -q);\quad q = \frac{5c^2}{2h^2} \quad \ldots [26]$$

where ce_n and se_n are Mathieu functions of the first kind, and Fek_n and Gek_n are modified Mathieu functions of the second kind. The behavior of these functions is such that as $q \to 0$, ce_n and se_n, by virtue of their periodicity in π, 2π, reduce to $\cos n\eta$ and $\sin n\eta$; while Fek_n and Gek_n become proportional to Bessel functions or modified Bessel functions (depending on whether q is positive or negative) as ξ tends to infinity. Furthermore, for small values of ξ, the function Fek_n remains finite, while Gek_n becomes infinite.

Plain Bending and Pure Twist of an Infinite Plate With an Elliptic Hole

Let us consider plain bending of an infinite plate with an elliptic hole. As will be seen later, the results for the case of pure twist may be deduced directly from those of plain bending.

For the case of plain bending, the boundary conditions are

$$M_x = M_0 \text{ or } 0,\ M_{xy} = 0,\ V_x = 0 \text{ at } x = \pm\infty \quad \ldots [27a, b, c]$$

$$M_y = 0 \text{ or } M_0,\ M_{yx} = 0,\ V_y = 0 \text{ at } y = \pm\infty \quad \ldots [28a, b, c]$$

[7] Reference (19), chapter 9 and Appendix III.

depending on whether the uniform stress couple M_0 at infinity is applied about the y or x-axis, respectively. Also

$$M_\xi = M_{\xi\eta} = V_\xi = 0 \text{ at } \xi = \xi_0 \quad \ldots [29a, b, c]$$

The Boundary Conditions [27] and [28] in elliptic co-ordinates may be written as

$$M_\xi = \frac{1}{2}M_0(1 + \Gamma\cos 2\eta) \quad \ldots [30a]$$

$$M_{\xi\eta} = -\frac{\Gamma}{2}M_0 \sin 2\eta \quad \ldots [30b]$$

$$V_\xi = 0 \quad \ldots [30c]$$

where $\Gamma = \pm 1$, depending on whether M_0 is applied about the y or x-axis, respectively.

The conditions at infinity, as well as the existing solution of the classical theory (13), suggest the following form for Dw

$$Dw = \bar{E}_0 + \bar{F}_0\xi + \frac{c^2}{8}A_0(\cosh 2\xi + \cos 2\eta) + (\bar{E}_2 e^{-2\xi} + \bar{F}_2 e^{2\xi})\cos 2\eta - \frac{c^2}{16}A_2(e^{-2\xi} + \cos 2\eta) \quad \ldots [31]$$

Although by Equation [2], χ is a linear combination of Equations [23] and [26], in view of the boundary conditions at the hole ($\xi = \xi_0$), the form of ψ_1 given by Equation [26] is not suitable in the present problem. Instead, we write

$$\chi = C^{(2)}(q)\frac{\mathrm{Gek}_2(\xi, -q)}{\mathrm{Gek}_2(\xi_0, -q)}\,\mathrm{se}_2(\eta, -q) + A_2 e^{-2\xi}\sin 2\eta \quad \ldots [32]$$

To determine the coefficient $C^{(2)}(q)$, we proceed as follows: From the condition $[V_\xi]_{\xi=\xi_0} = 0$, we have

$$\left.\begin{aligned} C^{(2)}\,\mathrm{se}_2'(\eta, -q) &= -2A_2 e^{-2\xi_0}\cos 2\eta \\ C^{(2)}\,\mathrm{se}_2(\eta, -q) &= -A_2 e^{-2\xi_0}\sin 2\eta \end{aligned}\right\} \quad \ldots [33]$$

where prime denotes derivative, and ξ_0 refers to the boundary of the hole. By orthogonality property of se_2 and its derivative,[8] we have

$$C^{(2)}\int_0^{2\pi}[\mathrm{se}_2'(\eta, -q)]^2 d\eta = -2A_2 e^{-2\xi_0}\int_0^{2\pi}\mathrm{se}_2'(\eta, -q)\cos 2\eta d\eta$$

Substituting

$$\mathrm{se}_2(\eta, -q) = \sum_{r=0}^{\infty}(-1)^r B^{(2)}_{2r+2}\sin(2r+2)\eta$$

into the last equation and making use of the first of Equations [33], there results

$$C^{(2)} = -\frac{4A_2 e^{-2\xi_0}B^{(2)}_2}{\sum_{r=0}^{\infty}(2r+2)^2[B^{(2)}_{2r+2}]^2} \quad \ldots [34]$$

where $B^{(2)}_{2r+2}$ are the Fourier coefficients in the expansion of $\mathrm{se}_2(\eta, -q)$ in $\sin(2r+2)\eta$.

After some lengthy calculations, we obtain the following expressions[9] for the stress-couples and the shear resultant V_η

[8] Reference (19), §2.18 and §2.19.

[9] The ratio $\frac{\mathrm{Gek}_2'(\xi, -q)}{\mathrm{Gek}_2(\xi_0, -q)}$ in Equations [35] is abbreviated as $\frac{\mathrm{Gek}_2'}{\mathrm{Gek}_2}$.

$$-\frac{4}{c^4}J^4M_\xi=\left\{A_2\left[\frac{1-3\nu}{8}-\frac{1}{2}e^{-2\xi}\left(\cosh 2\xi+\frac{1-\nu}{2}\sinh 2\xi\right)\right.\right.$$
$$\left.-\frac{3h^2}{5c^2}e^{-2\xi}\left(2+\frac{\mathrm{Gek}_2'}{\mathrm{Gek}_2}\right)\right]-\frac{6}{c^2}(1-\nu)(E_2e^{-2\xi}+F_2e^{2\xi})$$
$$\left.-\frac{2}{c^2}(1-\nu)F_0\sinh 2\xi+A_0(1+\nu)\left(\frac{3}{4}+\frac{1}{2}\sinh^2 2\xi\right)\right\}$$
$$+\cos 2\eta\left\{A_2\left[\frac{e^{-2\xi}+\nu\cosh 2\xi}{2}+\frac{4h^2}{5c^2}e^{-2\xi}\cosh 2\xi\left(2+\frac{\mathrm{Gek}_2'}{\mathrm{Gek}_2}\right)\right]\right.$$
$$+\frac{4}{c^2}(1-\nu)E_2e^{-2\xi}(\sinh 2\xi+2\cosh 2\xi)$$
$$\left.+\frac{4}{c^2}(1-\nu)F_2e^{2\xi}(2\cosh 2\xi-\sinh 2\xi)-A_0(1+\nu)\cosh 2\xi\right\}$$
$$+\cos 4\eta\left\{A_2\left[-\frac{1+\nu}{8}-\frac{h^2}{5c^2}e^{-2\xi}\left(2+\frac{\mathrm{Gek}_2'}{\mathrm{Gek}_2}\right)\right]\right.$$
$$\left.-\frac{2}{c^2}(1-\nu)(E_2e^{-2\xi}+F_2e^{2\xi})+A_0\frac{1+\nu}{4}\right\}\quad\ldots[35a]$$

$$-\frac{4}{c^4}J^4M_\eta=\left\{A_2\left[-\frac{3-\nu}{8}+e^{-2\xi}\left(\nu\cosh 2\xi+\frac{1-\nu}{4}\sinh 2\xi\right)\right.\right.$$
$$\left.+\frac{3h^2}{5c^2}e^{-2\xi}\left(2+\frac{\mathrm{Gek}_2'}{\mathrm{Gek}_2}\right)\right]+\frac{6}{c^2}(1-\nu)(E_2e^{-2\xi}$$
$$\left.+F_2e^{2\xi})+\frac{2}{c^2}(1-\nu)F_0\sinh 2\xi+A_0(1+\nu)\left(\frac{1}{4}+\frac{1}{2}\cosh^2 2\xi\right)\right\}$$
$$+\cos 2\eta\left\{A_2\left[\frac{\cosh 2\xi+\nu e^{-2\xi}}{2}-\frac{4h^2}{5c^2}e^{-2\xi}\cosh 2\xi\left(2+\frac{\mathrm{Gek}_2'}{\mathrm{Gek}_2}\right)\right]\right.$$
$$-\frac{4}{c^2}(1-\nu)E_2e^{-2\xi}(\sinh 2\xi+2\cosh 2\xi)$$
$$\left.-\frac{4}{c^2}(1-\nu)F_2e^{2\xi}(2\cosh 2\xi-\sinh 2\xi)-A_0(1+\nu)\cosh 2\xi\right\}$$
$$+\cos 4\eta\left\{A_2\left[-\frac{\nu}{4}+\frac{h^2}{5c^2}e^{-2\xi}\left(2+\frac{\mathrm{Gek}_2'}{\mathrm{Gek}_2}\right)\right]\right.$$
$$\left.-\frac{2}{c^2}(1-\nu)(E_2e^{-2\xi}+F_2e^{2\xi})+A_0\frac{1+\nu}{4}\right\}\quad\ldots[35b]$$

$$-\frac{4}{c^4}\frac{1}{(1-\nu)}J^4M_{\xi\eta}=\sin 2\eta\left\{A_2\left[-\frac{e^{-2\xi}+\sinh 2\xi}{4}\right.\right.$$
$$+\frac{h^2e^{-2\xi}}{5(1-\nu)c^2}\left[2\sinh 2\xi\left(2+\frac{\mathrm{Gek}_2'}{\mathrm{Gek}_2}\right)\right.$$
$$\left.\left.+\cosh 2\xi\left(4-\frac{\mathrm{Gek}_2''}{\mathrm{Gek}_2}\right)\right]\right]-\frac{2}{c^2}F_0$$
$$+\frac{4}{c^2}E_2e^{-2\xi}(\sinh 2\xi+2\cosh 2\xi)$$
$$\left.+\frac{4}{c^2}F_2e^{2\xi}(\sinh 2\xi-2\cosh 2\xi)\right\}$$
$$+\sin 4\eta\left\{A_2\left[-\frac{h^2e^{-2\xi}}{10(1-\nu)c^2}\left(4-\frac{\mathrm{Gek}_2''}{\mathrm{Gek}_2}\right)\right]\right.$$
$$\left.-\frac{2}{c^2}(E_2e^{-2\xi}-F_2e^{2\xi})\right\}\quad\ldots[35c]$$

$$JV_\eta=A_2e^{-2\xi}\left(2+\frac{\mathrm{Gek}_2'}{\mathrm{Gek}_2}\right)\sin 2\eta\quad\ldots[35d]$$

Substituting the foregoing expressions in the Boundary Conditions [29] and [30], the following expressions for the constants in Equation [31] are obtained

$$A_0=-\frac{M_0}{1+\nu}\quad\ldots[36a]$$

$$F_2=-\Gamma\frac{M_0}{16(1-\nu)}\quad\ldots[36b]$$

$$A_2=\frac{1}{\Delta}\left[\frac{8(1-\nu)}{c^2}F_2e^{2\xi_0}\sinh 2\xi_0-\frac{1+\nu}{2}A_0\sinh 2\xi_0\right]\quad\ldots[36c]$$

$$E_2=\frac{1}{\Delta}\frac{c^2}{4(1-\nu)}e^{2\xi_0}\left\{\frac{4(1-\nu)}{c^2}F_2\left[\frac{1-\nu}{4}e^{2\xi_0}\sinh 2\xi_0\right.\right.$$
$$\left.\left.-\frac{2h^2}{5c^2}\sinh 2\xi_0\left(2+\frac{\mathrm{Gek}_2'(\xi_0,-q)}{\mathrm{Gek}_2(\xi_0,-q)}\right)\right]-\frac{1+\nu}{4}A_0\sinh 2\xi_0\right\}$$
$$\quad\ldots[36d]$$

$$F_0=\frac{1}{\Delta}\frac{c^2}{2}\left\{\frac{2}{c^2}F_2(1+\nu)\sinh 2\xi_0\right.$$
$$+\frac{1+\nu}{2(1-\nu)}A_0\left[\frac{1}{2}e^{-2\xi_0}\sinh 2\xi_0-\frac{3+\nu}{4}\sinh 2\xi_0\cosh 2\xi_0\right.$$
$$\left.\left.-\frac{2h^2}{5c^2}e^{-2\xi_0}\sinh^2 2\xi_0\left(2+\frac{\mathrm{Gek}_2'(\xi_0,-q)}{\mathrm{Gek}_2(\xi_0,-q)}\right)\right]\right\}\quad\ldots[36e]$$

where

$$\Delta=-\left[\frac{3+\nu}{4}\sinh 2\xi_0\right.$$
$$\left.+\frac{2h^2}{5c^2}e^{-2\xi_0}\sinh 2\xi_0\left(2+\frac{\mathrm{Gek}_2'(\xi_0,-q)}{\mathrm{Gek}_2(\xi_0,-q)}\right)\right]$$

Denoting by α and β the ratios h/a and b/a (a and b being the semimajor and semiminor axes of the boundary $\xi=\xi_0$), respectively, we obtain from Equations [35] and [36] the following expressions for M_η on the boundary of the hole

$$\frac{M_\eta(\xi_0)}{M_0}=\frac{2}{Q}\left\{\frac{1+\nu}{16}\Gamma\left[-(1-\beta^2)[8\beta-6(1+\nu)(1+\beta^2)]\right.\right.$$
$$-4\cos 2\eta[(1-\beta^2)^2+(1+\beta^2)(1+\beta)^2]$$
$$\left.+2\cos 4\eta[(1-\beta^2)(1+\beta)^2]\right]$$
$$+\left[\frac{1}{4}(1-\beta^2)^2+\frac{1+\nu}{2}\beta+\frac{(1+\beta^2)^2}{2}\right.$$
$$\left.+\frac{\alpha^2(3+2\beta+3\beta^4)}{5(1+\beta)^2}\left(2+\frac{\mathrm{Gek}_2'}{\mathrm{Gek}_2}\right)\right]$$
$$-\cos 2\eta\left[(1+\beta^2)(1-\beta^2)+\frac{1+\nu}{2}\beta(1-\beta^2)\right.$$
$$\left.+\frac{4\alpha^2}{5}\frac{1-\beta}{1+\beta}(1+\beta^2)\left(2+\frac{\mathrm{Gek}_2'}{\mathrm{Gek}_2}\right)\right]$$
$$\left.+\cos 4\eta\left[\frac{(1-\beta^2)^2}{4}+\frac{\alpha^2}{5}(1-\beta)^2\left(2+\frac{\mathrm{Gek}_2'}{\mathrm{Gek}_2}\right)\right]\right\}\quad\ldots[37]$$

where

$$Q = \left[\frac{3+\nu}{2} + \frac{4\alpha^2}{5}\frac{1}{(1+\beta)^2}\left(2 + \frac{\mathrm{Gek}_2'}{\mathrm{Gek}_2}\right)\right]\left[(1+\beta^2) - \cos 2\eta(1-\beta^2)\right]^2$$

This expression has its greatest value at $\eta = \pi/2$ when $\Gamma = 1$. Hence

$$k_B = \frac{M_\eta\left(\xi_0, \frac{\pi}{2}\right)}{M_0} = 1 + \frac{\frac{1+\nu}{8}[3\nu + 10\beta + 6\beta^2 - 3\nu\beta^4]}{(3+\nu) + \frac{8}{5}\frac{\alpha^2}{(1+\beta)^2}\left(2 + \frac{\mathrm{Gek}_2'}{\mathrm{Gek}_2}\right)} \quad \ldots\ldots [38]$$

Similarly, by Equations [35] and [36], $V_\eta(\xi_0, \eta)$ is given by

$$\frac{V_\eta(\xi_0, \eta)}{M_0/a} = \frac{2\sqrt{2}\,[(1-\beta) - \Gamma(1+\beta)]\left(2 + \frac{\mathrm{Gek}_2'}{\mathrm{Gek}_2}\right)\sin 2\eta}{\left[(3+\nu) + \frac{8}{5}\frac{\alpha^2}{(1+\beta)^2}\left(2 + \frac{\mathrm{Gek}_2'}{\mathrm{Gek}_2}\right)\right](1+\beta)\left[(1+\beta^2) - (1-\beta^2)\cos 2\eta\right]^{1/2}} \quad \ldots\ldots [39]$$

which has its maximum value at $\eta = \pi/4$, when $\Gamma = 1$. Thus

$$\frac{\left[V_\eta\left(\xi_0, \frac{\pi}{4}\right)\right]_B}{M_0/a} = \frac{-4\sqrt{2}\,\beta\left(2 + \frac{\mathrm{Gek}_2'}{\mathrm{Gek}_2}\right)}{(1+\beta)(1+\beta^2)^{1/2}\left[(3+\nu) + \frac{8}{5}\frac{\alpha^2}{(1+\beta)^2}\left(2 + \frac{\mathrm{Gek}_2'}{\mathrm{Gek}_2}\right)\right]} \quad \ldots\ldots [40]$$

Having the results for the case of plain bending, the stress-concentration factor k_T for the case of infinite plate with an elliptic hole subjected to uniform twisting couple M_0 at infinity may be deduced as follows: Since the stresses and displacements in the state of pure twist may be expressed by suitable superposition of plain positive bending about the y-axis and a plain negative bending about the x-axis, it follows that

$$k_T = [k_B]_{\Gamma=1} - [k_B]_{\Gamma=-1} \quad \ldots\ldots [41]$$

Thus, by Equation [37], the greatest value of $M_{\xi\eta}(\xi_0)/M_0$ at $\eta = \pi/2$ is

$$k_T = \frac{(1+\nu)\left[\left(2 + \frac{3}{4}\nu\right) + \frac{1}{2}\beta + \frac{3}{2}\beta^2 - \frac{3}{4}\nu\beta^4\right]}{(3+\nu) + \frac{8}{5}\frac{\alpha^2}{(1+\beta)^2}\left(2 + \frac{\mathrm{Gek}_2'}{\mathrm{Gek}_2}\right)} \quad \ldots [42]$$

The maximum value of $V_\eta(\xi_0)/(M_0/a)$ for the case of pure twist occurs also at $\eta = \pi/4$ and is given by

$$\frac{\left[V_\eta\left(\xi_0, \frac{\pi}{4}\right)\right]_T}{M_0/a} = \frac{-4\sqrt{2}\left(2 + \frac{\mathrm{Gek}_2'}{\mathrm{Gek}_2}\right)}{(1+\beta^2)^{1/2}\left[(3+\nu) + \frac{8}{5}\frac{\alpha^2}{(1+\beta)^2}\left(2 + \frac{\mathrm{Gek}_2'}{\mathrm{Gek}_2}\right)\right]} \quad \ldots [43]$$

Solution in Limiting Cases—Numerical Example

When a confocal ellipse of semimajor axis r tends to a circle with this radius, $\xi \to \infty$ and $c \to 0$ such that $\frac{1}{2}ce^{\xi} \to r$. Then[10]

$$\pi\,\mathrm{Gek}_2(\xi, -q) \to s_2 K_2\left(\frac{\sqrt{10}}{h}r\right)$$

$$\pi\,\mathrm{Gek}_2'(\xi, -q) \to s_2' k_1 r K_2'\left(\frac{\sqrt{10}}{h}r\right)$$

where $k_1 r = q^{1/2}e^{\xi}$.

With reference to Equations [38] and [42], we note that as $\beta \to 1$

$$\frac{\mathrm{Gek}_2'(\xi_0, -q)}{\mathrm{Gek}_2(\xi_0, -q)} \to \mu\frac{K_2'(\mu)}{K_2(\mu)}$$

where

$$\mu = \frac{\sqrt{10}}{h}a$$

and K_2 is modified Bessel function of the second kind. Thus Expressions [38] and [42] for $\beta = 1$ reduce to

$$k_B = \left[1 + \frac{2(1+\nu)K_2(\mu)}{(1+\nu)K_2(\mu) + 2K_0(\mu)}\right],$$

$$k_T = \frac{4(1+\nu)K_2(\mu)}{(1+\nu)K_2(\mu) + 2K_0(\mu)}$$

which are the same as those given previously by Reissner (2). Similarly, the Expressions [40] and [43] for the shear resultant V_η become

$$\frac{\left[V_\eta\left(a, \frac{\pi}{4}\right)\right]_B}{M_0/a} = \frac{1}{2}\frac{\left[V_\eta\left(a, \frac{\pi}{4}\right)\right]_T}{M_0/a} = -\frac{\frac{10}{\alpha^2}[K_2(\mu) - K_0(\mu)]}{(1+\nu)K_2(\mu) + 2K_0(\mu)}$$

Also, as $\alpha \to 0$, Equations [38] and [42] yield, respectively

$$k_B = 1 + \frac{(1+\nu)[3\nu + 10\beta + 6\beta^2 - 3\nu\beta^4]}{8(3+\nu)}$$

$$k_T = \frac{(1+\nu)\left[\left(2 + \frac{3}{4}\nu\right) + \frac{1}{2}\beta + \frac{3}{2}\beta^2 - \frac{3}{4}\nu\beta^4\right]}{(3+\nu)}$$

which are identical with the predictions of the classical theory (13).

As the recurrence relations for modified Mathieu functions of the second kind are not available in the literature, the results for small values of a/h, i.e., as $\alpha \to \infty$, may not be obtained from the form of Equations [38] and [42]. However, since for the case $\beta = 1$, the stress-concentration factors in the limit of vanishing hole radius to plate thickness (a/h), as given in (2), were equal to

[10] Reference (19), p. 369.

stress-concentration factors in plane stress, one would suspect that as $a/h \to 0$, Equations [38] and [42] become $(1 + 2/\beta)$ and $(1 + \beta)^2/\beta$, respectively.

Figs. 2 and 3 show a plot of the stress concentration and $\frac{V_\eta\left(\xi_0, \frac{\pi}{4}\right)}{M_0/a}$ for both plain bending and pure twist. In both cases, $\beta = b/a$ is taken as $^3/_4$ and Poisson's ratio is assumed to be $^1/_3$.

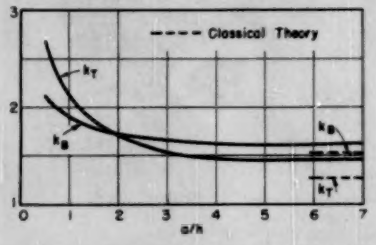

FIG. 2 STRESS-CONCENTRATION FACTORS VERSUS RATIO OF HOLE SEMIMAJOR AXIS TO PLATE THICKNESS ($^1/_2 \leq a/h \leq 7$) FOR BOTH PLAIN BENDING AND PURE TWIST; $b/a = 3/4$ AND $\nu = 1/3$

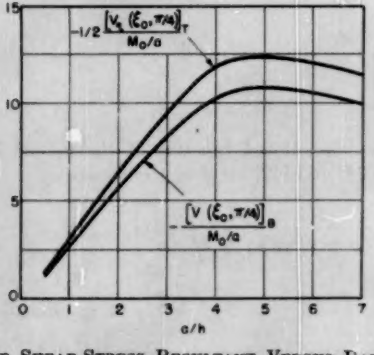

FIG. 3 EDGE SHEAR-STRESS RESULTANT VERSUS RATIO OF HOLE SEMIMAJOR AXIS TO PLATE THICKNESS ($^1/_2 \leq a/h \leq 7$) FOR BOTH PLAIN BENDING AND PURE TWIST; $b/a = 3/4$ AND $\nu = 1/3$

Also indicated in Fig. 2 are the predictions of the classical theory. In computing the quantity

$$\frac{\mathrm{Gek}_2'(\xi_0, -q)}{\mathrm{Gek}_2(\xi_0, -q)}$$

the series representation involving product of Bessel functions[11] was used, since this representation converges rapidly. It was observed by Reissner that for the case $\beta = 1$, the maximum shear resultant V_η in pure twist is only twice as much as the corresponding quantity in plain bending. A glance at Fig. 3 reveals that for $\beta < 1$, this deviation between the two increases further, as might be expected. It is also interesting to note that the values of the stress-concentration factors in Fig. 2 are smaller (for the range of a/h plotted) than the corresponding quantities for $\beta = 1$.

CONCLUSION

The solution given here is approximate in the sense that Equations [33] are not exactly fulfilled, as may be seen from the series expansion of $\mathrm{se}_2(\eta, -q)$. For an exact solution of the problem, the function χ, given by Equation [2], must include the entire second sum in Equation [26], and this becomes progressively more important as the elliptic hole becomes more slender.

Finally, it may be mentioned that the results given here can be used to obtain the solution of the corresponding stress-concentration problem of an elliptic inclusion.

[11] Reference 19, §8.30.

ACKNOWLEDGMENT

The author wishes to thank the Horace H. Rackham School of Graduate Studies at the University of Michigan for a faculty research grant which made completion of this investigation possible. Also, the author is indebted to Messrs. R. M. Cooper and J. C. Rowley for assistance with a portion of the computation and checking some formulas.

BIBLIOGRAPHY

1 "On the Theory of Bending of Elastic Plates," by E. Reissner, *Journal of Mathematics and Physics*, vol. 23, 1944, pp. 184–191.

2 "The Effect of Transverse Shear Deformation on the Bending of Elastic Plates," by E. Reissner, JOURNAL OF APPLIED MECHANICS, Trans. ASME, vol. 67, 1945, p. A-69.

3 "On the Bending of Elastic Plates," by E. Reissner, *Quarterly of Applied Mathematics*, vol. 5, 1947, pp. 55–68.

4 Discussion of reference (2), by J. N. Goodier, JOURNAL OF APPLIED MECHANICS, Trans. ASME, vol. 68, 1946, p. A-251.

5 "On a Variational Theorem in Elasticity," by E. Reissner, *Journal of Mathematics and Physics*, vol. 29, 1950, pp. 90–95.

6 "On Reissner's Theory of Bending of Elastic Plates," by A. E. Green, *Quarterly of Applied Mathematics*, vol. 7, 1949, pp. 223–228.

7 "The Elastic Equilibrium of Isotropic Plates and Cylinders," by A. E. Green, Proceedings of the Royal Society of London, England, series A, vol. 195, 1949, pp. 533–552.

8 "Influence of Rotary Inertia and Shear on Flexural Motions of Isotropic Elastic Plates," by R. D. Mindlin, JOURNAL OF APPLIED MECHANICS, Trans. ASME, vol. 73, 1951, p. 31.

9 Discussion of reference (2), by D. C. Drucker, JOURNAL OF APPLIED MECHANICS, Trans. ASME, vol. 68, 1946, p. A-250.

10 "The Effect of a Rigid Circular Inclusion on the Bending of a Thick Elastic Plate," by R. A. Hirsch, JOURNAL OF APPLIED MECHANICS, Trans. ASME, vol. 74, 1952, pp. 28–32.

11 "Über eine Verfeinerung der Klassischen Theorie dunner schwach gebogener Platten," by V. Manfred Schafer, *Zeitschrift für Angewandte Mathematik und Mechanik*, vol. 32, 1952, pp. 161–171.

12 "On the Bending of Axially Symmetric Plates on Elastic Foundations," by P. M. Naghdi and J. C. Rowley, Proceedings of the First Midwestern Conference on Solid Mechanics, University of Illinois, 1953.

13 "The Influence of Circular and Elliptical Holes on the Transverse Flexure of Elastic Plates," by J. N. Goodier, *London Philosophical Magazine*, series 7, vol. 22, 1936, pp. 69–80.

14 "The Influence of Shape and Rigidity of an Elastic Inclusion on the Transverse Flexure of Thin Plates," by M. Goland, JOURNAL OF APPLIED MECHANICS, Trans. ASME, vol. 65, 1943, p. A-69.

15 "Stress Concentration Around an Open Circular Hole in a Plate Subjected to Bending Normal to the Plane of the Plate," by C. Dumont, NACA TN 740, 1939.

16 "An Extension of the Photoelastic Method of Stress Measurement to Plates in Transverse Bending," by J. N. Goodier and G. H. Lee, JOURNAL OF APPLIED MECHANICS, Trans. ASME, vol. 63, 1941, p. A-27.

17 "The Photoelastic Analysis of Transverse Bending of Plates in the Standard Transmission Polariscope," by D. C. Drucker, JOURNAL OF APPLIED MECHANICS, Trans. ASME, vol. 64, 1942, pp. A-161 to A-164.

18 "A Treatise on the Mathematical Theory of Elasticity," by A. E. H. Love, Dover Publications, New York, N. Y., 1944.

19 "Theory and Application of Mathieu Functions," by N. W. McLachlan, Oxford University Press, Oxford, England, 1947.

20 "On the Computation of Mathieu Functions," by Gertrude Blanch, *Journal of Mathematics and Physics*, vol. 25, 1946, pp. 1–20.

21 "Tables Relating to Mathieu Functions," prepared by the Computational Laboratory of the National Bureau of Standards, Columbia University Press, New York, N. Y., 1951.

A Refinement of the Theory of Buckling of Rings Under Uniform Pressure

By A. P. BORESI,[1] URBANA, ILL.

A general variational theory of elastic stability that was originated by E. Trefftz (1)[2] is applied to the problem of buckling of rings of rectangular cross section subjected to uniform external pressure. The theory is believed to be more rigorous than previous treatments of the problem, since it avoids conventional assumptions of curved-beam theory, such as the assumptions that plane sections remain plane and that radial stresses vanish. The classical result of Levy (2) is confirmed for a ring of infinitesimal thickness. New results are obtained which show the effect of the finite thickness of a ring on the coefficients in the buckling formula.

Introduction

RECENT refinements in the theory of cylindrical shells that were instituted by Epstein (3) and elaborated by Kennard (4) cast doubts on the validity of the usual assumption that normals to the middle surface of a shell remain straight and normal during deformation of the shell. These doubts are particularly pertinent for buckling problems, since the solutions of these problems prove to be extremely sensitive to approximations.

It is possible to free the theory of buckling from arbitrary physical assumptions, such as the assumptions that are commonly used in the theories of beams, plates, and shells, for an exact analytical theory of elastic stability was developed by E. Trefftz (1) in 1933. Surprisingly, this theory has received very little attention. In 1943 C. Lanczos, being unaware of Trefftz's work, developed the theory independently and applied it to the problem of buckling of cylindrical shells under axial compression, but his work was not published. Recently, Langhaar (5), being motivated by Lanczos' work, applied Trefftz's theory to the problem of torsional-flexural buckling of columns.

In the present paper Trefftz's theory is applied to the problem of buckling of rings of rectangular cross section under the action of uniform external pressure. Stevens (6) recently demonstrated that the buckling load of a ring is affected significantly if the external forces remain directed toward the original center of the ring instead of remaining normal to the surface of the ring when buckling occurs. Both types of loading (central loading and normal loading) are investigated in the present work. The results do not agree with Stevens' value of the buckling pressure, for central loading, but the discrepancy has been traced to an unfortunate error in sign in Stevens' analysis.

The ring under consideration is referred to cylindrical coordinates (r, θ, z). The plane-stress assumption ($\sigma_z = \tau_{rz} = \tau_{\theta z} = 0$) is used. Also, the radial and circumferential displacements (u, v) are assumed to be independent of z. Actually, neither of these assumptions is justified rigorously, unless $\nu = 0$. Slight departures from plane stress and slight anticlastic deformations of the curved surfaces (denoting dependence of the displacements on z) are known to occur in the bending of curved beams. For a wide ring, the anticlastic deformations probably are confined principally to strips near the edges, and our assumptions may then be expected to be fulfilled approximately. For a narrow ring, the anticlastic deformations alleviate the effect of Poisson's ratio, and the buckling pressure is determined approximately by the solution for the case $\nu = 0$, irrespective of the value of ν. Analogously, the flexural stiffness of a flat plate that is subjected to cylindrical bending is increased by the factor $1/(1 - \nu^2)$, whereas this factor does not appear in beam theory because of anticlastic deformations.

The method that is employed in the present study establishes upper and lower bounds that bracket the coefficient K in the buckling formula ($p_{cr} = KEI/r_0^3$) closely, and that actually coincide if the thickness of the ring approaches zero. Aside from the assumptions mentioned in the preceding paragraph, no approximations are used to establish these bounds, other than the neglecting of second-degree terms in the initial radial displacement ξ (i.e., the displacement before buckling occurs) in the expressions for the strain components. Quadratic terms in ξ presumably are negligible since previous theories neglect even the variation of ξ through the thickness of the ring. Consequently, the results obtained are believed to be accurate for the case $\nu = 0$. A positive value of Poisson's ratio actually provides a slight stabilizing effect. The magnitude of this effect may be estimated on the basis of the preceding argument concerning the influence of ν.

Résumé of Trefftz's Theory

Although the general theory, upon which the analysis of this paper is based, was implied in the works of Lagrange (7), and later in the works of Poincaré (8), it was first developed with specific reference to elastic stability by E. Trefftz. A brief summary of this theory is given here.

A stationary conservative mechanical system is in stable equilibrium if, and only if, its total potential energy V has a relative minimum; hence $\Delta V > 0$ for any small virtual displacement of the system that is consistent with the constraints. For an elastic system, $V = U + \Omega$, where U is the strain energy, and Ω is the potential energy of the external forces. Consequently, $\Delta V = \Delta U + \Delta\Omega$. For a system with linear elasticity

$$\Delta U = \delta U + \frac{1}{2!}\delta^2 U + \frac{1}{3!}\delta^3 U + \frac{1}{4!}\delta^4 U$$

where $\delta^n U$ (the nth variation of U) is the volume integral of a homogeneous polynomial of nth degree in the components of the virtual displacement vector and its first derivatives.

Similarly, for the change in potential energy of the external loads

$$\Delta\Omega = \delta\Omega + \frac{1}{2!}\delta^2\Omega + \ldots .$$

---

[1] Assistant Professor in Theoretical and Applied Mechanics, University of Illinois.

[2] Numbers in parentheses refer to the Bibliography at the end of the paper.

Contributed by the Applied Mechanics Division and presented at the Annual Meeting, New York, N. Y., Nov. 28–Dec. 3, 1954, of The American Society of Mechanical Engineers.

Discussion of this paper should be addressed to the Secretary, ASME, 29 West 39th Street, New York, N. Y., and will be accepted until April 11, 1955, for publication at a later date. Discussion received after the closing date will be returned.

Note: Statements and opinions advanced in papers are to be understood as individual expressions of their authors and not those of the Society. Manuscript received by ASME Applied Mechanics Division, July 8, 1953. Paper No. 54—A-2.

Accordingly, the virtual increment of total potential energy is

$$\Delta V = \delta U + \delta\Omega + \frac{1}{2!}\delta^2 U + \frac{1}{2!}\delta^2\Omega + \dots .$$

By the principle of virtual work, $\delta U + \delta\Omega = 0$ for any equilibrium configuration. Accordingly, if the virtual displacements are small, the sign of ΔV is controlled by the sign of $\delta^2 U + \delta^2\Omega$. Therefore equilibrium is stable if, and only if, $\delta^2 U + \delta^2\Omega > 0$ for all virtual displacements. Equilibrium becomes unstable if $\delta^2 U + \delta^2\Omega$ can take negative values for certain virtual displacements. In other words, buckling occurs when $\delta^2 U + \delta^2\Omega$ changes from positive definite character to indefinite character. Thus the question of stability resolves into a mathematical study of $\delta^2 U + \delta^2\Omega$.

For a ring subjected to small external pressure p, $\delta^2 U + \delta^2\Omega$ is positive definite, but for large p, $\delta^2 U + \delta^2\Omega$ is indefinite. It is desired to find the pressure at which the change from positive definite character to indefinite character occurs. This pressure is the buckling pressure p_{cr}.

Unfortunately, there seems to be no exact way to treat this mathematical problem. However, an upper bound for the buckling pressure may be obtained by letting the virtual displacements be prescribed functions that are judged to conform closely to the actual deformations that occur at buckling. Furthermore, a lower bound for the buckling pressure is obtained, if we perform an exact mathematical analysis of the problem using a simplified approximation of $\delta^2 V$ obtained by discarding or reducing certain terms in $\delta^2 V$ that are essentially positive.

Second Variation of Strain Energy

In an exact theory of buckling it is necessary to retain quadratic terms in the strain tensor. For rectangular co-ordinates the exact expression for the strain components are given by Love (9). However, in ring problems the use of polar co-ordinates is advantageous. The exact expressions for the strain components in polar co-ordinates may be obtained from the equivalent expressions in rectangular co-ordinates by a tensor transformation. Thus the expressions for the strain components in polar co-ordinates are

$$\epsilon_r = \xi_r + \frac{1}{2}\xi_r^2 + \frac{1}{2}\eta_r^2$$

$$\epsilon_\theta = \frac{\xi}{r} + \frac{\eta_\theta}{r} + \frac{1}{2}\left(\frac{\xi_\theta - \eta}{r}\right)^2 + \frac{1}{2}\left(\frac{\xi + \eta_\theta}{r}\right)^2$$

$$\gamma_{r\theta} = \eta_r + \frac{\xi_\theta - \eta}{r} + \xi_r\left(\frac{\xi_\theta - \eta}{r}\right) + \eta_r\left(\frac{\xi + \eta_\theta}{r}\right) \dots [1]$$

where (ξ, η) are the displacement components in the r, θ directions, respectively, and the r, θ subscripts on ξ, η denote partial derivatives.

Let (ξ, η) be the displacement vector that defines the given equilibrium configuration. Let (u, v) be the incremental virtual displacement vector. Then the total displacement vector is $(\xi + u, \eta + v)$, Fig. 1. Substituting the total displacement vector $(\xi + u, \eta + v)$ into Equations [1], we obtain the following expressions for the strain components (since $\eta = 0$, $\xi_\theta = 0$)

$$\epsilon_r + \Delta\epsilon_r = \xi_r + u_r + \frac{1}{2}(\xi_r + u_r)^2 + \frac{1}{2}(v_r)^2$$

$$\epsilon_\theta + \Delta\epsilon_\theta = \frac{\xi}{r} + \frac{u}{r} + \frac{v_\theta}{r} + \frac{1}{2}\left(\frac{u_\theta - v}{r}\right)^2 + \frac{1}{2}\left(\frac{\xi + u + v_\theta}{r}\right)^2$$

$$\gamma_{r\theta} + \Delta\gamma_{r\theta} = v_r + \frac{u_\theta}{r} - \frac{v}{r} + (\xi_r + u_r)\left(\frac{u_\theta - v}{r}\right) + v_r\left(\frac{\xi + u + v_\theta}{r}\right) \dots [2]$$

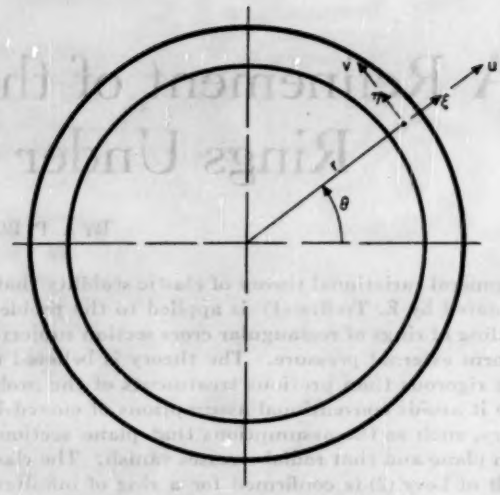

Fig. 1 The Total Displacement Vector $(\xi + u, \eta + v)$

where $\Delta\epsilon_r$, $\Delta\epsilon_\theta$, $\Delta\gamma_{r\theta}$ are the incremental strains due to the virtual displacement vector (u, v).

It is convenient to write

$$\Delta\epsilon_r = \delta\epsilon_r + \frac{1}{2}\delta^2\epsilon_r$$

$$\Delta\epsilon_\theta = \delta\epsilon_\theta + \frac{1}{2}\delta^2\epsilon_\theta$$

$$\Delta\gamma_{r\theta} = \delta\gamma_{r\theta} + \frac{1}{2}\delta^2\gamma_{r\theta} \dots [3]$$

where $\delta\epsilon_r$, $\delta\epsilon_\theta$, $\delta\gamma_{r\theta}$ are linear forms in (u, v) and their derivatives, and $\delta^2\epsilon_r$, $\delta^2\epsilon_\theta$, $\delta^2\gamma_{r\theta}$ are quadratic forms in the same variables. By Equations [2]

$$\epsilon_r = \xi_r + \frac{1}{2}\xi_r^2$$

$$\delta\epsilon_r = u_r(1 + \xi_r)$$

$$\delta^2\epsilon_r = u_r^2 + v_r^2$$

$$\epsilon_\theta = \frac{\xi}{r} + \frac{1}{2}\left(\frac{\xi}{r}\right)^2$$

$$\delta\epsilon_\theta = \left(\frac{u + v_\theta}{r}\right)\left(1 + \frac{\xi}{r}\right)$$

$$\delta^2\epsilon_\theta = \left(\frac{u_\theta - v}{r}\right)^2 + \left(\frac{u + v_\theta}{r}\right)^2$$

$$\gamma_{r\theta} = 0$$

$$\delta\gamma_{r\theta} = v_r\left(1 + \frac{\xi}{r}\right) + \left(\frac{u_\theta - v}{r}\right)(1 + \xi_r)$$

$$\delta^2\gamma_{r\theta} = 2u_r\left(\frac{u_\theta - v}{r}\right) + 2v_r\left(\frac{u + v_\theta}{r}\right) \dots [4]$$

We assume that $\sigma_r = \tau_{rz} = \tau_{\theta z} = 0$, and that the radial and circumferential displacements are independent of z (see Introduction). Then the strain energy of a ring of inner radius a, outer radius b, and width L is

$$U = \frac{EL}{2(1 - \nu^2)}\int_0^{2\pi}\int_a^b \left[\epsilon_r^2 + \epsilon_\theta^2 + 2\nu\epsilon_r\epsilon_\theta + \frac{1}{2}(1 - \nu)\gamma_{r\theta}^2\right] r\, dr\, d\theta$$

where E and ν are Young's modulus and Poisson's ratio, respectively. Substitution of $\epsilon_r + \Delta\epsilon_r$, $\epsilon_\theta + \Delta\epsilon_\theta$, and $\gamma_{r\theta} + \Delta\gamma_{r\theta}$ for ϵ_r, ϵ_θ, and $\gamma_{r\theta}$ yields

$$U + \Delta U = \frac{EL}{2(1-\nu^2)} \int_0^{2\pi} \int_a^b \left[\left(\epsilon_r + \delta\epsilon_r + \frac{1}{2}\delta^2\epsilon_r \right)^2 + \left(\epsilon_\theta + \delta\epsilon_\theta + \frac{1}{2}\delta^2\epsilon_\theta \right)^2 + 2\nu \left(\epsilon_r + \delta\epsilon_r + \frac{1}{2}\delta^2\epsilon_r \right) \times \left(\epsilon_\theta + \delta\epsilon_\theta + \frac{1}{2}\delta^2\epsilon_\theta \right) + \frac{1}{2}(1-\nu) \times \left(\gamma_{r\theta} + \delta\gamma_{r\theta} + \frac{1}{2}\delta^2\gamma_{r\theta} \right)^2 \right] r\, dr\, d\theta$$

Now, $\Delta U = \delta U + (1/2!)\delta^2 U + \ldots$, where δU is the integral of a linear form in (u, v) and their derivatives, $\delta^2 U$ is the integral of a quadratic form in (u, v) and their derivatives, and so on.

Consequently

$$\frac{1}{2}\delta^2 U = \frac{EL}{2(1-\nu^2)} \int_0^{2\pi} \int_a^b \left[\epsilon_r \delta^2\epsilon_r + (\delta\epsilon_r)^2 + \epsilon_\theta \delta^2\epsilon_\theta + (\delta\epsilon_\theta)^2 + \nu(\epsilon_r \delta^2\epsilon_\theta + 2\delta\epsilon_r \delta\epsilon_\theta + \epsilon_\theta \delta^2\epsilon_r) + \frac{1}{2}(1-\nu)(\delta\gamma_{r\theta})^2 \right] r\, dr\, d\theta \ldots [5]$$

Substituting Equations [4] into Equation [5] and neglecting quadratic terms in ξ_r and ξ/r as compared to unity, we get

$$\delta^2 U = \frac{EL}{(1-\nu^2)} \int_0^{2\pi} \int_a^b \left\{ u_r^2 \left(1 + 3\xi_r + \nu \frac{\xi}{r} \right) + v_r^2 \left(\frac{1-\nu}{2} + \xi_r + \frac{\xi}{r} \right) + \left(\frac{u_\theta - v}{r} \right)^2 \left(\frac{1-\nu}{2} + \xi_r + \frac{\xi}{r} \right) + \left(\frac{u + v_\theta}{r} \right)^2 \left(1 + \frac{3\xi}{r} + \nu\xi_r \right) + \left(1 + \xi_r + \frac{\xi}{r} \right) \times \left[2\nu u_r \left(\frac{u + v_\theta}{r} \right) + (1-\nu) v_r \left(\frac{u_\theta - v}{r} \right) \right] \right\} r\, dr\, d\theta \ldots [6]$$

It is worth noting that if quadratic terms in Equations [2] are neglected, $\delta^2 U$ (Equation [6]) is always positive definite. Hence, if $\delta^2\Omega = 0$, $\delta^2 V = \delta^2 U > 0$. Accordingly, the phenomenon of buckling, in general, does not lie within the scope of linear theory of elasticity.

The displacement component ξ is obtained from the elastic theory of thick-walled cylinders (10). The radial displacement of a point at the distance r from the center of the ring is

$$\xi = -\frac{Aa^2}{r} - Br$$

where

$$A = \frac{(1+\nu)b^2(p_o - p_i)}{E(b^2 - a^2)}$$

$$B = \frac{(1-\nu)(p_o b^2 - p_i a^2)}{E(b^2 - a^2)}$$

p_o, p_i are external and internal pressures, respectively.

For $p_i = 0$, let $p_o = p$. Then

$$\xi = -P\left(r + \frac{1+\nu}{1-\nu}\frac{a^2}{r} \right) \ldots [7]$$

where

$$P = \frac{1-\nu}{E} \frac{b^2}{b^2 - a^2} p = \frac{(1-\nu)p}{Ek} \ldots [8]$$

with

$$k = 1 - (a/b)^2 \ldots [8a]$$

Substitution of Equation [7] into Equation [6] gives (with $a = 1$)

$$\delta^2 U = \frac{EL}{(1-\nu^2)} \int_0^{2\pi} \int_1^b \left\{ \left[1 - P(3+\nu) + \frac{P(3-\nu)(1+\nu)}{r^2(1-\nu)} \right] u_r^2 + \left(\frac{1-\nu}{2} - 2P \right) v_r^2 + \left(\frac{1-\nu}{2} - 2P \right) \left(\frac{u_\theta - v}{r} \right)^2 + \left[1 - P(3+\nu) - \frac{P(3-\nu)(1+\nu)}{r^2(1-\nu)} \right] \left(\frac{u + v_\theta}{r} \right)^2 + 2\nu(1-2P) \times \left(\frac{u + v_\theta}{r} \right) u_r + (1-\nu)(1-2P) \left(\frac{u_\theta - v}{r} \right) v_r \right\} r\, dr\, d\theta \ldots [9]$$

Second Variation of Potential Energy of External Pressure

(a) *Normally Directed Pressure.* If the ring is loaded normally (e.g., by hydrostatic pressure), the virtual work of the external forces is $\Delta\Omega = pL\,\Delta A$, where ΔA is the change of the area enclosed by the outer circle $r = b$ due to the virtual displacements (u, v).

Since $\Delta\Omega = \delta\Omega + 1/2(\delta^2\Omega) + \ldots$ and $\Delta A = \delta A + 1/2(\delta^2 A) + \ldots$, the second variation of the potential energy of the external load is $\delta^2\Omega = pL\,\delta^2 A$. The term $\delta^2 A$ is most conveniently determined with the aid of rectangular co-ordinates (x, y), Fig. 2.

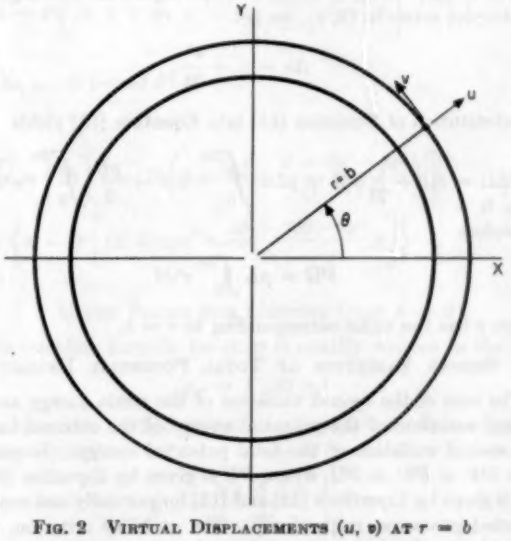

Fig. 2 Virtual Displacements (u, v) at $r = b$

In terms of the virtual displacements (u, v), the (x, y)-components of displacement are

$$u' = u\cos\theta - v\sin\theta$$

$$v' = u\sin\theta + v\cos\theta$$

where (u, v) are evaluated for $r = b$.

The original (x, y)-co-ordinates of the particle under consideration are $x_0 = b\cos\theta$, $y_0 = b\sin\theta$. After the virtual displacements (u, v), the particle is located at $x = x_0 + u'$, $y = y_0 + v'$ or

$$x = b\cos\theta + u\cos\theta - v\sin\theta$$

$$y = b\sin\theta + u\sin\theta + v\cos\theta \ldots [10]$$

Evaluation of the line integral $\oint x\, dy$ around the ring yields

$$A + \Delta A = \oint x\,dy \quad [11]$$

Substituting Equations [10] into Equation [11] and retaining only the quadratic terms in (u, v) and their derivatives, we obtain

$$\delta^2 A = 2\int_0^{2\pi} (u\cos\theta - v\sin\theta + u_\theta \sin\theta + v_\theta \cos\theta)(u\cos\theta - v\sin\theta)d\theta$$

Accordingly, for normally directed loading, the second variation of the potential energy of the external load is

$$\delta^2\Omega = 2pL\int_0^{2\pi} (u\cos\theta - v\sin\theta + u_\theta \sin\theta + v_\theta \cos\theta)(u\cos\theta - v\sin\theta)d\theta \quad [12]$$

where u and v have the values corresponding to $r = b$.

(*b*) *Centrally Directed Pressure.* Conceivably, the mechanism of loading may be such that the loads are always directed toward the center of the ring (see Introduction for description of central loading). For this type loading, the second variation of the potential energy of the external load may be obtained from the work performed in moving the load from its original position to its position after virtual displacement (u, v). This work is equal to the change in potential energy of the external load.

When the virtual displacements (u, v) are imposed, the radius b undergoes the change Δb. Hence the change in potential energy of the external load is

$$\Delta\Omega = pLb\int_0^{2\pi} \Delta b\,d\theta \quad [13]$$

But $(b + \Delta b)^2 = (b + u)^2 + v^2$. Solving for Δb and neglecting third-order terms in (u, v), we get

$$\Delta b = u + \frac{v^2}{2b} \quad [14]$$

Substitution of Equation [14] into Equation [13] yields

$$\Delta\Omega = \delta\Omega + \frac{1}{2!}\delta^2\Omega = pLb\int_0^{2\pi} u\,d\theta + \frac{pL}{2}\int_0^{2\pi} v^2 d\theta$$

Therefore

$$\delta^2\Omega = pL\int_0^{2\pi} v^2 d\theta \quad [15]$$

where v has the value corresponding to $r = b$.

Second Variation of Total Potential Energy

The sum of the second variation of the strain energy and the second variation of the potential energy of the external loads is the second variation of the total potential energy. In general, then $\delta^2 V = \delta^2 U + \delta^2\Omega$, where $\delta^2 U$ is given by Equation [9] and $\delta^2\Omega$ is given by Equations [12] and [15] for normally and centrally directed pressures, respectively. The stability criterion, in all cases, is that $\delta^2 V$ be positive definite for all virtual displacements (u, v), excepting rigid-body displacements.

Displacement Functions and Corresponding Expressions For Second Variations

The virtual displacement components (u, v) must have period 2π in θ. Consequently, they may be represented by uniformly convergent Fourier series in θ, in which the coefficients are functions of r, i.e.

$$u = \frac{1}{2}a_0 + \sum_{n=1}^{\infty}(a_n\cos n\theta + c_n \sin n\theta)$$

$$v = \frac{1}{2}d_0 + \sum_{n=1}^{\infty}(b_n \sin n\theta - d_n \cos n\theta) \quad [16]$$

To preclude a translation and a rotation of the ring, respectively, we set

$$a_1 = c_1 = 0$$

$$d_0 = 0 \quad [17]$$

Substitution of Equations [16] into Equations [9], [12], and [15] and integration with respect to θ yields the second variation of the potential energy in the form

$$\delta^2 V = \sum_{n=0}^{\infty}(A_n + B_n) \quad [18]$$

where A_n is an integral (with respect to r) of a quadratic form in (a_n, b_n) and their first derivatives, and B_n is an integral (with respect to r) of a quadratic form in (c_n, d_n) and their first derivatives.

Since A_n and B_n contain only terms of order n in (a_n, b_n, c_n, d_n), a necessary and sufficient condition that $\delta^2 V$ be positive definite is that each term in the series (Equation [18]) be positive definite. The terms of order 0 and 1 are found to be irrelevant since they are positive definite in the significant range of P. For $n > 1$, the terms A_n and B_n are identical, except that the independent functions in A_n are (a_n, b_n), whereas the independent functions in B_n are (c_n, d_n). Consequently, a necessary and sufficient condition that $A_n + B_n$ be positive definite is that A_n alone be positive definite. The fundamental mode of buckling corresponds to A_2. This is a mode in which the ring assumes a doubly symmetrical oval form. In this case we obtain for the second variation of the strain energy (where $a_2 = f(r)$, $b_2 = g(r)$ and all other coefficients are disregarded)

$$\delta^2 U = \frac{\pi EL}{1-\nu^2}\int_1^b \left\{\left[1 - P(3+\nu) + \frac{P(3-\nu)(1+\nu)}{r^2(1-\nu)}\right](f')^2 + \left(\frac{1-\nu}{2} - 2P\right)(g')^2 + \left(\frac{1-\nu}{2} - 2P\right)\left(\frac{2f+g}{r}\right)^2 + \left[1 - P(3+\nu) - \frac{P(3-\nu)(1+\nu)}{r^2(1-\nu)}\right]\left(\frac{f+2g}{r}\right)^2 + 2\nu(1-2P)\left(\frac{f+2g}{r}\right)f' - (1-\nu)(1-2P)\left(\frac{2f+g}{r}\right)g'\right\} r\,dr \quad [19]$$

Note that the coefficients are linear functions of P and rational functions of r. The integrand in Equation [19] is a quadratic form in f, g, f', g' that is positive definite for $P \leqq 0$.

Let $f(b) = \alpha$, $g(b) = \beta$; then the second variation of the potential energy of the external loads (Equations [12] and [15]) is as follows:

For normal loading

$$\delta^2\Omega = \pi pL(\alpha^2 + 4\alpha\beta + \beta^2) \quad [20]$$

For central loading

$$\delta^2\Omega = \pi pL\beta^2 \quad [21]$$

In all cases, the second variation of the potential energy is

$$\delta^2 V = \frac{\pi EL}{1-\nu^2}(N - PD) + \delta^2\Omega$$

where

$$N = \int_1^b \left[(f')^2 + \frac{1}{2}(1-\nu)(g')^2 + \frac{1}{2}(1-\nu)\left(\frac{2f+g}{r}\right)^2 + \left(\frac{f+2g}{r}\right)^2 + 2\nu f'\left(\frac{f+2g}{r}\right) - (1-\nu)g'\left(\frac{2f+g}{r}\right)\right] r\,dr \quad [22]$$

$$D = \int_1^b \left\{\left[3 + \nu - \frac{(3-\nu)(1+\nu)}{r^2(1-\nu)}\right](f')^2 + 2(g')^2 + 2\left(\frac{2f+g}{r}\right)^2 + \left[3 + \nu + \frac{(3-\nu)(1+\nu)}{r^2(1-\nu)}\right]\left(\frac{f+2g}{r}\right)^2 + 4\nu f'\left(\frac{f+2g}{4}\right) - 2(1-\nu)g'\left(\frac{2f+g}{r}\right)\right\} r\,dr \quad [23]$$

From Equation [8], $p = (kEP)/(1-\nu)$ where $k = 1 - (1/b^2)$ (with $a = 1$). Hence, after canceling the irrelevant term $\pi EL/(1-\nu^2)$, we obtain

$$\delta^2 V = N - PD + \begin{cases}(1+\nu)kP(\alpha^2 + 4\alpha\beta + \beta^2) & \text{normal loading} \\ (1+\nu)kP\beta^2 & \text{central loading}\end{cases} \quad [24]$$

The integral D is positive definite since the integrand is a positive definite quadratic function of f, g, f', g'. The integral N cannot take negative values since the minimum value of the integrand for arbitrary values of f, g, f', g' is zero. Hence there exists a constant $P_{cr} > 0$, such that $\delta^2 V$ is positive definite for $P < P_{cr}$, and indefinite for $P > P_{cr}$. For $P = P_{cr}$, $\delta^2 V$ is positive semidefinite; i.e., for certain nonzero functions (f, g), $\delta^2 V$ vanishes, but there are no functions (f, g) for which $\delta^2 V$ is negative. P_{cr} determines the value p_{cr} of the external pressure p (see Equation [8]).

If f and g are linear combinations of specified functions, $\delta^2 V$ reduces to a quadratic form in the coefficients. An upper bound for P_{cr} is the value P^r for which this quadratic form becomes indefinite.

Approximations to (u, v) may be obtained with the aid of the assumption that the ring buckles without shear. By Equation [21] this condition is approximated by

$$v_\theta + \frac{u_\theta - v}{r} = 0 \quad [25]$$

Since $u = f(r)\cos 2\theta$, $v = g(r)\sin 2\theta$, Equation [25] becomes

$$g' = \frac{2f+g}{r} \quad [26]$$

A simple solution of Equation [26] is

$$f = B, \quad g = Ar - 2B \quad [27]$$

where A and B are constants. Adopting these functions for (f, g) we obtain an upper bound for P_{cr}.

Substitution of Equation [27] into Equation [24] yields, for normally directed pressure

$$\delta^2 V = \left\{2kb^2 - P\left[(6+2\nu)kb^2 + \frac{(12-4\nu)(1+\nu)}{1-\nu}m\right]\right\}A^2 - 12h\left\{1 - P\left[(3+\nu) + \frac{(3-\nu)(1+\nu)}{b(1-\nu)}\right]\right\}AB + 9\left\{m - P\left[(3+\nu)m + \frac{(11-5\nu)(1+\nu)}{6(1-\nu)}k\right]\right\}B^2 \quad [28]$$

where $m = \log_e b$.

Equation [28] may be written in the form

$$\delta^2 V = a_{11}A^2 + 2a_{12}AB + a_{22}B^2 \quad [29]$$

where a_{11} is the coefficient of A^2 in Equation [28], and so on. By the theory of quadratic forms, $\delta^2 V$ is positive definite if, and only if

$$a_{11} > 0, \quad \begin{vmatrix} a_{11} & a_{12} \\ a_{12} & a_{22}\end{vmatrix} > 0 \quad [30]$$

The ring buckles if either of the conditions of Equation [30] is violated for any positive value of P. Ordinarily, a_{11} is positive. Hence an upper bound P^r of P_{cr} for normally directed pressure is the smallest root of the determinantal equation

$$\begin{vmatrix} 2kb^2 - P\left[(6+2\nu)kb^2 + \frac{(12-4\nu)(1+\nu)}{1-\nu}m\right] & 2h\left[1 - P\left(3 + \nu + \frac{(3-\nu)(1+\nu)}{(1-\nu)b}\right)\right] \\ 2h\left[1 - P\left(3 + \nu + \frac{(3-\nu)(1+\nu)}{(1-\nu)b}\right)\right] & m - P\left[(3+\nu)m + \frac{(11-5\nu)(1+\nu)}{6(1-\nu)}k\right]\end{vmatrix} = 0 \quad [31]$$

Similarly, for centrally directed pressure, an upper bound P^r is the smallest root of

$$\begin{vmatrix} 2kb^2 - P\left[(6+2\nu)kb^2 + \frac{(12-4\nu)(1+\nu)}{(1-\nu)}m\right] & 2h\left[3 - P\left(8 + 2\nu + \frac{8+6\nu-2\nu^2}{(1-\nu)b}\right)\right] \\ 2h\left[3 - P\left(8 + 2\nu + \frac{8+6\nu-2\nu^2}{(1-\nu)b}\right)\right] & 9\left\{m - P\left[(3+\nu)m + \frac{19+18\nu-\nu^2}{18(1-\nu)}k\right]\right\}\end{vmatrix} = 0 \quad [32]$$

Upper Bound for Limiting Case $h \to 0$

The buckling formula for rings is usually written in the form

$$p_{cr} = K_{cr}EI/r_0^3 \quad [33]$$

where $r_0 = (a+b)/2$, $I = h^3/12$, and $h = b - a$. If $a = 1$, these equations yield

$$K_{cr} = \frac{3(b+1)^4}{2b^3}\frac{P_{cr}}{h^3} \quad [34]$$

Consequently

$$\lim_{h\to 0} P_{cr}/h^3 = \text{const} > 0$$

For $h \to 0$, $b \to 1$, Equation [34] reduces to

$$K_{cr} = 24 \lim_{h\to 0}\frac{P_{cr}}{h^3} \quad [35]$$

We obtain an upper bound for

$$\lim_{h\to 0} P_{cr}/h^3 \text{ (hence for } K_{cr})$$

by expanding Equations [31] and [32] in powers of h and determining

$$\lim_{h\to 0} P/h^3$$

Thus for normally directed pressure ($\nu = 0$), the limiting case $h \to 0$ yields an upper bound K' that coincides with the result of the classical theory $K_{cr} = 3.0$. For $\nu = 0.30$, the limiting case $h \to 0$ yields

$$K' = \frac{3.0}{1 - \nu^2} = 3.2967 \ldots\ldots\ldots\ldots [36]$$

For centrally directed pressure (Equation [32]) and $\nu = 0$, we obtain the upper bound

$$K' = 4.5 \ldots\ldots\ldots\ldots [37]$$

For this case, Stevens (6) obtained $K_{cr} = 2.25$; however, he would have obtained $K_{cr} = 4.5$ except for an error in sign.

Numerical Results for Upper Bound

Equations [31], [32], and [34] provide upper bounds for K_{cr}. In addition to the limiting case $h \to 0$, these equations have been solved numerically for the values of P corresponding to $h = 0.05$ and 0.10. Two values of ν were used; $\nu = 0$ and $\nu = 0.30$. The results of these computations are given in Tables 1 and 2. These data were used to plot the curves for the upper bound K' in Fig. 5.

Lower Bound for Critical Pressure

In Equation [23] let us replace 1/2 in the coefficient of $(f')^2$ by

TABLE 1 VALUES OF P'/h^3 AND K' FOR $h/a = 0$, 0.05, 0.10

Normally Directed Pressure

h/a	ν	P'/h^3	K'
0	0	0.1250[a]	3.00
	0.3	0.0962[a]	3.29
0.05	0	0.1244	2.99
	0.3	0.0956	3.29
0.10	0	0.1237	2.98
	0.3	0.0950	3.28

[a] These numbers are $\lim_{h \to 0} P/h^3$.

TABLE 2 VALUES OF P'/h^3 AND K' FOR $h/a = 0$ 0.05, 0.10

Centrally Directed Pressure, $\nu = 0$

h/a	P'/h^3	K'
0	0.1875[a]	4.50
0.05	0.1740	4.18
0.10	0.1618	3.90

[a] This number is $\lim_{h \to 0} P/h^3$.

$1/b^2$, and let us replace $1/r^2$ in the coefficient of $(f + 2g)^2/r^2$ by 1. Thus the positive definite character of $\delta^2 V$ is weakened since we have reduced a positive term and increased a negative term. By performing an exact analysis with this "weakened" expression for $\delta^2 V$, we obtain a lower bound P' for P_{cr}.

Let the weakened expression for $\delta^2 U$ be J. Let $r = e^x$, $b = e^m$. Then

$$J = \int_0^m \Big\{(1 - sP)\dot{f}^2 + \left(\frac{1-\nu}{2} - 2P\right)\dot{g}^2 + 2\nu(1 - 2P)\dot{f}f + [3 - 2\nu - P(8 + t)]f^2 + 4\nu(1 - 2P)\dot{f}g - 2(1 - \nu) \times (1 - 2P)\dot{g}f + \left[\frac{9-\nu}{2} - P(2 + 4t)\right]g^2 - (1 - \nu) \times (1 - 2P)\dot{g}g + [6 - 2\nu - P(8 + 4t)]fg\Big\} dx \ldots\ldots [38]$$

where dots denote derivatives with respect to x, and

$$s = 3 + \nu - \frac{(3 - \nu)(1 + \nu)}{(1 - \nu)b^2}$$

$$t = 3 + \nu + \frac{(3 - \nu)(1 + \nu)}{1 - \nu}$$

There exists $P' \leqq P_{cr}$ such that $J + \delta^2\Omega$ is positive definite for $P < P'$ and indefinite for $P > P'$. For $P < P'$, $J + \delta^2\Omega > 0$ for all nonzero functions (f, g). For $P > P'$, there exist functions (f, g) such that $J + \delta^2\Omega < 0$. For $P = P'$, there exist nonzero functions (f, g) such that $J + \delta^2\Omega = 0$, but there are no functions (f, g) such that $J + \delta^2\Omega < 0$. In other words, when $P = P'$, $J + \delta^2\Omega$ attains the minimum value zero for certain nonzero functions (f, g). Hence there exist $(f, g) \not\equiv 0$ such that $\delta(J + \delta^2\Omega) = 0$. Accordingly, the vanishing of the first variation of $J + \delta^2\Omega$ is a necessary condition for $P = P'$. Since it leads to a unique result, it is also sufficient, if a solution of the problem exists.

If the functions (f, g) take variation (μ, ϵ), the first variation of $J + \delta^2\Omega$ is

$$\delta(J + \delta^2\Omega) = [(1 - sP)2\dot{f} + 2\nu(1 - 2P)(f + 2g)]\mu\Big|_0^m + [(1 - \nu - 4P)\dot{g} - (1 - \nu)(1 - 2P)(2f + g)]\epsilon\Big|_0^m + \int_0^m \Big\{\Big[-(1 - sP)2\ddot{f} + 2[3 - 2\nu - P(8 + t)]f - 2(1 + \nu)(1 - 2P)\dot{g} + 2[3 - \nu - P(4 + 2t)]g\Big]\mu + \Big[-\left(\frac{1-\nu}{2} - 2P\right)2\ddot{g} + 2\left[\frac{9-\nu}{2} - P(2 + 4t)\right]g + 2(1 + \nu)(1 - 2P)\dot{f} + 2[3 - \nu - P(4 + 2t)]f\Big]\epsilon\Big\} dx + \begin{cases} 2(1 + \nu)k\,P[(\alpha + 2\beta)\mu + (2\alpha + \beta)\epsilon]\,\big|^m \\ \text{for normally directed pressure} \\ 2(1 + \nu)kP\beta\epsilon\,\big|^m \\ \text{for centrally directed pressure} \end{cases} \equiv 0 \ldots [39]$$

The integral term in Equation [39] must be identically zero for all variations μ, ϵ; hence the coefficients of μ, ϵ must be identically zero. This condition leads to the Euler equations

$$\left.\begin{aligned} &(1 - sP)\ddot{f} - [3 - 2\nu - P(8 + t)]f + (1 + \nu)(1 - 2P)\dot{g} - [3 - \nu - P(4 + 2t)]g = 0 \\ &\left(\frac{1-\nu}{2} - 2P\right)\ddot{g} - \left[\frac{9-\nu}{2} - P(2 + 4t)\right]g - (1 + \nu)(1 - 2P)\dot{f} - [3 - \nu - P(4 + 2t)]f = 0 \end{aligned}\right\} \ldots [40]$$

The terms outside the integral must be zero identically also. This condition leads to the natural boundary conditions. Hence the natural boundary conditions depend on the type of loading. For normally directed loading they are

$$\begin{aligned} &(1 - sP)\dot{f}(0) + \nu(1 - 2P)[f(0) + 2g(0)] = 0 \\ &(1 - sP)\dot{f}(m) + [\nu(1 - 2P) + (1 + \nu)kP][f(m) + 2g(m)] = 0 \\ &(1 - \nu - 4P)\dot{g}(0) - (1 - \nu)(1 - 2P)\,[2f(0) + g(0)] = 0 \\ &(1 - \nu - 4P)\dot{g}(m) - [(1 - \nu)(1 - 2P) - 2k(1 + \nu)P][2f(m) + g(m)] = 0 \ldots [41] \end{aligned}$$

For centrally directed loading they are

$$\begin{aligned} &(1 - sP)\dot{f}(0) + \nu(1 - 2P)[f(0) + 2g(0)] = 0 \\ &(1 - sP)\dot{f}(m) + \nu(1 - 2P)[f(m) + 2g(m)] = 0 \\ &(1 - \nu - 4P)\dot{g}(0) - (1 - \nu)(1 - 2P)[2f(0) + g(0)] = 0 \\ &(1 - \nu - 4P)\dot{g}(m) - (1 - \nu)(1 - 2P)[2f(m) + g(m)] + 2(1 + \nu)kPg(m) = 0 \ldots [42] \end{aligned}$$

The general solution of the Euler equations (Equations [40]) is a sum of terms of the following type: $f = Ae^{nx}$, $g = Be^{nx}$. Substitution of these expressions into the Euler equations yields

$$\left.\begin{aligned}&\{(1-sP)n^2-[3-2\nu-P(8+t)]\}A+\{(1+\nu)\\&\quad\times(1-2P)n-[3-\nu-P(4+2t)]\}B=0\\&\{(1+\nu)(1-2P)n+[3-\nu-P(4+2t)]\}A\\&-\left\{\left(\frac{1-\nu}{2}-2P\right)n^2-\left[\frac{9-\nu}{2}-P(2+4t)\right]\right\}B=0\end{aligned}\right\}\quad[43]$$

Existence of a solution other than $f = g = 0$ requires that the determinant of the coefficients of the A and B vanish. Hence

$$(1-sP)\left(\frac{1-\nu}{2}-2P\right)n^4-\left\{5(1-\nu)-\left[\frac{9-\nu}{2}(t+s)+8-16\nu-4\nu^2\right]P+(12-8\nu-4\nu^2)+2(t+s)+4stP^2\right\}n^2+\frac{9}{2}(1-\nu)-\left[18+\frac{9}{2}t(1-\nu)\right]P+18tP^2=0\quad\ldots\ldots[44]$$

Denote the roots of Equation [44] by $n_1(P)$, $n_2(P)$, $-n_1(P)$, and $-n_2(P)$. These roots are real in the significant range $0 < P \leqq P''$. The general solution of the Euler equations now becomes

$$\left.\begin{aligned}f&=A_1e^{n_1x}+A_2e^{n_2x}+A_3e^{-n_1x}+A_4e^{-n_2x}\\g&=B_1e^{n_1x}+B_2e^{n_2x}+B_3e^{-n_1x}+B_4e^{-n_2x}\end{aligned}\right\}\quad\ldots\ldots[45]$$

where the B's are defined in terms of the A's (from Equations [43]) by the equation

$$B_i=2\frac{(1+\nu)(1-2P)n_i+3-\nu-P(4+2t)}{(1-\nu-4P)n_i^2-[9-\nu-2P(2+4t)]}A_i\quad[46]$$
$$i=1,2,3,4$$

The solution of the Euler equations must satisfy the natural boundary conditions (Equations [41] and [42]). Substitution of Equations [45] and [46] into Equations [41] or [42] gives a set of equations of the form

$$\sum_{i=1}^{4}\sum_{j=1}^{4}a_{ij}A_j=0\quad\ldots\ldots[47]$$

For the existence of a solution other than the trivial solution $f = g = 0$, the determinant of the coefficients of the A must be identically zero. Thus, in all cases, the characteristic equation for P is

$$F(P)=|a_{ij}|=0\quad\ldots\ldots[48]$$

This equation for P is highly transcendental, and it must be solved numerically. Fortunately, it happens that Equation [48] has only one real root. On the basis of the foregoing reasoning, this root is a lower bound P'.

Lower Bound For Limiting Case $h \to 0$

For $\nu = 0$, the function F (Equation [48]) has a simple pole at $P = 0$. This is eliminated by multiplying the first column of Equation [48] by P. The graph of the function PF has the general form shown in Fig. 3. We seek the intercept of the curve with the P-axis. As $h \to 0$, the intercepts approach the origin and the asymptote approaches $P = 1/6$. However, P/h^2 approaches a limit greater than zero. This limit may be obtained by expansion of PF in powers of h. The first step is to expand each of the terms a_{ij} in powers of h and to write PF in the form

$$PF=|A_{ij}+PB_{ij}|=0\quad\ldots\ldots[49]$$

Since $P \to 0$ as $h \to 0$, we may expand to first powers in P. Thus

$$PF=|A_{ij}|+P\sum\sum B_{ij}\,\mathrm{cof}\,A_{ij}$$

where cof A_{ij} denotes the cofactor of A_{ij} in the determinant $|A_{ij}|$. Hence the zero of PF is given by

$$P=-\left[\sum_{i=1}^{4}\sum_{j=1}^{4}B_{ij}\overline{A}_{ij}\right]^{-1}\quad\ldots\ldots[50]$$

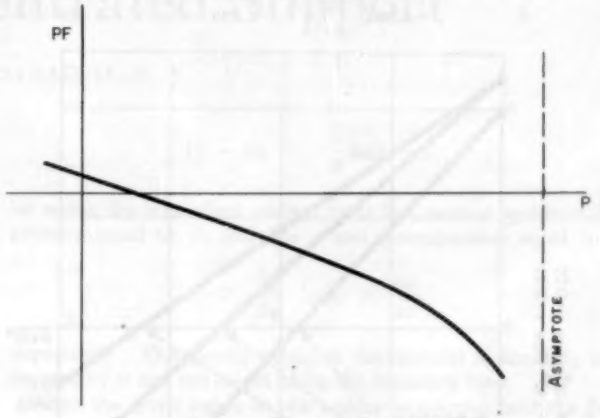

Fig. 3 General Form of Function PF

where $\overline{A}_{ij}$ is the normalized cofactor of A_{ij} in the determinant $|A_{ij}|$.

Further power-series expansion of Equation [50] and division by h^2 yields for the normally directed pressure

$$\lim_{h\to 0}P/h^2=1/8$$

and for the centrally directed pressure

$$\lim_{h\to 0}P/h^2=\frac{3}{16}$$

Hence, by Equation [35], for normally directed pressure

$$\lim_{h\to 0}K'=3.00$$

and for centrally directed pressure

$$\lim_{h\to 0}K'=4.50$$

The evaluation of the limiting case is much more involved for the lower bound than for the upper bound.

Numerical Results for Lower Bound

Calculations for the lower bound K' for $h/a = 0.10$ and for $\nu = 0$ and $\nu = 0.30$ have been performed numerically. Since only the ratio h/a is significant, we set $a = 1$. The values of b, k, and m, corresponding to given values of h, are obtained from $b = 1 + h$, $k = 1 - 1/b^2$, $m = \log_e b$.

Because of the sensitive nature of the characteristic determinant F (Equation [48]), the calculations for the lower bound P' were carried out to ten significant figures (the capacity of the standard ten-place keyboard desk calculator).

As the lower bound P' is restricted to the range $0 < P' < P''$, it is necessary merely to calculate the value of F for several small positive values of P. Then, if a curve of F versus P is plotted, the value $P = P'$ for which $F = 0$ may be determined by graphical interpolation. For $\nu = 0$, F has a simple pole at $P = 0$. Hence for this case, it is necessary to plot the modified characteristic determinant PF versus P to obtain, in a convenient manner, a sufficiently accurate value for P'. For the range of interest, the curve is nearly straight, and only a few points need be plotted (generally three points are adequate).

TABLE 3 VALUES OF F AND PF FOR $P = 0$, 0.001, 0.002
CP = centrally directed pressure
NP = normally directed pressure

	$\nu = 0$		$\nu = 0.3$
$P \times 10^3$	CP($PF \times 10^4$)	NP($PF \times 10^4$)	NP ($F \times 10^2$)
0	4.491	4.491	4.042
1	1.741	0.868	−0.289
2	−1.054	−2.730	−5.080

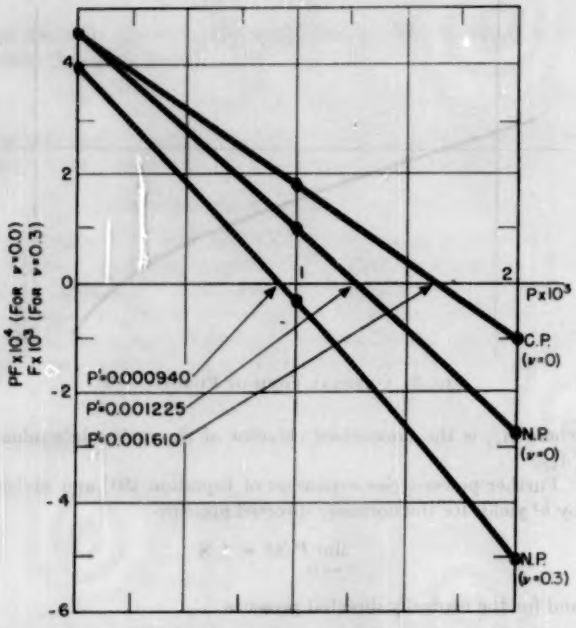

FIG. 4 GRAPHICAL INTERPOLATION FOR LOWER BOUND P'
(Normal pressure = NP; central pressure = CP; $h/a = 0.10$.)

The results of the computations are given in Table 3 and the data are plotted in Fig. 4. The values $P = P'$ for which P (or PF) = 0 were read directly from these graphs. The values of P' are correct seemingly to four significant figures (from a more expanded scale than that of Fig. 4). The values P' were substituted into Equation [34]. Thus lower bounds K' for the buckling pressures were obtained. These lower bounds were used to plot the K'-curves in Fig. 5. The data for K' are summarized in Tables 4 and 5.

TABLE 4 VALUES OF P'/h^2 AND K' FOR $h/a = 0$, 0.10
Normally Directed Pressure

h/a	ν	P'/h^2	K'
0	0	0.1250[a]	3.00
	0.3	0.0961[a]	3.29
0.10	0	0.1225	2.95
	0.3	0.0940	3.24

[a] These numbers are $\lim_{h \to 0} P'/h^2$.

TABLE 5 VALUES OF P'/h^2 and K' for $h/a = 0$, 0.10
Centrally Directed Pressure
$\nu = 0$

h/a	P'/h^2	K'
0	0.1875[a]	4.50
0.10	0.1610	3.88

[a] This number is $\lim_{h \to 0} P'/h^2$.

CONCLUSIONS

The computed upper and lower bounds K'' and K' of K_{cr} are given as functions of h/a and ν by graphs in Fig. 5 for normally and centrally directed pressures applied at the outside of the ring. (K_{cr} is defined by the equation $p_{cr} = K_{cr}EI/r_0^3$, where I is the moment of inertia of the cross section, and r_0 is the radius of the centroidal axis.) These graphs are an extension of the older theories which merely give the value of K_{cr} for $h/a = 0$.

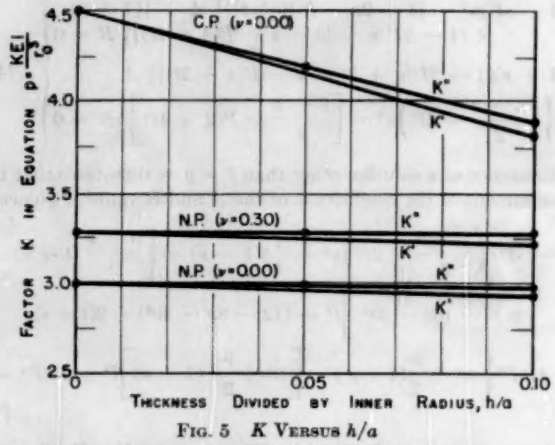

FIG. 5 K VERSUS h/a
(Normally directed pressure = NP; centrally directed pressure = CP; upper bound = K''; lower bound = K'.)

For normally directed pressure and $\nu = 0$, in the limiting case $h \to 0$, the results of this theory coincide with the results derived by Levy in 1884 ($K_{cr} = 3$). For $\nu = 0.3$, the limiting case $h \to 0$ yields $K_{cr} = 3/(1 - \nu^2) = 3.296 \ldots$. For $\nu = 0.3$ and all other values of h that were examined, one obtains K_{cr} approximately by multiplying the value of K_{cr} for $\nu = 0$ by the ratio $1/(1 - \nu^2)$. However, because of the assumptions mentioned in the introduction, the effects of ν have not been determined rigorously.

The results for centrally directed pressure have not been obtained previously and, in the limiting case $h \to 0$ ($\nu = 0$), $K_{cr} = 4.5$. This result, as well as the curves, Fig. 5, are believed to be new.

ACKNOWLEDGMENT

This paper is a condensation of a thesis presented in partial fulfillment of the requirements for the degree of Doctor of Philosophy in Theoretical and Applied Mechanics in The Graduate College of the University of Illinois, 1953.

The author is indebted to his adviser, Dr. H. L. Langhaar, not only for suggesting the problem, but especially for his extensive help and for his acute interest in and his benevolent attitude toward the author's efforts.

BIBLIOGRAPHY

1 "Zur Theorie der Stabilität des Elastischen Gleichgewichts," by E. Treffts, *Zeitschrift für Angewandte Mathematik und Mechanik*, vol. 13, 1933, p. 160.

2 "Mémoire sur un nouveau cas intégrable du problème de l'élastique et l'une de ses applications," by Maurice Levy, *Journal Math. et Applications*, (Liouville), Series 3, vol. 10, 1884, pp. 5–42.

3 "On the Theory of Elastic Vibrations in Plates and Shells," by P. S. Epstein, *Journal of Mathematics and Physics*, vol. 21, 1942, p. 198.

4 "The New Approach to Shell Theory: Circular Cylinders," by E. H. Kennard, Trans. ASME, vol. 75, 1953, p. 33.

5 "On Torsional-Flexural Buckling of Columns," by H. L. Langhaar, *The Journal of the Franklin Institute*, vol. 255, February, 1953, p. 101.

6 "The Stability of a Compressed Elastic Ring. . .," by G. W. H. Stevens, *Quarterly Journal of Mechanics and Applied Mathematics*, vol. 5, 1952, p. 221.

7 "Mécanique Analytique," by J. L. Lagrange, Paris, France, 1788.

8 "Sur L'Equilibre d'une Masse Fluide," by H. Poincaré, *Acta Mathematica*, vol. 7, 1885, p. 259.

9 "The Mathematical Theory of Elasticity," by A. E. H. Love, Dover Publications, New York, N. Y., 1944, p. 60.

10 "Theory of Elasticity," by S. Timoshenko and J. N. Goodier, McGraw-Hill Book Company, Inc., New York, N. Y., second edition, 1951, p. 58.

Gravitational Stresses in a Circular Ring Resting on Concentrated Support

By YI-YUAN YU,[1] SYRACUSE, N. Y.

Muschelišvili's complex variable method in two-dimensional elasticity has been extended by the present author to solve a few gravitational stress problems. A further problem of a heavy circular ring resting on a concentrated support is solved by the same method in the present paper. The two analytic functions which constitute the solution of the problem are determined. A numerical example is given for a ring the radii of which are in the ratio of 1 to 2.

Introduction

MUSCHELIŠVILI'S complex variable method in two-dimensional elasticity (1, 2)[2] has been extended by the present author (3, 4) to solve a few gravitational stress problems. A further problem of a heavy circular ring resting on a concentrated support will be solved by the same method in the present paper. Since the problem will be considered on the basis of the linear theory of elasticity, it actually represents the problem of a ring resting on a horizontal plane.[3] The extension of the problem into that of a heavy ring supported by any number of concentrated forces also can be carried out easily.

Method

For details of the method the reader may refer to the two previous papers (3, 4). Only the final results will be repeated here.

The boundary equation for the first fundamental boundary-value problem in two-dimensional elasticity involving body forces has the form

$$\varphi_1(z) + z\bar{\varphi}_1'(\bar{z}) + \bar{\psi}_1(\bar{z}) = i\int(\tau_x + i\tau_y)ds - \int V_1(z)dz \quad [1]$$

which holds true along the boundary C of a body in the complex plane of $z = x + iy$. In the equation $\varphi_1(z)$ and $\psi_1(z)$ are the two analytic functions for the particular state of stress, τ_x and τ_y are the x and y-components of the surface force on the boundary, and V_1 is the body-force potential. For body forces due to gravity acting in the negative y-direction we have

$$V_1 = wy = -\frac{1}{2}iw(z - \bar{z})$$

for which the equivalent surface force is a normal hydrostatic pressure equal to V_1 and has x and y-components equal to

$$-V_1\frac{dy}{ds} \quad \text{and} \quad V_1\frac{dx}{ds}$$

respectively. The specific weight of the material of the body is denoted by w and the length along the boundary by s.

When the given region in the z-plane is mapped into the ζ-plane and the boundary C onto γ by means of the mapping function

$$z = \omega(\zeta)$$

the boundary Equation [1] is transformed into

$$\varphi(\zeta) + \frac{\omega(\zeta)}{\bar{\omega}'(\bar{\zeta})}\bar{\varphi}'(\bar{\zeta}) + \bar{\psi}(\bar{\zeta}) = f_1 + if_2 \text{ (on } \gamma) \quad [2]$$

in which $\varphi(\zeta)$ and $\psi(\zeta)$ are the transformed forms of $\varphi_1(z)$ and $\psi_1(z)$, and $f_1 + if_2$ represents the transformed expression of the right-hand side of Equation [1].

Normal stresses $\tau_{\rho\rho}$, $\tau_{\theta\theta}$ and shearing stress $\tau_{\rho\theta}$ with reference to the polar co-ordinates (ρ, θ) may be computed by means of the following expressions

$$\left.\begin{aligned}\tau_{\rho\rho} + \tau_{\theta\theta} &= 2[\Phi(\zeta) + \bar{\Phi}(\bar{\zeta})] + 2V(\zeta)\\ \tau_{\theta\theta} - \tau_{\rho\rho} + 2i\tau_{\rho\theta} &= \frac{2\zeta^2}{\rho^2\bar{\omega}'(\bar{\zeta})}[\bar{\omega}(\bar{\zeta})\Phi'(\zeta) + \omega'(\zeta)\Psi(\zeta)]\end{aligned}\right\} \quad [3]$$

in which

$$\Phi(\zeta) = \frac{\varphi'(\zeta)}{\omega'(\zeta)}, \quad \Psi(\zeta) = \frac{\psi'(\zeta)}{\omega'(\zeta)}$$

and $V(\zeta)$ is the transformed form of $V_1(z)$.

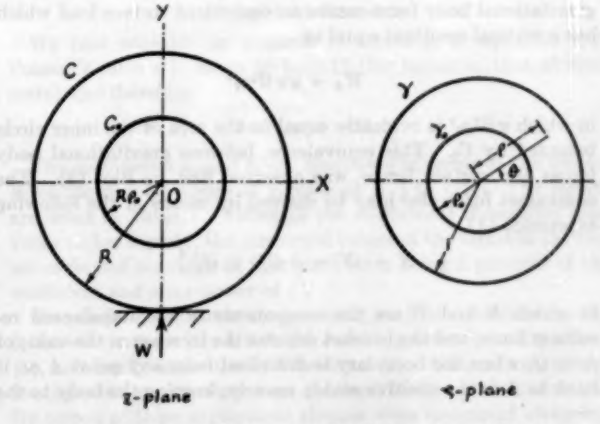

Fig. 1 Ring in z-Plane and Its Mapping in ζ-Plane

---

[1] Associate Professor of Mechanical Engineering, Syracuse University; formerly Assistant Professor, Department of Applied Mechanics, Washington University, St. Louis, Mo. Assoc. Mem. ASME.

[2] Numbers in parentheses refer to Bibliography at end of paper.

[3] A Summary of the present paper will appear in the Proceedings of the Eighth International Congress on Theoretical and Applied Mechanics under the title, "Gravitational Stresses in a Circular Ring Resting on a Horizontal Plane."

Contributed by the Applied Mechanics Division and presented at the Annual Meeting, New York, N. Y., November 28–December 3, 1954, of The American Society of Mechanical Engineers.

Discussion of this paper should be addressed to the Secretary, ASME, 29 West 39th Street, New York, N. Y., and will be accepted until April 11, 1955, for publication at a later date. Discussion received after the closing date will be returned.

Note: Statements and opinions advanced in papers are to be understood as individual expressions of their authors and not those of the Society. Manuscript received by ASME Applied Mechanics Division, November 12, 1952. Paper No. 54—A-7.

Heavy Ring Problem

Let R and $R\rho_0$ be the respective radii of the outer and inner boundaries C and C_0 of the concentric circular ring section in the z-plane, ρ_0 being a coefficient smaller than unity. Co-ordinate axes are chosen as shown in Fig. 1. The only surface load on the ring is a concentrated force equal to the weight W of the ring acting in the positive y-direction at the point $z = -iR$. When the ring is mapped into the ζ-plane by means of the function

$$z = \omega(\zeta) = R\zeta \quad \ldots\ldots [4]$$

the boundaries C and C_0 are mapped respectively onto the unit circle γ and another concentric circle γ_0 having a radius equal to ρ_0. The point of application of the concentrated force W is mapped into the point $\zeta = -i$.

Since surface forces τ_x and τ_y on both boundaries are zero everywhere except at the supporting point, the function $f_1 + if_2$ becomes

$$f_1 + if_2 = -\int V_1(z)dz = \frac{iw}{2}\int (z - \bar{z})dz = \frac{1}{2}\, iwR^2 \int (\zeta - \bar{\zeta})d\zeta$$

$$= \left\{ \begin{array}{ll} \dfrac{1}{2}\, iwR^2\rho_0^2\left(\dfrac{\sigma^2}{2} - \log \sigma\right) & (\text{on } \gamma_0) \\ \dfrac{1}{2}\, iwR^2\left(\dfrac{\sigma^2}{2} - \log \sigma\right) & (\text{on } \gamma) \end{array} \right\} \quad \ldots\ldots [5]$$

in which we have written $\zeta = \rho e^{i\theta}$ and $\sigma = e^{i\theta}$.

The analytic functions $\varphi(\zeta)$ and $\psi(\zeta)$ for the present problem have the following forms

$$\left. \begin{aligned} \varphi(\zeta) &= -\frac{iW}{2\pi}\log(\zeta + i) - \frac{iW_0}{2\pi(\kappa+1)}\log\zeta + \varphi^0(\zeta) \\ \psi(\zeta) &= -\frac{iW}{2\pi}\log(\zeta + i) + \frac{iW}{2\pi}\,\frac{i}{\zeta + 1} - \kappa\frac{iW_0}{2\pi(\kappa+1)}\log\zeta + \psi^0(\zeta) \end{aligned} \right\} \quad \ldots\ldots [6]$$

each of which is composed of three parts. The first part, consisting of the term including W, accounts for the singularity due to the concentrated vertical force at $\zeta = -i$. When the ring is supported at more than one point, similar terms should be included for each of the additional concentrated forces (3).

In the case of a multiply connected region, terms having logarithmic singularities also will be introduced into the analytic functions as a result of a nonvanishing resultant surface force on one of the inner boundaries.[4] Although there is no actual surface load on the inner boundary C_0 of the ring in the present case, the gravitational body force causes an equivalent surface load which has a vertical resultant equal to

$$W_0 = w\pi R^2\rho_0^2$$

in which $\pi R^2\rho_0^2$ is evidently equal to the area of the inner circle bounded by C_0. This equivalence, between gravitational body forces and surface forces, was observed first by Biot (5). The equivalent force also may be derived by means of the following expression (1)

$$X + iY = -i[f_1 + if_2]_A^A$$

in which X and Y are the components of the unbalanced resultant force, and the bracket denotes the increase in the value of $f_1 + if_2$ when the boundary is described from any point A on it back to A in the positive sense; namely, keeping the body to the left. Now the body force has contributed to $f_1 + if_2$ on C_0 an amount equal to, according to Equation [5]

$$\frac{1}{2}\, iwR^2\rho_0^2\left(\frac{\sigma^2}{2} - \log\sigma\right)$$

therefore

$$X + iY = -i\left[\frac{1}{2}\, iwR^2\rho_0^2\left(\frac{\sigma^2}{2} - \log\sigma\right)\right]_A^A = w\pi R^2\rho_0^2 = W_0$$

Terms involving this quantity are thus introduced into the functions as given in Equations [6]. The constant κ in these terms is a function of Poisson's ratio ν and, in the case of plane strain

$$\kappa = 3 - 4\nu$$

The third and last part of each function consists of the last term in each expression and represents the part of the function which is analytic in the entire region. Because the region is ring-shaped, this part is in the form of Laurent's series which contains both positive and negative powers of ζ; thus, we may write

$$\varphi^0(\zeta) = \sum_{-\infty}^{\infty} a_k\zeta^k, \quad \psi^0(\zeta) = \sum_{-\infty}^{\infty} b_k\zeta^k \quad \ldots\ldots [7]$$

The constant coefficients a_k and b_k, which are in general complex, remain to be determined.

Determination of Coefficients

The coefficients a_k and b_k will be determined by means of the boundary Equation [2]. With the mapping function $\omega(\zeta)$ given in Equation [4], and the two forms of the function $f_1 + if_2$ in Equation [5], we may write the boundary equations for the boundaries γ_0 and γ as follows

$$\left. \begin{aligned} &\varphi(\rho_0\sigma) + \rho_0\sigma\bar{\varphi}'(\rho_0\bar{\sigma}) + \bar{\psi}(\rho_0\bar{\sigma}) = \frac{1}{2}\, iwR^2\rho_0^2\left(\frac{\sigma^2}{2} - \log\sigma\right) \quad (\text{on } \gamma_0) \\ &\varphi(\sigma) + \sigma\bar{\varphi}'(\bar{\sigma}) + \bar{\psi}(\bar{\sigma}) = \frac{1}{2}\, iwR^2\left(\frac{\sigma^2}{2} - \log\sigma\right) \quad (\text{on } \gamma) \end{aligned} \right\} \quad \ldots [8]$$

Substituting Equations [6] and [7] into [8] and reducing yields

$$\sum_{-\infty}^{\infty} a_k\rho_0^k\sigma^k + \sum_{-\infty}^{\infty} k\bar{a}_k\rho_0^k\sigma^{-k+2} + \sum_{-\infty}^{\infty}\bar{b}_k\rho_0^k\sigma^{-k}$$

$$= \frac{iwR^2\rho_0^2(\kappa-1)}{4(\kappa+1)}\sigma^2 - \frac{iW}{2\pi}\left[\sum_1^{\infty}\frac{1}{k}(i\rho_0)^k\sigma^k + \sum_1^{\infty}\frac{1}{k}(-i\rho_0)^k\sigma^{-k} + \sum_0^{\infty}(-i\rho_0)^k\sigma^{-k} + \sum_0^{\infty}(-i\rho_0)^{k+1}\sigma^{-k+1}\right]$$

[4] Reference (2), p. 255.

$$\sum_{-\infty}^{\infty} a_k\sigma^k + \sum_{-\infty}^{\infty} k\bar{a}_k\sigma^{-k+2} + \sum_{-\infty}^{\infty} \bar{b}_k\sigma^{-k} = \left[\frac{iW}{4\pi} + \frac{iW\rho_0(\kappa-1)}{4\pi(\kappa+1)}\right]\sigma^2 + \frac{W}{2\pi}\sigma$$

We equate the coefficients of the different powers of σ on both sides of the first equation

$$(a_1+\bar{a}_1)\rho_0^2 + \bar{b}_{-1} = \frac{W\rho_0^2}{\pi} \quad (\text{for } \sigma)$$

$$a_2\rho_0^4 + \bar{b}_{-2} = \left[\frac{iwR^2(\kappa-1)}{4(\kappa+1)} + \frac{iW}{4\pi}\right]\rho_0^4 \quad (\text{for } \sigma^2)$$

$$a_k\rho_0^{2k} - (k-2)\bar{a}_{-(k-2)}\rho_0^2 + \bar{b}_{-k} = -\frac{iW}{2\pi}\frac{1}{k}(i)^k\rho_0^{2k} \quad (\text{for } \sigma^k,\ k \leqslant 3)$$

$$a_{-k}\rho_0^{-2k} + (k+2)\bar{a}_{k+2}\rho_0^2 + \bar{b}_k = \frac{iW}{2\pi}(-i)^k\left(\frac{1}{k}+1\right) + \frac{iW}{2\pi}(-i)^{k+2}\rho_0^2 \quad (\text{for } \sigma^{-k},\ k \leqslant 1)$$

Similarly, from the second equation

$$a_1 + \bar{a}_1 + \bar{b}_{-1} = \frac{W}{2\pi} \quad (\text{for } \sigma) \qquad [9]$$

$$a_2 + \bar{b}_{-2} = \frac{iwR^2\rho_0^2}{4}\frac{\kappa-1}{\kappa+1} + \frac{iW}{4\pi} \quad (\text{for } \sigma^2) \qquad [10]$$

$$a_k - (k-2)\bar{a}_{-(k-2)} + \bar{b}_{-k} = 0 \quad (\text{for } \sigma^k,\ k \leqslant 3) \qquad [11]$$

$$a_{-k} + (k+2)\bar{a}_{k+2} + \bar{b}_k = 0 \quad (\text{for } \sigma^{-k},\ k \leqslant 1) \qquad [12]$$

Coefficients b_k may be eliminated from these two sets of equations; thus

$$(a_1+\bar{a}_1)(1-\rho_0^2) = \frac{W}{2\pi}(1-2\rho_0^2) \qquad [13]$$

$$a_2(1-\rho_0^4) = \frac{iwR^2(\kappa-1)}{4(\kappa+1)}\rho_0^2(1-\rho_0^2) + \frac{iW}{4\pi}(1-\rho_0^4) \qquad [14]$$

$$a_k(1-\rho_0^{2k}) - (k-2)\bar{a}_{-(k+2)}(1-\rho_0^2) = \frac{W}{2\pi}(i)^{k+1}\frac{\rho_0^{2k}}{k} \quad (k \leqslant 3) \qquad [15]$$

$$a_{-k}(1-\rho_0^{-2k}) + (k+2)\bar{a}_{k+2}(1-\rho_0^2) = \frac{W}{2\pi}(-i)^{k+1}\left(\frac{1}{k}+1-\rho_0^2\right) \quad (k \leqslant 1)$$

Replacing k by $(k-2)$ in the last equation and formulating the conjugate of the result, we have

$$\bar{a}_{-(k-2)}(1-\rho_0^{-2k+4}) + ka_k(1-\rho_0^2) = \frac{W}{2\pi}(i)^{k+1}\left(\rho_0^2 - \frac{k-1}{k-2}\right) \quad (k \leqslant 3) \qquad [16]$$

With Equations [13] to [16] we are now in a position to determine the coefficients a_k.

Since stresses are prescribed at the boundary in the present problem, $\varphi^0(\zeta)$ is determined to within an expression (1)

$$\alpha_0 + i\beta_0 + i\beta_1\zeta$$

α_0, β_0, and β_1 being real constants; thus we may choose a_0 and the imaginary part of a_1 to be zero. The real part of a_1 is determined by Equation [13], from which we obtain

$$a_1 = \frac{W}{2\pi}\frac{1-2\rho_0^2}{2(1-\rho_0^2)} \qquad [17]$$

Equation [14] gives a_2 directly

$$a_2 = \frac{W}{2\pi}\frac{i}{2}\left(1 + \frac{\kappa-1}{\kappa+1}\frac{\rho_0^2}{1-\rho_0^4}\right) \qquad [18]$$

The rest of the coefficients $a_3, a_4, \ldots, a_{-1}, a_{-2}, \ldots$ may be obtained in pairs by solving Equations [15] and [16] simultaneously; the results are

$$\left.\begin{aligned} a_k &= \frac{\overline{W}}{2\pi}\frac{i^{k+1}}{k}\frac{[\rho_0^{2k} - (k-1)^2\rho_0^4 + k(2k-3)\rho_0^2 - k(k-1)]}{[(1-\rho_0^{2k})(1-\rho_0^{-2k+4}) + k(k-2)(1-\rho_0^2)^2]} \\ a_{-(k-2)} &= \frac{W}{2\pi}\frac{i^{-(k-2)}}{k-2}\frac{[\rho_0^{2k} + (k-2)\rho_0^2 - (k-1)]}{[(1-\rho_0^{2k})(1-\rho_0^{-2k+4}) + k(k-2)(1-\rho_0^2)^2]} \end{aligned}\right\} (k \leqslant 3) \qquad [19]$$

Once a_k is known, b_k may be computed easily by means of Equations [9] to [12]. The first two of these equations yields

$$\left.\begin{aligned} b_{-1} &= \frac{W}{2\pi}\frac{\rho_0^2}{1-\rho_0^2} \\ b_{-2} &= -\frac{iW}{2\pi}\frac{(\kappa-1)}{(\kappa+1)}\frac{\rho_0^4}{2(1-\rho_0^4)} \end{aligned}\right\} \qquad [20]$$

Equations [11] and [12] give the rest of the coefficients b_k in terms of a_k as follows

$$\left.\begin{aligned} b_{-k} &= -\bar{a}_k + (k-2)a_{-(k-2)} \quad (k \leqslant 3) \\ b_k &= -\bar{a}_{-k} - (k+2)a_{k+2} \quad (k \leqslant 1) \end{aligned}\right\} \qquad [21]$$

Coefficient b_0 may be taken to be zero, for $\psi^0(\zeta)$ is determined to within an arbitrary constant (1).

Hence we have determined all the coefficients in the two series in Equations [7]. Substituting the results into Equations [6] yields the two analytic functions $\varphi(\zeta)$ and $\psi(\zeta)$ which determine completely the state of stress for the present problem.

Numerical Example

We now consider an example in which ρ_0 is equal to 1/2. Poisson's ratio ν is taken to be 0.15 (for instance, that of concrete), and therefore

$$\kappa = 3 - 4\nu = 2.40$$

The coefficients a_k and b_k are computed in terms of the weight W of the ring by means of Equations [17] to [21]. The results are listed in Table 1. Although the coefficients themselves converge rather rapidly, the numerical values of the terms in the two series do not converge as fast (each term being a product of the coefficient and some power of ζ).

To compute the stress components, we first substitute a_k and b_k into Equations [7], insert the resulting series into Equations [6], and finally make use of Equations [3]. General expressions for the stress components were obtained for the present example. By means of these expressions stresses were computed along five

TABLE 1 VALUES OF COEFFICIENTS a_k AND b_k

k	$\frac{2\pi}{W} a_k$	$\frac{2\pi}{W} a_{-k}$	$\frac{2\pi}{W} b_k$	$\frac{2\pi}{W} b_{-k}$
1	0.33333	1.3704	−4.51860	0.3333
2	0.55469i	−0.11954i	−0.84346i	−0.01373i
3	1.04940	−0.019868	0.24452	0.3210
4	0.18098i	0.004141i	0.07894i	−0.0581i
5	−0.04493	$0.0^{2}947$	−0.02587	−0.01467
6	$-0.01247i$	$-0.0^{2}225i$	$-0.00835i$	$0.004098i$
7	0.00356	$-0.0^{4}546$	0.00264	0.001175
8	$0.001016i$	$0.0^{4}1338i$	$0.0^{4}816i$	$-0.0^{4}336i$
9	$-0.0^{3}287$	$0.0^{5}328$	$-0.0^{3}247$	$-0.0^{4}952$
10	$-0.0^{4}803i$	$-0.0^{5}811i$	$-0.0^{4}739i$	$0.0^{4}267i$
11	$0.0^{4}222$	$-0.0^{5}200$	$0.0^{4}217$	$0.0^{4}732$
12	$0.0^{4}609i$	$0.0^{4}497i$	$0.0^{4}631i$	$-0.0^{4}202i$
13	$-0.0^{5}1656$	$0.0^{5}1232$	.....	$-0.0^{5}550$
14	$-0.0^{4}448i$	$-0.0^{5}306i$		$0.0^{5}149i$
15	$0.0^{5}1202$	$-0.0^{5}760$		$0.0^{5}400$
16	$0.0^{5}322i$	$0.0^{5}1888i$		$-0.0^{5}106i$
17	$-0.0^{5}855$	$0.0^{10}471$		$-0.0^{5}285$
18	$-0.0^{5}227i$	$-0.0^{10}117i$		$0.0^{5}755i$
19	.....	.....		.....

sections across the ring, namely, at $\theta = 0°$, $\pm 45°$, and $\pm 90°$, respectively. Results are tabulated in Table 2 and plotted as shown in Fig. 2.

TABLE 2 VALUES OF STRESSES

Section	ρ	$\frac{\pi R}{W} \tau_{\theta\theta}$	$\frac{\pi R}{W} \tau_{\rho\rho}$	$\frac{\pi R}{W} \tau_{\rho\theta}$
$\theta = +90°$	0.5	+ 6.1184	0	0
	0.6	+ 2.7728	+ 0.6140	0
	0.7	+ 0.8343	+ 0.5658	0
	0.8	− 0.5762	+ 0.3720	0
	0.9	− 1.7802	+ 0.1725	0
	1.0	− 2.9110	0	0
$\theta = +45°$	0.5	+ 0.4936	0	0
	0.6	+ 0.0283	+ 0.0475	−1.2860
	0.7	− 0.1664	+ 0.0062	−1.3972
	0.8	− 0.3038	+ 0.0172	−1.0776
	0.9	− 0.4312	− 0.0256	−0.5795
	1.0	− 0.5872	0	0
$\theta = 0°$	0.5	− 8.8960	0	0
	0.6	− 4.5840	− 0.8664	−0.7195
	0.7	− 2.0033	− 0.8540	−0.7744
	0.8	− 0.1128	− 0.6019	−0.6002
	0.9	+ 1.4739	− 0.2989	−0.3274
	1.0	+ 2.9288	0	0
$\theta = -45°$	0.5	− 6.3258	0	0
	0.6	− 3.5150	− 0.4047	+1.9038
	0.7	− 2.2816	− 0.2025	+2.0124
	0.8	− 1.3540	− 0.0362	+1.4826
	0.9	− 0.5013	+ 0.0997	+0.7611
	1.0	+ 0.5716	0	0
$\theta = -90°$	0.5	+14.1922	0	0
	0.6	+ 5.2182	− 0.5882	0
	0.7	+ 1.6512	− 3.5921	0
	0.8	− 0.5909	− 8.2162	0
	0.9	− 2.5539	−19.2380	0
	1.0	− ∞	− ∞	0

BIBLIOGRAPHY

1 "Praktische Lösung der fundamentalen Randwertaufgaben der Elastizitätstheorie in der Ebene für einige Berandungsformen," by N. Muschelišvili, *Zeitschrift für angewandte Mathematik und Mechanik*, vol. 13, 1933, pp. 264–282.

2 "Mathematical Theory of Elasticity (mimeographed lecture notes)," by I. S. Sokolnikoff, Brown University, Providence, R. I., 1941.

3 "Heavy Disk Supported by Concentrated Forces," by Yi-Yuan Yu, *Quarterly of Applied Mathematics*, vol. 10, 1952, pp. 280–284.

4 "Gravitational Stresses on Deep Tunnels," by Yi-Yuan Yu, *Journal of Applied Mechanics*, Trans. ASME, vol. 74, 1952, pp. 537–542.

5 "Distributed Gravity and Temperature Loading in Two-Dimensional Elasticity Replaced by Boundary Pressure and Dislocations," by M. A. Biot, *Journal of Applied Mechanics*, Trans. ASME, vol. 57, 1935, pp. A-41-45.

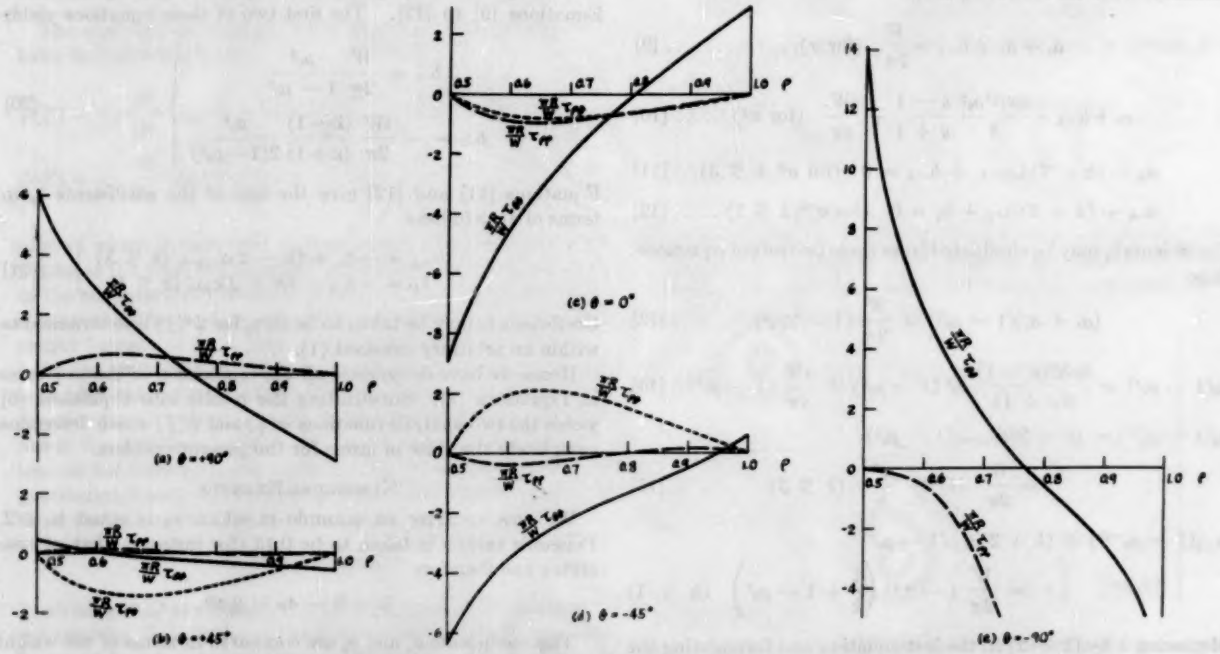

FIG. 2 (*Left, center, and right*) STRESSES ALONG SECTIONS ACROSS RING

Harmonic Oscillations of Nonlinear Two-Degree-of-Freedom Systems[1]

By T. C. HUANG,[2] CHICAGO, ILL.

In this paper an investigation is made of equations governing the oscillations of a nonlinear system in two degrees of freedom. Analyses of harmonic oscillations are illustrated for the cases of (1) the forced oscillations with nonlinear restoring force, damping neglected; (2) the free oscillations with nonlinear restoring force, damping neglected; and (3) the forced oscillations with nonlinear restoring force, small viscous damping considered. Amplitudes of oscillations and frequency equations are derived based on the mathematically justified perturbation method. Response curves are then plotted.

Introduction

THE purpose of this paper is to present a simple method of procedure to treat some simultaneous differential equations of second order which govern the oscillations of a nonlinear system in two degrees of freedom. For example, such a system can be used to represent a rubber-ring torsional vibration damper. The author treats three forms of such simultaneous equations which correspond to those different cases to be presented. In each case there will be an arbitrary small nonlinear term.

The procedure used in this investigation is referred to as "perturbation method." For a single-degree-of-freedom system, the procedure of this method has been well described.[3] Mathematical justification of this method or of the existence of the perturbation series, in general, is well established for systems with one degree[4] and two degrees[5] of freedom. It follows that the periodic solutions of these equations with frequency equal to that of the driving force are known to exist.

In the investigation of problems of nonlinear oscillations, we are generally interested in the periodic solutions. The principle of superposition which is applicable to linear system cannot be applied. Besides, subharmonics[6] no longer can be neglected.

Development of Solutions

Periodic solutions are known to exist for differential equations governing oscillations of a system in two degrees of freedom having small nonlinear terms. In the development of such periodic solutions for some special cases of these equations, the perturbation method will be used. Solutions of the problem are then successive approximations in nature.

The direct use of the perturbation series in obtaining the solutions has the difficulty of secular terms, i.e., terms in which the time t appears explicitly in the expression. Obviously, the existence of these terms, which tend to grow indefinitely as $t \to \infty$, destroys the periodicity one is seeking. This difficulty can be avoided by a change from the old period to the new, or corrected ones. Such modification of the period will be illustrated in the next section.

In the cases of forced oscillations, it is convenient to assume that the amplitude of the applied force is also small in the order of the small nonlinear term. This means that our development is one in the neighborhood of a linear free oscillation.

Further details of development will be explained briefly in the first case of the following three examples in the analyses of harmonic oscillations. Any difference arising due to small viscous damping will be mentioned in the third case.

Examples in Analysis of Harmonic Oscillations

Case 1 Forced Oscillations With Nonlinear Restoring Force, Damping Neglected. The system in this case is shown in Fig. 1.

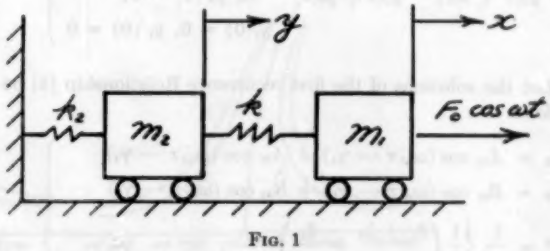

Fig. 1

It is assumed that the spring constant k is nonlinear such that the two equations of equilibrium take the form

$$\left.\begin{aligned} m_1\ddot{x} + k_1(x-y) + \epsilon_0(x-y)^3 &= F_0 \cos \omega t \\ m_2\ddot{y} - k_1(x-y) - \epsilon_0(x-y)^3 + k_2 y &= 0 \end{aligned}\right\} \quad \ldots [1]$$

where $k = k(k_1, \epsilon_0)$, $|\epsilon_0| \ll k_1 > 0$, and $F_0 = \epsilon_0 F$

Before applying the perturbation method, let a new independent variable τ replace t through the relation $\tau = \omega t$. Equations [1] become

$$\left.\begin{aligned} \omega^2 m_1 x'' + k_1(x-y) + \epsilon_0(x-y)^3 &= F_0 \cos \tau \\ \omega^2 m_2 y'' - k_1(x-y) - \epsilon_0(x-y)^3 + k_2 y &= 0 \end{aligned}\right\} \quad \ldots [2]$$

The dot or prime on a quantity means differentiation with respect to t or τ, respectively.

---

[1] Based on part of a thesis submitted to the University of Illinois in June, 1952, in partial fulfillment of the requirement for the degree of Doctor of Philosophy.

[2] Formerly University Fellow, University of Illinois, Urbana, Ill.; now with International Harvester Company, Manufacturing Research Department, Chicago, Ill.

[3] "Vibration Problems in Engineering," by S. Timoshenko, D. Van Nostrand Company, Inc., New York, N. Y., 1937, sections 25 and 26.

[4] "Nonlinear Vibrations," by J. J. Stoker, Interscience Publishers, Inc., New York, N. Y., 1950, Appendix 1.

[5] "Nonlinear Mechanics," by N. Minorsky, Edwards Brothers, Inc., Ann Arbor, Mich., 1947, section 47.

[6] "Subharmonic Oscillations in Nonlinear Systems of Two Degrees of Freedom," by T. C. Huang, Proceedings of the Second U. S. National Congress of Applied Mechanics, 1954

Contributed by the Applied Mechanics Division and presented at the Annual Meeting, New York, N. Y., November 28–December 3, 1954, of The American Society of Mechanical Engineers.

Discussion of this paper should be addressed to the Secretary, ASME, 29 West 39th Street, New York, N. Y., and will be accepted until April 11, 1955, for publication at a later date. Discussion received after the closing date will be returned.

Note: Statements and opinions advanced in papers are to be understood as individual expressions of their authors and not those of the Society. Manuscript received by ASME Applied Mechanics Division, July 31, 1953. Paper No. 54—A-19.

Let the perturbation series be as follows

$$\left.\begin{aligned} x &= x_0 + \epsilon x_1 + \epsilon^2 x_2 + \cdots\cdots\cdots \\ y &= y_0 + \epsilon y_1 + \epsilon^2 y_2 + \cdots\cdots\cdots \\ \omega &= \omega_0 + \epsilon\omega_1 + \epsilon^2\omega_2 + \cdots\cdots\cdots \end{aligned}\right\} \quad \cdots [3]$$

or $$\omega^2 = \omega_0^2 + \epsilon 2\omega_0\omega_1 + \epsilon^2(\omega_1^2 + 2\omega_0\omega_2) + \cdots$$

where $\epsilon = \epsilon_0/m_1$ and $|\epsilon| \ll 1$. Substituting these series into Equations [2] and equating terms containing the same power of ϵ from the resulting equations, the following sets of recurrence relationships are obtained

$$\left.\begin{aligned} \omega_0^2 x_0'' + \frac{k_1}{m_1}(x_0 - y_0) &= 0 \\ \omega_0^2 y_0'' - \frac{k_1}{m_2}(x_0 - y_0) + \frac{k_2}{m_2} y_0 &= 0 \end{aligned}\right\} \quad \cdots\cdots [4]$$

$$\left.\begin{aligned} \omega_0^2 x_1'' + \frac{k_1}{m_1}(x_1 - y_1) &= -2\omega_0\omega_1 x_0'' - (x_0 - y_0)^3 + F\cos\tau \\ \omega_0^2 y_1'' - \frac{k_1}{m_2}(x_1 - y_1) + \frac{k_2}{m_2} y_1 &= -2\omega_0\omega_1 y_0'' + \frac{m_1}{m_2}(x_0 - y_0)^3 \end{aligned}\right\} \quad \cdots [5]$$

. . . . . .

. . . . . .

$x(\tau)$ and $y(\tau)$ are required to satisfy the following two sets of conditions, respectively

$$\left.\begin{aligned} &(a)\ x_i(\tau + 2\pi) = x_i(\tau);\ x_0(0) = A,\ x_0'(0) = 0; \\ &\qquad x_i(0) = 0,\ x_i'(0) = 0 \\ &(b)\ y_i(\tau + 2\pi) = y_i(\tau);\ y_0(0) = B,\ y_0'(0) = 0; \\ &\qquad y_i(0) = 0,\ y_i'(0) = 0 \end{aligned}\right\} \quad \cdots [6]$$

Let the solutions of the first recurrence Relationship [4] be as follows

$$\left.\begin{aligned} x_0 &= A_{01}\cos(\omega_{n1}\tau - \gamma_1) + A_{02}\cos(\omega_{n2}\tau - \gamma_2) \\ y_0 &= B_{01}\cos(\omega_{n1}\tau - \gamma_1) + B_{02}\cos(\omega_{n2}\tau - \gamma_2) \\ \omega_n^2 &= \frac{1}{\omega_0^2}\left\{\frac{1}{2}\left(\frac{k_1 + k_2}{m_2} + \frac{k_1}{m_1}\right) \pm \left[\frac{1}{4}\left(\frac{k_1 + k_2}{m_2} + \frac{k_1}{m_1}\right)^2 - \frac{k_1 k_2}{m_1 m_2}\right]^{1/2}\right\} \end{aligned}\right\} \quad \cdots [7]$$

where ω_n is defined as a dimensionless angular frequency. Conditions [6] require

$$\omega_n(\tau + 2\pi) = \omega_n\tau + 2\pi \quad \cdots\cdots [8]$$

hence

$$\omega_n = 1 \quad \cdots\cdots [9]$$

It follows that

$$\left.\begin{aligned} x_0 &= A\cos\tau \\ y_0 &= B\cos\tau \end{aligned}\right\} \quad \cdots\cdots [10]$$

and

$$\omega_0^2 = \frac{1}{2}\left(\frac{k_1 + k_2}{m_2} + \frac{k_1}{m_1}\right) \pm \left[\frac{1}{4}\left(\frac{k_1 + k_2}{m_2} + \frac{k_1}{m_1}\right)^2 - \frac{k_1 k_2}{m_1 m_2}\right]^{1/2} \quad \cdots\cdots [11]$$

Equation [11] is also the square of the two natural frequencies of the system if the small nonlinearity is neglected. It explains why $\omega_n = 1$ is chosen in Equation [9], because $\cos\omega_n(\tau + 2\pi) = \cos(\omega_n\tau + 2\pi)$ holds whenever ω_n is equal to any integer.

In solving the second recurrence relationship, substitute Equations [10] and their second derivatives with respect to τ into Equations [5]. This yields

$$\left.\begin{aligned} \omega_0^2 x_1'' + \frac{k_1}{m_1}(x_1 - y_1) &= \left[2\omega_0\omega_1 A - \frac{3}{4}(A - B)^3 + F\right]\cos\tau - \frac{1}{4}(A - B)^3\cos 3\tau \\ \omega_0^2 y_1'' - \frac{k_1}{m_2}(x_1 - y_1) + \frac{k_2}{m_2} y_1 &= \left[2\omega_0\omega_1 B + \frac{3}{4}\frac{m_1}{m_2}(A - B)^3\right]\cos\tau + \frac{1}{4}\frac{m_1}{m_2}(A - B)^3\cos 3\tau \end{aligned}\right\} \quad \cdots [12]$$

The periodicity conditions for x_1 and y_1 require that the coefficients of $\cos\tau$ be zero, since otherwise the secular term is bound to appear in the solution. Hence

$$\left.\begin{aligned} 2\omega_0\omega_1 A - \frac{3}{4}(A - B)^3 + F &= 0 \\ 2\omega_0\omega_1 B + \frac{3}{4}\frac{m_1}{m_2}(A - B)^3 &= 0 \end{aligned}\right\} \quad \cdots\cdots [13]$$

This gives the value of $2\omega_0\omega_1$ and the frequency equation is

$$\omega^2 = \omega_0^2 + \epsilon\frac{3}{4}\left(1 + \frac{m_1}{m_2}\right)(A - B)^3 - \epsilon\frac{F}{A - B} \quad \cdots [14]$$

Equations [13] constitute two conditions on ω_1, A, and B. One condition is used in the form for the value of $2\omega_0\omega_1$; the other condition implies that in our initial conditions, A can be arbitrarily prescribed, while B has its value determined by A. After equating the coefficients of $\cos\tau$ to zero in Equations [12], the solutions that satisfy Conditions [6] are

$$\left.\begin{aligned} x_1 &= Q(k_2 m_1 - 9\omega_0^2 m_1 m_2)(A - B)^3(\cos\tau - \cos 3\tau) \\ y_1 &= Q9\omega_0^2 m_1^2(A - B)^3(\cos\tau - \cos 3\tau) \end{aligned}\right\} \quad \cdots [15]$$

where

$$1/Q = 4[(k_1 - 9\omega_0^2 m_1)(k_1 + k_2 - 9\omega_0^2 m_2) - k_1^2]$$

The complete solutions up to the first order of ϵ after changing to the original variable finally take the form

$$\left.\begin{aligned} x &= A\cos\omega t + \epsilon Q(k_2 m_1 - 9\omega_0^2 m_1 m_2)(A - B)^3(\cos\omega t - \cos 3\omega t) + \cdots \\ y &= B\cos\omega t + \epsilon Q9\omega_0^2 m_1^2(A - B)^3(\cos\omega t - \cos 3\omega t) + \cdots \end{aligned}\right\} \quad \cdots [16]$$

The method of procedure from this point on should be clear.

Case 2 Free Oscillations With Nonlinear Restoring Force, Damping Neglected. This is a special case of the previous case with $F = 0$. The equations of motion are as follows

$$\left.\begin{aligned} m_1\ddot{x} + k_1(x-y) + \epsilon_0(x-y)^3 &= 0 \\ m_2\ddot{y} - k_1(x-y) - \epsilon_0(x-y)^3 + k_2 y &= 0 \end{aligned}\right\} \quad \ldots\ldots [17]$$

in which the same nonlinearity is assumed as that in the first case. The frequency equation up to the first order of ϵ is

$$\omega^2 = \omega_0^2 + \epsilon \frac{3}{4}\left(1 + \frac{m_1}{m_2}\right)(A-B)^2 \ldots\ldots [18]$$

Solutions of x and y take the same form as Equations [16], but the results will be different from the case of forced oscillation. This is because ω in these two cases is different due to the dependence of ω on F.

Case 3 Forced Oscillation With Nonlinear Restoring Force, Small Viscous Damping Considered. This case is shown in Fig. 2.

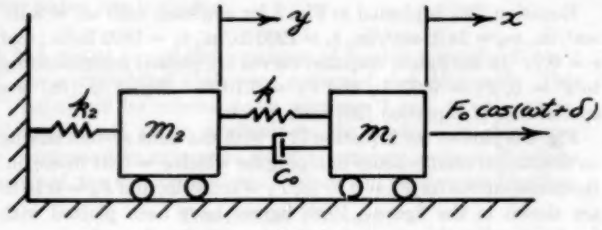

FIG. 2

With the same small nonlinear restoring force as that assumed in the first case, the equations of equilibrium are

$$\left.\begin{aligned} m_1\ddot{x} + c_0(\dot{x}-\dot{y}) + k_1(x-y) + \epsilon_0(x-y)^3 &= F_0\cos(\omega t+\delta) \\ m_2\ddot{y} - c_0(\dot{x}-\dot{y}) - k_1(x-y) - \epsilon_0(x-y)^3 + k_2 y &= 0 \end{aligned}\right\} \ldots [19]$$

where δ is the phase difference between driving force and x, and $c_0 = \epsilon_0 c$. Proceeding in the same manner as in the first case, i.e., introducing a new variable, applying the perturbation series, the following recurrence relationships are obtained

$$\left.\begin{aligned} \omega_0^2 x_0'' + \frac{k_1}{m_1}(x_0 - y_0) &= 0 \\ \omega_0^2 y_0'' - \frac{k_1}{m_2}(x_0 - y_0) + \frac{k_2}{m_2} y_0 &= 0 \end{aligned}\right\} \ldots\ldots [20]$$

$$\left.\begin{aligned} \omega_0^2 x_1'' + \frac{k_1}{m_1}(x_1 - y_1) &= -c\omega_0(x_0' - y_0') \\ &\quad - 2\omega_0\omega_1 x_0'' - (x_0 - y_0)^3 + F\cos(\tau+\delta) \\ \omega_0^2 y_1'' - \frac{k_1}{m_2}(x_1 - y_1) + \frac{k_2}{m_2} y_1 &= \frac{m_1}{m_2} c\omega_0(x_0' - y_0') \\ &\quad - 2\omega_0\omega_1 y_0'' + \frac{m_1}{m_2}(x_0 - y_0)^3 \\ \cdots\cdots\cdots\

Equations [23] and their first and second derivatives are then substituted in the second recurrence relationship. As the periodic conditions for x_1 and y_1 require that the coefficients of $\sin\tau$ and $\cos\tau$ be zero, four equations are obtained in this case. From these equations we have the value of $2\omega_0\omega_1$ and the frequency equation is

$$\omega^2 = \omega_0^2 + \epsilon\left(1+\frac{m_1}{m_2}\right)\left(\frac{3}{4}D^2+\frac{3}{4}B^2\sin^2\nu-\frac{c\omega_0 B\sin\nu}{D}\right)-\epsilon\frac{F\cos\delta}{D} \quad \ldots\ldots [24]$$

where

$$D = A - B\cos\nu$$

If there is no damping $c = 0$, then $\delta = \nu = 0$, and Equation [24] reduces to Equation [14]. In addition to $2\omega_0\omega_1$, the other three quantities which will be determined from these four equations are B, δ, and ν. It follows that in the initial Conditions [22] only A is prescribed arbitrarily, while other quantities are determined from it. From equations of second recurrence relationship with vanishing coefficients of $\sin\tau$ and $\cos\tau$ the solutions x_1 and y_1 that satisfy Conditions [22] are obtained. The complete solutions with original variable up to the first order of ϵ finally take the following form

$$\left.\begin{aligned} x &= A\cos\omega t + \epsilon Q(k_2 m_1 - 9\omega_0^2 m_1 m_2)\\ &\quad [R_1(\cos 3\omega t - \cos\omega t) - R_2\sin 3\omega t] + \ldots\\ y &= B\cos(\omega t - \nu) + \epsilon Q 9\omega_0^2 m_1^2\\ &\quad [R_1(\cos 3\omega t - \cos\omega t) - R_2\sin 3\omega t] + \ldots \end{aligned}\right\} \quad [25]$$

where

$$R_1 = -D^2 + 3B^2 D\sin^2\nu$$
$$R_2 = 3BD^2\sin\nu - B^2\sin^2\nu$$

Response Curves

In order to plot the response curves, frequency Equations [14] and [24] are rewritten as follows

$$\omega = \omega_0 + \frac{\epsilon}{2\omega_0}\frac{3}{4}\left(1+\frac{m_1}{m_2}\right)(A-B)^2 - \frac{\epsilon}{2\omega_0}\frac{F}{A-B} \quad [26]$$

$$\omega = \omega_0 + \frac{\epsilon}{2\omega_0}\left(1+\frac{m_1}{m_2}\right)\frac{3}{4}(D^2+B^2\sin^2\nu) - \frac{\epsilon}{2\omega_0}\frac{1}{D}\left[F\cos\delta + \left(1+\frac{m_1}{m_2}\right)c\omega_0 B\sin\nu\right] \quad [27]$$

Equation [26] is plotted in Fig. 3 for a system with $m_1 = 8$ lb-sec^2/in., $m_2 = 24$ lb-sec^2/in., $k_1 = 1200$ lb/in., $k_2 = 1800$ lb/in., and $\epsilon = 0.1$. In the figure, response curves are plotted corresponding to $F = 0$, $F_1 = 0.07$ lb, and $F_2 = 0.10$ lb. Equation [18] is a special case of Equation [26] with $F = 0$.

Fig. 4 is plotted for Equation [27] with the same system having an additional small viscous damping for which $c = 0.01$ lb-sec/in. Response curves for $F_1 = 0.07$ lb, $F_2 = 0.085$ lb, and $F_3 = 0.10$ lb are shown in the figure. Both figures have been plotted with hard and soft spring characteristics, i.e., $\epsilon > 0$ and $\epsilon < 0$.

Acknowledgment

This paper is based on a part of author's thesis written under the supervision of Dr. N. O. Myklestad, formerly Professor of Theoretical and Applied Mechanics, University of Illinois. The author is heartily grateful to his valuable guidance. The author's thanks also are tendered to Prof. H. J. Schrader for his kind encouragement.

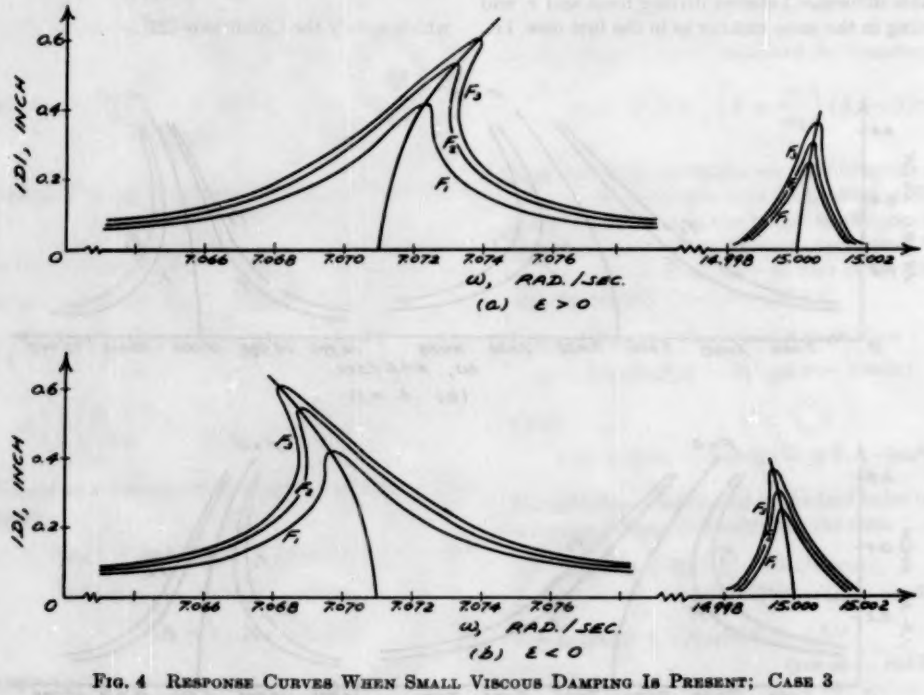

Fig. 4 Response Curves When Small Viscous Damping Is Present; Case 3

Cylindrical Shells: Energy, Equilibrium, Addenda, and Erratum

By E. H. KENNARD,[1] WASHINGTON, D. C.

The strain energy in a homogeneous cylindrical shell of uniform thickness is calculated from equations obtained by Epstein's method. The indeterminateness of the equations of equilibrium is further discussed and simplified forms of these equations and of the expressions for the stress resultants are given. Addenda and an erratum to a prior paper are included.

IN a recent paper[2] the equations of motion given by Epstein for a cylindrical shell were rederived and discussed. This paper will be referred to as reference 2 and, to save space, will be assumed to be available to the reader. In this paper the corresponding expression for strain energy in the shell will be given and the equations of equilibrium will be discussed further.

The Strain Energy

In deriving the equations of motion in reference 2 for a homogeneous cylindrical shell of uniform thickness h and median radius R, the co-ordinates used were x parallel to the axis, $s = R\phi$, where ϕ is the azimuth angle about the axis, and r, the distance from the axis; the corresponding components of displacement of any point of the median surface are u, v, w, with w taken positive outward. General expressions were obtained for the displacement of any point in the shell, from which expressions are easily derived for the six components of strain $\epsilon_x, \epsilon_s, \epsilon_r, \gamma_{xr}, \gamma_{sr}, \gamma_{xs}$ and for the corresponding six stresses $\sigma_1, \sigma_2, \sigma_3, \tau_1, \tau_2, \tau_3$. The strain energy U per unit area of the median surface can then be found by substituting in the usual formula

$$U = \frac{1}{2}\int_{R-h/2}^{R+h/2} (\epsilon_x\sigma_1 + \epsilon_s\sigma_2 + \epsilon_r\sigma_3 + \gamma_{sr}\tau_1 + \gamma_{xr}\tau_2 + \gamma_{xs}\tau)\frac{r}{R}\,dr$$

Evaluation of the integral is laborious if all terms arising directly from applied load on the faces of the shell are included. However, these terms are of very unequal interest. Let τ_1^+ and τ_2^+ denote applied shearing stresses in the x and s-directions, and σ_3^+ the normal stress on the outer surface of the shell and τ_1^-, τ_2^-, σ_3^- corresponding quantities on the inner surface, and for convenience write

$$P_1 = \tau_1^+ - \tau_1^-,\ P_2 = \tau_2^+ - \tau_2^-,\ P_3 = \sigma_3^+ - \sigma_3^-$$

$$S_1 = \frac{1}{2}(\tau_1^+ + \tau_1^-),\ S_2 = \frac{1}{2}(\tau_2^+ + \tau_2^-),\ S_3 = \frac{1}{2}(\sigma_3^+ + \sigma_3^-)$$

(In reference 2, Z_1, Z_2, Z_3 were written for P_1/h, P_2/h, P_3/h). Thus, for uniform pressure p, $\sigma_3^+ = \sigma_3^- = S_3 = -p$. Now, indirectly through the influence of boundary conditions, the net loads P_1, P_2, P_3 usually evoke, in thin curved shells, elastic stresses greatly exceeding the direct load terms S_1, S_2, S_3; and loading in shear is rare in practice. Hence the work was shortened by omitting all terms containing h^2 or h^3 and also either S_1 or S_2 or their derivatives. Therefore the h^2 or h^3 terms in the formulas may not be sufficiently accurate for flat plates with shearing loads on their faces.

Evaluation of the integral for U then gives, as far as terms of order h^3 but with omission of h^3S_1 or h^3S_2 or a derivative of these quantities, for the shell either at rest or in motion

$$U = U_m + U_b \qquad [1]$$

$$U_m = hE_s\left[\frac{1}{2}(1-\nu^2)u_x^2 + \frac{1}{2}\left(\nu u_x + v_s + \frac{w}{R}\right)^2 + \frac{1}{4}(1-\nu)(u_s + v_x)^2\right] + \frac{\theta h}{E_s}\left[S_1^2 + S_2^2 + \frac{1}{2}\theta(1-2\nu)S_3^2\right] \qquad [1a]$$

$$U_b = \frac{1}{24}h^3E_s\Big\{w_{xx}^2 + w_{ss}^2 + 2\nu w_{xx}w_{ss} + 2(1-\nu)w_{xs}^2 + \theta\nu(u_{xxx} + v_{xxs})(u_x + \nu v_s + \nu wR^{-1}) + \theta\nu(u_{xss} + v_{sss})(\nu u_x + v_s + wR^{-1}) + \theta w_{xx}[-(2-3\nu-3\nu^2)u_xR^{-1} - \nu(1-5\nu)v_sR^{-1} + \nu(1+3\nu)wR^{-2}] + \theta w_{ss}[2\nu(1+\nu)u_xR^{-1} + 4\nu v_sR^{-1} + 2(1+\nu)wR^{-2}] + \theta^2(\nu u_x + \nu v_s + wR^{-1})[(1+\nu)(\nu u_x + wR^{-1}) + 2\nu v_s]R^{-2} + \nu(u_{xxs} + v_{xss})(u_s + v_x) + w_{xs}u_sR^{-1} - (3-4\nu)w_{xs}v_xR^{-1} + \frac{1}{2}(1-\nu)(u_s^2R^{-2} + 3v_x^2R^{-2})\Big\}$$

$$+ \frac{1}{24}h^3\{\theta^2(1-2\nu)(\nu u_x + v_s + wR^{-1})P_3(hR)^{-1} + \theta^2(1-2\nu)[2\nu(u_{xxx} + u_{xss} + v_{xxs} + v_{sss}) + 2\nu^2w_{xx}R^{-1} + 2\nu w_{ss}R^{-1} + (2-5\nu)(\nu u_x + v_s + wR^{-1})R^{-2}]S_3 + 2\theta(u_x + \nu v_s + \nu wR^{-1})P_1h^{-1} + 2\theta(\nu u_x + v_s + wR^{-1})P_2h^{-1} + (u_s + v_x)(P_1 + P_2)h^{-1} - \theta(1-2\nu)[\theta(u_x + \nu v_s + \nu wR^{-1})S_{3xx} + \theta(\nu u_x + v_s + wR^{-1})S_{3ss} + (u_s + v_x)S_{3xs}]\}$$

$$+ \frac{1}{24}\theta h^3E_s^{-1}\Big\{[2P_1^2 + 2P_2^2 + \theta(1-2\nu)P_3^2]h^{-2} - \theta^2(3-4\nu)(1-2\nu)^2S_3^2R^{-2} + 2\theta(1-2\nu)[(\theta P_{1x} + \theta P_{2s} + 2P_3R^{-1})h^{-1} + \theta^2\nu^2(S_{3xx} + S_{3ss})]S_3 - 2\theta^2(1-2\nu)^2S_3\rho E_s^{-1}\frac{\partial^2}{\partial t^2}S_3\Big\} \qquad [1b]$$

---

[1] Physicist, David Taylor Model Basin.

[2] "The New Approach to Shell Theory: Circular Cylinders," by E. H. Kennard, JOURNAL OF APPLIED MECHANICS, Trans. ASME, vol. 75, 1953, pp. 33–40.

Contributed by the Applied Mechanics Division and presented at the Annual Meeting, New York, N. Y., November 28–December 3, 1954, of THE AMERICAN SOCIETY OF MECHANICAL ENGINEERS.

Discussion of this paper should be addressed to the Secretary, ASME, 29 West 39th Street, New York, N. Y., and will be accepted until April 11, 1955, for publication at a later date. Discussion received after the closing date will be returned.

NOTE: Statements and opinions advanced in papers are to be understood as individual expressions of their authors and not those of the Society. Manuscript received by ASME Applied Mechanics Division, May 14, 1953. Paper No. 54—A-10.

Here E is Young's modulus, ν is the Poisson ratio, ρ the density of the material, t the time, and $\theta = 1/(1-\nu)$, $E_* = E/(1-\nu^2)$. All quantities refer to the middle surface.

The membrane energy U_m and the first four terms of the bending energy U_b agree with expressions found by all other authors. Thereafter, however, the discrepancy in U_b is so large that detailed comparison is rather pointless. The differences undoubtedly are due in large part to the conventional neglect of the bending of normals to the middle surface and of the Poisson contraction of these normals.

Approximate Expression for U

The expression given in Equation [1] for the strain energy U appears to be correct in so far as terms of order h^3, except for the omission here of terms in U_b containing S_1 or S_2. It is hard to imagine, however, that so lengthy an expression will ever be used in practical applications. Fortunately, in particular cases many terms can be shown to be negligibly small, the choice of terms varying from one case to another. It also is possible, in fact, to derive in the following way a simplified expression for U_b that represents an approximation valid for all cases; this expression may be useful as a starting point for further reduction in special cases.

Any term in U_b that is always sufficiently small in comparison with the whole of U_m certainly can be dropped. An example is the term containing $u_x^2R^{-2}$ which is only $(\nu^2/[12(1-\nu)^2])(h^2R^{-2})$ as large as the first term containing u_x^2 in U_m, and the latter term cannot exceed U_m itself since the remaining terms in U_m are necessarily positive. Hence, provided hR^{-1} is small enough, the term in question can be dropped from U_b.

For other terms the reasoning has to be more indirect. If a term $(\nu u_x + v_s + wR^{-1})^2R^{-2}$ occurred in the first $\{\ \}$ in U_b, it would contribute only $(1/12)\ (h^2/R^2)$ as much as the similar term in U_m. Now

$$(v_s + wR^{-1})^2 = [(\nu u_x + v_s + wR^{-1}) - \nu u_x]^2 \leq 2(\nu u_x + v_s + wR^{-1})^2 + 2\nu^2 u_x^2$$

Hence the contribution of a term $(v_s + wR^{-1})^2R^{-2}$ in the first $\{\ \}$ in U_b could not exceed $U_m h^2R^{-2}[(2/12) + 2\nu^2/[12(1-\nu^2)]]$ or, at the worst, since $\nu < 0.5$, $(1/4)\ (h^2R^{-2})U_m$. Again, $|u_x(v_s + w/R)| = [u_x^2(v_s + wR^{-1})^2]^{1/2}$ so that a term $u_x(v_s + wR^{-1})R^{-2}$ could not contribute numerically more than $0.2\ h^2R^{-2}U_m$.

Extending such reasoning to include $(u_s + v_x)^2$, it is easily seen that any one of the following six quantities, if occurring divided by R^2 in the proper $\{\ \}$ in U_b, would contribute to U numerically less than $(U_m/3)h^2R^{-2}$

$$u_x^2,\quad (v_s + wR^{-1})^2,\quad (u_s + v_x)^2,\quad u_x(v_s + wR^{-1}),\quad u_x(u_s + v_x),\quad (v_s + wR^{-1})\ (u_s + v_x),\quad S_1^2,\quad u_xS_1,\quad (v_s + wR^{-1})S_2,\quad (u_s + v_x)S_2$$

Furthermore, instead of h^2R^{-2}, one of the operators $h^2\partial^2/\partial x^2$, $h^2\partial^2/\partial s^2$, or $h^2\partial^2/\partial x\partial s$ may occur in such comparisons; for, in a valid thin-shell theory these operators must have, in general, a heavily diminishing effect, in order to justify omitting terms of higher order in h (see reference 2). Thus $h^2u_{xxx}u_x$ is at most points small relative to u_xu_x or u_x^2, just as $h^2u_x^2R^{-2}$ is. In general, a quantity formed by imposing one of the three operators upon one factor of any one of the six quantities just listed, when occurring in a $\{\ \}$ in U_b, will make a contribution to U much smaller than U_m. Further examples are the products $u_{xxx}(v_s + wR^{-1})$, $u_{xxx}(u_s + v_x)$.

Using these results, certain terms in U_b can be dropped; they contain additional coefficients such as $\theta\nu$ but these are all of moderate magnitude relative to unity.

It is also permissible to multiply one of the negligible quantities by an arbitrary number of moderate size and then to add or subtract it from the quantity in a $\{\ \}$ in U_b; in this way further simplifications can be effected. For example, the term $\theta\nu v_{xx}u_x$ can be eliminated from the first $\{\ \}$ by subtracting $\theta\nu u_x(v_{xxx} + w_{xx}R^{-1})$, with a concomitant change in the coefficient of $w_{xx}u_xR^{-1}$, from $-\theta(2 - 3\nu - 3\nu^2)$ to $-\theta(2 - 2\nu - 3\nu^2)$. The error thereby introduced into U will equal at most a minute fraction of U_m.

By means of this latter device, the expression for U_b can be simplified into many alternative approximate forms, between which free choice may be made. The following form has certain attractive features

$$\begin{aligned}
U_b = \frac{1}{24}h^3E_*\Big\{ & w_{xx}^2 + w_{ss}^2 + 2\nu w_{xx}w_{ss} + 2(1-\nu)w_{xs}^2 \\
& + \theta w_{xx}[-(2 - 2\nu - 3\nu^2)u_xR^{-1} - \nu(1-4\nu)v_sR^{-1} \\
& + \nu(1+2\nu)wR^{-2}] + \theta w_{ss}[\nu(2+\nu)u_xR^{-1} + 3\nu v_sR^{-1} \\
& + (2+\nu)wR^{-2}] - \frac{3}{2}\theta\nu v_s^2R^{-2} + \frac{1}{2}\theta(2+\nu)w^2R^{-4} \\
& - \theta\nu(2+\nu)u_xv_sR^{-2} + (1-\nu)\Big[w_{xs}(u_sR^{-1} - 3v_xR^{-1}) \\
& + \frac{1}{2}u_s^2R^{-2} + \frac{3}{2}v_x^2R^{-2}\Big]\Big\} + \frac{1}{24}h^3\{\theta^2(1-2\nu)\ (\nu u_x \\
& + v_s + wR^{-1})P_3(hR)^{-1} + 2\theta(u_x + \nu v_s + \nu wR^{-1})P_{1x}h^{-1} \\
& + 2\theta(\nu u_x + v_s + wR^{-1})P_{2s}h^{-1} + (u_s + v_x)\ (P_{1s} + P_{2x})h^{-1} \\
& - 2\theta^2\nu(1-2\nu)w_{xx}S_3R^{-1}\} \\
& + \frac{1}{24}\theta h^3E_*^{-1}\Big\{[2P_1^2 + 2P_2^2 + \theta(1-2\nu)P_3^2]h^{-2} \\
& + 2\theta(1-2\nu)\ (\theta P_{1x} + \theta P_{2s} + 2P_3R^{-1})S_3h^{-1} \\
& - 2\theta^2(1-2\nu)^2S_3\frac{\rho}{E_*}\frac{\partial^2}{\partial t^2}S_3\Big\} \quad [2]
\end{aligned}$$

Here, as before, terms containing S_1 or S_2 are missing.

Near special points on the shell the simplification, of course, may not be fully justified, just as $h^2u_{xxx}u_x$ cannot be small relative to u_x^2 where $u_x = 0$. The effect of such points on the integral for the total strain energy, however, should be very small.

In particular cases, additional terms may be dropped. For example, the only reason that the three terms of $(u_s + v_x)^2$ or $u_s^2 + 2u_sv_x + v_x^2$ cannot be treated separately lies in the possibility that $u_x = 0$, $u_s = -v_x$, $v_s + wR^{-1} = 0$, so that $U_m = 0$. In this case $2u_sv_x$ cancels the sum, $u_s^2 + v_x^2$; and comparison of another term with u_s^2 or v_x^2 would imply nothing as to its magnitude relative to U_m. If, however, it is clear in a given case that the ratio $2u_sv_x/(u_s^2 + v_x^2)$ is everywhere much less than -1, or approaches -1 only near a few points, then the terms in U_b containing either u_s^2 or v_x^2 can be dropped. Similarly, if $2v_swR^{-1}/(v_s^2 + w^2R^{-2})$ is generally much less than -1, terms in v_s^2, w^2R^{-2}, or v_swR^{-1} may be dropped from U_b. If all such terms are dropped, there remain in U_b only the usual terms for a plate and additional terms containing the first power of w_{xx}, w_{ss}, or w_{xs}.

It may be remarked that, if w is taken positive toward the axis, then all terms that are linear in w or its derivatives are reversed in sign.

Equations of Equilibrium

Equations of equilibrium in terms of displacement can be found by setting $\ddot{u} = \ddot{v} = \ddot{w} = 0$ in the equations of motion. Complete expressions for these were not given in reference 2; they will be indicated in the Appendix to this paper. The equa-

tions of equilibrium obtained from the equations of motion complete through terms of order h^2 are

$$u_{xx} + (1/2)(1-\nu)u_{ss} + (1/2)(1+\nu)v_{xs} + \nu w_x R^{-1} + E_s^{-1}(P_1 h^{-1} + S_1 R^{-1} + \theta\nu S_{1s}) + (1/24)\theta^2 h^2[2\nu^2(u_{xxxx} + u_{xxss} + v_{xxxs} + v_{xsss}) - (2 - 5\nu + \nu^2)w_{xxx}R^{-1} + (1 - \nu + 4\nu^2 - 2\nu^3)w_{xss}R^{-1} - \nu(2 - 9\nu + 6\nu^2)u_{xx}R^{-2} + (1-\nu)^2 u_{ss}R^{-2} - (2 - 7\nu + 5\nu^2 - \nu^3)v_{xs}R^{-2} - (2 - 9\nu + 6\nu^2)w_x R^{-2}] + (1/24)\theta^2 h^2 E_s^{-1}[(2 - 3\nu^2)P_{3x}(hR)^{-1} + \theta(2 - 13\nu + 24\nu^2 - 12\nu^3)S_{3x}R^{-2} + (2 - \nu + \nu^2)P_{1xx}h^{-1} + (1-\nu)^2 P_{1ss}h^{-1} + (1+\nu)P_{2xs}h^{-1} + 2(3 - 5\nu + \nu^2)S_{1xs}R^{-1} - 2(1-\nu)^2 S_{1ss}R^{-1} + (3 - 13\nu + 10\nu^2)S_{2ss}R^{-1} - \theta(1 - 3\nu + 3\nu^2 - 3\nu^3)(S_{3xxx} + S_{3xss})] = 0 \quad [3a]$$

$$v_{ss} + (1/2)(1-\nu)v_{xx} + (1/2)(1+\nu)u_{xs} + w_s R^{-1} + E_s^{-1}(P_2 h^{-1} + 2S_2 R^{-1} + \theta\nu S_{1s}) + (1/24)\theta^2 h^2[2\nu^2(u_{xxxs} + u_{xsss} + v_{xxss} + v_{ssss}) - (3 - 9\nu + 6\nu^2 - 2\nu^3)w_{xxs}R^{-1} + \nu(3-\nu)w_{sss}R^{-1} - (3 + \nu - 17\nu^2 + 12\nu^3)u_{xs}R^{-2} - (10 - 23\nu + 12\nu^2)v_{ss}R^{-2} - (10 - 26\nu + 15\nu^2)w_s R^{-2}] + (1/24)\theta^2 h^2 E_s^{-1}[-12(1-\nu)^2 S_2 R^{-2} + (5 - 7\nu + \nu^2)P_{2s}(hR)^{-1} + \theta(4 - 28\nu + 49\nu^2 - 24\nu^3)S_{2s}R^{-2} + (1+\nu)P_{1ss}h^{-1} + (1-\nu)^2 P_{2xx}h^{-1} + (2 - \nu + \nu^2)P_{2ss}h^{-1} + 2(3 - 6\nu + 2\nu^2)S_{1ss}R^{-1} + 5(1-\nu)^2 S_{2xx}R^{-1} + 3(1-\nu)(2 - 5\nu)S_{2ss}R^{-1} - \theta(1 - 3\nu + 3\nu^2 - 3\nu^3)(S_{3xxs} + S_{3sss})] = 0 \quad [3b]$$

$$\nu u_x R^{-1} + v_s R^{-1} + wR^{-2} - E_s^{-1}[P_3 h^{-1} + \theta(1-2\nu)S_3 R^{-1} + S_{1x} + S_{2s}] + (1/24)\theta^2 h^2[2(1-\nu)^2(w_{xxxx} + 2w_{xxss} + w_{ssss}) + 3\nu^2 u_{xxx}R^{-1} + (4 - 5\nu + \nu^2 + 3\nu^3)u_{xss}R^{-1} + (2 - 7\nu + 11\nu^2 - 3\nu^3)v_{xxs}R^{-1} + (6 - 12\nu + 9\nu^2)v_{sss}R^{-1} + (2 - 2\nu + \nu^2 + 2\nu^3)w_{xx}R^{-2} + (10 - 17\nu + 10\nu^2)w_{ss}R^{-2} + 2(1-\nu)(1+3\nu)(\nu u_x R^{-2} + wR^{-2}) + 5\nu(1-\nu)v_s R^{-2}] + (1/24)\theta^2 h^2 E_s^{-1}[(1-\nu)P_3(hR^2)^{-1} - 2(1 + \nu - 6\nu^2)S_3 R^{-3} - (4 - 10\nu + 3\nu^2)P_{1s}(hR)^{-1} + \nu(2+\nu)P_{2s}(hR)^{-1} + (1-\nu)(2 - 7\nu)S_{1s}R^{-2} + 3(2 - 9\nu + 8\nu^2)S_{2s}R^{-2} - (1-\nu)(2-\nu)(P_{3xx} + P_{3ss})h^{-1} - \theta(2 - 6\nu + 6\nu^2 - 5\nu^3)S_{3xx}R^{-1} - \theta(5 - 22\nu + 29\nu^2 - 15\nu^3)S_{3ss}R^{-1} - 3(1-\nu)(2-\nu)(S_{1xxx} + S_{1xss} + S_{2xxs} + S_{2sss})] = 0 \quad [3c]$$

Indeterminateness of Equilibrium Equations

It is a remarkable fact that an application of the usual variational method to the strain-energy U yields equations of equilibrium in terms of displacement whose h^2 terms are not the same as those in Equations [3 *a*, *b*, *c*]. Furthermore, if the complete expressions for the resultant stress forces and couples are substituted into the usual dynamical conditions for equilibrium, the result is still a different set of h^2 terms. The possibility of such discrepancies appears to arise from an actual indeterminateness in the form of the equations of equilibrium when these are carried out through a certain order of powers of h.

The indeterminateness is due to the fact that each of the equations is of the form $M + h^2 N = 0$, so that the membrane part M, inclusive of load terms, is actually itself of order h^2. If, now, bM is added to N, where b is any number, the result is $M + h^2(N + bM)$ or $M + h^2 N - h^4 bN$. Terms of order h^4, however, were dropped in deriving the equations; hence for consistency, provided b is not numerically large relative to unity, the new term $-bh^4 N$ reasonably may be ignored. In this way N may be changed extensively in form. Furthermore, any derivative of M may be used instead of M; or any combination of the M's occurring in the three equations may be used. As was stated in reference 2, the procedure can be justified on the basis of the "thin-shell assumptions," provided that the quantity added to N is not multiplied by a positive power of the radius R. Multiplication by R may introduce the operator $R\partial/\partial x$ or $R\partial/\partial s$, whose effect on the magnitude of the quantity operated upon is unknown.

By such maneuvers it is found to be possible (at least if $P = S = 0$ and presumably in general) to convert any one of the three forms of the h^2 terms just mentioned into either of the other two, thus establishing the consistency of the three forms. It seems to be impossible to say which of these forms will give a result approximating most closely the unknown result that would be obtained from an exact application of three-dimensional analysis.

The h^2 terms also can be thrown by the same procedure into many other alternative forms. The solutions of a given problem obtained with use of these various forms will all differ only by terms of order h^4. Now a little reflection shows that, if equations already contain an unknown error and changes are made in them by which a second error is introduced that is larger than the first but of unknown sign, then the expectation of error is thereby increased. Nevertheless, it seems reasonable to expect that moderate arbitrary simplifications of the equations of equilibrium may be made by the procedure just outlined without increasing the error seriously, and with the possibility that it is decreased.

In addition to the parts of the left-hand members of Equations [3 *a*, *b*, *c*] that do not contain h^2, the following four expressions are especially useful for modifying the equations; they represent linear combinations of the parts just mentioned or of their derivatives, and are likewise of order h^2 (and actually equal to zero in membrane theory), as are also their further derivatives

$$(1): (u_{xx} + v_{xs})R^{-1} + 2\theta E_s^{-1}[P_2(hR)^{-1} + 2S_2 R^{-2} + P_3 h^{-1} + S_{3s}R^{-1} + S_{1xx} + S_{2ss}]$$

$$(2): u_{xxx}R^{-1} + \xi\theta E_s^{-1}[(P_{1x} - P_{2s})(hR)^{-1} + (S_{1x} - 2S_{2s})R^{-2} + (\nu P_{3xx} - P_{3ss})h^{-1} + (2\nu S_{3xx} - S_{3ss})R^{-1} + \nu(S_{1xxx} + S_{2xxs}) - S_{1xss} - S_{2sss}]$$

$$(3): v_{sss}R^{-1} + w_{xx}R^{-2} - \xi\theta E_s^{-1}[\nu(P_{1x} - P_{2s})(hR)^{-1} + \nu(S_{1x} - 2S_{2s})R^{-2} + (P_{3xx} - \nu P_{3ss})h^{-1} + (1-\nu)S_{3xx}R^{-1} - \nu S_{3ss}R^{-1} + S_{1xxx} + S_{2xxs} - \nu S_{1xss} - \nu S_{2sss}]$$

$$(4): u_{xxx} + u_{xss} + v_{xxs} + v_{sss} + (\nu w_{xx} + w_{ss})R^{-1} + E_s^{-1}[(P_{1x} + P_{2s})h^{-1} + (S_{1x} + 2S_{2s})R^{-1} + \theta\nu(S_{3xx} + S_{3ss})]$$

Here $\xi = 1/(1+\nu)$.

As an example of the procedure, the quantities $u_{xx}R^{-2}$ and $w_s R^{-2}$ may be removed simultaneously from Equation [3*a*] by

adding inside the bracket the following expression, obtained by differentiating the first part of Equation [3c] and multiplying by $(2 - 9\nu + 6\nu^2)R^{-1}$

$$(2 - 9\nu + 6\nu^2)\{\nu u_{xx} + v_{xs} + w_x R^{-1} - E_s^{-1}[P_{3x}h^{-1} + \theta(1 - 2\nu)S_{3x}R^{-1} + S_{1xx} + S_{2xs}]\}R^{-1}$$

The coefficient of $v_{xs}R^{-2}$ is thereby changed from $-(2 - 7\nu + 5\nu^2 - \nu^3)$ to $-\nu(1 - \nu)(2 + \nu)$ and the coefficients of P_{3x}, S_{3x}, S_{1xx}, and S_{2xs} also are changed.

Simplified Equilibrium Equations

Among the many possible modified forms of the equations of equilibrium that can be obtained in the manner just described, the following equations are attractively simple in the load-free terms

$$u_{xx} + (1/2)(1 - \nu)u_{ss} + (1/2)(1 + \nu)v_{xs} + \nu w_x R^{-1} + E_s^{-1}(P_1 h^{-1} + S_1 R^{-1} + \theta\nu S_{3x}) + (1/24)\theta h^2[-(2 - 3\nu - 2\nu^2)w_{xxx}R^{-1} + (1 + 2\nu^2)w_{xss}R^{-1} + (1 - \nu)^2 u_{ss}R^{-2} - \nu(2 + \nu)v_{xs}R^{-2}] + (1/24)\theta h^2 E_s^{-1}[9\nu P_{3x}(hR)^{-1} + (2 + \nu)P_{1xs}h^{-1} + (1 - \nu)P_{1ss}h^{-1} + (1 + 2\nu)P_{2xs}h^{-1} + \theta(4 - \nu - 6\nu^2)S_{1xx}R^{-1} - 2(1 - \nu)S_{1ss}R^{-1} + \theta(1 - 4\nu)S_{2ss}R^{-1} - (1 - \nu)(S_{2xxx} + S_{1xss})] = 0 \quad [4a]$$

$$v_{ss} + (1/2)(1 - \nu)v_{xx} + (1/2)(1 + \nu)u_{xs} + w_s R^{-1} + E_s^{-1}(P_3 h^{-1} + 2S_2 R^{-1} + \theta\nu S_{3s}) + (1/24)\theta h^2[-3(1 - 2\nu)w_{xxs}R^{-1} + 3\nu w_{sss}R^{-1} - 3(1 - \nu)^2 u_{xs}R^{-2} - 3\nu v_{ss}R^{-2}] + (1/24)\theta h^2 E_s^{-1}[-12(1 - \nu)S_2 R^{-2} - (5 - 14\nu)P_{3s}(hR)^{-1} - 6(1 - \nu)S_{3s}R^{-2} + (1 + 2\nu)P_{1ss}h^{-1} + (1 - \nu)P_{2xx}h^{-1} + (2 + \nu)P_{2ss}h^{-1} - \theta(4 - 14\nu + 13\nu^2)S_{1ss}R^{-1} + 5(1 - \nu)S_{2xx}R^{-1} - \theta(4 - 5\nu + 4\nu^2)S_{2ss}R^{-1} - (1 - \nu)(S_{3xxx} + S_{1xss})] = 0 \quad [4b]$$

$$\nu u_x R^{-1} + v_s R^{-1} + wR^{-2} - E_s^{-1}[P_3 h^{-1} + \theta(1 - 2\nu)S_3 R^{-1} + S_{1s} + S_{2s}] + (1/24)\theta h^2[2(1 - \nu)(w_{xxxs} + 2w_{xsss} + w_{ssss}) - (4 - 2\nu + \nu^2)v_{xxs}R^{-1} + (4 - \nu)w_{sss}R^{-2} - (2 + \nu)v_s R^{-3}] + (1/24)\theta h^2 E_s^{-1}[3(1 + 2\nu)P_3(hR^2)^{-1} - \xi\theta(4 - 8\nu - 4\nu^2 + 5\nu^3)P_{1x}(hR)^{-1} - \xi\theta(8 - 6\nu - 8\nu^2 + 9\nu^3)P_{2s}(hR)^{-1} + \xi\theta(4 + \nu - 7\nu^2 - \nu^3)S_{1x}R^{-2} - \xi\theta(8 + 7\nu - 5\nu^2 + 2\nu^3)S_{2s}R^{-2} + \xi\theta\nu(1 + 3\nu - \nu^2)P_{3xx}h^{-1} - \xi\theta(4 + \nu - 4\nu^2 + 2\nu^3)P_{3ss}h^{-1} + 3\xi\nu^2 S_{3xx}R^{-1} - \xi\theta(7 - 4\nu - 7\nu^2 + 7\nu^3)S_{3ss}R^{-1} - \xi\theta(4 - 3\nu - 7\nu^2 + 3\nu^3)(S_{1xxx} + S_{2xxs}) - \xi\theta(8 - \nu - 8\nu^2 + 4\nu^3)(S_{1xss} + S_{2sss})] = 0 \quad [4c]$$

The distinction should be noted carefully that, whereas Equations [4 *a*, *b*, *c*] for equilibrium stand on about the same footing in regard to accuracy as do Equations [3 *a*, *b*, *c*], Equation [2] for the energy represents an approximation that is presumably less accurate than Equation [1*b*]. This approximate expression for the energy would lead in turn, by the variational method, to a set of approximate equations of equilibrium, but these appear to be of no interest. It also may be remarked that, in contrast to the equilibrium equations, the equations of motion appear to be determinate. The only way to simplify them is by some procedure of approximation, of which a bold example was given at the end of reference 2.

From the practical standpoint, Equations [4 *a*, *b*, *c*] are still fantastically complicated. Fortunately, most of the load terms usually will be either zero or negligible. Furthermore, all of the displacement terms except those containing fourth derivatives of w are necessarily small relative to one of the membrane terms in the same equation, in the sense specified by the thin-shell assumptions of reference 2. In practice, therefore, sufficient accuracy often will be achieved by the common device of simply dropping these small terms, the u and v-equations being thereby reduced to the membrane terms alone. In special cases even the remaining three h^2 terms in the w-equation also will be small. If, however, the displacement approximates the purely transverse type to be discussed presently, terms must be dropped with caution. Many of the load terms, if not zero in a given case, can be dropped systematically for similar reasons; otherwise it is necessary to show that in the particular case at hand they are unimportant. Two cases merit special discussion.

Axisymmetric Nontorsional Case. $v = 0$, all s-derivatives zero, $P_2 = S_2 = 0$. For this case, Equations [4*a*, *c*] reduce to

$$u_{xx} + \nu w_x R^{-1} + E_s^{-1}(P_1 h^{-1} + S_1 R^{-1} + \theta\nu S_{3x}) - (1/24)\theta h^2\{(2 - 3\nu - 2\nu^2)w_{xxx}R^{-1} - E_s^{-1}[9\nu P_{3x}(hR)^{-1} + (2 + \nu)P_{1xx}h^{-1} + \theta(4 - \nu - 6\nu^2)S_{1xx}R^{-1} - (1 - \nu)S_{3xxx}]\} = 0 \quad [5a]$$

$$\nu u_x R^{-1} + wR^{-2} - E_s^{-1}[P_3 h^{-1} + \theta(1 - 2\nu)S_3 R^{-1} + S_{1x}] + (1/12)h^2 w_{xxxx} + (1/24)\theta h^2 E_s^{-1}[3(1 + 2\nu)P_3(hR^2)^{-1} - \xi\theta(4 - 8\nu - 4\nu^2 + 5\nu^3)P_{1x}(hR)^{-1} + \xi\theta(4 + \nu - 7\nu^2 - \nu^3)S_{1x}R^{-2} + \xi\theta\nu(1 + 3\nu - \nu^2)P_{3xx}h^{-1} + 3\xi\nu^2 S_{3xx}R^{-1} - \xi\theta(4 - 3\nu - 7\nu^2 + 3\nu^3)S_{1xxx}] = 0 \quad [5b]$$

In this particular case, further simplification is possible, as was shown for the displacement terms only in reference 2. The equations can be solved for u_{xx} and w_x/R, after differentiating the second. The expression thus found for w_x/R is then of order h^2 and, differentiated twice more, may be substituted for w_{xxx}/R, terms in h^4 being dropped. Multiplication by R is involved in solving for w_x/R, but all h^4 terms introduced by the substitution for w_{xxx}/R are easily seen to be of order $h^2\partial^2/\partial x^2$ relative to h^2 terms. The result is the following pair of equations

$$(1 - \nu^2)u_{xx} + E_s^{-1}(P_1 h^{-1} + S_1 R^{-1} + \nu R P_{3x}h^{-1} + 2\nu S_{3x} + \nu R S_{1xx}) - (1/24)h^2\{2\nu R w_{xxxxx} - E_s^{-1}[6\nu P_{3x}(hR)^{-1} + (2 + 5\nu)P_{1xx}h^{-1} + (4 + \nu)S_{1xx}R^{-1} - (2 - \nu)RP_{3xxx}h^{-1} - 3(1 - \nu)S_{3xxx} - \theta(2 - 7\nu + 3\nu^2)RS_{1xxxx}]\} = 0 \quad [6a]$$

$$(1 - \nu^2)w_x R^{-1} - E_s^{-1}[\nu P_1 h^{-1} + \nu S_1 R^{-1} + RP_{1x}h^{-1} + (1 - \nu)S_{3x} + RS_{1xx}] + (1/24)h^2\{2Rw_{xxxxx} + E_s^{-1}[3(1 + 3\nu)P_{3x}(hR)^{-1} - \theta(4 - 6\nu - \nu^2)P_{1xx}h^{-1} + \theta(4 - 3\nu - 4\nu^2)S_{1xx}R^{-1} + 3\theta\nu RP_{3xxx}h^{-1} + 3\nu S_{3xxx} - \theta(4 - 5\nu)RS_{1xxxx}]\} = 0 \quad [6b]$$

Most of the load terms in these equations are of course uninteresting. The solution will contain additive constants in w and u_x

that must be chosen to fit Equation [5b] and the boundary conditions. The equations agree with the results given in Sec. 81 of Timoshenko's "Theory of Plates and Shells" except for small corrections included here in the load terms.

Purely Transverse Case. $u = 0$, all x-derivatives zero, $P_1 = S_1 = 0$. In this case dropping further terms is dangerous because the membrane displacement parts of the equations are not independent; it is possible, in fact, to eliminate these terms entirely. At the same time, in the h^2 bracket of the w equation, let $-v_2/R^2$ be replaced by w/R^4 by the usual process of modification. This could have been done equally well in the original process of simplification.

The result is a differential equation for w alone

$$w_{,xxxx} + 2w_{,xx}R^{-2} + w_{,\theta\theta}R^{-4} - 12(h^2E_2)^{-1}[P_2(hR)^{-1} + 2S_2R^{-2} + P_{3,\theta}h^{-1} + S_{1,x}R^{-1} + S_{2,\theta\theta}] + (1/2)\theta E_{,\theta}^{-1}[12(1-\nu)S_2R^{-2} + 6(1-\nu)P_{3,\theta}(hR^2)^{-1} + 2(2-\nu)S_{1,x}R^{-3} - \xi\theta(10 - 5\nu - 10\nu^2 + 8\nu^3)P_{2,\theta\theta}(hR)^{-1} - 6\xi\theta(1 + \nu - \nu^2)S_{2,\theta\theta}R^{-2} - \xi\theta(4 + \nu - 4\nu^2 + 2\nu^3)P_{3,\theta\theta\theta}h^{-1} - 3\xi\theta(2 - \nu - 2\nu^2 + 2\nu^3)S_{2,\theta\theta\theta}R^{-1} - \xi\theta(8 - \nu - 8\nu^2 + 4\nu^3)S_{2,\theta\theta\theta\theta}] = 0$$

If $P_2 = S_2 = 0$, this equation can at once be integrated once, and for a shell unloaded on its faces it can be integrated completely.

Simplified Stress Resultants

Formulas were given in reference 2 for the ten resultant stress forces or moments, whose values may be needed at least at the boundaries of the shells. The complete load terms were not given, however, hence they will be cited in the Appendix. In the case of equilibrium, these expressions, being likewise accurate only through order h^2, can be modified by the same procedure that has been described for the equations of equilibrium. The errors thus introduced are again of order h^4 and hence very unlikely to be important, with a possibility that the total error is decreased.

One possible form of the expressions for the resultants that may be obtained in this manner, somewhat simpler in the displacement terms than the original, is the following; the notation is that of reference 2, and the shell is assumed to be in equilibrium

$$N_x = \theta\nu hS_2 + hE_x(u_{,x} + \nu v_{,\theta} + \nu wR^{-1}) + (1/24)\theta h^3E_x[-\nu(1-\nu)(u_{,xxx} + v_{,xx\theta}) - (2 - 3\nu - 2\nu^2)w_{,xxx}R^{-1} + \nu(1 + 2\nu)w_{,\theta\theta}R^{-1} - \nu(2 + \nu)v_{,\theta}R^{-2}] + (1/24)\theta h^3[9\nu P_3(hR)^{-1} + (2 + \nu)P_{1,x}h^{-1} + 3\nu P_{2,\theta}h^{-1} + \theta(4 - \nu - 6\nu^2)S_{1,x}R^{-1} - \theta\nu(2 + \nu)S_{2,\theta}R^{-1} - (1-\nu)S_{1,xx} - \nu S_{2,x\theta}] \quad [7a]$$

$$N_\theta = \theta\nu hS_2 + hE_\theta(\nu u_{,x} + v_{,\theta} + wR^{-1}) + (1/24)\theta h^3E_\theta[-\nu(1-\nu)(u_{,xxx} + v_{,xx\theta}) + \nu(1 + 2\nu)w_{,xx}R^{-1} + (2 + \nu)(w_{,\theta\theta}R^{-1} - v_{,\theta}R^{-2})] + (1/24)\theta h^3[3(1 + 2\nu)P_3(hR)^{-1} + 3\nu P_{1,x}h^{-1} + \xi(2 + 2\nu + \nu^2)P_{2,\theta}h^{-1} + \xi\theta(2 + 3\nu - 6\nu^2 - 5\nu^3)S_{1,x}R^{-1} + (2 + \nu)P_{2,\theta}h^{-1} + \theta(2 - 5\nu^2)S_{1,x}R^{-1} - \theta\nu(5 - 2\nu)S_{2,\theta}R^{-1} - \nu S_{2,xx} - (1-\nu)S_{2,\theta\theta}] \quad [7b]$$

$$N_{x\theta} = (1/2)(1-\nu)hE_x(u_{,\theta} + v_{,x}) + (1/24)h^3E_x[\nu(u_{,xx\theta} + v_{,x\theta\theta}) - (1 - 2\nu)w_{,x\theta}R^{-1} + (1-\nu)v_{,x}R^{-2}] + (1/24)h^3[P_{1,\theta}h^{-1} + P_{2,x}h^{-1} + 3S_{2,x}R^{-1} - \theta(1 - 2\nu)S_{2,x\theta}] \quad [7c]$$

$$N_{\theta x} = (1/2)(1-\nu)hE_\theta(u_{,\theta} + v_{,x}) + (1/24)h^3E_\theta[\nu(u_{,x\theta} + v_{,x\theta\theta}) + w_{,x\theta}R^{-1} + (1-\nu)u_{,\theta}R^{-2}] + (1/24)h^3[P_{1,\theta}h^{-1} + P_{2,x}h^{-1} - 2S_{1,\theta}R^{-1} + S_{2,x}R^{-1} - \theta(1 - 2\nu)S_{2,x\theta}] \quad [7d]$$

$$Q_x = hS_1 - (1/12)h^3E_x[w_{,xxx} + w_{,x\theta\theta} + (1-\nu)u_{,x\theta}R^{-1} - \nu w_{,xx}R^{-1}] + (1/12)h^3[2P_1(hR)^{-1} - S_1R^{-2} + \theta(2-\nu)S_{1,xx} + S_{1,\theta\theta} + \theta S_{2,x\theta}] \quad [7e]$$

$$Q_\theta = hS_2 - (1/12)h^3E_\theta[w_{,xxx} + w_{,x\theta\theta} + w_{,\theta}R^{-2} + (1/2)(3-\nu)u_{,x\theta}R^{-1} + (1/2)v_{,xx}R^{-1}] + (1/12)h^3[-6S_2R^{-2} - 3P_{3,\theta}h^{-1} - \theta(2-\nu)S_{2,\theta}R^{-1} - \theta(2 - 3\nu)S_{1,x\theta} + S_{2,xx} - \theta(1 - 2\nu)S_{2,\theta\theta}] \quad [7f]$$

$$M_x = -(1/12)h^3E_x[w_{,xx} + \nu w_{,\theta\theta} - (1-\nu^2)u_{,x}R^{-1} - \nu v_{,\theta}R^{-1}] + (1/12)h^3[\nu P_3h^{-1} + 2\nu S_1R^{-1} + \theta(2-\nu^2)S_{1,x} + \theta\nu(2-\nu)S_{2,\theta}] \quad [7g]$$

$$M_\theta = -(1/12)h^3E_\theta(\nu w_{,xx} + w_{,\theta\theta} - v_{,\theta}R^{-1}) + (1/12)h^3[-P_{3,\theta}h^{-1} - \theta(1-2\nu)S_{1,x} + \theta S_{2,\theta}] \quad [7h]$$

$$M_{x\theta} = -(1/12)h^3E_x(1-\nu)(w_{,x\theta} - v_{,\theta}R^{-1}) + (1/12)h^3(S_{1,\theta} + S_{2,x}) \quad [7i]$$

$$M_{\theta x} = -(1/12)h^3E_\theta(1-\nu)[w_{,x\theta} + (1/2)u_{,\theta}R^{-1} - (1/2)v_{,x}R^{-1}] + (1/12)h^3(S_{1,\theta} + S_{2,x}) \quad [7j]$$

When substituted in the usual conditions for equilibrium, these resultants do not quite produce the simplified Equations [4 *a*, *b*, *c*], but the differences can be shown in the usual way to be of order h^4. There does not seem to be any objection in principle to the use of Equations [7*a* to *j*] to express boundary conditions in conjunction with the use of Equations [4 *a*, *b*, *c*], or, for that matter, with the original Equations [3 *a*, *b*, *c*].

Appendix

Equations of motion complete through terms of order h^2 (including load terms omitted in reference 2)[3] are as follows. Let [3*a*], [3*b*], [3*c*] denote the left-hand members of the equations of equilibrium, Equations [3 *a*, *b*, *c*], respectively. Then, two dots denoting as usual double differentiation with respect to the time

$$\rho\ddot{u} = E_x[3a] - (1/24)\theta^2h^2\rho E_x^{-1}[2(1-\nu)\ddot{P}_1h^{-1} + 4(1-\nu)\ddot{S}_1R^{-1} - \theta(1-2\nu)(1-3\nu)\ddot{S}_{2,x}] \quad [8a]$$

$$\rho\ddot{v} = E_\theta[3b] - (1/24)\theta^2h^2\rho E_\theta^{-1}[2(1-\nu)\ddot{P}_2h^{-1} + 10(1-\nu)\ddot{S}_2R^{-1} - \theta(1-2\nu)(1-3\nu)\ddot{S}_{1,x}] \quad [8b]$$

$$\rho\ddot{w} = -E_\theta[3c] - (1/24)\theta^2h^2\rho E_\theta^{-1}[(1-2\nu)\ddot{P}_3h^{-1} + \theta(2 - 9\nu + 10\nu^2)\ddot{S}_2R^{-1} + 2(2-3\nu)(\ddot{S}_{1,x} + \ddot{S}_{2,\theta})] \quad [8c]$$

Similarly, to make Equations [13*a* to *j*] of reference 2 for the stress resultants complete through terms of order h^2 there must be added on the right side, in the equation representing the following quantity indicated in parentheses, respectively

[3] In the partial equivalent of [8*b*] in reference 2, the coefficients of $Z_{2,\theta}$ and $S_{2,\theta}$ are slightly in error.

$$(N_\theta): \quad (1/24)\theta^2h^3[\nu(5-6\nu)P_3(hR)^{-1} - \theta\nu(4-11\nu+6\nu^2)S_3R^{-2} + 2P_{1z}h^{-1} + 2\nu(2-\nu)P_{2\theta}h^{-1} + 2(2-2\nu-\nu^2)S_{1z}R^{-1} - 4\nu(1-\nu)S_{2\theta}R^{-1} - \theta(1-3\nu+2\nu^2-2\nu^3)S_{1zz} - \theta\nu(1-3\nu)S_{2\theta\theta} - 2\theta\nu(1-2\nu)\rho E_\theta^{-1}S_3]$$

$$(N_z): \quad (1/24)\theta^2h^3[(1-2\nu^2)P_3(hR)^{-1} - \theta(2-\nu-10\nu^2+8\nu^3)S_3R^{-2} + 2\nu(2-\nu)P_{1z}h^{-1} + 2P_{2z}h^{-1} - 2\nu S_{1z}R^{-1} - 2(1+3\nu-4\nu^2)S_{2z}R^{-1} - \theta\nu(1-3\nu)S_{2zz} - \theta(1-3\nu+2\nu^2-2\nu^3)S_{1\theta\theta} - 2\theta\nu(1-2\nu)\rho E_z^{-1}S_3]$$

$$(N_{z\theta}): \quad (1/24)h^3[P_{1\theta}h^{-1} + P_{2z}h^{-1} + 3S_{2z}R^{-1} - \theta(1-2\nu)S_{1z\theta}]$$

$$(N_{\theta z}): \quad (1/24)h^3[P_{1z}h^{-1} + P_{2\theta}h^{-1} - 2S_{1z}R^{-1} + S_{2z}R^{-1} - \theta(1-2\nu)S_{1z\theta}]$$

$$(Q_\theta): \quad (1/12)\theta h^3[2(1-\nu)P_1(hR)^{-1} - (1-\nu)S_1R^{-2} + P_{2\theta}h^{-1} + \theta(1-2\nu)S_{2z}R^{-1} + (3-\nu)S_{1zz} + (1-\nu)S_{1\theta\theta} + 2S_{2z\theta} - 2\rho E_\theta^{-1}S_1]$$

$$(Q_z): \quad (1/12)\theta h^3[(1-\nu)P_3(hR)^{-1} - 4(1-\nu)S_3R^{-2} + P_{2z}h^{-1} + \theta(2-7\nu+4\nu^2)S_{3z}R^{-1} + 2S_{1z\theta} + (1-\nu)S_{2zz} + (3-\nu)S_{2\theta\theta} - 2\rho E_z^{-1}S_3]$$

$$(M_\theta): \quad (1/12)\theta h^3[\nu P_3h^{-1} + \theta\nu(2-3\nu)S_3R^{-1} + 2S_{1z} + 2\nu S_{2\theta}]$$

$$(M_z): \quad (1/12)\theta h^3[\nu P_3h^{-1} + \theta(1-2\nu)S_3R^{-1} + 2\nu S_{1z} + 2S_{2\theta}]$$

$$(M_{z\theta} \text{ and } M_{\theta z}): \quad (1/12)h^3(S_{1\theta} + S_{2z})$$

Remarks on Donnell's Equations[1]

By JOSEPH KEMPNER,[2] BROOKLYN, N. Y.

Flügge's set of differential equations of equilibrium for circular cylindrical shells is expressed in a form analogous to the Donnell equations. The results of solutions of the two sets of equations for a simply supported cylinder under a centrally applied, uniformly distributed radial line load over a generator segment, as well as under sinusoidally applied line loads, are in very good agreement for the particular geometry investigated.

DONNELL's equations for the analysis of circular cylindrical shells have been known for the past 20 years.[3] Recently they have been used to calculate deflections and stresses caused by lateral loads.[4] It is interesting to note that for this purpose the equations can be derived by making suitable approximations to the strains as in Donnell's report[3] without any additional order-of-magnitude arguments. If the membrane and bending and twisting strains in the cylinder are expressed in the same manner as in the usual plane-stress theories of infinitesimal stretching and bending of thin flat plates except for the circumferential membrane strain, and the latter is assumed to be represented by the relation

$$\epsilon_\varphi = (\partial v/\partial\varphi) - w \qquad [1]$$

where v and w, respectively, are the ratios of the circumferential and inward radial displacements to the cylinder radius and φ is the circumferential angular co-ordinate, calculation of the total potential energy of the system and its variation with respect to v, w, and the nondimensional axial displacement u results in the following equations

$$\nabla^4 w - (1-\nu^2)(1/Ek^2)\sigma_\varphi - (a^3/D)q = 0 \qquad [2]$$

$$(\partial\sigma_x/\partial x) + (\partial\tau_{x\varphi}/\partial\varphi) + (a/h)X = 0 \qquad [3]$$

$$(\partial\tau_{x\varphi}/\partial x) + (\partial\sigma_\varphi/\partial\varphi) + (a/h)\Phi = 0 \qquad [4]$$

In Equations [2] to [4] E is Young's modulus, ν is Poisson's ratio, a and h, respectively, are the cylinder radius and wall thickness, $D = (1/12)Eh^3/(1-\nu^2)$, $k^2 = (1/12)(h/a)^2$, x is the distance measured in the axial direction along a generator divided by a, σ_x, σ_φ, and $\tau_{x\varphi}$, respectively, are the axial, circumferential, and shear membrane stresses, and q, X, and Φ, respectively, are applied surface loads in the inward radial, axial, and circumferential directions. The analysis does not include terms required for buckling problems.[5]

When expressed in terms of displacements only, Equations [2] to [4] appear as

$$\nabla^4 w + (1/k^2)(w - \dot{v} - \nu u') - (a^3/D)q = 0 \qquad [5]$$

$$u'' + (1/2)(1-\nu)\ddot{u} + (1/2)(1+\nu)\dot{v}' - \nu w' + (a^3/D)k^2X = 0 \qquad [6]$$

$$\ddot{v} + (1/2)(1-\nu)v'' + (1/2)(1+\nu)\dot{u}' - \dot{w} + (a^3/D)k^2\Phi = 0 \qquad [7]$$

in which a prime after a symbol indicates differentiation with respect to x and a dot over a symbol indicates differentiation with respect to φ. After differentiation and elimination, these equations can be written in the usual form of Donnell's equations.[3]

$$\nabla^8 w + (1/k^2)(1-\nu^2)w^{iv} - (a^3/D)\{\nabla^4 q + \ddot{X}' - \nu X''' - (2+\nu)\dot{\Phi}'' - \dddot{\Phi}\} = 0 \qquad [8]$$

$$\nabla^4 u = \nu w''' - \ddot{w}' - (a^3/D)k^2\{X'' + [2/(1-\nu)]\ddot{X} - [(1+\nu)/(1-\nu)]\dot{\Phi}''\} \qquad [9]$$

$$\nabla^4 v = (2+\nu)\dot{w}'' + \dddot{w} + (a^3/D)k^2\{[(1+\nu)/(1-\nu)]\dot{X}' - [2/(1-\nu)]\Phi'' - \ddot{\Phi}\} \qquad [10]$$

A more accurate set of differential equations, corresponding to Equations [5] to [7], is given by Flügge[7] and Biezeno and Grammel.[8] It is

$$\nabla^4 w + 2\ddot{w} + w + (1/2)(3-\nu)\dot{v}'' + u''' - (1/2)(1-\nu)\ddot{u}' + (1/k^2)(w - \dot{v} - \nu u') - (a^3/D)q = 0 \qquad [11]$$

$$u'' + (1/2)(1-\nu)\ddot{u} + (1/2)(1+\nu)\dot{v}' - \nu w' + k^2[w''' - (1/2)(1-\nu)\ddot{w}' + (1/2)(1-\nu)\ddot{u}] + (a^3/D)k^2X = 0 \qquad [12]$$

$$\ddot{v} + (1/2)(1-\nu)v'' + (1/2)(1+\nu)\dot{u}' - \dot{w} + k^2[(1/2)(3-\nu)v'' + (3/2)(1-\nu)v''] + (a^3/D)k^2\Phi = 0 \qquad [13]$$

After differentiation and elimination, this set of equations can be expressed in a form analogous to the Donnell equations

---

[1] Submitted to the Knolls Atomic Power Laboratory, which is operated by the General Electric Company for the U. S. Atomic Energy Commission, Contract No. W-31-109 Eng-52.

[2] Assistant Professor of Aeronautical Engineering, Polytechnic Institute of Brooklyn.

[3] "Stability of Thin Walled Tubes Under Torsion," by L. H. Donnell, NACA Technical Report No. 479, 1933.

[4] "Line Load Applied Along Generators of Thin-Walled Circular Cylindrical Shells of Finite Length," by N. J. Hoff, J. Kempner, and F. V. Pohle, *Quarterly of Applied Mathematics*, vol. 11, January, 1954, p. 411.

Contributed by the Applied Mechanics Division and presented at the Annual Meeting, New York, N. Y., November 28–December 3, 1954, of THE AMERICAN SOCIETY OF MECHANICAL ENGINEERS.

Discussion of this paper should be addressed to the Secretary, ASME, 29 West 39th Street, New York, N. Y., and will be accepted until April 11, 1955, for publication at a later date. Discussion received after the closing date will be returned.

NOTE: Statements and opinions advanced in papers are to be understood as individual expressions of their authors and not those of the Society. Manuscript received by ASME Applied Mechanics Division, March 9, 1954. Paper No. 54—A-28.

[5] It may be noted that the strain-displacement relations referred to can be obtained from those of Flügge[6] if h is considered to be very much smaller than a.

[6] "Statik und Dynamik der Schalen," by W. Flügge, Julius Springer, Berlin, Germany, 1934, p. 115.

[7] Ibid., p. 118.

[8] "Technische Dynamik," by C. B. Biezeno and R. Grammel, Julius Springer, Berlin, Germany, 1939, p. 469.

$$\nabla^8 w + 2\nu(1 + 3k^2)w^{vi} + [6 + 3k^2(2 - \nu + \nu^2)]\ddot{w}^{iv} + [2(4 - \nu) + (7 - 5\nu)k^2 + 3(1 - \nu)k^4]\ddot{\ddot{w}}'' + 2(1 + k^2)\dddot{\dddot{w}} + (1/k^2)(1 + 3k^2)(1 + k^2 - \nu^2)w^{iv} + [2 + (1/2)(1 - \nu)(1 + k^2)(4 + 3k^2)]\ddot{w}'' + (1 + k^2)\ddot{\ddot{w}} + k^2\{(2 - 3k^2)w^{viii} + (1/2)[(11 - 3\nu) + 9(1 - \nu)k^2]\ddot{w}^{vi} + [3(2 - \nu) - \nu^2k^2]\dddot{\dddot{w}}^{iv} + (1/2)[(7 - 3\nu) + 3(1 - \nu)k^2]\ddot{\ddot{w}}'' + \ddot{\ddot{w}}\ddot{\ddot{w}}\} - (a^3/D)\{\nabla^4 q + \ddot{X}' - \nu(1 + 3k^2)X''' + k^2[(1 + 3k^2)X^v - \ddot{\ddot{X}}' - (3/2)(1 - \nu)k^2\ddot{X}'''] - (2 + \nu)\dot{\Phi}'' - (1 + k^2)\ddot{\ddot{\Phi}} + 2k^2\dot{\Phi}^{iv} + k^2[2 + (1/2)(3 - \nu)k^2]\dddot{\dddot{\Phi}}''\} = 0 \quad \ldots\ldots [14]$$

$$\nabla^{*4}u = (1 + 3k^2)\nu w''' - \ddot{w}' + k^2[\ddot{\ddot{w}}' - (1 + 3k^2)w^v + (3/2)(1 - \nu)k^2\ddot{w}'''] - (a^3/D)k^2\{(1 + 3k^2)X'' + [2/(1 - \nu)]\ddot{X} - [(1 + \nu)/(1 - \nu)]\dot{\Phi}'\} \quad [15]$$

$$\nabla^{*4}v = (2 + \nu)\dot{w}'' + (1 + k^2)\dddot{\dddot{w}} - 2k^2\{\dot{w}^{iv} + [1 + (1/4)(3 - \nu)k^2]\ddot{\ddot{w}}''\} + (a^3/D)k^2\{[(1 + \nu)/(1 - \nu)]\dot{X}' - [2/(1 - \nu)]\Phi'' - (1 + k^2)\ddot{\Phi}\} \quad \ldots\ldots [16]$$

where

$$\nabla^{*4} = \nabla^4 + 3k^2(\partial^4/\partial x^4) + (k^2/2)(4 + 3k^2)(1 - \nu)(\partial^4/\partial x^2\partial\varphi^2) + k^2(\partial^4/\partial\varphi^4)$$

These equations, which can be simplified somewhat if $k^2 \ll 1$, are just as exact as the original set given by Flügge from which they were derived. It is difficult to say how good an approximation to them the Donnell Equations [8] to [10] are. Obviously Equations [8] to [10] are inaccurate when a circular cylinder deflects slightly into an elliptic shape. However, when there are many waves around the circumference, these equations should be satisfactory.[3]

It appears that the equations are also useful in calculating deflections and stresses when the loads are applied to comparatively small regions of the shell. In such cases the deflections are localized and can be represented by series comprising many higher harmonics.[4]

A particular problem has been worked out numerically to prove the adequacy of the Donnell equations by way of example. It consisted of a simply supported cylinder, free from applied loads except for a centrally located, uniformly distributed inward-radial line load over a segment of the generator $\varphi = 0$. The Donnell Equations [8] to [10] as well as the "exact" Equations [14] to [16] were solved by the method described by Hoff, Kempner, and Pohle.[4]

Numerical Problem

The line load was represented by the Fourier series

$$(2P^*/\pi\delta)\sum_{m=1,3,\ldots}^{\infty}(1/m)\sin(m\pi\delta/L)\cos(m\pi ax/L) \quad \ldots [17]$$

in which 2δ is the distance over which the load is distributed, L is the cylinder length, P^* is the resultant load, and x is the nondimensional axial co-ordinate measured from the mid-point of the generator $\varphi = 0$. The defining parameters were chosen as

$$a = 35 \text{ in.}, \quad h = 0.625 \text{ in.}, \quad L = 140 \text{ in.}$$

$$E = 30 \times 10^6 \text{ psi}, \quad \nu = 0.3, \quad 2\delta = 7 \text{ in.}$$

The deflection w, axial moment resultant M_x, circumferential moment resultant M_φ, and membrane stresses σ_x and σ_φ were computed at $x = 0$, $\varphi = 0$ from solutions of both the "exact" equations and the Donnell equations. The results are presented in Table 1. Also in Table 2 comparisons are presented of the first six Fourier components obtained from both sets of equations for the displacement and circumferential moment resultant at $x = 0$, $\varphi = 0$. The results show that for short cylinders loaded over small regions of their surface the simple Donnell equations are quite adequate for the determination of the deflections and the stresses in the neighborhood of the loads.

TABLE 1 COMPARISONS OF RESULTS OF SOLUTIONS OF "EXACT" AND APPROXIMATE SHELL EQUATIONS

(All quantities are computed at $x = 0$, $\varphi = 0$)

	From solution of "exact" Eq. [14]–[16]	From solution of Donnell Eq. [8]–[10]
$(w/P^*) \times 10^6$	0.169	0.160
M_x/P^*	0.107	0.106
M_φ/P^*	0.196	0.196
σ_x/P^*	−0.424	−0.412
σ_φ/P^*	−0.370	−0.377

TABLE 2 COMPARISONS OF FOURIER COMPONENTS OF DISPLACEMENT AND CIRCUMFERENTIAL MOMENT RESULTANT AT $x = 0$, $\varphi = 0$

	$(w_m/P^*) \times 10^6$		$M_{\varphi m}/P^*$	
m	Eq. [14] to [16]	Eq. [8] to [10]	Eq. [14] to [16]	Eq. [8] to [10
1	0.112	0.104	0.0501	0.0497
3	0.0219	0.0214	0.0282	0.0282
5	0.0107	0.0106	0.0213	0.0213
7	0.00675	0.00669	0.0174	0.0174
9	0.00473	0.00470	0.0147	0.0147
11	0.00346	0.00345	0.0126	0.0126

Temperature Distribution and Efficiency of a Heat Exchanger Using Square Fins on Round Tubes[1]

By H. ZABRONSKY,[2] NEW YORK, N. Y.

Formulas are obtained for the temperature and fin efficiency of a heat exchanger consisting of round tubes with square fins. Curves are presented for the fin efficiency as a function of tube radius, all other parameters remaining fixed, and also for the temperature distribution in one particular fin.

Nomenclature

The following nomenclature is used in the paper:

a = side of a square fin, ft
A = area of a square fin, sq ft
b = fin half-thickness, ft
c = $(h/bk)^{1/2}$
D = plane region of single fin
grad T = gradient of T
h = film coefficient of heat transfer, Btu/hr sq ft deg F
$I_n(x)$ = modified Bessel function of first kind and order n
k = thermal conductivity, Btu/hr ft deg F
$K_n(x)$ = modified Bessel function of second kind and order n
p = tube radius, ft
q = rate of heat flow through an element of fin
r, θ = polar co-ordinates
s = arc length
S = surface area
$T(x, y)$ = temperature at the point (x, y) of fin
T_0 = constant temperature of tube walls
$W = \frac{a}{2} - p$
x, y = rectangular co-ordinates
ΔT = Laplacian of $T = \frac{\partial^2 T}{\partial x^2} + \frac{\partial^2 T}{\partial y^2}$
ϕ = fin efficiency
$\frac{\partial}{\partial n}$ = derivative normal to curve

Introduction

This paper treats the problem of the transfer of heat between two fluids in a heat exchanger composed of round tubes with square fins. The fins are arranged as shown in Fig. 1. The fins shown in the figure are all from a single metallic sheet which is large compared to the diameter of a single tube. Advantage is taken of this fact by assuming that the fin sheet is infinite in extent. This assumption affects the results very little and simplifies the problem mathematically. No assumptions regarding the relative size of a single fin and the tube diameter are made.

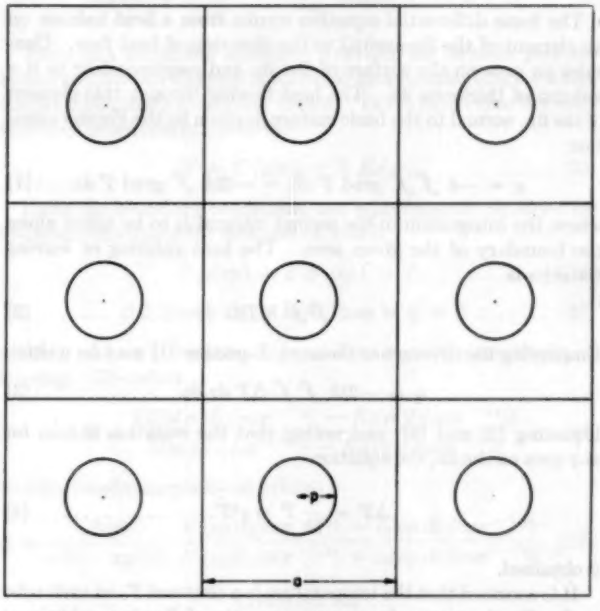

Fig. 1 Round Tubes With Square Fins

The use of fins in heat exchangers increases the heat flow per unit of basic surface. The average surface temperature of the fins tends to approach the temperature of the surrounding fluid. Thus a temperature gradient exists in the fins and the heat flow is less than it would be if the fin temperature were constant throughout. The "fin efficiency" is defined to be the ratio of the amount of heat transferred to the amount of heat which would be transferred if the fin had a constant temperature throughout.

Fin efficiencies have been determined for fins of various shapes[3] where the fin is symmetric with respect to the axis of the tube, but the case treated here apparently has not been treated heretofore.

Mathematical Treatment—Assumptions

The mathematical analysis is based on the following assumptions which are common to most previous investigations:[3]

1 Steady state persists.
2 Fin material is homogeneous and isotropic.
3 There are no energy sources within the fin, the heat being supplied from within the tubes.

[3] "Efficiency of Extended Surface," by K. A. Gardner, Trans. ASME, vol. 67, 1945, pp. 621–631.

---

[1] This paper was written at K-25, Oak Ridge, Tenn.; work performed under Contract No. W-7405-eng-26, Report No. K-929, issuance date August 15, 1952; published by permission of the Atomic Energy Commission, Oak Ridge, Tenn.

[2] Design Engineer, Ford Instrument Company, New York, N. Y.

Contributed by the Applied Mechanics Division and presented at the Annual Meeting, New York, N. Y., November 28–December 3, 1954, of The American Society of Mechanical Engineers.

Discussion of this paper should be addressed to the Secretary, ASME, 29 West 39th Street, New York, N. Y., and will be accepted until April 11, 1955, for publication at a later date. Discussion received after the closing date will be returned.

Note: Statements and opinions advanced in papers are to be understood as individual expressions of their authors and not those of the Society. Manuscript received by ASME Applied Mechanics Division, July 9, 1953. Paper No. 54—A-12.

4 The heat-transfer coefficient is the same over all of the fin surfaces.

5 The thermal conductivity of the fin material is a constant.

6 The temperature of the surrounding fluid is constant and the temperature of the tube wall is constant.

7 The fin thickness is so small compared to its height that temperature gradients, normal to the fin surface, may be neglected.

8 The heat transfer through the outermost edge of the fin is negligible compared to that passing through the sides.

Derivation of Basic Differential Equation and Boundary Conditions

The basic differential equation results from a heat balance on an element of the fin normal to the direction of heat flow. Consider an area on the surface of the fin and corresponding to it a volume of thickness $2b$. The heat flowing through this element of the fin, normal to the basic surface, is given by the Fourier equation

$$q = -k \iint \text{grad } T \, dS = -2bk \int \text{grad } T \, ds \quad [1]$$

where the integration in the second integral is to be taken along the boundary of the given area. The heat entering or leaving the sides is

$$q = -2 \iint h \, T dx \, dy \quad [2]$$

Employing the divergence theorem, Equation [1] may be written

$$q = -2bk \iint \Delta T \, dx \, dy \quad [3]$$

Equating [2] and [3], and noting that the equation is true for any area on the fin, the equation

$$\Delta T = \frac{h}{bk} T = c^2 T \quad [4]$$

is obtained.

It is assumed that the temperature is a constant T_0 on each tube wall. Furthermore, by symmetry, the following additional boundary conditions are obtained:

$$\left.\begin{aligned} &\frac{\partial T}{\partial x} = 0; \quad x = 0, \quad p \leqq y \leqq \frac{a}{2} \\ &\frac{\partial T}{\partial x} = 0; \quad x = \frac{a}{2}, \quad 0 \leqq y \leqq \frac{a}{2} \\ &\frac{\partial T}{\partial y} = 0; \quad y = 0, \quad p \leqq x \leqq \frac{a}{2} \\ &\frac{\partial T}{\partial y} = 0; \quad y = \frac{a}{2}, \quad 0 \leqq x \leqq \frac{a}{2} \end{aligned}\right\} \quad [5]$$

Solution of the Equation. Owing to the fact that the same conditions hold for any square the solution of Equation [4] must be an even doubly periodic function which is constant on the circles

$$(x - ma)^2 + (y - na)^2 = p^2, \quad (m = 0, \pm 1, \pm 2, \ldots; \quad n = 0, \pm 1, \pm 2, \ldots)$$

Even double periodicity is a condition of symmetry which automatically fulfills Equation [5].

If $T(x, y)$ is the solution of the problem for $\Delta T = T$, then $T(cx, cy)$ is the solution of $\Delta T = c^2 T$. In polar co-ordinates $\Delta T = T$ becomes

$$\frac{\partial^2 T}{\partial r^2} + \frac{1}{r}\frac{\partial T}{\partial r} + \frac{\partial^2 T}{\partial \theta^2} = T \quad [6]$$

Since $T = T_0$ on the circle $r = p$, a solution of Equation [6], which is a function of r alone, is sought. Equation [6] then simplifies to

$$\frac{d^2 T}{dr^2} + \frac{1}{r}\frac{dT}{dr} - T = 0 \quad [7]$$

Equation [7] has the two independent solutions

$$I_0(r) = \sum_{n=0}^{\infty} \frac{\left(\frac{r}{2}\right)^{2n}}{(n!)^2} \quad [8]$$

$$K_0(r) = \int_1^{\infty} e^{-rt}(t^2 - 1)^{-1/2} dt \; (r > 0) \quad [9]$$

$I_0(r)$ is an entire function which behaves somewhat like e^r as r tends to infinity. $K_0(r)$, on the other hand, behaves like $\log 1/r$ near $r = 0$ and tends to zero very rapidly as r tends to infinity.[4] In fact

$$K_0(r) \sim \left(\frac{\pi}{2}\right)^{1/2} \frac{e^{-r}}{r^{1/2}}. \quad [10]$$

The expression on the right of Equation [10] is, moreover, an extremely accurate approximation to $K_0(r)$ even for relatively "small" values of r.[4]

The function

$$T(x, y) = \sum_{-\infty}^{\infty} \sum_{-\infty}^{\infty} K_0 \{c[(x - ma)^2 + (y - na)^2]^{1/2}\} \quad [11]$$

is an even doubly periodic solution of $\Delta T = c^2 T$, which converges uniformly and absolutely in any closed region excluding the points (ma, na) and behaves like

$$-\ln\{c[(x - ma)^2 + (y - na)^2]^{1/2}\}$$

in the neighborhood of the point (ma, na). Owing to the extremely rapid convergence of $K_0(r)$ to the limit zero as r tends to infinity, $T(x, y)$ is nearly constant on the circles

$$(x - ma)^2 + (y - na)^2 = p^2$$

On the circle $r = 0.075417$, for instance, the values of $T(x, y)$ for $\theta = 90$ deg and $\theta = 45$ deg are 1.115 and 1.106, respectively. Therefore an accurate solution of the problem is given by the function $T_0 T(x, y)/M$ where M is the mean value of $T(x, y)$ on the circle $x^2 + y^2 = p^2$. The following addition theorem for Bessel functions is now used to find the mean value of $T(x, y)$[5]

$$K_0(w) = K_0(Z) I_0(z) + 2 \sum_{m=1}^{\infty} K_m(Z) I_m(z) \cos m\phi \quad [12]$$

where

$$w = (Z^2 + z^2 - 2Zz \cos u)^{1/2}$$

Now

$$T(x, y) = \sum_{-\infty}^{\infty} \sum_{-\infty}^{\infty} K_0\{c[(x - ma)^2 + (y - na)^2]^{1/2}\}$$

$$= \sum_{-\infty}^{\infty} \sum_{-\infty}^{\infty} K_0\{c[r^2 - 2ra(m^2 + n^2)^{1/2} \cos(\theta - \psi) + a^2(m^2 + n^2)]^{1/2}\} \quad [13]$$

where $\psi = \arctan (n/m)$. Substituting

$$Z = ac(m^2 + n^2)^{1/2}, \; z = cr, \text{ and } u = \theta - \psi$$

[4] "Theory of Bessel Functions," by G. N. Watson, Cambridge, England, 1922, p. 202.

[5] Ibid., pp. 358-359.

Equation [12] becomes

$$K_0\{c[r^2 - 2ra(m^2 + n^2)^{1/2}\cos(\theta - \psi) + a^2(m^2 + n^2)]^{1/2}\} \quad [14]$$

$$= K_0[ac(m^2 + n^2)^{1/2}]I_0(cr) + 2\sum_{l=1}^{\infty} K_l[ac(m^2 + n^2)^{1/2}]\, I_l(cr) \cos l(\theta - \psi)$$

Therefore the mean value of $T(x, y)$ on the circle $x^2 + y^2 = p^2$ is

$$K_0(cp) + I_0(cp) \sum_{-\infty}^{\infty} \sum_{-\infty}^{\infty}{}' K_0[ac(m^2 + n^2)^{1/2}] \quad [15]$$

The prime in the double summation indicates that the term for $m = n = 0$ is omitted. Therefore the temperature $T(x, y)$, at any point of the fin is given by the formula

$$T(x, y) = \frac{T_0 \sum_{-\infty}^{\infty} \sum_{-\infty}^{\infty} K_0\{c[(x - ma)^2 + (y - na)^2]^{1/2}\}}{I_0(pc) \sum_{-\infty}^{\infty} \sum_{-\infty}^{\infty}{}' K_0[ac(m^2 + n^2)^{1/2}] + K_0(pc)} \quad [16]$$

It should be emphasized that the transition from Equation [6] to Equation [7] is a simplification which results in a satisfactory approximation. Equation [11] does not exactly represent the boundary condition $T = T_0$ on $r = p$. Equation [16] is a smoothing of Equation [11] which fulfills the foregoing boundary condition even more accurately.

The fin efficiency may now be computed by evaluating the expression

$$\frac{1}{AT_0}\int_D\int T(x, y)\, dx\, dy \quad [17]$$

where A is the area of a square fin and D represents the plane region of a single fin, over which the integration is to be performed. The fin efficiency may be obtained directly, using Green's formula and the addition Theorem [12]

$$\int_D\int (V\,\Delta T - T\,\Delta V)\, dx\, dy = -\int\left(V\frac{\partial T}{\partial n} - T\frac{\partial V}{\partial n}\right)d \quad [18]$$

Let $V = 1$. Then, since $\Delta V = 0$, $\partial V/\partial n = 0$, $\Delta T = c^2T$, and $\partial T/\partial n$ vanishes on the sides of the square, Equation [18] simplifies to

$$c^2\int\int T(x, y)\, dx\, dy = -\int_{\substack{0 \\ D \\ (r=p)}}^{2\pi} \frac{\partial T}{\partial n}\, r\, d\theta \quad [19]$$

Now, making use of Equation [14]

$$\int_{\substack{0 \\ (r=p)}}^{2\pi} \frac{\partial K_0}{\partial r}\{c[r^2 - 2ra(m^2 + n^2)^{1/2}\cos(\theta - \psi) + a^2(m^2 + n^2)]^{1/2}\}\, d\theta$$

$$= 2\pi K_0\,[ac(m^2 + n^2)^{1/2}]I_0'\,(cp)$$

Therefore the fin efficiency is given by the formula

$$\phi = \frac{-2\pi p}{c^2(1 - \pi p^2)T_0} \frac{K_0'(cp) + I_0'(cp) \sum_{-\infty}^{\infty} \sum_{-\infty}^{\infty}{}' K_0[ac(m^2 + n^2)^{1/2}]}{K_0(cp) + I_0(cp) \sum_{-\infty}^{\infty} \sum_{-\infty}^{\infty}{}' K_0[ac(m^2 + n^2)^{1/2}]} \quad [20]$$

Since

$$I_1(x) = I_0'(x), \quad K_1(x) = -K_0'(x) \quad [21]$$

the final answer may be written

$$\phi = \frac{2\pi p}{c(1 - \pi p^2)T_0} \frac{K_1(cp) - I_1(cp) \sum_{-\infty}^{\infty} \sum_{-\infty}^{\infty}{}' K_0[ac(m^2 + n^2)^{1/2}]}{K_0(cp) + I_0(cp) \sum_{-\infty}^{\infty} \sum_{-\infty}^{\infty}{}' K_0[ac(m^2 + n^2)^{1/2}]} \quad [22]$$

There is a surprising similarity between the formula just obtained and the fin efficiency of an equal-area circular ring for which the same boundary conditions obtain. In the latter case the solution may be written in the form

$$T = C\,I_0(cr) + B\,K_0(cr) \quad [23]$$

Using the boundary conditions, two equations are obtained for the determination of the constants C and B

$$C\,I_0(cp) + B\,K_0(cp) = T_0 \quad [24]$$

$$C\,I_0'(ca\pi^{-1/2}) + B\,K_0'(ca\pi^{-1/2}) = 0 \quad [25]$$

where p and $a\pi^{-1/2}$ are the inner and outer radii, respectively, of the ring. Therefore

$$T = \frac{T_0[I_0(cr)K_1(ca\pi^{-1/2}) - K_0(cr)I_1(ca\pi^{-1/2})]}{I_0(cp)K_1(ca\pi^{-1/2}) - K_0(cp)I_1(ca\pi^{-1/2})} \quad [26]$$

and the fin efficiency may be written

$$\phi = \frac{2\pi P}{c(1 - \pi p^2)T_0} \frac{K_1(cp)I_1(ca\pi^{-1/2}) - I_1(cp)K_1(ca\pi^{-1/2})}{K_0(cp)I_1(ca\pi^{-1/2}) + I_0(cp)K_1(ca\pi^{-1/2})} \quad [27]$$

Conclusions

In calculations based upon this type of fin-and-tube arrangement it is customary to assume that the efficiency is the same as that of a round fin of the same area. In Table 1 the efficiencies for the square fin and equal-area round fin are calculated in terms of the variable radius p, all other parameters remaining fixed. In a practical case, under consideration, the following values were used

$$T_0 = 100\ \text{C}$$
$$a = 0.375\ \text{ft}$$
$$c = 7.44/\text{ft}$$

TABLE 1 COMPARISON BETWEEN FIN EFFICIENCY OF ROUND TUBES WITH SQUARE FINS AND WITH EQUAL-AREA ROUND FINS

($a = 0.375$ ft, $c = 7.44$/ft)

p	Fin efficiency (square fin), per cent	Fin efficiency (equal-area circular fin), per cent
0.001875	17.4	17.5
0.003750	20.5	20.5
0.005625	22.6	22.7
0.007500	24.4	24.5
0.009375	26.5	26.5
0.018750	33.7	33.8
0.028125	39.8	40.0
0.037500	45.3	45.5
0.046875	50.3	50.5
0.056250	55.2	55.5
0.065625	59.8	60.2
0.075525	64.3	64.8
0.084375	68.3	68.9
0.093750	72.3	72.9
0.103125	76.3	77.0
0.112500	79.6	80.6
0.121875	82.8	84.0
0.131250	85.6	87.0
0.140625	88.3	90.0
0.150000	90.3	92.4

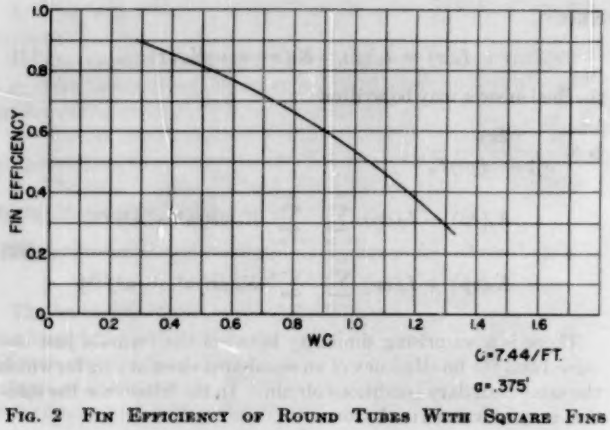

FIG. 2 FIN EFFICIENCY OF ROUND TUBES WITH SQUARE FINS

Table 1 shows that this assumption is a good one even for a fairly wide range of values of p.

Table 1 and Fig. 2 also show that the fin efficiency decreases very sharply as the tube radius decreases, as would be expected.

Fig. 3 shows the temperature variation of a fin for $p = 0.075417$ ft, where T_0, a, c, have the same values as before.

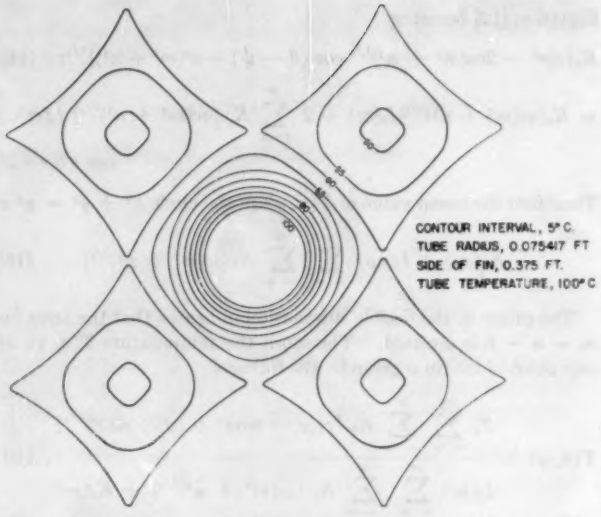

FIG. 3 LINES OF CONSTANT TEMPERATURE FOR ROUND TUBES WITH SQUARE FINS

Approximate Stress Functions for Triangular Wedges

By I. K. SILVERMAN,[1] DENVER, COLO.

The variational method is used to determine expressions for approximate stress functions for determining the effect of a third boundary to an infinite triangular wedge. The approximate function is a solution of a Euler-Lagrange total differential equation of the variational calculus with the constants of integration determined from the condition of least work. The approximate function yields zero stresses on the sloping faces of the wedge but furnishes correction stresses on the third boundary.

Introduction

THE state of stress in triangular-shaped bodies, Fig. 1, under the usual assumptions of elasticity has been determined for many cases of loading (1, 2, 3).[2] The solutions are in the form of Airy stress functions which satisfy the boundary conditions on the two faces of the wedge. Solutions are exact when the bounding faces are of infinite extent. The stresses may be obtained within the wedge if the displacements and stresses on the third boundary are those given by the Airy functions for the infinite wedge.

In practice this third-boundary condition is never met. In the case of a triangular dam the third boundary is furnished by an elastic foundation. Under the assumption of a rigid foundation the boundary conditions at the third face require zero displacements. It is thus seen that the solutions of the infinite wedge no longer hold throughout the body and especially so in the neighborhood of the third boundary. However, under the usual proportions for triangular dams, for example, Saint Venant's principle may be invoked to apply the wedge solutions in those regions removed from the disturbing boundary.

Eigenfunctions for Triangular Wedges

The existence of certain "eigen" or "characteristic" functions which may be used to evaluate the disturbing effect of a third boundary was noted by J. H. Brahtz (4). These functions were derived by considerations of the complex variable and also may be derived by assuming functions of the form

$$F = r^{n+1} f(\theta) \quad \ldots\ldots [1]$$

The differential equation for $f(\theta)$ is

$$\frac{d^4 f}{d\theta^4} + 2(n^2 + 1)\frac{d^2 f}{d\theta^2} + (n^2 - 1)^2 f = 0 \quad \ldots\ldots [2]$$

the solution of which is

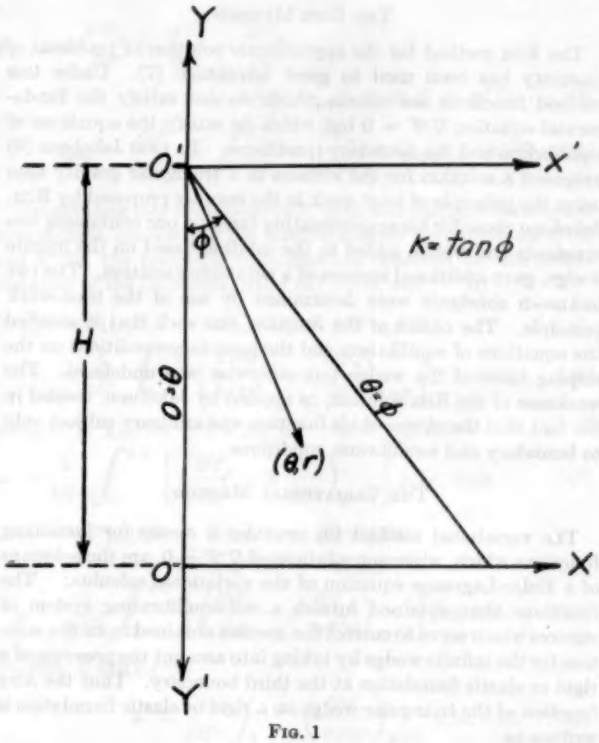

Fig. 1

$$f = r^{n+1}[c_1 \cos(n-1)\theta + c_2 \sin(n-1)\theta + c_3 \sin(n+1)\theta + c_4 \cos(n+1)\theta] \quad \ldots\ldots [3]$$

The boundary conditions are formulated so that the function [1] gives zero loads on the boundaries $\theta = 0$ and $\theta = \phi$, Fig. 1. A set of homogeneous equations (5) is obtained, the solution of which depends on the roots of an auxiliary equation

$$n^2 \sin^2 \phi = \sin^2 n\phi \quad \ldots\ldots [4]$$

The final form of the function is given by

$$F = \sum_n K_n r^{n+1}[n \cos n\theta \sin\theta + m \sin n\theta \sin\theta - \sin n\theta \cos\theta] \quad \ldots\ldots [5]$$

in which

$$n^2 \sin^2 \phi = \sin^2 n\phi \quad \ldots\ldots [5a]$$

and

$$m = \cot\phi - n \cot n\phi \quad \ldots\ldots [5b]$$

It is seen that an infinite number of "free" constants K_n are available to meet any number of conditions at the third boundary. Use of this function in the study of triangular dams resting on elastic foundations has been made (6). However, the numerical calculations associated with the roots of Equation [4] and the

---

[1] Engineer, U. S. Bureau of Reclamation.

[2] Numbers in parentheses refer to the Bibliography at the end of the paper.

Contributed by the Applied Mechanics Division and presented at the Annual Meeting, New York, N. Y., November 28–December 3, 1954, of The American Society of Mechanical Engineers.

Discussion of this paper should be addressed to the Secretary, ASME, 29 West 39th Street, New York, N. Y., and will be accepted until April 11, 1955, for publication at a later date. Discussion received after the closing date will be returned.

Note: Statements and opinions advanced in papers are to be understood as individual expressions of their authors and not those of the Society. Manuscript received by ASME Applied Mechanics Division, July 31, 1953. Paper No. 54—A-14.

extremely cumbersome expressions for stresses and displacements make Equation [5] an extremely tedious tool. Moreover, the determination of the free constants K_n involves the solution of sets of simultaneous equations, the number of which depends upon the number of elastic or stress conditions to be satisfied at the third boundary. The free constants also may be determined by application of the least-work principle or by the use of least squares.

The Ritz Method

The Ritz method for the approximate solution of problems of elasticity has been used to great advantage (7). Under this method functions are chosen which do not satisfy the fundamental equation $\nabla^4 F = 0$ but which do satisfy the equations of equilibrium and the boundary conditions. In 1930 Jakobsen (8) proposed a solution for the stresses in a triangular gravity dam using the principle of least work in the manner proposed by Ritz. Jakobsen chose for his approximating function one containing two constants and which, added to the solution based on the infinite wedge, gave additional stresses of a parabolic variation. The two unknown constants were determined by use of the least-work principle. The choice of the function was such that it satisfied the equations of equilibrium and the boundary conditions on the sloping faces of the wedge but otherwise was undefined. The weakness of the Ritz solution, as applied by Jakobsen, resided in the fact that the choice of his function was arbitrary subject only to boundary and equilibrium conditions.

The Variational Method

The variational method (9) provides a means for furnishing functions which, while not solutions of $\nabla^4 F = 0$, are the solutions of a Euler-Lagrange equation of the variational calculus. The functions thus obtained furnish a self-equilibrating system of stresses which serve to correct the stresses obtained from the solution for the infinite wedge by taking into account the presence of a rigid or elastic foundation at the third boundary. Thus the Airy function of the triangular wedge on a rigid or elastic foundation is written as

$$\phi = F_e + F = F_e + g(x, y)f(y) \quad \ldots\ldots [6]$$

where F_e is the solution for the infinite wedge satisfying $\nabla^4 F_e = 0$; $g(x, y)$ is a known function of (x, y); and $f(y)$ is a function of y yet to be determined. The function $g(x, y)$ is chosen so that the following boundary conditions are identically satisfied for all $f(y)$:

Along the vertical face ($x = 0$), Fig. 1

$$\left.\begin{array}{r} \sigma_x = 0;\ \tau = 0 \text{ for all values of y} \\ \text{Along the sloping face} \\ \sigma_x = -\tau k;\ k\sigma_y = -\tau \text{ for all values of } y \end{array}\right\} \quad \ldots [7]$$

where $k = \tan \phi$.

The principle of least work is utilized to determine the function $f(y)$ through the minimization of the energy integral

$$V = \frac{1}{2E} \int\int \{\phi_{xx}^2 + \phi_{yy}^2 - 2\nu\phi_{xx}\phi_{yy} + 2(1 + \nu)\phi_{xy}^2\}\, dx\, dy \quad \ldots\ldots [8]$$

The variation of the integral is

$$\delta V = \frac{1}{E} \int\int \{\phi_{xx}\delta\phi_{xx} + \phi_{yy}\delta\phi_{yy} - \nu\phi_{xx}\delta\phi_{yy} - \nu\phi_{yy}\delta\phi_{xx} + 2(1 + \nu)\phi_{xy}\delta\phi_{xy}\}\, dx\, dy \quad \ldots [9]$$

Integration by parts yields

$$\delta V = \frac{1}{E} \int_{x_0}^{x_1} \int_{y_0}^{y_1} \nabla^4\phi\, \delta\phi\, dx\, dy + \frac{1}{E} \int_{y_0}^{y_1} dy \{(\phi_{xx} - \nu\phi_{yy})\delta\phi_x - (\phi_{xxx} + (\nu + 2)\phi_{xyy})\delta\phi\}_{x_0}^{x_1} + \frac{1}{E} \int_{x_0}^{x_1} dx \{(\phi_{yy} - \nu\phi_{xx})\delta\phi_y - (\phi_{yyy} - \nu\phi_{xxy})\delta\phi + 2(1 + \nu)\phi_{xy}\delta\phi_x\}_{y_0}^{y_1} \quad \ldots [10]$$

From Equation [6]

$$\delta\phi = g(x, y)\delta f;\ \delta\phi_x = g_x\delta f;\ \delta\phi_y = g_y\delta f + g\delta(f') \quad \ldots [11]$$

The function $g(x, y)$ which satisfies the boundary conditions [7] is taken as

$$g(x, y) = \frac{Ax^3}{6} + \frac{Bx^3}{2}(H - y) + \frac{x^4}{12(H - y)} + \frac{x^5}{20(H - y)^2} \quad \ldots\ldots [12]$$

where

$$A = -k(1 + 0.9k);\ B = k^2\left(\frac{1}{6} + \frac{k}{5}\right) \quad \ldots\ldots [13]$$

It follows that

$$g_x = \frac{Ax^2}{2} + Bx(H - y) + \frac{x^3}{3(H - y)} + \frac{x^4}{4(H - y)^2} \quad \ldots [14]$$

$$g_y = -\frac{Bx^2}{2} + \frac{x^4}{12(H - y)^2} + \frac{x^5}{10(H - y)^3} \quad \ldots\ldots [15]$$

At the limit $y_1 (y = H, x = 0)$

$$\delta\phi = g(0, H)\delta f = 0 \quad \ldots\ldots [16]$$

$$\delta\phi_x = g_x(0, H)\delta f = 0 \quad \ldots\ldots [17]$$

$$\delta\phi_y = g_y(0, H)\delta f + g(0, H)\delta(f') = 0 \quad \ldots\ldots [18]$$

At the limit $y_0 (y = 0, x = x)$

$$\delta\phi = g(x, 0)\delta f = \left(\frac{Ax^3}{6} + \frac{BHx^3}{2} + \frac{x^4}{12H} + \frac{x^5}{20H^2}\right)\delta f(0) \quad \ldots [19]$$

$$\delta\phi_x = g_x(x, 0)\delta f = \left(\frac{Ax^2}{2} + BHx + \frac{x^3}{3H} + \frac{x^4}{4H^2}\right)\delta f(0) \quad \ldots [20]$$

$$\delta\phi_y = g_y(x, 0)\delta f(0) + g(x, 0)\delta f'(0) = \left(-\frac{Bx^2}{2} + \frac{x^4}{12H^2} + \frac{x^5}{10H^3}\right)\delta f(0) + \left(\frac{Ax^3}{6} + \frac{BHx^3}{2} + \frac{x^4}{12H} + \frac{x^5}{20H^2}\right)\delta f'(0) \quad \ldots [21]$$

At the limit $x_0 (x = 0, y = y)$

$$\delta\phi = g(0, y)\delta f = 0 \quad \ldots\ldots [22]$$

$$\delta\phi_x = g_x(0, y)\delta f = 0 \quad \ldots\ldots [23]$$

$$\delta\phi_y = g_y(0, y)\delta f + g(0, y)\delta f' = 0 \quad \ldots\ldots [24]$$

At the limit $x_1 [x = k(H - y), y]$

$$\delta\phi = g[k(H - y), y]\delta f = 0 \quad \ldots\ldots [25]$$

$$\delta\phi_x = g_x[k(H - y), y]\delta f = 0 \quad \ldots\ldots [26]$$

$$\delta\phi_y = g_y[k(H - y), y]\delta f + g[k(H - y), y]\delta f' = 0 \quad \ldots [27]$$

Using the values of the variations at the limits, Equation [10] becomes

$$\delta V = \frac{1}{E}\int_{x_0}^{x_1}\int_{y_0}^{y_1} \nabla^4\phi\delta\phi dx\,dy - \frac{1}{E}\int_{x_0}^{x_1} dx\,\{(\phi_{yy} - \nu\phi_{xx})\delta\phi_y - (\phi_{yyy} - \nu\phi_{xxy})\delta\phi + 2(1+\nu)\phi_{xy}\delta\phi_x\}_{y_0} \quad [28]$$

For the minimization of the energy integral, $\delta V = 0$, and the following double and single integrals vanish independently

$$\int_{x_0}^{x_1}\int_{y_0}^{y_1} \nabla^4\phi\delta\phi dx\,dy = 0 \quad [29]$$

$$\int_{x_0}^{x_1} [(\phi_{yy} - \nu\phi_{xx})\delta\phi_y]_{y_0} dx = 0 \quad [30]$$

$$\int_{x_0}^{x_1} [(\phi_{yyy} - \nu\phi_{xxy})\delta\phi]_{y_0} dx = 0 \quad [31]$$

$$\int_{x_0}^{x_1} (\phi_{xy}\delta\phi_x)_{y_0} dx = 0 \quad [32]$$

where

$$(\delta\phi_y)_{y_0},\ (\delta\phi)_{y_0},\ \text{and}\ (\delta\phi_x)_{y_0}$$

are given by Equations [21], [19], and [20], respectively.

Since $\nabla^4 F_e = 0$

$$\nabla^4\phi = \nabla^4(gf) = \nabla^4 gf + 4(g_{yyy} + g_{xxy})f' + (6g_{yy} + 2g_{xx})f'' + 4g_y f''' + gf^{IV} \quad [33]$$

Equation [29] becomes

$$\int_0^H \delta f dy \int_0^{k(H-y)} \nabla^4\phi g(x, y)dx = 0 \quad [29a]$$

and because of the arbitrariness of the variation δf it follows that

$$k^3\psi_3(H-y)^3 f^{IV} + 4\psi_3 k^2(H-y)^2 f''' + \psi_2(H-y)^2 f'' + 4\psi_1(H-y)f' + 2\psi_1 f = 0 \quad [34]$$

where the ψ-function of k is defined in the Appendix. Equation [34] is of the Euler-Cauchy type and its solution is

$$f(y) = c_1(H-y)^{r_1} + c_2(H-y)^{r_2} + c_3(H-y)^{r_3} + c_4(H-y)^{r_4} \quad [35]$$

where r_1, r_2, r_3, and r_4 are the roots of the auxiliary equation

$$r^4 + a_1 r^3 + a_2 r^2 + a_3 r + a_4 = 0 \quad [36]$$

where a_1, a_2, a_3, and a_4 are functions of the $\psi(k)$ functions as defined in the Appendix. It follows that

$$f(0) = c_1 H^{r_1} + c_2 H^{r_2} + c_3 H^{r_3} + c_4 H^{r_4} \quad [37]$$

$$f'(0) = -c_1 r_1 H^{r_1-1} - c_2 r_2 H^{r_2-1} - c_3 r_3 H^{r_3-1} - c_4 r_4 H^{r_4-1} \quad [38]$$

$$f''(0) = c_1 r_1(r_1-1)H^{r_1-2} + c_2 r_2(r_2-1)H^{r_2-2} + c_3 r_3(r_3-1)H^{r_3-2} + c_4 r_4(r_4-1)H^{r_4-2} \quad [39]$$

$$f'''(0) = -c_1 r_1(r_1-1)(r_1-2)H^{r_1-3} - c_2 r_2(r_2-1)(r_2-2)H^{r_2-3} - c_3 r_3(r_3-1)(r_3-2)H^{r_3-3} - c_4 r_4(r_4-1)(r_4-2)H^{r_4-3} \quad [40]$$

Evaluation of the integrals [30], [31], and [32] is obtained by the use of [19], [20], [21], and the following expressions, evaluated for $y = 0$

$$\sigma_x = \phi_{yy} = \frac{\partial^2 F_e}{\partial y^2} + \frac{\partial^2 F}{\partial y^2} = \frac{\partial^2 F_e}{\partial y^2} + (g_{yy}f + 2g_y f' + gf'') \quad [41]$$

$$\sigma_y = \phi_{xx} = \frac{\partial^2 F_e}{\partial x^2} + \frac{\partial^2 F}{\partial x^2} = \frac{\partial^2 F_e}{\partial x^2} + g_{xx}f \quad [42]$$

$$\tau = -\phi_{xy} = -\frac{\partial^2 F_e}{\partial x\partial y} - \frac{\partial^2 F}{\partial x\partial y} = -\frac{\partial^2 F_e}{\partial x\partial y} - (g_{xy}f + g_x f') \quad [43]$$

$$\phi_{yyy} = \frac{\partial^3 F_e}{\partial y^3} + \frac{\partial^3 F}{\partial y^3} = \frac{\partial^3 F_e}{\partial y^3} + (g_{yyy}f + 3g_{yy}f' + 3g_y f'' + gf''') \quad [44]$$

$$\phi_{xxy} = \frac{\partial^3 F}{\partial x^2\partial y} + \frac{\partial^3 F_e}{\partial x^2\partial y} = \frac{\partial^3 F_e}{\partial x^2\partial y} + (g_{xxy}f + g_{xx}f') \quad [45]$$

Substituting into Equations [30], [31], and [32], performing the integrations, considering the arbitrariness of the variations $\delta f(0)$ and $\delta f'(0)$, the following equations are obtained for the determination of the constants $f(0)$, $f'(0)$, $f''(0)$, and $f'''(0)$

$$(k^6\chi_5 - \nu k^2\chi_{10})f(0) + k^4 H\chi_6 f'(0) + k^4 H^2\chi_7 f''(0) = -\frac{1}{kH^5}\int_0^{kH}\left[\left(\frac{\partial^3 F_e}{\partial y^3} - \nu\frac{\partial^3 F_e}{\partial x^2}\right)_{y=0}\right] g(x, 0)dx \quad [46]$$

$$(k^6\chi_{12} - \nu k^2\chi_{16})f(0) + k^4 H\chi_{13} f'(0) + k^4 H^2\chi_{14} f''(0) = -\frac{1}{kH^4}\int_0^{kH}\left[\left(\frac{\partial^3 F_e}{\partial y^3} - \nu\frac{\partial^3 F_e}{\partial k^2}\right)_{y=0}\right] g_y(x, 0)dx \quad [47]$$

$$(k^6\chi_{17} - \nu k^2\chi_{20})f(0) + (k^4\chi_{18} - \nu\chi_{10})k^2 H f'(0) + k^4 H^2\chi_{19} f''(0) + k^4 H^3\chi_7 f'''(0) = -\frac{1}{kH^4}\int_0^{kH}\left[\left(\frac{\partial^3 F_e}{\partial y^3} - \nu\frac{\partial^3 F_e}{\partial x^2\partial y}\right)_{y=0}\right] g(x, 0)dx \quad [48]$$

$$k^2\chi_3 f(0) + k^3 H\chi_3 f'(0) = -\frac{1}{kH^4}\int_0^{kH}\left(\frac{\partial^2 F_e}{\partial x\partial y}\right)_{y=0} g_x(x, 0)dx \quad [49]$$

The χ-functions of k are given in the Appendix. The following steps are required for the determination of the approximate stress functions:

1 Evaluation of the χ-functions in the Appendix for various values of the argument k. The χ-functions are functions of the top angle and are therefore independent of the external loads.

2 Evaluation of the ψ-functions in the Appendix which are functions of k only so long as the F_e-function satisfies $\nabla^4 F_e = 0$. If F_e is not a solution $\nabla^4 F_e = 0$ the ψ-functions will depend upon the external loads which will appear in the evaluation of the Integral [29a].

3 Determination of the a_1, a_2, a_3, and a_4 functions in the Appendix.

4 Solving of the roots r_1, r_2, r_3, and r_4 of Equation [36].

5 Simultaneous solution of Equations [46] to [49], inclusive, for the values of $f(0)$, $f'(0)$, $f''(0)$, and $f'''(0)$.

6 Using the values of $f(0)$, $f'(0)$, and $f'''(0)$ thus determined, the values for $c_1 \ldots c_4$ are obtained from the simultaneous solutions of Equations [37] to [40], inclusive.

7 The total stresses are then defined by Equations [41], [42], and [43]. It is to be noted that the values of $c_1 \ldots c_4$ are not needed for the determination of the stresses along $y = 0$ since for $y = 0$

$$\sigma_x = \left(\frac{\partial^2 F_e}{\partial y^2}\right)_{y=0} + [g_{yy}(x, 0)f(0) + 2g_y(x, 0)f'(0) + g(x, 0)f''(0)] \quad [50]$$

$$\sigma_y = \left(\frac{\partial^2 F_s}{\partial x^2}\right)_{y=0} + g_{xx}(x, 0)f(0) \ldots\ldots\ldots [51]$$

$$\tau = -\left(\frac{\partial^2 F_s}{\partial x \partial y}\right)_{y=0} - [g_{xy}(x, 0)\, f(0) + g_x(x, 0)f'(0)] \ldots [52]$$

Triangular Wedge Under Hydrostatic Load

The solution for the stresses in a triangular wedge subject to an external hydrostatic load was first solved by Lévy (2). It is of technical importance in the analysis of gravity dams. The Airy Function for the (x, y)-co-ordinate system of Fig. 1 is

$$F_s = \frac{wx^2}{2K^2}(H - y) + \frac{wy^2}{6}(y - 3H) - \frac{wx^3}{3k^2} \ldots\ldots [53]$$

where w = unit weight of the fluid. The right-hand sides of Equations [46] to [49], inclusive, are designated R_1, R_2, R_3, and R_4 and on performing the differentiations and integrations

$$\left.\begin{aligned} R_1 &= w[k^2\chi_4 + \nu(\chi_8 - 2\chi_9)] \\ R_2 &= w[k^2\chi_{11} + \nu(\chi_{11} - 2\chi_{13})] \\ R_3 &= -w\chi_4[k^2 + \nu] \\ R_4 &= w\chi_1 \end{aligned}\right\} \ldots\ldots\ldots [54]$$

where

$$\chi_4 = \chi_8 = -\chi_1 = \frac{2k^2 + 3k^3}{720}$$

$$\chi_9 = \frac{3.5k^2 + 5.4k^3}{2520}$$

$$\chi_{11} = -\frac{2k^2 + 3k^3}{180} = 4\chi_1$$

$$\chi_{13} = -\frac{35k^2 + 54k^3}{5040} = -5\chi_9$$

For a top angle of 45 deg, $k = 1$, and the shape constants A, B, and χ are the following

$$A = -1.9;\ B = \frac{11}{30}$$

$$\chi_2 = -\frac{4.1867}{2016};\ \chi_3 = +\frac{4.1867}{5040};\ \chi_5 = \frac{1634}{4{,}989{,}600}$$

$$\chi_6 = -\frac{2409.4}{4{,}989{,}600};\ \chi_7 = \frac{344.2}{4{,}989{,}600};\ \chi_{10} = -\frac{2.0933}{2520}$$

$$\chi_{12} = -\frac{13{,}985.5}{4{,}989{,}600};\ \chi_{15} = \frac{158{,}823.05}{6{,}237{,}000};\ \chi_{14} = 0.5\chi_6$$

$$\chi_{16} = -2.5\chi_{10}$$

The load constants are

$$\chi_1 = -\frac{1}{144};\ \chi_9 = \frac{89}{25{,}200}$$

The simultaneous solution of Equations [46], [47], and [49] yield the values of $f(0)$ and $f'(0)$ which are as follows

$$f'(0)H = \frac{w}{144}\left[\frac{\chi_{14}\left(\frac{175 - 3\nu}{175} + \frac{\chi_5}{\chi_2} - \nu\frac{\chi_{10}}{\chi_2}\right) - \chi_7\left(\frac{190\nu - 700}{175} + \frac{\chi_{12}}{\chi_2} - \nu\frac{\chi_{16}}{\chi_2}\right)}{\chi_{14}\left(\chi_6 - \frac{\chi_3}{\chi_2}\chi_5 + \nu\chi_{10}\frac{\chi_3}{\chi_2}\right) - \chi_7\left(\chi_{12} - \frac{\chi_3}{\chi_2}\chi_{12} + \nu\chi_6\frac{\chi_3}{\chi_2}\right)}\right]$$

and

$$f(0) = -\frac{\chi_3}{\chi_2}f'(0)H - \frac{w}{144\chi_2}$$

Numerically, for $\nu = 0$

$$f'(0)\,H = +0.08928w$$

$$f(0) = +3.3770w$$

The simultaneous solution of Equations [46] to [49], inclusive, will furnish values for $f(0)$, $f'(0)$, $f''(0)$, and $f'''(0)$ which in turn will serve to determine the constants $c_1 \ldots c_4$ of Equations [37] to [40]. Of more interest are the stresses at the base $y = 0$ of a triangular wedge as a result of the imposing of boundary conditions [30], [31], and [32]. The σ_y and τ stress for $y = 0$ are obtained from Equations [42] and [43] and are expressed as follows

$$\sigma_y = wH\left(1 - 2\frac{x}{H}\right) + Hf(0)\left[B + A\left(\frac{x}{H}\right) + \left(\frac{x}{H}\right)^2 + \left(\frac{x}{H}\right)^3\right] \ldots\ldots [55]$$

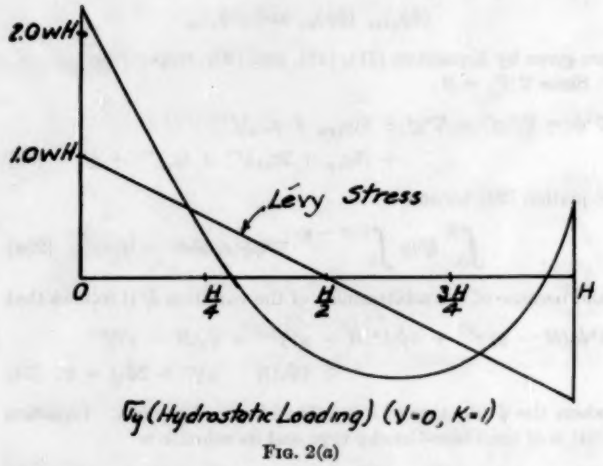

Fig. 2(a)

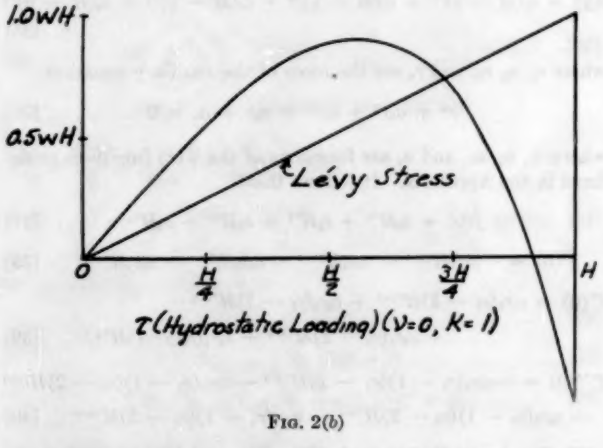

Fig. 2(b)

$$\tau = wH\left(\frac{x}{H}\right) - Hf(0)\left[\frac{1}{2}\left(\frac{x}{H}\right)^4 + \frac{1}{3}\left(\frac{x}{H}\right)^3 - B\left(\frac{x}{H}\right)\right] - H^2f'(0)\left[B\left(\frac{x}{H}\right) + \frac{A}{2}\left(\frac{x}{H}\right)^2 + \frac{1}{3}\left(\frac{x}{H}\right)^3 + \frac{1}{4}\left(\frac{x}{H}\right)^4\right] \quad \ldots . [56]$$

The resultant stresses σ_y and τ for the case $k = 1$ and $\nu = 0$ are

$$\sigma_y = wH\left\{\left(1 - 2\frac{x}{H}\right) + 3.377\left[-1.9\frac{x}{H} + \left(\frac{x}{H}\right)^2 + \left(\frac{x}{H}\right)^3 + \frac{11}{30}\right]\right\}$$

$$\tau = wH\left\{\left(\frac{x}{H}\right) - 3.337\left[\frac{1}{2}\left(\frac{x}{H}\right)^4 + \frac{1}{3}\left(\frac{x}{H}\right)^3 - \frac{11}{30}\left(\frac{x}{H}\right)\right] - 0.08928\left[\frac{1}{4}\left(\frac{x}{H}\right)^4 + \frac{1}{3}\left(\frac{x}{H}\right)^2 - 0.95\left(\frac{x}{H}\right)^3 + \frac{11}{30}\left(\frac{x}{H}\right)\right]\right\}$$

The results are plotted in Figs. 2(*a*) and 2(*b*).

BIBLIOGRAPHY

1 "Treatise on the Mathematical Theory of Elasticity," by A. E. H. Love, fourth edition, Cambridge University Press, New York, N. Y., 1927.

2 "Sur l'équilibre élastique d'un barrage en maçonnerie a section triangulaire," by M. Lévy, Comptes Rendus, vol. 127, 1898, pp. 10–15.

3 "Plain Strain in a Wedge With Applications to Masonry Dams," by S. D. Carothers, Proceedings of the Royal Society of Edinburgh, Scotland, vol. 33, 1913, pp. 292–306.

4 "Stress Function and Photoelasticity Applied to Dams," by J. H. A. Brahtz, Trans. ASCE, vol. 101, 1936, p. 1254.

5 Ibid., p. 1280.

6 "Effect of the Relative Foundation Rigidity on the Stresses in a Gravity Dam, With Application to the Grand Coulee Dam," by I. K. Silverman, C. N. Zangar, J. E. Soerens, and J. H. A. Brahtz, Technical Memorandum No. 494, U. S. Bureau of Reclamation, November, 1935.

7 "Theory of Elasticity," by S. Timoshenko, McGraw-Hill Book Co., Inc., New York, N. Y., 1934, p. 152.

8 "Stresses in Gravity Dams by Principle of Least Work," by B. F. Jakobsen, Trans. ASCE, vol. 96, 1932, pp. 489–513.

9 "Distribution of Stress in Built-In Beams of Narrow Rectangular Cross Section," by F. B. Hildebrand and Eric Reissner, JOURNAL OF APPLIED MECHANICS, Trans. ASME, vol. 64, 1942, p. A-108.

Appendix

ψ-FUNCTION OF k

$$2(H-y)^2k^3\psi_1(k) = \int_0^{k(H-y)} g\nabla^4\varphi dx$$

$$(H-y)^3k^3\psi_2(k) = \int_0^{k(H-y)} g^2 dx$$

$$(H-y)^4k^3\psi_3(k) = \int_0^{k(H-y)} gg_y\, dx$$

$$(H-y)^4k^3\psi_4(k) = \int_0^{k(H-y)} (g_{yyy} + g_{xxy})g\, dx$$

$$(H-y)^5k^3\psi_5(k) = \int_0^{k(H-y)} (6g_{yy} + 2g_{xx})g\, dx$$

$$\psi_1(k) = \frac{k^2(1890k^6 + 2046k^5 + 8470k^4 + 9105k^3 + 13{,}332k^2 + 13{,}860k + 4620)}{1{,}663{,}200}$$

$$\psi_2(k) = \frac{k^4(248.4k^3 + 330k + 110)}{9{,}979{,}200}$$

$$\psi_3(k) = \frac{k^2(5454k^4 + 9174k^3 + 3850k^2 - 28{,}512k - 23{,}760)}{2{,}851{,}200}$$

$$\psi_4(k) = \frac{k^4(1512k^4 + 1815k^3 + 3058k^2 + 3300k + 1100)}{3{,}326{,}400}$$

$$\psi_5(k) = \frac{-k^2(47{,}628k^6 + 83{,}457k^5 + 308{,}374k^4 + 642{,}312k^3 + 133{,}056k^2 - 277{,}200)}{4{,}989{,}600}$$

a-FUNCTION OF $\psi(k)$

$$a_1 = -\left(6 + \frac{b}{a}\right)$$

$$a_2 = 11 + \frac{3b}{a} + \frac{c}{a}$$

$$a_3 = -\left(6 + 2\frac{b}{a} + \frac{c}{a} + \frac{d}{a}\right)$$

$$a_4 = \frac{e}{a}$$

$$a = k^3\psi_2$$

$$b = 4k^3\psi_3$$

$$c = \psi_5$$

$$d = 4\psi_4$$

$$e = 2\psi_1$$

χ-FUNCTION OF k

$$\chi_2 = \frac{1}{k^3H^4}\int_0^{kH} g_{xy}(x,0)g_x(x,0)dx = -\frac{k^4(1.52k^2 + 2.0k + 0.67)}{2016}$$

$$\chi_3 = \frac{1}{k^3H^5}\int_0^{kH} g_x^2(x,0)dx = \frac{k^4(1.52k^2 - 103k + 105.67)}{5040}$$

$$\chi_5 = \frac{1}{k^7H^5}\int_0^{kH} g_{yy}(x,0)g(x,0)dx = \frac{k^2(567k^5 + 792k + 275)}{4{,}989{,}600}$$

$$\chi_6 = \frac{2}{k^5H^6}\int_0^{kH} g_y(x,0)g(x,0)dx = \frac{k^3(-7{,}106.4k^3 + 15{,}477k^2 + 6{,}545k - 17{,}325)}{4{,}989{,}600}$$

$$\chi_7 = \frac{1}{k^5H^7}\int_0^{kH} g^2(x,0)dx = \frac{k^4(124.2k^3 + 165k + 55)}{4{,}989{,}600}$$

$$\chi_{10} = \frac{1}{k^3H^5}\int_0^{kH} g_{xx}(x,0)g(x,0)dx = -\frac{k^4(0.76k^3 + k + 0.33)}{2520} = 0.4\chi_7$$

$$\chi_{12} = \frac{1}{k^2H^4}\int_0^{kH} g_{yy}(x,0)g_y(x,0)dx = -\frac{5103k^4 + 6682.5k^3 + 2200k^2}{4,989,600}$$

$$\chi_{13} = \frac{2}{k^5H^5}\int_0^{kH} g_y^2(x,0)dx = -\frac{k^2(19,845k^4 + 34,906.95k^3 + 15,125k^2 - 124,740k - 103,960)}{6,237,000}$$

$$\chi_{14} = \frac{\chi_6}{2}$$

$$\chi_{16} = \frac{1}{k^3H^4}\int_0^{kH} g_{xx}(x,0)g_y(x,0)dx = \frac{k^4(7.6k^2 + 10k + 3.33)}{10,080} = -\chi_2$$

$$\chi_{17} = \frac{1}{k^2H^4}\int_0^{kH} g_{yyy}(x,0)g(x,0)dx = \frac{k^2(1512k^2 + 1815k + 550)}{3,326,400}$$

$$\chi_{18} = \frac{3}{k^2H^5}\int_0^{kH} g_{yy}(x,0)g(x,0)dx = \frac{k^2(567k^2 + 792k + 275)}{1,663,200} = 3\chi_6$$

$$\chi_{19} = \frac{3}{2}\chi_6$$

$$\chi_{20} = \frac{1}{k^3H^4}\int_0^{kH} g_{xxy}(x,0)g(x,0)dx = \frac{k^4(7.6k^2 + 10k + 3.33)}{10,080} = -\chi_2$$

Brief Notes*

On the recommendations of the Executive Committee of the ASME Applied Mechanics Division, it has been decided to initiate a section devoted to brief notes on technical matters in mechanics. These notes must not be longer than 750 words (about 2½ double-spaced typewritten pages, including figures) and will be subject to the usual review procedure prior to publication. After approval such notes will be published in the next issue of the Journal. The notes should be submitted to the Secretary of the ASME Applied Mechanics Division.

Clamped Semicircular Plate Under Uniform Bending Load

BY S. WOINOWSKY-KRIEGER,[1] QUEBEC CITY, CANADA

The semicircular plate subjected to bending usually is considered as a particular case of a sectorial plate and one introduces polar co-ordinates to discuss the deflection of the plate and the corresponding distribution of stresses. If the semicircular plate is clamped along the boundary the application of approximate methods[2,3,4] becomes necessary to this end. It is worthy of note that a rather simple exact solution can be given in this latter case by making use of bipolar instead of polar co-ordinates.

CONSIDER a plate bounded by the semicircle $x^2 + y^2 = a^2$ $(y > 0)$ and the diameter $y = 0$. Let us introduce curvilinear co-ordinates u, v by putting $x + iy = a \tan {}^1/_2(u + iv)$, that is

$$x = \frac{a \sinh u}{\cosh u + \cos v} \quad y = \frac{a \sin v}{\cosh u + \cos v} \qquad \ldots\ldots [1]$$

The straight edge now is given by $v = 0$, the curved edge by $v = \pi/2$, and the corners of the plate by $u = \pm \infty$. Denoting the flexural rigidity of the plate by D and the intensity of the uniform load by q, let the elastic surface of the plate be of the form

$$w = w_0 + w_1 \qquad \ldots\ldots [2]$$

where

$$w_0 = \frac{q}{64D}(a^2 - x^2 - y^2)^2 \qquad \ldots\ldots [3]$$

is the deflection of a clamped circular plate concentric with the given plate and carrying the same load q. Furthermore, putting

$$w_1 = -\frac{qa^4}{8D(\cosh u + \cos v)} \int_0^\infty \frac{\Omega \lambda \cos \lambda u \, d\lambda}{\sinh \pi\lambda \left(\sinh^2 \frac{\pi\lambda}{2} - \lambda^2\right)} \qquad \ldots\ldots [4]$$

in which

$$\Omega = \sinh\left[\lambda\left(\frac{\pi}{2} - v\right)\right]\left(\sinh \frac{\pi\lambda}{2} \cos v + \lambda \cosh \frac{\pi\lambda}{2} \sin v\right) - \lambda^2 \cosh \lambda v \cos v \qquad \ldots\ldots [5]$$

the homogeneous differential equation of the bent plate

$$\left[(\cosh u + \cos v)^2 \left(\frac{\partial^2}{\partial u^2} + \frac{\partial^2}{\partial v^2}\right)\right]^2 w_1 = 0 \qquad \ldots\ldots [6]$$

is satisfied as well.

Next, let us consider the conditions on the boundary. The gradient $\partial w_0/\partial n$ in the direction of the normal n is zero on both edges of the semicircular plate and the deflection w_0 vanishes on its curved edge. It is readily shown that the same holds for the quotient $\partial w_1/\partial v$ (to which the gradient $\partial w_1/\partial n$ is proportional) and for the deflection w_1. Thus it remains to consider the deflection on the straight edge of the plate. Taking into account that $a^2 - x^2 - y^2 = 2a^2/(\cosh u + 1)$ and $\Omega = \sinh^2(\pi\lambda/2) - \lambda^2$ for $y = v = 0$ the deflection in question can be written as

$$w = \frac{qa^4}{16D(\cosh u + 1)^2} - \frac{qa^4}{8D(\cosh u + 1)} \int_0^\infty \frac{\lambda \cos \lambda u \, d\lambda}{\sinh \pi\lambda} \qquad \ldots\ldots [7]$$

The value of the latter integral being ${}^1/_2(\cosh u + 1)^{-1}$ the result is zero; hence the solution given by Equations [2], [3], and [4] satisfies the differential equation $\Delta\Delta w = q/D$ as well as the required conditions on the boundary of the plate.

The maximum deflection occurs, according to Hassé, at $x = 0$, $y = 0.486$, i.e., at $u = 0$, $v = 0.905$. The solution here given yields for this deflection the value of

$$0.002021 qa^4/D$$

against

$$0.002022 qa^4/D$$

obtained by Hassé and

$$0.0020202 qa^4/D$$

found by Conway and Huang.

The maximum bending moment of the plate is the radial moment M_v at the center of the straight edge $(u = v = 0)$. Using the well-known general formulas[5] for the moments expressed in bipolar co-ordinates, one finds at that point

$$M_v = -\frac{qa^2}{2} \int_0^\infty \frac{(\lambda^2 + 1)\lambda^2 d\lambda}{\sinh \pi\lambda \left(\sinh^2 \frac{\pi\lambda}{2} - \lambda^2\right)} = -0.0731 qa^2 \qquad \ldots\ldots [8]$$

while the clamping moment at the center of the curved edge $(u = 0, v = \pi/2)$ proves to have the value of only $-0.0584 qa^2$.

---

[1] Professor of Structural Engineering, Laval University.

[2] "Strength of a Semicircular Plate," by R. Kuno, *Journal of the Society of Mechanical Engineers of Japan*, vol. 37, 1934, p. 101.

[3] "The Bending of a Uniformly Loaded Clamped Plate in the Form of a Circular Sector," by H. R. Hassé, *Quarterly Journal of Mechanics and Applied Mathematics*, vol. 3, 1950, p. 271.

[4] "The Bending of Uniformly Loaded Sectorial Plates with Clamped Edges," by H. D. Conway and M. K. Huang, JOURNAL OF APPLIED MECHANICS, Trans. ASME, vol. 74, 1952, p. 5.

[5] See, for instance, "Die strenge Berechnung von Kreisplatten unter Einzellasten," by W. Flügge, Julius Springer, Berlin, Germany, 1928, p. 15.

* Discussion of papers in Brief Notes should be addressed to the Secretary, ASME, 29 West 39th Street, New York, N. Y., and will be accepted until April 11, 1955, for publication at a later date. Discussion received after the closing date will be returned.

NOTE: Statements and opinions advanced in papers are to be understood as individual expressions of their authors and not those of the Society. Manuscript received by ASME Applied Mechanics Division, October 18, 1954.

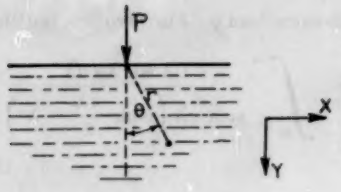

FIG. 1

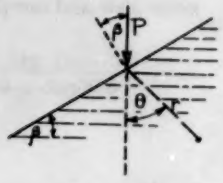

FIG. 2

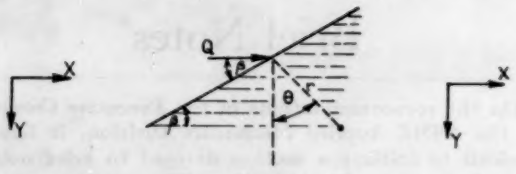

FIG. 3

FIG. 4

FIG. 5

Note on the Orthotropic Half Plane Subjected to Concentrated Loads

BY H. D. CONWAY,[1] ITHACA, N. Y.

THE stress system induced by a concentrated load acting either normally or tangentially to the edge of an orthotropic half plane has been given,[2] it being assumed that one of the principal axes of orthotropy is parallel to the edge of the half plane. The object of this note is to show how this solution can be generalized to the case when the edge of the half plane is inclined at an arbitrary angle to the principal axes of orthotropy.

Considering an orthotropic half plane, the direction of the edge of which corresponds to a principal axis of orthotropy and loaded as shown in Fig. 1, the stress system induced is

$$\sigma_r = \frac{P(\alpha_1 + \alpha_2)}{\pi r} \frac{\cos\theta}{(\alpha_1^2 \sin^2\theta + \cos^2\theta)(\alpha_2^2 \sin^2\theta + \cos^2\theta)},$$

$$\sigma_\theta = \tau_{r\theta} = 0 \quad \ldots\ldots [1]$$

where α_1^2 and α_2^2 are functions of the elastic constants given, with the usual notation,[2] by

$$\alpha_1^2\alpha_2^2 = S_{11}/S_{22}, \quad \alpha_1^2 + \alpha_2^2 = (S_{66} + 2S_{12})/S_{22}$$

[1] Professor of Mechanics, Cornell University.

[2] "Some Problems of Orthotropic Plane Stress," by H. D. Conway, JOURNAL OF APPLIED MECHANICS, Trans. ASME, vol. 75, 1953, pp. 72–76.

Manuscript received by ASME Applied Mechanics Division, June 25, 1954.

Because of the nature of this solution, it can easily be shown that the boundary of the half plane can be rotated relative to the principal axes of orthotropy as shown in Fig. 2, and the stress system is still given by Equation [1].

If α_1 and α_2 in Equation [1] are replaced, respectively, by their reciprocals, the principal axes of orthotropy are reversed and it follows that the stresses in Fig. 3 are given by

$$\sigma_r = \frac{Q\alpha_1\alpha_2(\alpha_1 + \alpha_2)}{\pi r} \frac{\sin\theta}{(\alpha_1^2 \sin^2\theta + \cos^2\theta)(\alpha_2^2 \sin^2\theta + \cos^2\theta)},$$

$$\sigma_\theta = \tau_{r\theta} = 0 \quad \ldots\ldots [2]$$

By suitable choice of the relationships between P and Q and superposing the systems in Figs. 2 and 3, the solution can be found for the cases when the edge is subjected either to normal or to tangential loads. In this way it is found that the stresses in Fig. 4 are given by

$$\sigma_r = \frac{N(\alpha_1 + \alpha_2)}{\pi r} \frac{\cos\beta\cos\theta + \alpha_1\alpha_2 \sin\beta\sin\theta}{(\alpha_1^2 \sin^2\theta + \cos^2\theta)(\alpha_2^2 \sin^2\theta + \cos^2\theta)},$$

$$\sigma_\theta = \tau_{r\theta} = 0 \quad \ldots\ldots [3]$$

whereas those for Fig. 5 are

$$\sigma_r = \frac{T(\alpha_1 + \alpha_2)}{\pi r} \frac{\sin\beta\cos\theta - \alpha_1\alpha_2 \cos\beta\sin\theta}{(\alpha_1^2 \sin^2\theta + \cos^2\theta)(\alpha_2^2 \sin^2\theta + \cos^2\theta)},$$

$$\sigma_\theta = \tau_{r\theta} = 0 \quad \ldots\ldots [4]$$

Discussion

Analysis of Plastic Deformation in a Steel Cylinder Striking a Rigid Target[1]

CARLO RIPARBELLI.[2] It is important to notice in the second approach to the problem (Equations [9] and [15]) the introduction of an excess of stress $\sigma - \sigma_0$. As shown by Sokolowsky and others, this is the fundamental parameter determining the plastic-flow rate. This is not considered in references (2) and (3) of the paper, based upon the assumption of validity of the static stress-strain relation during impact. Therefore the conclusion that this assumption is confirmed does not appear clear. Also, it is not clear how the excess of stress computed from the momentum relation compares with the stress-strain curves in Figs. 1 and 2 of this discussion.

It seems that the stress-strain relation in Figs. 1 and 2 of the paper corresponds to the geometric relation of section area enlarging with the negative elongation of the bar. In the second approach, the excess of stress is determined from the momentum consideration and added to the static constant stress. It seems that in both ways the equation of flow of the material is omitted.

It may be shown that the same plastic-strain distribution presented in the experiments can be obtained without assuming that the static stress-strain relation be valid in the presence of high strain rates, but rather distinguishing between the two strain components, elastic and plastic.

An increment of stress $\Delta\sigma$ is related to an increment of elastic strain Δe_e according to Hooke's law and to the nature of the stress, determined by electric forces associated with the positions of the atoms in the crystals. Therefore the elastic component Δe_e is simultaneous with $\Delta\sigma$.

A strain increment Δe observed during a time interval δt is believed to be the resultant of the elastic component Δe_e and of the plastic component Δe_p.

$$\Delta e = \Delta e_e + \Delta e_p \text{ (Fig. 1)}$$

The plastic component Δe_p is the resultant of the plastic flow during the time δt, i.e.

$$\Delta e_p = \dot{e}_p \delta t$$

The time rate of plastic flow $\dot{e}_p$ can be considered to be a function of the stress (and of some other parameter here neglected). These relations simply describe the dependence of the stress-strain relation upon the time rate of strain.

The time rate of plastic strain $\dot{e}_p$ is determined by the full value of the stress σ, compared to which, for a sufficiently small δt, the increment $\Delta\sigma$ is negligible.

Also, the plastic flow of a bar element (Fig. 2, herewith) is essentially a relaxation process and it occurs without addition to the momentum of the element itself. The elastic-strain component and therefore the stress determine the increase of momentum.

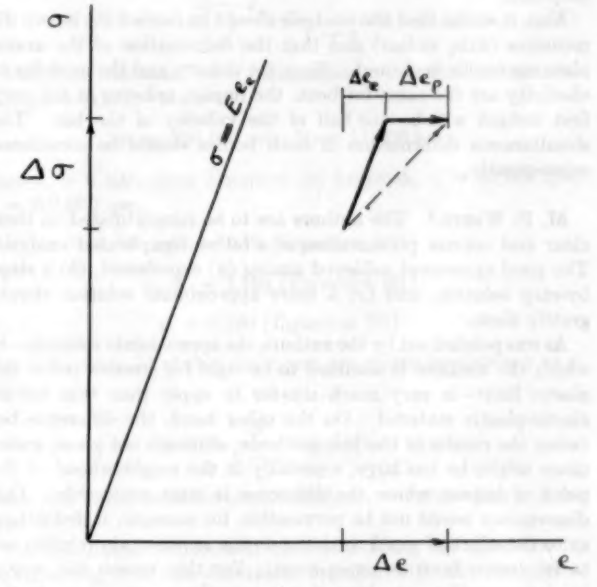

FIG. 1

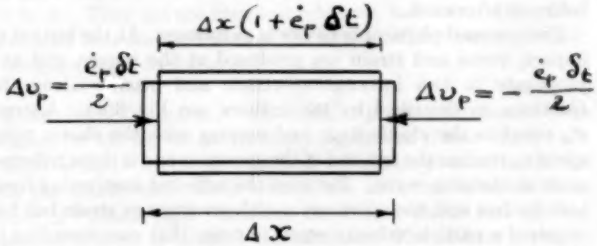

FIG. 2

The plastic component does not. Therefore Equations [1] and [2] in the paper should rather be written

$$\Delta\sigma = \rho c \Delta v_e$$

$$\Delta v_e = c \Delta e_e$$

and Equation [3]

$$c^2 = \frac{1}{\rho}\frac{\Delta\sigma}{\Delta e_e} = \frac{E}{\rho}$$

This interpretation is consistent with the experimental data of Sternglass and Stuart, of the writer, and several others. The plastic flow of the element of bar considered may be written in terms of the relative velocity of its end sections. Hence these are sources of stress-relieving waves propagating in both directions. If only for the sake of discussion the Sokolowsky relation is assumed to be valid as well as the one-dimensional scheme, i.e.

$$\dot{e}_p = k(\sigma - \sigma_0)$$

With k = const, σ_0 const, the exponential plastic-strain distribu-

[1] By E. H. Lee and S. J. Tupper, published in the March, 1954, issue of the JOURNAL OF APPLIED MECHANICS, Trans. ASME, vol. 76, pp. 63–70.

[2] Graduate School of Aeronautical Engineering, College of Engineering, Cornell University, Ithaca, N. Y.

tion is readily obtained, as indicated in Figs. 13 and 14 of the paper. By assuming $k = 0.5$ sec.$^{-1}$in^{2}lb^{-1} the maxima of 20 and 40 per cent at the origin are obtained. This value for k is very high compared to those obtained at low strain rates, so that the simple linear relation assumed should be modified.

The writer believes that only the direct measure of the forces present can give some light on the reliability of the theories proposed.

Also, it seems that the analysis should be carried out in two dimensions (axis, radius) and that the deformation of the armor plate cannot be neglected. Since the density and the modulus of elasticity are the same for both, the impact velocity at the very first instant will be one half of the velocity of the bar. The simultaneous deformation of both bodies should be considered subsequently.

M. P. White.[3] The authors are to be congratulated on their clear and concise presentation of a rather complicated analysis. The good agreement achieved among (a) experiment, (b) a step-by-step solution, and (c) a more approximate solution should gratify them.

As was pointed out by the authors, the approximate solution—in which the medium is assumed to be rigid for stresses below the elastic limit—is very much simpler to apply than that for an elastic-plastic material. On the other hand, the difference between the results of the two methods, although not great, sometimes might be too large, especially in the neighborhood of the point of impact where the difference is most noticeable. This discrepancy would not be permissible, for example, if deductions as to the effect of rapid straining on the stress-strain relation are to be drawn from an experiment. For this reason the writer has attempted to combine the two methods, assuming elastic-plastic behavior during the early stages of impact and rigid-plastic behavior afterward.

The assumed physical behavior is as follows: At the instant of impact, stress and strain are produced at the impact end and propagate in two increments—elastic and plastic—along the specimen, as described by the authors, see Fig. 3(a). A stress σ_o, equal to the elastic limit and moving with the elastic wave speed c_o, reaches the free end of the specimen and is there reflected as an unstressing wave. Between the reflected unstressing front and the free end, the specimen is without stress or strain but has acquired a particle velocity equal to twice that corresponding to the elastic limit stress σ_o, see Fig. 3(b). Moving relatively slowly from the impact end is a plastic stress-strain increment $\sigma_i - \sigma_o$, of which the maximum stress equals the impact stress σ_i, see Figs. 3(a and b). At point x_1 (distance measured from the free end) the forward moving plastic increment and the reflected elastic wave meet

$$x_1/L = \frac{c_o - c_i}{c_o + c_i} \quad \ldots\ldots\ldots\ldots\ldots\ldots [1]$$

where $c_o^2 = E/\rho$ and $c_i^2 = \dfrac{\sigma_i - \sigma_o}{\rho(e_i - e_o)}$

(Note that i refers to conditions associated with the initial impact and o to the elastic limit.)

Following this meeting, a set of wave increments—some elastic, some plastic—will move in both directions from the point x_1, as shown in Fig. 3(c). These increments will be reflected again and again at the ends of the specimen and in the interior, as described by the authors.

In order to simplify the analysis it is assumed that at this instant the elastic modulus E, and therefore the elastic wave speed c_o, become infinite. Thus the first waves proceeding from x_1 consist of a plastic element and two infinite-speed elastic elements. The elastic waves are reflected an infinite number of times and therefore can change the state of stress in the specimen immediately to any extent. On the other hand, a stress increment with infinite speed cannot affect the velocity of the material over which it passes. It follows that only by the plastic increment is the material velocity changed.

Fig. 3(d) shows the assumed variations of stress and strain shortly after the meeting of the waves at x_1. The portion of the specimen toward the impact end has the impact velocity V_i, while the rest of the specimen has a velocity $2V_o$. The condition of continuity of velocity on both sides of x_1 (the authors' Equation [5]) yields the relation

$$\frac{\sigma_1 - \sigma_o}{c_1} = \frac{\sigma_i - \sigma_o}{c_i} - \frac{\sigma_o}{c_o} = \rho V_i - 2\frac{\sigma_o}{c_o} \quad \ldots\ldots [2]$$

which is used to find the stress jump $\sigma_1 - \sigma_o$ that exists imme-

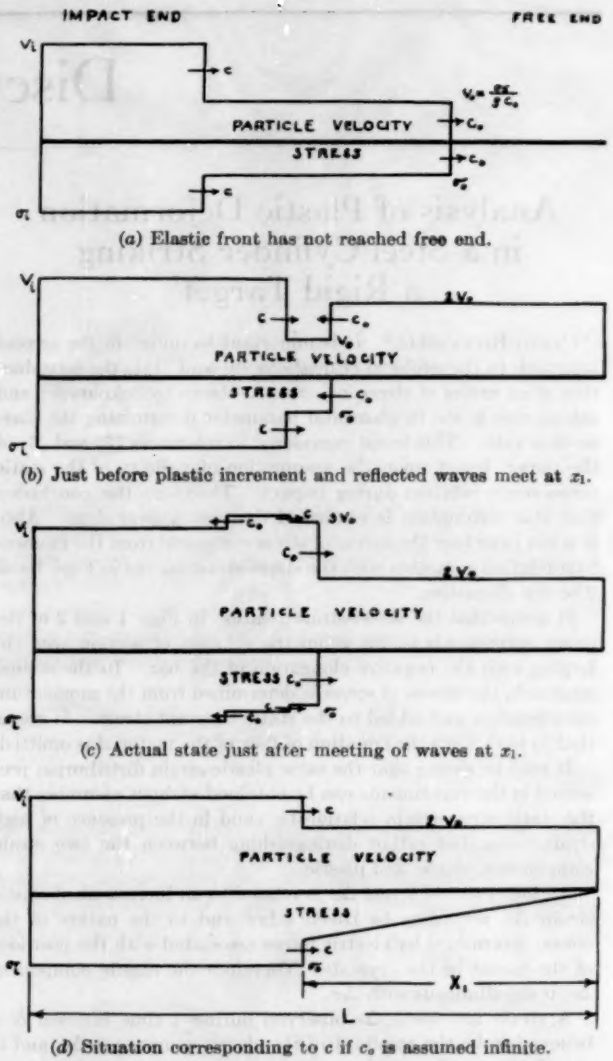

(a) Elastic front has not reached free end.

(b) Just before plastic increment and reflected waves meet at x_1.

(c) Actual state just after meeting of waves at x_1.

(d) Situation corresponding to c if c_o is assumed infinite.

Fig. 3 First Stages of Wave Propagation in Specimen—One End Free, the Other Subjected to Constant Axial Velocity V_i, Suddenly Imposed

[3] Head, Department of Civil Engineering, University of Massachusetts, Amherst, Mass.

diately after the meeting of waves at x_1. In this equation, c_1 is the speed of the shock increment $\sigma_1 - \sigma_o$.

From this time on the behavior may be described by the authors' Equations [6 to 15] which refer to a specimen being brought to rest. However, instead of this, relations are used here that correspond to the case of a specimen initially at rest and put into motion by a velocity imposed at one end. These equations continue to apply until the entire specimen has a velocity equal to the initial impact velocity V_i. The equations of motion are

$$\rho x \frac{dV}{dt} = \sigma_o \quad \ldots\ldots [3]$$

(acceleration of free end; see Equation [10] of paper)

$$\frac{dx}{dt} = -c \quad \ldots\ldots [4]$$

(speed of shock = rate of decrease of x)

$$c^2 = \frac{\sigma - \sigma_o}{\rho e} \quad \ldots\ldots [5]$$

(Lagrangian speed of shock; see Equation [3] of paper)

$$V_i - V = c_o \quad \ldots\ldots [6]$$

(see Equation [2] of paper.)

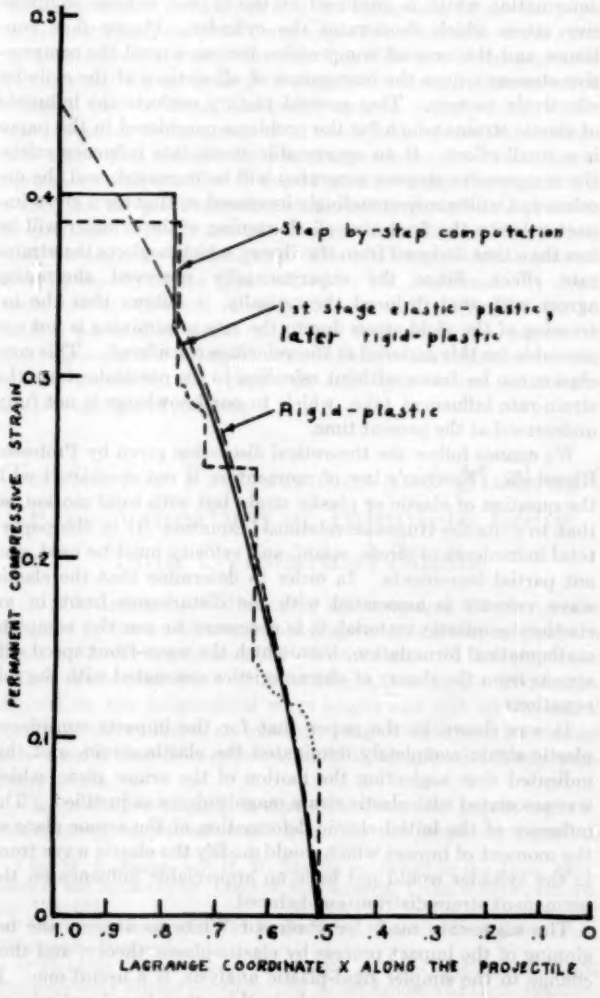

FIG. 4 CALCULATED PERMANENT STRAIN DISTRIBUTION DUE TO 335 FPS IMPACT

The initial conditions at $t = 0$ (corresponds to time of meeting at x_1) are

$$\sigma = \sigma_1, \quad e = e_1, \quad x = x_1, \quad V = 2\,V_o$$

where σ_1 is given by Equation [2] of this discussion.

The plastic part of the stress-strain relation used by the authors is

$$\frac{\sigma - \sigma_o}{\sigma_o} = \frac{e}{1 - e} \quad \ldots\ldots [7]$$

Numerical Solution. For comparison, the authors' second example is taken. Here

$$\sigma_o = 250{,}000 \text{ psi}; \quad V_i = 11{,}200 \text{ ips}$$

Then $e_i = 0.400$; from Equation [5] herewith, $c_i = 23{,}800$ ips; $c_o = 202{,}000$ ips

$$x_1/L = 0.79 \text{ (Equation [1])}$$

$$\sigma_1/\sigma_o = 1.491 \text{ (Equation [2])}$$

$$e_1 = 0.329 \text{ (Equation [7])}$$

Equations [3 to 7] of this discussion are solved to obtain x as a function of e

$$(x/L)^2 = \frac{A}{1 - e} \exp 1/(1 - e)$$

where A is found from the condition that $e = 0.329$ when $x/L = 0.79$.

The calculated distribution of strains along the specimen is shown in Fig. 4 of this discussion, together with the two corresponding curves from the authors' Fig. 11. It can be seen that the difference between the two approximations is quite small for $x < 0.79$. They are not identical relations, however. (The disagreement between the values of the initial uniform strains is due to computational divergences.)

ALEXANDER YORGIADIS.[4] The authors present two theoretical methods for solving the problem of longitudinal plastic impact of cylindrical bars. In the first method, or "elastic-plastic" method, both the elastic and plastic strains are analyzed, while in the second or "plastic-rigid" method, the smaller elastic strains are neglected in order to simplify the solution. The authors present some experimental results which show that these methods are reasonably accurate.

The elastic-plastic method of analysis presented by the authors is by no means a new method. In 1948 DeJuhasz[5] presented a general and extensive derivation of this method and used it to solve several problems of plastic one-dimensional impact for materials with various plastic stress-strain curves. The problems treated in Figs. 7 and 10 of the paper are covered by problem 13 and Fig. 19 in the foregoing reference. This is the case of plastic impact of a bar of finite length against a rigid target, with the material of the bar having a yield point which increases as a result of prior stressing. Diagrams 19(*b*) in the reference, and Figs. 7 and 10 in the paper, are all the same, "time-location" charts, in which a point denotes a certain cross section x of the bar at a certain time τ. DeJuhasz derived the basic wave equations and developed additional diagrams which enable better visualization of the entire phenomenon of elastic and plastic impact.

[4] Sandia Corporation, Albuquerque, N. M. Mem. ASME.

[5] "Graphical Analysis of Impact of Bars Stressed Above the Elastic Range," by K. J. DeJuhasz, presented before the Seventh International Congress of Applied Mechanics, September, 1948, at London, England, and published in the *Journal of The Franklin Institute*, vol. 248, July, 1949, pp. 15–48, and August, 1949, pp. 113–142.

Probably the most important of these diagrams is the "diagram of state" or velocity-stress diagram which enables graphical solution of equations such as Equations [1] to [5], inclusive, in the paper. The points on this diagram can be obtained either by geometrical construction, or by calculation if greater accuracy is needed. In both cases, this diagram makes it easier to follow the sequence of events occurring as a result of passage of a wave front, or intersection of wave fronts.

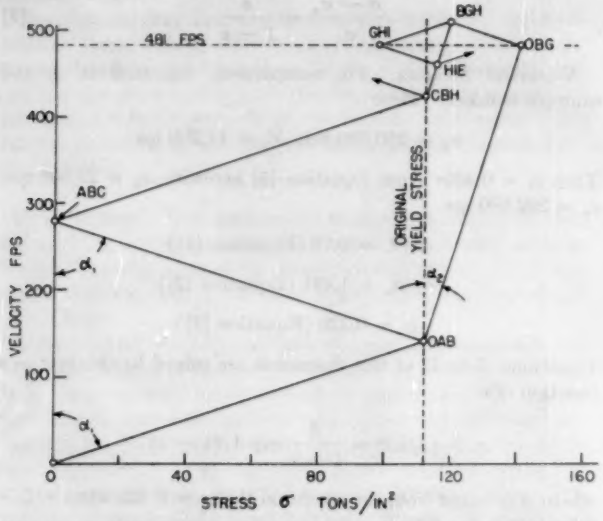

FIG. 5 DIAGRAM OF STATE FOR IMPACT OF ALLOY-STEEL BAR ABOVE ITS ELASTIC LIMIT; PROBLEM IN FIG. 7 OF PAPER

(Tan α_1 = 0.798 ton/in.^{2} per fps represents the wave factor in the elastic range. Tan α_2 = 0.084 ton/in.^{2} per fps, is the wave factor for the plastic range AB of Fig. 2 in paper.)

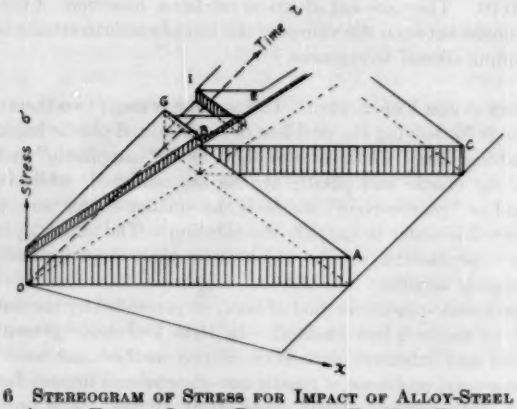

FIG. 6 STEREOGRAM OF STRESS FOR IMPACT OF ALLOY-STEEL BAR ABOVE ELASTIC LIMIT; PROBLEM IN FIG. 7 OF PAPER

The diagram of state presented in Fig. 5 of this discussion applies to the problem in Fig. 7 of the paper. Each point on this diagram represents the velocity and stress existing in a certain "domain" in the time-location diagram of Fig. 7. For example, triangular domain O-A-B in Fig. 7 has a stress and velocity equal to co-ordinates of point marked O-A-B in Fig. 5 of the discussion. Other points in this diagram define the other domains. The procedure for construction of this diagram will not be explained since it is fully covered in the reference.[5]

Dynamic phenomena in a bar subjected to impact can be described completely by giving the co-ordinates of state for every cross-section "x" and for every instant of time. Such three-dimensional diagrams are known as "stereograms." DeJuhasz[5] has prepared such diagrams to show variation of stress, velocity, displacement under various impact conditions. The stereogram of stress for the problem in Fig. 7 of author's paper is presented in Fig. 6 of this discussion. Three-dimensional models of plaster or wood can be built for still clearer representation of the phenomena.

AUTHORS' CLOSURE

We wish to express our appreciation to the discussers for the detailed consideration they have given to the paper.

We feel that Professor Riparbelli has misunderstood certain aspects of the theory presented in the paper. For example, the stress difference ($\sigma - \sigma_0$) in Equation [9] of the paper is merely the difference in nominal stress associated with the plastic flow occurring at the wave front of strain discontinuity. Values on both sides are in accordance with the static stress-strain relation, so that this stress difference does not represent an "excess" stress in the sense to which he refers. The whole analysis of the paper is based consistently on the use of the static stress-strain relation. Nevertheless, it was possible to draw the conclusion that the experimental results confirmed this assumption and would not have agreed with a theory which included an appreciable influence of the strain rate in increasing the stress for plastic flow. The reason for this can be seen by considering the process of impact in a general way as follows: When the cylinder strikes the target the deformation which is produced by the impact induces compressive stress which decelerates the cylinder. Plastic flow continues and the over-all compression increases until the compressive stresses reduce the momentum of all sections of the cylinder effectively to zero. This general picture neglects the influence of elastic strains which for the problems considered in the paper is a small effect. If an appreciable strain-rate influence exists, the compressive stresses generated will be increased, and the deceleration will be correspondingly increased, so that for a given impact velocity the final over-all shortening of the cylinder will be less than that deduced from the theory which neglects the strain-rate effect. Since the experimentally observed shortening agrees with that deduced theoretically, it follows that the increasing of the yield stress due to the rate of straining is not appreciable for this material at the velocities considered. This conclusion can be drawn without reference to the particular form the strain-rate influences take, which to our knowledge is not fully understood at the present time.

We cannot follow the theoretical discussion given by Professor Riparbelli. Newton's law of momentum is not associated with the question of elastic or plastic strain but with total motion, so that to write the Hugoniot relations (Equation [1] in the paper) total increments of stress, strain, and velocity must be used, and not partial increments. In order to determine that the elastic wave velocity is associated with the disturbance front in an elastic-viscoplastic material, it is necessary to use the complete mathematical formulation, from which the wave-front speed will appear from the theory of characteristics associated with the full equations.

It was shown in the paper that for the impacts considered plastic strain completely dominated the elastic strain, and this indicated that neglecting the motion of the armor plate, which was associated with elastic strain magnitudes, was justified. The influence of the initial elastic deformation of the armor plate at the moment of impact which would modify the elastic wave front in the cylinder would not have an appreciable influence on the permanent strain distribution deduced.

The suggestion made by Professor White to analyze the beginning of the impact process by elastic-plastic theory, and then change to the simpler rigid-plastic analysis, is a useful one. It provides a more accurate analysis than that based entirely on plastic-rigid theory without appreciable additional complication.

It seems to us that the discrepancy in the strain magnitude adjacent to the impact face shown in Fig. 4 of the discussion may be associated with the fact that maximum strain is plotted for Professor White's analysis, whereas Figs. 8 and 11 of the paper depict permanent residual strain. The maximum strain after impact corresponding to the permanent strain shown in Fig. 11 of the paper is 0.4, which agrees with the example presented by Professor White.

We feel that the reference to the work by K. J. DeJuhasz mentioned by Dr. Yorgiadis forms a useful complement to the paper. The graphical method of analysis which he applied to problems of the propagation of plastic waves for materials which have a piecewise linear stress-strain relation concave toward the strain axis provides a useful illustration of the methods used in the paper under discussion. However, Dr. DeJuhasz' paper does not include the analysis given in the paper under discussion, nor does it attempt the same objective. We discuss a particular material which was found to have a concave upward stress-strain curve so that theories of the type considered by Dr. DeJuhasz had to be modified to allow for shock formation according to one-dimensional theory, with the wave velocities at a prescribed strain magnitude not given by the gradient of the stress-strain curve there, but by the shock conditions across the finite stress increment occurring. The use of the Hugoniot relations is of course the same as that in footnote 5 of the discussion, but in the paper under discussion the plastic wave speed is a function of the stress on both sides of the shock front. The objective of the paper was to carry out the analysis according to the measured stress-strain relation, and to check the result against experimental impact tests to assess the accuracy of a theory which is one-dimensional and which does not contain a strain-rate influence. Satisfactory agreement with this theory was obtained. Since the variation in velocity of the plastic shock fronts is not large, it would probably be permissible to assume an average value which would be held fixed throughout the analysis. The resulting calculation would then be exactly of the type treated by Dr. DeJuhasz. It would seem well worth while to carry this out and to compare the resulting permanent strain with that deduced in the paper. If good agreement is obtained, and we believe that this can reasonably be expected, this procedure will provide an alternative simpler method of analysis.

Tables for Frequencies and Modes of Free Vibration of Infinitely Long Thin Cylindrical Shells[1]

G. B. Warburton.[2] The writer has compared the frequencies obtained by the authors with those derived by another method in a paper by R. N. Arnold and G. B. Warburton.[3] In that paper the cylinders considered are of finite length, but as the frequencies depend on the longitudinal wave length and not on the actual length of the cylinder, an infinitely long cylinder can be treated as a special case of a cylinder of finite length with freely supported ends.

The method is similar to that of the authors' paper, but the strain-energy expression used to derive the frequency equation contains the terms due to bending. The frequencies depend on the number of circumferential waves, the ratio of the thickness to the mean radius of the shell, and the ratio of the longitudinal wave length to the mean radius. For a particular set of values of these three functions, there are three frequencies. The paper[3] shows that for vibrations associated with the lowest frequency both bending and stretching of the cylinder walls occur, but only stretching occurs for those associated with the two higher frequencies. For the former type of vibration, which is of most practical significance, curves are plotted showing the variation of a dimensionless factor, proportional to frequency, with the ratio of the mean circumference to the longitudinal wave length for various values of the number of circumferential waves and the ratio of the thickness to the mean radius. Experimental work is also included; there is good agreement between the calculated and measured values of frequency for cylinders of various dimensions.

These frequency curves help to explain the anomaly mentioned by the authors. When the mean radius is small compared with the longitudinal wave length, the frequency increases as the number of circumferential waves increases. As $j\ (= \pi a/L)$ increases, the frequency curves for different values of n and a particular value of h/a cross. This effect is most marked for small values of h/a. For example, if $h/a = 0.002$, the frequency decreases as n increases from 2 to 9 for any value of j greater than 2.2; if $h/a = 0.01$ and $j = 3.5$, the frequency decreases as n increases from the value 2, reaches a minimum corresponding to $n = 7$, and then increases with further increase of n. (The paper[3] considers only flexural vibrations of the walls of the cylinder; i.e., $n \geqslant 2$.)

This behavior is governed by the distribution of the strain energy between bending and stretching. For particular values of j and h/a and for a given maximum radial displacement, the energy due to bending increases as n increases, but that due to stretching decreases. The frequency is approximately proportional to the square root of the total strain energy. When j is small, the stretching energy is negligible in comparison with the energy of bending for any value of n. (In the limit as $j \to 0$, the frequencies of this type of vibration are given by the theory of inextensional deformation of a thin cylinder due to Rayleigh.[4]) As a result, the distribution of energy of bending controls the frequency, and the latter increases with increase of n. As j increases, the energy of stretching becomes comparable with that of bending. Because of the different method of variation of the two strain-energy components with n, the total strain energy decreases as n increases from $n = 2$, has a minimum value, and then increases with further increase of n. For low values of n the energy of stretching predominates but for higher values that of bending is more important. The value of n at which the total strain energy (and thus the frequency) is a minimum depends on the values of j and h/a.

The foregoing remarks apply only to the modes of vibration corresponding to the lowest root of the frequency equation, for which W is greater than U and V. For the two higher roots, the maximum displacements occur in the longitudinal or tangential directions, all the strain energy is due to stretching, and the frequency increases as n increases, because the stretching energy increases with n for these modes.

The values of the lowest root of the frequency equation depend on the expression used for the strain energy due to bending. However, this effect is small; this is shown in Table 1 of this discussion, where values of the frequency factor, $\omega a \sqrt{m/(Gh)}$, derived by four different methods, are given for various modes. In A the frequencies are derived from the authors' tables, values of

[1] By M. L. Baron and H. H. Bleich, published in the June, 1954, issue of the Journal of Applied Mechanics, Trans. ASME, vol. 76, pp. 178–184.

[2] Lecturer, Department of Engineering, University of Edinburgh, Edinburgh, Scotland.

[3] "Flexural Vibrations of the Walls of Thin Cylindrical Shells Having Freely Supported Ends," by R. N. Arnold and G. B. Warburton, Proceedings of the Royal Society of London, England, series A, vol. 197, 1949, pp. 238–256.

[4] "Theory of Sound," by Lord Rayleigh, second edition, Macmillan and Company, Ltd., London, England, 1894, vol. 1, p. 417.

$$K\sqrt{1+\frac{K^2h^2}{K^2a^2}}$$

being calculated for various values of h/a. Corresponding values obtained from the analysis in the paper[3] are given in B. In that paper strain expressions given by Timoshenko[5] are used; the corresponding expression for the strain energy of bending is

$$P_2 = \frac{E}{24(1-\nu^2)}\frac{h^3}{a^3}\iint [a^4w_{xx}^2 + (w_{\theta\theta}+v_\theta)^2 + 2\nu a^2 w_{xx}(w_{\theta\theta}+v_\theta) + 2(1-\nu)a^2(w_{x\theta}+v_x)^2]\,dz\,d\theta$$

In C the writer gives the frequencies obtained by using the method of the above paper with the strain energy of bending given by Equation [3] of the authors' paper; i.e., Flügge's strain expressions are used. In D some frequency factors have been derived from the equations of motion of a thin cylindrical shell given by Epstein,[6] who considered a thin shell to be a limiting case of a thick shell. Thus, as there are less simplifying assumptions, this method should give frequencies nearest to the true values. However, Epstein's expressions contain more terms than those of Timoshenko or Flügge, and thus more arithmetical work is required to obtain the frequencies.

The table shows that there is good agreement between the frequencies derived by the different methods. Comparing frequencies from B and C with those of D, it is seen that the effect on frequency of simplifying the strain expressions is small. For some of the modes included in the table, the strain energy is mainly due to stretching, but for others the energy due to bending predominates. The authors' values for the ratios V/U and W/U are, in effect, those for a shell in which $h/a \to 0$, as the strain energy of bending is neglected in obtaining them. However, these ratios depend only on the nodal pattern and not on h/a, so that the wave forms assumed for the modes, in which bending energy is appreciable, are accurate; thus the authors' values of frequency are accurate.

TABLE 1 VALUES OF FREQUENCY FACTOR, $\omega a\sqrt{\frac{m}{Gk}}$

(Lowest frequency, $\nu = 0.3$)

Method	L/a	n	h/a = 1/100	1/20	1/10
A Baron and Bleich	1	2	1.104	1.121	1.261
	1	6	0.4039	0.7948	2.179
	10	2	0.03712	0.05653	0.1385
	10	6	0.1690	0.5631	1.689
B Arnold and Warburton	1	2	1.103	1.120	1.257
	1	6	0.4038	0.7936	2.169
	10	2	0.03710	0.05644	0.1380
	10	6	0.1690	0.5630	1.686
C From Flügge's expressions	1	2	1.103	1.120	1.260
	1	6	0.4040	0.7946	2.175
	10	2	0.03712	0.05651	0.1384
	10	6	0.1690	0.5630	1.688
D From Epstein's equations	1	2	.....	.....	1.254
	1	6	.....	.....	2.183
	10	2	.....	.....	0.1382
	10	6	.....	.....	1.695

Although the authors claim that their method is accurate only up to $h/a = 1/20$, it can be seen from the table that the method can be used for higher values of h/a without appreciable loss of accuracy. Expressions for the strain energy depend on h/a being small, but due to the good agreement between theoretical and experimental work previously mentioned, it can be assumed that the strain-energy expressions are accurate up to $h/a = 1/10$.

The writer considers that the authors' method of determining the frequencies corresponding to the lowest root is just as complex as a full solution including bending effects. The authors' paper is an interesting application of the Rayleigh principle to the theory of vibrations of thin cylinders. This principle also has been applied to obtain the frequencies of vibration of thin cylinders of finite length with fixed or partially fixed ends.[7] For these conditions the longitudinal wave form is not sinusoidal and is not known exactly, but because of Rayleigh's principle, accurate values of frequency can be determined by assuming an approximate wave form.

Authors' Closure

The authors are in full agreement with the discusser's comments. It is of particular interest that the experiments referred to indicate that the tables in the paper are valid up to a thickness ratio 1:10.

The authors have to comment, however, on the final paragraph of the discussion, stating that their method is just as complex as a full solution including bending effects. There appears to be a misunderstanding on the discusser's part. It is not the authors' claim to have presented a novel method at all as the basic equations were already well known; the purpose of the paper is to present numerical tables of the frequencies. These tables are considerably simpler in the manner obtained than if they had been derived from one of the available full solutions including bending effects. In the latter case each of the tables for the fundamental frequencies would have to consist of a number of tables equal to the number of h/a ratios to be considered. The authors' procedure is for this reason better suited for the purpose of obtaining tables of frequencies.

Stresses in a Metal Tube Under Both High Radial Temperature Variation and Internal Pressure[1]

J. H. Faupel.[2] The authors have worked out a rather complicated system for calculating stresses in tubes subjected simultaneously to thermal gradients and internal pressure. We would like to ask if the authors have applied their methods to experimental models and, in particular, how the condition of initial yielding and final bursting are predicted, since these are extremely important engineering quantities with respect to cylinders.

It would appear that, at least for the initial yield and final burst quantities, a limit design procedure could be employed which would remove most of the complexity of the mathematics involved and at the same time provide answers within perhaps 15 to 20 per cent of the actual values which would be of prime interest to designers of such types of vessels.

We would propose that the actual thermal stresses involved would be critical only for the initial yield; these stresses at the bore of the cylinder can be calculated by methods given by Timoshenko. These stresses plus the stresses induced by internal pressure then combine in accordance with the von Mises criterion to cause yielding. The yield pressure is thus

[3] "Theory of Plates and Shells," by S. Timoshenko, first edition, McGraw-Hill Book Company, Inc., New York, 1940, p. 439.

[6] "On the Theory of Elastic Vibrations in Plates and Shells," by P. S. Epstein, *Journal of Mathematics and Physics*, vol. 21, 1942, pp. 198–209. The equations are also given in "The New Approach to Shell Theory: Circular Cylinders," by E. H. Kennard, Journal of Applied Mechanics, Trans. ASME, vol. 75, 1953, pp. 33–40.

[7] "The Flexural Vibrations of Thin Cylinders," by R. N. Arnold and G. B. Warburton, Proceedings of The Institution of Mechanical Engineers (A), vol. 167, 1953, pp. 62–80.

[1] By C. C. Chang and W. H. Chu, published in the June, 1954, issue of the Journal of Applied Mechanics, pp. 101–108.

[2] Research Project Engineer, Engineering Research Laboratory, Engineering Department, E. I. du Pont de Nemours and Company, Inc., Wilmington, Del. Mem. ASME.

$$p_y^2\left[\frac{R^2}{R^2-1}\right]^2 + p_y\left[\frac{R^2}{R^2-1}\right]\sigma_h' + \frac{1}{3}\left\{(\sigma_h')^2 + (\sigma_z')^2 - \sigma_z'\sigma_h' - \sigma_y^2\right\} = 0$$

where

R = ratio of outside to bore radius
p_y = yield pressure, psi
σ_h' = thermal hoop stress at bore, psi
σ_z' = thermal longitudinal stress at bore, psi
σ_y = yield strength of material in tension, psi (at temperature)

The only point of real concern is the value of the yield strength of the material, σ_y, which is not constant through the material because of the thermal gradient. However, by the limit design procedure we would use only the yield strength of the material at the bore location corrected for modulus variation throughout the rest of the cylinder wall. Thus, if the average modulus is E', and the modulus at the bore is E, the yield value used would be

$$\sigma_y \frac{E'}{E}$$

For final bursting we would use a system similar to that discussed in a recent publication.[3]

$$p_b = \frac{2\sigma_y}{\sqrt{3}} \ln R \left(2 - \frac{\sigma_y}{\sigma_u}\right)$$

where

p_b = bursting pressure, psi
σ_y = yield strength of material in tension, psi
σ_u = ultimate tensile strength of material, psi

For bursting, the thermal stresses would not enter the calculation and σ_y and σ_u would be the average values across the wall.

For the case of steady temperature up to about 350 C we have found predictions of yield and bursting to agree quite well with calculated values; we have no data for the case of thermal gradients, however, and would be interested in the comments of the author.

Authors' Closure

First of all, the authors should like to point out that their theory holds for the elastic range only, and cannot be applied to the problems of initial yielding and bursting pressure without further extension. However, the authors would endeavor to comment on these important design problems in the following.

In case the temperature gradient is very large the temperature effects on the modulus of elasticity E and the thermal-expansion coefficient a' are appreciable, whence the method of calculation proposed by Mr. Faupel is difficult to justify. The initial yielding pressure may be calculated by the von Mises criterion

$$\sigma_y = \left\{\frac{1}{2}\left[(\sigma_{11}-\sigma_{22})^2 + (\sigma_{22}-\sigma_{33})^2 + (\sigma_{33}-\sigma_{11})^2\right]\right\}^{1/2}$$

where

$$\sigma_{11}\,(=\sigma_{11}^{(1)}+\sigma_{11}^{(2)}),\quad \sigma_{22}\,(=\sigma_{22}^{(1)}+\sigma_{22}^{(2)}),\quad \sigma_{33}\,(=\sigma_{33}^{(1)}+\sigma_{33}^{(2)})$$

are given in the authors' paper. (Note that the internal pressure enters the equation through the terms $\sigma^{(2)}$.) In this calculation, a few terms of the series solution given in the paper will be sufficient since the parameter z usually takes fairly small values. As σ_y decreases with increasing temperature and the thermal compression at the inner wall increases with increasing temperature gradient, the following possibilities of initial yielding due to internal pressure and temperature gradient may occur (let $p_0 \leqq 0$)

(*a*) Initial "tensile yielding" near outer boundary
(*b*) Initial "compression yielding" at inner wall
(*c*) Initial tensile yielding at inner wall
(*d*) Both (*a*) and (*b*) occur
(*e*) Both (*a*) and (*c*) occur.

As far as the bursting pressure p_b is concerned, the authors do not agree with the statement that "for bursting the thermal stresses would not enter the calculation." For rough estimation, perhaps, some formula similar to Mr. Faupel's expression could be used. Based on the same assumptions implied by his work,[4] one would have (cf footnote 5)

$$p_b \leqq K\left[\int_{r_i}^{r_0} \frac{2}{\sqrt{3}}\frac{\sigma_u(r)}{r}\,dr + p_0\right] + (1-K)\left[\int_{r_i}^{r_0}\frac{\sigma_y(r)}{r}\,dr + p_0\right]$$

where σ_u and σ_y (e.g., Fig. 1 in the paper), both functions of temperature could be obtained experimentally and an appropriate coefficient $K(0 \leqslant K \leqslant 1)$ remains to be determined. When there is no temperature gradient σ_u and σ_y are constants. If $K = \frac{\sigma_y}{\sigma_u}$, the foregoing equation reduces to

$$p_b = \frac{2}{\sqrt{3}}\left(2 - \frac{\sigma_y}{\sigma_u}\right)\ln\frac{r_0}{r_i}$$

When there is temperature gradient across the wall, Faupel proposed that the average values of σ_u and σ_y be used in the last expression. It is doubtful that this formula is approximately valid under high temperature gradient.

The investigations on thermal stresses in thick-wall cylinders under high-temperature gradient are still at an infant stage. Further theoretical and experimental developments are urgently needed.

The Stresses in a Flat Curved Bar Resulting From Concentrated Tangential Boundary Loads[1]

S. Woinowsky-Krieger.[2] The paper offers an example of a solution which, being not rigorous, basically provides results quite satisfactory for technical purposes. As a matter of fact, the authors, in order to apply the Fourier-integral method to the problem in question, replace the given open ring by a spiral of a constant curvature and an infinite length. It seems rather difficult to figure out a physical model of such a bar having at the

[3] "Influence of Residual Stress on Behavior of Thick-Wall Closed-End Cylinders," by J. H. Faupel and A. R. Furbeck, Trans. ASME, vol. 75, 1953, pp. 345–354.

[4] "Influence of Residual Stress on Behavior of Thick-Wall Closed-End Cylinders," by J. H. Faupel and A. R. Furbeck, Trans. ASME, vol. 75, 1953, pp. 345–354.

[5] "Theory of Flow and Fracture of Solids," by A. Nadai, vol. 1, second edition, McGraw-Hill Book Company, Inc., New York, N. Y., 1950, chapter 30.

[1] By N. G. Wu and C. W. Nelson, published in the June, 1954, issue of Journal of Applied Mechanics, pp. 151–159.

[2] Professor of Structural Engineering, Laval University, Quebec, Canada.

same time a section with a finite width and a finite depth. As for the reactive forces, their effect on the section $\phi = 0$ under consideration remains virtually unaffected by their infinite angular distance from $\phi = 0$ as compared with a finite one. This fact is quite in accordance with the principle of Saint Venant, provided the bar remains slender. No objection can be made to the very effective method by which the infinite integrals have been evaluated, a method already used in a previous paper.[5]

Another consideration suggested by the paper is the following: As C. W. Nelson points out[3] the Fourier-series solution is convenient to use for values of a/b up to 0.5 or even more. For a/b close to unity it should be possible, however, to split the stresses in the vicinity of the section $\phi = 0$ into two parts: (1) Stresses depending on the local effect of the load and essentially the same as those in a straight beam, and (2) stresses obtainable from the elementary theory of the curved rod and depending of course on the end conditions. This method not only has been applied by F. Seewald[4] in investigating the stresses in straight beams but also by the writer in determining the stress distribution in thick elastic plates under concentrated loads.[5] The solution of the problem as given in the present paper would then be justified in a range between some value $a/b > 0.5$ and some other less than unity.

As for the determination of stresses due to the elementary theory of bending, several methods may be effective for this purpose, particularly the Fourier-integral method. A special form of this method has been used in several recent papers.[6] The stresses just mentioned should be obtainable also by some limiting procedure similar to that used in the paper for another purpose. However, this procedure should consider as fixed not the difference $(b - a)$, but some radius of the ring, say, the inner radius a.

Authors' Closure

The authors wish to thank Professor Woinowsky-Krieger for the interest evidenced by his discussion and for the constructive criticisms contained therein.

The suggestion that the stresses in the vicinity of $\phi = 0$ be presented as made up of two parts is a good one and this might well be done exactly in the way that Professor Woinowsky-Krieger suggests for $\frac{a}{b}$ very close to unity. The authors would like to point out that the procedure, modified slightly, can be extended to values of $\frac{a}{b}$ considerably less than unity. This can be accomplished by splitting the stresses into two parts as follows:

(1) Stresses depending on the local effect of the load and essentially the same as those in a straight beam, and (2) stresses obtained from a proper combination of H. Golovin's two solutions expressed by Equations [25] and [26] of the paper and applicable, respectively, to Figs. 3(a) and 3(b) of the paper. The reason why the authors prefer this method of splitting the stresses into two parts $\left(\text{for } \frac{a}{b} \text{ not extremely close to unity}\right)$ rather than the method proposed $\left(\text{for } \frac{a}{b} \text{ very close to unity}\right)$ by Professor Woinowsky-Krieger can be explained best by means of an example. Consider the cross section $\phi = 90$ deg in Fig. 1(a) of the paper for the case $\frac{a}{b} = 0.7$. At this cross section, the circumferential stress at the inner boundary from Equation [30] can be shown to be

$$(\sigma_{\phi I})_{r=a} = -15.8828 \frac{P}{(b-a)} \quad \ldots\ldots [1]$$

The stress at the same point corresponding to (2) as specified in the foregoing can be calculated from Equation [35] of the paper and the result is

$$\text{Part (2) of } (\sigma_{\phi I})_{r=a} = -15.8828 \frac{P}{(b-a)} \quad \ldots\ldots [2]$$

Thus by subtracting Equation [2] from Equation [1] it is found that

$$\text{Part (1) of } (\sigma_{\phi I})_{r=a} = 0.0000 \frac{P}{(b-a)} \quad \ldots\ldots [3]$$

and it is clear that the local effect of the load is practically zero at

$$\phi = 90 \text{ deg } (\Phi = 4.404) \text{ for } \frac{a}{b} = 0.7.$$

By the elementary theory[7] of bending of curved bars, sometimes called Winkler's Theory, the circumferential stress for the loading shown in Fig. 1(a) is found to be (for $\phi > 0$)

$$\sigma_{\phi I} = \frac{P \cos\phi}{(b-a)} - \frac{P}{(b-a)} \frac{\left[\left(\frac{b+a}{2r}\right)\cos\phi - \frac{a}{r}\right]\left(r - \frac{b-a}{\ln\frac{b}{a}}\right)}{\left(\frac{a}{2} + \frac{b}{2} - \frac{b-a}{\ln\frac{b}{a}}\right)} \quad \ldots\ldots [4]$$

and the value at $\phi = 90$ deg, $r = a$, for $\frac{a}{b} = 0.7$, is

$$-15.8577 \frac{P}{b-a}$$

If this value were used for Part (2) of $(\sigma_{\phi I})_{r=a}$, then Part (1) of the same stress would come out different from zero and this might lead to the erroneous conclusion that there was still an appreciable local effect of the load at the cross section $\phi = 90$ deg.

Although the stresses were not split into two parts in the original paper, the reader can still separate out Part (1) of the stress, i.e. the local effect of the load, from the total stress in at least some of the figures accompanying the paper. For example, in Fig. 5 of the paper, the stresses indicated by the curves at negative values of Φ are entirely Part (1) stresses since the Part (2) stresses for the case shown are zero at negative values of Φ. The complete curve of Part (1) stresses versus Φ for this case is antisymmetrical about the line $\Phi = 0$.

The authors found that the paper by H. Jung, mentioned in the discussion, contains an interesting application of the Fourier-integral method. However, with two methods available for expressing Part (2) of the stresses as explained above, no attempt was made to apply the procedure used by Jung in the present problem.

---

[3] "A Fourier Integral Solution for the Plane-Stress Problem of a Circular Ring With Concentrated Radial Loads," by C. W. Nelson, Journal of Applied Mechanics, Trans. ASME, vol. 73, 1951, pp. 173–182.

[4] "Die Spannungen und Formänderungen von Balken mit rechteckigem Querschnitt," by F. Seewald, Abhandlungen aus dem Aerodynamischen Institut an der Technischen Hochschule Aachen, Germany, vol. 7, 1927, pp. 11–33.

[5] "Der Spannungszustand in dicken elastischen Platten," by S. Woinowsky-Krieger, *Ingenieur Archiv*, vol. 4, 1933, p. 312.

[6] "Ein Beitrag zur Berechnung von Knicklasten," by H. Jung, *Zeitschrift für angewandte Mathematik und Mechanik*, vol. 31, 1951, pp. 142–148.

[7] "Strength of Materials, Part II," by S. Timoshenko, D. Van Nostrand Company, Inc., New York, N. Y., second edition, 1941, pp. 65–69.

Transmission of Tension From a Bar to a Plate[1]

EDGAR KRAHN.[2] The authors have shown what part of the tension applied to the bar or strip is transmitted to the edge of the plate.

It has been observed before that the calculation leads to reasonable results only if part of the tension is applied to the edge and consequently the equation given by E. Reissner (1)[3] has to be amended to[4]

$$\frac{1}{2bt_1(x)E_1}\left[P-\alpha P-2b\int_0^x q(\xi)d\xi\right]=\frac{1}{t_2E_2}\left[\frac{\alpha P}{2b}K(x,0)+\int_0^a q(\xi)K(x,\xi)d\xi\right]\quad\ldots\ldots[1]$$

where $t_1(x)$ is the variable thickness of the bar and α is the part of the tension applied at the edge of the plate and depends on the details of the attachment of the bar.

The theorem proved by the authors solves the question of determining α.

Except for $K(x, 0)$ and $K(x, \xi)$ which are different, as will be explained, the other symbols in Equation [1], herewith, are those of the paper under discussion.

The bar is supposed to be shaped so that the load transmitted to the plate at $x = a$ is zero or negligible.

If the tension is calculated as if the bar were attached to the plate along a line only, then $K(x, 0)$ and $K(x, \xi)$ have singularities at $x = 0$ and $x = \xi$, respectively.

These singularities can be avoided assuming the contact along a narrow strip instead of a line and calculating the mean strain over the width of the strip.

If a unit force is applied at (ξ, η) in the direction of the negative x-axis then the strain at (x, y) is (5)

$$\frac{1}{\pi tE}\frac{1+\nu}{2}\left\{\frac{x-\xi}{r_1^4}[(x-\xi)^2-\nu(y-\eta)^2]+\frac{x+\xi}{r_2^4}\{(x+\xi)^2+2x\xi-\nu[(y-\eta)^2+2\xi^2]\}+\nu\frac{2\xi(y-\eta)^2}{r_2^4}-(1+\nu)\frac{8x\xi(x+\xi)(y-\eta)^2}{r_2^6}\right\}$$
$$+\frac{1}{\pi tE}\frac{1-\nu}{4}\left\{(1+\nu)\frac{x-\xi}{r_1^2}+\frac{3x+\xi-\nu(x+3\xi)}{r_2^2}-(1+\nu)\frac{4x(y-\eta)^2}{r_2^4}\right\}\quad\ldots\ldots[2]$$

where

$$r_1^2=(x-\xi)^2+(y-\eta)^2 \text{ and } r_2^2=(x+\xi)^2+(y-\eta)^2$$

Regarding the shear force at $x = \xi$ as constant over the width of the strip $-b \leqq y \leqq b$ and integrating with respect to η, one gets the strain at (x, y) induced by the stress at ξ. Integrating then with respect to y and dividing by $2b$ one gets the average strain at x induced by the stress at ξ. That gives the function

$$\frac{1}{tE}K(x,\xi)=\frac{1}{\pi tE}\left\{(1-\nu^2)\tan^{-1}\frac{2b}{x-\xi}+(1-\nu)^2\tan^{-1}\frac{2b}{x+\xi}-\frac{(1+\nu)(1-3\nu)}{8b}(x-\xi)\log\left[1+\left(\frac{2b}{x-\xi}\right)^2\right]+\left[\frac{1+6\nu-3\nu^2}{8b}(x+\xi)-\frac{(1+\nu)^2}{4b}\xi\right]\log\left[1+\left(\frac{2b}{x+\xi}\right)^2\right]+(1+\nu)^2\frac{x\xi}{x+\xi}\frac{2b}{(x+\xi)^2+4b^2}\right\}\quad\ldots\ldots[3]$$

which remains finite.

In the case that the force is applied at the edge one has

$$\frac{1}{tE}K(x,0)=\frac{1}{\pi tE}\left\{\frac{\nu}{b}x\log\left(1+\frac{4b^2}{x^2}\right)+2(1-\nu)\tan^{-1}\frac{2b}{x}\right\}\quad\ldots\ldots[4]$$

which remains finite at $x = 0$.

Equations [3] and [4] of this discussion are the functions $K(x, 0)$ and $K(x, \xi)$ appearing in Equation [1].

M. Z. v. KRZYWOBLOCKI.[5] The following reference may be added to the bibliography given by the authors:

"Action d'une force concentrée sur la plague indéfinie à l'aide d'une barre rigide de section circulaire," by F. Szelagowski, Arch. Méc. Appl. Gdansk, vol. 3, 1951, pp. 99–105 (Polish, French summary).

AUTHORS' CLOSURE

Mr. Krahn's discussion contributes to the subject on certain points which were passed over lightly or altogether in the paper. Replacement of the single-line load of the integral equation by a band load with uniform distribution of load as to the width of the strip, as in Mr. Krahn's analysis, was considered in an attempt to improve the agreement with the test results. A curve was worked out on the basis of uniform-width distribution, corresponding to the calculated curve in Fig. 5 of the paper which is of course for the line-load assumption. It lay well above the calculated curve in Fig. 5—for instance, at $x = 2$ the ordinate was 44 per cent, and at $x = 5$ it was 27 per cent.

It seems to the authors that in principle there is no strong reason for preferring the band load with uniform distribution to the line load. The theorem of the first section of the paper, that in (indefinitely) thin plates of equal Poisson's ratios the load will be transmitted as peripheral line load, means that there will in the idealized test specimen be two parallel line loads along the two edges of the strip. In a real specimen (not indefinitely thin) each of these line loads is of course to be interpreted as an idealization of load occupying a width of the order of the strip or plate *thickness*. This suggests that in our specimen, which has a strip-width to strip-thickness ratio of 8 (not mentioned in the paper), the distribution of the actual bond shear would be heavily concentrated toward each end of the width, and accordingly, very far from uniform. There must also be cross forces since the Poisson contraction of the strip will be interfered with by the plate. In a real joint, rather than a monolithic test specimen, the line forces could be forces transmitted by the edge welding, and the bonding over the interface might be absent. It is conceivable that calculations in terms of two line loads, one for each long edge of the strip, matching strip and plate strain along the

[1] By J. N. Goodier and C. S. Hsu, published in the June, 1954, issue of JOURNAL OF APPLIED MECHANICS, Trans. ASME, vol. 76, pp. 147–150.

[2] U. S. Naval Ordnance Laboratory, White Oak, Silver Spring, Md.

[3] Numbers in parentheses refer to the Bibliography at the end of the paper.

[4] "Note on the Stress Distribution in a Stiffened Semi-Infinite Sheet," by E. Krahn, Admiralty Research Laboratory, Teddington, England, Note ALR/N1/Maths 4.57, August, 1952.

[5] Professor of Gasdynamics and Theoretical Aerodynamics Department of Aeronautical Engineering, University of Illinois, Urbana, Ill.

middle line, could yield better agreement with tests. No calculations of this type were performed.

The authors are grateful to both discussers for the items they have added to the bibliography.

Method of Computing Principal Strains[1]

F. A. McCLINTOCK.[2] The author's algebraic derivation is of interest. Equivalent and perhaps simpler equations were derived from Murphy's graphical construction[3] and reported in the Proceedings of the Society for Experimental Stress Analysis, vol. 9, 1951, pp. 209–210.

Stresses and Deformation of Flanged Shells[1]

C. O. RHYS.[2] The general method of making calculations of strains and stresses in flanged shells, i.e., considering the different deformations set up in the flange and shell, if they were separated, and finding the forces and moments required to bring them together, is well known to be a sound procedure. As the authors point out, this often involves stresses of considerable magnitude. These are stated to be dealt with by the use of adequate fillets best determined by experimental methods; presumably such methods are found to be satisfactory.

Something analogous to the use of fillets might be mentioned here. There is sometimes a sudden sharp change of radius of curvature in a shell fabricated all in one piece. When the change of curvature really is sudden, going from, say, r to R at one point, discontinuity stresses are set up, and such stresses, calculated on the basis of a sudden change, show good agreement with experimental results. It sometimes happens, however, that the stress as obtained from measured strains is considerably less than that obtained by calculations made on the sudden change basis. The explanation seems to be that the change from r to R actually takes place over a short distance in a gradual manner, more or less modifying the effect of an abrupt boundary between the two curvatures, somewhat as a fillet reduces the effect of a sharp corner in a casting or where two different shaft diameters come together. A gradual change from r to R could be used to cut down discontinuities in shell, but, in general, manufacturing methods do not permit this to be done with sufficient accuracy, as obviously can be done for the flange and knuckle considered in the paper.

However, it is indicated that care should be taken to see that the structure is sufficiently strong at points where high stress concentration might take place. This seems, in effect, to nullify the authors' assumption (d) since, to do this, stress concentration must be taken into account.

No definition seems to be given of the term "attenuation length," [3a, b]. This seems to be what, in the Pressure Vessel Research Committee work (Bibliography 8), is called the "instantaneous wave length" divided by twice pi. This instantaneous wave length is expressed by

$$L = 2\pi/N$$

where N^{-1} is equal to the l of the paper. In the damped sinusoidal curves the variable n can be replaced by Ns where s is the x of the paper (though it is usually measured from the flange and not the apex). This is done in the reference (1c) mentioned and also in reference (8), giving

$$F_2 = e^{-Ns} \sin Ns, \text{ etc.}$$

Term s being known, Ns would be the corresponding angle (in radians or ratio) for the F-functions. In the numerical example given in the paper, s from flange to knuckle would be $12\sqrt{2} = 17$, so that Ns, with Poisson's ratio equal to 0.3, would be

$$Ns = [(3)(0.91)]^{0.25}(17)/\sqrt{[(78)\sqrt{2(0.375)}]} = 3.4 \text{ radians} \quad \ldots\ldots [1]$$

which would correspond with values of the F-functions in or near their second loops, where they would be relatively small, so that discontinuity effects of the flange and knuckle on each other would be slight.

As a check on this, the l calculated in the paper as 5 in. would give $N = 0.2$, so that Ns would be $(0.2)(17) = 3.4$ radians.

Actually this is somewhat greater than 3.4, since N increases as r decreases, giving a greater Ns in the same length s. When this is taken into consideration, Ns has to be replaced by $\int Nds$ over the length s considered. For a 45-deg cone, this is

$$[2.57/\sqrt{h}]\,[\sqrt{R} - \sqrt{R - s}] \quad \ldots\ldots [2]$$

R being the $\bar{r}/\sin\phi$ of the paper. This would give

$$[2.57/0.61][10.5 - 9.65] = 3.58 \text{ radians} \quad \ldots\ldots [3]$$

which is only slightly greater than for Equation [1] of this discussion, as there is not much difference in $r/\sin\phi$ from flange to knuckle, but for a relatively large change in r the difference would be considerable.

The foregoing has been gone into somewhat fully in order to get a clear idea of the term attenuation length, and to see whether it agrees with the definition "wave length divided by twice pi." An error involved in using [3a, b] would be on the safe side, that is, as compared with Equation [2] of this discussion.

HERBERT SAUNDERS.[3] The authors are to be congratulated on their splendid effort in accomplishing the solution of a flanged noncircular shell. Most of the work reported in the literature has been concerned mainly with circular shells. There are several methods of flange solutions but many are conservative in the evaluation of flanged shells where weight is at a premium. The writer would like to know if any tests have been made corroborating the authors' work. The main objection to this paper is the introduction of symbols not presently used in the literature which makes it difficult to follow the authors' paper.

AUTHORS' CLOSURE

The interesting comments of Messrs. Rhys and Saunders are much appreciated. Obviously, it is important to relate newly introduced terminology to older ones, and the authors—who failed to explain the term "attenuation length"—are indebted to Mr. Rhys for clarifying the notion. The analysis presented in the paper accounts only for tensile stresses (σ_s is constant) and bend-

[1] By N. J. Taleb, published in the June, 1954, issue of the JOURNAL OF APPLIED MECHANICS, Trans. ASME, vol. 76, pp. 197–198.

[2] Assistant Professor of Mechanical Engineering, Massachusetts Institute of Technology, Cambridge, Mass. Assoc. Mem. ASME.

[3] "A Graphical Method for Evaluation of Principal Strains From Normal Strains," by Glenn Murphy, JOURNAL OF APPLIED MECHANICS, Trans. ASME, vol. 67, 1945, p. A-209.

[1] By G. Horvay and I. M. Clausen, Jr., published in the June, 1954, issue of the JOURNAL OF APPLIED MECHANICS, Trans. ASME, vol. 76, pp. 109–116.

[2] Retired, 1947. Mem. ASME.

[3] Research Engineer, Grumman Aircraft Engineering Corporation, Bethpage, Long Island, N. Y. Mem. ASME.

ing stresses (σ_x varies linearly across a cross section) in the shell. When there is departure from linear variation, then the σ_x stress trajectories necessarily bunch in part of the cross section; the ratio of the trajectory density near the outer (or inner) surface of the shell to the density corresponding to linear variation gives the stress-concentration factor. Changes in cross section or contour, unless prevented by suitable fillets, are always accompanied by stress concentration. In shells one may regard the situation as a polar-symmetric analog of the two-dimensional elbow.[4] Experimental evidence which distinguishes between discontinuity stresses and stress concentration is meager, mostly because very sharp corners usually are not found in shells.

The authors wish to express their appreciation also to the reviewer of the paper for questioning their use—without proof—of the centroid (at radius R) of the flange cross section as rotational center, irrespective of the radius at which the shell is connected (at which the shell moment is applied) to the flange. An argument based on the idea of minimum strain energy of a configuration readily establishes the desired result. A more illuminating proof proceeds as follows: Write inner and outer radii of the flange in the form $a = R(1 - \eta)$, $b = R(1 + \eta)$, and let a moment $M = 1$ lb-in/in be transmitted to the flange at the inner radius a. We shall show that the radial displacement $u(r)$, at locations $r = a, R, b$ of the flange mid-plane, is given, to lowest terms in η and φ_c by

$$u(a) = \frac{1}{2}\,\eta\varphi_c^2, \quad u(R) = -\frac{2 + 5\mu}{12}(\eta\varphi_c)^2, \quad u(b) = -\frac{1}{2}\,\eta\varphi_c^2 \qquad \ldots\ldots [4]$$

where $\varphi_c = \varphi(R)$ is the rotation angle at the flange centroid. Equation [4] reveals that, to the extent that η^2 is negligible, the flange center does not move radially, in spite of the fact that the moment M is applied in the most eccentric location, at radius $R(1 - \eta)$.

The formula for the rotation $\varphi(r)$ of a ring due to moment M applied at $r = a$ is well known[5]

$$\varphi(r) = \frac{a^2 b^2(1 + \mu) + r^2(1 - \mu)}{2Rr}\,\frac{M}{EI} \ldots\ldots [5a]$$

which we write briefly as

$$\varphi = \frac{C_1}{2}\,r + \frac{C_2}{r} \ldots\ldots [5b]$$

Inserting this expression into the equation for radial displacement[6]

$$\frac{d}{dr}\left[\frac{1}{r}\,\frac{d}{dr}\,(ru)\right] = -\,\frac{1 - \mu}{2r}\,\varphi^2 - \varphi\,\frac{d\varphi}{dr} \ldots\ldots [6]$$

one finds

$$u = \frac{1 - \mu}{4}\,Ar + \frac{1 + \mu}{4}\,\frac{B}{r} - \frac{3 - \mu}{64}\,C_1^2 r^3 - \frac{1 - \mu}{4}\,C_1 C_2\, r \ln r - \frac{1 + \mu}{4}\,C_2^2\,\frac{\ln r}{r} \ldots\ldots [7]$$

where

$$\left.\begin{aligned} A &= -\frac{1}{2}\,\frac{1 + \mu}{1 - \mu}\,C_1 C_2 + \frac{C_1^2 R^2}{8} - \frac{1}{2}\,\frac{C_2^2}{R^2} \\ &\quad + \eta^2\left(\frac{1}{6}\,C_1 C_2 + \frac{C_1^2 R^2}{8} - \frac{C_2^2}{6R^2}\right) + \ldots \\ B &= \frac{1}{2}\,C_1 C_2 R^2 + \frac{1}{2}\,\frac{1 - \mu}{1 + \mu}\,C_2^2 + \frac{C_1^2}{16}\,R^4 \\ &\quad + \eta^2\left(-\frac{C_1^2}{8}\,R^4 - \frac{5}{6}\,R^2 C_1 C_2 - \frac{7}{6}\,C_2^2\right) + \ldots \end{aligned}\right\} \ldots [8]$$

From these expressions the foregoing stated results, Equations [4], follow at once.

On the Equations of Motion of Cylindrical Shells[1]

R. Bart[2] and G. D. Galletly.[3] We would like to congratulate the authors on their interesting paper concerning the various approximations that have been used in cylindrical shell theory and would like to make the following observations concerning the formulas used by them for the change of curvature ϑ_s and twist ϑ_{xs}:

If, as is suggested in footnote 9 of the paper, their Equations [6] are substituted into Equations [4] and then z/a is neglected in comparison to unity, one obtains the following expressions for the moments

$$\left.\begin{aligned} M_x &= D\left[-\left(\frac{\partial^2 w}{\partial x^2} + \frac{1}{a}\,\frac{\partial u}{\partial x}\right) - \nu\left(\frac{\partial^2 w}{\partial s^2} + \frac{1}{a}\,\frac{\partial v}{\partial s}\right)\right] \\ M_s &= D\left[-\left(\frac{\partial^2 w}{\partial s^2} + \frac{w}{a^2}\right) - \nu\,\frac{\partial^2 w}{\partial x^2}\right] \\ M_{xs} &= \frac{D(1 - \nu)}{2}\left[-2\,\frac{\partial^2 w}{\partial x\,\partial s} - \frac{2}{a}\,\frac{\partial v}{\partial x}\right] \\ M_{sx} &= \frac{D(1 - \nu)}{2}\left[-2\,\frac{\partial^2 w}{\partial x\,\partial s} - \frac{1}{a}\,\frac{\partial v}{\partial x} + \frac{1}{a}\,\frac{\partial u}{\partial s}\right] \end{aligned}\right\} \ldots [1]$$

Equations [1] of this discussion agree with those obtained by Reissner and others[3] when due account is taken of the different sign conventions used.

Osgood and Joseph,[4] by purely geometrical considerations, obtained for the changes of curvature and twist

$$\vartheta_x = -\,\frac{\partial^2 w}{\partial x^2}, \quad \vartheta_s = -\left(\frac{\partial^2 w}{\partial s^2} + \frac{w}{a^2}\right), \quad \vartheta_{xs} = -\,2\,\frac{\partial^2 w}{\partial x\,\partial s} - \frac{1}{a}\,\frac{\partial v}{\partial x} + \frac{1}{a}\,\frac{\partial u}{\partial s} \ldots\ldots [2]$$

In the derivation of Equations [2] the usual assumption was made that normals to the undeformed middle surface remain normal to the deformed middle surface and suffer no extension.

---

[4] Illustrated in "Formulas for Stress and Strain," by R. J. Roark, McGraw-Hill Book Company, Inc., New York, N. Y., Case XVII, 9, 1943 edition.

[5] "Theory of Plates and Shells," by S. Timoshenko, McGraw-Hill Book Company, Inc., New York, N. Y., 1940, p. 63.

[6] Ibid., p. 331.

[1] By P. M. Naghdi and J. G. Berry, published in the June, 1954, issue of the Journal of Applied Mechanics, Trans. ASME, vol. 76, pp. 160–166.

[2] Structural Research Engineer, Navy Department, David Taylor Model Basin, Washington, D. C.

[3] "Note on the Expressions for the Strains in a Bent Thin Shell," by Eric Reissner, *American Journal of Mathematics*, vol. 64, 1942, p. 769.

[4] "On the General Theory of Thin Shells," by W. R. Osgood and J. A. Joseph, Journal of Applied Mechanics, Trans. ASME, vol. 72, 1950, p. 397.

(The changes of curvature and twist were defined as the coefficients of z in the expressions for the components of strain.)

If the deformation of the middle surface is inextensional, then the following relations hold

$$\frac{\partial u}{\partial x} = 0, \quad \frac{\partial v}{\partial s} = \frac{w}{a}, \quad \frac{\partial v}{\partial x} = -\frac{\partial u}{\partial s} \qquad [3]$$

Substitution of the Relations [3] into Equations [1] and [2] yields

$$\left.\begin{aligned} M_x &= D\left[-\frac{\partial^2 w}{\partial x^2} - \nu\left(\frac{\partial^2 w}{\partial s^2} + \frac{w}{a^2}\right)\right] \\ M_s &= D\left[-\left(\frac{\partial^2 w}{\partial s^2} + \frac{w}{a^2}\right) - \nu\frac{\partial^2 w}{\partial x^2}\right] \\ M_{xs} = M_{sx} &= \frac{D(1-\nu)}{2}\left[-2\frac{\partial^2 w}{\partial x \partial s} - \frac{2}{a}\frac{\partial v}{\partial x}\right] \end{aligned}\right\} \qquad [1a]$$

and

$$\vartheta_x = -\frac{\partial^2 w}{\partial x^2}, \quad \vartheta_s = -\left(\frac{\partial^2 w}{\partial s^2} + \frac{w}{a^2}\right), \quad \vartheta_{xs} = -2\frac{\partial^2 w}{\partial x \partial s} - \frac{2}{a}\frac{\partial v}{\partial x} \qquad [2a]$$

Thus, with the use of Equations [3], herewith, the expressions for the changes of curvature, obtained by neglecting z/a in comparison to unity, after Equations [6] of the paper have been substituted into Equations [4], agree with those derived by Osgood and Joseph. As noted by the authors, the expression for twist ϑ_{xs} also agrees with that derived by Love and Timoshenko.

Use of the Relations [3] of this discussion also would bring ϑ_{xs} given by Equation [2a], into line with that used by the authors. However, we prefer to use the expression

$$\vartheta_s = -\left(\frac{\partial^2 w}{\partial s^2} + \frac{w}{a^2}\right) \qquad [4]$$

as then it is immediately obvious that the change in curvature, when the cylinder undergoes a uniform radial displacement w, is $-w/a^2$ to the first order. This is in contradistinction to the authors' (also Love's and Timoshenko's) expression for ϑ_s, where they write

$$\vartheta_s = -\left(\frac{\partial^2 w}{\partial s^2} + \frac{1}{a}\frac{\partial v}{\partial s}\right) \qquad [4a]$$

and the change in curvature would now appear to be zero, unless one knew that in deriving Equation [4a] the conditions of an inextensional middle surface had been utilized.

We should appreciate any comments that the authors may wish to make on the foregoing remarks.

Authors' Closure

The authors appreciate the comments of Drs. Bart and Galletly. However, it appears that they may have overlooked one or two points concerning the stress couple-displacement relations of shell theory.

First, it should be noted that the form of the stress couple-displacement relations does not depend at all on the set of quantities usually referred to as "changes of curvatures." The form of these relations depends solely on the approximations introduced when Equations [6] of the paper are substituted into Equations [4c]. Once the stress couple-displacement relations have been obtained it is desirable (although not necessary), as a matter of convenience and for the sake of brevity perhaps, to introduce the so-called changes in curvatures; hence these quantities must not be regarded as fundamental in the theory.

The expressions for the changes in curvatures of a surface (here the middle surface) may be obtained from differential geometry alone. When the displacements of the surface are small the changes in curvatures (to the first order in the displacement components) are

$$\left.\begin{aligned} \varphi_x &= \frac{\partial^2 w}{\partial x^2}, \quad \varphi_s = \frac{\partial^2 w}{\partial s^2} + \frac{1}{a}\frac{\partial v}{\partial s} - \frac{1}{a}e_s \\ \varphi_{xs} &= 2\frac{\partial^2 w}{\partial x \partial s} + \frac{2}{a}\frac{\partial v}{\partial x} - \frac{1}{a}e_{xs} \end{aligned}\right\} \qquad [5]$$

where e_s and e_{xs}, the strains of the middle surface are given by

$$e_s = \frac{\partial v}{\partial s} - \frac{w}{a}, \quad e_{xs} = \frac{\partial v}{\partial x} + \frac{\partial u}{\partial s}$$

Apart from a negative sign, which is determined by the positive stress-couple convention, Equations [5] of this closure agree with Equations [2] of the discussion. The fact that Equations [5] are identical with the coefficients of z in the expressions for the strains (Equation [6] of the paper) is a consequence of the neglect of shear deformation and normal stress in the classical theory. With this in mind, it seems logical to consistently associate the coefficients of z in the strains with a set of quantities we may call the changes in curvatures, even though these do not necessarily agree with Equations [5].

As was emphasized in the text of the paper, Love's first approximation was adopted, and the changes in curvatures obtained from the foregoing procedure are consistent with this approximation. Furthermore, nowhere has the assumption of inextensibility been made nor can our results be obtained from Equations [5] by assuming inextensibility.

In view of the foregoing, it is not surprising that our expression for φ_s does not agree with Equation [4] of the discussion. Drs. Bart and Galletly have chosen to use the exact form of φ_s as given by Equations [5]. However, as was pointed out in the second paragraph, this has no significance in so far as the stress couple-displacement relations are concerned.

In conclusion, we repeat that it is the approximations which are introduced into the definitions of the strains and the stress couples that affect the stress couple-displacement relations and not the so-called changes in curvatures.

On the Thickness of Normal Shock Waves in a Perfect Gas[1]

H. G. Elrod, Jr.,[2] and S. Jarvis.[3] We are currently working on the problem of the interaction of a shock wave with a boundary layer[4] and, therefore, have had occasion to study the continuum theory of shock structure. Several portions of the present paper appear to us to contain incorrect implications, or to lack clarity, and we offer the following analysis for comment by the authors.

To discuss the items in question, let us first write the following differential equation, valid for a perfect gas having constant specific heats and Prandtl number

[1] By A. H. Shapiro and S. J. Kline, published in the June, 1954, issue of the Journal of Applied Mechanics, Trans. ASME, vol. 76, pp. 185–192.

[2] Assistant Professor, Case Institute of Technology, Cleveland, Ohio. Assoc. Mem. ASME.

[3] Research Assistant, Case Institute of Technology, Cleveland, Ohio.

[4] The writers wish to acknowledge support for their work from the Office of Ordnance Research, United States Army.

$$\frac{2}{3}q''(z) + \left[Q'(q) + \frac{1}{k}\left(\frac{1-k}{2} - \frac{2}{3}\Pr\right)\right]q'(z) = \Pr Q \quad [1]$$

where

$$q \equiv u^2 \quad [2]$$

$$z \equiv \int_0^x \frac{m\,dx}{\mu} \quad [3]$$

$$Q \equiv \frac{k+1}{2k}(u_1 - u)(u - \alpha u_1) \quad [4]$$

$$\alpha \equiv \frac{k-1}{k+1} + \frac{2}{k+1}\frac{1}{M_1^2} \quad [5]$$

At the point of minimum viscous stress,[5] $u''(z) = 0$. This condition is equivalent to setting $u''(x) = 0$ in the authors' Equation [6] where the viscosity derivative has been omitted. It is a convenient condition to use, in conjunction with the following definition of shock-thickness Reynolds number

$$\mathrm{Re} \equiv \frac{(u_2 - u_1)\rho_1 u_1}{\left(\mu \dfrac{du}{dx}\right)_{\min}} = \frac{\frac{4}{3}(p_2 - p_1)}{|\text{viscous stress}|_{\max}} \quad [6]$$

Now at the point of minimum stress Equation [1], herewith, becomes

$$\frac{8k}{3\Pr}u'(z)^2 - 2(Du^*)u'(z) + (k+1)(u^* - u_1)(u^* - \alpha u_1) = 0 \quad [7]$$

with

$$D \equiv \frac{4}{3} + \frac{2k}{\Pr} - \frac{k+1}{2\Pr}(1+\alpha)\frac{u_1}{u^*} \quad [8]$$

When the foregoing quadratic equation is solved, and the resulting value of $u'(z)$ employed in Equation [6], we have

$$\mathrm{Re} = \frac{(u_2 - u_1)Du^*}{(k+1)(u^* - u_1)(u^* - \alpha u_1)}\left[1 \pm \sqrt{1 - \frac{8k(k+1)}{3\Pr}\frac{1}{D^2}\frac{(u^* - u_1)(u^* - u_1)}{u^{*2}}}\right] \quad [9]$$

For all finite values of thermal conductivity the over-all flow from uniform conditions at $-\infty$ to uniform conditions at $+\infty$ is adiabatic, so that the Rankine-Hugoniot relation $u_2 = \alpha u_1$ is valid. Examination of Equations [9] and [8] discloses, then, that an exact answer for Re can be found whenever the correct value of the velocity (u^*) at the point of minimum stress is known. Thus a consideration of various empirical velocity profiles is not especially pertinent to the prediction of shock Reynolds numbers. In particular, absolutely no significance should be attributed to the agreement between the authors' Equation [19b] and Becker's result for $\Pr = 3/4$, since the authors borrowed Becker's value of u^* for their own analysis.

Except for the case of $\Pr = 3/4$, agreement between the authors' Equation [19b] and other known exact answers is not forced and lends some confidence to its use as an interpolation formula. There are special reasons for this extended agreement. Let us consider the form which Equation [1], herewith, assumes for the various special cases cited. For brevity, we shall restrict ourselves to cases of finite viscosity, so that a one-to-one correspondence between x and z exists.

[5] This viscous stress is negative.

Case A. $\Pr = 3/4$

$$\frac{2}{3}q''(z) + Q'(z) - \frac{3}{4}\left[\frac{2}{3}q'(z) + Q\right] = 0 \quad [10]$$

The equation is exact. Uniformity of infinity demands that

$$\frac{2}{3}q'(z) + Q = 0 \quad [11]$$

Case B. $\Pr \to \infty$; μ, C_p, finite; $\lambda \to 0$

$$\frac{2}{3}q'(z) + kQ = 0 \quad [12]$$

Case C. $Q \to 0$ (weak shock); C_p, μ, k finite: Order-of-magnitude analysis yields

$$q''(z) \ll q'(z);\ Q'(q) \ll \frac{1}{k}\left(\frac{1-k}{2} - \frac{2}{3}\Pr\right) \quad [13]$$

$$\therefore \left(\frac{4}{3} + \frac{k-1}{\Pr}\right)q'(z) + 2kQ = 0 \quad [14]$$

Case D. $\gamma \to 1$; μ finite; $C_p \to \infty$

$$\frac{2}{3}q''(z) + Q'(z) - \Pr\left[\frac{2}{3}q'(z) + Q\right] = 0 \quad [15]$$

The equation is exact. A satisfactory first integral is

$$\frac{2}{3}q'(z) + Q = 0 \quad [16]$$

In all of the special cases considered, a first integral of Equation [1] of this discussion can be found in the form

$$q'(z) = 2uu'(z) = K(u - u_1)(u - u_2) \quad [17]$$

where K, a constant, varies from case to case. For all these cases the following equation is valid when $u''(z) = 0$

$$u^* = \sqrt{u_1 u_2} \quad [18]$$

We see, therefore, the reason for the extended agreement of the authors' Equation [19] with known analytical results. Moreover, we see that it lies solely in their happy formulation for u^*.

The results of the authors' paper are based on their guess that Equation [18] will hold well enough for general Prandtl number and shock strength in a perfect-gas continuum. Whereas their guess may be satisfactory in the normal range of Prandtl number, it becomes incorrect for some shocks of finite strength and small Prandtl number, where u^* must be less than the geometric mean of the two velocity extremes. Some indication of this fact is provided by the failure of the authors' Equation [19] to give an infinite shock Reynolds number for allowable values of M_1^* when $\Pr^* \to 0$.

We have been applying normal-shock analyses, such as that of the authors', to the estimation of oblique-shock thicknesses. Since the standard formulations for fluid flow are in Newtonian mechanics, a uniform translation of a co-ordinate system parallel to the "surface" of a rectilinear shock will not introduce new "forces," and oblique-shock solutions are thereby obtained. Such solutions probably represent the asymptotic behavior of oblique shocks at suitable distances from solid surfaces. They indicate that in certain experiments concerning shock-boundary-layer interaction, the two transition thicknesses are of comparable magnitude.

F. S. SHERMAN.[6] This paper brings to the theoretical study of the thickness of normal shock waves a cleverly conceived approximate method of analysis the results of which both summarize and exceed those more tediously obtained in several previous papers. Within the framework of the Navier-Stokes equations for a perfect gas, Equation [19] of the paper appears to give a satisfactory accounting for the separate or combined effects of all the significant parameters such as Mach number Prandtl number, and specific-heat ratio. The choice of dimensionless groupings, reference of gas properties to the "critical" temperature T^*, and discussion of the effects of variable viscosity are very satisfying, having much in common with the treatment of Puckett and Stewart.

Two serious questions remain unanswered, however, concerning the practical applicability of the theoretical results obtained. Both of these are properly mentioned in the present paper but have been subjected to considerable recent probing along both theoretical and experimental lines.

The first of these questions asks for the upper limit of shock strength for proper application of the Navier-Stokes relations for a monatomic gas, for which no possible relaxation effects can exist to confuse the picture. In pursuit of an answer, Wang-Chang,[7] Zoller,[8] and Grad[9] have turned to the kinetic theory of gases, seeking solutions to the Burnett equations[10] in the first two instances, and to the "thirteen moment"[11] equations in the last. Their results generally deviate significantly from those obtained by the Navier-Stokes equations when M_1 is greater than 1.5, the shock thicknesses calculated from the kinetic theory being larger than those predicted in the present paper. Grad's paper gives a particularly fine summary and critique of the problem, including in his analysis a new method of obtaining the shock profile in analytic form as a series expansion in the shock strength.

The second question was raised by the experimental data produced by the Metcalf Laboratory Group at Brown University, which suggests that the Navier-Stokes perfect-gas formulation of the problem may be in considerable error for a diatomic gas due to relaxation effects in the rotational degrees of freedom of the diatomic molecule. Since the reference to this work which is indicated by Shapiro and Kline, there has been at least one further report from the Metcalf Laboratory,[12] extending the scope of their work and confirming earlier results. In the meanwhile, an entirely different type of experimental determination of shock-wave thicknesses has been undertaken at the University of California, utilizing the low-density wind tunnel at Berkeley. The results of the latter tests are still being analyzed, but already have indicated general confirmation of the Brown University results, both with respect to the good agreement with Navier-Stokes theory for a monatomic gas, and to the systematic deviations from theory in a diatomic gas. In addition, it has been noted at Berkeley that the shapes of shock profiles for a given Mach number are completely similar in air and helium, with no apparent oddities of the air profile which could be attributed to relaxation phenomena.

In summary, it appears that the present paper gleans all that profitably may be obtained from the Navier-Stokes perfect-gas approach to the calculation of normal shock-wave thicknesses. In combination with recent papers dealing with more complex equations derived from the kinetic theory of gases, it probably brings about a fairly accurate prediction of the state of affairs in a shock wave in a monatomic gas. Preliminary experimental evidence suggests, however, that shocks in diatomic gases may not be so simply described, and that a profitable field for further theoretical study is still open, particularly to anyone who can devise a method of analysis for the shock transition in a gas with short, but significant, relaxation times.

L. N. TAO.[13] The authors derived a general approximation of the normal shock-thickness problem based on an assumption of velocity distribution. It is interesting in that the results show such excellent agreement with others.

However, such a result may also be obtained without the assumption of velocity distribution. Since

$$\frac{d}{dx}(u^2) \equiv 2u\frac{du}{dx}$$

$$\frac{d^2}{dx^2}(u^2) \equiv 2u\left(\frac{d^2u}{dx^2}\right) + 2\left(\frac{du}{dx}\right)^2$$

guided by the definition of a shock-wave thickness[14]

$$\delta = \frac{u_2 - u_1}{\left(\frac{du}{dx}\right)_{x=0}}$$

and the requirements (e) and (f), stated by the authors, we obtain

$$\left(\frac{du}{dx}\right)_{x=0} = \frac{c^*}{\delta}\left(\frac{1}{M_1^*} - M_1^*\right)$$

$$\left(\frac{d(u^2)}{dx}\right)_{x=0} = 2\frac{c^{*2}}{\delta}\left(\frac{1}{M_1^*} - M_1^*\right)$$

and

$$\left(\frac{d^2(u^2)}{dx^2}\right)_{x=0} = 2\frac{c^{*2}}{\delta^2}\left(\frac{1}{M_1^*} - M_1^*\right)^2$$

These equations are exactly the same as the authors' Equations [9b], [9c], and [9d] with the substitution of b from Equation [11]. Hence any function that obeys the conditions (a) to (e) as given by the authors will yield the identical results. For example, a set of inverse tangent functions is proposed as the velocity distribution

$$x \leqslant 0 \qquad u = c^* + (c^* - u_1)\frac{2}{\pi}\tan^{-1}(ax)$$

$$x \geqslant 0 \qquad u = c^* + (c^* - u_2)\frac{2}{\pi}\tan^{-1}\left(\sqrt{\frac{u_1}{u_2}}\,ax\right)$$

where a is associated with δ by the expression

$$a\delta = \frac{\pi}{2}\frac{M_1^* + 1}{M_1^*}$$

---

[6] Low Pressures Project, Institute of Engineering Research, University of California, Berkeley, Calif.

[7] "On the Theory of the Thickness of Shock Waves," by C. S. Wang-Chang, University of Michigan, Department of Engineering Research, Report UMH-3-F, (APL/JHU CM-503), 1948.

[8] "Zur Struktur des Verdichtungstosses," by K. Zoller, *Zeitschrift für Physik*, vol. 130, 1951, p. 1.

[9] "The Profile of a Steady Plane Shock Wave," by H. Grad, Comm. on Pure and Applied Mathematics, vol. 5, 1952, pp. 257–300.

[10] "Mathematical Theory of Non-Uniform Gases," by S. Chapman and T. Cowling, Cambridge University Press, Cambridge, England, 1939.

[11] "On the Kinetic Theory of Rarefied Gases," by H. Grad, Comm. on Pure and Applied Mathematics, vol. 2, 1950.

[12] "The Shape and Thickness of Shock Fronts in Argon, Hydrogen, Nitrogen and Oxygen," by E. F. Greene and D. F. Hornig, ONR-061-041, Technical Report No. 4, Metcalf Research Laboratory, Brown University, Providence, R. I., August, 1952.

[13] Research and Development Department, Worthington Corporation, Harrison, N. J.

[14] All the symbols are the same as used by the authors.

The values of

$$\left(\frac{du}{dx}\right)_{x=0}, \left(\frac{d(u^2)}{dx}\right)_{x=0}, \text{ and } \left(\frac{d^2(u^2)}{dx^2}\right)_{x=0}$$

are the same for both error integral and inverse tangent functions and therefore the same results are derived.

To conclude, it would appear that the authors' solution, in so far as $c^{*2} = u_1u_2$ [requirement (f) in the paper] holds, is applicable only at the boundary points, i.e., at $x = -\infty, +\infty$, and 0. No direct or reliable information can be extracted for the region of $-\infty < x < 0$ and $0 < x < +\infty$.

L. MEYERHOFF.[15] The problem of calculating the thickness of a shock wave is treated by Professors Shapiro and Kline in this paper. In the course of the analysis a Reynolds number-type parameter is introduced as a basis for comparing the variation of this thickness parameter with a variation of the Prandtl number of the initial flow. The comparison showed only a small influence of the initial Prandtl number. However, the actual (dimensional) thickness of the wave does change appreciably with initial Prandtl number or initial temperature; i.e., the Prandtl number, for air, is temperature dependent. This increase of dimensional thickness is shown in Fig. 3 in the writer's paper[16] to which the authors refer. The actual thickness of a shock wave is usually defined by

$$\text{Thickness, } \delta, = \frac{u_0 - u_1}{du/dx} \quad \ldots\ldots\ldots\ldots\ldots [19]$$

where

u_0 = initial supersonic velocity
u_1 = Rankine-Hugoniot final velocity
du/dx = slope at shock-wave center, defined by $d^2u/dx^2 = 0$
x = co-ordinate, e.g., centimeters

Fig. 3 of the writer's paper[16] shows calculated curves of the velocity through the shock wave versus the x-co-ordinate. These curves are calculated for an initial Mach number $\mathbf{M} = 2.0$ and identical initial mass flow. For one curve, the initial Prandtl number $\mathbf{P}_r$ is 0.75 and for the other $\mathbf{P}_r$ is 0.657. A straightforward comparison of shock-wave thickness, based on definition (1), obtained from these curves, shows the curve for $\mathbf{P}_r = 0.657$ gives three times the thickness of the $\mathbf{P}_r = 0.75$ curve. In order to obtain this change of initial Prandtl number for air, it is necessary to change the initial temperature; that is, the available experimental data show $\mathbf{P}_r$ to be a function of temperature. Of course it is apparent that this change of initial temperature from 0 to 500 C will produce a marked change in the coefficients of viscosity and conductivity. The change of these values can be used to explain further the lengthened wave shown in Fig. 3.[16]

In an oversimplified way, the situation between the Reynolds number-type thickness versus the dimensional thickness is perhaps analogous to the case of an airplane flying at 660 mph at 35,000 ft and 760 mph at sea level. In both cases the Mach number is 1.0, but the actual speed relative to the ground is 100 mph greater at sea level. Likewise, the Reynolds-number shock-thickness parameter is the same for the two flows in the writer's Fig. 3, but the thickness of the wave, in centimeters, for $\mathbf{P}_r = 0.657$, according to definition [19] is larger.

The Reynolds-number parameter for shock waves is based on a constant value of the viscosity coefficient, while in fact, this coefficient must vary appreciably through the wave, with the corresponding change in temperature.

Concerning the definition of the shock thickness in terms of the velocity, it may be pointed out that such a thickness also could be based on the change of pressure, density, temperature, or even entropy within the wave. It is pointed out, for example, in the writer's paper[16] that inside the shock, at $\mathbf{M}_0 = 4.0$, the velocity gradient for variable gas properties may be about 27 times greater than the corresponding temperature gradient.

In passing, it may be of interest to note that a calculation scaled from Fig. 6 in the paper,[16] at $\mathbf{M}_0 = 4.0$, indicates surprisingly, that the velocity shock thickness is about five times greater than the temperature thickness. Fig. 6 of the paper[16] compares, for the same initial flow conditions, the velocity versus the x-co-ordinate inside the shock wave for the cases of constant and varying gas properties along the flow. The initial Prandtl number is 0.75 for these two curves. It is found, as stated in the paper, that the thickness of the shock wave is about $2^1/_2$ times greater than that for constant gas properties. It is also about this same thickness greater than the mean free path of the molecules. It may be of interest to examine the effect of varying gas properties on the shock thickness for a range of initial Mach numbers and initial Prandtl numbers.

AUTHORS' CLOSURE

The authors wish to thank Professor Elrod and Mr. Jarvis, and also Mr. Tao, for demonstrating that the only feature of the assumed velocity profile which influences the calculated shock-thickness Reynolds number is the value of u at the point where $d^2u/dx^2 = 0$. If the authors may be permitted to restate the arguments of the foregoing writers in what appears to be the simplest form, Equation [6] of the paper shows that, at the point where $d^2u/dx^2 = 0$, the value of du/dx depends only on the value of u; in which case Equations [10] and [12] of the paper reveal that Rey depends only on the value of u at the point of inflection of the velocity profile. Therefore any velocity profile for which the value of u is chosen as $\sqrt{u_1u_2}$ at the point where $d^2u/dx^2 = 0$ will give results identical with those of the paper. The authors plead guilty to having displayed good intuition but in all modesty they must also admit that the choice of $\sqrt{u_1u_2}$ could hardly have been avoided in view of Becker's exact solution! Nevertheless, the proofs given by Elrod and Jarvis, particularly for the cases of Prandtl number other than $^3/_4$, are very enlightening in the sense that they illuminate why the results of the authors are in such remarkable agreement with all the previously known limiting solutions. Thus the results of Elrod and Jarvis strengthen the results of the authors by showing that the most critical assumption of the paper is, in fact, correct for a very wide range of circumstances.

The remark of Professor Elrod and Mr. Jarvis that Equation [19] of the paper fails to show that $\text{Rey} \to \infty$ as $\text{Pr}^* \to 0$ is incorrect, as they will find from the authors' Table 1 and a more careful study of Equation [19] that Rey does indeed become infinite as Pr^* approaches zero (but note that δ does not necessarily become infinite). Thus it would still appear that the solution presented by the authors is in agreement with all of the limit points and limiting solutions at present available.

What Mr. Tao means by his final paragraph is not clear, for the authors had no intention of solving for the velocity profile (in fact, their method precludes such) but only for the shock thickness.

Regarding Dr. Meyerhoff's discussion of the effect of Prandtl number on shock thickness, the authors cannot help but feel that he is only further buttressing the misleading impression of the importance of Pr which he gave in his earlier paper.[16] The example

[15] Research Group Leader, Department of Aeronautical Engineering and Applied Mechanics, Polytechnic Institute of Brooklyn, Brooklyn, N. Y.

[16] An extension of "The Theory of the One-Dimensional Shock-Wave Structure," by Leonard Meyerhoff, *Journal of the Aeronautical Sciences*, vol. 17, 1950, pp. 775–786.

given by Dr. Meyerhoff compared (if this is the suitable word under the circumstances) the shock thicknesses in air for two cases having the same values of M_1 and $\rho_1 u_1$, but different values of T_1, p_1, Pr, and k. Since, as shown in the authors' paper, Rey depends only weakly on Pr and k, it is to be expected that the two values of Rey will be nearly alike, and indeed they are within 4 per cent of each other. However, it follows from the definition of Rey that the two shock thicknesses will be quite different because of the differences in T_1 and p_1. Putting the cart before the horse, Dr. Meyerhoff states that the change of viscosity with temperature *further* explains the threefold increase[17] of shock thickness as Pr increases from 0.657 to 0.750. The fact is that, of the roughly 100 per cent increase shown by Meyerhoff's Fig. 3 (15), 96 per cent is accounted for by the changes in p_1 and T_1, 3 per cent is accounted for by the change in k, and only the remaining 1 per cent can be attributed to the variation in Pr.

Also in reply to Dr. Meyerhoff, it is noted that the definition of shock-thickness Reynolds number does *not* depend on a constant viscosity coefficient. The authors have shown in the paper that the great majority of the effect of variable properties, including all of the qualitative effects cited by Dr. Meyerhoff, are explicable solely on the basis of the difference in properties between the upstream values and the values at the center of the shock wave where the viscous and heat-transfer effects are concentrated. This type of effect can be accounted for within the framework of the method given by the authors in an extremely simple fashion.

The authors are particularly indebted to Dr. Sherman for his fine discussion showing the relationship of the continuum results to the kinetic-theory results for a monatomic gas, mentioning the problem of relaxation effects in complex molecules and the difficulties of handling them theoretically, and describing his excellent experimental results bearing on both these points. Since the submission of his comments Professor Sherman has apparently carried his excellent work somewhat farther as shown in his published work.[18] It is particularly important to note that Sherman concludes, in answer to his own question mentioned here, that the shock structure can be adequately described by the Navier-Stokes equations for both monatomic and diatomic gases, at least to $M_1 = 2$, provided that the bulk (or second) coefficient of viscosity is taken to be zero for the case of the monatomic gas but equal to approximately two thirds of the ordinary viscosity for the case of the diatomic gas. Thus Sherman provides the start toward information not only on shock structure but also on the very fundamental questions which have so long been unanswered concerning the Navier-Stokes stress formulation.

[17] Actually a scaling of Meyerhoff's Fig. 3 (15) shows a twofold increase.

[18] "A Low-Density Wind-Tunnel Study of Shock Wave Structure and Relaxation Phenomena in Gases," by F. S. Sherman, Report No. HE-150-122, University of California, Berkeley, Institute of Engineering Research, NACA Contract NAw 6287.

Bending of Isotropic Thin Plates by Concentrated Edge Couples and Forces[1]

W. A. NASH.[2] The author has presented a clear and concise exposition of Muschelišvili's complex variable approach to plate problems where the faces of the plate are free from normal forces. In this case the governing equation for deflections is biharmonic and its solution may be represented in terms of two analytic functions of a complex variable. The general procedure presents deflections, bending moments, and transverse shears in terms of these two functions. Although the principles of this approach are relatively straightforward, practical difficulties arise when it becomes necessary to determine a mapping function which maps the boundary of the plate into a unit circle. The author has extended this technique by developing rather elegant methods for treating concentrated edge loadings in the general case and by virtue of this has presented closed-form solutions to three interesting problems in circular-plate theory.

The choice of a circular plate was certainly a logical starting point in applying the complex variable approach to the problem of concentrated edge loadings because of the simplicity of the mapping function. The writer, however, questions whether it will be possible to obtain solutions for more than a few additional plate contours because of the difficulty of determining a mapping function.

Several years ago the writer presented a solution[3] to the problem of a generalized edge loading acting on a plate of elliptical contour. The technique employed there was to expand the loading in a Fourier series, using elliptical co-ordinates, and consequently any distributed or concentrated loading could be treated. Convergence of the series for deflections and moments was reasonably satisfactory. The special case of a circular plate could of course be readily treated by this technique for any concentrated loading. It would have been interesting for the author to compare the facility with which he can obtain results from his method with those obtainable from this writer's approach.

Further, the technique developed by the writer[3] is readily applicable to certain multiply-connected regions, whereas mapping functions for such contours would be extremely difficult to determine.

K. S. PISTER.[4] The author's interesting paper on the transverse flexure of plates by edge loading is based upon the method developed by Kolossoff and Muschelišvili for problems of plane elasticity and later extended to plate problems by Lechnitzky. Solutions of problems in either of these areas by this method generally have been limited to the following: Finite plane slices (or plates) that can be mapped conformally on the interior of a unit circle or upon a circular annulus; infinite plane slices (or plates) with cutouts that can be mapped on the infinite region exterior to a unit circle. In either case the mapping function must be relatively simple, or an approximate polynomial mapping function substituted, if heavy computations are to be avoided. Some examples of solutions of these types are included in the author's introduction. Additional results for an infinite plate with a cutout in the form of a circle, ellipse, square with rounded corners, or triangle with rounded corners, have been given by Holgate.[5,6] Edge loadings considered in his papers were flexural couples distributed around all edges, cylindrical bending about one axis, and uniform twist about one axis. Both isotropic and aeolotropic plates have been treated by him using complex variable methods similar to those used extensively by Stevenson and Green. These techniques, although apparently

[1] By Y. Y. Yu, published in the June, 1954, issue of the JOURNAL OF APPLIED MECHANICS, Trans. ASME, vol. 76, pp. 129–139.

[2] Associate Professor, Department of Engineering Mechanics, University of Florida, Gainesville, Fla. Mem. ASME.

[3] "Bending of an Elliptical Plate by Edge Loading," by W. A. Nash, JOURNAL OF APPLIED MECHANICS, Trans. ASME, vol. 72, 1950, pp. 269–274.

[4] Assistant Professor of Civil Engineering, University of California, Berkeley, Calif. Assoc. Mem. ASME.

[5] "The Transverse Flexure of Perforated Isotropic Plates," by S. Holgate, Proceedings of the Royal Society of London, England, series A, vol. 185, January–April, 1946, pp. 35–49.

[6] "The Transverse Flexure of Perforated Aeolotropic Plates," by S. Holgate, Proceedings of the Royal Society of London, England, series A, vol. 185, January–April, 1946, pp. 50–69.

developed independently, are basically the same as those of Muschelišvili.

In pointing out the similarity between the plate problems considered by him and their analogs in plane elasticity, the author indicates an analogy of considerable interest and importance. As is well known, the first boundary-value problem of plate theory is analogous to the second boundary-value problem of plane elasticity, and the second boundary-value problem of plate theory is analogous to the first of plane elasticity. Considerable experimental use of the latter analogy has been made for determining plane-stress fields by edge loading and measuring the curvatures of the analogous plate. Details of this application of the analogy may be found in the papers of Westergaard[7] and Mindlin.[8] Generalization of the analogy for mixed boundary-value problems has been given by Southwell.[9] In the writer's opinion the use of these analogies has been all too infrequent. It appears that a number of problems of interest in the flexure of plates can be deduced readily from existing solutions of plane elasticity problems.

Author's Closure

The author[10] wishes to thank Professors Nash and Pister for their interest in the paper. He agrees with Professor Nash in that it would be interesting to compare results obtainable by the complex variable method and by the method developed by Professor Nash. In addition to the several types of regions listed by Professor Pister, to which the complex variable method is applicable, Muschelišvili[11] also investigated extensively problems related to the elastic half-plane, and Tiffen[12] discussed rather thoroughly the plane stress problems in infinite strips. Muschelišvili further indicated how the method may be applied to simply-connected regions bounded by arbitrary contours and to regions bounded by several contours.

In connection with Southwell's paper,[9] the author would like to point out that a special case of Southwell's combined extensional-flexural analog is an immediate consequence of writing the boundary equations in the complex form. Thus the boundary equations for the two fundamental problems in generalized plane stress systems are, during the absence of body forces

$$\varphi_1(z) + z\varphi_1'(\bar{z}) + \bar{\psi}_1(\bar{z}) = \frac{1}{2E}\left(\frac{\partial F}{\partial x} + i\,\frac{\partial F}{\partial y}\right) \quad [1]$$

$$\frac{3-\nu}{1+\nu}\,\varphi_1(z) - z\varphi_1'(\bar{z}) - \bar{\psi}_1(\bar{z}) = \frac{1}{2(1+\nu)}\,(u+iv) \quad [2]$$

in which F is Airy's stress function and u and v are the displacement components in the x and y-directions. Similar equations for plates free from lateral loading are

$$\varphi_1(z) + z\bar{\varphi}_1'(\bar{z}) + \bar{\psi}_1(\bar{z}) = \frac{1}{2}\left(\frac{\partial w}{\partial x} + i\,\frac{\partial w}{\partial y}\right) \quad [3]$$

$$\frac{3+\nu}{1-\nu}\,\varphi_1(z) - z\bar{\varphi}_1'(\bar{z}) - \bar{\psi}_1(\bar{z}) = -\frac{1}{2D(1-\nu)} \int_0^s \left[M\nu + i\int_0^s \left(Q_\nu + \frac{\partial H_{\nu s}}{\partial s}\right) ds \right] (dx + i\,dy) \quad [4]$$

The right-hand sides of Equations [1] and [2] are purposely written in a form slightly different from the usual one given by Muschelišvili so that the results may easily be compared with Southwell's. By introducing Southwell's quasi-displacements U and V it may be shown that Equation [4] becomes

$$\frac{3+\nu}{1-\nu}\,\varphi_1(z) - z\bar{\varphi}_1'(\bar{z}) - \bar{\psi}_1(\bar{z}) = \frac{1}{2(1-\nu)}\,(U+iV) \quad [5]$$

By comparing Equations [1] and [2] with [3] and [5] it is seen that (*a*) F/E corresponds with w, (*b*) ν in Equation [2] corresponds with $-\nu$ in Equation [5], and (*c*) u and v correspond with U and V. These conclusions are the same as Southwell's for the case in which body forces and lateral loads are absent. All of Southwell's conclusions may also be verified by means of the complex representation for the general case in which body forces and lateral loading are present in the respective elasticity and plate problems. The result will be reported separately.

Finally, the author would like to take the opportunity to acknowledge receipt of the reprints of three papers[13] sent to him recently by Prof. Kyuichiro Washizu of the University of Tokyo, who is now at M.I.T. All three papers are on the application of the complex variable method to plate problems. In the first of these the problem of a circular plate under concentrated edge forces is also discussed. The boundary equation used is of a different form and may be obtained by differentiating the foregoing Equation [4]. The analytic functions for the general case are determined.

A Method for Determining the Internal Damping of Machine Members[1]

B. J. Lazan.[2] The author has made a fine contribution which should aid considerably in clarifying the design significance of internal damping in members.

We at Minnesota have been using an approach almost identical to that outlined by the author, doing so not because of magneto-mechanical damping effects but for other reasons. About two years ago it was decided to convert average damping procured in rotating-beam equipment to the specific damping energy, or that associated with a specific stress. In doing so it becomes necessary

[7] "Graphostatics of Stress Functions," by H. M. Westergaard, Trans. ASME, vol. 56, 1934, pp. 141–150.

[8] "The Analogy Between Multiply-Connected Slices and Slabs," by R. D. Mindlin, *Quarterly of Applied Mathematics*, vol. 4, 1946, pp. 279–290.

[9] "On the Analogues Relating Flexure and Extension of Flat Plates," by R. V. Southwell, *Quarterly Journal of Mechanics and Applied Mathematics*, vol. 3, part 3, September, 1950, pp. 257–270.

[10] Now Associate Professor of Mechanical Engineering, Syracuse University, Syracuse, New York.

[11] "Some Basic Problems of the Mathematical Theory of Elasticity," by N. I. Muschelišvili, translated by J. R. M. Radok, P. Noordhoff Ltd., Groningen, Holland, 1953.

[12] "Generalized Plane Stress Problems in Infinite Elastic Strips," by R. Tiffen, *Quarterly Journal of Mechanics and Applied Mathematics*, vol. 6, 1953, pp. 344–356.

[13] "On the Bending of Isotropic Plates," by Kyuichiro Washizu, Transactions of the Japan Society of Mechanical Engineers, vol. 18, no. 68, 1952, pp. 41–47. (In Japanese with English summary.)

"A Note on the Two-Dimensional Stresses of Orthogonally Aeolotropic Plates," by Kyuichiro Washizu, Transactions of the Japan Society of Mechanical Engineers, vol. 18, no. 68, 1952, pp. 47–51. (In Japanese with English summary.)

"On the Bending of Orthogonally Aeolotropic Plates," by Kuyichiro Washizu, Proceedings of the First Japan National Congress for Applied Mechanics, 1951, pp. 157–162.

[1] By A. W. Cochardt, published in the September, 1954, issue of the Journal of Applied Mechanics, Trans. ASME, vol. 76, 1954, pp. 257–262.

[2] Professor and Head of the Department of Mechanics and Materials, University of Minnesota, Minneapolis, Minn. Mem. ASME.

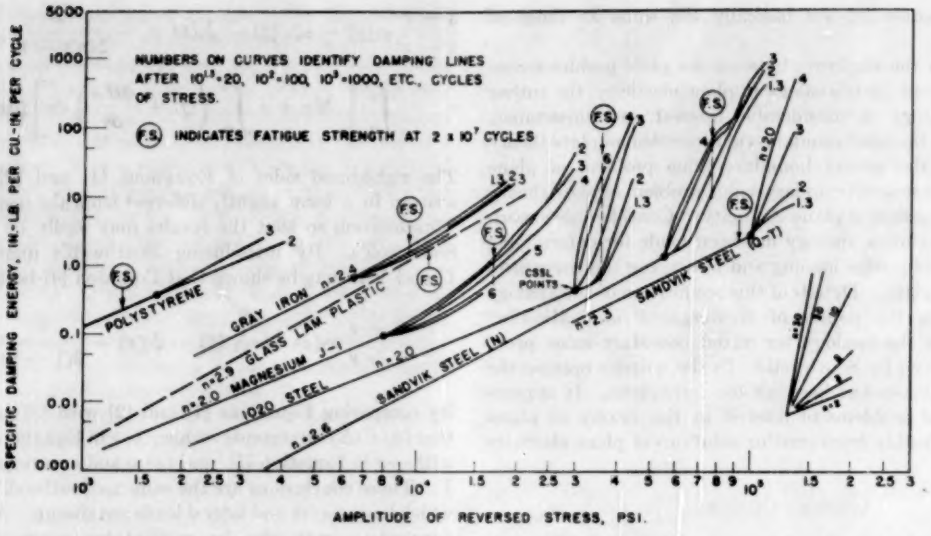
NUMBERS ON CURVES IDENTIFY DAMPING LINES AFTER $10^{1.3}$=20, 10^2=100, 10^3=1000, ETC., CYCLES OF STRESS.
FS INDICATES FATIGUE STRENGTH AT 2 x 10^7 CYCLES
SPECIFIC DAMPING ENERGY, IN-LB PER CU-IN PER CYCLE
AMPLITUDE OF REVERSED STRESS, PSI.
POLYSTYRENE
GRAY IRON n=2.4
GLASS LAM. PLASTIC n=2.9
MAGNESIUM J-1 n=2.0
1020 STEEL n=2.0
SANDVIK STEEL (N) n=2.6
CSSL POINTS
SANDVIK STEEL (Q-T) n=2.3

FIG. 1 SPECIFIC DAMPING ENERGY OF VARIOUS MATERIALS AS A FUNCTION OF AMPLITUDE OF REVERSED STRESS

to consider the stress distribution or volume-stress[3] function of the rotating-beam specimen along the lines discussed by the author. This conversion to specific damping-energy unit is highly desirable not only to express damping in more basic units which can be used more directly in calculations, but also for another reason to be discussed. This discussion also will attempt to clarify the nature of the damping versus stress relationship with special reference to the generality of the exponential relationship discussed in the paper.

Fig. 1 of this discussion shows the specific damping energy, determined from the total or average damping energy, plotted as a function of amplitude of reversed stress. For the materials diagrammed the log-damping versus log-stress curve is a straight line up to a certain critical point identified by the black dot and called the cyclic stress-sensitivity limit. Beyond this critical point, two things generally happen in metallic materials; (*a*) there is usually a change, sometimes abrupt, in the slope of the curve, and (*b*) damping becomes sensitive to a number of prior stress cycles. Therefore, above this point it becomes necessary to represent the damping-stress relationship by means of a family of curves, one curve for each stress history prior to damping measurement. Fig. 1 also indicates the location of fatigue strength of the individual materials by means of the FS flags. Observe that the cyclic stress-sensitivity limit generally falls in a range from 0.6 to 0.9 of the fatigue strength, although values as low as 0.5 and as high as 1.1 have been observed.

It is apparent that for some materials, for example the glass laminate, the exponential relationship between damping and stress continues over the entire stress range covered. For still other materials, for example gray iron and magnesium up to the fatigue strength, the exponential relationship is exact in the low stress region and is a good approximation in the high stress region. For still other materials, for example 1020 mild steel and the Sandvik steel normalized, a very abrupt slope discontinuity occurs at the cyclic stress-sensitivity limit and a single exponential relationship cannot be used. And for still other materials, for example Sandvik steel quenched and tempered, this discontinuity does not occur until beyond the fatigue strength; therefore the exponential relationship can be used to the fatigue strength.

These trends in damping versus stress relationship are far less pronounced in average damping curves than in specific damping curves. In fact, for specimens with sharp stress drop-off, the "large volume at low stress" effects may so camouflage the "small volume at high stress" effects as to completely mask the trends discussed in the foregoing. It is for this reason, as well as that brought out by the author, that it becomes necessary to use volume-stress functions for data reduction.

The data just presented indicate that for many materials (magneto-mechanical materials excluded) the use of a simple exponential volume-stress function is permissible over a rather wide range of stress. The exponential relationship greatly simplifies calculating. Its use is therefore justifiable in many cases. Furthermore, it permits separating terms that clarify general trends and enables rather significant generalizations to be made which may be valuable for design guidance (author's reference 1).

In the Minnesota work it was found that for the cases where simplifying assumptions cannot be made, a graphical method for finding the total damping of a member was preferred to a curve-fitting and mathematical approach. Also, the fundamental terms making up the resonance amplification factor were separated somewhat differently as indicated by the following equation

$$A_r = \left[\frac{\pi S_m^2}{ED}\right] K_v = K_m K_v$$

where

A_r = resonance-amplification factor
S = stress at any point
S_m = maximum stress in part
E = modulus of elasticity
D = specific damping energy at stress S in-lb/cu in/cycle
D_m = specific damping energy at stress S_m
V = volume having a stress less than a specified value
K_v = volume-stress factor which defines the effect of shape and stress distribution on the resonance amplification of the part.[4] Its value is

[3] "Damping, Elasticity, and Fatigue Properties of Unnotched and Notched N-155 at Room and Elevated Temperatures," by L. J. Demer and B. J. Lazan, WADC Technical Report 53-70, February, 1953. Also presented before American Society for Testing Materials, in June, 1953, and to be published in Proceedings of that society.

[4] In the author's reference (1) A_r is expressed in terms of cross-sectional shape factor K_c and longitudinal stress-distribution factor K_s. It can be shown that $K_s K_c = K_v$.

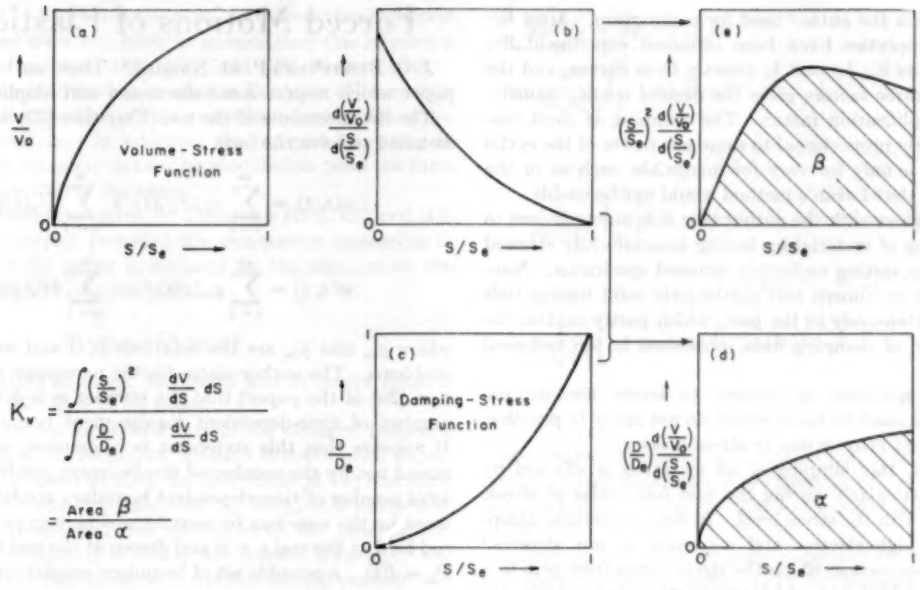

FIG. 2 GRAPHICAL METHOD FOR DETERMINING THE VOLUME-STRESS FACTOR K_v FOR A PART HAVING COMPLICATED STRESS DISTRIBUTION

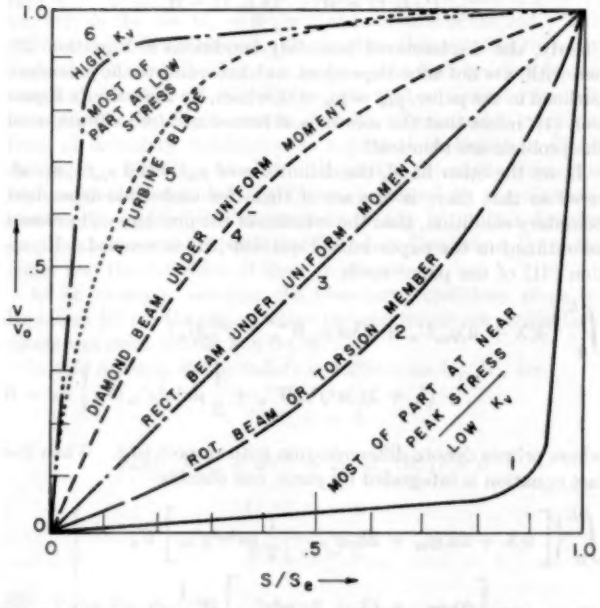

FIG. 3 VOLUME-STRESS FUNCTIONS FOR VARIOUS TYPES OF MEMBERS

$$K_v = \frac{\int \left(\frac{S}{S_m}\right)^2 \frac{dV}{dS}\, dS}{\int \frac{D}{D_m} \frac{dV}{dS}\, dS}$$

K_m = material factor which defined the constants of materials of importance in the resonance condition. $K_m = \pi S_m^2/ED$

If one is concerned with the resonance fatigue-failure problem then S_m may be replaced by S_e (the fatigue strength of the material) and D_m by D_e (the damping energy at the fatigue strength). Under these conditions the material factor $K_m = \pi S_e^2/ED$, and K_v may be determined[5] by the graphical method outlined in Fig. 2, herewith. Recognizing that the "damping-stress function" in this figure is the same as the author's "energy-absorption function," and the "volume-stress function" is related to his "stress-distribution function," it is seen that the two approaches are quite identical.

The question regarding which is more important, low stress damping or high stress damping, does not have a simple answer as already pointed out by the author. Fig. 3 of this discussion is intended to help clarify this point. This figure shows the volume-stress function, on a unitless basis, for various types of members from "1" which (like a tension-compression member) is almost entirely at near peak stress, to "6" which (like a severely notched member) is mostly at low stress. Most parts encountered in engineering practice would probably fall between these two extremes, as shown by curves 2, 3, 4, and 5. In general, it may be stated that in parts having volume-stress functions approaching 1 the high stress damping would dominate in parts exposed to resonant fatigue conditions. However, in parts having volume-stress function approaching 6 the low stress damping would dominate. In between these two extremes, both are important.

ALEXANDER YORGIADIS.[6] The author presents a new and useful method of finding the damping properties of members by a combination of experimental and analytical procedures. The principal advantage of the author's method over previous methods is in analyzing members made of materials having irregular damping properties that cannot be expressed by simple mathematical relationships. The author's Equations [6], [7], and [10] can be solved by graphical, numerical as well as mathematical methods.

This method, however, is more laborious than others, such as

[5] "Status Report 53-1 on Properties of Materials and Joints Under Alternating Force," by B. J. Lazan, Wright Air Development Center, February, 1953.

[6] Sandia Corporation, formerly Chief Engineer, Sonntag Scientific Corporation, Greenwich, Conn. Mem. ASME.

that of Lazan which the author used for comparison. After the basic material properties have been obtained experimentally, Lazan[7] reads factors k_m, k_s, and k_e directly from curves, and the product of these three factors gives the desired result; namely, the resonance-amplification factor. The damping of most materials is very nearly proportional to some nth power of the cyclic stress, so that it is only for very few materials, such as in the author's example, that Lazan's method would not be usable.

The writer disagrees with the author that it is more efficient to determine damping of material by testing nonuniformly stressed specimens than by testing uniformly stressed specimens. Nonuniformly stressed specimens and particularly solid torsion rods have been used extensively in the past, which partly explain the lack of correlation of damping data, published in the technical literature.

This type of specimen is subject to errors because too many assumptions must be made which do not apply in practice. The most important error is due to stress history.

To some extent, the damping of all materials is affected by stress history, particularly during the first few cycles of stress. This effect varies with the stress level. In some materials, damping increases at high stresses and decreases at low stresses.[8] Using a torsion specimen in which the stress varies from zero to a maximum would yield results which are of little value in determining basic material properties since one effect may possibly neutralize another. A second source of error is the assumption that the modulus of elasticity of the specimen is constant throughout the stress range of zero to a maximum. Usually, and particularly at high stresses, the modulus of elasticity is appreciably less than at low stress levels, so that the calculated stress is somewhat higher than the true stress at the outer fibers.

Apart from these critical comments, the writer feels that the author's method is a very valuable added tool in the hands of those who are engaged in the analysis of damping in machine members.

Author's Closure

The author would like to thank Professor Lazan and Dr. Yorgiadis for their remarks. While he agrees with what has been pointed out by Professor Lazan, he does not share all of Dr. Yorgiadis' views. Dr. Yorgiadis is of the opinion that "the damping of most materials is very nearly proportional to some nth power of the cyclic stress." This may be true for a certain range of stress, but is certainly not true in the lower stress range[9] and is also often not the case at high stresses as is best illustrated by Professor Lazan's Fig. 1. However, as Professor Lazan and the author have pointed out, it is sometimes of advantage to use the simple n-power relationship. This, of course, depends upon the particular stress system and the particular material.

Two methods are mentioned in the paper for determining the energy absorption function $\Delta U(\sigma)$. It is admitted that it is often questionable whether the indirect method is more "efficient" than the direct method; for example, in torsion it may be preferable to determine the damping curve on a hollow specimen rather than on a solid one.

Finally, the author agrees with Dr. Yorgiadis that the accuracy of the method can be increased by considering in the analysis the change of elastic modulus with stress.

[7] "Effect of Damping Constants and Stress Distribution on the Resonance Response of Members," by B. J. Lazan, Journal of Applied Mechanics, Trans. ASME, vol. 75, 1953, pp. 201–209.

[8] Reference in author's paper.

[9] "Internal Friction in Metals," by A. S. Nowick, *Progress in Metal Physics*, vol. 4, 1953, p. 1, Interscience Publishers Inc., New York, N. Y.

Forced Motions of Elastic Rods[1]

J. G. Berry[2] and P. M. Naghdi.[3] There are two points in this paper which require some discussion and amplification.

The displacements of the rod (Equation [23] of the paper) are assumed to have the form

$$\left.\begin{aligned} u(z,t) &= \sum_{i=1}^{m} g_{iu}(z)f_i(t) + \sum_{n=1}^{\infty} U_n(z)q_n(t) \\ w(z,t) &= \sum_{i=1}^{m} g_{iw}(z)f_i(t) + \sum_{n=1}^{\infty} W_n(z)q_n(t) \end{aligned}\right\} \quad \ldots\ldots [1]$$

where g_{iu} and g_{iw} are the solutions $u(z)$ and $w(z)$ of m statics problems. The author states (in the paragraph preceding Equation [20] of the paper) that the number m is determined by the number of time-dependent displacement boundary conditions. It appears that this statement is incomplete, since m is determined not by the number of displacement conditions but by the total number of time-dependent boundary conditions. That this must be the case can be seen by a simple example: Consider a rod held at the end $z = 0$ and driven at the end $z = L$ by a force $P_z = f(t)$. A possible set of boundary conditions in this case is

$$u(0,t) = w(0,t) = 0$$

$$P_z(L,t) = f(t), \quad Q(L,t) = 0 \quad \ldots\ldots [2]$$

Clearly, the displacement boundary conditions in Equation [2], herewith, are not time-dependent and, according to the procedure outlined in the paper, $g_{iu} = g_{iw} = 0$, which, by the writer's Equation [1], infers that the solutions of forced and free vibrations of the problem are identical!

If, on the other hand, the definitions of $g_{iu}(z)$ and $g_{iw}(z)$ are altered so that there is one set of them for each time-dependent boundary condition, then the solution of the problem will proceed as outlined in the paper until Equation [31] is reached. Equation [31] of the paper reads

$$\int_0^L \Big\{ 4(\lambda+\mu)g_{iu}U_n + 2\lambda a(g_{iu}W'_n + g'_{iw}U_n) + (\lambda+2\mu)a^2 g'_{iw}W'_n + \frac{1}{2}\mu\kappa^2 a^2 g'_{iu}U'_n \Big\}\, dz = 0$$

where primes denote differentiation with respect to z. When the last equation is integrated by parts, one obtains

$$\left.\begin{aligned} &\int_0^L \Big\{ \Big[4(\lambda+2\mu)g_{iu} + 2\lambda a g'_{iw} - \frac{1}{2}\mu\kappa^2 a^2 g''_{iu} \Big] U_n \\ &\qquad - \Big[2\lambda a g_{iu} + (\lambda+2\mu)a^2 g'_{iw} \Big] W_n \Big\}\, dz \\ &+ \Big[2\lambda a g_{iu} W_n + (\lambda+2\mu)a^2 g'_{iw} W_n + \frac{1}{2}\mu\kappa^2 a^2 g'_{iu} U_n \Big]_0^L \end{aligned}\right\} \quad \ldots [3]$$

The integral in Equation [3] vanishes due to the equilibrium equations of the statics problems (Equation [20] of the paper). However, the last bracket in Equation [3] does not vanish unless all of the boundary conditions are displacement conditions, for only in

[1] By G. Herrmann, published in the September, 1954, issue of the Journal of Applied Mechanics, Trans. ASME, vol. 76, 1954, pp. 221–224.

[2] Instructor in Engineering Mechanics, University of Michigan, Ann Arbor, Mich. Assoc. Mem. ASME.

[3] Professor of Engineering Mechanics, University of Michigan, Ann Arbor, Mich. Assoc. Mem. ASME.

this case will $U_n = W_n = 0$ at the ends. It follows that Equation [31] of the paper does not hold, in general, and this requires a modification of Equations [33], [34], and [38] of the paper.

It can be shown that the last bracket in Equation [3] is exactly the negative of that portion of the generalized force which arises from the end loadings. In addition, the integral appearing in Equation [26] of the paper cannot be modified to yield the form given by Equation [33] of the paper.

The general solution, as given by Equations [41], [42], and [43] of the paper, is correct provided the summation appearing in Equation [39] of the paper is replaced by the negative of the integral appearing in Equation [26].

Author's Closure

The author wishes to thank Mr. Berry and Professor Naghdi for the attention they gave to his paper.

The author does not agree with any of the changes, proposed by the discussers, of the procedure outlined in the original paper.

First, there is no need to alter the definitions of the functions g_{iu} and g_{iw}. The discussers state that $g_{iu} = g_{iw} = 0$ infers that the solutions of forced and free vibrations of the problem are identical. This conclusion is clearly not correct, since $q_n(t)$ will be different in these two cases, as is evident from Equation [40] of the paper.

The second item taken up by the discussers concerns Equation [31] of the paper and they state that it does not hold in general, but only in the case $U_n = W_n = 0$ at both ends of the rod. This statement also is not correct. Integrating this equation by parts, discussers' Equation [3] is obtained. The last bracket in this equation vanishes not only in the case that all boundary conditions are on the displacements, but for all admissible combinations of boundary conditions, as expressed in Equation [3] of the paper. This last bracket in Equation [3] of the discussion represents the work done by forces, produced by the displacements g_{iu}, g_{iw}, in the displacements U_n, W_n. This bracket vanishes in accordance with the Boundary Conditions [3] of the paper and the definition of these functions.

As an example, consider the boundary conditions given by Equation [21] of the paper, where two conditions are on displacements and two conditions on forces.

In this example the boundary conditions on U_n, W_n are

$$U_n(0, t) = 0$$

$$2a\lambda U_n(0, t) + a^2(\lambda + 2\mu)W_n'(0, t) = 0$$

$$U_n'(l, t) = 0$$

$$W_n(l, t) = 0$$

and on g_{iu}, g_{iw}

$$g_{iu}(0, t) = 1$$

$$2a\lambda g_{iu}(0, t) + a^2(\lambda + 2\mu)g_{iw}'(0, t) = 0$$

$$g_{iu}'(l, t) = 0$$

$$g_{iu}(l, t) = 0$$

Clearly, the last bracket in Equation [3] of the discussion vanishes, and no modification of Equations [33], [34], and [38] of the paper is required.

Further, the author does not share the discussers' finding that the integral appearing in Equation [26] of the paper cannot be modified to yield the form given by Equation [33] of the paper. In fact, writing in all detail

$$\int_0^l [g_{iu} U_n + 2g_{iw} W_n]\, dz$$

$$= \frac{1}{\rho\omega_n{}^2 a^2}\int_0^l \Big\{ g_{iu}\,[-a^2x^2\mu U_n'' + 8(\lambda + \mu)U_n + 4a\lambda W_n'] + 2g_{iw}\,[-2a\lambda U_n' - a^2(\lambda + 2\mu)W_n'']\Big\}\, dz$$

$$= \frac{1}{\rho\omega_n{}^2 a^2}\int_0^l \Big\{ 8(\lambda + \mu)g_{iu}\, U_n + a^2x^2\mu g_{iu}'U_n' + 4a\lambda g_{iu}W_n' + 4a\lambda g_{iw}'U_n + 2a^2(\lambda + \mu)g_{iw}'\, W_n'\Big\}\, dz$$

$$+ \frac{1}{\rho\omega_n{}^2 a^2}\Big[-a^2\kappa^2\mu g_{iu}U_n' - 4a\lambda g_{iw}U_n - 2a^2(\lambda + 2\mu)g_{iw}W_n'\Big]_0^l$$

where use has been made of Equation [13] of the paper. The last integral vanishes on account of Equation [31] of the paper and the last bracket is equal to the right-hand side of Equation [33] of the paper.

Lastly, consider the example suggested by the discussers, the boundary conditions being given by Equation [2] of the discussion. In this case $m = 0$ and no functions g_{iu}, g_{iw} need to be introduced. The functions U_n, W_n have to be determined from the Equations [20] of the paper, together with the boundary conditions

$$U(0, t) = 0$$

$$W(0, t) = 0$$

$$2a\lambda U(l, t) + a^2(\lambda + 2\mu)W'(l, t) = 0$$

$$U'(l, t) = 0$$

Next, from Equation [38] of the paper, we find

$$H_1 = H_2 = H_3 = 0$$

$$H_4 = 2\pi\, W_n(l)f(t)$$

and from Equation [39] of the paper

$$Q_n{}^* = \frac{\omega_n{}^2}{2T_{n\,\max}}\, 2\pi\, W_n(l)f(t)$$

Thus the solution is given by

$$\left.\begin{aligned} u(z, t) &= \sum_{n=1}^{\infty} U_n(z)q_n(t) \\ w(z, t) &= \sum_{n=1}^{\infty} W_n(z)q_n(t) \end{aligned}\right\} \quad \ldots\ldots\ldots\ldots [4]$$

where, by Equation [41] of the paper

$$\left.\begin{aligned} q_n(t) &= A_n \cos \omega_n t + B_n \sin \omega_n t \\ &\quad + \frac{\omega_n \pi W_n(l)}{T_{n\,\max}}\int_0^t f(t) \sin \omega_n(t - \tau)d\tau \end{aligned}\right\} \quad \ldots [5]$$

This completes the formal solution of the simple problem suggested by the discussers, employing the procedure outlined in the paper, and, clearly, no modifications of this procedure are required.

Concluding, it should be pointed out that the objections raised by the discussers, relative to the validity of the procedure outlined in the paper, are not related to the fact that radial inertia and radial shear stress are taken into account in the author's

study of forced motions of elastic rods. In fact, when these additional effects are neglected, that is, when the motions are governed by the classical rod theory, and in the absence of time-dependent boundary displacements, the procedure of the paper is standard textbook material. The problem suggested by the discussers has been worked out in detail in the case of classical rod theory,[4] by precisely the same method. Noting that in that case

$$W_n(z) = \sin \frac{n\pi z}{2l}$$

$$\omega_n = \frac{n\pi}{2l}\sqrt{\frac{E}{\rho}}$$

$$T_{n\,max} = \frac{\omega_n^2\,\pi\rho a^2 l}{4}$$

and that the quantities $f(t)$ and $\pi\rho a^2$, respectively, stand for $S/2\pi$ and $A\gamma/g$, respectively, in Timoshenko's notation, the solution contained in Equations [4] and [5] reduces readily to the one given in Timoshenko's text.

On Bending of a Flat Slab Supported by Square-Shaped Columns and Clamped[1]

YI-YUAN YU.[2] The author is to be congratulated for having made another contribution on the design of plates. Regarding the moments at the support the author concludes: "By the theory here established the moments $M_\theta = \nu M_\rho$ become secondary as compared with the moments M_ρ, . . ." Perhaps it should be indicated more explicitly that this result is solely due to the assumption of a rigidly clamped edge of the flat slab at the support. Along the tangential direction of the clamped edge the curvature of the slab is zero; therefore $M_\theta = \nu M_\rho$. This relation holds true for supporting columns of any shape and should be verified by computational results obtained by any method.

A similar situation occurs in the case of rigid-core problems in two-dimensional elasticity. At the boundary between a rigid core and its surrounding plane, where complete bond is assumed to exist, the normal strain along the tangential direction of the boundary is zero. By Hooke's law the ratio between the two normal stress components σ_θ and σ_ρ becomes a constant and is equal to ν in the case of plane stress. This was pointed out by the writer in an earlier paper.[3]

AUTHOR'S CLOSURE

The author is much indebted to Prof. Yi-Yuan Yu for his comment. The fact that the relation $M_\theta = \nu M_\rho$ between the tangential and the radial moments along the edge of the support could be foreseen without application of any special theory admittedly has not been stressed enough in the paper. This result in itself could therefore be considered as trivial. Not trivial, however, may be the data obtained for the absolute magnitude of the bending moments along the edge as well as the moments throughout the panel of the slab.

Creep Tests of Rotating Disks at Elevated Temperature and Comparison With Theory[1]

L. F. COFFIN.[2] The authors have presented a very interesting comparison of the derived and measured creep deformation in a biaxially stressed body. This represents a considerable contribution to the subject matter of a complex but important engineering problem. Whether one agrees or disagrees with the authors' analysis, the experimental information will be of inestimable value for those looking for proof or disproof of their own particular theory on the subject.

The writer notes that stress distributions of Figs. 2 and 4 are obtained for the steady-state solution, i.e., when the contribution of the elastic part of the strain at any point becomes vanishingly small, such that stresses can be related to strain rates only. On the basis of the stress distributions so calculated, the strains at the bore of the rotating disk are found from creep deformations of test coupons tested at the same stress level for the same time. From this strain, the strain values are found elsewhere in the disk. It was then found that the strains calculated by the Mises criterion are low, while good agreement is found for a solution using the maximum-shear theory. The better agreement of the maximum-shear theory is attributed to anisotropy in the material.

While anisotropy is undoubtedly important, another explanation can be found for the unsatisfactory agreement of the Mises criterion. This pertains to the neglect of the transient stress solution. When the disk is first rotated, the stress is actually elastic throughout the disk. Through the process of time-dependent plastic flow, the stress distribution is gradually transformed to the steady-state solution reported. At the bore, the tangential stress, initially quite high, is reduced by plastic flow, until the steady-state condition is reached. Consequently, more flow occurs at the bore than would be found if the steady-state stresses were applied at the start. At the rim, the elastic stress is less than the steady-state and the total strain developed there is correspondingly less than that found for a steady-state solution. Although the authors have found that the transient condition is of short duration, nevertheless, the transient strains produced thereby cannot be neglected.

Since the strains found throughout the tube are based on the bore tangential strain, the strains calculated in Figs. 7, 8, and 9, are all too low by this transient-bore tangential strain. When this quantity is taken into account, it may well be that the Mises criterion gives better agreement than is found in the paper. The inclusion of this transient condition and the gradual transfer of stresses and strains with time to the steady-state case were reported for a thick-walled cylinder under internal pressure.[3] Such a study would be of interest here to clarify this point.

F. A. MCCLINTOCK.[4] In Figs. 7, 8, and 9 of the paper, "scatter

[4] "Vibration Problems in Engineering," by S. Timoshenko, D. Van Nostrand Company, Inc., New York, N. Y., second edition, 1937, pp. 314-315.

[1] By S. Woinowsky-Krieger, published in the September, 1954, issue of the JOURNAL OF APPLIED MECHANICS, Trans. ASME, vol. 76, pp. 263–270.

[2] Associate Professor, Department of Mechanical Engineering, Syracuse University, Syracuse, N. Y. Assoc. Mem. ASME.

[3] "Solution for the Exterior of a General Ovaloid Under Arbitrary Loading and Its Application to Square Rigid Core Problems," by Yi-Yuan Yu, Proceedings of the First U. S. National Congress of Applied Mechanics, 1952, pp. 227–237.

[1] By A. M. Wahl, G. O. Sankey, M. J. Manjoine, and E. Shoemaker, published in the September, 1954, issue of the JOURNAL OF APPLIED MECHANICS, Trans. ASME, vol. 76, pp. 225–235.

[2] Research Associate, General Electric Company, Knolls Atomic Power Laboratory, Schenectady, N. Y. Mem. ASME.

[3] "Primary Creep in the Design of Internal Pressure Vessels," by L. F. Coffin, Jr., P. R. Shepler, and G. S. Cherniak, JOURNAL OF APPLIED MECHANICS, Trans. ASME, vol. 71, 1949, pp. 229–241.

[4] Assistant Professor of Mechanical Engineering, The Massachusetts Institute of Technology, Cambridge, Mass. Assoc. Mem. ASME.

bands" are shown to indicate the uncertainty in the results due to scatter. A better idea of the uncertainty can be obtained if statistical theory is used to make estimates from the data. Aside from fixed errors, assume that the "true value" to be estimated is the mean value that would be obtained from tests on the population of all possible disks. As an example, consider the data of Fig. 8 at 180 hr. Assume that at this time the population of the logarithms of the creep of all possible disks is distributed according to a normal or Gaussian distribution function. The assumption of a Gaussian distribution permits the use of common statistical techniques, and the logarithm is introduced to exclude the possibility of negative creep.

The estimation can be made with the aid of Student's t distribution, which describes how far the mean of a small sample may be from the mean of the population, without requiring exact knowledge of the standard deviation of the population.[5]

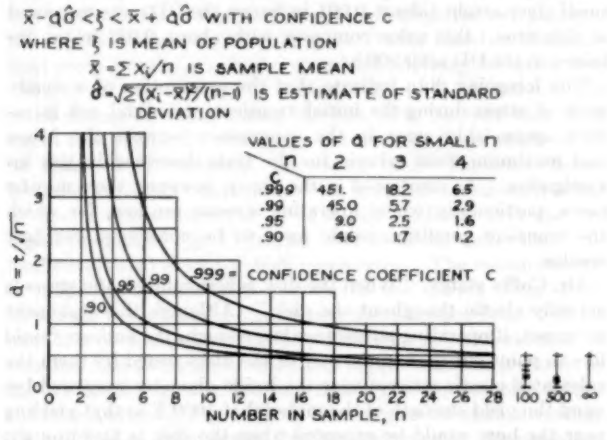
$\bar{x} - a\hat{\sigma} < \xi < \bar{x} + a\hat{\sigma}$ WITH CONFIDENCE C
WHERE ξ IS MEAN OF POPULATION
$\bar{x} = \Sigma x_i/n$ IS SAMPLE MEAN
$\hat{\sigma} = \sqrt{\Sigma(x_i - \bar{x})^2/(n-1)}$ IS ESTIMATE OF STANDARD DEVIATION
VALUES OF a FOR SMALL n
n 2 3 4
C
.999 451. 18.2 6.5
.99 45.0 5.7 2.9
.95 9.0 2.5 1.6
.90 4.6 1.7 1.2
$a = t/\sqrt{n}$
.90
.95
.99
.999 = CONFIDENCE COEFFICIENT C
0 2 4 6 8 10 12 14 16 18 20 22 24 26 28 100 500 ∞
NUMBER IN SAMPLE, n

FIG. 1 CONFIDENCE LIMITS FOR MEAN; NORMALLY DISTRIBUTED POPULATION

Fig. 1 of this discussion presents the distribution in the form most convenient for this problem. For the three disks shown in Fig. 8 at 180 hr, the mean $\log_{10}$ (creep), $\bar{x}$, is —0.852 and the estimate of the standard deviation of the population, $\hat{\sigma}$, is 0.085. If 95 per cent confidence is desired, that is, if a statistical technique is used which gives a correct answer 95 per cent of the time it is applied, then from Fig. 1, $a = 2.49$ and the estimate of ξ, the mean $\log_{10}$ (creep) for the population, is

$$-1.064 < \xi < -0.640 \qquad \text{(95 per cent confidence)}$$

From the antilogarithm of the limits just obtained one can conclude with 95 per cent confidence that the true value for creep on the inner diameter at 180 hr lies between 0.086 and 0.23 in. (If the creep itself, rather than its logarithm, had been assumed normally distributed, the 95 per cent confidence interval would have been 0.074 to 0.21 in.)

It is well that the authors tested three disks; Fig. 1 of this discussion shows how much broader an interval would have been obtained had only two disks been tested. On the other hand, the precision of the estimate increases rather slowly when the sample size is greater than four.

Returning to the case at hand, the confidence limits which were obtained show that the uncertainty due to scatter is considerably greater than that indicated by the scatter band of Fig. 8 of the paper. It also must be borne in mind that possible lack of statistical control between disks, and the presence of fixed errors due to the method of testing and interpreting the results will increase the uncertainty beyond that obtained from the foregoing statistical procedure. Therefore the conclusions of the paper probably should be accepted with more reservation than is indicated by the scatter bands of Figs. 7, 8, and 9.

M. H. LEE WU.[6] The problem of rotating disks at elevated temperature under creep is an important and a complicated one. The authors are to be complimented for their investigation on the problem, especially for their fine work in correlating the experimental data with theory.

One of the authors' conclusions is that the theoretically calculated creep strains and strain rates in the rotating disk at 1000 F, by using a power function approximating the average tensile-creep test data based on Mises theory, may be much lower than the experimental values, and that those based on the maximum-shear theory are on the safe side. The writer agrees with this conclusion, but it is believed that the degree of disagreement or agreement may not be fully represented by Fig. 9 of the paper.

From Fig. 9 of the paper, it can be seen that the theoretically calculated tangential strain based on the maximum-shear theory falls almost in the middle of the scatter band of the test results, while those obtained from Mises theory are far below the scatter band. In view of the fact that even for the thin tube at room temperature, the stress-strain relations based on the maximum-shear theory for biaxial tensions are not exactly the same as those for the uniaxial tension. The agreement between experimentally and theoretically obtained strains based on maximum-shear theory for rotating disks at high temperature is then not to be expected to be as good as that shown in Fig. 9 of the paper. Also, from the thin-tube test data (constant stress ratio at room temperature) obtained by Dr. Osgood,[7] it is indicated that the deformation theory (for constant stress ratio, Mises theory is the same as deformation theory) and the maximum-shear theory provide the upper and lower bounds, respectively, and the scattering for the two theories is about the same. A comparison [8,9] of the theoretical and experimental bursting speed of a rotating disk at room temperature by using deformation theory shows the same tendency, and the deviation between theoretical and experimental results is small. It is possible then that the theoretical strains obtained by the authors based on the two theories are lower than they should be due to some other factors.

The results may be affected by the following factors: (1) The authors measured strains for both tensile creep test and disk creep test by stopping the test periodically. It is mentioned in the paper that there is no effect on tensile creep test due to such unloading. However, it may have some effect on creep test of rotating disk, because the stress distribution in the tensile specimen is uniform but the stress distribution in the rotating disk is nonuniform. (2) Some effects also may be introduced because of the difficulty of maintaining a constant true stress through the creep test. (3) The anisotropy of the disk material also may have some effect on the results, but in the writer's opinion, it may not be so large

[5] "Introduction to Mathematical Statistics," by P. G. Hoel, John Wiley & Sons, Inc., New York, N. Y., 1947, pp. 144–145.

[6] Research Supervisor, Department of Mechanical Engineering, Polytechnic Institute of Brooklyn, Brooklyn, N. Y. Mem. ASME.

[7] "Combined-Stress Tests on 24S-T Aluminum-Alloy Tubes," by W. R. Osgood, JOURNAL OF APPLIED MECHANICS, Trans. ASME, vol. 69, 1947, pp. A-147–A-153.

[8] "General Plastic Behavior and Approximate Solutions of Rotating Disk in Strain Hardening Range," by M. H. Lee Wu, NACA TN 2367, May, 1951.

[9] "A Simple Method of Determining Plastic Stresses and Strains in Rotating Disks With Nonuniform Metal Properties," by M. H. Lee Wu, JOURNAL OF APPLIED MECHANICS, Trans. ASME, vol. 74, 1952, pp. 489–495.

as the authors expected. (4) The theoretical strain distributions are obtained by multiplying the tangential strain at the inner radius by the ratio of strains to the tangential strain at the inner radius (Fig. 3 of the paper). For simplicity, this ratio of strain was referred to as "proportionate strain,"[9] and will be also used in the present discussion. Any error in tangential strain at the inner radius would affect the whole strain distribution. From Fig. 12 of the paper, it can be seen that the stress obtained by power function approximation is higher than the experimental value in some places, especially around $\bar{\sigma} = 32{,}000$ psi. Higher stresses give a higher value of rotating speed for a given tangential strain at the inner radius. In other words, it gives a lower calculated tangential strain for a given rotating speed. A small error in rotating speed may mean a large deviation in tangential strain at the inner radius, and thereby affect the whole strain distribution. Therefore the strain obtained based on the maximum-shear theory may be much lower than it should be.[10] Other approximations involved in the theoretical analysis also may affect the results. If all these effects can be reduced to a minimum, the theoretical strains obtained by maximum-shear theory and Mises theory also may provide upper and lower bound for the rotating disk at high temperature. Further investigations on this subject would be of great interest.

Fig. 3 of the paper shows that the proportionate strain distributions of a rotating disk with hole obtained by Mises theory and by maximum-shear theory for $n = 6$ to 9 are the same. In an NACA report,[10] calculations were made for three rotating disks, whose inner and outer radius ratio were equal to 0.0356, 0.0804, and 0.188, made of Inconel X at room temperature; the radius ratio of 0.188 is very close to the radius ratio considered by the authors, $1.25/6 = 0.208$. Therefore the proportionate strain distribution for a disk having radius ratio equal to 1.25/6 for Inconel X at room temperature may be obtained by extrapolating the results calculated for the three disks.[10] The results compare closely to those of the authors, although the values of n of the disk materials for both cases are quite different. This is a further confirmation of the previously obtained fact[8] that the proportionate strain distributions are essentially independent of the materials. The writer takes some space to discuss this fact because it is important to the solutions of a group of plastic problems, and it is also utilized by the authors in the theoretical analysis.

The work performed by the authors is a valuable contribution to the field. The problem is a very complicated one; there are so many effects involved, and it is very difficult to exclude these effects. The authors should be congratulated for having supplied a great deal of information to the field.

Authors' Closure

The authors wish to express their appreciation to Dr. Coffin, Professor McClintock, and Dr. Wu for their interesting and pertinent discussions. These bring out several important points not fully covered in the paper.

Dr. Coffin suggests that better agreement with the Mises criterion might have been obtained if the additional plastic flow occurring during the transient period (in which the initial stress distribution changes into the steady-state plastic distribution) is taken into account, and that a further study of this would be of interest. As mentioned in the paper, the duration of this transient period was estimated by calculation to be only a few hours. The strains during this time were calculated, in effect, by assuming that the steady-state stress distribution is present, by taking into account the high initial creep rate which occurs during the first few hours as shown by the tension-creep tests. All the plastic strain occuring during this initial period is therefore not neglected in the analysis but only that part responsible for the relaxation of stress near the inside diameter of the disk. Since this stress relaxation occurs only in a localized region near the bore, the additional strain neglected by using the steady-state solution would be of the order of the elastic strain only and therefore very small compared to bore strains around 10 per cent reached during the course of the spin test. An approximate calculation of this additional strain based on a power function relation ($n = 5$) between stress and creep rate also indicates values of the order of the elastic strain and therefore negligible. Further evidence in support of this conclusion is given by the measurements on disk No. 12 after $6^1/_2$ hr of operation (corresponding approximately to the transient interval) which show creep strains about the same as those calculated based on the maximum-shear criterion and assuming the steady-state stress distribution. Also, a relatively small creep strain (about 0.001 in/in. on the OD) was measured at this time; this value compares with about 0.021 in/in. obtained at the OD after 900 hr.

The foregoing data indicate that the assumption of a steady state of stress during the initial transient period did not introduce appreciable error in the comparison between the Mises and maximum-shear criteria for the tests described in this investigation. As mentioned in the paper, however, there may be cases, particularly where operating stresses are low, for which the transient condition would have to be considered for best results.

Dr. Coffin states: "When the disk is first rotated, the stress is actually elastic thoughout the disk." Although this statement is correct, if operating stresses are low enough, the authors would like to point out that in the case of the disks tested by them the calculated elastic stresses near the inside diameter were well beyond the yield strength of the material at 1000 F so that yielding near the bore would be expected when the disk is first brought up to speed. Hence, in our case, the stresses were not completely elastic even at the start of the test; this condition of initial local yielding also occurs frequently in practical applications.

Professor McClintock correctly points out that the "mean of a small sample" may differ from the "true value" or "mean of the population," and that this difference for 95 per cent confidence may exceed the limits of the scatter bands of the data from the three disks tested. It turns out that these scatter bands correspond approximately to the 75 per cent confidence limits. The conclusions of the paper, however, need not be altered since they contain the reservation that "in the absence of such (more conclusive) data it is suggested that a conservative course in design is to apply the maximum-shear theory since this will give larger creep deformations, i.e., values on the safe side, as compared with those obtained using the Mises criterion."

The authors are indebted to Dr. Wu for a very comprehensive discussion. Regarding the tests on aluminum tubes made by Dr. Osgood[7] and cited by Dr. Wu, the authors feel that short-time load-deformation tests under combined stress at normal temperature and with variable loading may give quite different results (in so far as comparison of the Mises and maximum-shear criteria is concerned) than long-time creep tests at high temperature and at essentially constant stress. Although it is of considerable interest that Dr. Wu finds good agreement between the results of her analysis (based on the Mises criterion) and the experimentally determined bursting speeds of rotating disks,[8] it is the authors' opinion that a comparison of strength theories based on an analysis of short-time bursting tests of disks at room temperature would not necessarily apply to the case of creep deformations in long-time spin tests of disks at elevated temperature.

[10] "Analysis of Plane-Plastic-Stress Problems With Axial Symmetry in Strain-Hardening Range," by M. H. Lee Wu, NACA Report 1021, 1951 (formerly NACA TN 2217, 1950).

The points brought out by Dr. Wu in the fourth paragraph of her discussion will now be discussed:

1 Regarding the effect of periodic stopping and starting of the disks, as indicated in the paper, tests were made on two tension-creep specimens under the same intermittent loading and heating cycles as in the spin tests 1 and 2. These showed that such effects, if present, were not large. Although as mentioned by the discusser, the stress is not constant throughout the disk, as shown in Fig. 4 of the paper, for $n = 8$ the steady-state stress distribution along a radius does not vary too much from a constant value. Hence it is the authors' opinion that the variable stress distribution in the disk combined with the intermittent loading and heating condition will not affect the comparison between the Mises and maximum-shear criteria to any great extent.

2 Regarding the effect of not maintaining constant stress in the tension-creep tests, the authors wish to point out that all of the test points shown in Fig. 12 of the paper, except the two points at the highest stress (31,500 psi approx.), were based on constant-load creep tests in which the stress did not vary by more than about 3 per cent during the course of the test. Because of this small change in stress during the test, it is believed that these strain-rate values are practically the same as those which would be obtained for constant true-stress tests. However, recent tension-creep data obtained on this material at constant stress by one of the authors (M. J. Manjoine) indicate that the two highest points of Fig. 12 (which were obtained under constant-load conditions) show too high creep rates. The reason for this is probably because that portion of the curves from which these data were obtained was too near the transition point. These more recent data (which may be published later) indicate that for constant true stress the actual curve is practically that shown by the full line in Fig. 12 or 180 hr. Hence it is the authors' opinion that the full lines of Fig. 12 (based on the power-function relation) are valid for constant stress conditions even up to stresses somewhat beyond 32,000 psi.

3 Regarding the effects of anisotropy of the material: Since the paper was written, some further creep-test results (to be published later) have been obtained by one of the authors (M. J. Manjoine). These data were obtained from specimens cut out in a direction perpendicular to the plane of the disk. The results indicate that the effects of anisotropy, for strains corresponding to those present in the spin tests, are not so great as had been expected. (This is in agreement with Dr. Wu's discussion.) Average creep rates in the axial direction of the disks, based on these tests, were about 20 to 40 per cent greater than those obtained in the tangential direction. This amount of anisotropy does not appear to be sufficient to account for the relatively large differences between average test results and those obtained using the Mises criterion.

4 Dr. Wu mentions that the actual strain rate at 32,000 psi may be considerably greater than the value based on the power-function relation (represented by the straight lines in Fig. 12) which was used in the theoretical calculation. This opinion is no doubt based on the fact that the two highest points of Fig. 12 (at around 31,500 psi) show higher creep rates than those given by the power-function relation. However, as pointed out previously, more recent creep-test data obtained at constant stress indicate that these two points (which were obtained from constant-load test data) are too high for constant-stress conditions and that the true curve is best represented by the straight lines of Fig. 12 which were used in the analysis. This is true even for stresses somewhat beyond 32,000 psi. Hence it is believed that any error introduced by using the power-function relation is small and therefore will not invalidate the comparison between the Mises and maximum-shear criteria given in the paper.

In conclusion, the authors wish to emphasize that their main objective in carrying out this investigation was not to establish a general strength theory which is correct under all conditions but rather to develop a reasonably simple method of analysis which would give good results for design use when applied to the calculation of creep deformations in rotating disks at high temperatures. As stated in the paper, it appears that the analysis described, involving the use of the maximum-shear theory, will give closest agreement with average spin-test results for the material tested. Nevertheless, the authors believe that further spin tests using other high-temperature materials are necessary before general conclusions may be drawn.

Book Reviews

Elliptic Integrals

HANDBOOK OF ELLIPTIC INTEGRALS FOR ENGINEERS AND PHYSICISTS. By Paul F. Byrd and Morris D. Friedman. Springer-Verlag, Berlin, Germany, 1954; Lange, Maxwell & Springer, Ltd., London, England, New York, N. Y., 1954. Cloth, 6 × 9 in., xii and 355 pp., 22 figs., $9.85.

REVIEWED BY A. ALI KHEIRALLA[1]

THIS work goes far toward supplying engineers and physicists with an effective means of utilizing the elliptic integrals and elliptic functions which arise in so many important physical problems.

Over 3000 integrals and formulas are presented and systematically arranged to facilitate rapid usage. The notations of Legendre and Jacobi are used throughout except for an appendix on Weierstrassian elliptic integrals and elliptic functions.

There is a 43-page introductory section which summarizes the definitions and most important properties of the functions and could be used as a review or initial approach to the subject. Then follow 145 pages of tables for the reduction of integrals with algebraic, trigonometric, or hyperbolic integrands to Jacobian elliptic functions. Tables of integrals of the latter and of their inverses and of elliptic integrals of the third kind are given. Short sections on repeated integrals, Laplace transforms, and hyperelliptic integrals are also presented. The final sections deal with integrals of elliptic integrals, derivatives, and series expansions.

Appendixes on the Theta functions, pseudo-elliptic integrals, and the afore-mentioned Weierstrassian elliptic functions and elliptic integrals are included.

Finally there are six place tables of numerical values.

The material is well organized and the printing generally well executed in spite of a rather long errata list.

Steam and Gas Turbines

THEORY AND DESIGN OF STEAM AND GAS TURBINES. By John F. Lee. McGraw-Hill Book Company, Inc., New York, N. Y., 1954. Cloth, 6 × 9 in., illus., xiii and 502 pp., $9.

REVIEWED BY H. HEGETSCHWEILER[2]

THIS book may be classified as a textbook on the thermodynamic design of steam and gas turbines as well as other components of thermal power plants.

The student will appreciate the wide use of basic thermodynamics and aerodynamics in the discussion of practical phenomena. Such derivations are enjoyably clear and easy to follow. The neophyte engineer will welcome the chapters on present practice and basic mechanical aspects.

The power specialist will find, in this book, useful design information on the various components of thermal power plants. He will be reminded that basic theory can produce and explain practical results.

The scope of this book appears to be well selected. The two chapters on combustion and regeneration, which might be considered as falling outside of the theory and design of steam and gas turbines, will prove to be most helpful in over-all plant studies. An additional chapter on thermal power-plant economics would be a welcome addition to later editions. There specialists as well as students could be shown how improvements in efficiency of thermal power plants are capitalized and evaluated, dollarwise; or what outages cost, and so on. An illustrative list of cost figures of station equipment would be needed.

The author, probably by nature more of the scientific type, experienced difficulties in handling some practical aspects. For instance, reheat steam power plants are being used not because of improved moisture conditions in the last stages but because the improvement in efficiency due to reheat warrants the additional expenditure and complication of the power station. Also, the terms "impulse" and "reaction" staging were carried through the book to a degree where the unfamilar reader may believe that there are either zero reaction or 50 per cent reaction steam turbines. In practical design any intermediate degree of reaction is being used. Today's most efficient United States steam power stations are equipped with turbines having from 5 to 20 per cent reaction in their high-pressure stages and up to 50 per cent reaction in the low-pressure stages.

It appears that efficiencies of large thermal power plants can be improved substantially by combining steam and gas turbines. Gains, of the order of magnitude of those realized by reheat, are expected. A concerted effort of the gas-turbine, steam-turbine, and boiler-design specialists will be necessary to arrive at a practical solution of this project. Here, the book under review will serve as a valuable link between specialists.

Engineering Mechanics

ENGINEERING MECHANICS. By Linton E. Grinter. The Macmillan Company, New York, N. Y., 1953. Cloth, 6 × 9¼ in., xix and 408 pp., figs., $5.75.

REVIEWED BY E. H. LEE[3]

THIS is a first textbook in engineering mechanics. The first half of the book comprises a rather full discussion of statics with chapters on statics, components and resultants of coplanar forces, equilibrium of coplanar forces, structural analysis, friction and coplanar machine forces, force groups in space, and moments of inertia of areas and bodies. An historical introduction is included. Plane problems are considered extensively by both analytical and graphical means, and an appreciable number of three-dimensional problems are also treated. The second half of the book commences with two long chapters on kinematics, the first concerned with particle motion and the second with motion of rigid bodies. A single chapter of about 40 pages covers the dynamics of particles and rigid bodies using Newton's second law and D'Alembert's principle. Short chapters follow on work and energy, impulse and momentum, vibration and balancing, and the principle of virtual work.

The book includes a wealth of engineering examples which are well illustrated by clear figures. Specimen computation sheets

[1] Lessells and Associates, Inc., Boston, Mass.

[2] Supervisor, Tb. Steam Design and Proposition Engineering, Large Steam Turbine-Generator Department, General Electric Company, Schenectady, N. Y. Assoc. Mem. ASME.

[3] Chairman, Division of Applied Mathematics, Brown University, Providence, R. I. Mem. ASME.

are given for some of the problems as a guide for the students' own work.

In the reviewer's opinion the full and satisfactory treatment of statics leaves an inadequate treatment of dynamics. The latter also contains some misleading or incorrect statements which the student studying this field for the first time will find confusing. For example, the statement about moving axes on page 281, and the statement on page 305 about the invariance of acceleration of bodies connected by an inextensible cable. The components along the cable are only invariant if the line of action of the cable remains fixed in direction. Thus the reviewer feels that the book is suitable only for courses mainly concerned with statics, in which study of dynamics plays a secondary role.

Theory of Games and Statistical Decisions[4]

THEORY OF GAMES AND STATISTICAL DECISIONS. By David Blackwell and M. A. Girshick. John Wiley & Sons, Inc., New York, N. Y., 1954. Cloth, 6 × 9 in., xii and 355 pp., illustrated, $7.50.

REVIEWED BY EDWARD C. VARNUM[5]

WRITTEN by academicians for academicians, this book is designed as a text for graduate students in statistics. The reviewer feels it has little value for a practicing engineer or a manufacturing executive anxious to apply game theory immediately to industrial problems.

Defining a two-person zero-sum game $G(X, Y, M)$ as a payoff function M over the product space X by Y of players' strategies, the authors give examples and continue by describing pure value, mixed extension, minimax strategy, game matrices, good strategy, convex sets and functions, along with many definitions from point-set topology. Statistical games are introduced as special cases in which the players are nature and the statistician. After defining sample spaces, random variables, probability distributions, expected values, decision functions, and risk functions, theorems concerning their use are developed. Further topics include utility, principles of choice, optimal strategies, Bayes solutions, sequential games, and comparison of experiments.

Nonlinear Vibrations

ACTES DU COLLOQUE INTERNATIONAL DES VIBRATIONS NON LINÉAIRES. Publications Scientifiques et Techniques du Ministere de L'Air. Magasin C.T.O., Paris, France, 1953. Paper bound, 7 × 10½ in., 296 pp., illus., 1800 Fr.

REVIEWED BY A. ALI KHEIRALLA[6]

THIS publication contains 21 papers presented at the International Colloquium of 1951 on Non-Linear Vibrations. Most of these are printed simultaneously in French and some other language (English, German, or Italian). Although many of the articles are of high quality, considerations of space prevent mention of more than a few papers of engineering interest.

The paper of Prof. R. Grammel on nonlinear vibrations with infinitely many degrees of freedom discusses the deviation of characteristic frequencies of systems whose stress-strain relation contains a cubic term in strain in addition to the usual linear one given by Hooke's Law. Detailed examples given are torsional vibrations of a circular cylinder and bending vibrations of a prismatic rod.

An article of Prof. J. J. Stoker investigates periodic oscillations of nonlinear systems with infinitely many degrees of freedom. Discussions of certain degenerate cases in which the sufficiency condition of the Poincaré theory does not hold are presented. The equation of the vibrating string

$$\frac{\partial^2 u}{\partial x^2} - \frac{\partial^2 u}{\partial t^2} = \epsilon f(u, x, \omega(\epsilon)t)$$

with $T(\epsilon) = 2\pi + \epsilon\eta(\epsilon)$ is reduced to an integral equation and the difficulties of establishing the existence of solutions are mentioned. Finally, an analog of Duffing's equation in the case of the stretched string is discussed.

Dr. P. Draminsky's paper on the occurrence of dangerous subharmonics in the torsional vibrations of crankshafts treats a system with periodically varying stiffness and a forcing term of the same frequency and phase. A lower bound for the damping necessary to avoid these vibrations is obtained and the practical example of a dynamo driven by a spring-coupled diesel locomotive is presented. Equations with stiffness linear or quadratic in displacement are also discussed and applied to vibrations of springs.

Other articles include contributions by J. Haag, R. Mazet, G. Borg, L. E. Zachrisson, E. Mettler, J. P. Schouten, A. W. Gilles, B. Van der Pol, H. G. Cohen, D. Graffi, L. Collatz, W. Wasow, N. Minorsky, Th. Vogel, L. Gauthier, L. Amerio, P. Vernotte, and C. Ferrari.

Wave Motion and Vibration Theory

WAVE MOTION AND VIBRATION THEORY. Volume 5, Proceedings of the Fifth Symposium in Applied Mathematics of the American Mathematical Society, held at Carnegie Institute of Technology, June 16–17, 1952. Editor, Albert E. Heins; Editorial Committee: R. V. Churchill, Eric Reissner, A. H. Taub. McGraw-Hill Book Co., New York, N. Y., 1954. Cloth, 6¾ × 10 in., 169 pp., figs., $7.

REVIEWED BY G. K. BATCHELOR[7]

THIS volume of fifteen papers delivered at a meeting in 1952 continues the series of publications by the American Mathematical Society. It is rather a mixed bag of papers, since the title seems to have been interpreted in such a way as to include large sections of fluid dynamics, solid mechanics, acoustics, and related differential-equation theory. But for those whose digestions are good, and can cope with a transition from a paper on the diffusion of tides into permeable rock to one on Liénard's differential equation, there are some good things in the volume. Only about four of the papers have the *general* character that one hopes to find in papers presented at a symposium, which is perhaps a pity. Presumably, scientists gather together chiefly in order to clarify their minds and enlarge their horizons, and it seems likely that this can be done best by talking about those aspects of their work that are common to a whole section of their subject. For some reason (related to the strong emphasis in the U. S. A. on the purely mathematical aspects of research in mechanics and theoretical physics?), speakers seem reluctant to talk uninhibitedly about the direction of their work, to speculate (or is this a naughty word?), and to say those interesting things that are usually reserved for informal occasions. One contributor makes some stimulating remarks about how the Sommerfeld radiation condition ought to be formulated—and, being of general significance, I shall remember his point long after I have forgotten the content of other, specialized papers in the volume—but

[4] This review was reprinted from *Applied Mechanics Reviews*, November, 1954, p. 473, Review No. 3458.

[5] Head, Operations Research, Barber-Colman Company, Rockford, Ill.

[6] Lessells and Associates, Inc., Boston, Mass.

[7] Lecturer in Mathematics, Cambridge University, Cambridge, England.

nearly spoils the pleasure of the listener or reader by saying "the writer would not have set down these remarks—which are of a character so obvious that they must also have occurred to many others—if it were not . . ." I think we are fortunate that he did set them down, and I think his diffidence is misplaced.

Turning briefly to the particular contents of the volume, there is first an invaluable survey of the present state of the problem of stability of quasi-plane parallel flow of a fluid by C. C. Lin, who has contributed so many of the developments himself. Research on this problem is in the closing stages and this article can be recommended for those who want a condensed account of what has happened during the thirty years of active work. A review of results obtained for the stability of quite different flow systems, including cases in which the fluid is an electrical conductor and a magnetic field is present, is contributed by S. Chandrasekhar. These two papers, a less substantial review of significant observations of the Mach reflection of shock waves by W. Bleakney, and a discussion of radiation conditions by J. J. Stoker, are the papers that seem to have most general interest. Of the remaining papers, those by N. W. McLachlan, A. Weinstein, and S. Lefschetz are on special differential equations, and there are papers on plane waves incident on a circular disk, on two contiguous half planes of different materials, and on a "soft" obstacle, by H. Levine, by A. E. Heins and H. Feshbach, and by E. W. Montroll and J. M. Greenberg, respectively. P. R. Garabedian contributes a paper on axially symmetric cavity flow, and then finally there are three papers with more appeal to physically-minded readers: G. F. Carrier and W. H. Munk on the diffusion of tides into permeable rock, E. H. Lee on wave propagation in helical compression springs with allowance for coil closure, and R. J. Duffin and A. Schild on the effect of small constraints on the natural frequencies of a vibrating system.

Heat Conduction

HEAT CONDUCTION: With Engineering, Geological and Other Applications. By Leonard R. Ingersoll, Otto J. Zobel, and Alfred C. Ingersoll. The University of Wisconsin Press, 811 State Street, Madison, Wis., 1954. Cloth, 6 × 9 in., xiii and 325 pp., figs, $5.

REVIEWED BY T. P. TORDA[8]

THIS book is a revision of the 1948 McGraw-Hill edition and the principal changes are additions of two new chapters. One of the chapters deals with the "heat pump," or the theory of year-round air conditioning using the ground as a source (or sink) of heat. The other new chapter treats drying and soil consolidation. Though most workers in the field are familiar with the two previous editions of the book, it might be useful to review the contents of the new edition.

The present edition has fourteen chapters, thirteen appendixes, and an index. The first chapter is an introduction giving the symbols used, a very brief historical note, some basic definitions, the fields of application, units and dimensions, and values of some of the constants used.

In the following chapters (2 through 6), the Fourier conduction equation is derived, the heat conduction is treated in steady-one-dimensional and steady- more than one-dimensional problems, and periodic flow of heat in one dimension is discussed. The Fourier trigonometric series are developed, the Fourier integral introduced, and harmonic analyzers discussed.

Chapters 7 to 9 treat linear flow of heat and flow of heat in more than one dimension. The infinite and semi-infinite solid, the slab, the radiating rod, radial flow of heat, heat sources and sinks, spherical problems, the infinite circular cylinder, and the general case of heat flow in an infinite medium are treated.

Chapter 10 discusses the formation of ice. Chapter 11 gives auxiliary methods for treating heat-conduction problems, i.e., the method of isothermal surfaces and flow lines, electrical methods, solutions from tables and curves, the Schmidt method, the relaxation method, and the step method.

Chapter 12 deals with methods of measuring thermal-conductivity constants. The theory of earth heat exchangers for the heat pump is given in chapter 13, and that of drying and soil consolidation in chapter 14.

The appendixes contain tables of constants, indefinite, and definite integrals, values of various functions and integrals, and miscellaneous formulas.

Little emphasis is placed on purely mathematical derivations and on proofs of uniqueness, existence, and convergence theorems. The reader is referred to standard classical references for such topics. The aim of the book is, primarily, to contribute to applied mathematics and applied mechanics and it fulfills this aim excellently. Both the student and the engineer will find this work very useful, since the general treatment of problems is given (setting up and solution) as well as illustrations chosen from many fields of engineering endeavor. Tables of newly evaluated functions and extensions of old tables are given which will prove valuable to those working in the field.

An excellent list of 200 references is given in the last appendix.

The reviewer wishes to congratulate the authors for their valuable contribution.

Gas Dynamics of Thin Bodies

GAS DYNAMICS OF THIN BODIES. By F. I. Frankl and E. A. Karpovich. Translated from the Russian by M. D. Friedman. Interscience Publishers, Inc., New York, N. Y., 1954. Cloth, 6 × 9 in., 33 figs., index, viii and 175 pp., $5.75.

REVIEWED BY ASCHER H. SHAPIRO[9]

THIS little book of 175 pages is a comprehensive treatise on the mathematical theory of the aerodynamics of slender bodies moving at high speeds through a perfect gas. The treatment is limited to nonviscous irrotational flow. What makes it possible to consider thin bodies as a class is that in the motions considered there are only small perturbations from a condition of uniform, streaming flow, and this fact justifies the omission of perturbation terms of second order and higher in the equations of motion. The resulting differential equations for the perturbation quantities then prove to be linear (except at transonic and hypersonic speeds), with concomitant simplifications in mathematical treatment. Practically speaking, not much is lost by considering only slender bodies inasmuch as the aerodynamic drag of bodies which are not slender is excessive at high speeds.

Written by mathematicians, the volume has a highly mathematical flavor. Clearly, the objective of the authors has been to set out the various mathematical procedures which have been developed for obtaining solutions at subsonic and supersonic speeds, and for a variety of aerodynamic geometries of a single partial differential equation: the linearized equation of the perturbation velocity potential. Considering its mathematical spirit, it is not surprising that comparatively little attention is given in the book to assessing the accuracy of the theoretical results, that the emphasis is primarily on theoretical methods rather than on specific theoretical results, and that there is a

[8] Professor of Aeronautical Engineering, University of Illinois, Urbana, Ill.

[9] Professor of Mechanical Engineering, Massachusetts Institute of Technology, Cambridge, Mass. Mem. ASME.

complete absence of comparison between theory and experiment. The book will therefore find its audience among applied mathematicians and theoretical aerodynamicists.

Chapter 1 begins with a historical survey of the subject in which the authors rather perilously try to be good scientists by mentioning the contributions of all nationalities to the subject and at the same time try to be good Soviet citizens by aiming to convey the idea that the really important ideas and the best methods came from the U.S.S.R. In addition, the first chapter contains the mathematical formulation of the problem of linearized potential flow and introduces the elementary solution which forms the foundation of much that follows—the solution for the retarded potential of a point source.

Chapter 2 treats in great detail the subsonic and supersonic flows past bodies of revolution, and incorporates the effects of angle of attack and of longitudinal acceleration of the body. There is considered also the motion of elongated bodies not possessing axial symmetry. In this chapter the reader encounters one of the two diversions from mathematical theory appearing in the book—a page of shadowgraphs of a projectile flying at subsonic and supersonic speeds.

Chapter 3 considers steady motion of wings at subsonic and supersonic speeds. Wings of both infinite span and finite span are included.

In Chapter 4 the wing theory is extended to unsteady flows. In addition, the theory of high-speed propellers is presented.

Chapter 5 discusses the method of conical fields for supersonic flows past wings of infinite span and conical bodies.

By those with some training in the fundamentals of gas dynamics and with the necessary mathematical background (extending through the conventional college course titled "Advanced Calculus"), the book will be found clearly and well written. The translation is impeccable: Not only does it avoid the clumsy ghosts of foreign idioms which so often haunt translations, but it was evidently done by a scientist with a firsthand knowledge of the technical jargon of gas dynamics. The publishers have done an expert job of designing and producing the complicated text matter.

It seems likely that this book will for some time to come occupy an important niche in the literature on gas dynamics.

Thermal Stresses

WAERMESPANNUNGEN INFOLGE STATIONAERER TEMPERATURFELDER. By E. Melan and H. Parkus. Springer-Verlag, Vienna, Austria, 1953. Cloth, 6 × 9 in., 30 figs., tables, v and 114 pp., $4.40.

REVIEWED BY I. MALKIN[10]

THE determination of thermal stresses in various parts of engineering structures of numerous kinds, especially in mechanical engineering, is one of the fundamental problems, which the designing engineer faces in his daily work. While there is a great number of separate contributions to the subject in the technical literature, the book under review is, to the writer's knowledge, the first attempt of giving the interested public a concise but comprehensive presentation of a considerable variety of problems on temperature stresses in the form of a monograph. Within a comparatively small space the authors offer an abundance of useful information with illustrating examples, maintaining at the same time a high theoretical level in an easily readable exposition. Starting from the fundamentals they discuss thermal stresses in systems, consisting of one-dimensional elements, in ribs and plates under various heating and boundary conditions, in thick-walled tubes, to mention only some of the problems. Chapter 9 (pages 89–98), which deals with thermal stresses in shells of revolution with rotationally symmetrical temperature distribution, deserves special attention. This problem is of interest to designers of pressure vessels.

The problem of thermal stresses in pressure vessels has several phases. The determination of the temperature distribution in the shell of a pressure vessel is a rather involved problem of heat transfer influenced by many coefficients of heat transmission, especially if layers of insulating material are being used. Another difficult question is the influence of high temperatures, occurring in pressure vessels, on the magnitude of the stresses. The mathematical stress analysis is an important concluding step to which chapter 9 is a valuable contribution. It begins with a generalization of the well-known differential equations of H. Reissner and E. Meissner to include thermal effects. Then the particular solution is developed for the case of the cylindrical shell. The analysis is valid for moderate temperatures. A numerical example concludes the chapter.

The authors intend to add to the volume under review another one dealing with stress problems for nonstationary temperature distributions and with such characterized by high temperatures, at which elastoplastic conditions are to be expected. These are practically very important but rather difficult problems. The first volume justifies the hope that the second one will be a valuable contribution to the particular subject just indicated.

In conclusion, a very short comment on print and figures: They are both magnificent.

[10] Standards and Design Engineer, Foster Wheeler Corporation, New York, N. Y.

Dynamics and Thermodynamics

THE DYNAMICS AND THERMODYNAMICS OF COMPRESSIBLE FLOW. Vol. 1. By Ascher H. Shapiro. Ronald Press Company, New York, N. Y. 1953. Cloth, 6 × 9 in., xiii and 647 pp., 603 illus., $16.

REVIEWED BY W. R. HAWTHORNE[11]

IT IS rare that writers on compressible flow manage to present both the thermodynamics and the mechanics of the subject in a clear and logical fashion. The author has succeeded in this the first of two volumes in covering the fundamentals of one-dimensional flow and the introductory aspects of two and three-dimensional flow in an adequately rigorous and at the same time reasonably elementary fashion. The volume is divided into five parts. In part one the foundations of the dynamics of macroscopic fluid systems are described. The principles of conservation of mass and Newton's second law are carefully applied to flow through control volumes. The definitions and concepts of thermodynamics are followed by brief expositions of the first and second laws which are then applied to flow through control volumes. The thermodynamic relations for a perfect-gas are set down. A chapter is devoted to the velocity of sound, Mach cone, number and angle, similarity and optical methods of investigating compressible flows. The second part contains five chapters devoted to one-dimensional flow. The general features of isentropic and adiabatic flow are presented. Algebraic expressions are derived for a perfect gas and the use of tables explained; choking and the behavior of nozzles are discussed. The effect of deviations from the perfect-gas state is described. The next chapter deals with the normal shock using the Fanno and Rayleigh lines and developing the relations for a perfect gas. The formation and thickness of shocks and shocks in ducts and supersonic diffusers are included. Flow in constant-area ducts with friction forms the subject of the next chapter.

[11] Professor of Applied Thermodynamics, Cambridge University, Cambridge, England.

Adiabatic and isothermal flow is included and the chapter concludes with a brief summary of experimental measurements of friction coefficients. The next chapter deals with flow with heat-exchange and stagnation-temperature change. Condensation shocks and explosion waves are also included. The final chapter of this part contains the analysis of the simultaneous effects of area change, friction, heat transfer, reaction, mixing, change of phase, and molecular weight and specific heat. Numerical and graphical methods of integration are described and illustrated by examples of combined friction and heat transfer. The chapter concludes with a careful discussion of the conditions at the sonic point.

The third part, which is introductory to the parts on subsonic and supersonic flow in two and three dimensions which follow it, contains a derivation of the equations of motion and introduces the concepts of rotation, velocity potential, and stream function.

The first chapter of part four contains a clear and well-organized description of the application of the method of small perturbations to two-dimensional subsonic flow. The similarity laws of Gothert and Prandtl-Glauert are explained and illustrated by examples and experimental results. The hodograph equations are presented in the next chapter and applied to the derivation of the Kármán-Tsien pressure correction formula. The complex variable is introduced for the first time in a section dealing with profile-shape corrections. There is a chapter dealing with methods used by Janzen and Rayleigh, and Kaplan for calculating nearly exact solutions to two-dimensional subsonic-flow problems. Some of these solutions are given for comparison with experiment and more approximate methods. The experiments on airfoils at subsonic speeds do not perhaps do justice to the previous theory and introduce the shock before the reader is prepared for it.

The remaining chapter in part four deals with the development of Gothert's rule for three-dimensional subsonic flow and its application to bodies of revolution and wings of finite span. The chapter concludes with a brief introduction to the swept-back wing.

Part five contains three chapters dealing with two-dimensional supersonic flow. The first two deal with linear approximation, Mach waves, and their reflection and intersection. The analysis is applied to airfoil profiles and compared with experiment. The method of characteristics is introduced first by an extension of the linearized theory imagining small disturbances propagated along Mach lines, and secondly, by formal mathematical methods. The method is applied to examples such as compressor and turbines blades and supersonic wind-tunnel nozzles. Shear flow is also considered briefly in a section at the end of this chapter.

The last chapter deals with oblique shocks starting with the conventional theory and graphical representations. Numerous aspects of shock waves are presented with clear and adequate illustrations. There are examples of flow with shocks including jets, two-dimensional profiles, wakes, and of shock-boundary layer interaction. In spite of the brevity essential in presenting this material the reader will find this a satisfactory chapter.

Each chapter is followed by a number of well-chosen problems illustrating the textual material and there are two appendixes, one dealing with the theory of characteristics and the other containing useful tables of functions.

The author has set himself exacting standards of completeness, rigor, and lucidity. The result is particularly successful. The book's arrangement is logical and there is sufficient discussion of numerical methods to make it very useful to the engineer. To the expert the book will be refreshing without being altogether repetitious since the author has included some original work. The length of the book, 647 pages, is due to the author's desire to start from scratch. This painstaking interest in careful exposition has resulted in a first class, if expensive, textbook for the student.

Higher Transcendental Functions

HIGHER TRANSCENDENTAL FUNCTIONS. By the Staff of the Bateman Manuscript Project. McGraw-Hill Book Company, Inc., New York, N. Y.; Toronto, Ont.; London, England, 1953. Cloth, 6 × 9 in., Vol. 1, xxvi and 302 pp., $6.50; Vol. 2, xvii and 396 pp., $7.50.

PREPARED BY ERIC REISSNER[12]

THE present two volumes are part of a projected total of three volumes. The authors consider their work as a logical extension of the celebrated treatise on modern analysis by Whittaker and Watson. It seems safe to state that a perusal of the present work requires a level of mathematical maturity going considerably beyond that acquired through the study of books on advanced calculus. Briefly, these books collect in one place more or less widely scattered properties of functions many of which occur in the applications. Volume 1 deals with hypergeometric and confluent hypergeometric functions, with gamma functions, and Legendre functions. Volume 2 includes Bessel functions parabolic cylinder functions, incomplete gamma functions, orthogonal polynomials, and ellipitic integrals and functions.

The original impetus for this work were notes left by the late Prof. Harry Bateman for a projected "Guide to Special Functions." Upon his death in 1946, California Institute of Technology and the Office of Naval Research of the United States Navy arranged for a project to complete Bateman's work. As project director they selected Professor Erdelyi, and as his associates, Professors Magnus, Oberhettinger, and Tricomi, all of whom are internationally known for their contributions to that field of mathematics which in present days is designated as classical analysis. It is natural to expect that under these circumstances there was produced a work of first-rate importance in classical analysis, and the reviewer feels that the authors have lived up to this expectation. The work, however, does not seem to live up to expectations when it comes to judging it from point of view of the research worker in the applications, such as mechanics of continua or particles. This reviewer has looked back upon his own studies in the field of mechanics, trying to visualize at what point availability of the present work would have lightened his task. He feels that in the majority of cases this work could not have lightened his task. (Conceivably, this may be a criticism to be leveled against the reviewer rather than against the books, depending on one's point of view.)

One regrets somewhat that a work of this importance was not type set by letter press. Considering the probable total cost of the project to all parties concerned, the educational institution, the government agency, the authors, and the publisher, the savings accomplished by this economy measure are possibly not in proportion to what they have done to the comfort of the reader.

[12] Professor of Mathematics, Massachusetts Institute of Technology, Cambridge, Mass.

Third U. S. National Congress of Applied Mechanics

Preliminary Announcement

The Third U. S. National Congress of Applied Mechanics will be held at Brown University, Providence, Rhode Island, during June 11–14, 1958. It is hoped that the scheduling of conflicting meetings can be avoided by this early announcement of the date chosen for the Congress. Further announcements concerning the preparation of papers will be made as the Congress draws nearer.

Inquiries regarding the Congress should be addressed to any of the following members of the Organizing Committee at Brown University, Providence, R. I.:

Professor D. C. Drucker, *Secretary*
Professor E. H. Lee, *Treasurer*
Professor W. Prager, *Chairman*